**UNIVERSIDADE ESTADUAL PAULISTA – UNESP**
**INSTITUTO DE QUÍMICA - Câmpus de Araraquara**

**LUIS CARLOS CHITIVA CHITIVA**

# METABOLOMIC STUDY OF THE CHEMICAL COMPOSITION OF BAMBOOS FROM THE GENUS *Guadua* (POACEAE) AND EXPLORATION OF THEIR BIOLOGICAL POTENTIAL

Bogotá – Colombia
Araraquara – São Paulo – Brazil
2024

**UNIVERSIDADE ESTADUAL PAULISTA**
**INSTITUTO DE QUÍMICA**
**PROGRAMA DE PÓS-GRADUAÇÃO EM QUÍMICA**

# METABOLOMIC STUDY OF THE CHEMICAL COMPOSITION OF BAMBOOS FROM THE GENUS *Guadua* (POACEAE) AND EXPLORATION OF THEIR BIOLOGICAL POTENTIAL

**LUIS CARLOS CHITIVA CHITIVA**

Thesis presented, under cotutelle, to the São Paulo State University (UNESP), Institute of Chemistry, Araraquara and Pontificia Universidad Javeriana (PUJ), to obtain the title of Doctor in Chemistry (UNESP) and Doctor in Biological Sciences (PUJ)

**Area of concentration:** Natural Products and Metabolomics

**Advisor:** PhD. Ian Castro Gamboa (UNESP)

**Advisor:** PhD. Geison Modesti Costa (PUJ)

**Co-advisor:** PhD. Juliet Angélica Prieto (PUJ)

Araraquara – São Paulo – Brazil
Bogotá – Colombia
2024

**PONTIFICIA UNIVERSIDAD JAVERIANA**
**FACULTAD DE CIENCIAS**
**DEPARTAMENTO DE QUÍMICA**
**DOCTORADO EN CIENCIAS BIOLÓGICAS**

# METABOLOMIC STUDY OF THE CHEMICAL COMPOSITION OF BAMBOOS FROM THE GENUS *Guadua* (POACEAE) AND EXPLORATION OF THEIR BIOLOGICAL POTENTIAL

**LUIS CARLOS CHITIVA CHITIVA**

Thesis presented, under cotutelle, to the Pontificia Universidad Javeriana (PUJ) and São Paulo State University (UNESP), Institute of Chemistry, Araraquara to obtain the title of Doctor in Biological Sciences (PUJ) and Doctor in Chemistry (UNESP)

**Advisor:** PhD. Geison Modesti Costa (PUJ)

**Advisor:** PhD. Ian Castro Gamboa (UNESP)

**Co-advisor:** PhD. Juliet Angélica Prieto (PUJ)

Bogotá – Colombia
Araraquara – São Paulo – Brazil
2024

Chitiva, Luis Carlos Chitiva
C543m Metabolomic study of the chemical composition of bamboos from the genus *Guadua* (Poaceae) and exploration of their biological potential / Luis Carlos Chitiva Chitiva – Araraquara: [s.n.], 2024
316 p.: il.

Thesis (doctor) – Universidade Estadual Paulista, Instituto de Química
Advisor: Ian Castro Gamboa
Advisor: Geison Modesti Costa
Co-advisor: Juliet Angélica Prieto

1. Bamboo. 2. *Guadua*. 3. Metabolomics. 4. Metabolites. 5. Bioactive compounds. I. Title.

Sistema de geração automática de fichas catalográficas da Unesp. Biblioteca do Instituto de Química, Araraquara. Dados fornecidos pelo autor(a).

Essa ficha não pode ser modificada

**NOTA DE ADVERTENCIA**

**Artículo 23 de la Resolución No. 13 de Julio de 1946**

“La Universidad no se hace responsable por los conceptos emitidos por sus alumnos en sus trabajos de tesis. Solo velará porque no se publique nada contrario al dogma y a la moral católica y porque la tesis no contenga ataques personales contra persona alguna, antes bien se vea en ellas el anhelo de buscar la verdad y la justicia”

**NOTA**

“Esta tesis doctoral se ha realizado teniendo en cuenta las normativas establecidas de los programas en el convenio de cooperación para la cotutela de tesis doctorales conducente al doble título de doctor firmado entre las universidades”.
Por la Pontificia Universidad Javeriana (Bogotá, Colombia), título de Doctor en Ciencias Biológicas y por la Universidad Estatal Paulista (Araraquara, Brasil), título de Doctor en Química.

**NOTE**

"This doctoral thesis has been carried out taking into account the established regulations of the programs in the cooperation agreement for the cotutelle of doctoral theses leading to the double doctoral degree signed between the universities".
From the Pontificia Universidad Javeriana (Bogotá, Colombia), Doctor in Biological Sciences and from the São Paulo State University (Araraquara, Brazil), Doctor in Chemistry.

**OBSERVAÇÃO**

"Esta tese de doutorado foi realizada levando em consideração os regulamentos estabelecidos dos programas no acordo de cooperação para os doutorados em cotela de tese, levando ao título duplo de doutorado assinado entre as universidades".
Pela Pontifica Universidad Javeriana (Bogotá, Colômbia), Título de Doutor em Ciências Biológicas e pela Universidade Estadual Paulista (Araraquara, Brasil), Título de Doutor em Química.

## POTENTIAL IMPACT OF THIS RESEARCH

This study provides a deep understanding of the chemical composition and biological activity of bamboos of the genus *Guadua*, driving new scientific research and technological developments in biomedicine and biotechnology. The identification of bioactive compounds with antioxidant, anti-inflammatory and cytotoxic properties open opportunities to develop new pharmaceutical and therapeutic products, positively impacting public health and generating new economic opportunities in the pharmaceutical industry. The innovative metabolomic approach used in this study can be applied to other medicinal plants, promoting the identification of new bioactive compounds and the development of medicinal and therapeutic applications. This work provides valuable knowledge that can be incorporated into educational and research programs at universities and research centers, encouraging the training of new researchers and collaborative projects. In addition, it highlights the cultural importance of bamboos of the genus *Guadua*, promoting their preservation and sustainable use. The results of this study interest the international scientific community, facilitating collaboration between researchers from different countries and promoting the global dissemination of knowledge. Finally, research can significantly impact the local and regional communities where these bamboos grow, promoting their sustainable use and biodiversity conservation, and contributing to the development of public policies and conservation programs at the national level.

## IMPACTO POTENTIAL DE ESTA PESQUISA

Este estudo proporciona uma compreensão profunda da composição química e atividade biológica dos bambus do gênero *Guadua*, impulsionando novas pesquisas científicas e desenvolvimentos tecnológicos em biomedicina e biotecnologia. A identificação de compostos bioativos com propriedades antioxidantes, anti-inflamatórias e citotóxicas abre oportunidades para desenvolver novos produtos farmacêuticos e terapêuticos, impactando positivamente a saúde pública e gerando novas oportunidades econômicas na indústria farmacêutica. A abordagem metabolômica inovadora utilizada neste estudo pode ser aplicada a outras plantas medicinais, promovendo a identificação de novos compostos bioativos e o desenvolvimento de aplicações medicinais e terapêuticas. Este

trabalho fornece conhecimento valioso que pode ser incorporado em programas educacionais e de pesquisa em universidades e centros de pesquisa, incentivando a formação de novos pesquisadores e projetos colaborativos. Além disso, destaca a importância cultural dos bambus do gênero *Guadua*, promovendo sua preservação e uso sustentável. Os resultados deste estudo interessam à comunidade científica internacional, facilitando a colaboração entre pesquisadores de diferentes países e promovendo a disseminação global do conhecimento. Finalmente, a pesquisa pode impactar significativamente as comunidades locais e regionais onde esses bambus crescem, promovendo seu uso sustentável e a conservação da biodiversidade, e contribuindo para o desenvolvimento de políticas públicas e programas de conservação em nível nacional.

UNIVERSIDADE ESTADUAL PAULISTA

Câmpus de Araraquara

## CERTIFICADO DE APROVAÇÃO

TÍTULO DA TESE: METABOLOMIC STUDY OF THE CHEMICAL COMPOSITION OF BAMBOOS FROM THE GENUS Guadua (POACEAE) AND EXPLORATION OF THEIR BIOLOGICAL POTENTIAL

**AUTOR: LUIS CARLOS CHITIVA CHITIVA**
**ORIENTADOR(A): IAN CASTRO GAMBOA**
**COORIENTADOR: GEISON MODESTI COSTA**

Aprovado como parte das exigências para obtenção do Título de Doutor em Química, pela Comissão Examinadora:

Prof. Dr. IAN CASTRO GAMBOA (Participaçao Presencial)
Departamento de Bioquimica e Quimica Organica / Instituto de Quimica – UNESP – Araraquara

Prof. Dr. GEISON MODESTI COSTA (Participaçao Presencial)
Departamento de Química / Pontificia Universidad Javeriana - Bogotá - Colombia

Prof. Dr. NORBERTO PEPORINE LOPES (Participaçao Virtual)
Departamento de Física e Química / Faculdade de Ciências Farmacêuticas - USP - Ribeirão Preto

Prof. Dr. JOSÉ ALFREDO IGLESIAS JIMÉNEZ (Participaçao Presencial)
Biologia / Pontificia Universidad Javeriana

Prof. Dr. ALAN CESAR PILON (Participaçao Presencial)
Departamento de Bioquimica e Quimica Organica / Instituto de Química - UNESP - Araraquara

Prof. Dr. DIEGO RICARDO MUÑOZ CENDALES (Participaçao Presencial)
Química / Universidad Salesiana

Araraquara, 19 de julho de 2024

**METABOLOMIC STUDY OF THE CHEMICAL COMPOSITION OF BAMBOOS FROM THE GENUS *Guadua* (POACEAE) AND EXPLORATION OF THEIR BIOLOGICAL POTENTIAL**

**LUIS CARLOS CHITIVA CHITIVA**

**APROBADO**

**PhD. Geison Modesti Costa**
DIRECTOR PUJ

**PhD. Ian Castro Gamboa**
DIRECTOR UNESP

**PhD. Juliet Angélica Prieto**
CO-DIRECTORA PUJ

**PhD. Norberto Peporine Lopes**
JURADO

**PhD. Martha Zuluaga**
JURADO

**PhD. Diego Ricardo Muñoz**
JURADO

**PhD. José Alfredo Iglesias**
JURADO

**PhD. Alan Cesar Pilon**
JURADO

**CURRICULUM VITAE**

## Identification

**Name:** Luis Carlos Chitiva Chitiva
**Date of birth:** 18/06/1992
**Nationality:** Colombian
**Name in bibliographic citations:**Chitiva- Chitiva, L. C.; Chitiva, L. C.
**Curriculum Lattes:** http://lattes.cnpq.br/8935150467809395
**ORCID:** https://orcid.org/0000-0003-1422-5545
**Another identifier:**
https://scienti.minciencias.gov.co/cvlac/visualizador/generarCurriculoCv.do?cod_rh=0000021579

## Academic education

**2020-2024** Doctorate in Chemistry
Universidade Estadual Paulista, UNESP, São Paulo, Brazil
Doctorate in Biological Sciences
Pontificia Universidad Javeriana, PUJ, Bogotá, Colombia
Title: Metabolomic study of the chemical composition of bamboos from the genus *Guadua* (Poaceae) and exploration of their biological potential.
Advisor: PhD. Ian Castro Gamboa (UNESP)
Advisor: PhD. Geison Modesti Costa (PUJ)
Co-advisor: PhD. Juliet Angélica Prieto (PUJ)

**2017-2019** Master in Chemistry
Universidad Nacional de Colombia, UNAL, Bogotá, Colombia
Title: Search for antifungal substances for the control of phytopathogenic fungi from chemical constituents present in *Piper pesaresanum.*
Advisor: PhD. Oscar Javier Patiño Ladino
Co-advisor: PhD. Fabian Harvey López Vallejo

**2009-2015** Bachelor in Chemistry
Universidad Distrital Francisco José de Caldas, Bogotá, Colombia
Title: Contribution to the phytochemical study of leaves of the plant species *Senna reticulata* (Fabaceae) and evaluation of their antioxidant activity.
Advisor: MSc. William Fernando Castrillón Cardona
Co-advisor: MSc. Javier Andrés Matulevich Pelaez

## Complementary academic training

**2022-2023** Scholarship-Internship of cotutelle of doctoral thesis
Universidade Estadual Paulista, UNESP, São Paulo, Brazil

Title: Metabolomic study of the chemical composition of bamboos from the genus *Guadua* (Poaceae) and exploration of their biological potential.
Advisor: PhD Ian Castro Gamboa
Scholarship holder from: CNPq 23038.000776/2017-54

**2019-2020** Diploma in Instrumental Analytical Chemistry
Khymos

**2018-2019** Scholarship-Internship Program for Young Researchers and Innovators
Universidad Nacional de Colombia, UNAL, Bogotá, Colombia
Title: Bioprospecting in species of the *Piper* genus for the control of *Moniliophthora roreri*.
Advisor: Luis Enrique Cuca Suárez
Scholarship holder from: Ministerio de Ciencia Tecnología e Innovación (MINCIENCIAS) 287-2018

## Disciplines taken during the doctorate

1. Chemical Safety in Laboratories (2 credits), **concept A**
2. Integrated Metabolomics (3 credits), **concept A**
3. Mass spectrometry as an important tool in multiomics analysis (3 credits), **concept A**

## Full articles published in journals

1. CHITIVA, L. C., SANTAMARÍA-TORRES, M. A., REZENDE-TEIXEIRA, P., BORLOT, J. R. P. D. O., ROMAGNA, R. D. A., LONDOÑO, X., KITAGAWA, R. R., COSTA-LOTUFO, L., PRIETO.RODRÍGUEZ, J. A., CASTRO-GAMBOA, I., & COSTA, G. M. (2024). Uncovering Metabolic Alterations in HCT-116 Colon Cancer Cells upon Exposure to Bamboo Leaf Extract Obtained from *Guadua incana* Londoño. *Molecules*, 29(13), 2985.

2. QUEJADA, L. F., HERNANDEZ, A. X., CHITIVA, L. C., BRAVO-CHAUCANÉS, C. P., VARGAS-CASANOVA, Y., FARIA, R. X., COSTA, G. M., & PARRA-GIRALDO, C. M. (2024). Unmasking the Antifungal Activity of *Anacardium occidentale* Leaf Extract against Candida albicans. *Journal of Fungi*, 10(7), 464.

3. BRAVO-CHAUCANÉS, C. P., CHITIVA, L. C., VARGAS-CASANOVA, Y., DIAZ-SANTOYO, V., HERNÁNDEZ, A. X., COSTA, G. M., & PARRA-GIRALDO, C. M. (2023). Exploring the Potential Mechanism of Action of Piperine against *Candida albicans* and Targeting Its Virulence Factors. *Biomolecules*, 13(12), 1729.

4. VILLAMARIN-RAAD, D. A., LOZANO-PUENTES, H. S., CHITIVA L. C., COSTA, G. M., DÍAZ-GALLO, S. A., DÍAZ-ARIZA, L. A. (2023). Changes in phenolic profile, total phenols and total flavonoids content of *Guadua angustifolia* Kunth plants under organic and conventional fertilization. *ACS Omega*, 8, 41223-41231.

5. VELÁSQUEZ, M. M., LATTIG, M. C., CHITIVA, L. C., COSTA, G. M., SUTACHAN, J. J., & ALBARRACIN, S. L. (2023). Dendritogenic Potential of the Ethanol Extract from *Lippia alba* Leaves in Rat Cortical Neurons. *Molecules*, 28(18), 6666.

6. LASSO, P., ROJAS, L., ARÉVALO, C., URUEÑA, C., NATALIA MURILLO, NOSSA, P., SANDOVAL, T., CHITIVA, L. C., BARRETO, A., COSTA, G. M. & FIORENTINO S. (2023). *Piper nigrum* extract suppresses tumor growth and enhances the antitumor immune response in murine models of breast cancer and melanoma. Cancer Immunology, Immunotherapy, 1-14.

7. VANEGAS ROMERO, M. ÁNGEL, CHITIVA, L. C., BRAVO-CHAUCANÉS, C. P., HERNÁNDEZ, A. X., PARRA-GIRALDO, C. M., & COSTA, G. M. (2023). Black-eyed Susan vine (*Thunbergia alata*): chemical and antifungal potential evaluation of an invasive plant species in Colombia. *Universitas Scientiarum*, 28(2), 217–229.

8. CHITIVA, L. C., LOZANO-PUENTES, H. S., LONDOÑO, X., LEÃO, T. F., CALA, M. P., RUIZ-SÁNCHEZ, E., DÍAZ-ARIZA, L. A., PRIETO-RODRÍGUEZ, J. A., CASTRO-GAMBOA, I. & COSTA, G. M. (2023). Untargeted metabolomics approach and molecular networking analysis reveal changes in chemical composition under the influence of altitudinal variation in bamboo species. *Frontiers in Molecular Biosciences*, 10, 1192088.

9. BRAVO-CHAUCANÉS, C. P., VARGAS-CASANOVA, Y., CHITIVA-CHITIVA, L. C., CEBALLOS-GARZÓN, A., MODESTI-COSTA, G., & PARRA-GIRALDO, C. M. (2022). Evaluation of anti-*Candida* potential of *Piper nigrum* extract in inhibiting growth, yeast-hyphal transition, virulent enzymes, and biofilm formation. *Journal of Fungi*, 8(8), 784.

10. CHITIVA-CHITIVA, L. C., LADINO-VARGAS, C., CUCA-SUÁREZ, L. E., PRIETO-RODRÍGUEZ, J. A., & PATIÑO-LADINO, O. J. (2021). Antifungal activity of chemical constituents from *Piper pesaresanum* C. DC. and derivatives against phytopathogen fungi of cocoa. *Molecules*, 26(11), 3256.

11. MATULEVICH-PELÁEZ, J. A., CASTRILLÓN-CARDONA, W. F., & CHITIVA-CHITIVA, L. C. (2017). Phytochemical study and evaluation of antioxidant capacity of leaves of *Senna reticulata* obtained in the Colombian Andean region. *Revista científica*, (29), 149-163.

12. PELÁEZ, J. A., CARDONA, W. F., CHITIVA, L. C., & DÍAZ, E. A. (2017). Caracterización química del aceite esencial de hojas de la especie vegetal *Senna reticulata* (Fabaceae). *Revista Facultad de Ciencias Básicas*, 13(2), 123-127.

**Participation in scientific events**

1. 20th Annual Conference of the Metabolomics Society – Metabolomics 2024, Osaka – Japan, June 16-20, 2024. Metabolomic analysis of chemical composition and

exploration of biological potential in bamboo of the genus *Guadua*. Luis Carlos Chitiva, Paula Rezende Teixeira, Hair Santiago Lozano-Puentes, Jessica Rodrigues Pereira de Oliveira Borlot, Rodrigo de Almeida Romagna, Rodrigo Rezende Kitagawa, Lucía Ana Díaz-Ariza, Ximena Londoño, Leticia Costa-Lotufo, Juliet Angélica Prieto, Geison Modesti Costa, Ian Castro-Gamboa. Oral presentation – Co-author.

2. 9th Brazilian Conference on Natural Products/XXXV RESEM, Salvador, Brazil, 24-27 de October 2023. Metabolomics Approach Applied to the Analysis of the Chemical Composition of Bamboos Belonging to the Genus *Guadua* and its Correlation with Cytotoxic Activity. Luis Carlos Chitiva, Paula Rezende Teixeira, Ximena Londoño, Leticia V. Costa Lotufo, Juliet A. Prieto Rodríguez, Geison Modesti Costa, and Ian Castro Gamboa. Presentación oral – Autor.

3. IV Lamps Meeting (Latin American Metabolic Profiling Society, Cartagena, Colombia, 2-4 de noviembre, 2022. Untargeted phyto-metabolomics using LC-MS-QTOF reveals the influence of altitudinal variation in chemical composition of bamboo species. Luis Carlos Chitiva, Santiago Lozada, Tiago Leão, Mónica Cala, Juliet Angélica Prieto, Ian Castro-Gamboa, Geison Modesti Costa. Presentación poster – Autor.

4. IV Lamps Meeting (Latin American Metabolic Profiling Society, Cartagena, Colombia, 2-4 de noviembre, 2022. Metabolic profiling of ethanolic extracts from Colombian species of *Guadua* Kunth (Poaceae). Luis Carlos Chitiva, Ximena Londoño, Joao Bronzel, Juliana Rodrigues, Ian Castro-Gamboa, Geison Modesti Costa. Presentación poster – Autor.

5. 7 SIBGUADUA Séptimo Simposio Internacional del Bambú y la Guadua, Lima, Perú, 15-17 de septiembre, 2022. Análisis del perfil químico de *Guadua* spp. encontrada en guaduales colombianos. Luis Carlos Chitiva, Hair Santiago Lozano, Ximena Londoño, Juliet Angélica Prieto, Lucía Ana Díaz, Geison Modesti Costa. Presentación oral – Coautor.

6. I Congreso Internacional Programa GAT, Bogotá, Colombia, 30 de noviembre y 1 de diciembre, 2021. Perfil metabólico preliminar de extractos vegetales con posible potencial citotóxico. Luis Carlos Chitiva, Laura Rojas, Susana Fiorentino, Juliet Angélica Prieto, Geison Modesti Costa. Presentación oral – Autor.

7. 8th Brazilian Conference on Natural Products/XXXIV RESEM, Goiás, Brazil, 9-12 de noviembre 2021. Cytotoxic activity and preliminary metabolic profile of Colombian plant extracts. Luis Carlos Chitiva, Laura Rojas, Susana Fiorentino, Juliet Angélica Prieto, Geison Modesti Costa. Presentación poster – Autor.

8. XVI Congreso La Investigación en la Pontificia Universidad Javeriana, Bogotá, Colombia, 15-16 de septiembre, 2021. Perfilamiento químico de plantas colombianas con posible potencial citotóxico. Luis Carlos Chitiva, Laura Rojas, Susana Fiorentino, Geison Modesti Costa. Presentación oral – Autor.

**Participation in supervisions**

1. Student: Miguel Quintero Correa. Research title: Chemotaxonomic contribution for three plant species of the genus *Piper* (Piperaceae) using HPTLC and CPC techniques. Pontificia Universidad Javeriana. Status: Completed Thesis. Biology Program. 2022. Supervisor: Prof. Dr. Geison Modesti Costa.

**DEDICATORY**

*A mi amada esposa,*
*quien me acompañó, apoyó y me brindó todo su amor*
*durante esta etapa de mi vida*

*A mis suegros y Tato por su apoyo incondicional*

*A mis padres, quienes me dieron la vida,*
*y a mi hermano, quien también me acompañó*
*en este andar de la vida*

*A todos ellos, gracias por confiar en mí*

**ACKNOWLEDGMENTS**

The time has come to express my deepest gratitude to all those who helped me develop this doctoral work. With your collaboration, it was possible to have achieved this.

First of all, I would like to thank my supervisors, Prof. Geison Modesti Costa (PUJ-Colombia) and Prof. Ian Castro Gamboa (UNESP-Brazil), for giving me the opportunity to work on this project, for having the patience in teaching me and supporting me in critical moments. I am very grateful to have completed my PhD under his excellent expertise and guidance. My great gratitude goes to my co-supervisor, Prof. Juliet Angélica Prieto, for her dedication and unconditional support.

I want to thank the GIFUJ research group for opening the doors to me and being able to develop this work. From there, my laboratory colleagues José, Leonardo, Santiago, Yohum, Kevin, and Andrea for all their collaboration.

I would like to thank the NUBBELÂNDIA group for opening the doors for me and being able to discover new things in metabolomics. From there, I want to thank Prof. João Bronzel, Prof. Juliana Rodrigues, Prof. Uenifer Couto, Prof. Nivaldo Boralle, and Prof. Lidiane Gaspareto for helping me with the instrumental analyses. I also want to thank my laboratory colleagues “Doutor Givaldo”, “Doutor Edelson”, Emanuel, Rafael, Lucas, Luiz, Yves, and Camila for all their teachings.

I especially want to thank Prof. Tiago Leão for sharing his expertise, knowledge, and collaboration during my stay at UNESP.

I also want to express deep gratitude to the research groups that played a fundamental part in carrying out the biological assays, mainly to the group *Laboratório de Farmacologia de Produtos Naturais Marinhos* of Prof. Leticia Costa Lotufo for opening the doors of the Laboratory to me and being able to carry out the cytotoxic assays. From there, I also thank Paula Rezende for all her collaboration and teachings.

I also thank the research group *Laboratório de Triagem Biológica de Produtos Naturais* of Prof. Rodrigo Kitawaga for their collaboration in the anti-inflammatory assays and from there to Jessica and Rodrigo for the biological trials carried out.

I would also like to thank Prof. Mónica Cala, leader of the MetCore group, for opening the doors to me and learning about the area of metabolomics during the collaboration stay.

I want to thank Prof. Ximena Londoño for her collaboration in sampling the *Guadua* species and all her teachings during my stay at El Paraiso del Bambú y la Guadua.

I want to thank Prof. Lucia Ana for allowing me to be part of the "*Guadua team*" and for the collaborations that resulted from it.

I especially want to thank my much-loved wife, Mary Andrea, for her unconditional love and support during this time and for her advice and collaboration in developing this work.

I thank my brother Andrés (Brous) and my parents, Elsa, and Luis, for their infinite love and support throughout my life.

I am grateful for approving the cotutelle agreement (Doctoral Thesis and Double Degree) between PUJ-Colombia and UNESP-Brazil, signed on June 21st, 2022.

I thank the Ministerio de Ambiente y Desarrollo Sostenible (MINAMBIENTE) for granting the contract to access genetic resources used in this study.

I thank the PUJ and the Colombia Científica program "*Generación de alternativas terapéuticas en cáncer a partir de plantas a través de procesos de investigación y desarrollo traslacional, articulados en sistemas de valor sostenibles ambiental y económicamente*" and the World Bank for the financial support throughout my doctorate.

Likewise, I want to thank Vicerrectoría de Investigación at the Pontificia Universidad Javeriana for contributing to the financial support of this research (Proposal ID 20834).

Finally, I thank the Instituto Nacional de Ciência e Tecnologia em Biodiversidade e Produtos Naturais (INCTBioNat) and Conselho Nacional de Desenvolvimento Científico e Tecnológico (CNPq) with contract number 23038.000776/2017-54 for the financial support.

*Muchas gracias a todos!!!*

*Muito obrigado a todos!!!*

## ABSTRACT

Bamboos belonging to the *Guadua* genus are recognized worldwide for their various applications in the ecological, social, economic, cultural, and medicinal fields. However, to date information on its chemical composition and biological activity is still unknown. In this context, the present work aimed to study the chemical composition and biological activity of bamboos of the *Guadua* genus through a metabolomic approach, with four main objectives: (1) evaluate the variations in the chemical composition under the influence of an altitudinal gradient and map chemical diversity using GNPS; (2) correlate chemical composition and biological activities for the identification of bioactive compounds; (3) evaluate metabolic alterations in HCT-116 cells after exposure to *G. incana* extract; and (4) isolate some bioactive compounds from the active extract of *G. incana*, guided by the metabolomic approach. The results obtained highlight that the first objective shows a significant increase in flavonoid composition at high altitudes. A great richness in the chemical diversity of these bamboos was also demonstrated. In the second objective, the presence of 49 compounds was identified in *Guadua* species, including flavonoids and cinnamic acid derivatives that showed a strong correlation with anti-inflammatory and antioxidant activities. Particularly, it was found that flavone glycosides presented a positive correlation with cytotoxic potential. In the third objective, an alteration of 99 metabolites was found in HCT-116 cells when treated with the active extract of *G. incana*, mainly associated with glutathione metabolism. Finally, in the fourth objective, a flavone glycoside corresponding to isoschaftoside was isolated that showed potent cytotoxic activity and a mixture of three flavones derived from apigenin. In conclusion, this study contributed important and robust scientific data to the knowledge of the chemical composition and the antioxidant, anti-inflammatory and cytotoxic potential of several species of the genus *Guadua* that had not yet been studied.

***Keywords:*** bamboo, *Guadua*, metabolomics, metabolomic profiling, molecular networks, metabolites, bioactive compounds, anti-inflammatory activity, antioxidant activity, cytotoxic activity, HCT-116 cells.

## RESUMO

Os bambus pertencentes ao gênero *Guadua* são reconhecidos mundialmente por suas diversas aplicações nas áreas ecológica, social, econômica, cultural e medicinal. Entretanto, até o momento, informações sobre sua composição química e atividade biológica ainda são desconhecidas. Neste contexto o presente trabalho teve como objetivo estudar a composição química e a atividade biológica de bambus do gênero *Guadua* através de uma abordagem metabolômica tendo quatro objetivos principais: (1) avaliar as variações na composição química sob a influência de um gradiente altitudinal e mapear a diversidade química usando GNPS; (2) correlacionar composição química e atividades biológicas para identificação de compostos bioativos; (3) avaliar alterações metabólicas em células HCT-116 após exposição ao extrato de *G. incana*; e (4) isolar alguns compostos bioativos do extrato ativo de *G. incana*, guiado pela abordagem metabolômica. Os resultados obtidos destacam que o primeiro objetivo destaca um aumento significativo na composição de flavonóides em grandes altitudes. Também foi demonstrada uma grande riqueza na diversidade química desses bambus. No segundo objetivo, foi identificada a presença de 49 compostos nas espécies de *Guadua*, incluindo flavonóides e derivados do ácido cinâmico que apresentaram forte correlação com atividades antiinflamatórias e antioxidantes. Particularmente, constatou-se que as flavonas glicosiladas apresentaram correlação positiva com o potencial citotóxico. No terceiro objetivo, foi encontrada alteração de 99 metabólitos em células HCT-116 quando tratadas com o extrato ativo de *G. incana*, principalmente associado ao metabolismo da glutationa. Por fim, no quarto objetivo, foram isoladas uma flavona glicosilada correspondente ao isoschaftosídeo que apresentou potente atividade citotóxica e uma mistura de três flavonas derivadas da apigenina. Concluindo, este estudo contribuiu com dados científicos importantes e robustos para o conhecimento da composição química e do potencial antioxidante, antiinflamatório e citotóxico de diversas espécies do gênero *Guadua* que ainda não haviam sido estudadas.



***Palavras-chave:*** bambu, *Guadua*, metabolômica, perfil metabolômico, redes moleculares, metabólitos, compostos bioativos, atividade anti-inflamatória, atividade antioxidante, atividade citotóxica, células HCT-116.

## RESUMEN

Los bambúes pertenecientes al género *Guadua* son reconocidos a nivel mundial por sus diversas aplicaciones en los ámbitos ecológico, social, económico, cultural y medicinal. Sin embargo, hasta la fecha aún se desconoce información sobre su composición química y actividad biológica. En este contexto, el presente trabajo tuvo como objetivo estudiar la composición química y actividad biológica de bambúes del género *Guadua* mediante un enfoque metabolómico, con cuatro objetivos principales: (1) evaluar las variaciones en la composición química bajo la influencia de un gradiente altitudinal y mapear la diversidad química mediante GNPS; (2) correlacionar la composición química y actividades biológicas para la identificación de compuestos bioactivos; (3) evaluar las alteraciones metabólicas en las células HCT-116 tras la exposición al extracto de *G. incana*; y (4) aislar algunos compuestos bioactivos a partir del extracto activo de *G. incana*, guiado por el enfoque metabolómico. Los resultados obtenidos resaltan que en el primer objetivo se destaca un aumento significativo en la composición de flavonoides a altitudes elevadas. También se demostró una gran riqueza en la diversidad química de estos bambúes. En el segundo objetivo, se identificó la presencia de 49 compuestos en las especies de *Guadua*, incluyendo flavonoides y derivados de ácidos cinámicos que mostraron una fuerte correlación con las actividades antiinflamatoria y antioxidante. Particularmente, se encontró que flavonas glucosiladas presentaron una correlación positiva con el potencial citotóxico. En el tercer objetivo, se encontraron una alteración de 99 metabolitos en las células HCT-116 cuando fueron tratadas con el extracto activo de *G. incana*, asociados principalmente con el metabolismo del glutatión. Finalmente, en el cuarto objetivo se aisló una flavona glucosilada correspondiente a isoschaftosido que mostró una potente actividad citotóxica y una mezcla de tres flavonas derivadas de apigenina. En conclusión, este estudio aportó importantes y robustos datos científicos al conocimiento de la composición química y del potencial antioxidante, antiinflamatorio y citotóxico de diversas especies del género *Guadua* que aún no habían sido estudiadas.



***Palabras clave***: bambú, *Guadua*, metabolómica, perfil metabolómico, redes moleculares, metabolitos, compuestos bioactivos, actividad antiinflamatoria, actividad antioxidante, actividad citotóxica, células HCT-116.

## RESUMO EXPANDIDO

O estudo abrangente de produtos naturais e compostos bioativos inspirou inovações importantes e poderosas na descoberta e no desenvolvimento de medicamentos. Esses produtos têm sido estudados há anos e as plantas têm sido a principal fonte de compostos usados na medicina, na farmacologia e na biologia. Não é de se surpreender que um número significativo de medicamentos prescritos seja derivado ou inspirado em produtos naturais e sigam sendo usados na medicina tradicional e moderna para o tratamento de várias doenças (DIAS; URBAN; ROESSNER, 2012; MUSHTAQ et al., 2018; PRIYA; SATHEESHKUMAR, 2020). Os efeitos medicinais benéficos das plantas podem estar relacionados às combinações de compostos químicos presentes que atuam de forma sinérgica. Assim, elas têm a capacidade de sintetizar estruturas químicas complexas e diversas que possuem vários efeitos terapêuticos de maneiras únicas, como antibióticos, antifúngicos, antivirais, antioxidantes, anticancerígenos etc., e servem para desafiar e inspirar pesquisas básicas e aplicadas (BONAM et al., 2018; KATIYAR et al., 2012; NEWMAN; CRAGG, 2020). Atualmente, os produtos naturais têm desempenhado um papel importante na descoberta e no desenvolvimento de medicamentos, especialmente para agentes anticâncer, de modo que grande parte desses medicamentos tem origem natural (CRAGG; PEZZUTO, 2016; KOPARDE; DOIJAD; MAGDUM, 2019).

As plantas de bambu pertencentes ao gênero *Guadua* são reconhecidas mundialmente por suas diversas aplicações ecológicas, sociais, econômicas, culturais, comerciais e medicinais. No entanto, até o momento, as informações sobre a composição química e o potencial biológico do metaboloma dessas espécies ainda são desconhecidas. Atualmente, existem abordagens abrangentes para o estudo de produtos naturais usando abordagens metabolômicas, inspirando contribuições importantes e inovadoras para a descoberta de compostos bioativos.

Nesse contexto, a presente pesquisa foi realizada em colaboração entre o Grupo de Investigación Fitoquímica Universidad Javeriana (GIFUJ), na Colômbia, e o Núcleo de Bioensaios, Biossíntese e Ecofisiologia de Produtos Naturais (NuBBE), no Brasil, no âmbito do Programa Científico GAT-Colombia, para estudar a diversidade da composição

química e explorar o potencial biológico dos bambus do gênero *Guadua* por meio de análise metabolômica, com o objetivo de contribuir para o conhecimento químico e biológico dessas bambus.

O desenvolvimento metodológico incluiu quatro etapas: Na primeira etapa, as variações na composição química sob a influência de um gradiente altitudinal de 111 amostras de plantas correspondentes a 12 espécies de bambu pertencentes aos gêneros *Guadua*, *Phyllostachys* e *Bambusa* foram avaliadas usando uma abordagem metabolômica não direcionada por cromatografia líquida acoplada à espectrometria de massa (LC-MS) e mapeamento da diversidade química por análise de rede molecular. Na segunda etapa, o perfil metabolômico de 30 extratos pertencentes a 10 espécies de *Guadua* foi realizado por LC-MS e espectroscopia de ressonância magnética nuclear de prótons ($^{1}$H-NMR) e correlacionado com a atividade biológica anti-inflamatória, antioxidante e citotóxica para a identificação de compostos bioativos. Na terceira etapa, as alterações metabólicas em células de câncer de cólon (HCT-116) induzidas pelo extrato de *G. incana* foram avaliadas usando uma abordagem metabolômica não direcionada por LC-MS e $^{1}$H-NMR para a exploração de possíveis mecanismos de ação. Na última etapa, um estudo fitoquímico orientado pela metabolômica e a bioatividade do extrato de *G. incana* foram realizados por cromatografia de partição centrífuga (CPC) para o isolamento de alguns marcadores químicos e biológicos.

Os resultados da primeira etapa nos permitiram determinar mudanças significativas na composição química das espécies de bambu sob a influência da altitude. Houve um aumento significativo na composição de flavonóides em altas altitudes, em contraste com as baixas altitudes, onde foi encontrado um aumento significativo no perfil de ácidos cinâmicos e derivados. Também foi demonstrada uma riqueza na diversidade química desses bambus, incluindo a presença de flavonoides glicosilados, derivados do ácido cinâmico, lignanas alcaloides, carboidratos e ácidos graxos. Na segunda etapa, 49 compostos foram identificados no metaboloma geral das espécies de *Guadua*, incluindo flavonoides e derivados do ácido cinâmico que mostraram uma forte correlação com atividades anti-inflamatórias, antioxidantes e citotóxicas. Com destaque para uma correlação positiva dos compostos vicentina-2, ácido clorogênico e ácido cafeico com

atividades anti-inflamatórias e antioxidantes. Além disso, estabeleceu-se que flavonas glicosiladas estavam positivamente correlacionadas com a atividade citotóxica em células HCT-116. Na terceira etapa, foram encontrados 57 metabólitos alterados no endometaboloma e 42 metabólitos alterados no exometaboloma das células HCT-116 após a exposição ao extrato de *G. incana*, que estão relacionados a diferentes vias metabólicas alteradas, principalmente associadas ao metabolismo da glutationa. Além disso, a análise metabolômica revelou que o extrato possivelmente inibe o crescimento do tumor, induzindo danos às células tumorais e promovendo a apoptose, a qual foi corroborada experimentalmente. Finalmente, na última etapa, foi isolada uma flavona glicosilada correspondente a isoschaftosido e uma mistura de três flavonas de núcleo apigenina. O isoschaftosido apresentou um potencial citotóxico com um valor de $IC_{50}$ de 13,26 µM, enquanto a mistura dos flavonoides apresentou um percentual de inibição de 94,35% a uma concentração de 50 µg/mL.

Em conclusão, nossas descobertas demonstram uma grande diversidade química nas diferentes espécies estudadas, relatando pela primeira vez diferentes metabólitos secundários. Além disso, são apresentados resultados biológicos inéditos, que são bastante promissores do ponto de vista farmacológico. Por fim, nosso estudo destaca a importância da aplicação de abordagens de análise de rede molecular e metabolômica para acelerar o processo de descoberta de novos compostos bioativos. À medida que avançamos na pesquisa dessas espécies, esperamos continuar contribuindo para o desenvolvimento de abordagens inovadoras que promovam um uso alternativo do bambu na Colômbia, gerando benefícios tanto para a sociedade quanto para a exploração do potencial químico e biológico dessas plantas, o que lhes pode conferir valor agregado.

## INDEX OF FIGURES

**Figure 1.1.** Importance of bamboo worldwide. ---- 41
**Figure 1.2.** Distribution of all woody bamboos (Bambuseae). ---- 42
**Figure 1.3.** Flavonoids reported (**1**-**30**) from bamboos (Poaceae family). ---- 48
**Figure 1.4.** Phenolic acids derivatives reported (**31**-**52**) from bamboos (Poaceae family). ---- 50
**Figure 1.5.** Lignans reported (**53**-**55**) from bamboos (Poaceae family). ---- 51
**Figure 1.6.** Phytosterols reported (**56**-**63**) from bamboos (Poaceae family). ---- 52
**Figure 1.7.** Coumarins reported (**64**-**69**) from bamboos (Poaceae family). ---- 53
**Figure 1.8.** Representative morphological characteristics of *Guadua* genus. ---- 59
**Figure 1.9.** Flavonoids isolated in leaves of *G. angustifolia*. ---- 61
**Figure 1.10.** Workflow used in the study of NPs. ---- 64
**Figure 1.11.** Workflow used in a targeted metabolomics study. ---- 65
**Figure 1.12.** Workflow used in an untargeted metabolomic study. ---- 66
**Figure 1.13.** Stages and development of CRC. ---- 72
**Figure 1.14.** Map showing the global incidence (A) and mortality (B) rates of colorectal cancer. ---- 73
**Figure 1.15.** Morphology of the HCT-116 ATCC cell line. ---- 74
**Figure 2.1.** Geographical distribution map showing the bamboo species studied. ---- 79
**Figure 2.2.** Schematic of the experiment analytical workflow used in this study. ---- 84
**Figure 2.3.** Score plots of the influence of direction compared low/high altitudes. ---- 86
**Figure 2.4.** Molecular networks analysis obtained from GNPS platform online. ---- 92
**Figure 2.5.** Hierarchical clustering with heatmap illustrating the differences in the metabolite abundance between low and high altitudes. ---- 93
**Figure 2.6.** Box plot for the altered metabolites corresponding to cinnamic acid derivatives and flavonoids. ---- 94
**Figure 2.7.** Molecular networking and dereplication of flavonoids comparing twelve bamboo species. ---- 95
**Figure 2.8. (A)** Pearson's correlations using pattern search of the top 25 metabolites between low and high altitude. ---- 96

**Figure 3.1.** Workflow of the metabolomics strategy implemented for the identification of candidate bioactive compounds. ---------- 119
**Figure 3.2.** HPTLC chromatographic profiles for **(A)** flavonoid aglycones and **(B)** flavonoid glycosides.---------- 121
**Figure 3.3.** Representative MolNetEnhancer mass spectral molecular networking of consortium showing the chemical CF_superclasses in negative **(A)** and positive **(B)** electrospray ionization modes of BLEs based on UHPLC-QTOF-MS. ---------- 123
**Figure 3.4.** Representative UHPLC-QTOF-MS base peak intensity chromatograms of the QC samples of the BLEs in negative **(A)** and positive **(B)** ions. ---------- 124
**Figure 3.5.** Stacked representative $^{1}$H-NMR spectra of BLEs are presented.---------- 128
**Figure 3.6.** Antioxidant activity is determined for BLEs. The ABTS and DPPH of the BLEs. ---------- 130
**Figure 3.7.** Determination of the percentage of chemical inhibition of NO by BLEs. -- 132
**Figure 3.8.** Cellular concentration of NO in the murine cell line RAW 264.7 stimulated with LPS after treatment with BLE.---------- 136
**Figure 3.9.** Percentage growth inhibition of BLEs evaluated at 50 and 5 µg/mL against HCT-116 (colorectal carcinoma) using MTT assay after 72 hours of exposure. -------- 137
**Figure 3.10.** Dose-response curves of the cytotoxicity of HCT-116 cells after 72 h treatment with the BLEs.---------- 139
**Figure 3.11.** Heatmap representation of the Pearson's simple correlation coefficients for the top 24 statistically differential metabolites and antioxidant activities monocation of ABTS and DPPH of BLEs. ---------- 141
**Figure 3.12.** Heatmap representation of the Pearson's simple correlation coefficients for the top 24 statistically differential metabolites and the anti-inflammatory activity of BLEs. ---------- 142
**Figure 3.13. (A)** OPLS-DA score plot demonstrating distinct separation between active (green) and inactive (blue) extracts against the colon cancer cell line (HCT-116). **(B)** S-loading plot depicting metabolites highly correlated with HCT-116 cytotoxicity.--------- 143
**Figure 3.14. A)** Hierarchical clustering analysis (HCA) with heatmap illustrating the difference in the compounds annotated abundance between active and inactive samples. ---------- 148

**Figure 3.15.** Bioactive molecular networking of the BLEs displays compounds that contribute most significantly to activity. ---------- 150
**Figure 4.1.** Schematic of the analytical workflow used in this cellular metabolomic study experiment.---------- 191
**Figure 4.2.** Molecular networking analysis of BLEGI highlighting flavonoids and other compounds, performed using the LC-MS/MS technique in negative mode.---------- 194
**Figure 4.3.** A) The cell viability after 72 h incubation at different concentrations. B) Dose-response curves of the cytotoxicity of HCT-116 cells after 72 h treatment with the BLEGI.---------- 199
**Figure 4.4.** Immunofluorescence of a-tubulin and DAPI in HCT 116 cells after 72 h of incubation with DMSO 0.1%, DOXO 0.2 µM and BLEGI 1.23 µg/mL. ---------- 200
**Figure 4.5.** A) Determination of the percentage of chemical $NO_2^-$ after treatment with BLEGI.---------- 202
**Figure 4.6.** OPLS-DA score plots comparing the BLEGI-treated group (green) versus the control group (purple) for LC-MS and $^1$H-NMR data of the A) endometabolome and B) exometabolome of HCT-116 cells. ---------- 204
**Figure 4.7.** Altered A) endo- and B) exometabolome metabolites among BLEGI-treated versus untreated cells. ---------- 206
**Figure 4.8.** Hierarchical clustering with a heatmap illustrating the differences in the abundance of metabolites found in A) endometabolome and B) exometabolome between BLEGI-treated cells and untreated cells. ---------- 207
**Figure 4.9.** Violin plot for the altered metabolites corresponding to BLEGI-treated and untreated cells.---------- 208
**Figure 4.10.** Metabolic pathway analysis based on the enrichment analysis procedure for metabolites found in the metabolome of HCT-116 cells after exposure to BLEGI.- 209
**Figure 4.11.** Schematic biochemical representation of the main altered metabolic pathways 72 hours after BLEGI treatment in HCT-116 cells. ---------- 215
**Figure 5.1.** UHPLC-DAD chromatogram for the ethanolic extract of G. incana leaves obtained at a wavelength of 364 nm and ultraviolet absorption spectra for 7 major flavonoids present in extract. ---------- 241

**Figure 5.2.** UHPLC-QTOF-MS base peak chromatogram (BPC) for the ethanolic extract of G. incana leaves obtained in A) negative and B) positive ionization modes. --------- 242
**Figure 5.3.** Percent growth inhibition of the four fractions obtained from the G. incana extract was evaluated at 50 and 5 µg/mL against HCT-116 using the MTT assay after 72 hours of exposure. ---------- 243
**Figure 5.4.** MS/MS spectra and proposed fragmentation pathway for isoschaftoside **1** isolated from G. incana leaves. ---------- 246
**Figure 5.5. A)** Cell viability after 72 hours of incubation at two concentrations: 5 and 50 µg/mL. B) Dose-response curve of the cytotoxicity in HCT-116 cells after 72 hours of treatment with isoschaftoside. ---------- 248

## INDEX OF TABLES

**Table 1.1.** Phytoconstituents reported for bamboo species. ..... 43
**Table 1.2.** Biological activity reported for bamboo species. ..... 55
**Table 1.3.** An overview of metabolomics studies in the HCT-116 cell line ..... 75
**Table 2.1.** Classification of bamboo species according to altitudinal range. ..... 80
**Table 2.2.** Significantly differential metabolites found the altitudinal variation. ..... 86
**Table 3.1.** Information for samples used in this study. ..... 108
**Table 3.2.** Evaluation of the cytotoxic effect of BLEs against RAW 264.7 macrophage cells. ..... 133
**Table 3.3.** Effect of BLEs on NO inhibition in LPS-stimulated RAW 264.7 macrophage cells. ..... 133
**Table 3.4.** Significantly differential major metabolites correlating with cytotoxic activity determined by OPLS-DA model for UHPLC-QTOF-MS and $^{1}$H-NMR analysis. ..... 144
**Table 4.1.** Metabolites tentatively identified in BLEGI using LC-MS/MS. ..... 196
**Table 5.1.** Compounds identified in the extract of G. incana. ..... 242

## INDEX OF ABREVIATIONS AND ACRONYMS

| | |
|---|---|
| **ABTS** | 2,2-Azinobis(3-Ethylbenzothiazoline-6-Sulfonic Acid) |
| **ACN** | Acetonitrile |
| **ANOVA** | Analysis Of Variance |
| **AOB** | Antioxidant Of Bamboo Leaves |
| **ATCC** | American Type Culture Collection |
| **BLE** | Bamboo Leaf Extract |
| **BLEs** | Bamboo Leaf Extracts |
| **BLEGI** | Bamboo Leaf Extract obtained from *Guadua incana* |
| **BPI** | Base Peak Intensity |
| **$CD_3OD$** | Deuterated methanol |
| **CGA** | Chlorogenic Acid |
| **CPC** | Centrifugal Partition Chromatography |
| **CQAs** | Caffeoylquinic Acids |
| **CRC** | Colorectal Cancer |
| **CV** | Coefficient of Variation |
| **DDA** | Data Dependent Acquisition |
| **DEPTQ** | Distortion Less Enhancement by Polarization Transfer with Quaternary Carbon Detection |
| **DMEM** | Dulbecco's Modified Eagle Medium |
| **DMSO** | Dimethyl Sulfoxide |
| **DOXO** | Doxorubicin hydrochloride |
| **DPPH** | 1,1-Diphenyl-2-Picrylhydrazyl |
| **EBuWat** | Ethyl Acetate-Butanol-Water |
| **EGFR** | Epidermal Growth Factor Receptor |
| **ESI** | Electrospray Ionization |
| **ESI-** | Negative Ionization Mode |
| **ESI+** | Positive Ionization Mode |
| **FA** | Formic Acid |
| **FBS** | Fetal Bovine Serum |
| **FC** | Fold Change |
| **FDR** | False Discovery Rate |
| **FIDs** | Free Induction Decays |
| **FRAP** | Ferric Reducing Antioxidant Power |
| **GC-MS** | Gas Chromatography-Mass Spectrometry |
| **GNPS** | Global Natural Products Social Molecular Networking |
| **GR** | Glutathione Reductase |
| **GSH** | Glutathione |
| **GSSH** | Glutathione Disulfide |
| **HCA** | Hierarchical Clustering Analysis |
| **HCT-116** | Human Colon Cancer Cell Line |

| | |
|---|---|
| **HPLC-DAD** | High-Performance Liquid Chromatography coupled with Diode Array Detector |
| **HPTLC** | High-Performance Thin Layer Chromatography |
| **HRMS** | High-Resolution Mass Spectrometry |
| **IAPs** | Inhibitors Of Apoptosis |
| **$IC_{50}$** | Half Maximal Inhibitory Concentration |
| **IFN-γ** | Interferon gamma |
| **iNOS** | Inducible Nitric Oxide Synthase |
| **JK** | Jack-Knife Confident Interval |
| **LC-MS** | Liquid Chromatography-Mass Spectrometry |
| **LC-QTOF-MS** | Liquid Chromatography Quadrupole Time-Of-Flight Mass Spectrometry |
| **L-NAME** | N(ω)-Nitro-L-Arginine Methyl Ester |
| **LP** | Lower Phase |
| **LPS** | Escherichia Coli Lipopolysaccharide |
| ***m/z*** | Mass/Charge Ratio |
| **MFs** | Molecular Families |
| **MS/MS** | Tandem Mass Spectrometry |
| **MTT** | 3-(4,5-Dimethylthiazol-2-Yl)-2,5-Diphenyl-2H-Tetrazolium Bromide |
| **MVA** | Multivariate Analyses |
| **NAD+** | Nicotinamide-Adenine Dinucleotide |
| **NAM** | Nicotinamide |
| **NMR** | Nuclear Magnetic Resonance Spectroscopy |
| **NNMT** | Nicotinamide N-Methyltransferase |
| **NP/PEG** | Natural Products-Polyethylenglycol Reagent |
| **NPS** | Sodium Nitroprusside |
| **NO** | Nitric oxide |
| **OPLS-DA** | Orthogonal Partial Least Squares Discriminant Analysis |
| **PCA** | Principal Component Analysis |
| **PLS-DA** | Partial Least Squares Discriminant Analysis |
| **QA** | Quinic Acid |
| **QC** | Quality Control |
| **RDA** | Retro-Diels-Alder |
| **RF** | Retention Factor |
| **ROS** | Reactive Oxygen Species |
| **SD** | Standard Deviation |
| **SEM** | Standard Error of The Mean |
| **STD** | Reference Standards |
| **TEAC** | Trolox Equivalent Antioxidant Capacity |
| **TF** | Total Flavonoids |
| **TLC** | Thin-Layer Chromatography |
| **TP** | Total Phenols |

| | |
|---|---|
| **UHPLC-HRMS** | Ultra-High Performance Liquid Chromatography Coupled to High Resolution Mass Spectrometry |
| **UHPLC-QTOF-MS/MS** | Liquid Chromatography Coupled with Quadrupole Time-Of-Flight Mass Spectrometry |
| **UP** | Upper Phase |
| **VIP** | Variable Importance in the Projection |
| **$^{1}$H-NMR** | Proton Nuclear Magnetic Resonance |
| **1-MNA** | 1-Methylnicotinamide |
| **2PY** | N1-Methyl-2-Pyridone-5-Carboxamide |
| **4PY** | N1-Methyl-4-Pyridone-3-Carboxamide |

**TABLE OF CONTENTS**

**GENERAL INTRODUCTION ..... 36**

**OBJECTIVES ..... 39**

GENERAL OBJECTIVE ..... 39
SPECIFIC OBJECTIVES ..... 39

**1 CHAPTER 1. STATE OF THE ART ..... 40**

PRESENTATION ..... 40
1.1 OVERVIEW OF BAMBOO SPECIES ..... 40
*1.1.1 Bambuseae tribe of tropical woody bamboos (Poaceae: Bambusoideae) ... 41*
*1.1.2 Phytochemical studies of bamboo species ..... 42*
*1.1.3 Biological activity of bamboo species ..... 53*
1.2 OVERVIEW OF *GUADUA* SPECIES ..... 58
*1.2.1 Phytochemical studies of Guadua species ..... 60*
*1.2.2 Biological activity of Guadua species ..... 61*
1.3 NEW STRATEGIES FOR THE STUDY AND DISCOVERY OF NPS ..... 62
*1.3.1 Metabolomics applied to the area of NPs ..... 63*
*1.3.2 Targeted and untargeted metabolomics approaches ..... 64*
*1.3.3 Analytical platforms used in metabolomics for the study of NPs ..... 67*
*1.3.4 Correlation analysis using chemometric approaches ..... 69*
1.4 GENERAL INFORMATION ON CANCER DISEASE ..... 69
*1.4.1 Colorectal cancer ..... 71*
*1.4.2 Global Epidemiology of CRC ..... 72*
*1.4.3 Study model: HCT-116 human colon cancer cell line ..... 73*
*1.4.4 Overview of metabolomic studies in the HCT-116 cell line ..... 74*

**2 CHAPTER 2. UNTARGETED METABOLOMICS APPROACH AND MOLECULAR NETWORKING ANALYSIS REVEAL CHANGES IN CHEMICAL COMPOSITION UNDER THE INFLUENCE OF ALTITUDINAL VARIATION IN BAMBOO SPECIES ... 78**

PRESENTATION ..... 78
2.1 MATERIALS AND METHODS ..... 78
*2.1.1 Study design ..... 78*
*2.1.2 Plant material collection and identification ..... 79*
*2.1.3 Metabolite extraction and sample preparation ..... 81*
*2.1.4 Untargeted metabolomics using LC-QTOF-MS ..... 81*
*2.1.5 Quality control samples ..... 82*
*2.1.6 Metabolomics data processing ..... 82*
*2.1.7 Statistical analysis ..... 82*

*2.1.8 Metabolite identification* ..... *83*
*2.1.9 Global natural products social molecular networking (GNPS) web platform workflow description* ..... *83*
2.2 RESULTS AND DISCUSSION ..... 85
*2.2.1 Chemical variation of bamboo species presented between low and high altitudes* ..... *85*
*2.2.2 Molecular networks and heatmap analyses reveal the chemical variation under the influence of altitudinal variation* ..... *90*
*2.2.3 Changes in the concentration and analysis of biosynthesis pathways of the most relevant metabolites in bamboo species* ..... *93*
*2.2.4 Molecular networking for chemical space mapping of the metabolome of bamboo species by MolNetEnhancer* ..... *94*
2.3 CONCLUSION ..... 98
SUPPLEMENTARY INFORMATION ..... 100

**3 CHAPTER 3. METABOLOMIC PROFILING OF *GUADUA* SPECIES AND ITS CORRELATION WITH ANTIOXIDANT, ANTI-INFLAMMATORY AND CYTOTOXIC ACTIVITIES ..... 107**

PRESENTATION ..... 107
3.1 MATERIALS AND METHODS ..... 107
*3.1.1 Chemical and reagents* ..... *107*
*3.1.2 Plant material and preparation of bamboo leaf extracts (BLEs)* ..... *108*
*3.1.3 Clean-up of the BLEs* ..... *109*
*3.1.4 Preparation of chemical standards and quality control (QC) samples* ..... *109*
*3.1.5 HPTLC data acquisition* ..... *110*
*3.1.6 HPLC-DAD data acquisition* ..... *110*
*3.1.7 UHPLC-QTOF-MS data acquisition* ..... *111*
*3.1.8 $^{1}$H-NMR data acquisition* ..... *112*
*3.1.9 GNPS classical molecular MS/MS network* ..... *112*
*3.1.10 Antioxidant activity* ..... *113*
*3.1.11 ABTS radical cation decolorization assay* ..... *113*
*3.1.12 DPPH free radical scavenging activity* ..... *113*
*3.1.13 Nitric oxide (NO) inhibitory assay* ..... *114*
*3.1.14 Macrophages cell culture and viability* ..... *114*
*3.1.15 Inhibition of NO produced by macrophages* ..... *115*
*3.1.16 Cell and cell cultures* ..... *115*
*3.1.17 MTT cell viability assay* ..... *116*
*3.1.18 Statistical analysis* ..... *117*
*3.1.19 Data processing and biochemometric analysis* ..... *117*
*3.1.20 Metabolite identification* ..... *118*

3.2 RESULTS AND DISCUSSION ..... 119
*3.2.1 HPTLC and HPLC-DAD phytochemical profiling analysis ..... 119*
*3.2.2 UHPLC-QTOF-MS-based metabolic fingerprinting analysis ..... 122*
*3.2.3 Flavonoids ..... 124*
*3.2.4 Phenolic acid derivatives ..... 126*
*3.2.5 NMR-based metabolomic fingerprinting analysis ..... 127*
*3.2.6 Antioxidant capacity of BLEs ..... 129*
*3.2.7 Anti-inflammatory activity of BLEs ..... 131*
*3.2.8 Cytotoxic activity of BLEs ..... 137*
*3.2.9 Correlation-based untargeted metabolomics analysis ..... 140*
*3.2.10 Bioactivity score-based molecular networking ..... 149*
3.3 CONCLUSION ..... 151
SUPPLEMENTARY INFORMATION ..... 152

**4 CHAPTER 4. UNCOVERING METABOLIC ALTERATIONS IN HCT-116 COLON CANCER CELLS UPON EXPOSURE TO BAMBOO LEAF EXTRACT OBTAINED FROM *GUADUA INCANA* LONDOÑO ..... 184**

PRESENTATION ..... 184
4.1 MATERIALS AND METHODS ..... 184
*4.1.1 Chemical and reagents ..... 184*
*4.1.2 Plant material, extraction, and chemical characterization ..... 185*
*4.1.3 Chemical characterization of the BLEGI ..... 185*
*4.1.4 Cell lines and culture conditions ..... 186*
*4.1.5 Cytotoxicity assay ..... 187*
*4.1.6 Immunofluorescence Analysis ..... 187*
*4.1.7 Nitric oxide (NO) inhibitory assay ..... 188*
*4.1.8 Macrophages cell culture and viability ..... 188*
*4.1.9 Inhibition of NO produced by macrophages ..... 189*
*4.1.10 Statistical analysis ..... 189*
*4.1.11 Untargeted metabolomic analysis ..... 190*
4.2 RESULTS AND DISCUSSION ..... 193
*4.2.1 Chemical Characterization of Extract ..... 193*
*4.2.2 Cell viability of HCT-116 cells ..... 199*
*4.2.3 Immunofluorescence assay ..... 199*
*4.2.4 Nitric Oxide (NO) Production Inhibition ..... 201*
*4.2.5 Untargeted endo- and exometabolome analysis ..... 202*
*4.2.6 Analysis of altered metabolites in HCT-116 cells ..... 204*
*4.2.7 Exploration of altered metabolic pathways in HCT-116 cells ..... 208*
4.3 CONCLUSION ..... 217
SUPPLEMENTARY INFORMATION ..... 218

**5 CHAPTER 5. CYTOTOXIC FLAVONE GLYCOSIDES FROM *GUADUA INCANA* LEAVES ..... 235**

PRESENTATION ..... 235
5.1 MATERIALS AND METHODS ..... 235
*5.1.1 General experimental procedures ..... 235*
*5.1.2 Plant material and extract preparation ..... 236*
*5.1.3 UHPLC-DAD-QTOF-MS analysis ..... 236*
*5.1.4 $^{1}$H-NMR data acquisition ..... 237*
*5.1.5 Extract fractionation and isolation of bioactive compounds ..... 237*
*5.1.6 Cell lines and maintance ..... 239*
*5.1.7 Cytotoxic activity ..... 239*
*5.1.8 Statistical analysis ..... 239*
5.2 RESULTS AND DISCUSSION ..... 240
*5.2.1 Chemical analysis of the crude extract and fractionation ..... 240*
*5.2.2 Cytotoxic activity of the fractions ..... 243*
*5.2.3 Isolation of flavonoids ..... 244*
*5.2.4 Cytotoxic activity of the compounds ..... 248*
5.3 CONCLUSION ..... 249
SUPPLEMENTARY INFORMATION ..... 250

**GENERAL DISCUSSION ..... 259**

**CONCLUSIONS ..... 274**

**PERSPECTIVES ..... 277**

**REFERENCES ..... 278**

**PARTICIPATION IN SCIENTIFIC EVENTS AND AWARDS ..... 303**

**PUBLICATIONS AND OTHER CONTRIBUTIONS ..... 308**

ARTICLE 1 ..... 308
ARTICLE 2 ..... 309
ARTICLE 3 ..... 310
ARTICLE 4 ..... 311
ARTICLE 5 ..... 312
ARTICLE 6 ..... 313
ARTICLE 7 ..... 314
ARTICLE 8 ..... 315
UNDERGRADUATE THESIS SUPERVISION ..... 316

## GENERAL INTRODUCTION

Natural products (NPs) are considered an important source of specialized bioactive metabolites, which have been applied in different fields, such as food, economic, and medicinal areas. In Latin America, specifically in Colombia, many plants have been reported as medicinal plants, which have the potential to possess active molecules with important therapeutic properties in various biological models. In this context, bamboo plants are known to be a source of valuable bioactive compounds with potential for unexplored and promising pharmacological activities. Bamboo species have traditionally been used as a construction material; however, it is important to highlight that most chemical and biological studies on bamboo have focused on the Asian continent, and notably in Latin America, chemical and biological studies for these species are limited, particularly in Colombia.

The genus *Guadua* are considered the most important Neotropical woody bamboos in Latin America, due to their extensive use in construction. They comprise approximately 34 species distributed in the tropical regions of Central and South America. Despite their importance, little is known about the chemical composition and biological potential of these species. Thus, only preliminary phytochemical studies have been carried out, reporting the presence of flavonoids, phenolic acid derivatives, terpenes, saponins, and alkaloids. Currently, the search for these compounds represents a great challenge due to the great chemical diversity present and the long periods of studies involved in traditional phytochemistry. Consequently, novel strategies have gained popularity in the last decades, such as the application of metabolomics based on various modern instrumental analytical techniques, *e.g.*, liquid chromatography coupled with mass spectrometry (LC-MS), gas chromatography coupled with mass spectrometry (GC-MS), and nuclear magnetic resonance spectroscopy (NMR), which allow for the collection of information on the chemical composition of crude extracts. Metabolomics is considered an important interdisciplinary field in the study of plants because it integrates several analytical tools with statistical analysis and biological activity studies. As a result, this strategy has allowed for the optimization of research times and the rapid identification of

secondary metabolites in plants, leading to the discovery of new biologically active substances. One of the advantages of this strategy is that, through the analysis of correlations between the bioactivity and the chemical composition of an extract, it is possible to assign the compounds, or group of compounds that contributing to the activity, facilitating their subsequent isolation and identification.

In this context, this work aims to study the chemical composition and biological potential of different extracts from bamboo leaves belonging to the genus *Guadua* through an untargeted metabolic approach to contribute to the chemical and biological knowledge of these underexplored bamboos of the South American continent. Therefore, the selection of *Guadua* species for the development of this work was based on the following criteria: 1) limited information on chemical composition and biological activity, 2) results of screening for antioxidant, anti-inflammatory and cytotoxic activities on the colon cancer cell line HCT-116 and 3) literature background. This study was part of the research results of a macroproject Programa GAT-Colombia Científica, in the proyect entitled "Aproximación biológica, fitoquímica y agronómica para la gestión de recursos vegetales con potencial farmacológico: Aporte a cadena de valor para el sector de los fitomedicamentos en Colombia" funded by Minciencias and World Bank.

This thesis is organized into five chapters. Chapter 1 presents a general literature review of bamboo species concerning their chemical composition and biological potential, as well as a review of the application of metabolomic approaches in the study of NPs. Additionally, a review of colorectal cancer (CRC) was carried out as the biological model selected for the development of this study. Chapter 2 presents the initial of the experimental results, with the study on changes in chemical composition under an altitudinal gradient using an untargeted metabolomic approach. Chapter 3 presents a correlation study based on the chemical composition of different species of the *Guadua* genus and their antioxidant, anti-inflammatory, and cytotoxic potential using a metabolomic approach. Chapter 4 presents the evaluation of metabolic alterations in HCT-116 colon cancer cells after exposure to a bamboo leaf extract from *G. incana*. Finally, Chapter 5 presents the isolation and chemical characterization of some

metabolites from the species *G. incana*, which was shown to have the most potent cytotoxic effect, guided by the metabolomic approach and biological activity.

## OBJECTIVES

### General objective

To explore the chemical composition and biological potential of bamboo leaf extracts (BLEs) belonging to the genus *Guadua* using an untargeted metabolomic approach.

### Specific objectives

- To evaluate changes in the chemical composition of different BLEs under the influence of an altitudinal gradient using an untargeted metabolomics approach.

- To establish a correlation between the chemical profiles and bioactivity of BLEs from *Guadua* species using a metabolomics approach based on LC-MS and $^{1}$H-NMR analyses.

- To evaluate changes in the metabolome of HCT-116 colon cancer cells treated with a bioactive BLE using an untargeted metabolomics approach based on LC-MS and $^{1}$H-NMR analyses.

- To isolate compounds with biological potential present in the most active BLE through a targeted phytochemical isolation supported by the metabolomic approach.

# 1 CHAPTER 1. State of the art

## Presentation

Chapter 1 presents a review of different bamboo species, covering phytochemical studies and reported biological activity. It also details the chemical and biological studies reported in the genus *Guadua*, to which the species under study belong. Additionally, this chapter provides a brief review of new strategies for the study and discovery of natural products, particularly focusing on the area of metabolomics and its approaches. Finally, it presents a review of the status of colorectal cancer, the main pathology addressed in this doctoral work.

## 1.1 Overview of bamboo species

Bamboos are species belonging to the grass family (Poaceae), Bambusoideae subfamily comprising approximately 1670 species grouped into 125 genera distributed in temperate and warm tropics in Asia, Africa, and Latin America. The subfamily is divided into three tribes: herbaceous bamboos (Olyreae), tropical woody bamboos (Bambuseae), and temperate woody bamboos (Arundinarieae) (Gagliano, et al., 2022; Vorontsova et al., 2016). Bamboos are widely used as a material in construction, handicrafts, food, paper making, ethanol production, cellulose, in the manufacture of household utensils, paper, and in medicinal uses (CHENG et al., 2023), considered of high economic, social, cultural and medicinal importance (Figure 1.1). Bamboos can be divided as woody or herbaceous presenting variations to the habitat in which they are found, a distinctive advantage of bamboo is its rapid growth and renewal of lignocellulosic biomass.

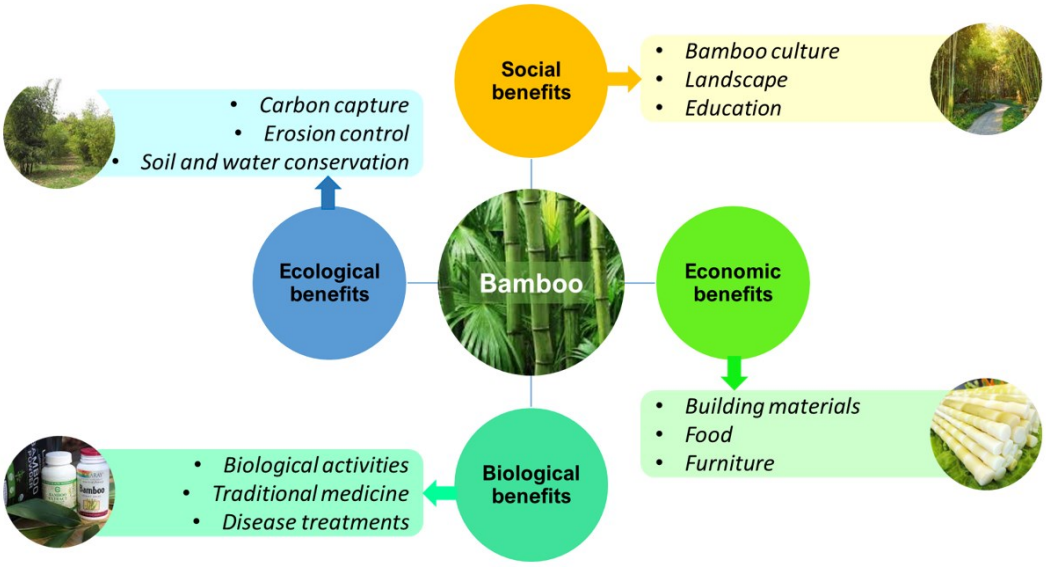



**Figure 1.1.** Importance of bamboo worldwide.

### 1.1.1 Bambuseae tribe of tropical woody bamboos (Poaceae: Bambusoideae)

Woody bamboos are characterized by having a woody, hard and hollow stem, they are perennial herbs, macro or monopodic, with developed rhizomes. Among the parts that characterize these plants contain a stem called culms, which is divided into nodes, and is characterized by having a space between the nodes called an internode, when the plant is young it is protected from cauline leaves, also consists of a rhizome with small secondary stems called roots. Of the Latin American countries, Brazil has the greatest diversity, followed by Colombia, Venezuela, Ecuador, Costa Rica, and Mexico (Figure 1.2) (LONDOÑO; RUIZ-SANCHEZ, 2024; RUIZ-SANCHEZ et al., 2021).

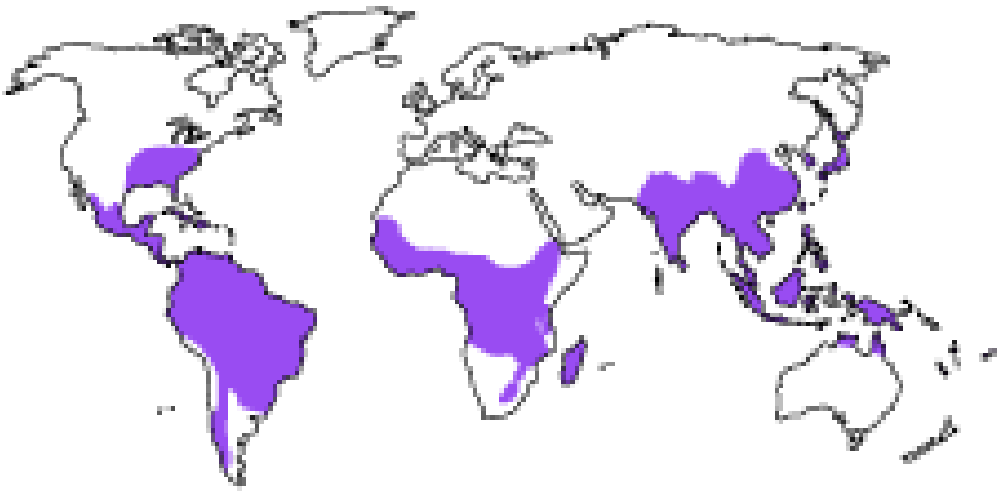


**Figure 1.2.** Distribution of all woody bamboos (Bambuseae) Figure from (BREDENOORD, 2024).

Bamboos are widely used in traditional Asian medicine for the treatment of respiratory diseases, gastrointestinal problems, hypertension, arteriosclerosis, cardiovascular diseases, and certain forms of cancer. Additionally, their therapeutic properties are highlighted to combat asthma, hemoptysis, maintain blood sugar levels, reduce cholesterol, address ulcers, and strengthen hair (WRÓBLEWSKA et al., 2018). In the Americas, little information is known about the traditional use of these plants; mostly they are used as construction material for housing (BREDENOORD, 2024).

### 1.1.2 Phytochemical studies of bamboo species

So far, various secondary metabolites have been reported in different bamboo species belonging to the Poaceae family. The chemical constituents commonly reported for these species include flavonoids, phenolic acids derivatives, lignans, phenylpropanoids, alkene glycosides, chromones, phytosterols, carotenoids and coumarins. Their names, plant sources and corresponding structures are shown in Table 1.1 and Figures 1.3 – 1.7. Primarily, in bamboos, phenolic compounds have been identified as main components, corresponding mainly to flavonoid glycosides of the *C*-glycoside type as chemical markers. These compounds have been reported for a wide variety of species, including *Phyllostachys nigra*, *Arundinaria gigantea*, *Bambusa balcooa*,

*Dendrocalamus hamiltonii*, *Dinochloa scandens*, *Fargesia robusta* and *Fargesia rufa* (Ma et al., 2020; Van Hoyweghen et al., 2012; Wang, et al., 2012). The main reports for each group of metabolites are described below.

**Table 1.1.** Phytoconstituents reported for bamboo species.

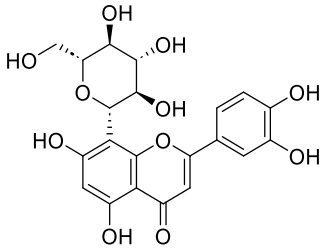
| No. | Compounds | Species | Plant part(s) | References |
|---|---|---|---|---|
| ***Flavonoids*** | | | | |
| **1** | Orientin | *Phyllostachys nigra* var. *henonis* | Leaves | (Zhang et al., 2008) |
| | | *Phyllostachys nigra* Munro | Leaves | (KIM et al., 2009) |
| | | *Phyllostachys pubescens* Mazel ex H. de Lehaie | Leaves | (SUN et al., 2010) |
| | | *Phyllostachys glauca* McClure | Leaves | (SUN et al., 2010) |
| | | *Pleioblastus yixingensis* S.L. Chen et S.Y. Chen | Leaves | (SUN et al., 2010) |
| | | *Phyllostachys nigra* | Leaves | (VAN HOYWEGHEN et al., 2012) |
| | | *Phyllostachys edulis* | Leaves | (SHAO et al., 2020) |
| **2** | Isoorientin | *Sasa borealis* | Leaves | (PARK et al., 2007) |
| | | *Phyllostachys nigra* Munro | Leaves | (KIM et al., 2009) |
| | | *Sasa quelpaertensis* Nakai | Leaves | (SULTANA; LEE, 2010) |
| | | *Phyllostachys nigra* var. *henonis* | Leaves | (ZHANG et al., 2008) |
| | | *Fargesia robusta* var. *Pingwu* | Leaves | (VAN HOYWEGHEN et al., 2010) |
| | | *Phyllostachys pubescens* Mazel ex H. de Lehaie | Leaves | (SUN et al., 2010) |
| | | *Pleioblastus yixingensis* S.L. Chen et S.Y. Chen | Leaves | (SUN et al., 2010) |
| | | *Bambusa textilis* McClure | Leaves | (WANG et al., 2012b) |
| | | *Sasa veitchii* | Leaves | (VAN HOYWEGHEN et al., 2012) |
| | | *Phyllostachys variegatus* | Leaves | (VAN HOYWEGHEN et al., 2012) |
| | | *Phyllostachys nigra* | Leaves | (VAN HOYWEGHEN et al., 2012) |
| | | *Phyllostachys humilis* | Leaves | (VAN HOYWEGHEN et al., 2012) |
| | | *Fargesia robusta* 'Pingwu' | Leaves | (VAN HOYWEGHEN et al., 2012) |
| | | *Fargesia rufa* 'Green Panda' | Leaves | (VAN HOYWEGHEN et al., 2012) |
| | | *Arundinaria gigantea* | Leaves | (VAN HOYWEGHEN et al., 2012) |
| | | *Phyllostachys edulis* | Leaves | (SHAO et al., 2020) |
| **3** | Vitexin | *Phyllostachys nigra* var. *henonis* | Leaves | (ZHANG et al., 2008) |
| | | *Phyllostachys nigra* Munro | Leaves | (KIM et al., 2009) |
| | | *Phyllostachys glauca* McClure | Leaves | (SUN et al., 2010) |
| | | *Pleioblastus yixingensis* S.L. Chen et S.Y. Chen | Leaves | (SUN et al., 2010) |
| | | *Phyllostachys edulis* | Leaves | (SHAO et al., 2020) |
| **4** | Isovitexin | *Phyllostachys nigra* var. *henonis* | Leaves | (ZHANG et al., 2008) |
| | | *Phyllostachys pubescens* Mazel ex H. de Lehaie | Leaves | (SUN et al., 2010) |
| | | *Phyllostachys glauca* McClure | Leaves | (SUN et al., 2010) |
| | | *Bambusa balcooa* | Leaves | (VAN HOYWEGHEN et al., 2012) |
| | | *Phyllostachys nigra* | Leaves | (VAN HOYWEGHEN et al., 2012) |
| | | *Phyllostachys edulis* | Leaves | (SHAO et al., 2020) |
| **5** | Luteolin-7-glucoside | *Phyllostachys nigra* var. *henonis* | Leaves | (HU; ZHANG; KITTS, 2000) |

| | | | | |
|---|---|---|---|---|
| **6** | Isoorientin 2"-*O*-a-L-rhamnoside | *Sasa borealis* | Leaves | (PARK et al., 2007) |
| **7** | Tricin 7-O-b-D-glucopyranoside | *Sasa borealis* | Leaves | (PARK et al., 2007) |
| **8** | Apigenin 6-C-b-D-xylopyranosyl-8-*C*-b-D-glucopyranoside | *Sasa borealis* | Leaves | (PARK et al., 2007) |
| **9** | Kurilensin A | *Sasa kurilensis* var. *gigantea* | Leaves | (HASEGAWA et al., 2008) |
| **10** | Kurilensin B | *Sasa kurilensis* var. *gigantea* | Leaves | (HASEGAWA et al., 2008) |
| **11** | Tricin-4´-*O*-b-D-glucopyranoside | *Sasa kurilensis* var. *gigantea* | Leaves | (HASEGAWA et al., 2008) |
| **12** | Tricin-5-*O*-b-D-glucopyranoside | *Sasa kurilensis* var. *gigantea* | Leaves | (HASEGAWA et al., 2008) |
| | | *Fargesia robusta* var. *Pingwu* | Leaves | (VAN HOYWEGHEN et al., 2010) |
| **13** | Luteolin-6-*C*-(6"-*O*-*trans*-caffeoylglucoside) | *Phyllostachys nigra* Munro | Leaves | (KIM et al., 2009) |
| **14** | Vittariflavone | *Phyllostachys nigra* Munro | Leaves | (KIM et al., 2009) |
| **15** | Tricin | *Phyllostachys nigra* Munro | Leaves | (KIM et al., 2009) |
| | | *Sasa quelpaertensis* Nakai | Leaves | (SULTANA; LEE, 2010) |
| **16** | Tricin-7-*O*-glycoside | *Sasa quelpaertensis* Nakai | Leaves | (SULTANA; LEE, 2010) |
| **17** | Tricitin-3',4',5'-tri-*O*-methyl-7-*O*-b-glucopyranoside | *Sasa quelpaertensis* Nakai | Leaves | (SULTANA; LEE, 2010) |
| **18** | Farobin A | *Fargesia robusta* var. *Pingwu* | Leaves | (VAN HOYWEGHEN et al., 2010) |
| **19** | Farobin B | *Fargesia robusta* var. *Pingwu* | Leaves | (VAN HOYWEGHEN et al., 2010) |
| **20** | Cassiaoccidentalin A | *Bambusa chungii* | Leaves | (YUAN et al., 2021) |
| **21** | Cassiaoccidentalin B | *Fargesia robusta* var. *Pingwu* | Leaves | (VAN HOYWEGHEN et al., 2010) |
| | | *Bambusa chungii* | Leaves | (YUAN et al., 2021) |
| **22** | Isoorientin 4"-*O*-b-D-xylopyranoside | *Bambusa textilis* McClure | Leaves | (WANG et al., 2012b) |
| **23** | Isoorientin 2"-*O*-a-L-rhamnoside | *Bambusa textilis* McClure | Leaves | (WANG et al., 2012b) |
| **24** | Rutin | *Dendrocalamus hamiltonii* | Leaves | (VAN HOYWEGHEN et al., 2012) |
| **25** | Schaftoside | *Phyllostachys pracecox* | Shoots | (JIANG et al., 2019) |
| | | *Phyllostachys edulis* | Shoots | (WANG et al., 2022b) |
| **26** | Tamarixetin | *Phyllostachys heterocycla* var. *pubescens* | Shoots | (ABDELHAMEED et al., 2021) |
| **27** | Apigenin 6-C-a-L-arabinopyranoside-8-C-b-D-xylopyranoside | *Phyllostachys edulis* | Shoots | (WANG et al., 2022b) |
| **28** | Chrysin 6-*C*- arabinoside 8-*C*-glucoside | *Phyllostachys edulis* | Shoots | (WANG et al., 2022b) |
| **29** | Chrysin 6-*C*-glucoside 8-*C*- arabinoside | *Phyllostachys edulis* | Shoots | (WANG et al., 2022b) |
| **30** | Catechin | *Bambusa vulgaris* | Shoots | (AKHTAR; PATOWARY, 2022) |
| ***Phenolic compounds*** | | | | |
| **31** | Chlorogenic acid | *Phyllostachys nigra* var. *henonis* | Leaves | (HU; ZHANG; KITTS, 2000) |
| | | *Bambusa vulgaris* | Shoots | (AKHTAR; PATOWARY, 2022) |
| | | *Phyllostachys pracecox* | Shoots | (JIANG et al., 2019) |
| **32** | Caffeic acid | *Phyllostachys nigra* var. *henonis* | Leaves | (HU; ZHANG; KITTS, 2000) |
| | | *Bambusa vulgaris* | Shoots | (AKHTAR; PATOWARY, 2022) |
| **33** | *N*-*p*-coumaroylserotonin | *Sasa quelpaertensis* Nakai | Leaves | (SULTANA; LEE, 2009) |
| **34** | *N*-feruloylserotonin | *Sasa quelpaertensis* Nakai | Leaves | (SULTANA; LEE, 2009) |
| **35** | *p*-coumaric acid | *Sasa quelpaertensis* Nakai | Leaves | (SULTANA; LEE, 2009) |
| | | *Phyllostachys pracecox* | Shoots | (JIANG et al., 2019) |
| **36** | *p* -hydroxybenzoic acid | *Sasa quelpaertensis* Nakai | Leaves | (SULTANA; LEE, 2010) |
| | | *Phyllostachys pracecox* | Shoots | (JIANG et al., 2019) |
| **37** | 3-hydroxy-1-(4-hydroxy 3,5-dimethoxyphenyl)-1-propanone | *Sasa quelpaertensis* Nakai | Leaves | (SULTANA; LEE, 2010) |
| **38** | Gallic acid | *Phyllostachys pracecox* | Shoots | (JIANG et al., 2019) |
| **39** | Neochlorogenic acid | *Phyllostachys pracecox* | Shoots | (JIANG et al., 2019) |
| **40** | 3-*p*-Coumaroylquinic acid | *Phyllostachys pracecox* | Shoots | (JIANG et al., 2019) |
| **41** | Cryptochlorogenic acid | *Phyllostachys pracecox* | Shoots | (JIANG et al., 2019) |
| **42** | 3-*O*-Feruloylquinic acid | *Phyllostachys pracecox* | Shoots | (Jiang et al., 2019) |
| **43** | Syringic acid | *Phyllostachys pracecox* | Shoots | (JIANG et al., 2019) |
| **44** | 5-*p*-Coumaroylquinic acid | *Phyllostachys pracecox* | Shoots | (JIANG et al., 2019) |
| **45** | 3-*O*-Caffeoylshikimic acid | *Phyllostachys pracecox* | Shoots | (JIANG et al., 2019) |
| **46** | 5-*O*-Feruloylquinic acid | *Phyllostachys pracecox* | Shoots | (JIANG et al., 2019) |

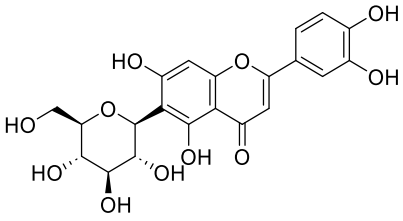
| | | | | |
|---|---|---|---|---|
| **47** | Ferulic acid | *Phyllostachys pracecox* | Shoots | (JIANG et al., 2019) |
| **48** | 1,3-Dicaffeoyl quinic acid | *Phyllostachys pracecox* | Shoots | (JIANG et al., 2019) |
| **49** | 3,5-Dicaffeoyl quinic acid | *Phyllostachys pracecox* | Shoots | (JIANG et al., 2019) |
| **50** | 7-hydroxy, 5-methoxy, methyl cinnamate | *Phyllostachys heterocycla* var. *pubescens* | Shoots | (ABDELHAMEED et al., 2021) |
| **51** | 3,4-dihydroxybenzoic acid | *Phyllostachys heterocycla* var. *pubescens* | Shoots | (ABDELHAMEED et al., 2021) |
| **52** | Methyl ferulate | *Phyllostachys heterocycla* var. *pubescens* | Shoots | (ABDELHAMEED et al., 2021) |
| ***Lignans*** | | | | |
| **53** | Phyllostadimers A | *Phyllostachys edulis* | Stems | (SUGA et al., 2003) |
| **54** | Phyllostadimers B | *Phyllostachys edulis* | Stems | (SUGA et al., 2003) |
| **55** | 4-keto- pinoresinol | *Phyllostachys heterocycla* var. *pubescens* | Shoots | (ABDELHAMEED et al., 2021) |
| ***Phytosterols*** | | | | |
| **56** | Daucosterol | *Sasa quelpaertensis* Nakai | Leaves | (SULTANA; LEE, 2010) |
| **57** | (6'-*O*-octadeca-8",11"-dienoyl)-sitosterol-3-*O*-*b*-D-glucoside | *Phyllostachys heterocycla* var. *pubescens* | Shoots | (ABDELHAMEED et al., 2020) |
| **58** | stigmast-4-en-3-one | *Phyllostachys heterocycla* var. *pubescens* | Shoots | (ABDELHAMEED et al., 2020) |
| **59** | 6-*b*-hydroxy-24-ethyl-cholest-4-en-3-one | *Phyllostachys heterocycla* var. *pubescens* | Shoots | (ABDELHAMEED et al., 2020) |
| **60** | 6-α-hydroxycholest-4-en-3-one | *Phyllostachys heterocycla* var. *pubescens* | Shoots | (ABDELHAMEED et al., 2020) |
| **61** | *β*-sitosterol | *Phyllostachys heterocycla* var. *pubescens* | Shoots | (ABDELHAMEED et al., 2020) |
| **62** | (6'-*O*-palmitoyl)-sitosterol-3-*O*-b-D-glucoside | *Phyllostachys heterocycla* var. *pubescens* | Shoots | (ABDELHAMEED et al., 2020) |
| **63** | *b*-sitosterol-3-O-*b*-D-glucoside | *Phyllostachys heterocycla* var. *pubescens* | Shoots | (ABDELHAMEED et al., 2020) |
| ***Coumarins*** | | | | |
| **64** | Skimin | *Sasa argenteastriatus* | Leaves | (WANG et al., 2013) |
| | | *Phyllostachys propinqua* | Leaves | (WANG et al., 2013) |
| **65** | Scopolin | *Dendrocalamus giganteus* | Leaves | (WANG et al., 2013) |
| | | *Bambusa pervariabilis* | Leaves | (WANG et al., 2013) |
| **66** | Scopoletin | *Dendrocalamus giganteus* | Leaves | (WANG et al., 2013) |
| | | *Bambusa pervariabilis* | Leaves | (WANG et al., 2013) |
| | | *Phyllostachys nidularia* | Leaves | (WANG et al., 2013) |
| | | *Phyllostachys sulphurea* | Leaves | (WANG et al., 2013) |
| | | *Sasa argenteastriatus* | Leaves | (WANG et al., 2013) |
| | | *Phyllostachys spectabilis* | Leaves | (WANG et al., 2013) |
| | | *Pseudosasa japonica* | Leaves | (WANG et al., 2013) |
| | | *Phyllostachys aureosulcata* | Leaves | (WANG et al., 2013) |
| | | *Pleioblastus fortunei* | Leaves | (WANG et al., 2013) |
| | | *Phyllostachys propinqua* | Leaves | (WANG et al., 2013) |
| | | *Phyllostachys nigra* | Leaves | (WANG et al., 2013) |
| **67** | Umbelliferone | *Sasa argenteastriatus* | Leaves | (WANG et al., 2013) |
| | | *Pleioblastus fortunei* | Leaves | (WANG et al., 2013) |
| | | *Phyllostachys propinqua* | Leaves | (WANG et al., 2013) |
| | | *Phyllostachys nigra* | Leaves | (WANG et al., 2013) |
| **68** | Coumarin | *Phyllostachys propinqua* | Leaves | (WANG et al., 2013) |
| | | *Phyllostachys nigra* | Leaves | (WANG et al., 2013) |
| **69** | Pimpinellin | *Pseudosasa japonica* | Leaves | (WANG et al., 2013) |
| ***Phenylpropanoids*** | | | | |
| **70** | 3-*O*-*p*-coumaroyl-1-(4-hydroxy-3,5-dimethoxyphenyl)-1-propanone | *Sasa quelpaertensis* Nakai | Leaves | (SULTANA; LEE, 2009) |
| **71** | 3-*O*-*p*-coumaroyl-1-(4-hydroxy-3,5-dimethoxyphenyl)-1-*O*-b-gulco-pyranosylpropanol | *Sasa quelpaertensis* Nakai | Leaves | (SULTANA; LEE, 2009) |
| ***Alkene glycosides*** | | | | |
| **72** | (*E*)-3-hexenyl-b-glucopyranoside | *Sasa quelpaertensis* Nakai | Leaves | (SULTANA; LEE, 2010) |
| ***Chromones*** | | | | |
| **73** | Saikochromone A | *Sasa quelpaertensis* Nakai | Leaves | (SULTANA; LEE, 2010) |
| ***Carotenoids*** | | | | |
| **74** | Lutein | *Sasa quelpaertensis* Nakai | Leaves | (SULTANA; LEE, 2010) |

### 1.1.2.1 Flavonoids

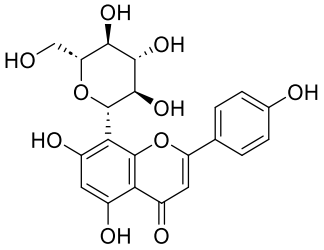
Flavonoids are phenolic compounds widely reported in bamboos. They are mainly found in all organs, especially in leaves, shoots and culms, playing a crucial role in antioxidant defense (VAN HOYWEGHEN; DEFORCE; HEYERICK, 2010). In general, in the genera e.g., *Phyllostachys*, *Sasa*, *Pleioblastus*, *Fargesia*, *Bambusa*, *Arundinaria* and *Dendrocalamus*, the composition of flavonoids is primarily represented by glycosides of flavones and flavonols (**1**-**30**).



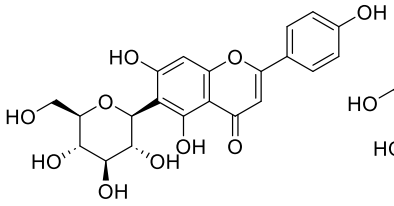
**1**



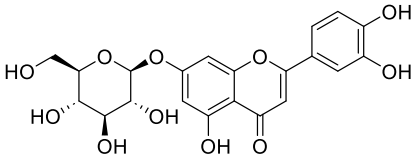
**2**



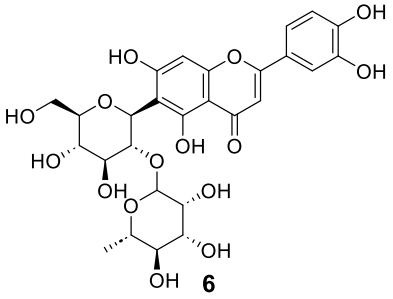
**3**



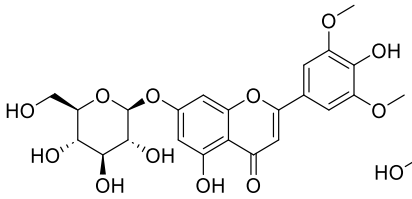
**4**



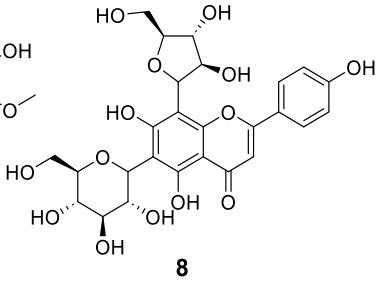
**5**



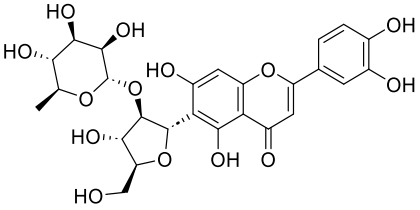
**6**



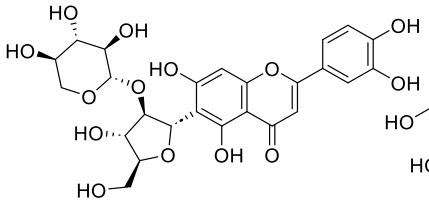
**7**



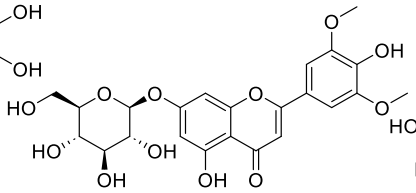
**8**



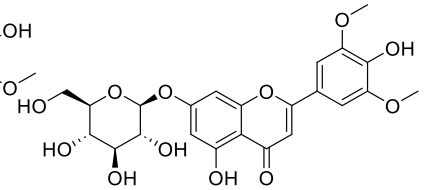
**9**



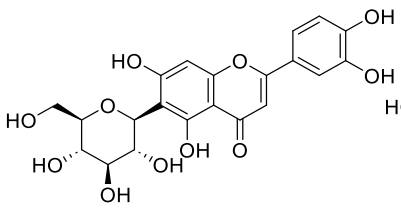
10



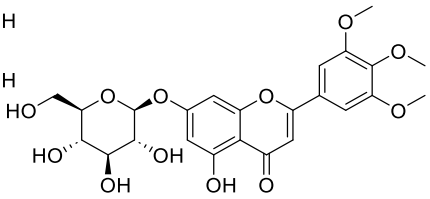
11



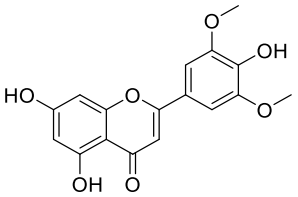
12



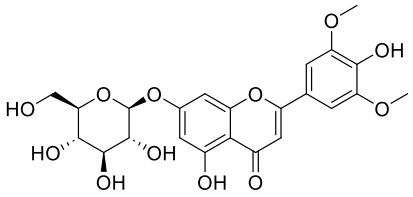
13



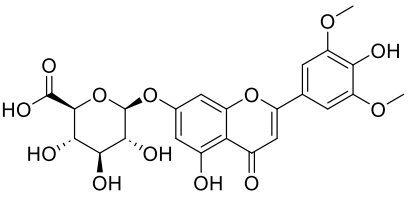
14



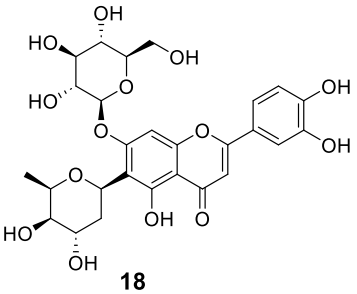
15



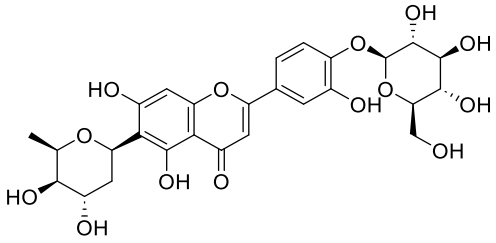
16



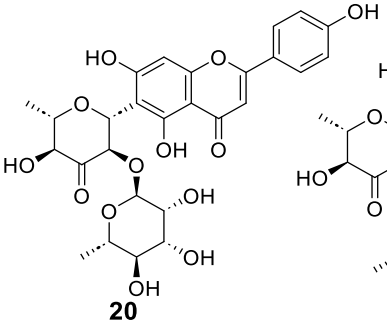
17



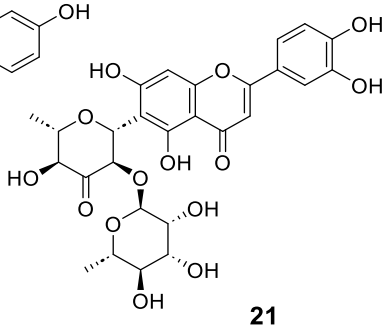
18



19



20



21

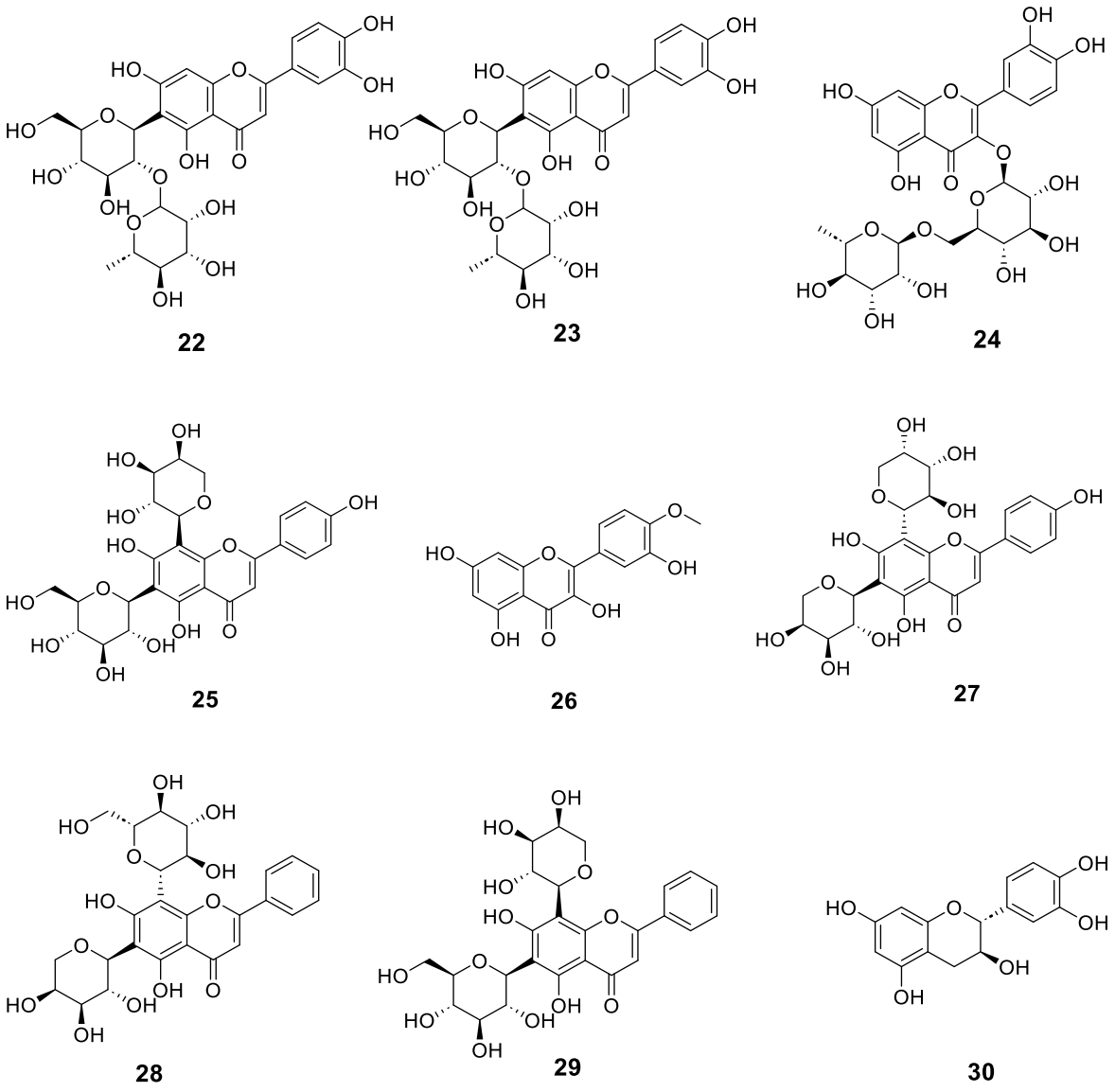
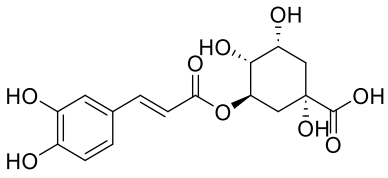



**Figure 1.3.** Flavonoids reported (**1**-**30**) from bamboos (Poaceae family).

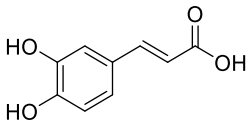
### 1.1.2.2 Phenolic acids derivatives

Phenolic acid derivatives are also predominant compounds in bamboo species, with antioxidant and antibacterial properties (ANDRESSA ALMEIDA FARIAS et al., 2024). The most representative compounds are those derived from caffeic (**32**), *p*-coumaric (**35**) and ferulic (**47**) acids. Furthermore, other reports have highlighted that the main phenolic acids present in bamboo leaves are chlorogenic (**31**), neochlorogenic (**39**) and

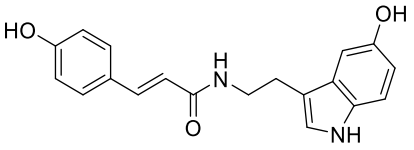
cryptochlorogenic (**41**) acids (Kumbhare, 2009; Ma et al., 2020). Other related phenolic acids (**31**-**52**) are described in Figure 1.4.



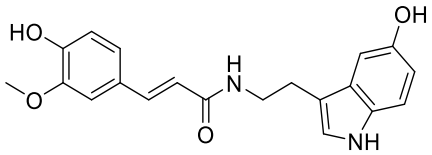
**31**



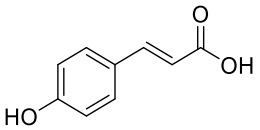
**32**



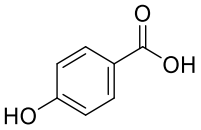
**33**



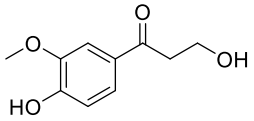
**34**



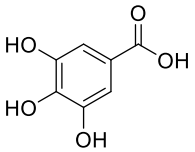
**35**



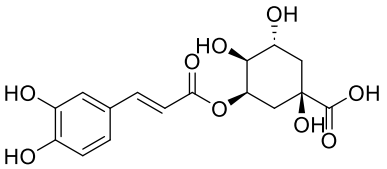
**36**



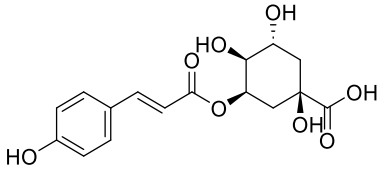
**37**



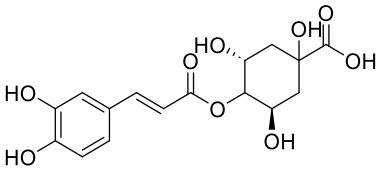
**38**



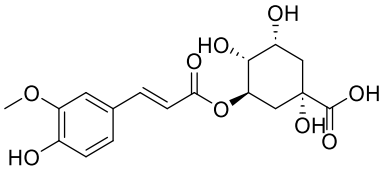
**39**



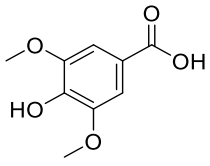
**40**



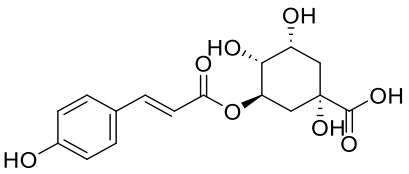
**41**



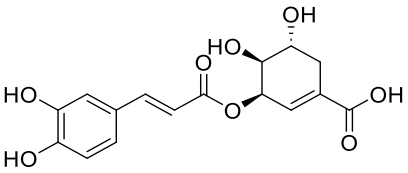
**42**



**43**



**44**



**45**

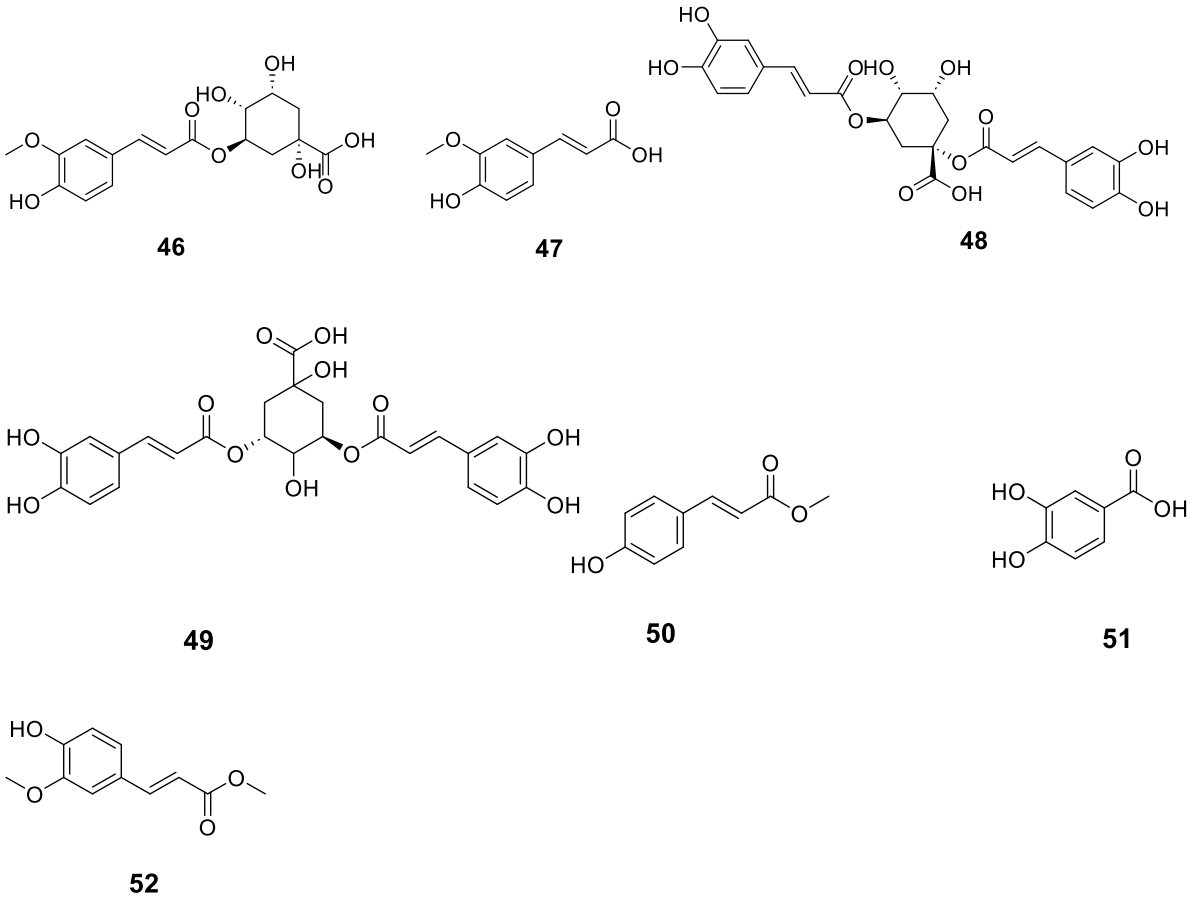
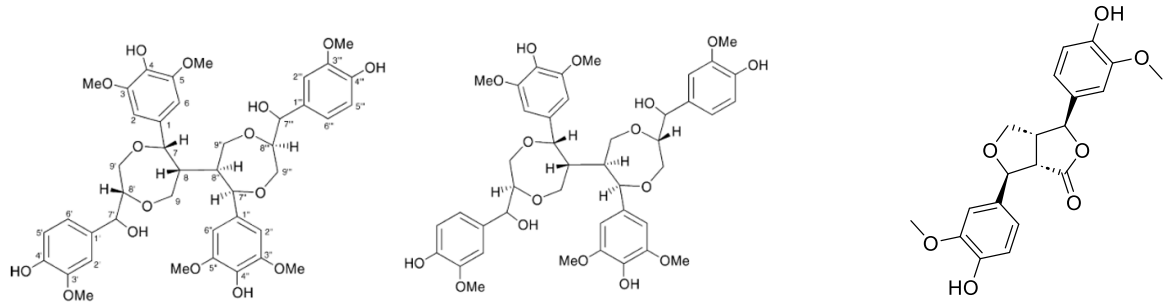



**Figure 1.4.** Phenolic acids derivatives reported (**31**-**52**) from bamboos (Poaceae family).

### 1.1.2.3 Lignans

Lignans are widely distributed in angiosperms and gymnosperms plants. Several lignans are known to have antimitotic, antitumor, and antiviral activity. However, these secondary metabolites are not as commonly found in bamboo plants, although dimeric lignans (**53**-**55**) have been reported for some species such as *Phyllostachys edulis* and *Phyllostachys heterocycla* var. *pubescens* (ABDELHAMEED et al., 2021; SUGA et al., 2003).

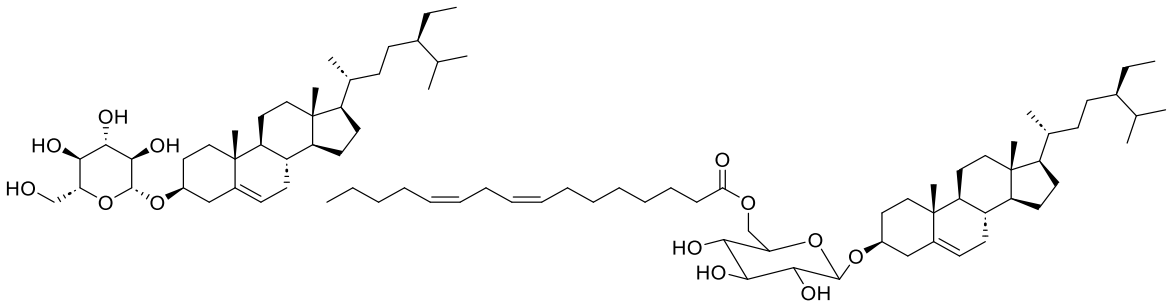


**53** **54** **55**

**Figure 1.5.** Lignans reported (**53**-**55**) from bamboos (Poaceae family).

### 1.1.2.4 Phytosterols

Phytosterols are common compounds found mainly in bamboo leaves and culms. They are characterized by having C28 and C29 carbon steroids in their main scaffold. Phytosterols have important functions, such as stabilizing the phospholipid bilayer of plant cell membranes. The most abundant and commonly found phytosterols in bamboos include *β*-sitosterol (**61**), campesterol, and stigmasterol. Particularly, the species *Phyllostachys heterocycla* var. *pubescens* contains phytosterol-glucoside-fatty acid derivatives at the hydroxyl position (**56**-**63**) (ABDELHAMEED et al., 2020).



**56** **57**

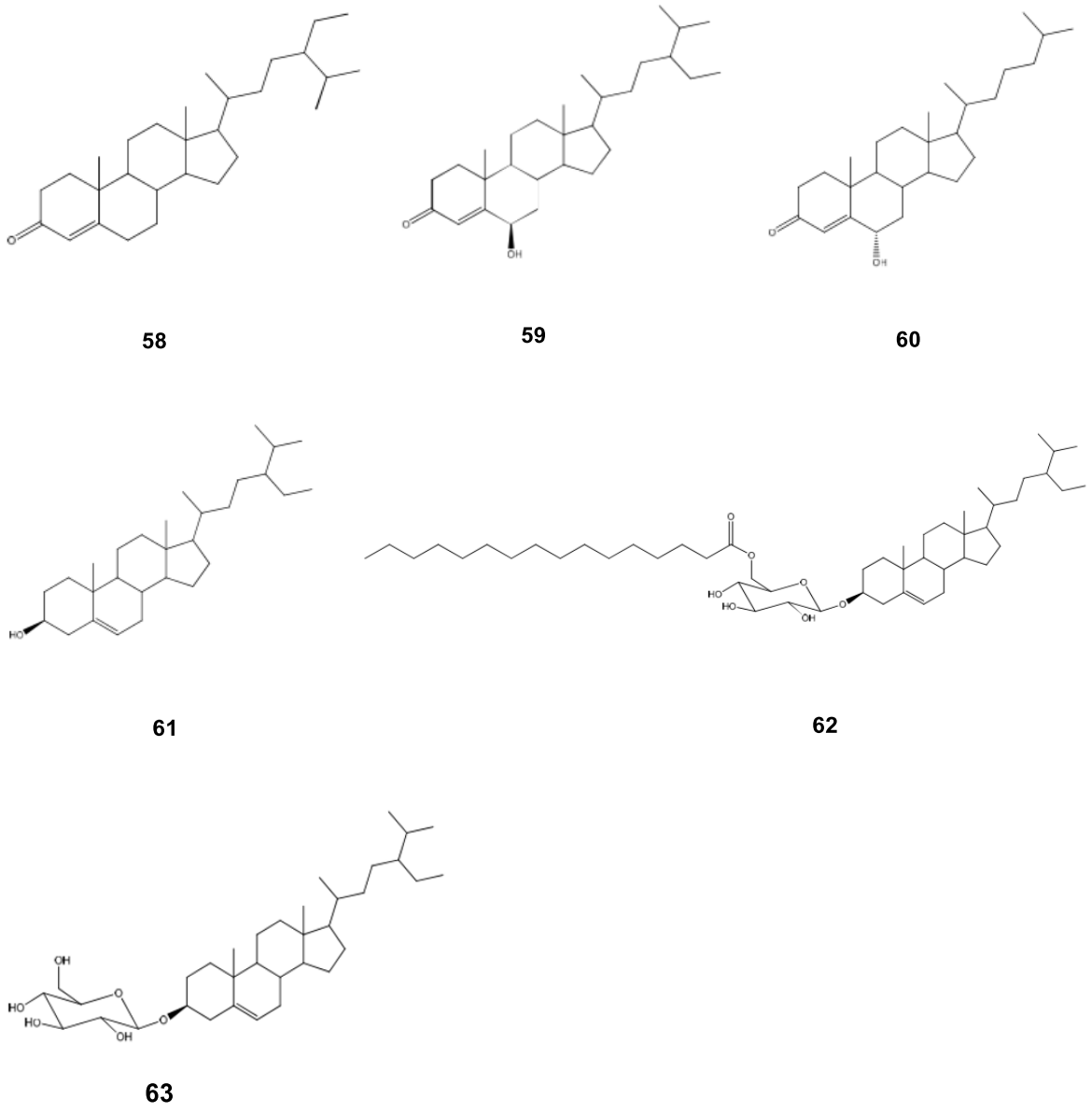



**Figure 1.6.** Phytosterols reported (**56**-**63**) from bamboos (Poaceae family).

### 1.1.2.5 Coumarins

Coumarins are known as benzopyrones, commonly found in many plants. Notably, in several species of bamboo, i.e., *Dendrocalamus giganteus*, *Bambusa pervariabilis*, *Phyllostachys nidularia*, *Phyllostachys sulphurea*, *Sasa argenteastriatus*, *Phyllostachys spectabilis*, *Pseudosasa japonica*, *Pseudosasa aureosulcata*, *Pleioblastus fortunei*,

*Pleioblastus propinqua*, and *Phyllostachys nigra*, the presence of various coumarins has been found (**64**-**69**) (WANG et al., 2013). These metabolites have been discovered to be responsible for a wide spectrum of pharmacological activities, including anticoagulant, anti-inflammatory, anticancer, and antibacterial effects, among others (SHARIFI-RAD et al., 2021).

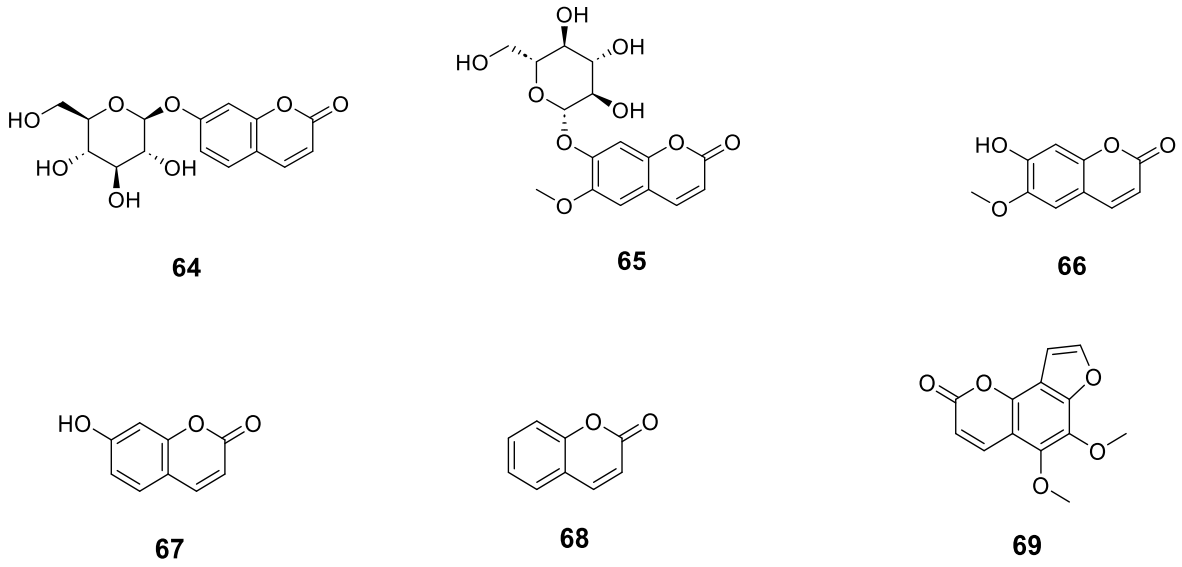



**Figure 1.7.** Coumarins reported (**64**-**69**) from bamboos (Poaceae family).

### 1.1.2.6 Other compounds

Other less common compounds reported in bamboo are related to the presence of phenylpropanoids (**70**-**71**), alkene glycosides (**72**), chromones (**73**) and carotenoids (**74**). Most of them are also related to some biological properties related to anti-inflammatory, cytotoxic, antioxidant effects (SILVA et al., 2018).

## 1.1.3 Biological activity of bamboo species

The most relevant activities reported for bamboos are mainly antifungal (OWOLABI; LAJIDE; MOSES OWOLABI, 2015), antibacterial (TANAKA et al., 2014), antiallergic (TANAKA et al., 2014), antioxidant (VAN HOYWEGHEN et al., 2014), photoprotective (WRÓBLEWSKA et al., 2019), anti-inflammatory (YANG et al., 2017) and

cytotoxic (ABDELHAMEED et al., 2020, 2021). The information in this section is organized by plant species, organ used, type of biological activity, and method evaluated, including the most representative references found for different bamboo species (Table 1.2).

According to the previous section, which highlights the chemical diversity present in different bamboo species, these molecules have been the basis for various biological activity studies with great potential. The general antioxidant activity of bamboos is particularly notable due to their high composition of phenolic compounds. Most of these molecules are potential antioxidants that protect against reactive oxygen species (ROS), helping to prevent diseases related to oxidative stress, such as cancer, cardiovascular diseases, neurodegenerative diseases, and inflammatory disorders (TUNDIS et al., 2023; WRÓBLEWSKA et al., 2019).

Another important activity in bamboo species is their anti-inflammatory potential evaluated *in vitro*, which is associated with cancer and plays a key role in tumor development and progression. Studies highlight the anti-inflammatory activity through the nitric oxide (NO) inhibition assay, a key signaling molecule in the inflammation process (VANINI; KASHFI; NATH, 2015). Furthermore, NO is usually considered a proinflammatory mediator in different cellular models. It is important to highlight that the inhibition of the NO molecule may represent a significant therapeutic advance in the treatment of inflammatory diseases (KIM, 2020).

The cytotoxic activity of bamboo species has also been reported, particularly for *Sasa quelpaertensis*, *Phyllostachys heterocycla*, *Melocanna baccifera* and *Phyllostachys edulis*, against different tumor cell models, including HCT-116, HepG2, HeLa, A549, MCF-7, MCF-10A, SIHA, and C6. It is highlighted that the content of compounds related to flavonoids and some sterols is responsible for the cytotoxic potential (ABDELHAMEED et al., 2020).

**Table 1.2.** Biological activity reported for bamboo species.

| Species | Organ used | Activity evaluated | References |
|---|---|---|---|
| *Bambusa vulgaris* Schrad. Ex J.C. Wendl. | Leaves | Antifungal<br>• *Aspergillus niger*<br>• *Verticillium albo-atrum*<br>Antibacterial<br>Gram positive<br>• *Bacillus cereus*<br>• *Staphylococcus aureus*<br>Gram negative<br>• *Escherichia coli*<br>• *Klebsiella pneumoniae* | (OWOLABI; LAJIDE; MOSES OWOLABI, 2015) |
| *Phyllostachys pubescens* | Leaves, branches, culms, rhizomes, and roots | Melanin biosynthesis assay<br>Antioxidant<br>• ORAC<br>• ABTS<br>Antibacterial<br>• *Staphylococcus aureus*<br>Antiallergic<br>Immunoglobulin E production assay | (TANAKA et al., 2014) |
| *Sasa quelpaertensis* Nakai | Leaves and culms | Tyrosinase inhibition assay | (SULTANA; LEE, 2009) |
| | Leaves | Cytotoxic<br>HCT-116 cell line<br>• Cell viability (Trypan blue)<br>• Cell cycle analysis<br>• Nitrite production (Griess reaction)<br>• Caspase 3 activity assay | (Kim, 2020) |
| *Fargesia robusta* | Leaves | Antioxidant<br>• DPPH<br>• TEAC<br>• ORAC | (VAN HOYWEGHEN et al., 2010) |
| *Phyllostachys nigra* | Leaves | Antioxidant<br>• DPPH<br>• TEAC | (VAN HOYWEGHEN et al., 2012) |
| *Phyllostachys nigra* | Leaves | Inhibition of transcription factor NF-kB and cyclooxygenase | (VAN HOYWEGHEN et al., 2014) |
| *Sasa veitchii* | Leaves | Antioxidant<br>• DPPH<br>• TEAC | (VAN HOYWEGHEN et al., 2014) |
| *Sasa veitchii* | Leaves | Inhibition of transcription factor NF-kB and cyclooxygenase | (VAN HOYWEGHEN et al., 2014) |

| | | | |
|---|---|---|---|
| *Dendrocalamus hamiltonii* | Leaves | Antioxidant<br>• DPPH<br>• TEAC | (VAN HOYWEGHEN et al., 2014) |
| *Dinochloa scandens* | Leaves | Antioxidant<br>• DPPH<br>• TEAC | (VAN HOYWEGHEN et al., 2014) |
| *Guadua amplexifolia* | Leaves | Antioxidant<br>• DPPH<br>• TEAC | (VAN HOYWEGHEN et al., 2014) |
| *Phyllostachys humilis* | Leaves | Antioxidant<br>• DPPH<br>• TEAC | (VAN HOYWEGHEN et al., 2014) |
| *Pleioblastus variegatus* | Leaves | Antioxidant<br>• DPPH<br>• TEAC | (VAN HOYWEGHEN et al., 2014) |
| *Pseudosasa japonica* | Leaves | Antioxidant<br>• DPPH<br>• TEAC | (VAN HOYWEGHEN et al., 2014) |
| *Fargesia rufa* | Leaves | Antioxidant<br>• DPPH<br>• TEAC | (VAN HOYWEGHEN et al., 2014) |
| *Arundinaria gigantea* | Leaves | Antioxidant<br>• DPPH<br>• TEAC | (VAN HOYWEGHEN et al., 2014) |
| *Bambusa balcooa* | Leaves | Antioxidant<br>• DPPH<br>• TEAC | (VAN HOYWEGHEN et al., 2014) |
| *Neosinocalamus affini* | Leaves | Antioxidant<br>• DPPH<br>• ABTS<br>Nitric oxide-scavenging assay<br>• Griess reagent | (LUO et al., 2015) |
| *Sasa coreana* Nakai | Leaves | Anti-inflammatory (Nitrite production)<br>RAW 264.7 murine macrophage cell line<br>3T3-L1 preadipocytes<br>• Griess reagent<br>Antidioapogenic | (YANG et al., 2017) |
| *Merostachys pluriflor* | Leaves and culms | Antioxidant<br>• DPPH<br>• FRAP<br>• ABTS<br>Determination of iron chelating reduction<br>Determination of oxygen radical scavenging capacity | (GAGLIANO; GROMBONE-GUARATINI; FURLAN, 2018) |

| | | | |
|---|---|---|---|
| | | Antioxidant<br>• DPPH<br>Photoprotective evaluation | (WRÓBLEWSKA et al., 2019) |
| *Chusquea bambusoides* Rupr. ex Döll | Leaves and culms | Antioxidant<br>• DPPH<br>Photoprotective evaluation | (WRÓBLEWSKA et al., 2019) |
| *Chusquea capituliflora Trin.* var. *pubescens* McClure | Leaves and culms | Antioxidant<br>• DPPH<br>Photoprotective evaluation | (WRÓBLEWSKA et al., 2019) |
| *Aulonemia aristulata* (Döll) McClure. | Leaves and culms | Antioxidant<br>• DPPH<br>Photoprotective evaluation | (WRÓBLEWSKA et al., 2019) |
| *Chusquea meyeriana* Rupr. | Leaves and culms | Antioxidant<br>• DPPH<br>Photoprotective evaluation | (WRÓBLEWSKA et al., 2019) |
| *Phyllostachys heterocycla* var. *Pubescens* | Shoot | Cytotoxic<br>HepG2<br>HeLa<br>A549<br>MCF-7<br>MCF-10A<br>• MTT | (ABDELHAMEED et al., 2020) |
| | Shoot | Cytotoxic<br>HepG2<br>HeLa<br>A549<br>MCF-7<br>THP-1<br>• MTT<br>EGFR Inhibition | (ABDELHAMEED et al., 2021) |
| *Melocanna baccifera* (Roxb.) Kurz | Leaves and frutis | Cytotoxic<br>SIHA<br>MCF-7<br>MCF-10A<br>C6<br>• MTT<br>• Flow cytometric evaluation<br>Acetylcholinesterase inhibition | (GOVINDAN et al., 2019) |
| *Phyllostacys edulis* J. Houz | Leaves and sheath | Cytotoxic<br>HepG2<br>• MTT<br>Anti-inflammatory<br>THP-1 monocytes<br>• MTT | (TUNDIS et al., 2023) |

## 1.2 Overview of *Guadua* species

The genus *Guadua* is native to the Neotropics and belongs to the family Poaceae, subfamily Bambusoideae and tribe Bambuseae. It extends from Mexico through all the countries of Central and South America to Argentina, except for Chile. It comprises about 34 species, of which four species and one variety are economically representative in Colombia: *G. amplexifolia*, *G. superba*, *G. weberbaueri*, *G. angustifolia,* and *G. angustifolia* var. bicolor. Bamboo is a perennial herb that belongs to the group of angiosperms, which grow very well in tropical and subtropical areas, being very adaptable (CÉSPEDES PRIETO et al., 2020; MEJÍA GALLÓN et al., 2011). The species of this genus are woody and reach their highest degree of development under mesophytic conditions at altitudes not exceeding 1500 m. Temperature is a limiting factor in its latitudinal and altitudinal distribution; it does not withstand prolonged periods below 0 °C and does not grow well in areas where precipitation is less than 1200 m per year (LONDOÑO, 2011). In Colombia, most of the *Guadua* populations grow between 0-1000 meters above sea level, occupying diverse habitats in the tropical rainforest and very humid premontane forest vegetation formations. At the morphological level, the distinctive characteristics of the genus are its lateral branches with well-developed spines and culms with internodes covered with trichomes (Figure 1.8).




**Figure 1.8.** Representative morphological characteristics of *Guadua* genus. a. *Guadua angustifolia*; b. *G. incana*; c. *G. lynnclarkiae*; d. *G. sarcocarpa*; e. *G. takahashiae*; f. *G. uncianata*; g. *G. weberbaueri*. Figure from (LONDOÑO, 2024).

In different countries, such as China and Japan, the culms and vinegar obtained from guadua have been traditionally used for the treatment of human ailments. For example, to cure allergies, dermatitis, diabetes, facilitate hair growth, cure acne, hypertension, fevers, detoxifications, and the treatment of certain forms of cancer, etc. They are also widely used for agricultural activities (MEJÍA GALLÓN et al., 2011). In Colombia, *Guadua* is basically but widely used in construction and handicrafts. It is also extensively utilized by rural producers as an economic alternative in the coffee region (MOSQUERA et al., 2016). Studies show that bamboo species are known as the "vegetable steel" or the "green gold of the 21$^{st}$ century" since they are crucial for construction, providing high resistance to traction and compression. Additionally, bamboo has become an alternative to mitigate the effects caused by climate change and has been used to replace illicit crops in different areas of the country (ACOSTA-LEAL et al., 2021; CÉSPEDES PRIETO et al., 2020).

*Guadua angustifolia* Kunth is the bamboo of America and is the most representative species in our country due to the demand and better acceptance by the productive sector. This is attributed to its easy propagation capacity, fast growth, usefulness, and tradition in working its products. It also holds potential in the areas of construction, furniture making, handicrafts, paper making, and as an environmental improver (CUELLAR BAHAMON, 2016; ESPINOSA PÉREZ, 2004). It is also the most ecologically, socially, economically, culturally, and commercially important species. That is why it is considered one of the most valuable forest resources in the country (MOSQUERA MARTÍNEZ et al., 2012).

### 1.2.1 Phytochemical studies of *Guadua* species

Regarding the chemical composition, there are few reports to date for the genus *Guadua*. A wide variety of secondary metabolites, such as flavonoids, terpenes, triterpene, steroidal saponins, alkaloids and phenolic acid derivatives, observed by preliminary phytochemical analysis, have been described (ARBOLEDA ECHAVARRÍA; JARAMILLO YEPES; PALACIO TORRES, 2012; MOSQUERA MARTÍNEZ et al., 2012).

Morales and collaborators, in 2008, isolated and identified some flavonoids in polar extracts of leaves of *G. angustifolia*. In this study they determined the presence of flavonoids in aglycone and glycosidic forms, such as quercetin (**75**), kaempferol (**76**), violanthin (**77**), kaempferol-7-*O*-neohesperidoside (**78**), respectively (Figure 1.9) (MORALES NOREÑA; SANCHEZ VALLEJO, 2008). A GC-MS study of the compounds present in the vinegar obtained from *G. angustifolia*, led to the determination of different organic compounds corresponding to derivatives of phenolic compounds, organic acids, alcohols, cyclic ketones, furanic derivatives, and aromatic hydrocarbons, which were found in the acid, neutral and alkaline fractions prepared from the vinegar (Gallón et al., 2011). It is highlighted that for other species belonging to the genus *Guadua*, no phytochemical studies have been reported so far.

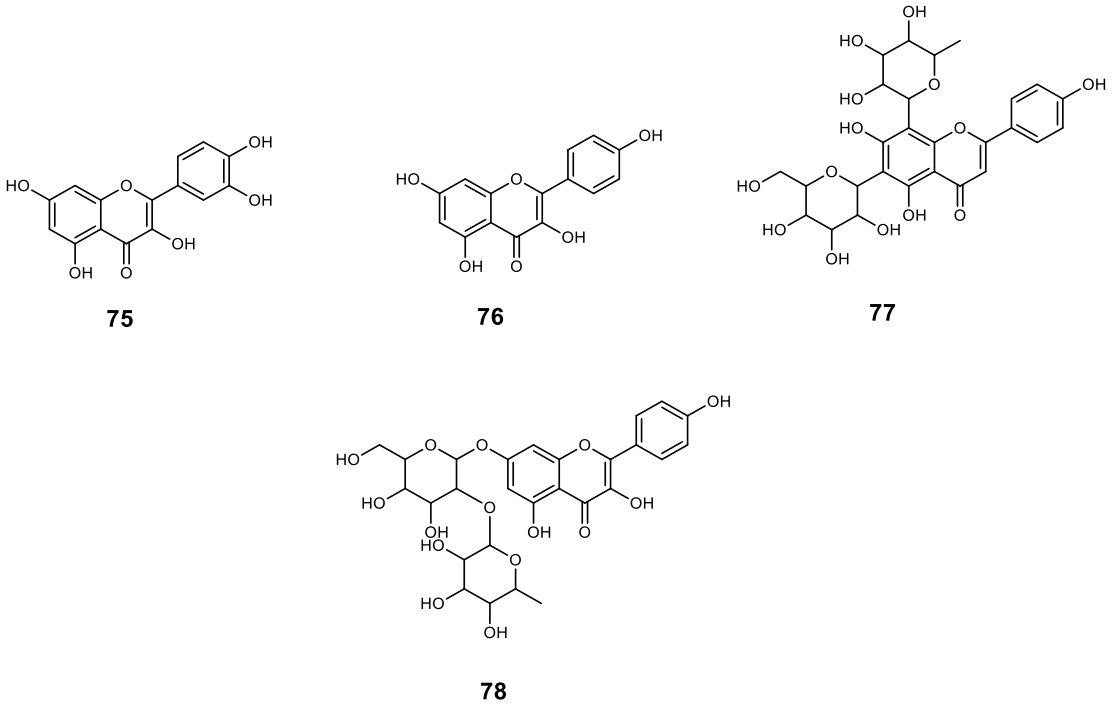



**Figure 1.9.** Flavonoids isolated in leaves of *G. angustifolia*.

### 1.2.2 Biological activity of *Guadua* species

Some studies of biological activity for *Guadua* species are reported in the literature, either of isolated compounds or of extracts and fractions. In this context, antioxidant and

antimicrobial activities have been reported for vinegar obtained from *G. angustifolia* leaves, activities mainly attributed to the high content of phenolic compounds. Additionally, the phenolic fraction obtained from this vinegar is recognized to have a high amount of antioxidant compounds that are considered important for the development of antiseptic products (ÁLVAREZ et al., 2015; GOMEZ et al., 2021; MEJÍA GALLÓN et al., 2011; MEJÍA GALLÓN; CADAVID TORRES; GALLARDO CABRERA, 2011; VALENCIA et al., 2011). The evaluation of the antioxidant activity was performed by the DPPH and ABTS methods to determine the free radical scavenging capacity of the extract. From the results, it was determined that all extracts obtained by different extraction methods (Soxhlet, ultrasound, and percolation) from the leaves of *G. angustifolia* showed antioxidant activity. Additionally, the ethanolic extracts showed antioxidant activity higher than 80 µmol Trolox/g extract (MOSQUERA et al., 2016; VALENCIA et al., 2011). The evaluation of the antiseptic activity was carried out by the agar diffusion method in Müller Hilton medium against two strains of *Pseudomonas aeruginosa* and *Staphylococcus aureus* bacteria using the vinegar obtained from *G. angustifolia*. The results indicated high sensitivity of *P. aeruginosa* and *S. aureus* bacteria to guadua vinegar at a pH lower than 4, with activity levels of 94.39% and 98.9%, respectively (Gallón et al., 2011).

### 1.3 New strategies for the study and discovery of NPs

The discovery of bioactive compounds from natural sources involves an extremely time-consuming process and the complexity of traditional methodologies. A classic strategy in natural products research begins with a biological activity screening of extracts to identify their biological potential, which is then fractionated to isolate and identify the active constituents. Advances in methodology and strategies have helped to streamline the discovery process, effectively shortening the classical process in identifying molecules of interest in active extracts. This metabolomics-inspired strategy employs analytical chemistry techniques, along with computational and statistical tools, to provide an overview of the metabolomic profile. (DEMARQUE et al., 2020; DEMARQUE; ESPINDOLA, 2021).

### 1.3.1 Metabolomics applied to the area of NPs

In general terms, metabolomics is understood as the simultaneous and global acquisition of chemical profiles corresponding to multiple metabolite concentrations and their systemic and cellular fluctuations in response to a biological system. This strategy pursues the analytical description of complex biological samples and attempts to characterize and quantify all small molecules in such samples. However, measuring the metabolome is a considerable analytical challenge (CASTRO et al., 2020; VERPOORTE; CHOI; KIM, 2010). This is due to the labile nature of metabolites, the widely dynamic and diverse range of many metabolites, the chemical complexity, and heterogeneous nature of metabolites, the lack of automated analytical techniques that can quantitatively measure many metabolites of unknown structure, and the throughput of measurements. Metabolomics is playing an increasingly important role in NPs research. This approach represents a new way of interrogating biological systems, as it is an unbiased data-driven approach that can lead to hypotheses and new biological insights. Thanks to technological advances in chromatography and spectrometry, metabolomics was initially applied in research fields such as biomedical and agricultural sciences. For several years now, it has been established as a novel strategy in the study of NPs. Advances in analytical instrumentation together with computational approaches allow the prediction of novel and important structures for the discovery of new drugs from a natural product (RINSCHEN et al., 2019; TAWFIKE; VIEGELMANN; EDRADA-EBEL, 2013; YULIANA et al., 2011). This modern approach can provide accurate information on the chemical composition of an extract, helping to prioritize secondary metabolites for further isolation, accelerate the processes of dereplication and annotation of unknown compounds. The workflow is summarized in Figure 1.10.

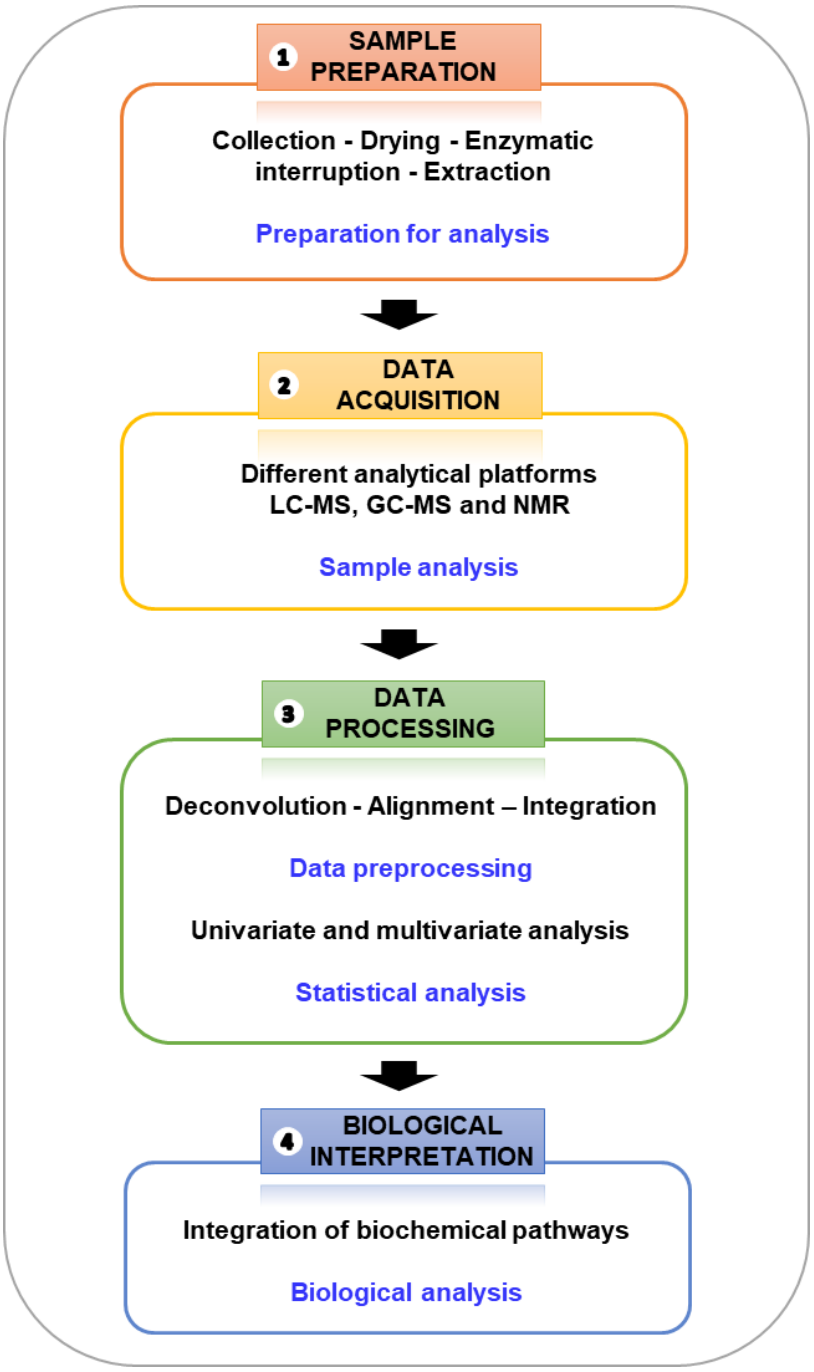



**Figure 1.10.** Workflow used in the study of NPs.

### 1.3.2 Targeted and untargeted metabolomics approaches

The metabolomics study can be performed using a targeted or untargeted approach. Targeted approaches can quantify specific classes or groups of metabolites,

whereas untargeted approaches aim to acquire as much metabolic information as possible. In targeted metabolomics, a defined set of metabolites is analyzed. In this case, laborious optimization work is required using commercial standards, which in most cases is limited by the high costs they present. The targeted approach generates the search for specific metabolites of certain molecules that are related to the disease or have been previously reported (Figure 1.11). It is used to validate specific biological pathways or confirm selected metabolites in an untargeted study. Additionally, it accurately detects and quantifies a small set of known metabolites (Bingol, 2018; Gorrochategui et al., 2016; Vinaixa et al., 2016; Wang et al., 2019).

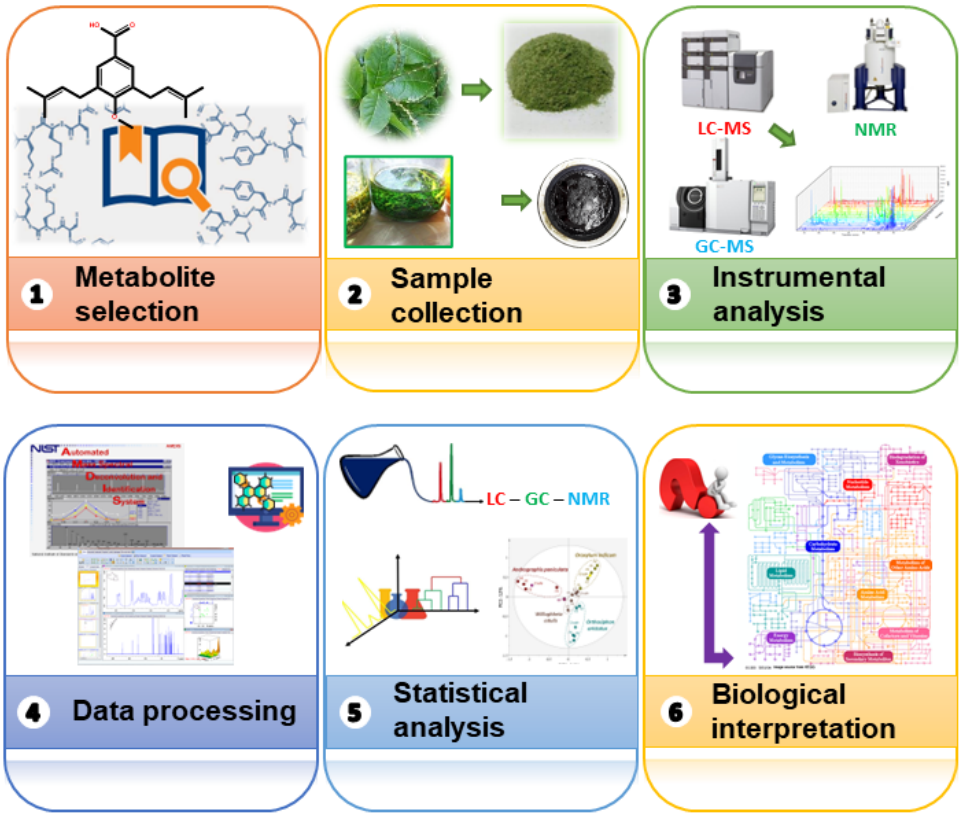



**Figure 1.11.** Workflow used in a targeted metabolomics study.

In untargeted metabolomics, all metabolites present in a sample are analyzed, and a profile is obtained to characterize the type of sample analyzed. This approach allows not only to characterize changes in the overall metabolic profile, but also to detect unknown metabolites (Figure 1.12). In this step, all the signals generated by the analysis are

entered into databases where we will try to recognize which metabolite they belong to. Although excellent progress has been made in building metabolomics databases with new metabolites obtained from plants, a significant part of the signals detected in untargeted studies are still not useful for identifying unknown substances, due to the absence of their spectra in the databases. Untargeted studies are very focused on the identification of known metabolites, especially when they are the biomarkers of a study (BINGOL, 2018; GORROCHATEGUI et al., 2016). Unlike targeted metabolomics, which is effective for testing specific hypotheses, the goal of untargeted metabolomics is to measure as many metabolites in the sample as possible. This plant-level assessment is very attractive because it can potentially allow the search for bioactive compounds while taking into account the complexity of the extracts (WANG et al., 2019).

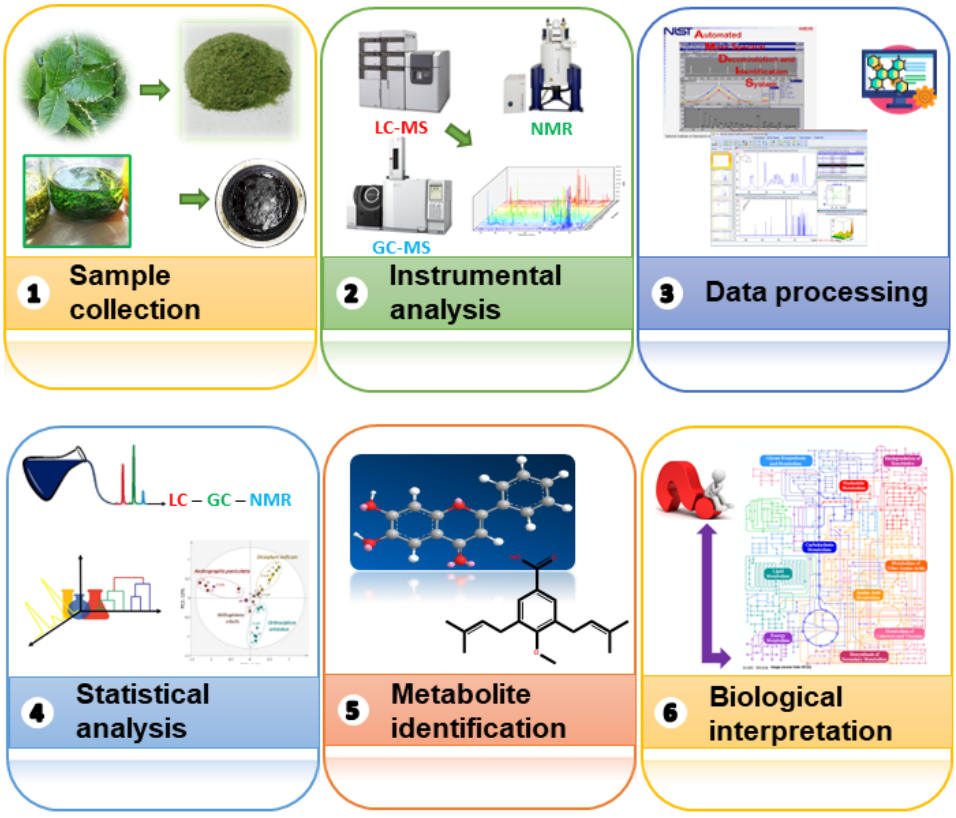



**Figure 1.12.** Workflow used in an untargeted metabolomic study.

### 1.3.3 Analytical platforms used in metabolomics for the study of NPs

The most successful analytical platforms used in this area have been mainly focused on nuclear magnetic resonance (NMR) and mass spectrometry (MS), the latter coupled with chromatographic separation techniques, such as liquid chromatography (LC) and gas chromatography (GC), and electrophoretical techniques, such as capillary electrophoresis (CE). This combination is generally used to obtain good sensitivity and resolution in the detection of metabolites (MARKLEY et al., 2017; PANDA; PARIDA; RANGANI, 2018). For several years, it has been evident that the number of publications using the two approaches was comparable, but recently, MS-based metabolomics has clearly surpassed NMR-based metabolomics. These platforms have provided the capability to obtain a global, rapid, and accurate assessment of metabolites within a plant extract (MARKLEY et al., 2017).

According to the focus of this thesis, an extension of LC-MS and NMR techniques for metabolomic studies of natural products is presented.

#### 1.3.3.1 LC-MS

MS-based omics techniques, including metabolomics and proteomics, are rapidly growing fields in systems biology that combine analytical and statistical methodologies for high-throughput analysis of molecule profiles. Large-scale experiments, coupled with a variety of statistical tools, have been used to identify specific biological changes and for the identification of compounds in plant samples, leading to the discovery of new molecules in plants (LUAN et al., 2018). LC-MS has become an established technique for metabolomics studies due to its ability to separate and detect a wide range of molecules with unparalleled sensitivity. Although the accuracy, resolution, and speed of instrumentation for LC-MS metabolomics have improved over the last decade, covering the complexity of the metabolome remains a major challenge (THEODORIDIS et al., 2020). MS has established itself in recent years as an essential tool in metabolite analysis and is considered a widely used technique in metabolomics studies due to its high sensitivity and selectivity. It is based on the detection of ions that are separated according

to their mass/charge ratio (*m/z*), when applying an electromagnetic field. This coupling is often used to obtain the most information about the metabolome of the study matrix in a clearer and simpler way. By combining these techniques, the discovery of new compounds from plants can be accelerated, as well as the identification of those that have been previously reported in the literature, allowing for a fast and accurate evaluation of a large amount of data. This constitutes a viable option for the identification of active compounds in plant extracts.

#### 1.3.3.2 NMR

NMR-based metabolite detection is based on the use of magnetic properties of atom nuclei under a magnetic field. NMR is a non-destructive method widely used to identify low molecular weight metabolites including metabolite fingerprinting, profiling, metabolic flux, and extraction of molecular structural information of the compound present in biological samples (KUMAR et al., 2017). This technique provides a window to rigorously observe and quantify all the most abundant compounds present in an extract, without the need for rigorous sample preparation or fractionation. In addition, it is indispensable when it is certain that compounds that are difficult to ionize or require derivatization are present. The short measurement time, rapid sample preparation, and the possibility of elucidating structures of known or unknown compounds in a complex mixture make this technique very useful. Proton Nuclear Magnetic Resonance ($^1$H-NMR) is the most widely used method in metabolomics, specifically in the area of NPs, due to its excellent reproducibility and its suitability for comparison of results with public databases (CVETKOVIĆ et al., 2020). The signals are grouped and then analyzed or matched with signal patterns corresponding to the metabolites expected to be present in the mixture (MARKLEY et al., 2017). This technique can be used independently or in combination with other analytical technologies, such as MS. These two techniques are complementary and contribute to high reproducibility and access to unambiguous structural information (DEBORDE et al., 2017).

### 1.3.4 Correlation analysis using chemometric approaches

Chemometric analysis allows the use of mathematical and statistical methods to design or select optimal measurement procedures and experiments, providing maximum information by analyzing the chemical data obtained on the aforementioned platforms (GORROCHATEGUI et al., 2016). In the analysis of the results, discriminant correlations and/or multivariate statistical analyses are generally used to identify possible bioactive compounds. To perform this type of analysis, the data treatment includes an initial stage of preprocessing or debugging of the information where the data is filtered, aligned, and normalized, followed by the interpretation of the results and putative identification of the compounds (CORNEJO-BÁEZ et al., 2019; YI et al., 2016). Multivariate data analysis methods fall into two main categories: unsupervised (PCA), for which only spectral data are collected for information; and supervised methods (PLS-DA, OPLS-DA), for which it is necessary to relate a qualitative or quantitative variable that is related to the spectral data. Generally, unsupervised analysis is a descriptive exploration of the data, in contrast to supervised analysis which allows a prediction to be made on a data set with a specific biological target. Furthermore, they can be successfully employed to find differential metabolites between active and inactive samples and thus predict potentially active compounds. This strategy compares samples (extracts and/or fractions) of the same or closely related species. Finally, this approach identifies compounds of interest and allows for dereplication, thus avoiding re-isolation of known compounds when this is not the objective (HUBERT; NUZILLARD; RENAULT, 2017; LUAN et al., 2018).

## 1.4 General information on Cancer disease

Cancer is defined as the uncontrolled growth of abnormal cells in the body and develops when the body's normal control mechanism stops working. Old cells usually do not die and instead grow uncontrollably, forming new, abnormal cells. These additional cells form a mass of tissue called a malignant tumor. This disease usually develops in any part of the human body through the formation of cancerous tumors that can be malignant and spread or invade nearby tissues(BLACKADAR, 2016; COOPER; HAUSMAN, 2007;

HANAHAN; WEINBERG, 2011). There are more than 100 types of cancer, and they are usually named after the organs or tissues they invade; however, they have been mainly categorized as: carcinomas, sarcomas, leukemias, lymphomas, among others. Carcinomas, which include approximately 90% of human cancers, are malignant tumors of epithelial cells. Sarcomas, which are rare in humans, are solid tumors of connective tissues, such as muscle, bone, cartilage, and fibrous tissues. Leukemias and lymphomas, which account for approximately 8% of malignant tumors in humans, arise in blood-forming cells and immune system cells, respectively. At the cellular level, cancer development is a multistep process involving mutation and selection of cells with progressively increasing capacity for proliferation, survival, invasion, and metastasis. The first step in the process is believed to be the initiation of a tumor because of a genetic alteration that leads to the abnormal proliferation of a single cell (BLACKADAR, 2016; COOPER; HAUSMAN, 2007).

Cell proliferation leads to the growth of a clonally derived tumor cell population. Tumor progression continues as additional mutations occur within the cells of the tumor population. Some of these mutations confer a selective advantage to the cell, such as faster growth, and the descendants of a cell carrying such a mutation will become dominant in the tumor population. The process is called clonal selection, as a new clone of tumor cells has evolved based on its increased growth rate or other properties (such as survival, invasion, or metastasis) that confer a selective advantage. Clonal selection continues during tumor development, so that tumors continually become faster growing and increasingly malignant (BLACKADAR, 2016; COOPER; HAUSMAN, 2007; HANAHAN, 2022; MCGURK, 2013).

According to World Health Organization (WHO), by 2023, approximately 9.6 million people will die from cancer. These deaths are mainly due to five behavioral and dietary risks such as high body mass index, low fruit and vegetable intake, lack of physical activity and tobacco and alcohol consumption. By the year 2022, a total of approximately 18 million people were registered as carriers of this disease, with lung cancer (11.6%), breast cancer (11.6%), colon cancer (10.2%), prostate cancer (7.1%), stomach cancer (5.7%),

liver cancer (4.7%), esophageal cancer (3.2%) and other types of cancers corresponding to 46%, respectively, of people suffering from this disease in the world. According to a study by Global Burden of Disease (GBD) in 2021 reported that the most common types of cancer are prostate, lung and colorectal cancer in men and breast, colorectal and lung cancer in women. In Colombia for the year 2022, it is estimated that colon cancer affected about 16 thousand people, with an annual incidence of 13 thousand new cases and 3 thousand deaths (ACS, 2022; AMERICAN CANCER SOCIETY, 2021).

### 1.4.1 Colorectal cancer

Colorectal cancer (CRC) is the third most common malignancy and the second leading cause of cancer deaths worldwide. CRC is a type of cancer that affects the colon (large intestine) or rectum. It is one of the most common types of cancer worldwide, causing serious harm and potentially leading to death. The risk of CRC increases with age and, in most cases, affects people over 50 years of age. The stages and development of CRC are mainly described in four phases: initiation, promotion, progression, and metastasis. Abnormal growth of tissue protruding from the epithelial cells of the colorectal mucosa forms a polyp, which can progress to a tumor. It is estimated that up to 18 years can pass between the development of a polyp and invasive cancer, which can be classified from stage 0 to stage IV, with stage IV being the most aggressive (Figure 1.13) (HOSSAIN et al., 2022). The severity of the disease and the treatment options are determined according to the stage of CRC. For instance, surgery could be used for stages 0 to II; stage III may require a combination of surgery and adjuvant chemotherapy; and stage IV may require surgery, chemotherapy, and targeted therapy.

Importantly, multiple risk factors have been linked to an increased risk of developing CRC. These risk factors include a medical history of cancer, inflammatory bowel disease, colon polyps, cholecystectomy, and diabetes mellitus (BHATT et al., 2023).

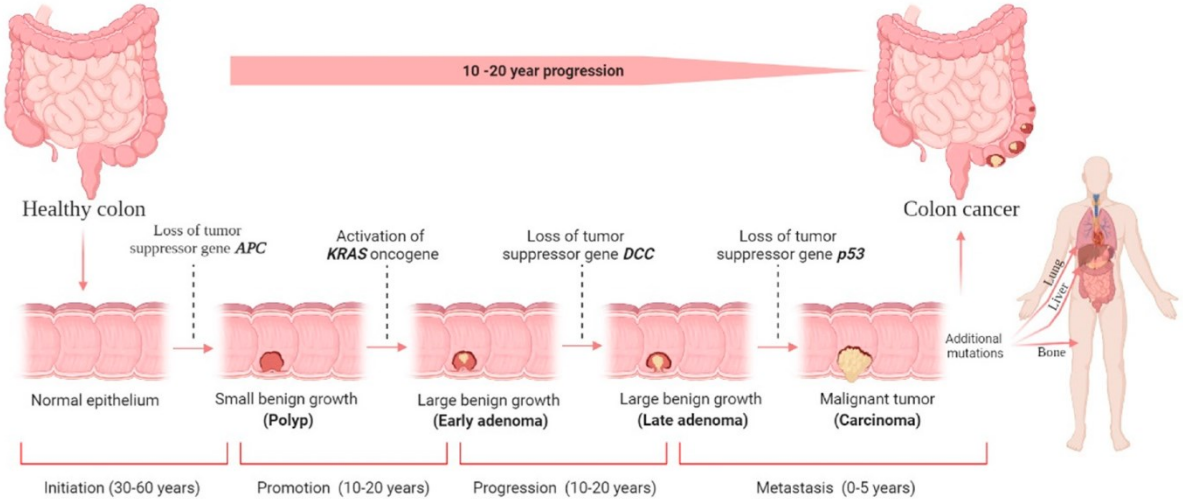



**Figure 1.13.** Stages and development of CRC. Four stages are highlighted in the development of CRC carcinogenesis: initiation, promotion, progression, and metastasis. Figure from (HOSSAIN et al., 2022).

### 1.4.2 Global Epidemiology of CRC

By 2023, this neoplasm accounted for 10% of cancer cases and 9.4% of deaths (GLOBOCAN, 2023; SUNG et al., 2021). According to the World Health Organization (WHO), high incidence rates of colorectal cancer were recorded mainly in Europe, Australia, and New Zealand, while high mortality rates were recorded in Eastern Europe. By 2040, the burden of CRC is projected to increase to 3.2 million new cases per year (a 63% increase) and 1.6 million deaths per year (a 73% increase) (Figure 1.14A-B). These forecasts may vary according to the level of socioeconomic development of each country and genetic and environmental factors (XI; XU, 2021). Despite advances and the availability of treatments such as radiotherapy, surgery, chemotherapy and metastatic therapies, colon cancer remains the second most lethal cancer, contributing to high mortality and morbidity rates. This situation is largely due to deficiencies in screening programs and therapeutic approaches, which coincides with increasing incidence rates. In addition, most of the patients suffering from this pathology develop drug resistance, decreasing the effectiveness of oncological treatments and culminating in the ineffectiveness of chemotherapy (BONAM et al., 2018; DEMAIN; VAISHNAV, 2011).

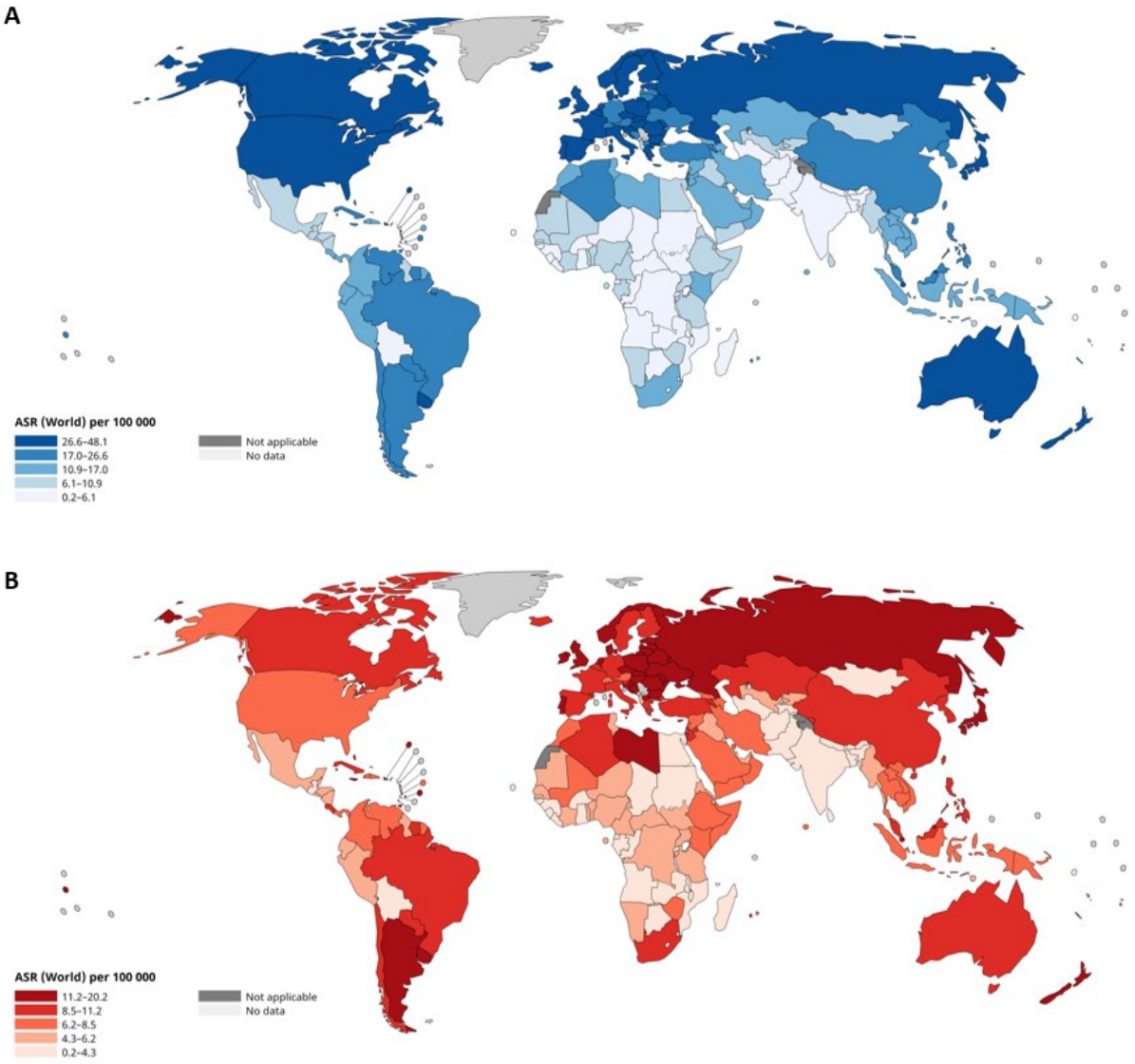



**Figure 1.14.** Map showing the global incidence (A) and mortality (B) rates of colorectal cancer standardized by age for countries on five continents, according to the latest figures from the WHO International Agency for Research on Cancer (reproduced from GLOBOCAN, 2023).

### 1.4.3 Study model: HCT-116 human colon cancer cell line

HCT116 cells were isolated from the colon of an adult male with colon cancer and have a mutation in codon 13 of the KRAS proto-oncogene, making them suitable transfection targets for gene therapy research. The cells have an epithelial morphology

and are adherent (Figure 1.15) (KAESER; PEBERNARD; IGGO, 2004; RAJPUT et al., 2008).

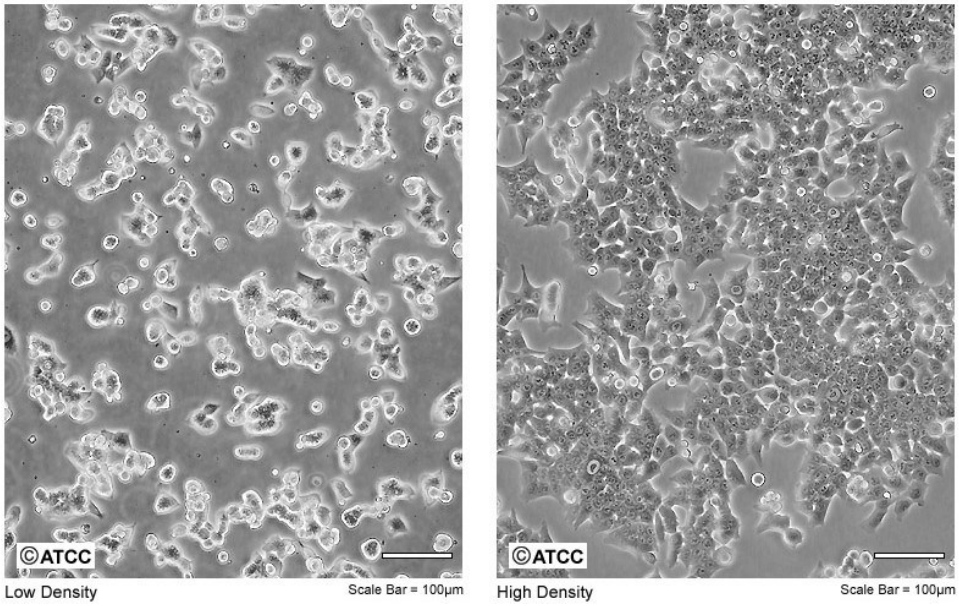



**Figure 1.15.** Morphology of the HCT-116 ATCC cell line. Image taken from https://www.atcc.org/products/ccl-247

### 1.4.4 Overview of metabolomic studies in the HCT-116 cell line

Currently, new approaches such as metabolomics have emerged to investigate metabolic alterations, enabling a comprehensive analysis of metabolites present in cells, biofluids, and tissues. Furthermore, metabolomics is considered a powerful tool for identifying metabolic fingerprints associated with exposure to drugs, substances, and plant extracts (Hounoum et al., 2016; Zhang et al., 2013). From the metabolomic studies reported so far on the HCT-116 cell line, researchers have studied the endometabolome treated with various drugs, isolated compounds, and plant extracts to understand their possible mechanisms of action. The use of various compounds isolated from natural sources is notable, including the diterpene flexibilide, soyasaponins I, and demethoxycurcumin (GAO et al., 2016; XIA et al., 2022; YOON et al., 2023a). Treatments with doxorubicin hydrochloride, a drug widely used in the treatment of various types of cancer, are also highlighted. Notably, the use of crude extracts from species such as *Curcuma longa* is emphasized (BENIWAL et al., 2023; YOON et al., 2023a). According to

the review, metabolomic studies involving crude extracts from natural sources are limited. Additionally, it is noted that metabolomic studies conducted on the HCT-116 cell line have primarily employed liquid chromatography techniques coupled with mass spectrometry (LC-MS) and nuclear magnetic resonance (NMR). Table 1.3 presents a summary of the metabolomic studies performed on HCT-116 cells.

**Table 1.3.** An overview of metabolomics studies in the HCT-116 cell line

| Treatment used | Source | Exposure time | Analytical platform | Metabolomic approach | Differential metabolites | Altered metabolic pathways | Reference |
|---|---|---|---|---|---|---|---|
| Flexibilide | Cembranoloide diterpene isolated from the soft coral *Sinularia flexibilis* | 5 μM during 24 h | UPLC-QTOF-MS | Untargeted metabolomics | C16 sphinganine, sphinganine, phytosphingosine, dihydroceramide, glutamate, glutamine, stearic acid, PC(16:1/16:0), phosphocholine (↓)<br>Sphingosine-1-phosphate, LysoPC(18:1), LysoPC(18:0), LysoPC(16:0), palmitic acid, palmitoyl N-isopropyl amide and stearamide (↑) | Sphingolipid, glycerophospholipid, fatty acid, glutamate, phenylalanine metabolism and TCA cycle | (GAO et al., 2016) |
| Soyasaponins I | Oleanane triterpenoid acquired from Nanjing Plant Origin Biological Technology | 161.4 μM during 24 h | UHPLC-Orbitrap-MS | Untargeted metabolomics | Xanthylic acid, triacetate lactone, 3-Methyl-L-tyrosine, vanillylmandelic acid, penbutolol, L-Lysine, arachidic acid, (R)-5,6-Dihydrothymine and 17a-Estradiol (↓)<br>Soyasaponin I, dodecanoic acid, N8-Acetylspermidine, 2-hydroxybutyric acid, L-Methionine, 5,6-Dihydro-5-fluorouracil, pantothenic acid, 2-pyrrolidinone, | Amino acid metabolism including "Protein digestion and absorption", "Aminoacyl-tRNA biosynthesis", "Central carbon metabolism in cancer", "Mineral absorption", "ABC transporters", and "Valine, leucine, and isoleucine | (XIA et al., 2022) |

| | | | | | | | |
|---|---|---|---|---|---|---|---|
| | | | | | hydroxyphenyllactic acid, biotin, 2-naphthylamine (↑) | biosynthesis" | |
| 2-(4-(Dimethylamino)phenyl)−2,3-dihydroquinazolin-4(1*H*)-one (**1**)<br><br>2-(2-Methoxy-4-nitrophenyl)−2,3-dihydroquinazolin-4(1*H*)-one (**2**) | 2,3-dihydroquinazolin-4(1H)-one analogues obtained from chemical synthesis | 1.4 µM during 72 h for (**1**)<br><br>24 µM during 72 h for (**2**) | LC-HRMS/MS | Untargeted metabolomics | Adenosine diphosphate (ADP), carnitine, spermine, phosphocreatine, cytosine, spermine and glutamine (↓)<br><br>Adenine, uridine and pipecolic acid, carnitine, and uridine (↑) | Amino acids biosynthesis and metabolism, redox homeostasis, energy related processes (*e.g.*, fatty acid oxidation, second Warburg like effect) and one-carbon and glutathione, and purine metabolism | (DAHABIYEH et al., 2023)v |
| Natural crude extract (**3**) Demethoxycurcumin (**4**) | Extract obtained from the rhizomes of the species *Curcuma longa* (Zingiberaceae)<br><br>β-diketone derived for curcumin, isolated from *C. longa* | 300 µg/mL during 48 h for (**3**)<br><br>20, 40 and 60 µM during 48 h for (**4**) | $^1$H-NMR (NOESY) 2D-NMR (COSY, HSQC) | Untargeted metabolomics | Aspartate, ATP, betaine, creatine, glutamate, lactate, dimethylamine, formate, glycerophosphocholine, myo-inositol, glucose, phosphocholine, and uridine (↓)<br><br>Alanine, arginine, glutathione (GSH), glycine, $NAD^+$, phenylalanine, lactate and uracil (↑) | Energy and glutathione metabolism | (YOON et al., 2023a) |
| Doxorubicin hydrochloride | Drug acquired from Sigma–Aldrich Chemicals | 0, 0.75, 1.5, and 7.5 µg/mL during 24 h | $^1$H-NMR | Untargeted metabolomics | Alanine, choline, taurine, o-phosphocholine, inosine, lysine, and phenylalanine (↓)<br><br>Glutamate, glutamine, sn-glycero-3-PCho, valine, methionine, isoleucine, acetate, and glucose (↑) | ATP production through glycolysis and oxidative phosphorylation | (GANESAN; PRABHAKARAN; VALSALA GOPALAKRISHNAN, 2022) |
| Natural crude extract | Extract obtained from the leaves of the species | 1.23 µg/mL during 72 h | LC-MS $^1$H-NMR | Untargeted metabolomics | Sphingosine, Glutathione, nicotinamide, carnitines, lysophosphatidylch | glutathione, TCA acid cycle, and lipoic acid metabolism | This thesis |

| | | | |
|---|---|---|---|
| | *Guadua incana* (Poaceae) | olines (LPC), phosphatidylethanolamines (PE), phosphatidylinositol (PI) (↓)<br><br>Glutathione disulfide, lysophosphatidylethanolamines (LPE), phosphatidylserines (PS) (↑) | |

TCA: Tricarboxylic acid, LC: Liquid Chromatography, UPLC: Ultra Performance Liquid Chromatography, UHPLC: Ultra High-Performance Liquid Chromatography, MS: Mass Spectrometry, $^{1}$H-NMR: Proton Nuclear Magnetic Resonance. Red indicates potential up-regulated metabolites (↑), while blue indicates potential down-regulated metabolites (↓).

# 2 CHAPTER 2. Untargeted metabolomics approach and molecular networking analysis reveal changes in chemical composition under the influence of altitudinal variation in bamboo species

## Presentation

Considering the lack of chemical and biological information for bamboos belonging to the genus *Guadua*, as evidenced in the review of the previous chapter, the experimental work of this thesis begins in this chapter, which presents a study of the chemical composition of 12 bamboo species under the influence of an altitudinal gradient using an untargeted metabolomics approach and mapping chemical diversity through molecular network analysis. The objective was to determine the differential metabolites in the different altitudinal ranges and establish the effect of variation on the chemical composition. Additionally, the study also aimed to identify which biosynthetic pathways were affected and whether they increased or decreased the production of the main metabolite families. This chapter corresponds to the publication:

*Frontiers in Molecular Biosciences*, 2023, 10, 1192088. DOI: 10.3389/fmolb.2023.1192088

## 2.1 Materials and methods

### 2.1.1 Study design

A completely random sampling method was implemented for the metabolomic study by selecting different collection sites in Colombian locations [Cundinamarca (CU), Nariño (NA), Putumayo (PU), and Quindío (QU)] situated at different altitudes, ranging from (0 to 3000 m). The geographical distributions of the collected species are shown in Figure 2.1. All samples were collected from natural bamboo in the period 2020 to 2022 (more details are provided in Supplementary Table S2.1).

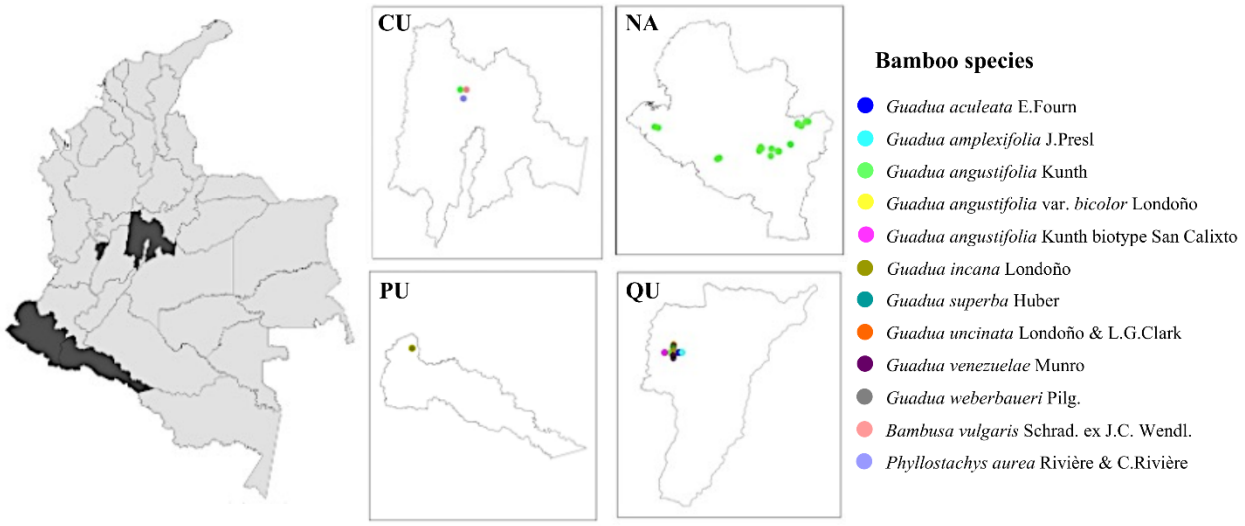



**Figure 2.1.** Geographical distribution map showing the bamboo species studied. Each mark corresponds to the place of collection of each specimen.

### 2.1.2 Plant material collection and identification

We collected a total of 111 leaf samples from the upper branches of 12 bamboo species, which were distributed across 40 different altitudes and collected under the same conditions. The collection was performed under the permit of the Contract for Access to Genetic Resources and Derived Products (Contract No. 212/RGE 0287-6) granted by the Ministry of the Environment and Sustainable Development to the Pontificia Universidad Javeriana (PUJ) and the Colombia Científica/GAT Program. Harvested bamboo leaves were immediately air-dried at room temperature and then ground into powder for extraction. Based on altitude, we divided the 111 leaf samples into two groups: the low altitude group (~0 to 1500 m; $n$ = 40) and high altitude group (~1500 to 3000 m; $n$ = 71), as indicated in Table 2.1. At least three individuals ($n$ = 3) were collected at each collection site, and voucher specimens were deposited in the (HPUJ) Herbarium of the Pontificia Universidad Javeriana.

**Table 2.1.** Classification of bamboo species according to altitudinal range.

| Plant scientific name | Sampling location | Altitude (m) | Group |
|---|---|---|---|
| *G. aculeata* E.Fourn. | Quindío, Montenegro | 1256 | Low |
| *G. amplexifolia* J.Presl | Quindío, Montenegro | 1256 | Low |
| *G. angustifolia* Kunth | Nariño, Tumaco | 18 | Low |
| | Nariño, Tumaco | 21 | Low |
| | Nariño, Ricaurte | 1053 | Low |
| | Nariño, Ricaurte | 1089 | Low |
| | Quindío, Montenegro | 1256 | Low |
| | Cundinamarca, Pacho | 1343 | Low |
| | Nariño, Samaniego | 1478 | Low |
| | Nariño, Samaniego | 1565 | High |
| | Nariño, Samaniego | 1588 | High |
| | Nariño, San Lorenzo | 1595 | High |
| | Nariño, La Unión | 1598 | High |
| | Nariño, Consacá | 1606 | High |
| | Nariño, Samaniego | 1606 | High |
| | Nariño, La Unión | 1610 | High |
| | Nariño, La Unión | 1631 | High |
| | Nariño, San Lorenzo | 1713 | High |
| | Nariño, Sandoná | 1720 | High |
| | Nariño, Sandoná | 1744 | High |
| | Nariño, San Lorenzo | 1779 | High |
| | Nariño, San Lorenzo | 1808 | High |
| | Nariño, San Lorenzo | 1826 | High |
| | Nariño, Chachagüí | 1857 | High |
| | Nariño, San Lorenzo | 1876 | High |
| | Nariño, San Lorenzo | 1930 | High |
| | Nariño, San Lorenzo | 1970 | High |
| | Nariño, La Florida | 2089 | High |
| | Nariño, La Florida | 2122 | High |
| | Nariño, La Florida | 2137 | High |
| *G. angustifolia* var. *bicolor* Londoño | Quindío, Montenegro | 1256 | Low |
| *G. angustifolia* Kunth biotype *San Calixto* | Quindío, Montenegro | 1256 | Low |
| *G. incana* Londoño | Putumayo, Mocoa | 604 | Low |
| | Quindío, Montenegro | 1256 | Low |
| *G. superba* Huber | Quindío, Montenegro | 1256 | Low |

| | | | |
|---|---|---|---|
| *G. uncinata* Londoño & L.G.Clark | Quindío, Montenegro | 1256 | Low |
| *G. venezuelae* Munro | Quindío, Montenegro | 1256 | Low |
| *G. weberbaueri* Pilg. | Quindío, Montenegro | 1256 | Low |
| *B. vulgaris* Schrad. ex J.C. Wendl. | Cundinamarca, Pacho | 1343 | Low |
| *P. aurea* Rivière & C.Rivière | Quindío, Montenegro | 1256 | Low |

### 2.1.3 Metabolite extraction and sample preparation

To extract the plant material (leaves), 300 mg of dried and ground samples were mixed with 10 mL of a solvent containing chloroform, methanol, and water (in a ratio of 5:2.5:2.5 *v*/*v*/*v*). The resulting mixture was then vortexed for 1 minute, sonicated for 20 minutes, and centrifuged at 5000 rpm and 20° C for 10 minutes. The liquid supernatant was filtered using PTFE syringe filters with a pore size of 0.22 µm (Thermo Scientific, Rockwood, TN), and stored at -80 °C until used for metabolomics analysis.

### 2.1.4 Untargeted metabolomics using LC-QTOF-MS

Untargeted metabolomics was conducted using an Agilent Infinity 1260 HPLC system coupled to an Agilent 6545 quadrupole time-of-flight (QTOF) mass spectrometer equipped with electrospray ion source (Waldbronn, Germany). 5 µL of the extracts were injected on a C18 column (Kinetex 100 x 2.1 mm, 2.6 µm) at 30 °C. The mobile phase employed in LC analyses was composed of 0.1 % formic acid in Milli-Q water (*v/v*) (Solvent A) and acetonitrile (Solvent B) with a constant flow of 400 µL/min. The gradient was set as follows: 3% for 1 min; 3-97% B in 15 min; 97% B for 2 min; the column was re-equilibrated for 6 min at the initial conditions. Full-scan MS1 and MS/MS spectra were acquired. Data mass spectra were acquired in negative ionization mode ($ESI^-$), in a mass range of *m/z* 80 – 1700 Da in data-dependent acquisition (DDA) mode. The QTOF instrument was operated in the 4 GHz (high resolution) mode. The parameters used for data acquisition were set as follows: nitrogen used as nebulizer gas with pressure at 52 psi, a capillary voltage of 3000 V, ion source temperature of 250 °C, dry gas flow at 12 L/min, and acquisition rate of one spectrum per second. MS/MS fragmentation was performed using a collision-induced dissociation energy of 20 eV. Throughout the

analysis, two reference masses were used for mass correction: *m/z* 112.9856 [$C_2O_2F_3(NH_4)$] and *m/z* 1033.9881($C_{18}H_{18}O_6N_3P_3F_{24}$).

### 2.1.5 Quality control samples

To evaluate system performance and reproducibility in sample analysis, multiple QC samples were created by pooling and mixing equal volumes of each extracted sample. To assess the instrument's robustness, pooled QC samples were injected before the sample analysis until system equilibration was achieved and after every ten randomized sample injections.

### 2.1.6 Metabolomics data processing

The LC-QTOF-MS raw data sets were processed using Agilent MassHunter Workstation Profinder software (B.10.0, Agilent Technologies) to extract molecular features for deconvolution, alignment, and integration. The data were manually inspected to eliminate noise and unrelated ions, and a presence filter was applied. For statistical analysis, features that were present in 100% of the samples for each altitudinal group and had a coefficient of variation (CV) of less than 20% in the QC were selected.

### 2.1.7 Statistical analysis

Univariate and multivariate analyses were conducted using MatLab (R2019b, MathWorks, Inc., Natick) and SIMCA 14.0 software (Umetrics, Umeå, Sweden), respectively. The multivariate analysis generated PCA and OPLS-DA models, which were validated using cross-validation less than 0.05 and evaluated based on $R^2X$ (change in X explained by the model), $R^2Y$ (the total of Y explained), and $Q^2$ (sum parameter in cross-validation). The significantly differential metabolites were identified by calculating the variable importance in the projection (VIP) greater than 1, with Jack-knife confident interval (JK) not including zero combined with FC > 2.0 or FC < 0.5. The annotated metabolites and their peak area were organized in a table (.csv), which was uploaded to MetaboAnalyst 5.0 software for statistical, functional, and integrative analysis of

metabolomics data (https://www.metaboanalyst.ca/). The software was used for visualization using heatmap clustering (PANG et al., 2022), normalized by Pareto scaling. Additionally, univariate analysis was performed to determine the *p*-value features.

### 2.1.8 Metabolite identification

Differential metabolite annotation was conducted by considering the precision of the mass (maximum error of mass ten ppm), isotopic pattern distribution, and adduct formation, using different public online databases such as METLIN (http://metlin.scripps.edu), KEGG (http://genome.jp/kegg), HMDB (https://hmdb.ca/), PubChem (https://pubchem.ncbi.nlm.nih.gov/) and ChEBI (https://www.ebi.ac.uk/chebi/) through the CEU Mass Mediator (http://ceumass.eps.uspceu.es/) tool. The identity of the metabolites was confirmed through MS/MS analysis, which included the use of MS-DIAL 4.80 (http://prime.psc.riken.jp/compms/msdial/main.html), MS-FINDER 3.52 (http://prime.psc.riken.jp/compms/msfinder/main.html), SIRIUS 5.5.7 (https://bio.informatik.uni-jena.de/software/sirius/), CFM-ID 4.0 (https://cfmid.wishartlab.com/) for in silico mass spectral fragmentation, GNPS web platform (https://gnps.ucsd.edu/ProteoSAFe/static/gnps-splash.jsp) and manual interpretation with the Agilent Mass Hunter Qualitative Analysis software (version 10.0). The metabolites were identified according to the metabolomics standards initiative (SCHYMANSKI et al., 2014).

### 2.1.9 Global natural products social molecular networking (GNPS) web platform workflow description

A molecular network was created using the online workflow (https://ccms-ucsd.github.io/GNPSDocumentation/) on the GNPS website (http://gnps.ucsd.edu). The precursor ion mass tolerance was set to 0.02 Da and an MS/MS fragment ion tolerance of 0.02 Da. A network was then created where edges were filtered to have a cosine score above 0.6 and more than four matched peaks. Further, edges between two nodes were kept in the network if and only if each of the nodes appeared in each other's respective top 10 most similar nodes. Finally, the maximum size of a molecular family was set to 0,

and the lowest-scoring edges were removed from molecular families until the molecular family size was below this threshold. The spectra in the network were then searched against GNPS spectral libraries. All matches kept between network spectra and library spectra were required to have a score above 0.6 and at least four matched peaks (WANG et al., 2016). To enhance chemical structural information within the molecular network, information from in silico structure annotations from GNPS Library Search, Network Annotation Propagation, Dereplicator were incorporated into the network using the GNPS MolNetEnhancer workflow (https://ccms-ucsd.github.io/GNPSDocumentation/molnetenhancer/). Chemical class annotations were performed using the ClassyFire chemical ontology (DA SILVA et al., 2018; DJOUMBOU FEUNANG et al., 2016; ERNST et al., 2019; MOHIMANI et al., 2017). The attribute table of the generated nodes was visualized in the Cytoscape software to analyze the molecular network. The data used for the analysis of molecular networks were deposited in the MassIVE Public GNPS database (http://massive.ucsd.edu) with the accession number MSV000090298. The workflow used in this study is summarized in Figure 2.2.

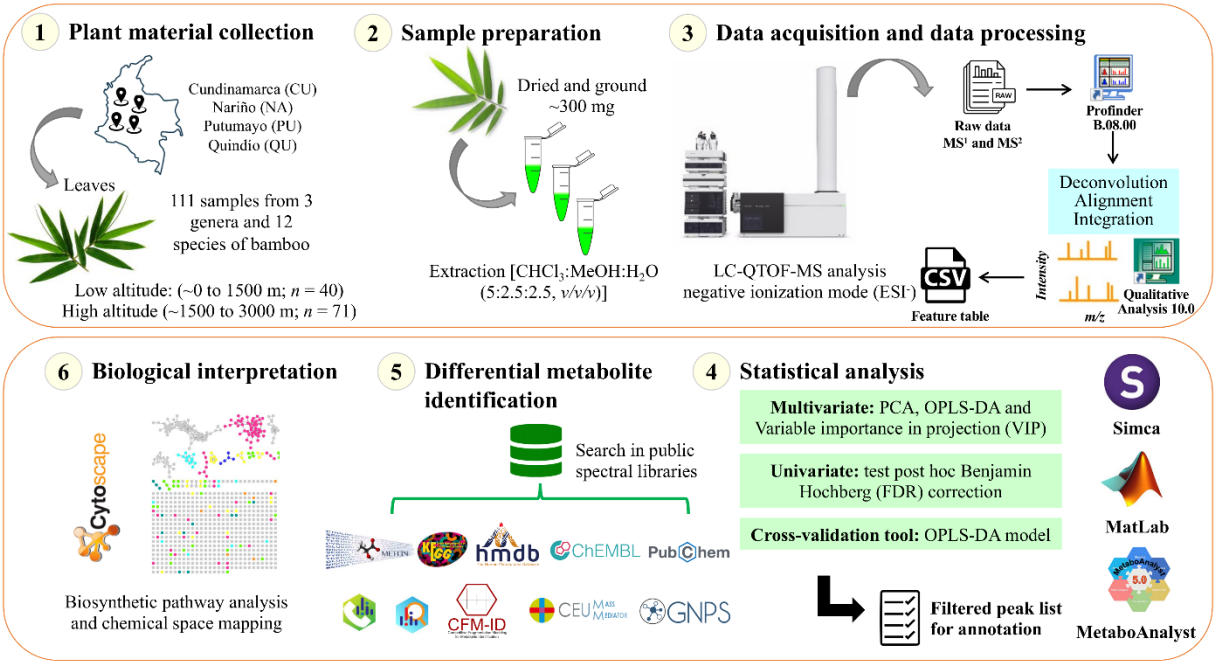



**Figure 2.2.** Schematic of the experiment analytical workflow used in this study.

## 2.2 Results and discussion

### 2.2.1 Chemical variation of bamboo species presented between low and high altitudes

The quality and stability of the instrument were assessed by conducting a principal component analysis (PCA) on the quality control samples. Supplementary Figure S2.1 shows a clustering of the QC samples, which indicates the analytical platform platform's reliability and the data's validity. To account for altitudinal variation, we performed PCA and orthogonal partial least squares discriminant analysis (OPLS-DA) models on samples classified into two altitude ranges. Based on this classification, we developed an unsupervised PCA model to observe trends between the two altitude groups. As depicted in Figure 2.3A, the PCA model showed an initial exploration of the data set, evidencing certain trends between the variables of the altitude groups.

Additionally, we constructed a supervised OPLS-DA model to differentiate between low and high altitude groups, with appropriate quality parameters, demonstrating complete separation of the groups. (Figure 2.3B). This allowed us to identify the significant variables that contributed to the separation between the groups, yielding a total of 89 significant variables with values (false discovery rate, FDR) < 0.05, VIP > 1, and FC > 2.0 (or < 0.5), as identified according to the metabolomics standards initiative (SCHYMANSKI et al., 2014). To validate the OPLS-DA model, we conducted permutation analysis, plotting $R^2$ and $Q^2$ of 200 permutation tests, as shown in Figure 2.3C.

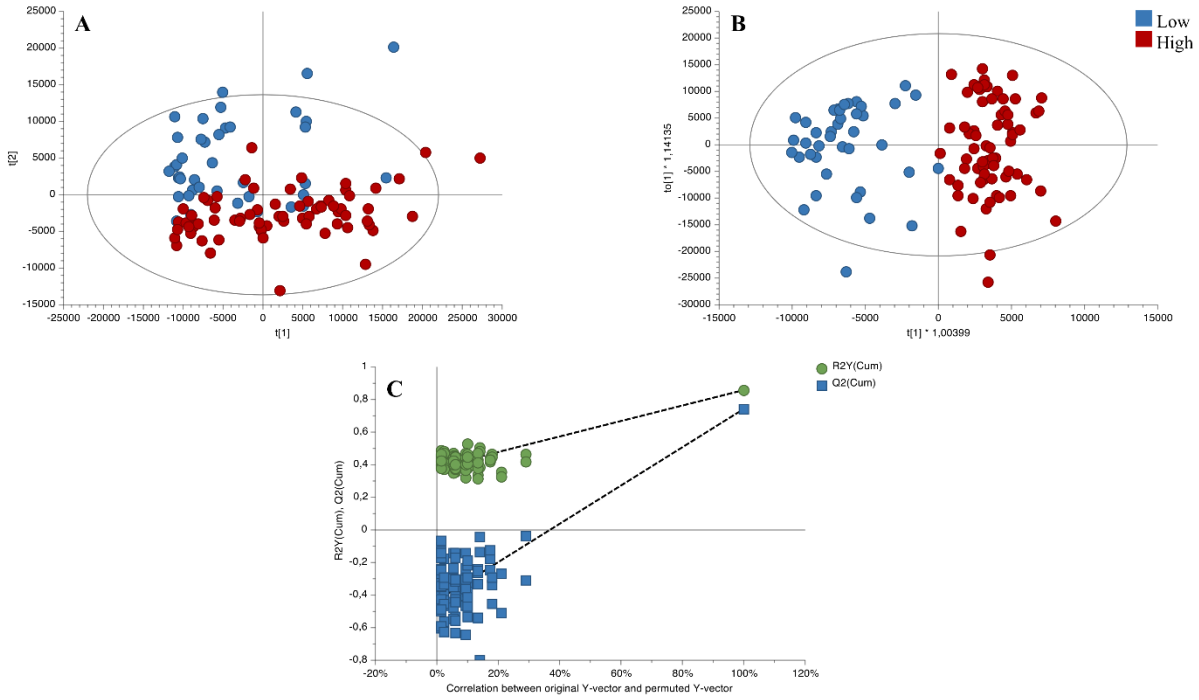



**Figure 2.3.** Score plots of the influence of direction compared low/high altitudes. **(A)** PCA score plot of total samples ($R^2X_{(cum)}$: 0.813; $Q^2_{(cum)}$: 0.54)**. (B)** OPLS-DA score plot of the low vs. high altitudes sample ($R^2X_{(cum)}$: 0.494; $R^2Y_{(cum)}$:0.858; $Q^2_{(cum)}$:0.742; CV-Anova: 9.61549e-27). **(C)** Cross-validation plot of the OPLS-DA model with 200 permutation tests. Low altitude (~0 to 1500 m; n = 40) and high altitude (~1500 to 3000 m; n = 71).

Table 2.2 presents the differential metabolites (89) that belong to various families, such as flavonoids (48%), fatty acids (19%), cinnamic acid derivatives (11%), unknown (6%), peptides (3%), glycosylated lignans (2%), alkaloids (2%), carboxylic acids (1%), phenolic compounds (1%), carbohydrates (1%), steroids (1%), glycosylated stilbenes (1%) and prenolipids (1%). The largest group of differentially expressed metabolites comprises flavonoids which are the most frequently reported metabolites for these species Many metabolites in this group showed an upward trend at higher altitudes, potentially contributing to the medicinal potential of these species.

**Table 2.2.** Significantly differential metabolites found the altitudinal variation.

| Compound name | Molecular formula | Molecular weight (g/mol) | RT (min) | Mass error (ppm) | Adduct | ID Level | [a]CV for QC (%) | Low vs. high altitude | | |
|---|---|---|---|---|---|---|---|---|---|---|
| | | | | | | | | [b]FC | [c]VIP | [d]*p*-value with FDR |

| | | | | | | | | | | |
|---|---|---|---|---|---|---|---|---|---|---|
| ***Flavonoids*** | | | | | | | | | | |
| Luteolin 6-*C*-glucoside 8-*C*-arabinoside | $C_{27}H_{30}O_{16}$ | 610.1534 | 5.17 | 1 | $[M-H]^-$ | 2 | 0.64 | 0.67 | 3.26 | 2.41E-02 |
| Quercetin 3,7-dirhamnoside | $C_{27}H_{30}O_{15}$ | 594.1585 | 5.39 | 1 | $[M-H]^-$ | 2 | 1.73 | 0.65 | 3.71 | 2.81E-04 |
| Kaempferol-3-*O*-rutinoside | $C_{27}H_{30}O_{15}$ | 594.1585 | 6.09 | 4 | $[M-H]^-$ | 4 | 0.86 | 0.77 | 2.34 | 1.70E-02 |
| Vitexin 6''-(3-hydroxy-3-methylglutarate) | $C_{27}H_{28}O_{14}$ | 576.1479 | 6.86 | 1 | $[M-H-H_2O]^-$ | 3 | 3.42 | 0.45 | 3.03 | 6.10E-05 |
| Maysin | $C_{27}H_{28}O_{14}$ | 576.1479 | 5.86 | 1 | $[M-H]^-$ | 2 | 3.53 | 0.53 | 3.58 | 1.47E-04 |
| Cassiaoccidentalin B | $C_{27}H_{28}O_{14}$ | 576.1479 | 6.72 | 2 | $[M-H]^-$ | 2 | 1.76 | 0.58 | 2.70 | 2.91E-04 |
| Nicotiflorin | $C_{27}H_{30}O_{15}$ | 594.1585 | 5.96 | 0 | $[M-H]^-$ | 2 | 2.95 | 0.68 | 1.88 | 8.91E-03 |
| Scutellarein 4'-methyl ether 7-glucuronide | $C_{22}H_{20}O_{12}$ | 476.0955 | 6.44 | 1 | $[M-H]^-$ | 2 | 1.46 | 0.44 | 2.68 | 3.25E-06 |
| Denticulaflavonol | $C_{35}H_{42}O_6$ | 558.2981 | 12.92 | 9 | $[M+Cl]^-$ | 2 | 0.94 | 0.26 | 2.03 | 7.02E-12 |
| Apigenin 7-[6''-(3-Hydroxy-3-methylglutaryl)glucoside] | $C_{27}H_{28}O_{14}$ | 576.1479 | 8.29 | 5 | $[M-H-H_2O]^-$ | 4 | 1.00 | 0.61 | 2.21 | 1.23E-03 |
| Quercetin 3-(2'',3'',4''-triacetylgalactoside) | $C_{27}H_{26}O_{15}$ | 590.1272 | 6.90 | 1 | $[M-H-H_2O]^-$ | 3 | 0.74 | 0.35 | 2.33 | 5.17E-07 |
| Hosloppin | $C_{22}H_{16}O_7$ | 392.0896 | 8.82 | 7 | $[M+HCOO-H]^-$ | 2 | 0.62 | 0.68 | 1.54 | 1.25E-03 |
| Vitexin 2''-*O*-rhamnoside* | $C_{27}H_{30}O_{14}$ | 578.1636 | 5.96 | 3 | $[M-H]^-$ | 2 | 0.58 | 0.67 | 1.87 | 1.41E-03 |
| Allivicin | $C_{27}H_{30}O_{16}$ | 610.1534 | 5.81 | 1 | $[M-H]^-$ | 2 | 1.38 | 0.75 | 2.35 | 2.99E-02 |
| Paniculatin | $C_{27}H_{30}O_{15}$ | 594.1585 | 6.86 | 0 | $[M-H-H_2O]^-$ | 4 | 2.88 | 0.50 | 2.42 | 1.24E-03 |
| 6''-*O*-(3-Hydroxy-3-methylglutaroyl)astragalin | $C_{27}H_{28}O_{15}$ | 592.1428 | 6.21 | 1 | $[M-H]^-$ | 2 | 1.60 | 0.58 | 1.31 | 3.73E-03 |
| Baicalin | $C_{21}H_{18}O_{11}$ | 446.0849 | 6.18 | 3 | $[M-H]^-$ | 4 | 2.31 | 0.47 | 1.59 | 2.05E-03 |
| 4'-*O*-Methylneobavaisoflavone 7-*O*-(2''-p-coumaroylglucoside) | $C_{36}H_{36}O_{11}$ | 644.2258 | 6.14 | 8 | $[M-H]^-$ | 3 | 0.63 | 2.14 | 1.37 | 8.96E-03 |
| Apigenin 7-[rhamnosyl-(1->2)-galacturonide] | $C_{27}H_{28}O_{15}$ | 592.1428 | 6.21 | 2 | $[M-H]^-$ | 4 | 2.60 | 0.66 | 1.09 | 2.01E-03 |
| Isorhamnetin 3-galactoside-7-rhamnoside | $C_{28}H_{32}O_{16}$ | 624.1690 | 5.52 | 2 | $[M-H]^-$ | 2 | 0.71 | 0.67 | 1.47 | 8.10E-03 |
| Violanthin | $C_{27}H_{30}O_{14}$ | 578.1636 | 6.51 | 4 | $[M-H]^-$ | 4 | 1.05 | 0.56 | 1.27 | 2.10E-05 |
| Eruberin B | $C_{30}H_{40}O_{15}$ | 640.2367 | 6.23 | 2 | $[M-H]^-$ | 3 | 1.81 | 5.15 | 1.07 | 9.72E-04 |
| Kaempferol 7-sophoroside | $C_{27}H_{30}O_{16}$ | 610.1534 | 5.17 | 6 | $[M-H]^-$ | 2 | 0.26 | 0.74 | 2.44 | 4.45E-02 |
| Vicenin 2* | $C_{27}H_{30}O_{15}$ | 594.1585 | 5.96 | 1 | $[M-H]^-$ | 2 | 3.76 | 0.74 | 1.74 | 2.13E-02 |
| Thonningianin B | $C_{35}H_{30}O_{17}$ | 722.1483 | 9.07 | 3 | $[M+HCOO-H]^-$ | 2 | 0.86 | 0.58 | 1.49 | 1.25E-04 |
| Bracteoside | $C_{22}H_{20}O_{12}$ | 476.0955 | 6.01 | 2 | $[M-H]^-$ | 4 | 5.58 | 0.48 | 1.07 | 4.91E-05 |

| | | | | | | | | | | |
|---|---|---|---|---|---|---|---|---|---|---|
| Orientin 2''-rhamnoside | $C_{27}H_{30}O_{15}$ | 594.1585 | 6.09 | 1 | $[M-H]^-$ | 2 | 0.77 | 0.74 | 2.47 | 6.33E-03 |
| 7,8,3',4'-Tetrahydroxyflavanone 7-(2,4,6-triacetylglucoside) | $C_{27}H_{28}O_{14}$ | 576.1479 | 6.72 | 1 | $[M-H]^-$ | 2 | 1.66 | 0.57 | 2.72 | 2.80E-04 |
| Epigallocatechin 3-gallate | $C_{22}H_{18}O_{11}$ | 458.0849 | 7.93 | 2 | $[M-H]^-$ | 2 | 2.83 | 0.45 | 1.15 | 3.29E-06 |
| Glychalcone A | $C_{22}H_{22}O_5$ | 366.1467 | 1.34 | 4 | $[M-H]^-$ | 4 | 1.85 | 0.48 | 1.29 | 6.72E-08 |
| Quercetin 3-(3'',6''-diacetylgalactoside) | $C_{25}H_{24}O_{14}$ | 548.1166 | 6.94 | 6 | $[M-H-H_2O]^-$ | 3 | 1.39 | 0.52 | 1.06 | 9.13E-05 |
| 2'',4''-Diacetylafzelin | $C_{25}H_{24}O_{12}$ | 516.1268 | 6.79 | 1 | $[M-H]^-$ | 3 | 0.39 | 0.73 | 2.54 | 3.65E-03 |
| Epigallocatechin 3-*O*-caffeate | $C_{24}H_{20}O_{10}$ | 468.1057 | 8.30 | 5 | $[M+HCOO-H]^-$ | 3 | 1.06 | 0.48 | 1.16 | 1.05E-06 |
| Cyanidin 3-rutinoside | $C_{27}H_{31}O_{15}$ | 595.1663 | 6.72 | 8 | $[M-H-H_2O]^-$ | 4 | 1.72 | 0.73 | 1.29 | 1.24E-02 |
| 5,7,3',4'-Tetrahydroxyflavanone 7-alpha-L-arabinofuranosyl-(1->6)-glucoside | $C_{26}H_{30}O_{15}$ | 582.1585 | 5.17 | 2 | $[M+HCOO-H]^-$ | 4 | 0.24 | 0.63 | 2.60 | 2.76E-03 |
| Isoorientin 2''-*O*-rhamnoside | $C_{27}H_{30}O_{15}$ | 594.1585 | 5.86 | 2 | $[M-H]^-$ | 4 | 1.15 | 0.60 | 2.82 | 1.20E-03 |
| Neosaponarin | $C_{27}H_{30}O_{15}$ | 594.1585 | 6.72 | 2 | $[M-H]^-$ | 4 | 0.99 | 0.64 | 2.92 | 1.85E-03 |
| Chamaemeloside | $C_{27}H_{28}O_{14}$ | 576.1479 | 6.08 | 1 | $[M-H]^-$ | 2 | 1.39 | 0.59 | 1.68 | 3.16E-05 |
| 5',5''',8,8''-Tetrahydroxy-3',3''',4',4''',7',7''-hexamethoxy-5,5''-biflavan | $C_{36}H_{38}O_{12}$ | 662.2363 | 5.90 | 8 | $[M-H-H_2O]^-$ | 3 | 0.33 | 0.61 | 1.45 | 1.39E-05 |
| Kaempferol 7-neohesperidoside | $C_{27}H_{30}O_{15}$ | 594.1585 | 6.09 | 1 | $[M-H]^-$ | 2 | 0.85 | 0.72 | 2.56 | 4.44E-03 |
| Saponarin* | $C_{27}H_{30}O_{15}$ | 594.1585 | 5.40 | 2 | $[M-H]^-$ | 2 | 1.32 | 0.69 | 2.78 | 7.22E-04 |
| Astragalin 7-rhamnoside | $C_{27}H_{30}O_{15}$ | 594.1585 | 6.54 | 1 | $[M-H-H_2O]^-$ | 3 | 1.66 | 0.51 | 1.61 | 5.64E-05 |
| Apigenin 7-glucuronide-4'-rhamnoside | $C_{27}H_{28}O_{15}$ | 592.1428 | 6.54 | 1 | $[M-H-H_2O]^-$ | 3 | 1.95 | 0.50 | 1.64 | 5.20E-05 |
| ***Fatty Acids*** | | | | | | | | | | |
| TriHODE | $C_{18}H_{32}O_5$ | 328.2250 | 8.07 | 1 | $[M-H]^-$ | 4 | 0.36 | 0.65 | 3.90 | 2.34E-08 |
| Sativic acid | $C_{18}H_{36}O_6$ | 348.2512 | 8.45 | 1 | $[M-H-H_2O]^-$ | 4 | 0.26 | 0.61 | 3.96 | 4.91E-13 |
| Coriolic acid | $C_{18}H_{32}O_3$ | 296.2351 | 11.70 | 1 | $[M-H]^-$ | 2 | 0.75 | 0.35 | 2.40 | 7.02E-12 |
| HoTrE | $C_{18}H_{30}O_3$ | 294.2195 | 11.20 | 1 | $[M-H]^-$ | 2 | 0.76 | 0.33 | 2.44 | 1.84E-12 |
| Dodecanedioic acid | $C_{12}H_{22}O_4$ | 230.1518 | 6.43 | 0 | $[M-H]^-$ | 2 | 0.45 | 0.67 | 1.88 | 1.95E-04 |
| TriHOME | $C_{18}H_{34}O_5$ | 330.2406 | 8.88 | 2 | $[M-H]^-$ | 4 | 1.37 | 0.48 | 1.30 | 3.66E-07 |
| Lauric acid | $C_{12}H_{22}O_3$ | 214.1569 | 8.39 | 1 | $[M-H]^-$ | 2 | 0.64 | 0.43 | 1.14 | 2.13E-07 |
| Undecylenic acid | $C_{11}H_{20}O_2$ | 184.1463 | 6.70 | 1 | $[M+HCOO-H]^-$ | 4 | 0.61 | 0.68 | 1.26 | 1.89E-03 |
| HpODE | $C_{18}H_{32}O_4$ | 312.2301 | 10.50 | 1 | $[M-H]^-$ | 4 | 1.25 | 0.46 | 1.02 | 1.74E-07 |
| HpOTrE | $C_{18}H_{30}O_4$ | 310.2144 | 10.09 | 1 | $[M-H]^-$ | 4 | 1.74 | 0.41 | 1.03 | 2.56E-07 |

| | | | | | | | | | | |
|---|---|---|---|---|---|---|---|---|---|---|
| Undecenoic acid | $C_{11}H_{20}O_2$ | 184.1463 | 8.07 | 1 | $[M+HCOO-H]^-$ | 4 | 0.87 | 0.65 | 1.23 | 3.88E-07 |
| Cascarillic acid | $C_{11}H_{20}O_2$ | 184.1463 | 8.45 | 1 | $[M+HCOO-H]^-$ | 4 | 0.88 | 0.53 | 1.43 | 5.49E-12 |
| Sorbic acid | $C_6H_8O_2$ | 112.0524 | 3.33 | 1 | $[M-H-H_2O]^-$ | 3 | 1.11 | 0.61 | 1.24 | 9.88E-07 |
| Malyngic acid | $C_{18}H_{32}O_5$ | 328.2250 | 9.08 | 2 | $[M-H]^-$ | 4 | 9.26 | 0.60 | 1.36 | 9.87E-07 |
| Fulgidic acid | $C_{18}H_{32}O_5$ | 328.2250 | 8.55 | 1 | $[M-H]^-$ | 4 | 1.53 | 0.56 | 1.01 | 1.06E-05 |
| Hydroxyjasmonic acid | $C_{12}H_{18}O_4$ | 226.1205 | 7.50 | 1 | $[M-H]^-$ | 2 | 0.83 | 0.61 | 1.04 | 3.25E-06 |
| Norlinolenic acid | $C_{17}H_{28}O_2$ | 264.2089 | 9.08 | 2 | $[M+HCOO-H]^-$ | 4 | 0.89 | 0.41 | 1.72 | 7.02E-12 |
| ***Cinnamic acid derivatives*** | | | | | | | | | | |
| *O*-Caffeoylquinic acid | $C_{25}H_{24}O_{12}$ | 516.1268 | 6.79 | 5 | $[M-H]^-$ | 2 | 0.26 | 0.77 | 2.16 | 5.80E-03 |
| *p*-Coumaroylquinic acid | $C_{16}H_{18}O_8$ | 338.1002 | 4.97 | 2 | $[M-H]^-$ | 4 | 1.22 | 4.38 | 1.15 | 2.61E-06 |
| *O*-Feruloyl-beta-D-glucose | $C_{16}H_{20}O_9$ | 356.1107 | 4.24 | 1 | $[M-H-H_2O]^-$ | 4 | 1.39 | 2.39 | 1.14 | 2.12E-03 |
| Dihydrocaffeic acid 3-*O*-glucuronide | $C_{15}H_{18}O_{10}$ | 358.0900 | 5.12 | 7 | $[M+HCOO-H]^-$ | 2 | 0.60 | 0.73 | 1.37 | 1.12E-02 |
| *O*-Feruloylgalactarate | $C_{16}H_{18}O_{11}$ | 386.0849 | 5.83 | 7 | $[M+HCOO-H]^-$ | 2 | 0.45 | 0.62 | 2.09 | 1.80E-06 |
| Caffeic acid 3-glucoside | $C_{15}H_{18}O_9$ | 342.0951 | 7.31 | 8 | $[M+HCOO-H]^-$ | 4 | 1.05 | 0.66 | 1.49 | 3.44E-03 |
| Dihydroferulic acid 4-*O*-glucuronide | $C_{16}H_{20}O_{10}$ | 372.1056 | 5.30 | 1 | $[M-H]^-$ | 4 | 0.83 | 2.96 | 1.51 | 3.60E-07 |
| 1-Caffeoyl-4-deoxyquinic acid | $C_{16}H_{18}O_8$ | 338.1002 | 5.28 | 1 | $[M-H]^-$ | 4 | 9.71 | 2.79 | 1.04 | 1.32E-02 |
| Quinic acid | $C_7H_{12}O_6$ | 192.0634 | 4.73 | 2 | $[M-H]^-$ | 2 | 0.91 | 5.05 | 1.42 | 3.14E-03 |
| 1-*O*-Sinapoylglucose | $C_{17}H_{22}O_{10}$ | 386.1213 | 5.48 | 1 | $[M-H]^-$ | 4 | 0.88 | 6.16 | 1.24 | 8.80E-09 |
| ***Unknown*** | | | | | | | | | | |
| Unknown 1 (396.036@4.25) | - | - | 4.25 | - | - | 5 | 1.89 | 0.32 | 2.27 | 1.54E-07 |
| Unknown 2 (586.0623@8.9) | - | - | 8.90 | - | - | 5 | 1.77 | 0.67 | 1.49 | 4.69E-04 |
| Unknown 3 (572.0832@8.44) | - | - | 8.44 | - | - | 5 | 0.45 | 0.79 | 1.02 | 1.65E-02 |
| Unknown 4 (255.989@8.9) | - | - | 8.90 | - | - | 5 | 1.36 | 0.66 | 1.11 | 8.14E-05 |
| Unknown 5 | $C_{27}H_{36}O_{12}$ | - | 6.14 | - | - | 4 | 0.88 | 2.10 | 1.36 | 1.02E-02 |
| Unknown 6 | $C_{27}H_{36}O_{12}$ | - | 5.90 | - | - | 4 | 0.39 | 0.61 | 1.80 | 2.56E-05 |
| ***Peptide*** | | | | | | | | | | |
| Tripeptide 1 | $C_{19}H_{25}N_3O_7$ | 407.1692 | 4.65 | 6 | $[M-H]^-$ | 3 | 1.16 | 9.13 | 1.62 | 2.22E-09 |
| Tripeptide 2 | $C_{19}H_{25}N_3O_7$ | 407.1692 | 4.55 | 7 | $[M-H]^-$ | 3 | 1.46 | 10.31 | 1.61 | 1.56E-10 |
| Tripeptide 3 | $C_{15}H_{20}N_4O_6$ | 352.1383 | 4.81 | 5 | $[M-H]^-$ | 4 | 1.09 | 4.36 | 1.89 | 1.84E-12 |
| ***Lignan glycosides*** | | | | | | | | | | |

| | | | | | | | | | | |
|---|---|---|---|---|---|---|---|---|---|---|
| Prupaside | $C_{27}H_{36}O_{12}$ | 552.2207 | 5.90 | 1 | $[M+HCOO-H]^-$ | 3 | 0.40 | 0.61 | 1.88 | 2.37E-05 |
| Citrusin B | $C_{27}H_{36}O_{13}$ | 568.2156 | 6.27 | 2 | $[M+HCOO-H]^-$ | 4 | 1.00 | 0.58 | 1.02 | 6.10E-05 |
| ***Alkaloid*** | | | | | | | | | | |
| 2'-Norberbamunine | $C_{35}H_{38}N_2O_6$ | 582.2730 | 8.51 | 5 | $[M+HCOO-H]^-$ | 4 | 1.30 | 0.39 | 1.07 | 4.43E-12 |
| Vomilenine | $C_{21}H_{22}N_2O_3$ | 350.1630 | 4.88 | 8 | $[M+Cl]^-$ | 4 | 0.50 | 1.36 | 1.44 | 1.04E-02 |
| ***Carboxylic acid*** | | | | | | | | | - | |
| 3,4,5-trihydroxy-6-(2-hydroxy-6-methoxyphenoxy)oxane-2-carboxylic acid | $C_{13}H_{16}O_9$ | 316.0794 | 2.06 | 2 | $[M-H]^-$ | 4 | 0.88 | 2.14 | 1.54 | 5.09E-04 |
| ***Phenols*** | | | | | | | | | | |
| Phenol glucuronide | $C_{12}H_{14}O_7$ | 270.0740 | 2.06 | 0 | $[M+HCOO-H]^-$ | 4 | 0.90 | 2.14 | 1.54 | 5.10E-04 |
| ***Carbohydrate*** | | | | | | | | | | |
| Ribulose | $C_5H_{10}O_5$ | 150.0528 | 0.60 | 0 | $[M-H]^-$ | 4 | 0.76 | 0.75 | 1.14 | 1.21E-03 |
| ***Steroid*** | | | | | | | | | | |
| Physalin L | $C_{28}H_{32}O_{10}$ | 528.1995 | 1.54 | 3 | $[M-H]^-$ | 2 | 1.11 | 0.40 | 1.08 | 1.07E-07 |
| ***Stilbene glycosides*** | | | | | | | | | | |
| Piceatannol 4'-galloylglucoside | $C_{27}H_{26}O_{13}$ | 558.1373 | 7.69 | 2 | $[M-H]^-$ | 3 | 2.60 | 0.36 | 1.23 | 2.24E-05 |
| ***Prenol lipids*** | | | | | | | | | | |
| Auxin b | $C_{18}H_{30}O_4$ | 310.2144 | 9.08 | 1 | $[M-H]^-$ | 4 | 1.13 | 0.41 | 1.81 | 7.07E-12 |

[a]CV, coefficient of variation in the metabolites in the QC samples; [b]FC, fold change in the comparison (average in low altitude/average in high altitude); [c]VIP, variable importance in projection; [d]*p*-value corresponding to the *p* values calculated by the Benjamini-Hochberg false discovery rate post hoc correction (FDR < 0.05); *Metabolites annotated with GNPS. RT: retention time; Confidence levels in annotation were as following: Level 1: Confirmed structure, Level 2: Probable structure, Level 3: Tentative candidate(s), Level 4: Unequivocal molecular formula, Level 5: Exact mass (SCHYMANSKI et al., 2014).

### 2.2.2 Molecular networks and heatmap analyses reveal the chemical variation under the influence of altitudinal variation

To explore the leading chemical classes, we created a molecular network using the GNPS platform, which enabled us to visualize the chemical space of the metabolome in these species. Figure 2.4A illustrates the molecular network analyzed in the MolNetEnhancer platform, revealing the classes of molecular families (MF) present in the metabolome. We identified seven groups of molecular families, including

phenylpropanoids and polyketides, lipids and lipid-like molecules, organic acid derivatives, lignans, neolignans and related compounds, alkaloids, and derivatives, organoheterocyclic compounds, and oxygenated organic compounds. However, due to the complexity of the metabolome in these species and the limitations of the spectral libraries, many of the nodes did not match any spectral reference. Therefore, it is crucial to continue exploring the chemical composition of these species, which is still limited in the literature. Notably, when we created a molecular network of the flavonoid cluster and compared the low vs. high altitude groups of the annotated compounds, we found that vitexin 2"-*O*-rhamnoside (FC = 1.494; *p*-value = 1.41E-03), saponarin (FC = 1.458; *p*-value = 7.22E-04), and vicenin 2 (FC = 1.360; *p*-value = 2.13E-02) (Supplementary Figure S2.2A-C) exhibited positive correlations at higher altitudes, confirming the statistical analysis performed previously (Figure 2.4B).

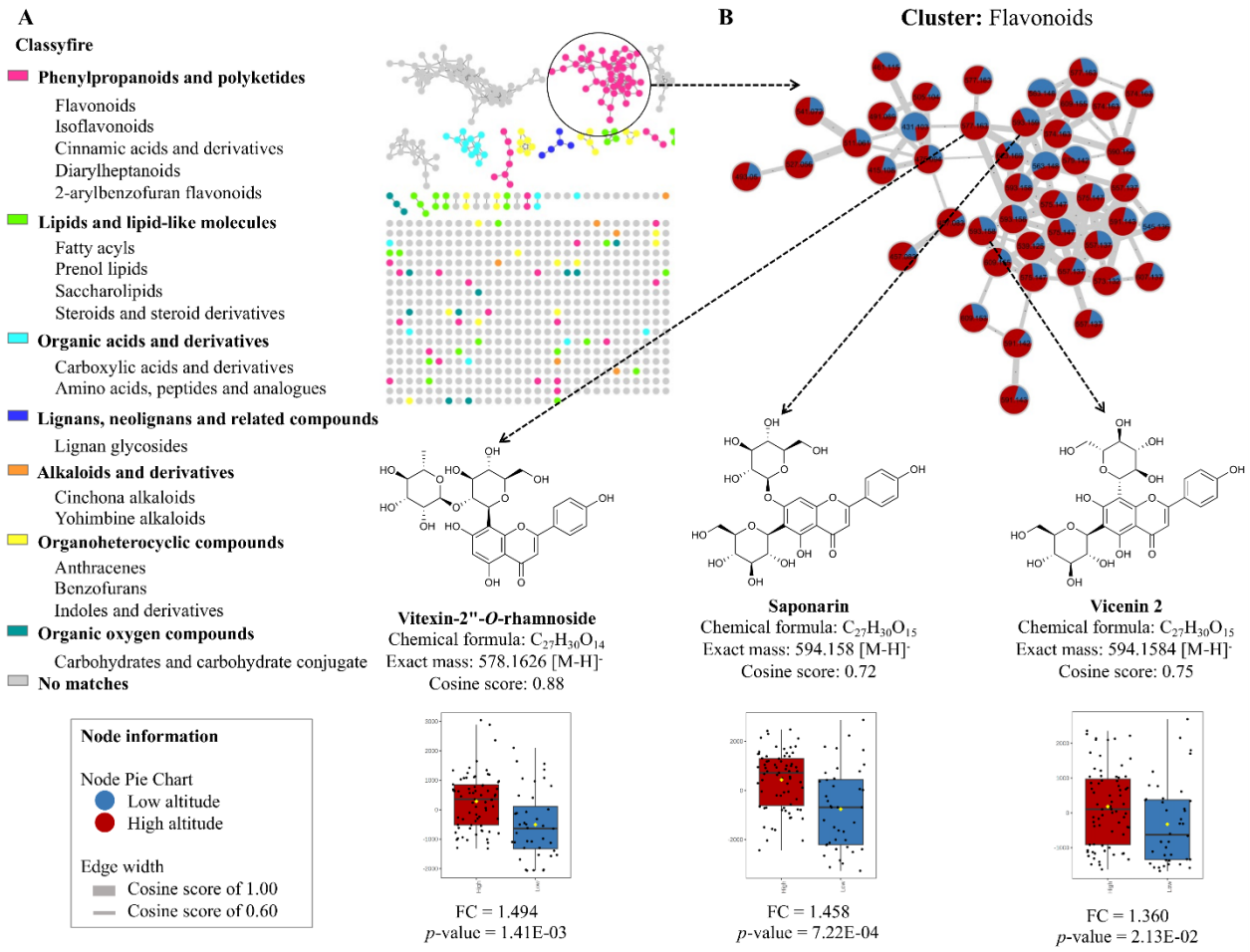



**Figure 2.4.** Molecular networks analysis obtained from GNPS platform online. **(A)** Identification of major classes of chemical constituents of bamboo species using MolNetEnhancer technique and GNPS molecular networking. Color of the node is set according to the chemical class using "Classyfire". **(B)** Molecular network of the flavonoid cluster comparing low altitude (blue) and high altitude (red).

By conducting hierarchical clustering analysis and generating a heatmap based on the two most relevant groups of annotated metabolites that exhibited significant changes with altitude (flavonoids and cinnamic acid derivatives), we identified two distinct groups that were associated with altitude. We found that each group exhibited different patterns in terms of chemical composition and levels of presence and abundance. Figure 2.5 depicts the clustering of the two altitudinal ranges evaluated, with the first cluster corresponding to the high altitude samples that exhibited a high accumulation of flavonoids, while the low altitude samples exhibited a high accumulation of cinnamic acid derivatives.

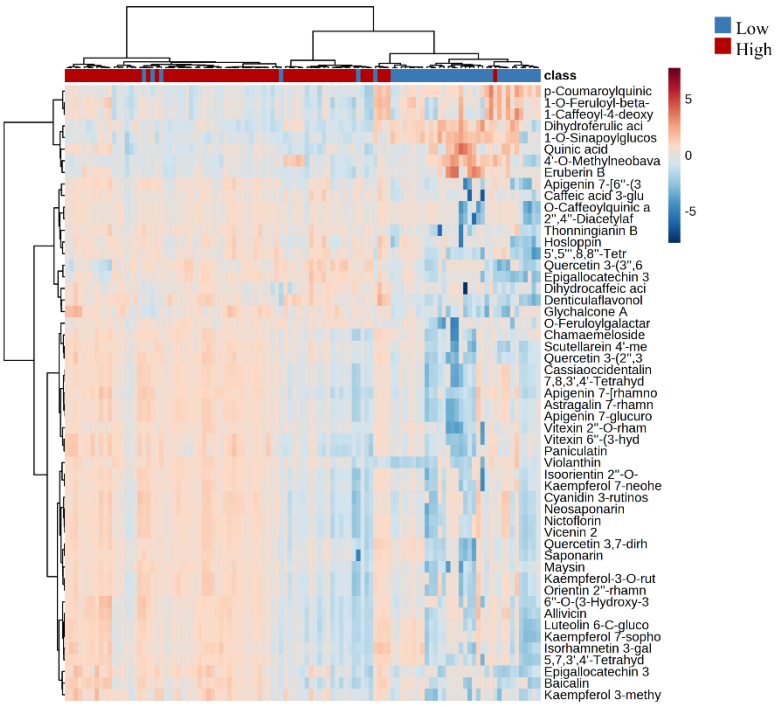



**Figure 2.5.** Hierarchical clustering with heatmap illustrating the differences in the metabolite abundance between low and high altitudes. The x-axis shows the clustering of all the samples, and the y-axis shows the clustering of the annotated flavonoids and cinnamic acid derivatives.

### 2.2.3 Changes in the concentration and analysis of biosynthesis pathways of the most relevant metabolites in bamboo species

The box plot shows the differential metabolites for the two altitude groups. In Figure 2.6 we present the fold change of the main metabolites that exhibited a significant change. We found that cinnamic acid derivatives and flavonoids showed a significant change with the low and high altitude groups, respectively. Our study also highlighted the significance of quinic acid (QA) is a major differential metabolite, which acts as a crucial precursor in the biosynthetic pathway of phenylpropanoids and is essential in the production of a diverse array of phenolic compounds.

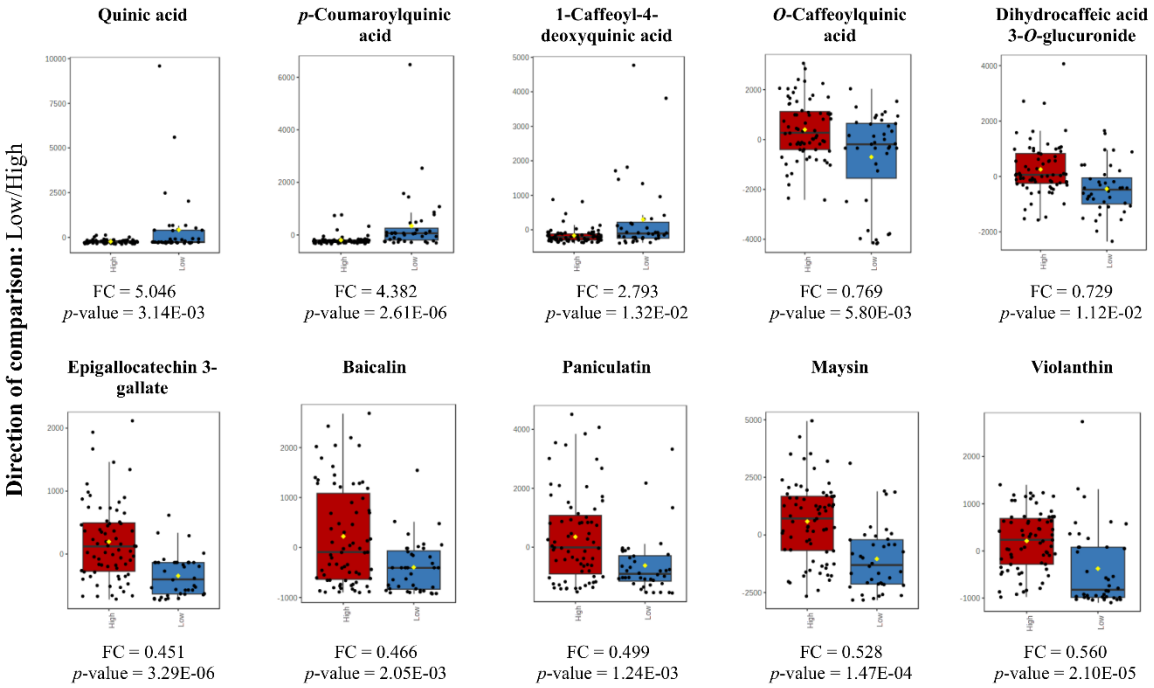



**Figure 2.6.** Box plot for the altered metabolites corresponding to cinnamic acid derivatives and flavonoids (*p*-value < 0.05) at low altitude (blue) and high altitude (red). Y-axes are represented as relative units. The data were normalized with respect to the total spectral area. Bar charts show normalized values (mean +/- one standard deviation). Boxes range from the 5% and 95% percentiles are indicated as error bars; individual data points are indicated by circles. The medians are indicated by horizontal lines within each box.

### 2.2.4 Molecular networking for chemical space mapping of the metabolome of bamboo species by MolNetEnhancer

To complement the study on the chemical composition of the global metabolome of bamboo species, a molecular network was constructed using the GNPS platform to compare other types of flavonoids that were not statistically significant among the twelve species studied. Four flavonoid *C*-glycosides (isorhamnetin 7-rhamnoside, isovitexin, isoschaftoside, and rhoifolin) and one flavonoid *O*-glycoside (cyanidin 3-*O*-sophoroside) were annotated (Figure S2.2D-H). It was observed that the *G. angustifolia* species was found to have an abundant profile of flavonoid *C*-glucosides, specifically of the compound isoschaftoside, which is functionally related to apigenin (Figure 2.7). In terms of flavonoid variation between species, isovitexin and isorhamnetin 7-rhamnoside were found in most species.

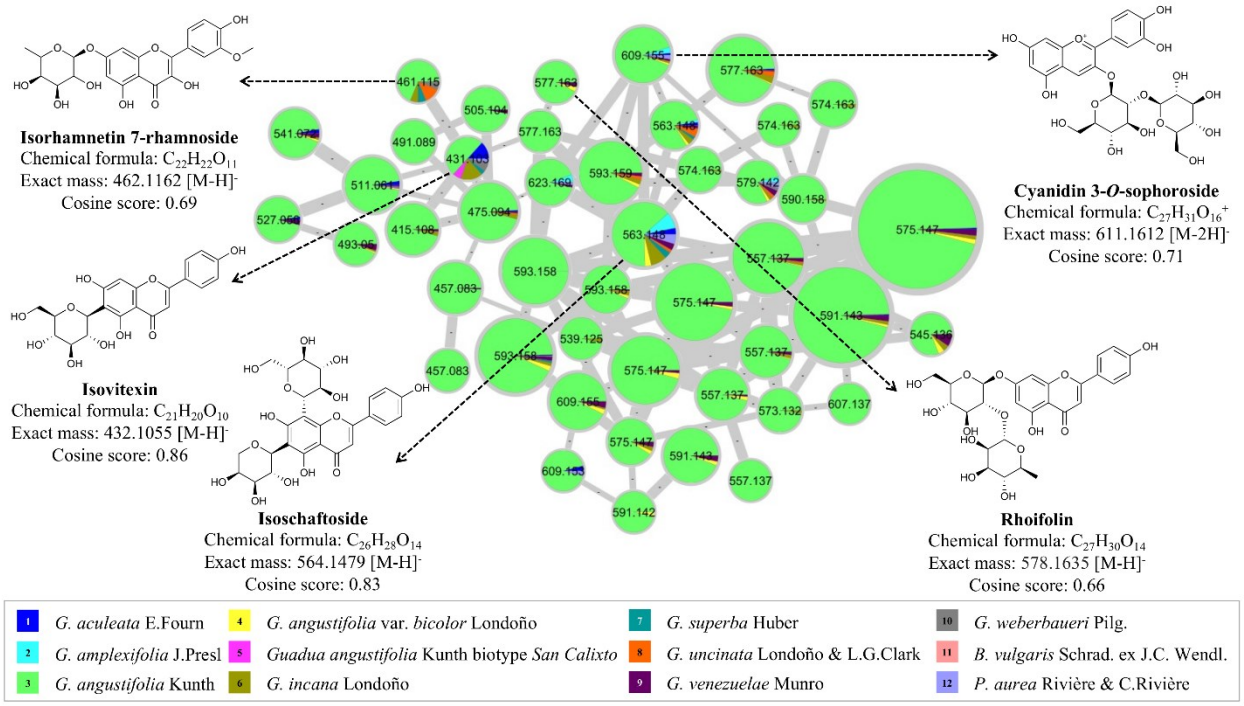



**Figure 2.7.** Molecular networking and dereplication of flavonoids comparing twelve bamboo species.

Our findings indicate that flavonoids significantly increased at high altitudes, while cinnamic acid derivatives exhibited an increasing trend at low altitudes. Notably, flavonoids from *G. angustifolia* showed a positive correlation with the high altitude group, as did cinnamic acid derivatives from *G. aculeata*, *G. amplexifolia*, *G. angustifolia* var. *bicolor*, *G. angustifolia* biotype San Calixto, *G. incana*, *G. superba*, *G. uncinata*, *G. venezuelae*, *B. vulgaris*, and *P. aurea* with low altitude (Figure 2.8). However, further research is needed to determine the exact nature of this correlation.

The effect of altitudinal variation on the chemical composition of the leaves of bamboo species is poorly documented. Previous studies have suggested that plants grown at high altitudes tend to have higher levels of flavonoids compared to those grown at low altitudes (WANG et al., 2020a; ZHOU et al., 2021). This phenomenon can be attributed to an increase of in ultraviolet radiation, illumination time and the delay of the phenophase of the plant, along with elevation, which is a protective mechanism that plants use against unfavorable environmental conditions (NI et al., 2013). In a recent study, Zhou

*et al*. in 2021 investigated the influence of an altitudinal gradient on the variation of flavonoids in *Agriophyllum squarrosum* and found that these metabolites were enriched at high altitudes (ZHOU et al., 2021). The study also demonstrated a strong positive correlation between the contents of flavonoids, such as quercetin, tricine, and rutin, and environmental variables, such as latitude, longitude, and precipitation gradients. These findings corroborate our results and provide valuable information on the variation in the chemical profile of bamboo under various abiotic factors such as altitude, temperature, light, and soil, etc.

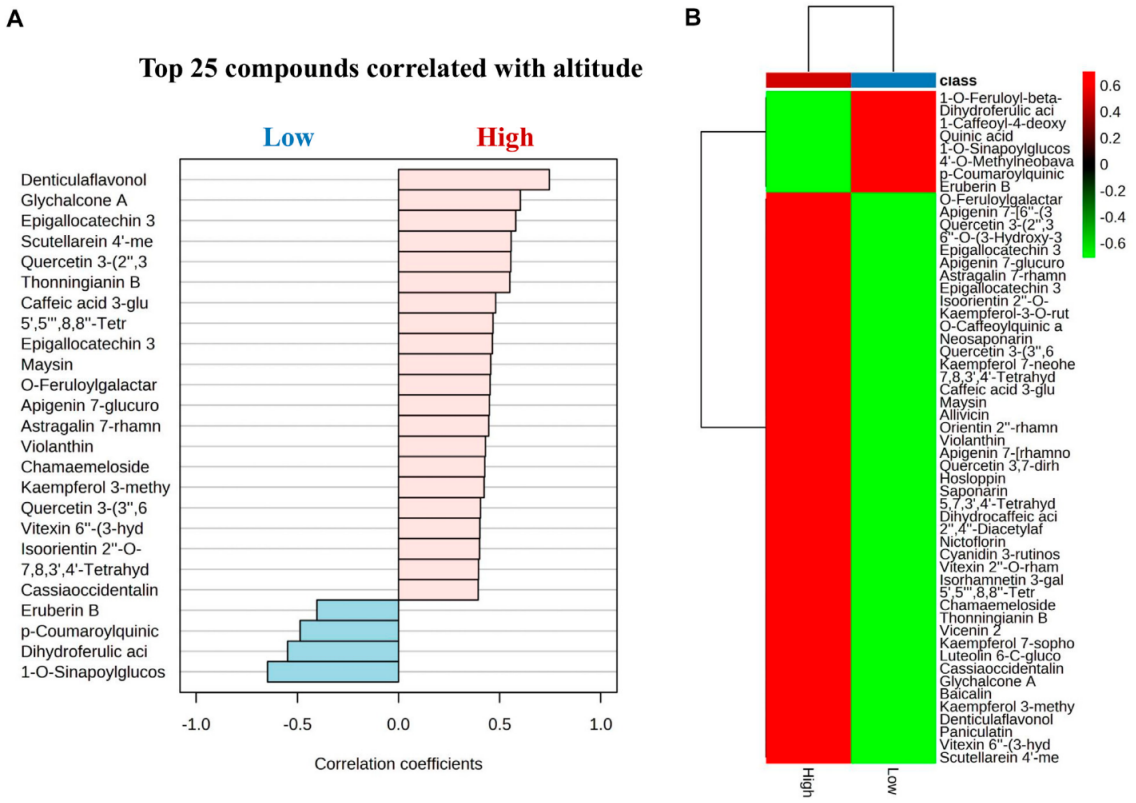



**Figure 2.8. (A)** Pearson's correlations using pattern search of the top 25 metabolites between low and high altitude. **(B)** Cluster heatmap based on correlation between flavonoids and acid cinnamic derivatives and the altitude variable. The analysis shows a positive (red) and negative (green) correlation with a *p*-value = 0.05 for all the metabolites.

The metabolic differences expressed in bamboo species between high and low altitudes provide valuable information about the ideal growing conditions to promote the production of phenolic compounds with important biological properties in medicine.

Moreover, the bamboo leaves have added value as are agro-industrial residues generated in the construction industry. Our results suggest that the accumulation of flavonoids at high altitudes is due to the adaptability of bamboo species to environmental conditions. These giant grasses biosynthesize flavonoid-type phenolic compounds that are used as defence and potential antioxidants (FALCONE FERREYRA; RIUS; CASATI, 2012; PANCHE; DIWAN; CHANDRA, 2016; WANG; LI; BI, 2018).

Notably, the phenylpropanoid biosynthesis pathway, which is the starting point for producing many essential compounds such as flavonoids, coumarins, lignans, and hydroxycinnamic acid conjugates (FRASER; CHAPPLE, 2011), is possibly the pathway that has been altered considering the results of this study. Flavonoid production occurs mainly through a diverse biosynthetic pathway involving the shikimate pathway and polyketide pathways (LIU et al., 2021; MOURADOV; SPANGENBERG, 2014). Interestingly, the phenylpropanoid biosynthetic pathway showed a significant change in the presence of QA, with a fold change of 5.05, VIP of 1.42, and a *p*-value with FDR 3.14E-03. QA is a metabolite that is closely related to the biosynthesis pathway of caffeoylquinic acids (CQAs) and are specialized bioactive metabolites that are derived from the phenylpropanoid biosynthesis pathway. Consequently, QA is a critical intermediate in the biosynthesis of many flavonoids through cinnamic acid, which is a necessary precursor (ALCÁZAR MAGAÑA et al., 2021; LIU et al., 2021). Furthermore, the study revealed interesting chemical diversity in these species, with a predominance of groups of metabolites that are flavonoids and cinnamic acid derivatives. The mapping of the chemical space (including information about known reference spectra) allowed for the visualization of a large part of the global chemical composition of these species. However, the GNPS platform had a low annotation rate, resulting in many no-matches.

To complement the study of changes in chemical composition under the influence of altitude, the molecular network was used to analyze the specific cluster for flavonoids, comparing low and high altitudes. The study showed that the flavonoids such as vitexin 2"-*O*-rhamnoside, vicenin 2, and saponarin had a positive tendency to increase at high altitudes. This finding suggests a close relationship between the concentration of phenolic

compounds (flavonoids and cinnamic acid derivatives) in bamboo species. The heatmap shows a clear difference in the content of flavonoids and cinnamic acid derivatives between the groups compared under the effect of the altitudinal gradient, which could serve as marker compounds for chemical classification. The metabolites exposed to the variable altitude showed a significant difference, indicating that environmental factors have previously influenced the genetic and chemical diversity of plants (PACHECO-HERNÁNDEZ et al., 2021).

The metabolome of various bamboo species was compared, it was found that *G. angustifolia* had a rich profile of *C*-glycoside flavonoids. Similar metabolites have been reported for other bamboo species such as *P. nigra* var. *henonis* (IBRAHIM et al., 2021; ZHANG et al., 2008), *P. pubescens* (TANAKA et al., 2014), and *B. vulgaris* (AKHTAR; PATOWARY, 2022). Some flavonoids were found to be shared among other species, such as *G. aculeata*., *G. angustifolia*, *G. angustifolia* biotype San Calixto, *G. incana*, *G. uncinata,* and *G. venezuelae*. Out of the twelve species analyzed, *B. vulgaris* and *P. aurea* were found to be the most studied species at the chemical level in Asia. However, considering the limited information available in the literature and the results obtained from the metabolomic analysis, this study presents an opportunity to explore the metabolome of these species further, especially those belonging to the genus *Guadua* and distributed in the Neotropical region.

## 2.3 Conclusion

This study employed an untargeted metabolomics approach and molecular networking analysis to assess changes in the chemical composition of bamboo species due to variations in altitude. The study revealed that high altitude had a significant influence on the increase of flavonoid profiles, while low altitude led to an increase in cinnamic acid derivatives profiles. The molecular network analysis further demonstrated the diverse chemical composition of these species, including flavonoid glycosides, cinnamic acid derivatives, lignans, alkaloids, carbohydrates, and fatty acids. Conducting metabolomic studies on bamboo can provide a detailed understanding of its chemical

composition and metabolic conservation, aiding in identifying patterns and trends in relation to environmental and cultivation factors. This information can help to enhance the production and quality of bamboo, identify bioactive compounds for natural health products, and improve sustainability, positively impacting the industry and the economy.

## Supplementary information

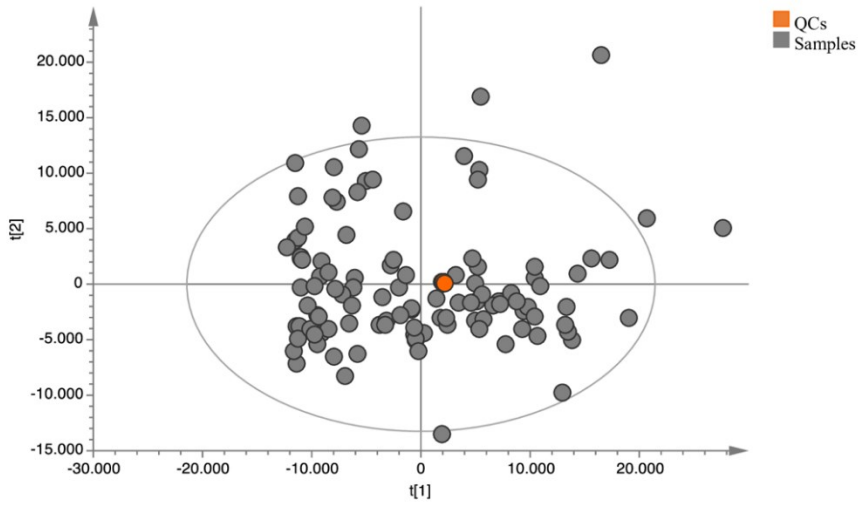
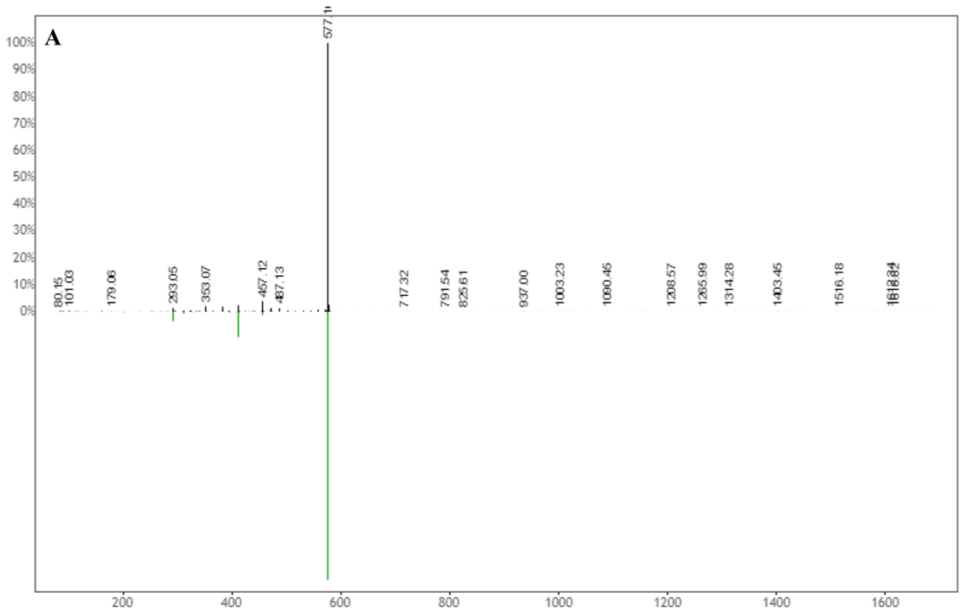
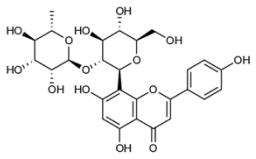
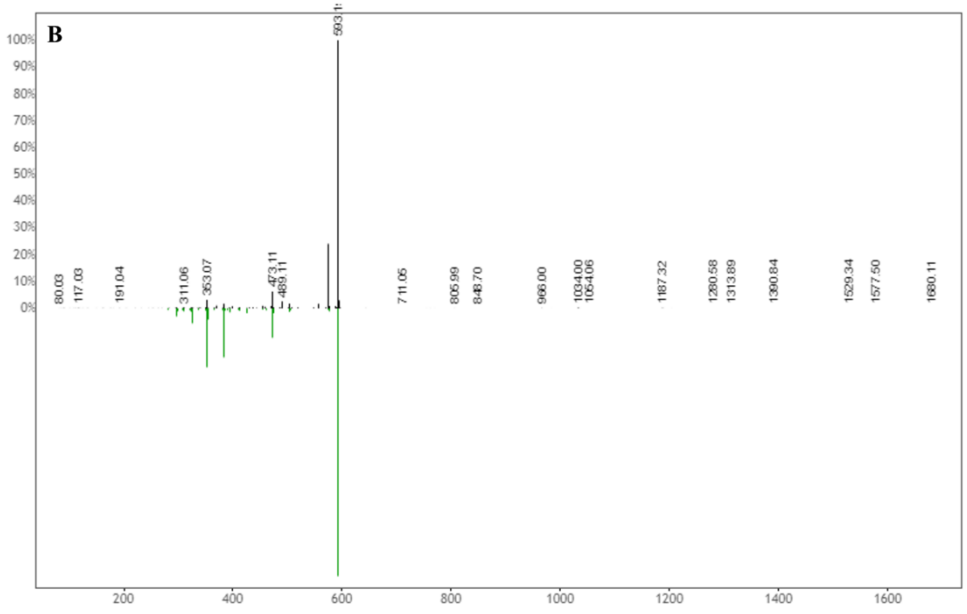


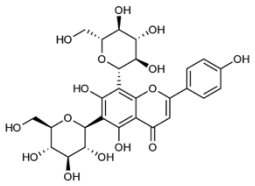

**Figure S2.1.** PCA score plot including quality controls (QCs) and all samples from LC-QTOF-MS analysis.



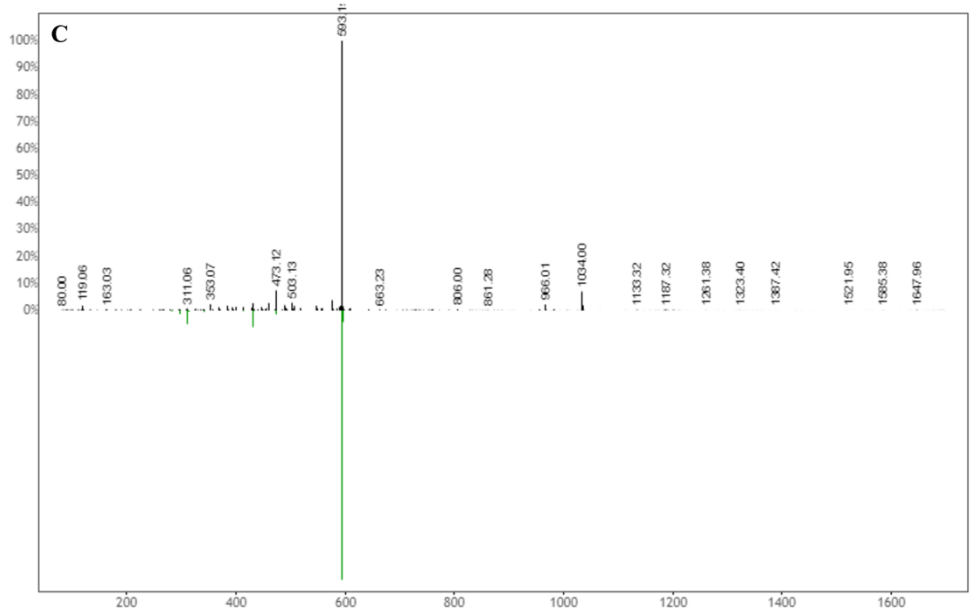



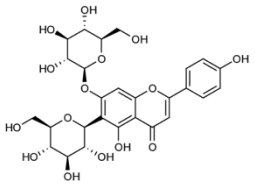
**Vitexin-2"-*O*-rhamnoside**
Chemical formula: $C_{27}H_{30}O_{14}$
Exact mass: 578.1626 [M-H]$^-$
Cosine score: 0.88



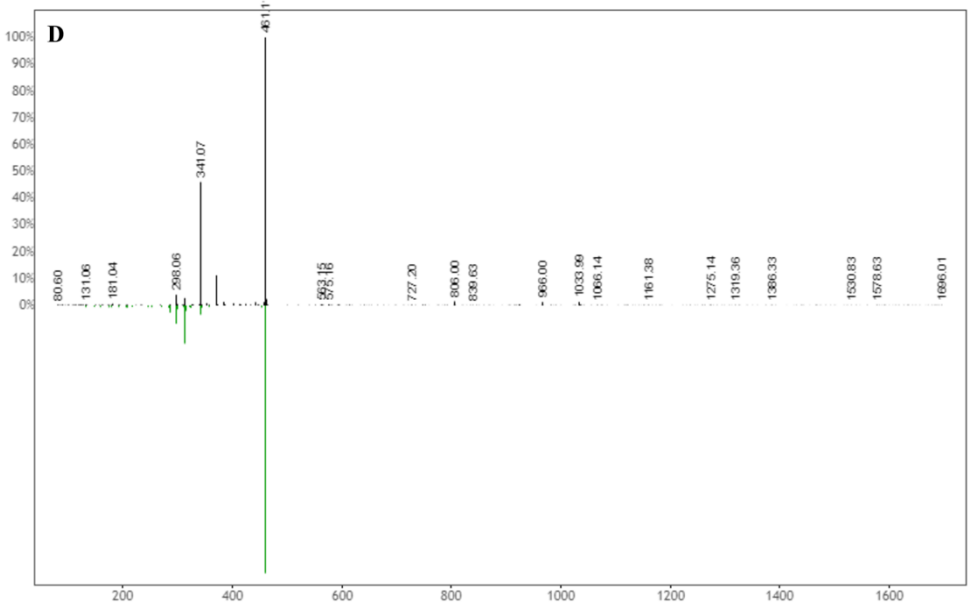



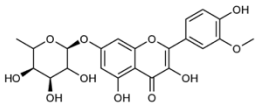
**Vicenin 2**
Chemical formula: $C_{27}H_{30}O_{15}$
Exact mass: 594.1584 [M-H]$^-$
Cosine score: 0.75



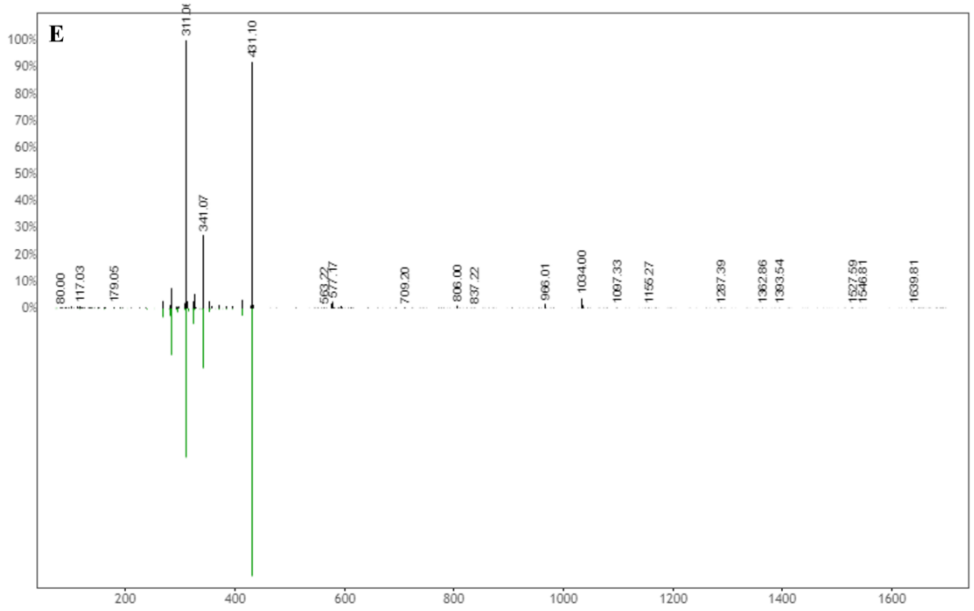



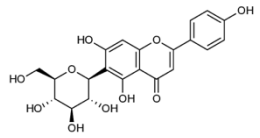
**Saponarin**
Chemical formula: $C_{27}H_{30}O_{15}$
Exact mass: 594.158 [M-H]$^-$
Cosine score: 0.72



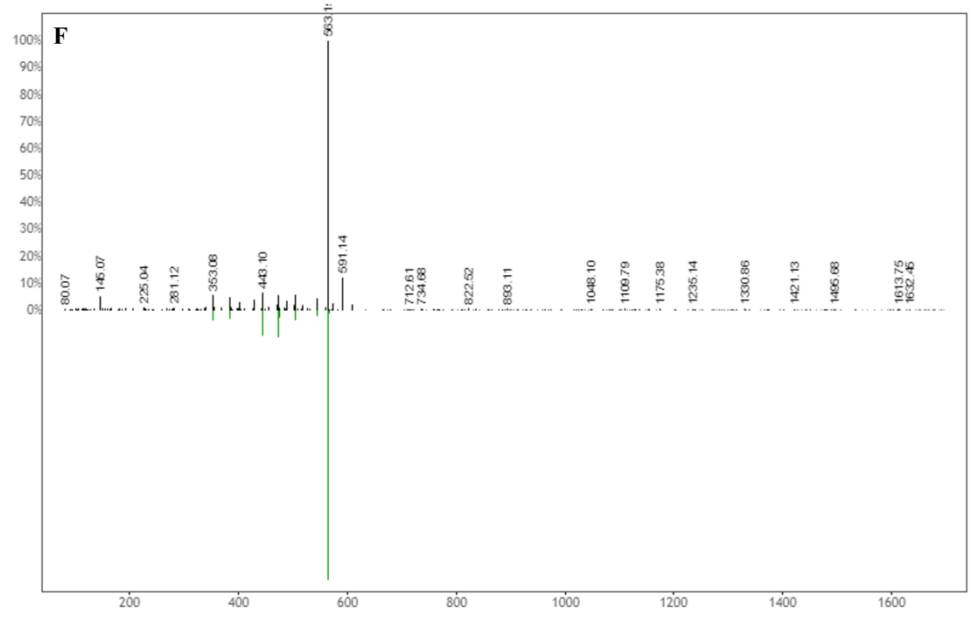



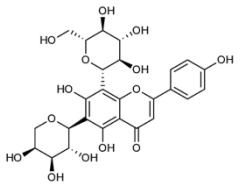
**Isorhamnetin 7-rhamnoside**
Chemical formula: $C_{22}H_{22}O_{11}$
Exact mass: 462.1162 [M-H]$^-$
Cosine score: 0.69



**Isovitexin**
Chemical formula: $C_{21}H_{20}O_{10}$
Exact mass: 432.1055 [M-H]$^-$
Cosine score: 0.86



**Isoschaftoside**
Chemical formula: $C_{26}H_{28}O_{14}$
Exact mass: 564.1479 [M-H]$^-$
Cosine score: 0.83

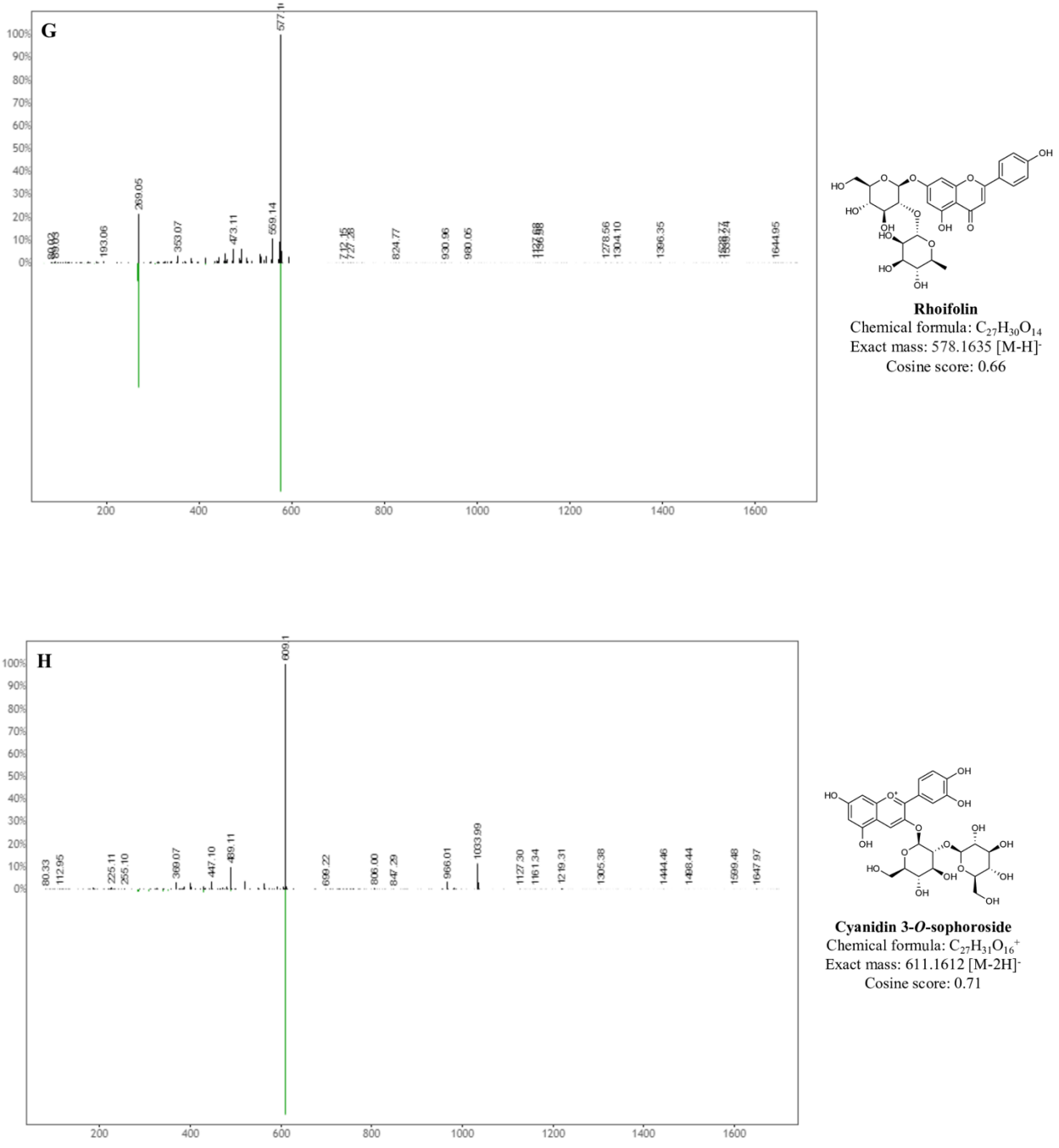



**Figure S2.2.** Dereplication of metabolites using Global Natural Social Molecular Networking (GNPS). The MS/MS spectrum match feature of GNPS showing the similarity of fragment peaks of the experimental and library data. **(A)** Vitexin-2"-*O*-rhamnoside, **(B)** Vicenin 2, **(C)** Saponarin, **(D)** Isorhamnetin 7-rhamnoside, **(E)** Isovitexin, **(F)** Isoschaftoside, (**G)** Rhoifolin, and **(H)** Cyanidin 3-*O*-sophoroside.

**Table S2.1.** List and information on the environmental variables of collection of the bamboo species used for the metabolomic study.

| Plant scientific name | Sampling location | Collection date | AMAT (°C) | AMET (°C) | AMIT (°C) | MP (mm) | RH (%) | Longitude | Latitude | Altitude (m) | Voucher number |
|---|---|---|---|---|---|---|---|---|---|---|---|
| *G. aculeata* E.Fourn. | Quindío, Montenegro | 12/2021 | 28.0 | 24.0 | 21.0 | 200-300 | 82.0 | -75.80102 | 4.52086 | 1256 | HPUJ-30736 |
| *G. amplexifolia* J.Presl | Quindío, Montenegro | 12/2021 | 28.0 | 24.0 | 21.0 | 200-300 | 82.0 | -75.80108 | 4.52083 | 1256 | HPUJ-30733 |
| *G. angustifolia* Kunth | Nariño, Tumaco | 01/2022 | 28.0 | 26.0 | 24.0 | 200-300 | 85.0 | -78.71333 | 1.56033 | 18 | HPUJ-30717 |
| | Nariño, Tumaco | 01/2022 | 28.0 | 26.0 | 24.0 | 200-300 | 85.0 | -78.67738 | 1.54900 | 21 | HPUJ-30717 |
| | Nariño, Ricaurte | 01/2022 | 24.0 | 20.0 | 16.0 | 400-600 | 75.0 | -78.05322 | 1.21986 | 1053 | HPUJ-30718 |
| | Nariño, Ricaurte | 01/2022 | 24.0 | 20.0 | 16.0 | 400-600 | 75.0 | -78.03030 | 1.23202 | 1089 | HPUJ-30718 |
| | Quindío, Montenegro | 12/2021 | 28.0 | 24.0 | 21.0 | 200-300 | 82.0 | -75.79944 | 4.51788 | 1256 | HPUJ-30731 |
| | Cundinamarca, Pacho | 09/2020 | 31.5 | 25.5 | 23.5 | 100-200 | 82.5 | -74.19519 | 5.18127 | 1343 | HPUJ-30740 |
| | Nariño, Samaniego | 01/2022 | 22.0 | 18.0 | 14.0 | 100-200 | 65.0 | -77.60819 | 1.31588 | 1478 | HPUJ-30719 |
| | Nariño, Samaniego | 01/2022 | 22.0 | 18.0 | 14.0 | 100-200 | 65.0 | -77.59416 | 1.34527 | 1565 | HPUJ-30719 |
| | Nariño, Samaniego | 01/2022 | 22.0 | 18.0 | 14.0 | 100-200 | 65.0 | -77.58619 | 1.33219 | 1588 | HPUJ-30719 |
| | Nariño, San Lorenzo | 01/2022 | 20.0 | 15.0 | 12.0 | 200-300 | 71.0 | -77.16970 | 1.56840 | 1595 | HPUJ-30721 |
| | Nariño, La Unión | 01/2022 | 21.0 | 18.0 | 12.0 | 200-300 | 63.0 | -77.12369 | 1.61061 | 1598 | HPUJ-30721 |
| | Nariño, Consacá | 01/2022 | 22.7 | 19.5 | 14.5 | 100-200 | 66.0 | -77.48802 | 1.25369 | 1606 | HPUJ-30720 |
| | Nariño, Samaniego | 01/2022 | 22.0 | 18.0 | 14.0 | 100-200 | 65.0 | -77.61022 | 1.30783 | 1606 | HPUJ-30719 |
| | Nariño, La Unión | 01/2022 | 21.0 | 18.0 | 12.0 | 200-300 | 73.0 | -77.10830 | 1.61391 | 1610 | HPUJ-30721 |
| | Nariño, La Unión | 01/2022 | 21.0 | 18.0 | 12.0 | 200-300 | 73.0 | -77.09472 | 1.61463 | 1631 | HPUJ-30721 |
| | Nariño, San Lorenzo | 01/2022 | 20.0 | 15.0 | 12.0 | 200-300 | 71.0 | -77.20347 | 1.59688 | 1713 | HPUJ-30721 |
| | Nariño, Sandoná | 01/2022 | 21.8 | 16.8 | 13.6 | 100-200 | 65.0 | -77.48088 | 1.32755 | 1720 | HPUJ-30719 |
| | Nariño, Sandoná | 01/2022 | 21.8 | 16.8 | 13.6 | 100-200 | 65.0 | -77.48088 | 1.32755 | 1744 | HPUJ-30719 |
| | Nariño, San Lorenzo | 01/2022 | 20.0 | 15.0 | 12.0 | 200-300 | 71.0 | -77.20711 | 1.58952 | 1779 | HPUJ-30721 |
| | Nariño, San Lorenzo | 01/2022 | 20.0 | 15.0 | 12.0 | 200-300 | 71.0 | -77.20669 | 1.58786 | 1808 | HPUJ-30721 |

| | | | | | | | | | | | |
|---|---|---|---|---|---|---|---|---|---|---|---|
| | Nariño, San Lorenzo | 01/2022 | 20.0 | 15.0 | 12.0 | 200-300 | 71.0 | -77.20700 | 1.58680 | 1826 | HPUJ-30721 |
| | Nariño, Chachagüí | 01/2022 | 20.6 | 17.5 | 12.3 | 100-200 | 60.0 | -77.28186 | 1.37486 | 1857 | HPUJ-30722 |
| | Nariño, San Lorenzo | 01/2022 | 20.0 | 15.0 | 12.0 | 200-300 | 71.0 | -77.20591 | 1.58616 | 1876 | HPUJ-30721 |
| | Nariño, San Lorenzo | 01/2022 | 20.0 | 15.0 | 12.0 | 200-300 | 71.0 | -77.16610 | 1.56820 | 1930 | HPUJ-30721 |
| | Nariño, San Lorenzo | 01/2022 | 20.0 | 15.0 | 12.0 | 200-300 | 71.0 | -77.16610 | 1.56820 | 1970 | HPUJ-30721 |
| | Nariño, La Florida | 01/2022 | 20.0 | 16.0 | 10.0 | 100-200 | 64.0 | -77.41291 | 1.30511 | 2089 | HPUJ-30719 |
| | Nariño, La Florida | 01/2022 | 20.0 | 16.0 | 10.0 | 100-200 | 64.0 | -77.41325 | 1.30041 | 2122 | HPUJ-30719 |
| | Nariño, La Florida | 01/2022 | 20.0 | 16.0 | 10.0 | 100-200 | 64.0 | -77.40380 | 1.30005 | 2137 | HPUJ-30719 |
| *G. angustifolia* var. b*icolor* Londoño | Quindío, Montenegro | 04/2022 | 29.0 | 23.0 | 18.0 | 200-300 | 80.0 | -75.80056 | 4.52018 | 1256 | HPUJ-30735 |
| *G. angustifolia* Kunth biotype San Calixto | Quindío, Montenegro | 04/2022 | 29.0 | 23.0 | 18.0 | 200-300 | 80.0 | -75.80041 | 4.52063 | 1256 | HPUJ-30737 |
| *G. incana* Londoño | Putumayo, Mocoa | 12/2021 | 26.0 | 22.5 | 20.0 | 100-200 | 85.0 | -76.66477 | 1.17730 | 604 | HPUJ-30723 |
| | Quindío, Montenegro | 12/2021 | 28.0 | 24.0 | 21.0 | 200-300 | 82.0 | -75.80013 | 4.52102 | 1256 | HPUJ-30723 |
| *G. superba* Huber | Quindío, Montenegro | 04/2022 | 29.0 | 23.0 | 18.0 | 200-300 | 80.0 | -75.80036 | 4.52100 | 1256 | HPUJ-30734 |
| *G. uncinata* Londoño & L.G.Clark | Quindío, Montenegro | 12/2021 | 28.0 | 24.0 | 21.0 | 200-300 | 82.0 | -75.80033 | 4.51816 | 1256 | HPUJ-30730 |
| *G. venezuelae* Munro | Quindío, Montenegro | 04/2022 | 29.0 | 23.0 | 18.0 | 200-300 | 80.0 | -75.80005 | 4.52057 | 1256 | HPUJ-30729 |
| *G. weberbaueri* Pilg. | Quindío, Montenegro | 04/2022 | 29.0 | 23.0 | 18.0 | 200-300 | 80.0 | -75.80057 | 4.52043 | 1256 | HPUJ-30738 |
| *B. vulgaris* Schrad. ex J.C. Wendl. | Cundinamarca, Pacho | 03/2021 | 31.5 | 25.5 | 23.5 | 100-200 | 82.5 | -74.19527 | 5.18138 | 1343 | HPUJ-30714 |
| *P. aurea* Rivière & C.Rivière | Quindío, Montenegro | 03/2021 | 28.0 | 24.0 | 21.0 | 200-300 | 82.0 | -74.19527 | 5.18138 | 1256 | HPUJ-30715 |

Annual Maximum Temperature - AMAT (°C), Annual Mean Temperature - AMET (°C), Annual Minimum Temperature - AMIT (°C), Monthly Precipitation - MP (Sampling Month) (mm), Relative Humidity - RH (%), Longitude, Latitude, and Altitude (m).

# 3 CHAPTER 3. Metabolomic profiling of *Guadua* species and its correlation with antioxidant, anti-inflammatory and cytotoxic activities

## Presentation

Considering the results of the previous chapter, where it was observed that bamboos belonging to the genus *Guadua*, found in natural environments of medium and high altitude, exhibited a high content of flavonoids, chapter 2 focuses on selecting 10 different species of the genus *Guadua* from various locations in Colombia. The objective was to establish a correlation study between the chemical composition and biological activities, specifically in terms of antioxidant, anti-inflammatory, and cytotoxic properties, through a metabolomic approach, to identify compounds related to those activities.

Part of these results were submitted to publication in *ACS Omega*, 2024. Al this time, the manuscript is undergoing final (minor) corrections for publication.

## 3.1 Materials and methods

### 3.1.1 Chemical and reagents

1,1-Diphenyl-2-picrylhydrazyl (DPPH), 2,2-azinobis(3-ethylbenzothiazoline-6-sulfonic acid) (ABTS), 6-hydroxy-2,5,7,8-tetramethylchroman-2-carboxylic acid (Trolox, Hoffman-La Roche) were purchased from Sigma Aldrich Co., (St. Louis, MO, USA). Methanol (MeOH), Acetonitrile (ACN), and formic acid (FA) HPLC grade were acquired from Merck (Darmstadt, Germany). Ultra-pure water was used throughout and was produced by a Milli-Q Ultra-pure water system with a resistivity of 18.2 MΩ .cm at 25 °C (Millipore, Bedford, USA). For the NMR experiments, methanol-$d_4$ (>99.8 atom % D) and deuterium oxide (>99.8 atom % D) were purchased from Sigma-Aldrich USA (St. Louis, MO, USA). Dimethyl sulfoxide (DMSO) was purchased from Panreac AppliChem. Gallic acid (purity: >98%), chlorogenic acid (purity: >98%), caffeic acid (purity: >98%), isoorientin (purity: >98%), ampelopsin (purity: >98%), rutin (purity: >98%), vitexin (purity: >98%), *p*-coumaric acid (purity: >98%), sinapic acid (purity: >98%), morin (purity: >98%), coumarin

(purity: >98%), quercetin (purity: >98%), cinnamic acid (purity: >98%), and naringenin (purity: >98%) were obtained from Sigma-Aldrich (St. Louis, MO, USA). All these compounds were used as reference standards. RPMI-1640 medium, fetal bovine serum (FBS), and penicillin-streptomycin were obtained from Gibco BRL (Grand Island, NY, USA).

### 3.1.2 Plant material and preparation of bamboo leaf extracts (BLEs)

Mature leaves obtained from the apical branches of 10 bamboo species belonging to the genus *Guadua* were collected from different locations in Colombia as described in Table 3.1. The voucher species were deposited in the Herbarium of the Pontificia Universidad Javeriana (HPUJ) and determined by Professor Néstor García. The plant materials were dried for 96 h, at 35 °C, in an oven with forced air circulation, followed by ground to a fine powder. The material obtained was subjected to a percolation process with ethanol (plant:solvent, 1:10 *w/v*) at room temperature for 24 h with solvent changes repeating four times. Subsequently, the extract solutions obtained were concentrated on a rotary evaporator under reduced pressure at an average temperature of 35 °C, providing the corresponding BLEs and stored at room temperature until used.

**Table 3.1.** Information for samples used in this study.

| Species | Collection place[a] | Samples code | Voucher number (HPUJ) | Number of samples[b] |
|---|---|---|---|---|
| *G. aculeata* Rupr. ex E. Fourn. | Quindío | *Gac-Q* (1) | HPUJ-30736 | 1 |
| *G. amplexifolia* J.Presl | Quindío | *Gam-Q* (1 to 3) | HPUJ-30733 | 3 |
| *G. angustifolia* Kunth | Cundinamarca | *Gan-C* (1 to 7) | HPUJ-30740 | 7 |
| | Nariño | *Gan-N* (1 to 6) | HPUJ-30722 | 6 |
| | Quindío | *Gan-Q* (1 to 2) | HPUJ-30731 | 2 |
| *G. angustifolia* Kunth biotype *San calixto* | Quindío | *Ganc-Q* (1) | HPUJ-30737 | 1 |

| | | | | |
|---|---|---|---|---|
| *G. angustifolia* var. *bicolor* Londoño | Quindío | *Ganb-Q* (1) | HPUJ-30735 | 1 |
| *G. incana* Londoño | Putumayo | *Gin-P* (1) | HPUJ-30723 | 1 |
| | Quindío | *Gin-Q* (1 to 2) | HPUJ-30723 | 2 |
| *G. superba* Huber | Quindío | *Gsu-Q* (1) | HPUJ-30734 | 1 |
| *G. uncinata* Londoño & L.G.Clark | Quindío | *Gun-Q* (1 to 3) | HPUJ-30730 | 3 |
| *G. venezuelae* Munro | Quindío | *Gve-Q* (1) | HPUJ-30729 | 1 |
| *G. weberbaueri* Pilg. | Quindío | *Gwe-Q* (1) | HPUJ-30738 | 1 |

[a] Information regarding collection sites is provided in Supplementary Material Table S2.2. [b] A total of 30 BLEs were prepared.

### 3.1.3 *Clean-up* of the BLEs

The BLEs were solubilized in methanol:water 95:5 (*v/v*) and a *clean-up* step were performed for biological test and chromatographic analyses. The extracts underwent a *clean-up* step in a solid phase extraction cartridge (Strata X, C18). In this procedure, first the cartridge is packed with 6 volumes (~5 mL) of HPLC grade methanol. Then, the cartridge was equilibrated with 6 volumes of methanol:water solution at 95% and the extract obtained in the previous step was applied. The elution was carried out with 3 mL of 95% methanol:water. The extract obtained was dried by rotary evaporation and stored at room temperature until used for analysis.

### 3.1.4 Preparation of chemical standards and quality control (QC) samples

Chemical standards solutions were prepared as 1 mg/mL solutions in methanol. Multiple QC samples were prepared by pooling and mixing equal volumes of each extracted sample to check system performance and reproducibility in sample analysis. To assess the robustness of the instrument, pooled QC samples were injected prior to the sample analysis until system equilibration was achieved and after every ten randomized sample injections.

### 3.1.5 HPTLC data acquisition

Analyses were performed on an HPTLC equipment (Camag, Muttenz, Switzerland), which included an autosampler (ATS 4), a developer (ADC), a derivatizer (DV), a development chamber, a visualization chamber, and VisionCATS software. Ten µL of the extracts (10 mg/mL in ethanol) were applied as 7 mm bands on the Silica gel 60 $F_{254}$ 10 x 10 cm (Merck, Darmstadt, Germany) plates. Plates were eluted with *n*-hexane/ethyl acetate/Formic acid 10/6/1 (*v/v/v*) for flavonoid aglycones and ethyl acetate/Formic acid/Acetic acid/water 100/11/11/27 (*v/v/v/v*) for flavonoid glycosides in a chamber (20 cm x 10 cm, Camag) followed by air dried. For derivatization, the following reagents were applied through automatic piezoelectric spraying: natural product reagent (1 g 2-aminoethyl diphenyl borate in 100 mL ethanol) (NP/PEG) at UV 365 nm. The software VisionCATS version 3.1.21109.3 controlled the instruments.

### 3.1.6 HPLC-DAD data acquisition

Samples were prepared by weighing 5 mg of each extract and solubilizing them with 1 mL methanol. The chromatograph used was a Shimadzu UFLC system (Shimadzu, Duisburg, Germany) coupled to a diode array detector (DAD, VIS-Shimadzu 1520 PC-Diode Array), pumps model 6-AD Shimadzu SCL-10VP control system, an in-line degasser, and an autosampler. Chromatographic separation was performed on a Luna® C18 column (150 x 4.6 mm, 5 µm, 100 Å) was used to carry on the chromatographic separation at 30 °C. The mobile phase used was eluent A (0.1% formic acid in water, *v/v*) and eluent B (0.1% formic acid in acetonitrile, *v/v*) with flow of 1 mL/min. Gradient elution was performed as follows: 0 to 40 min, 5% to 100% B; 40 to 50 min, 100% B; 50 to 53 min, 100% to 5% B and 53 to 63 min, 5% B. The wavelengths used were 274 and 365 nm, with spectra acquired in a range of 200 to 400 nm. Dereplication studies were performed compared retention times and UV spectrum.

### 3.1.7 UHPLC-QTOF-MS data acquisition

For UHPLC-QTOF-MS analysis, the BLEs were dissolved in methanol at a concentration of 1 mg/mL. Samples were further diluted with methanol to obtain a final concentration of 500 ppm. Analyses were performed on an ACQUITY UPLC System (Waters, Milford, MA, USA) coupled with a Waters Xevo G2-XS QToF Mass Spectrometer. An ACQUITY UPLC HSS T3 C18 column (2.1 × 100 mm, 1.8 µm) from Waters (Waters Corporation, Wexford, Ireland) was used to carry on the chromatographic separation at 30 °C. The mobile phases consisted of eluent A (Water 0.1% formic acid) and eluent B (Acetonitrile 0.1% formic acid) with flow rate of 0.5 mL/min. The gradient was programmed as follows: 10-100% B from 0 to 10 min, 100% B from 10 to 14 min, 100-5% B from 14 to 15 min, 5% B from 15 to 20 min. Mass spectrometry was performed on a Xevo G2-XS QToF instrument using electrospray ionization (ESI). Data mass spectra were acquired in ionization negative (ESI−) and positive (ESI+) modes, in a mass range of m/z 100–1500 Da in data dependent acquisition (DDA) mode at rate was set to 0.1 s scans, followed by an MS/MS scan of the most intense ions. For MS/MS fragmentation, a low collision energy ramp ranging from 10 to 40 eV and a high collision energy ramp ranging from 50 to 80 eV were applied to acquire the data in centroid format. The QTOF instrument was operated at a frequency of 6.0 GHz and 76.0 µs utilizing high resolution calibrated with the reference mass correction for Leucine-enkephalin ($C_{28}H_{37}N_5O_7$) was used as a lock mass compound in positive ion mode ($[M+H]^+$ = 556.2771) and negative ion mode ($[M-H]^-$ = 554.2615), respectively. The spectrometer parameters were as follows: capillary voltage was set to 2.2 kV (ESI−) or 2.6 kV (ESI+), cone voltage was set to 40 V, source temperature was maintained at 120 °C, cone gas was set to 50 L/h, and desolvation gas was set to 800 L/h at 300 °C. Retention time data compared between HPLC-DAD and UHPLC-QTOF-MS analyzes of the reference standards are detailed in Supplementary Material Table S3.3.

### 3.1.8 $^{1}$H-NMR data acquisition

To the BLEs were added 500 µL of methanol-*d*$_4$ ($CD_3OD$) and 200 µL of phosphate buffer ($KH_2PO_4$, 99% anhydrous) in deuterium oxide ($D_2O$) (pH 6.0) from Sigma-Aldrich USA Isotope with 99.8% purity, solution was sonicated (frequency of 50 kHz/20 min) and centrifugated (10.000 rpm/5 min), and 700 µL of the supernatant was transferred to a 5 mm NMR tubes for further 1D NMR analyses. $^{1}$H-NMR spectra were recorded at 25 °C on a Bruker Avance III HD 600 MHz spectrometer (Bruker, Karlsruhe, Germany) operating at a proton NMR frequency of 600.13 MHz. Each $^{1}$H NMR spectrum consisted of 128 scans using the following parameters: 0.16 Hz/point, pulse width (PW) = 30 (11.3 µs), and relaxation delay (RD) = 1.5 s. Free induction decays (FIDs) were Fourier transformed with a line broadening (LB) = 0.3 Hz. Deuterated methanol was used as the internal lock. Chemical shifts were expressed in δ (ppm), and coupling constants were reported in hertz. The $^{1}$H-NMR spectra of some reference standards were included in Supplementary Material Figure S3.7.

### 3.1.9 GNPS classical molecular MS/MS network

The MS/MS data files into mzML format were submitted to the GNPS online platform (http://gnps.ucsd.edu). The molecular networking (MN) of BLEs was obtained using parameters provided in the Supplementary Material, as shown in Table S3.3. For visualization of comprehensive chemical space were incorporated MolNetEnhancer tool. Chemical class annotations were performed using the ClassyFire chemical ontology. The MN for both negative and positive ionization modes are accessible at the GNPS Website under the following links:

Negative mode:
https://gnps.ucsd.edu/ProteoSAFe/status.jsp?task=d4d5f88562114bf0b1a6a8083ecfb166

Positive mode:
https://gnps.ucsd.edu/ProteoSAFe/status.jsp?task=f6f3a908473a462eb8822d718a087d8b

The attribute table of the generated nodes was visualized in the Cytoscape version 3.7.2 software to analyze the molecular network.

### 3.1.10 Antioxidant activity

The assays were carried out in triplicate for all the samples using a single extract concentration of 1 mg/mL (LOZANO-PUENTES et al., 2023) and determined by the azinobis-(ethylbenzothiazoline-6-sulphonic acid) (ABTS) radical scavenging method and scavenging of 1,1-diphenyl-2-picryl-hydrazyl (DPPH) radical assay.

### 3.1.11 ABTS radical cation decolorization assay

The ABTS assay was based on a previously described method (RE et al., 1999). Briefly, a solution of $ABTS^{\bullet+}$ (7 mM) was reacted with a solution of potassium persulfate (2.45 mM) and incubated overnight in the dark to obtain a dark-colored solution containing $ABTS^{\bullet+}$ radical cations. The working solution was prepared by diluting the $ABTS^{\bullet+}$ radical cations solution with methanol to obtain an absorbance of approximately 0.70 ± 0.02 at 745 nm. Then, 294 mL of the working solution was mixed with 6 mL of the extract and left to react for 30 min at room temperature in the dark. The absorbance was measured at 734 nm using a Varioskan Lux ThermoScientific microplate reader and compared with a Trolox calibration curve (0-400 mmol/L, $r^2$= 0.9705).

### 3.1.12 DPPH free radical scavenging activity

The antioxidant capacity of the BLEs was assessed through their ability to scavenge $DPPH^{\bullet}$ radicals, which were dissolved in a purple solution (SAEED; KHAN; SHABBIR, 2012). The stock solution was prepared by dissolving 24 mg DPPH in 100 mL methanol and stored at 20 °C until required. The working solution was obtained by diluting the DPPH solution with methanol to an absorbance of approximately 0.98 ± 0.02 at 517

nm using a spectrophotometer. Subsequently, 280 mL of the working solution was mixed with 20 mL of the extract and left to react for 30 min at room temperature in the dark. The absorbance was measured at 517 nm using a Varioskan Lux ThermoScientific microplate reader and compared with a Trolox calibration curve (0-400 mmol/L, $r^2$= 0.9709).

### 3.1.13 Nitric oxide (NO) inhibitory assay

In this essay, the methodology presented by Marcocci et al (MARCOCCI et al., 1994) with adaptations was used as a basis. The assay is based on the ability of sodium nitroprusside (NPS) molecules (commercial Neon code 02232; São Paulo, Brazil) to release NO spontaneously in PBS buffer when under the influence of light (BATES et al., 1995). NO, in turn, is transformed into nitrite ($NO_2^-$) when reacting with molecular oxygen in the medium and can therefore be quantified by adding Griess reagent (1% *w/v* sulfanilamide, 0.1% *w/v* of naphthyl ethylenediamine and 2.5% *v/v* of ortho-phosphoric acid) (Neon commercial code 02179, 01874 and 00232, respectively, São Paulo, Brazil) to form a pink chromophore with high absorption at 540 nm. To this end, NPS (1.25 mM) was prepared in phosphate buffer (0.1 M and pH 7.0) in the absence of light. In a 96-well plate, 50 µL of NPS and 50 µL of samples at different concentrations (25; 50, 100 and 200 µg/mL) were added and incubated for 40 minutes at room temperature with strong exposure to UV light. After incubation, 100 µL of Griess reagent was added and the reaction mixture was read at 540 nm. A calibration curve was also performed with sodium nitrite ($NaNO_2$) to represent the data in concentration of $NO_2^-$ formed (Figure S3.4).

### 3.1.14 Macrophages cell culture and viability

The murine macrophage cell line RAW 264.7 (ATCC TIB 71) was provided by the cell bank of Rio de Janeiro, Brazil. The cells were maintained in DMEM high glucose medium (Dulbecco's modified eagle medium) (Vitrocell code 02037, Campinas, Brazil) supplemented with 10% fetal bovine serum (FBS) (*v/v*) and incubated in an oven at 37 °C with atmosphere containing 5% $CO_2$ at different periods until reaching confluence of approximately 70-90%. Afterwards, the cells were removed with the aid of a cell scraper (RAW macrophages) and counted in a Neubauer chamber to obtain cell concentration

values. After removing the medium and washing 3 times with PBS, the cells were detached with a cell scraper and counted in a Neubauer chamber. 100 µL of medium containing approximately $50\times10^4$ cells/mL was distributed in microplates (96 wells) incubated under the same conditions as above. After 24 hours, the medium was removed, the wells were washed with PBS 3 times, and each well was treated with 3 concentrations of each sample (50 to 200 µg/mL) in triplicate. After incubation for 24 hours, cell viability was determined by the MTT test (Sigma-Aldrich, St. Louis, USA) (MOSMANN, 1983). The results were presented as mean ± standard deviation.

### 3.1.15 Inhibition of NO produced by macrophages

For NO assays, murine macrophage cultures RAW 264.7 (ATCC TIB-71) were used. Briefly, the cells were distributed in 96-well microplates at a concentration of $5 \times 10^5$ viable cells/well/mL in complete DMEM medium and incubated for 2h (37ºC/5%$CO_2$) for cell adhesion. After this period, the supernatant was discarded, and the cells were washed with sterile PBS. They were then stimulated with *Escherichia coli* Lipopolysaccharide (LPS) (SIGMA code L2630; St. Louis, MO, USA) at a concentration of 1 µg/mL, receiving, at the same time, different concentrations of samples (2 – 200 µg/mL) in supplemented DMEM, being the concentrations previously determined by the cytotoxicity assay. The plates were incubated overnight (37ºC/5%$CO_2$). After this period, culture supernatants were collected for detection and quantification of nitric oxide using the Griess method (GREEN et al., 1982). Data were presented in $NO_2^-$ concentration (mM), using a standard curve for $NaNO_2$. N(ω)-nitro-l-arginine methyl ester (L-NAME) was used as an inhibition control (Figure S3.5). Cytotoxicity evaluations were performed to determine the appropriate non-toxic concentrations of samples and after immunomodulatory assay through MTT method as described in item 3.319.

### 3.1.16 Cell and cell cultures

The human colorectal carcinoma cell line HCT-116 was acquired from the American Type Culture Collection (ATCC, Rockville, MD, USA) and ground under standard cell culture conditions (37 °C, 95% with 5% $CO_2$ atmosphere) in RPMI-1640

medium supplemented with 10% fetal bovine serum (FBS), 2 g/L of $NaHCO_3$, and 1% antibiotics (penicillin and streptomycin).

### 3.1.17 MTT cell viability assay

Colorimetric 3-(4,5-dimethylthiazol-2-yl)-2,5-diphenyltetrazolium bromide (MTT) assay was used to evaluate metabolic activity (MOSMANN, 1983). Almost $1x10^4$ cells per well were seeded in 96-well. 24 h after seeding, the cells were then treated with DMSO 0.05% (vehicle), doxorubicin 10 μM (control), and BLEs at a concentration of 50 and 5 μg/mL (treatments) and incubated at standard cell culture conditions for 72 h again. Subsequently, MTT solution (150 μL, 10%) was added to each control and treated and incubated at again for three h. The medium was then poured out, and solubilization of the crystal formazan dye was done in 200 □L DMSO. The Bio-Tek Synergy HTX multi-mode reader (BioTeck Instruments) was applied to read the absorbance at 570 nm. The percent growth inhibition was calculated by the following formula:

$$\%\ growth\ inhibition = \frac{Absorbance\ of\ sample}{Absorbance\ of\ control}\ \mathrm{x}\ 100$$

To determine dose-response curves (percentage cell survival versus concentration) and to obtain the $IC_{50}$ (the minimum concentration of each ethanol extract that provides 50% survival of HCT-116 cells) value the extracts that exceeded 85% inhibition of cell growth were prepared across a range of concentrations from 0.78 to 50 μg/mL, following the same procedure explained above. Data were determined in three independent biological replicates, each with technical quadruplicates. $IC_{50}$ curves and values of the extracts were calculated by using GraphPad Prism version 8.0.2 software (San Diego, CA, USA) using sigmoidal dose–response curve fitting (variable slope, four parameters).

### 3.1.18 Statistical analysis

All results are represented as the mean ± standard deviation (SD) of triplicate data. Differences observed between the doses were achieved by one-way analysis of variance (ANOVA) followed by Tukey's pot hoc test and values of * $p$ value ≤ 0.05 and ** $p$ value ≤ 0.01 were considered significant. Statistical analyses were performed using GraphPad Prism version 8 software (La Jolla, California, USA).

### 3.1.19 Data processing and biochemometric analysis

The raw UHPLC-QTOF-MS data files were converted into mzML format using the MSConvert tool from the ProteoWizard software (version 3.0, Palo Alto, CA, USA) to separate negative and positive ionization modes. The files were processed in MZmine version 2.53 (http://mzmine.github.io/download.html), including feature detection, chromatogram builder, deconvolution, deisotopes, alignment, filtering, and gap filling whose parameters summarized in Supplementary Material Table S3.4. The list of data information, including $t_R$-$m/z$ (characterize the detected ions) and normalized peak area were exported as .csv files and manually inspected to eliminate noise and presence filter was applied. The features that were present in 100% of the samples and had a coefficient of variation in the QC of less than 20% were used for statistical analysis.

The raw $^1$H NMR spectra were imported into NMRProcFlow version 1.4.20 (https://www.nmrprocflow.org) for ppm calibration, baseline correction, alignment, spectra bucketing, and data normalization whose parameters summarized in Supplementary Material Table S3.5. Regions at $\delta_H$ 4.85 – 4.95 and $\delta_H$ 3.25 – 3.35 ppm were removed from the analysis due to residual solvents signals of $D_2O$ and $CD_3OD$, respectively. Spectra bucketing utilized the intelligent bucketing method and variable size bucketing, encompassing the full range of $\delta_H$ 0.40 – 10.0 ppm.

Statistical analysis was performed with the SIMCA-P+ software version 13.0.3 (Umetrics, Umeå, Sweden). The multivariate analysis allowed the generation of the PCA, PLS-DA, and OPLS-DA models. The OPLS-DA model was validated by cross-validation

less than 0.05, and quality was evaluated based on parameters $R^2X$, $R^2Y$, and $Q^2$. The groups were compared to determine the significantly differential metabolites by calculating the variable importance in the projection (VIP) combined with FC > 2.0 or FC < 0.5. Annotated metabolites were organized in a table (.csv) containing the peak area were uploaded at MetaboAnalyst 5.0 software – statistical, functional, and integrative analysis of metabolomics data (https://www.metaboanalyst.ca/) was used visualization for heatmap clustering (PANG et al., 2022), normalized by Pareto scaling. Univariate analysis was performed to determine the *p*-value features.

### 3.1.20 Metabolite identification

Differential metabolite annotation was performed considering the precision of the mass (maximum error of mass 10 ppm), isotopic pattern distribution, and adduct formation, using different public online databases such as METLIN (http://metlin.scripps.edu), KEGG (http://genome.jp/kegg), HMDB (https://hmdb.ca/), PubChem (https://pubchem.ncbi.nlm.nih.gov/) and ChEBI (https://www.ebi.ac.uk/chebi/) through the CEU Mass Mediator (http://ceumass.eps.uspceu.es/) tool. The identity of the metabolites was confirmed through MS/MS analysis, which included the use of MS-DIAL 4.80 (http://prime.psc.riken.jp/compms/msdial/main.html), MS-FINDER 3.52 (http://prime.psc.riken.jp/compms/msfinder/main.html), SIRIUS 5.5.7 (https://bio.informatik.uni-jena.de/software/sirius/), CFM-ID 4.0 (https://cfmid.wishartlab.com/) for in silico mass spectral fragmentation, GNPS web platform (https://gnps.ucsd.edu/ProteoSAFe/static/gnps-splash.jsp) and manual interpretation with the MassLynx software version 4.01 (Waters Company, Milford, MA, USA). Additionally, were created *in-house* library was created with metabolites reported of bamboo species (Subfamily: Bambusoideae). The tentative identification of compounds was performed using the molecular masses, together with the fragmentation patterns, and data from literature. The metabolites were identified according to Metabolomics Standards Initiative (MSI) (BLAŽENOVIĆ et al., 2018). The workflow used in this study is summarized in Figure 3.1.

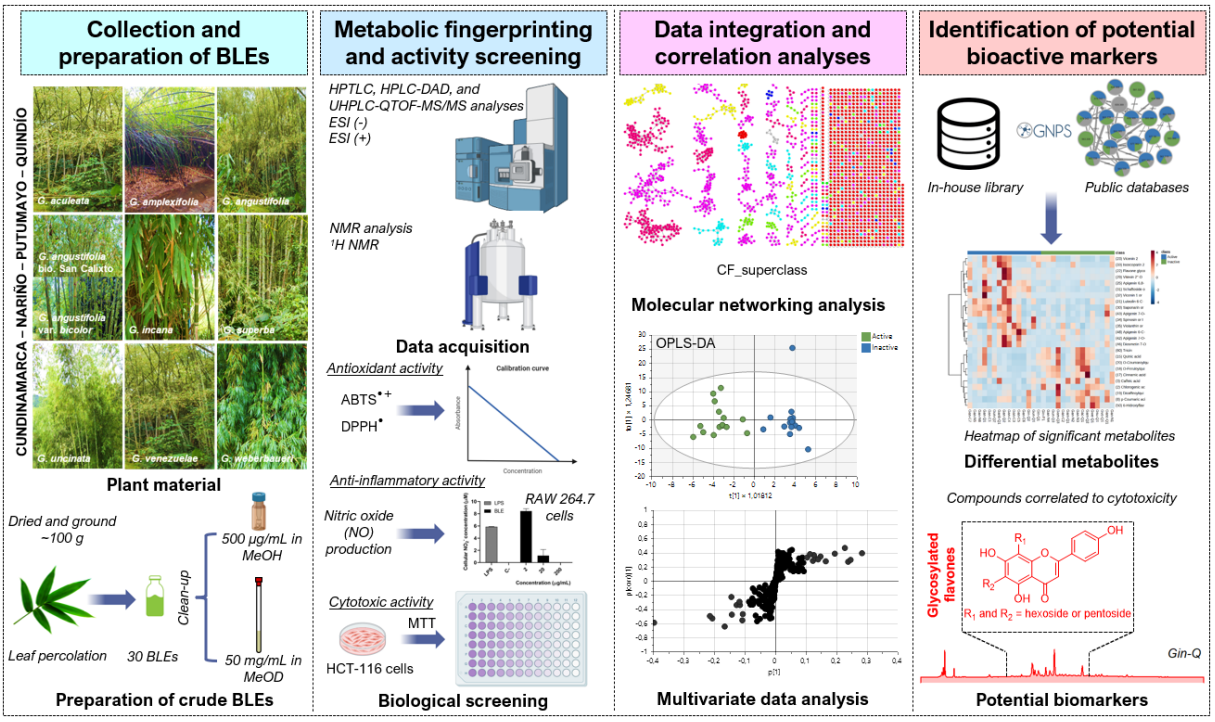



**Figure 3.1.** Workflow of the metabolomics strategy implemented for the identification of candidate bioactive compounds. All images were acquired at the author's expense using the results provided by Simca 18.0 and MetaboAnalyst 5.0. Some images were created using BioRender, while others were obtained from the internet under the rights of use granted by a Creative Commons License.

## 3.2 Results and discussion

### 3.2.1 HPTLC and HPLC-DAD phytochemical profiling analysis

A previous study conducted on bamboos belonging to the genus *Guadua*, using an untargeted metabolomics approach to determine the changes in chemical composition under the influence of altitudinal variation, showed that these bamboos have a high chemical composition, specifically of phenolic compounds, encompassing flavonoids in both their aglycone and glycosidic forms, accounting for 48% of their total chemical makeup (CHITIVA et al., 2023). These findings enabled us to conducted targeted chemical profiling in this study, aiming to dereplication for known compounds using specific commercial chemical standards related to flavonoids and phenolic acid derivatives (**1-14**) via high-performance thin-layer chromatography (HPTLC) and high-performance liquid chromatography coupled with diode array detector (HPLC-DAD).

Figure 3.3A-B shows the chromatographic profiles obtained by HPTLC for the extracts of *Guadua* species collected at thirteen distinct locations, as detailed in Table 2. Figure 3.2A presents the chemical profile of the flavonoid aglycones, while Figure 3.2B presents the flavonoid glycosides alongside the reference standards quercetin (**12**) and rutin (**6**), respectively.

Moreover, the plates were eluted based on the polarity of these compounds, then sprayed with the natural products-polyethylenglycol reagent (NP/PEG) and developed at a wavelength of UV-365 nm (WAGNER et al., 1996). From the results, it is evident that the extracts contain a limited number of flavonoid aglycones, while a higher quantity of flavonoid glycosides is emphasized, as confirmed by the presence of yellow and orange fluorescent bands. The retention factor ($R_f$) values for reference standards **12** and **6** were 0.58 and 0.62, respectively. *G. incana* (*Gin*-*Q*) is the species that exhibits a significant number of flavonoid glycosides compared to the other species, which are found in lower proportions. In this study, it was observed that flavonoid glycosides exhibit considerable variability among different extracts and are distinguished based on collection sites. This finding is consistent with earlier preliminary studies that revealed a higher accumulation of these compounds in these bamboos considered as giant grasses (MOSQUERA MARTÍNEZ et al., 2012).

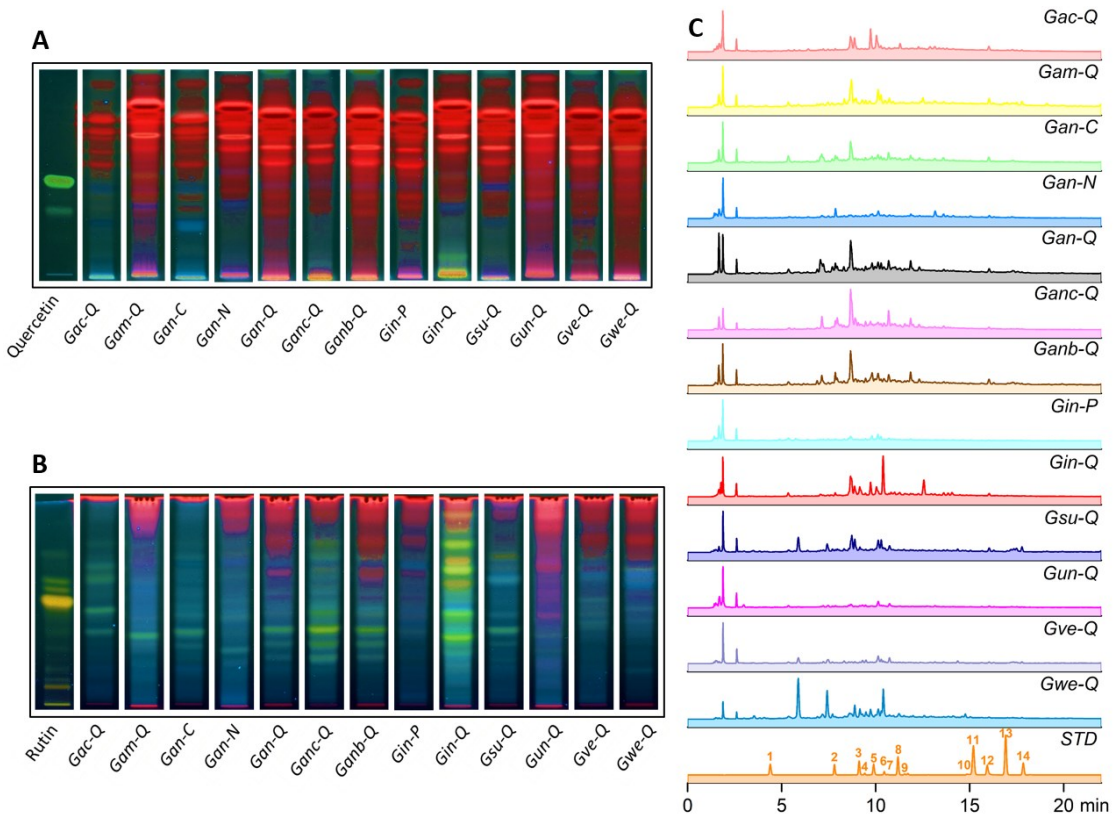



**Figure 3.2.** HPTLC chromatographic profiles for **(A)** flavonoid aglycones and **(B)** flavonoid glycosides. HPLC-PDA chromatograms of the BLEs were expanded from 0 to 23 minutes at **(C)** 274 nm. Chemical standards (STD): Gallic acid (**1**, $t_R$ = 4.36 min), Chlorogenic acid (**2**, $t_R$ = 7.72 min), Caffeic acid (**3**, $t_R$ = 9.08 min), Isoorientin (**4**, $t_R$ = 9.39 min), Ampelopsin (**5**, $t_R$ = 9.88 min), Rutin (**6**, $t_R$ = 10.42 min), Vitexin (**7**, $t_R$ = 10.56 min), *p*-Coumaric acid (**8**, $t_R$ = 11.15 min), Sinapinic acid (**9**, $t_R$ = 11.55 min), Morin (**10**, $t_R$ = 14.79 min), Coumarin (**11**, $t_R$ = 15.19 min), Quercetin (**12**, $t_R$ = 15.86 min), Cinnamic acid (**13**, $t_R$ = 16.84 min), and Naringenin (**14**, $t_R$ = 17.75 min). Column: Luna C18 column (150 x 4.6 mm, 5 µm, 100 Å); mobile phase: (A) 0.1% formic acid in water and (B) 0.1% formic acid in acetonitrile, 5-40% B (0-23 min); flow rate: 1 mL/min; detection wavelength: 274 nm. UV spectra were obtained by PDA detection. Chemical profiles were plotted by selecting one sample for each collection site and the different species (*n* = 13) according to the coding in Table 2.

Figure 3.2C shows the chromatographic profiles obtained by HPLC-DAD for the thirteen extracts. We emphasize that between 5 and 12 minutes, a significant portion of the chemical composition of these extracts is observed, primarily comprising flavonoid glycosides and phenolic acid derivatives. The identification of these compounds was confirmed through ultraviolet spectra analysis (Supplementary Material Figure S3.1). Most of the peaks exhibited two distinctive absorption bands characteristic of flavonoids, corresponding to band I (240-285 nm) and band II (300-560 nm) (FALCONE FERREYRA;

RIUS; CASATI, 2012; MA et al., 2011). The presence of phenolic acid derivatives was also determined by the characteristic band with a shoulder (sh) between 290-310 nm (HOLSER, 2012). From the dereplication study of BLEs, chlorogenic acid (CGA) (**2**) was identified in the *G. weberbaueri* species with a retention time ($t_R$ = 7.72 min) and an ultraviolet spectrum with absorption at 326 nm and a shoulder peak (sh) at 292 nm, which was compared with the commercial chemical standard and reports in the literature.(BELAY; GHOLAP, 2009) This compound is reported for the first time in this species. However, it has been previously reported in other bamboo species (CHENG et al., 2023; JIANG et al., 2019). The remaining reference compounds were not found in any of the other species. Nevertheless, it can be inferred that these species may contain compounds related to flavonoid glycoside and phenolic acid derivatives scaffolds, based on the absorption bands observed in the ultraviolet spectra (Supplementary Material Figure S3.1).

### 3.2.2 UHPLC-QTOF-MS-based metabolic fingerprinting analysis

A comprehensive metabolic fingerprinting was conducted on the BLEs using UHPLC-QTOF-MS in both negative and positive modes. Initially with the MS/MS data, an analysis was conducted on the GNPS platform to visualize the chemical composition of the global metabolome of BLEs. The comprehensive analysis in Figure 3.3A-B highlights the presence of molecular families (MF), mainly corresponding to phenylpropanoids and polyketides, lipids and lipid-like molecules, organic acids and derivatives, organoheterocyclic compounds, and organic oxygen compounds for both ionization modes. Notably, in the positive ionization mode, the MF of phenylpropanoids and polyketides, including flavonoids and derivatives of cinnamic, benzoic, and carboxylic acids, are most abundant. In contrast, in the negative ionization mode, the MF of lipids and related molecules predominates to a greater extent. However, the prevalence of phenylpropanoid and polyketide MFs also stands out. These findings are consistent with a recent study involving 111 bamboo plant samples, which confirmed the presence of some of the MFs reported here. Furthermore, they underscore the prevalence of

phenylpropanoid and polyketide MFs, indicating the presence of flavonoids and cinnamic acid derivatives, primarily (CHITIVA et al., 2023).

The structures of the compounds representing the major detected peaks are discussed below. The identification of the detected compounds was based on a search for the main molecular ions (MS) and on some of the informative fragmentations observed (MS/MS), along with the use of standards when available, retention data, UV absorption, comparison with literature data, GNPS web platform, and public databases.

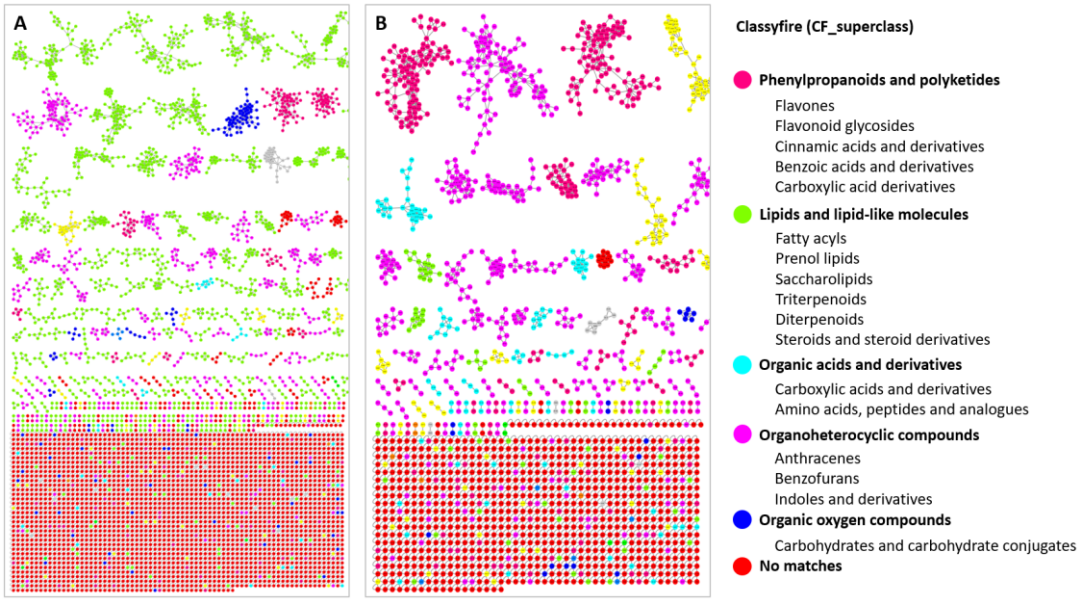



**Figure 3.3.** Representative MolNetEnhancer mass spectral molecular networking of consortium showing the chemical CF_superclasses in negative **(A)** and positive **(B)** electrospray ionization modes of BLEs based on UHPLC-QTOF-MS. This annotated based GNPS library matches with network annotation (NAP) and DEREPLICATOR outputs.

In the present work, 49 phytochemical compounds (**2**, **3**, **8**, and **15-60**) have been tentatively characterized in the BLEs. Notably, there is a presence of 40 flavonoids and 9 cinnamic acid and derivatives, listed in Supplementary Material Table S3.1 and represented with the retention time in the base peak intensity (BPI) chromatograms of the quality control (QC) samples of the extracts, presented in Figure 3.4A-B for the negative and positive ionization modes, respectively. Importantly, many of these compounds are being reported for the first time within the genus, marking novel discoveries. Furthermore,

certain compounds have been previously identified in other species of the subfamily Bambusoideae. The structures of the tentatively characterized compounds are presented in Supplementary Material Figure S3.2, where the MS/MS spectrum of several of them were determined based on the data obtained from UHPLC-QTOF-MS analysis of the studied extract, as illustrated in Supplementary Material Figure S3.3. An extensive study of some of the compounds characterized according to their families is described below.

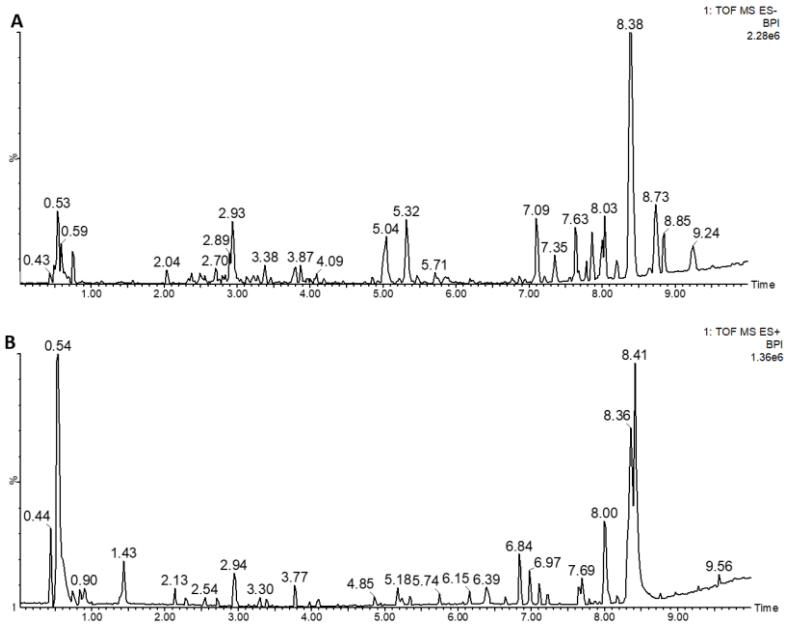



**Figure 3.4.** Representative UHPLC-QTOF-MS base peak intensity chromatograms of the QC samples of the BLEs in negative **(A)** and positive **(B)** ions. The retention times of the compounds that could be annotated in the BLEs are shown in Table S3.1.

### 3.2.3 Flavonoids

We report the identification of 40 flavonoids in the leaves of various extracts of *Guadua*. Of the identified scaffolds, five groups were found corresponding to 12 with apigenin skeleton (**23**, **25**, **29**, **30**, **31**, **32**, **34**, **35**, **42**, **43**, **48** and **54**), 5 with kaempferol skeleton (**36**, **37**, **38**, **57** and **58**), 3 with luteolin skeleton (**21**, **44** and **49**), 2 with quercetin skeleton (**39** and **40**), 2 with tricin skeleton (**51** and **60**) and 2 with naringenin skeleton (**52** and **53**). Most of them had *C*-glycosidized substituents at the C6 and C8 positions on the A-ring of the aglycone, while others had *O*-glycosidized substituents at the C7 and C3 positions of the corresponding aglycone. Flavonoids **33**, **41**, **45**, **46** and **47** also presented

*C*- and *O*-glycosidic substituents corresponding to other scaffolds, some of them with glycosidic substituents on the B-ring of the aglycone. The presence of three aglycones corresponding to one flavone **50** and 2 flavonols **55** and **59** was also identified. The presence of isoflavone **56** was also determined. Additionally, 5 compounds (**22**, **24**, **26**, **27**, and **28**) were found to be classified as unknown flavone glycosides based on their UV spectra and fragmentation patterns. These results were corroborated with the ultraviolet spectra obtained and compared with reports in literature where the range of flavones ($\lambda_{max}$ ≈ 275 and 335 nm), flavonols ($\lambda_{max}$ ≈ 275 and 355 nm), and flavanones ($\lambda_{max}$ ≈ 275 and 340 nm) is highlighted (GAGLIANO et al., 2022a).

Compound **31** exhibited a precursor ion at *m/z* 563.1406 $[M-H]^-$ and $MS^2$ fragments at *m/z* 473 $[M-H-90]^-$ derived from the possible loss of five water molecules, 443 $[M-H-120]^-$, 383 $[M-H-180]^-$, 353 $[M-H-210]^-$, 325 $[M-H-238]^-$, 297 $[M-H-266]^-$ derived from cross-ring cleavages of the respective sugars (hexoside and pentoside) present. Additionally, it displayed a precursor ion at *m/z* 565.1563 $[M+H]^+$ with $MS^2$ fragments at *m/z* 547 $[M+H-18]^+$, 529 $[M+H-36]^+$, 499 $[M+H-66]^+$, 457 $[M+H-108]^+$, 427 $[M+H-138]^+$, 379 $[M+H-186]^+$. These results were consistent with those reported by Jiang *et al*. in 2019, and the compound was identified as isoschaftoside (JIANG et al., 2019). This compound is a type of flavone *C*-glucoside previously reported in species such as *Phyllostachys pracecox*, *Phyllostachys edulis*, *Olyra glaberrina*, *Parodiolyra micrantha*, *Aulonemia aristulata*, *Filgueirasia arenicola*, *Filgueirasia cannavieira*, and *Merostachys pluriflora* (GAGLIANO et al., 2022a).

Compound **48** was identified as Apigenin 6-*C*-hexoside 7-*O*-hexoside with *m/z* 593.1511 $[M-H]^-$. The $MS^2$ fragment at *m/z* 473 $[M-H-120]^-$ is a typical loss of *C*-linked hexose and the base peak at *m/z* 431 $[M-H-162]^-$ refers to the loss of a hexose indicating an *O*-glycosylation. These two fragments show the presence of two hexose units identifying the apigenin scaffold. Additionally, fragments *m/z* 353, 341, 311, 283 derived from cross-ring cleavages of the hexoside part of the flavonoid glycosyl moiety and the loss of several water molecules, respectively. For bamboo species this compound is reported for the first time. This compound is a *C*,*O*-glycosidic flavone type reported in a

study conducted for leaf extracts of *Passiflora incarnata*, *Passiflora caerulea*, and *Passiflora alata* species. In this study, they demonstrated the potent cytotoxic effect of *P. alata* and *P. incarnata* extracts against human acute lymphoblastic leukemia CCRF-CEM, mainly attributed to the content of phenolic compounds, specifically to the high content of flavones C-glycosides with scaffold related to apigenin and luteolin (OZAROWSKI et al., 2018). According to the flavonoids identified and because the majority correspond to flavone *C*-glycosides (Supplementary Information Table S3.1) details the corresponding MS/MS fragment ions that for most of the molecules present the occurrence of the characteristic ions, e.g., $[M-H-150]^-$, $[M-H-120]^-$, $[M-H-90]^-$, $[M-H-66]^-$, $[M-H-60]^-$, and $[M-H-36]^-$, corresponding to the cross-ring cleavages of the hexoside and pentoside part of the flavonoid glycosyl moiety and characteristics of *C*-glycosides.

Compound **54** possesses a precursor ion *m/z* 269.0455 $[M-H]^-$ with $MS^2$ fragments *m/z* 151 $[M-H-188]^-$, 117 $[M-H-152]^-$, and 107 $[M-H-151-CO_2]^-$ corresponding to retro-Diels-Alder (RDA) cleavage accompanied by loss of $CO_2$. These results were consistent with those reported by Troalen *et al*. (2012), (TROALEN et al., 2014) and the compound was identified as apigenin. The quercetin scaffold derived from flavone *C*-glucosides presented the product ion *m/z* 301 $[M-H]^-$ mainly presents five $MS^2$ fragment ions with *m/z* 273 $[M-H-28]^-$, 179 $[M-H-122]^-$, 151 $[M-H-150]^-$, 121 $[M-H-180]^-$, and 107 $[M-H-194]^-$ being a product of RDA cleavage and CO and $CO_2$ loss, respectively. Some quercetin derivatives have been reported for bamboo species such as *G. angustifolia* (CHITIVA et al., 2023; MORALES NOREÑA; SANCHEZ VALLEJO, 2008). Bamboo species are known to accumulate phenolic compounds, mainly glycosylated flavones whose aglycones normally are apigenin, luteolin, and tricin. The most common flavonoids found in Asian bamboo species are the flavone *C*-glucosides (GROMBONE-GUARATINI et al., 2021; VAN HOYWEGHEN et al., 2010, 2012).

### 3.2.4 Phenolic acid derivatives

Nine phenolic acids were identified in BLEs of eight (8) *Guadua* species. Two phenolic acids including chlorogenic acid (CGA) (**2**), caffeic acid (**3**), and *p*-coumaric acid

(**8**) were identified by comparison with authentic standards. Additionally, based on literature reports, three other phenolic acid derivatives were also identified. Compounds **18**, **19**, and **20** were recognized as derivatives of caffeoylquinic acid (CQAs) and named *O*-Feruloylquinic acid, Dicaffeoylquinic acid, and *O*-Coumaroylquinic acid, respectively. Compounds **16** and **17** were identified to chemical class designated as not identified. Finally, compound **15** identified as quinic acid (QA) was present in all species. QA has been recently reported in *G. angustifolia* being one of the metabolites that showed a significant increase at high altitudes in these species.(CHITIVA et al., 2023)

Compound **2** presented the precursor ion M-H at *m/z* 353.0531 $[M-H]^-$ and showed $MS^2$ fragments at *m/z* 191 $[M-H-162]^-$, formed by the cleavage of the ester bond between the quinic acid and caffeic acid residues, and the ion *m/z* 179 [M-H-174] which loses a portion of carbon dioxide to produce the ion *m/z* 135 [M-H-44]. This report is consistent with the identification based on the $MS^2$ spectrum (Supplementary information Figure S3.3) of the CGA pattern, together with that reported by Reis Luz *et al*. (2018).(DOS REIS LUZ et al., 2018) Although chlorogenic acid is a new compound reported for 4 *Guadua* species, it has been found in other bamboo species such as *Sasa argenteastriatus*, *Phyllostachys nigra* var. *henonis* and *P. pubescens*.(CHOI et al., 2018; NI et al., 2012; TANAKA et al., 2014)

### 3.2.5 NMR-based metabolomic fingerprinting analysis

Representative $^1$H-NMR spectra obtained from BLEs are shown in Figure 3.5. The analysis of the $^1$H-NMR spectral dataset led to the identification of representative metabolite signals in the samples. Fingerprinting analysis revealed that BLEs mainly contained compounds related to three specific regions corresponding to aliphatic compounds, glycosidized compounds, and aromatic compounds. Signals in the region between $\delta_H$ 0.90 and 1.50 ppm were assigned to aliphatic compounds, specifically fatty acids and related molecules, determined by methyl ($-CH_3$) and methylene ($-CH_2$) proton signals, as confirmed by the allylic region of the aliphatic chains between $\delta_H$ 2.29 and 2.75 ppm.

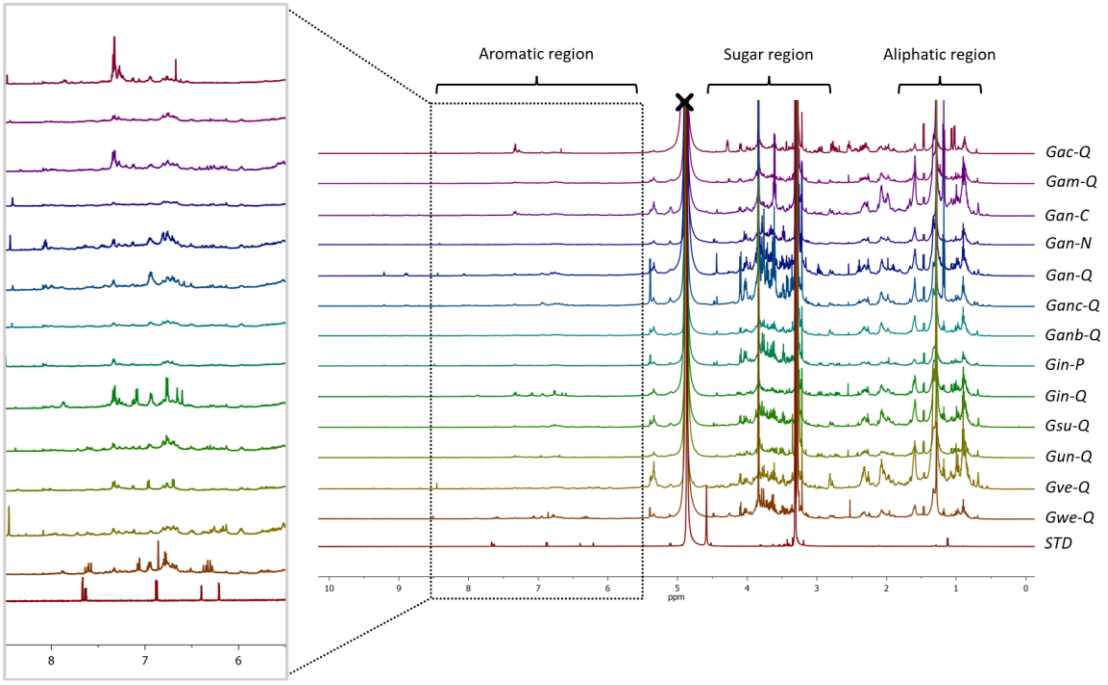



**Figure 3.5.** Stacked representative $^{1}$H-NMR spectra of BLEs are presented. The panels display the partial assignment of aliphatic ($\delta_H$ 0.90 – 1.50 ppm), sugar ($\delta_H$ 3.00 – 5.50 ppm), and aromatic ($\delta_H$ 6.50 – 8.55 ppm) regions, respectively. An expanded spectral region from $\delta_H$ 5.50 to 8.50 ppm is shown for aromatic compounds. Assignments were established by extracting signals with reference standards (STD) and base on literature reports on the NMR spectra.

The signals between $\delta_H$ 3.00 and 5.50 ppm assigned to glucoside compounds were primarily determined by the anomeric signals of the sugar compounds. Mainly, the anomeric protons of glucose in $\beta$ position with $\delta_H$ 4.58 (d, $J$ = 7.6 Hz) and in the $\alpha$ with $\delta_H$ 5.15 (d, $J$ = 3.5 Hz) were extracted and assigned. According to our results, this sugar is present in most of the flavonoids previously found and described in Supplementary Material Figure S3.2, confirming the respective structure annotations. It is important to note that, due to the nature of an extract, many of the signals overlap in the spectrum. However, some of the signals extracted in this study were confirmed and compared with available reference compounds. The $^{1}$H-NMR spectra in the aromatic region between $\delta_H$ 6.85 and 8.05 ppm revealed the presence of phenolic compounds, primarily related to flavonoids and phenolic acids. The presence of aromatic protons at $\delta_H$ 6.26 (d, $J$ = 2.20 Hz, 1H), 6.44 (d, $J$ = 2.22 Hz, 1H), 6.96 (d, $J$ = 8.90 Hz, 2H), and 7.84 (d, $J$ = 8.90 Hz, 2H) distinctive signals corresponding to a flavonoid-type scaffold derived from apigenin with

substitutions at the C6 and C8 positions particularly stands out. Representative $^{1}$H-NMR signals were assigned as described in Table 3.1.

### 3.2.6 Antioxidant capacity of BLEs

The results of the ABTS and DPPH assays are presented in Figure 3.6. Among the 30 extracts tested, most exhibited significant antioxidant potential at the tested concentration of 1 mg/mL. It is evident that these extracts displayed robust antioxidant activity in both the ABTS and DPPH assays, which can be attributed to their high phenolic compound content. The activity was expressed as µmol TE/g extract. Phenolic compounds constitute one of the main groups of compounds known to act as important antioxidants because they usually possess an aromatic ring that allows the stabilization and relocation of the unpaired electrons of their structure, thus facilitating the donation of hydrogen atoms and electrons from their hydroxyl groups.(PLATZER et al., 2022; ZEB, 2020) In our study, two methods were used to quantify the antioxidant capacity of the 30 selected BLEs. When considering the antioxidant activity determined by ABTS, the species with the highest values were *G. amplexifolia* J. Presl (*Gam-Q1*, *Gam-Q2*, and *Gam-Q3*), *G. angustifolia* (*Gan-C4*, *Gan-C7*, *Gan-N2*, *Gan-N4*, *Gan-N5*, *Gan-N6*, and *Gan-Q1*), *G. incana* (*Gin-P1*, *Gin-Q1*, and *Gin-Q2*), *G. uncinata* Londoño & L.G. Clark (*Gun-Q2*), and *G. venezuelae* Munro (*Gve-Q1*), with 149.7, 148.5, 146.6, 149.7, 124.0, 133.5, 140.4, 126.4, 122.0, 192.8, 145.2, 200.2, 144.9, 152.6, and 149.1 µmol TE/g extract, respectively. Regarding the antioxidant activity determined by DPPH in each of the BLEs, the extracts with the highest antioxidant values were *G. amplexifolia* (*Gam-Q1*), *G. angustifolia* (*Gan-C4* and *Gan-N1*), *G. angustifolia* (*Ganc-Q1*), *G. incana* (*Gin-Q1*), and *G. superba* Huber (*Gsu-Q1*), with 54.5, 48.1, 44.4, 50.7, 61.1, and 58.5 µmol TE/g extract, respectively. Phenolic compounds and flavonoids, widely distributed as secondary metabolites in most plants, are important due to their ability to act as antioxidants. Many phenolic compounds have been reported to possess potent antioxidant activity, which may also be associated with anticancer, antibacterial, antiviral, or anti-inflammatory properties to varying degrees.(ABOU BAKER, 2022; KUMAR; PANDEY, 2013; PANCHE; DIWAN; CHANDRA, 2016) The findings of this work demonstrate that BLEs possess

antioxidant potential, aligning with data collected for certain bamboo leaf species such as *G. angustifolia*(VALENCIA et al., 2011), which reported antioxidant capacity in their extracts at an evaluated concentration of 50 mg/mL. Another study determined the antioxidant potential of bamboo vinegar obtained through a pyrolysis process from *G. angustifolia*, showing a DPPH radical uptake of 940.2 µmol/L TEAC.(ARBOLEDA ECHAVARRÍA; JARAMILLO YEPES; PALACIO TORRES, 2012)

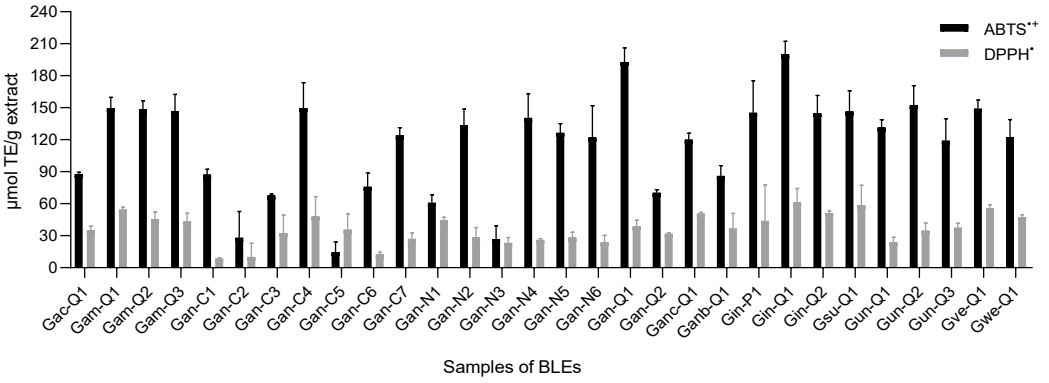
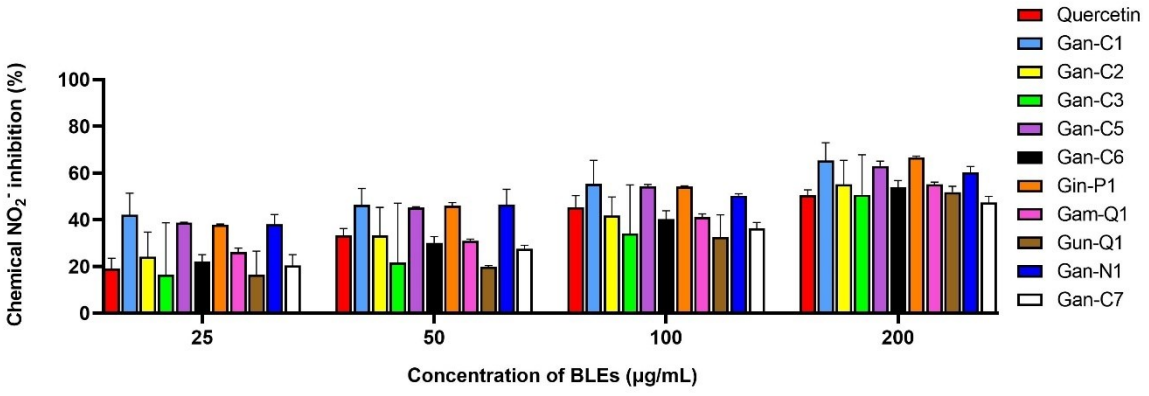



**Figure 3.6.** Antioxidant activity is determined for BLEs. The ABTS and DPPH of the BLEs results was expressed as µmol Trolox equivalents per gram of extract (µmol TE/g extract).

In addition to its use in Asian folk medicine, the dry leaves of *Sasa veitchii* bamboo are used as a source of antioxidant food supplements in Japan. In addition, the Chinese Food Additives Standardization Committee approved an extract of *Phyllostachys nigra* var. *henonis* known as antioxidant of bamboo leaves (AOB) as a novel kind of natural antioxidant, due to its potent antioxidant capacity attributed to phenolic compounds.(VAN HOYWEGHEN et al., 2010; VAN HOYWEGHEN; DEFORCE; HEYERICK, 2010) Such products derived from bamboo extracts, along with the increased production of reactive oxygen species (ROS), are believed to play a significant role in preventing disease development and reducing the impact of oxidative stress when disease occurs (CHOI et al., 2018; YU et al., 2019).

### 3.2.7 Anti-inflammatory activity of BLEs

Inflammation is a defense mechanism involving various physiological and pathological processes within an organism induced by tissue injury caused by biological, chemical, or physical damage. Activation of various immune cells (monocytes and macrophages) produces various inflammatory mediators, such as nitric oxide (NO), cyclooxygenase-2, prostaglandins E2 and other pro-inflammatory cytokines, including tumor necrosis factor-alpha (TNF-α) and interleukins. NO is strongly associated with inflammation, where uncontrolled production of these species is linked to several diseases, including cancer. Consequently, the effect of BLEs on NO inhibition was evaluated. Chemical NO levels were expressed as a percentage inhibition of nitrite ion ($NO_2^-$) determined spectrophotometrically by means of a calibration curve with sodium nitrite ($NaNO_2$) (Supplementary information Figure S3.4). Figure 3.7 shows the results of the percentage inhibition of chemical NO obtained from the BLEs at different concentrations of 25, 50, 100 and 200 µg/mL, respectively. The results show that the species corresponding to *G. angustifolia* (*Gan-C1*, *Gan-C5*, *Gan-N1*, *Gan-Q2* and *Ganc-Q1*), *G. incana* (*Gin-Q1*, *Gin-P1* and *Gin-Q2*), *G. uncinata* (*Gun-Q2*) and *G. superba* (*Gsu-Q1*) showed inhibition percentages higher than 60% at the maximum concentration evaluated (200 µg/mL).



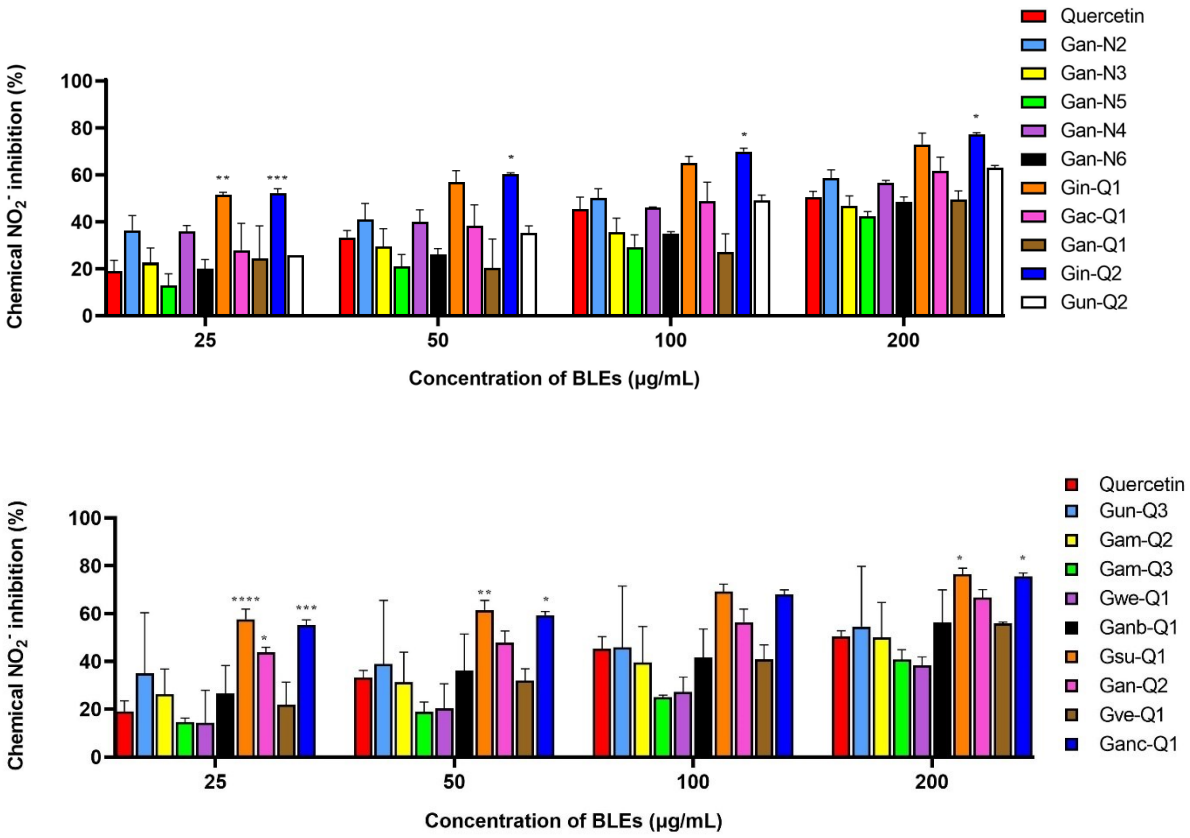



**Figure 3.7.** Determination of the percentage of chemical inhibition of NO by BLEs evaluated at four concentrations (25, 50, 100 and 200 µg/mL). One-way ANOVA analysis using Tukey's post hoc test was employed to indicate significance, denoted as follows: * $p < 0.05$, ** $p < 0.01$ and *** $p < 0.001$ compared to quercetin.

It is important to note that macrophages play a crucial role in inflammation processes and this cellular response is initiated by bacterial lipopolysaccharide (LPS), which is part of the outer membrane of gram-negative bacteria, interferon-γ (IFN-γ) and proinflammatory cytokines. Therefore, considering the previously determined anti-inflammatory potential, the effect of BLEs on RAW 264.7 macrophage cells was determined *in vitro*. Initially, we assessed the cytotoxic effect of BLEs on macrophage cells using a cell viability assay performed by MTT test. The results showed that none of the extracts exhibited cytotoxicity at the highest concentration evaluated (200 µg/mL). Table 3.2 presents the $IC_{50}$ values determined for each BLEs.

**Table 3.2.** Evaluation of the cytotoxic effect of BLEs against RAW 264.7 macrophage cells.

| Samples | $IC_{50}$ (µg/mL) | Samples | $IC_{50}$ (µg/mL) |
|---|---|---|---|
| *Gan-C1* | >200 | *Gin-P1* | >200 |
| *Gan-C2* | >200 | *Gac-Q1* | >200 |
| *Gan-C3* | >200 | *Gan-Q1* | >200 |
| *Gan-C5* | >200 | *Gin-Q2* | >200 |
| *Gan-C6* | >200 | *Gun-Q2* | >200 |
| *Gin-Q1* | >200 | *Gun-Q3* | >200 |
| *Gam-Q1* | >200 | *Gam-Q2* | >200 |
| *Gun-Q1* | >200 | *Gam-Q3* | >200 |
| *Gan-N1* | >200 | *Gwe-Q1* | >200 |
| *Gan-C7* | >200 | *Ganb-Q1* | >200 |
| *Gan-N2* | >200 | *Gsu-Q1* | >200 |
| *Gan-N3* | >200 | *Gan-Q2* | >200 |
| *Gan-N5* | >200 | *Gve-Q1* | >200 |
| *Gan-N4* | >200 | *Ganc-Q1* | >200 |
| *Gan-N6* | >200 | | |

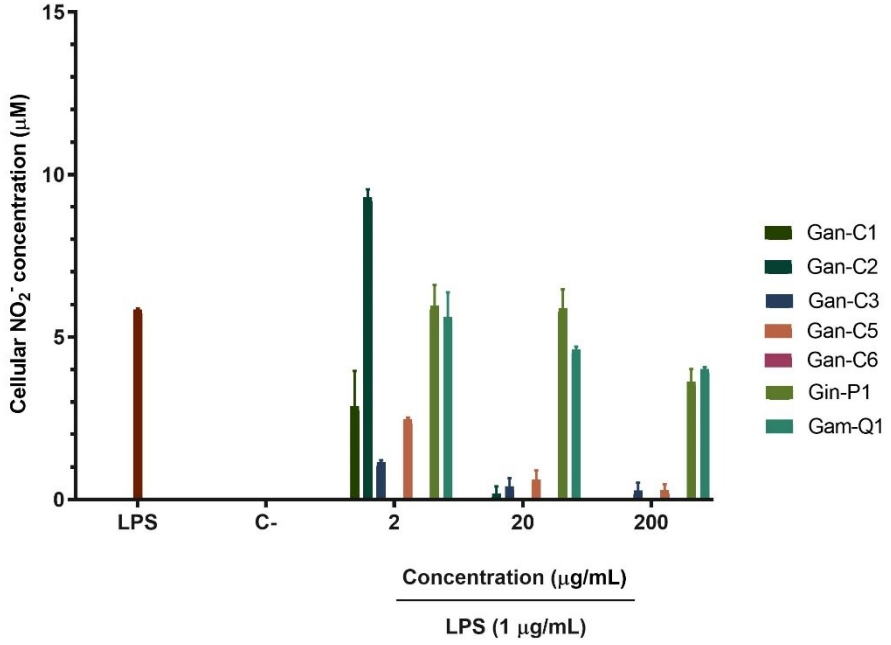
Cellular NO was also evaluated in RAW 264.7 macrophage cells. For cellular NO production inhibition tests, concentrations of 2, 20 and 200 µg/mL were used. The results are shown in % inhibition in Table 3.3 for each concentration. N(ω)-nitro-l-arginine methyl ester (L-NAME) was used as an inhibition control, and the results are presented in Supplementary information Table S3.2. The results demonstrate that the species *G. aculeata* (*Gac-Q1*), *G. angustifolia* (*Gan-C1*, *Gan-C6*, *Gan-N1*, *Gan-C7*, *Gan-N2*, *Gan-N3*, *Gan-N4*, *Gan-N5*, *Gan-N6*, *Ganb-Q1*, *Gan-Q2* and *Ganc-Q1*), *G. incana* (*Gin-Q1* and *Gin-Q2*), *G. uncinata* (*Gun-Q1*, *Gun-Q2* and *Gun-Q3*), *G. superba* (*Gsu-Q1*) and *G. venezuelae* (*Gve-Q1*) exhibited inhibition percentages higher than 85% at the maximum concentration evaluated (200 µg/mL).

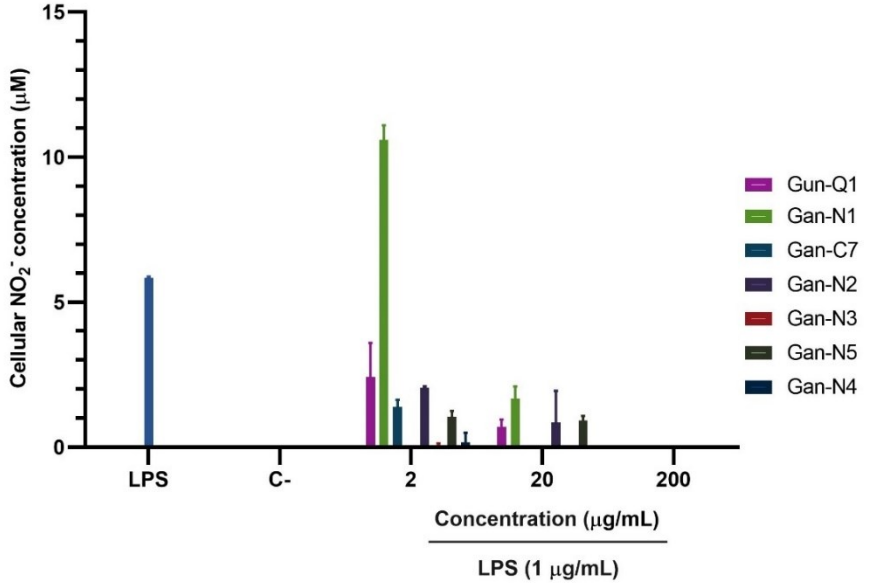
**Table 3.3.** Effect of BLEs on NO inhibition in LPS-stimulated RAW 264.7 macrophage cells.

| Samples | Concentrations tested (µg/mL) | | |
|---|---|---|---|
| | 2 | 20 | 200 |
| *Gan-C1* | 34.7 % ± 4.3 | 92.3 % ± 3.7 | 94.2 % ± 3.1 |
| *Gan-C2* | 0 | 67.7 % ± 3.5 | 74.5 % ± 3.6 |
| *Gan-C3* | 52.4 % ± 1.02 | 61.8 % ± 0.9 | 64.1 % ± 0.62 |
| *Gan-C5* | 31.4 % ± 1.02 | 60.9 % ± 4.6 | 65.9 % ± 2.8 |
| *Gan-C6* | 72.5 % ± 1.5 | 81.9 % ± 0.5 | 100 % ± 0.89 |
| *Gin-Q1* | 0 | 52.2 % ± 1.05 | 93.0 % ± 3.01 |
| *Gam-Q1* | 0 | 0 | 6.5 % ± 1.02 |
| *Gun-Q1* | 35.5 % ± 0.7 | 54.3 % ± 4.6 | 92.0 % ± 0.1 |

| | | | |
|---|---|---|---|
| *Gan-N1* | 0 | 41 % ± 0.1 | 97 % ± 2.7 |
| *Gan-C7* | 42 % ± 4.6 | 72 % ± 1.4 | 98.5 % ± 0.7 |
| *Gan-N2* | 29.5 % ± 0.7 | 63 % ± 2.8 | 100 % |
| *Gan-N3* | 75 % ± 1.4 | 100 % | 100 % |
| *Gan-N5* | 48 % ± 3.5 | 50.3 % ± 2.9 | 93.7 % ± 3.5 |
| *Gan-N4* | 67 % ± 4.2 | 82.5 % ± 3.5 | 84 % ± 1.4 |
| *Gan-N6* | 68.6 % ± 0.1 | 82.8 % ± 7.4 | 98.5 % ± 1.05 |
| *Gin-P1* | 0 | 0 | 15.6 % ± 5.0 |
| *Gac-Q1* | 61.7 % ± 5.8 | 100 % | 100 % |
| *Gan-Q1* | 60.4 % ± 0.74 | 66.4 % ± 1.05 | 79.9 % ± 1.3 |
| *Gin-Q2* | 84.3 % ± 0.1 | 85.8 % ± 5.2 | 86.6 % ± 1.05 |
| *Gun-Q2* | 67.5 % ± 3.7 | 78.4 % ± 2.11 | 85.3 % 3.4 |
| *Gun-Q3* | 70.1 % ± 0.1 | 75.3 % ± 5.2 | 100 % |
| *Gam-Q2* | 66.2 % ± 4.9 | 67.3 % ± 1.49 | 80.6 % ± 1.04 |
| *Gam-Q3* | 56.7 % ± 3.5 | 79.5 % ± 6.0 | 79.5 % ± 1.99 |
| *Gwe-Q1* | 65.4 % ± 4.9 | 72.9 % ± 4.4 | 80.6 % ± 2.5 |
| *Ganb-Q1* | 69.0 % ± 2.9 | 72.8 % ± 1.5 | 100 % |
| *Gsu-Q1* | 73.2 % ± 1.5 | 92.5 % ± 2.8 | 100 % |
| *Gan-Q2* | 66.5 % ± 3.5 | 84.1 % ± 3.5 | 100 % |
| *Gve-Q1* | 63.7 % ± 2.5 | 72.9 % ± 3.5 | 100 % |
| *Ganc-Q1* | 23.23 % ± 0.1 | 69.7 % ± 4.2 | 94.1 % ± 2.8 |

Figure 3.8 shows the NO concentrations (in μM) determined at different concentrations for the BLEs. It is noteworthy that at the maximum evaluated concentration of 200 μg/mL, the following species *G. aculeata* (*Gac-Q1*), *G. amplexifolia* (*Gam-Q3*), *G. angustifolia* (*Gan-C5*, *Gan-C3*, *Gan-N1*, *Gan -C7*, *Gan-N2*, *Gan-N3*, *Gan-N4*, *Gan-N2*, *Gan-Q1*, *Gan-N6*, *Gan-Q2* and *Ganc-Q1*), *G. uncinata* (*Gun-Q1*, *Gun-Q2* and *Gun- Q3*), *G. incana* (*Gin-P1* and *Gin-Q2*), *G. superba* (*Gsu-Q1*) and *G. venezuelae* (*Gve-Q1*) exhibited concentrations lower than 2 μM, indicating low levels of cellular NO concentrations in the RAW 264.7 macrophage cells.


15
10
5
0
Cellular $NO_2^-$ concentration (μM)
LPS
C-
2
20
200
Concentration (μg/mL)
LPS (1 μg/mL)
Gan-C1
Gan-C2
Gan-C3
Gan-C5
Gan-C6
Gin-P1
Gam-Q1


15
10
5
0
Cellular $NO_2^-$ concentration (μM)
LPS
C-
2
20
200
Concentration (μg/mL)
LPS (1 μg/mL)
Gun-Q1
Gan-N1
Gan-C7
Gan-N2
Gan-N3
Gan-N5
Gan-N4

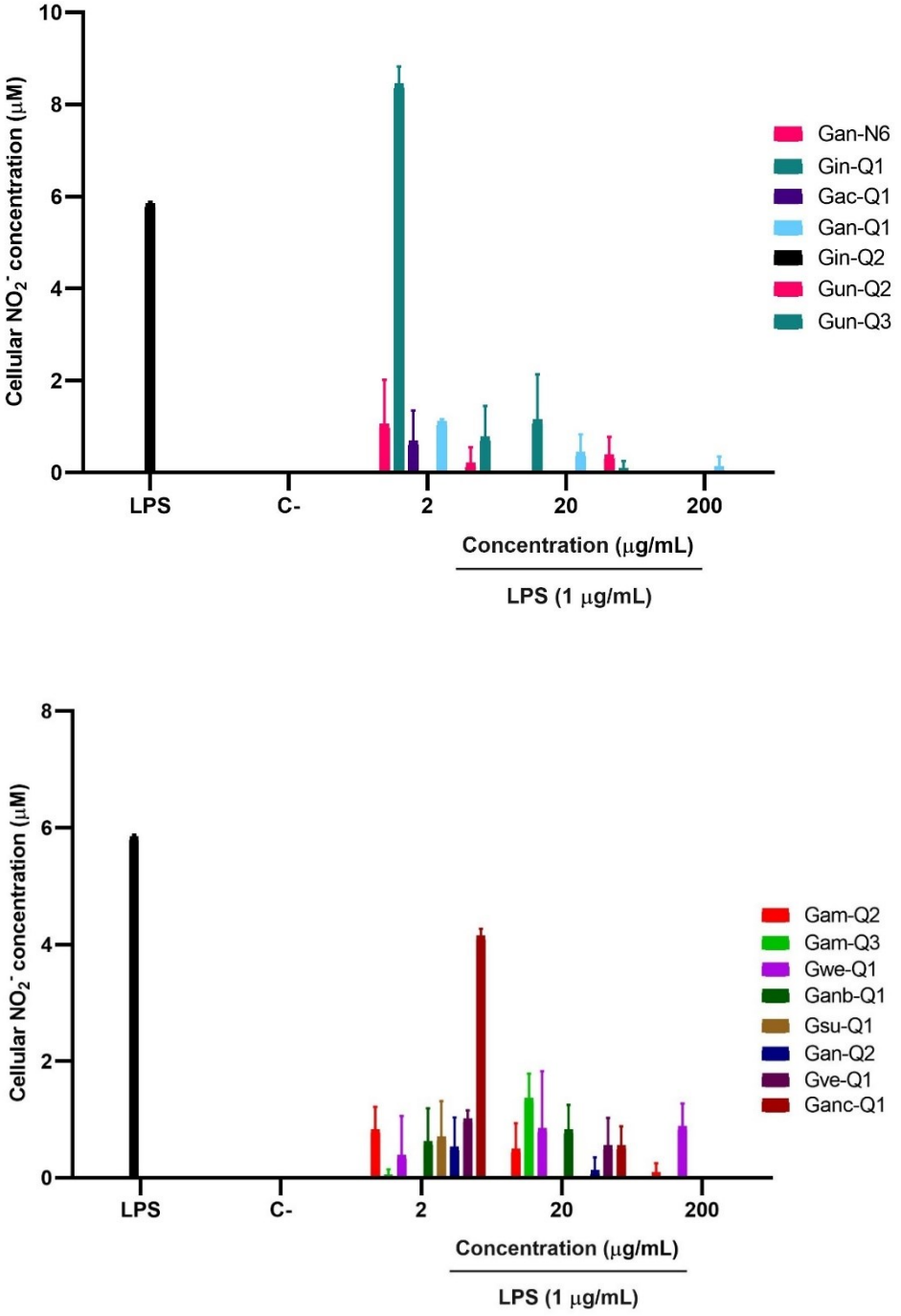



**Figure 3.8.** Cellular concentration of NO in the murine cell line RAW 264.7 stimulated with LPS after treatment with BLE, evaluated at three concentrations (2, 20 and 200 μg/mL).

In general, BLEs showed significant results in inhibition NO production, with most of the extracts exhibiting inhibition greater than 60%. This is considered an important

finding, given that NO is a factor involved in tumor progression. Considering the results obtained from chemical NO and cellular NO, it is possible to infer that the samples can capture NO and inhibiting iNOS (inducible nitric oxide synthase). This is the first report of anti-inflammatory activity described for these *Guadua* species.

### 3.2.8 Cytotoxic activity of BLEs

To determine the cytotoxic activity, two concentrations 5 and 50 µg/mL of the extracts were tested against HCT-116 colon cancer cells. Figure 3.9 shows the percentage inhibition of the exposure of each of the extracts against the cell line. Out of the thirty extracts evaluated against the cell line, it is notable that fifteen of them exhibited an inhibition percentage greater than 85%, meeting the criteria for activity established according to the National Cancer Institute (NCI) guidelines at the maximum evaluated concentration (50 µg/mL).(BAHARUM et al., 2014; NORDIN et al., 2018) It should be noted that *G. angustifolia* (*Gan-C4*) and *G. incana* (*Gin-Q1*) demonstrated the highest inhibition percentages in cell growth, with values of 97.7% and 96.1%, respectively.

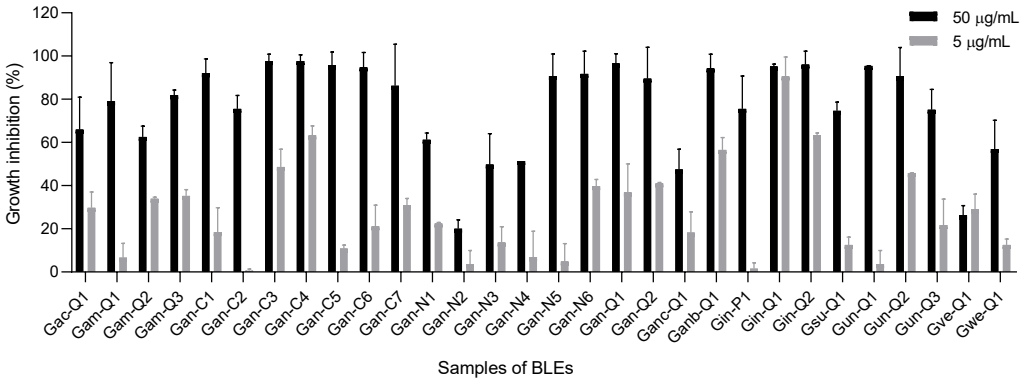



**Figure 3.9.** Percentage growth inhibition of BLEs evaluated at 50 and 5 µg/mL against HCT-116 (colorectal carcinoma) using MTT assay after 72 hours of exposure. The percentage inhibition was calculated based on the growth of untreated cells. Data presented as mean ± SEM (standard error of the mean) from three independent duplicate experiments. All experiments utilized 0.05% DMSO (vehicle) and doxorubicin (DOXO) as negative and positive controls, respectively. Samples are considered active with an inhibition percentage higher than 85%. An extract was deemed active if it exhibited an inhibition of tumor cell lines >85% at 50 µg/mL.

Figure 3.10 displays the dose-response curves featuring $IC_{50}$ values of the extracts. Overall, it is evident that *G. amplexifolia*, *G. angustifolia*, *G. angustifolia* var. *bicolor*, *G. incana*, and *G. uncinata* species exhibited a significant cytotoxic effect on HCT-116 colon cancer cell lines, with $IC_{50}$ values below 50 µg/mL. Conversely, *G. aculeate* E. Fourn., *G. angustifolia* biotype San Calixto, *G. superba*, *G. venezuelae*, and *G. weberbaueri* did not demonstrate such an effect, displaying $IC_{50}$ values above 50 µg/mL. According to the criteria established by the NCI, plant extracts are categorized into four groups: highly active ($IC_{50} \leq 20$ µg/mL), moderately active ($IC_{50} > 21$-49 µg/mL), and weakly active ($IC_{50} > 50$ µg/mL). Cytotoxic analysis revealed that five extracts, corresponding to *G. amplexifolia* (*Gam-Q3*), *G. angustifolia* (*Gan-C4* and *Gan-Q2*), and *G. incana* (*Gin-Q1* and *Gin-Q2*), demonstrated a high cytotoxic effect with $IC_{50}$ values of 14.1, 4.73, 11.34, 1.23, and 17.6 µg/mL, respectively. Additionally, ten extracts showed a moderate effect, including *G. amplexifolia* (*Gam-Q1*), *G. angustifolia* (*Gan-C1*, *Gan-C3*, *Gan-C7*, and *Gan-N6*), *G. angustifolia* var. *bicolor* (*Ganb-Q1*), *G. incana* (*Gin-P1*), and *G. uncinata* (*Gun-Q1*, *Gun-Q2*, and *Gun-Q3*), with $IC_{50}$ values of 41.6, 49.4, 27.8, 40.5, 32.2, 48.05, 44.9, 39.4, 36.1, and 48.6 µg/mL, respectively. The remaining fifteen extracts exhibited a weak cytotoxic effect. This is the first report describing the cytotoxic activity of eight (8) *Guadua* species extracts. We emphasize that, according to our results, these bamboos the *Guadua* species from this reserach represent a potential source for the search for cytotoxic candidates. Notwithstanding the absence of reports on this biological activity, it is noteworthy that, in general, bamboo species exhibit anticancer effects, which are directly associated with the high content of polyphenols found in these plants species.(CHENG et al., 2023; GAGLIANO et al., 2022b)

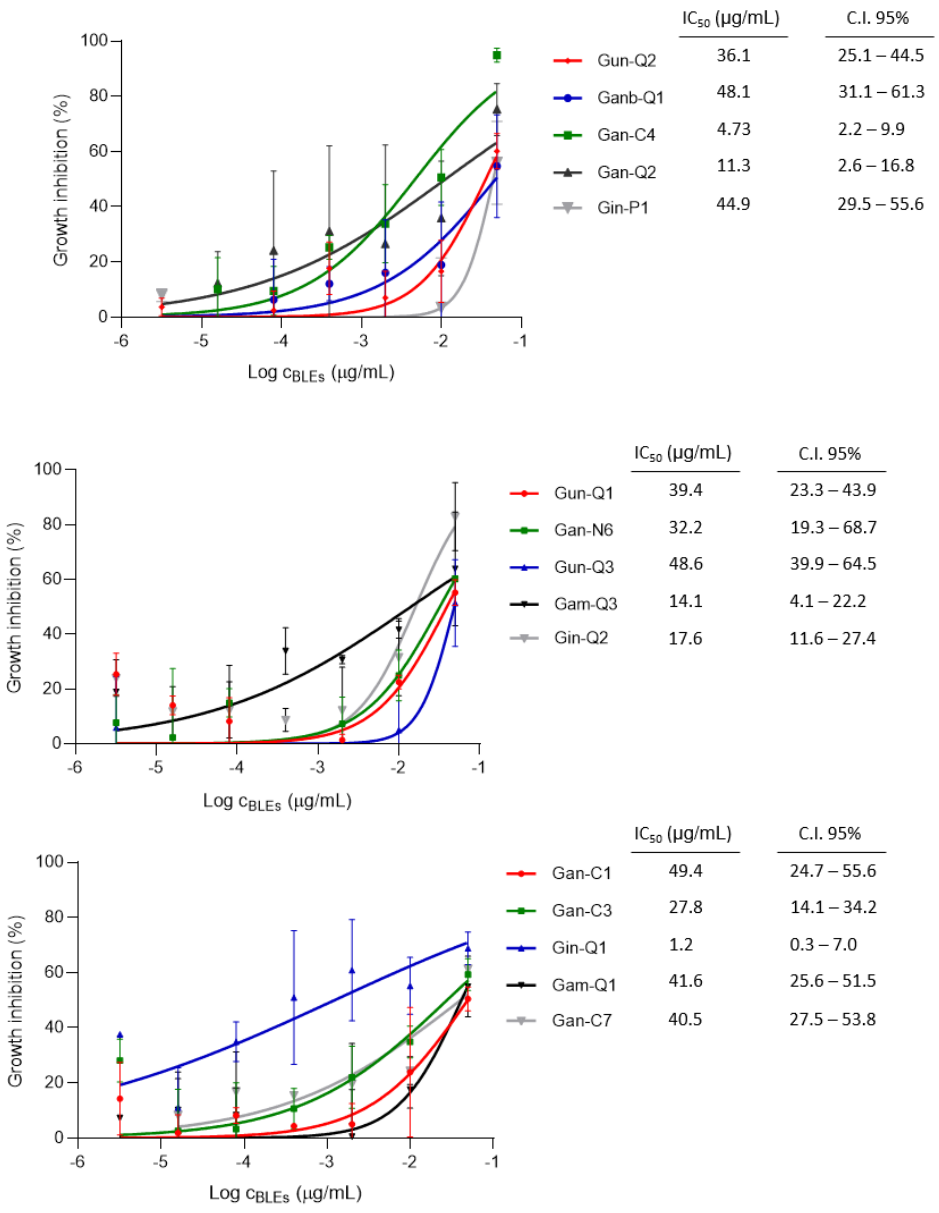



**Figure 3.10.** Dose-response curves of the cytotoxicity of HCT-116 cells after 72 h treatment with the BLEs using concentrations of 0.78-50 µg/mL. The data represent the mean of three independent biological replicates with at least technical duplicates ± SEM (standard error of the mean). All experiments employed 0.05% DMSO (vehicle) and doxorubicin (DOXO) ranging 0.00064 to 10 µM with $IC_{50}$ = 0.2 µM (C.I 95% 0.14 – 0.25) as negative and positive controls, respectively.

Previous studies in other bamboo species have reported cytotoxic activity, for example, in the crude methanol extract obtained from the skin of the shoots of the bamboo *Phyllostachys heterocycla*. The crude extract was evaluated against five cell lines-four of

them tumorigenic (HepG2, HeLa, A549, and MCF-7) and one non-tumorigenic cell line. The results showed that the crude extract presented a moderate cytotoxic effect against HepG2 and MCF-7, with $IC_{50}$ values of 48.4 and 38.9 µg/mL, respectively, while against HeLa it showed a weak effect with an $IC_{50}$ value of 50 µg/mL.(ABDELHAMEED et al., 2022) In a more recent study on *P. heterocycla* var. *pubescens*, the cytotoxic effect was evaluated against the crude methanol extract and the fractions obtained from *n*-hexane, ethyl acetate, and *n*-butanol, targeting five cell lines: HepG2, HeLa, A549, MCF-7, and THP-1. It was reported that the *n*-butanol fraction exhibited inhibition percentages exceeding 60% against all cell lines at the maximum concentration of 100 µg/mL. Notably, the *n*-butanol fraction demonstrated the highest inhibition at 94.31% against the HeLa cell line. (ABDELHAMEED et al., 2021)

### 3.2.9 Correlation-based untargeted metabolomics analysis

The correlation study based on the chemical composition of the extracts and antioxidant activity allowed us to determine that most of the BLEs showed high antioxidant capacity, which was related to the high content of phenolic compounds present in the eight (8) *Guadua* species. Notably, the extracts that had a high content of flavonoids, as determined by HPTLC and HPLC-DAD analyses, were the ones that exhibited the highest antioxidant capacity, with *G. incana* and *G. angustifolia* species standing out. Figure 3.11 shows the relationship between antioxidant activity values and the chemical composition of the BLEs through a Pearson's simple correlation coefficients. We can observe a positive statistical relationship between the two activity variables with respect to metabolites, with a correlation coefficient of 0.50 for most of them. We noticed a significant increase in both variables in relation to the activity, which is closely related to the composition.

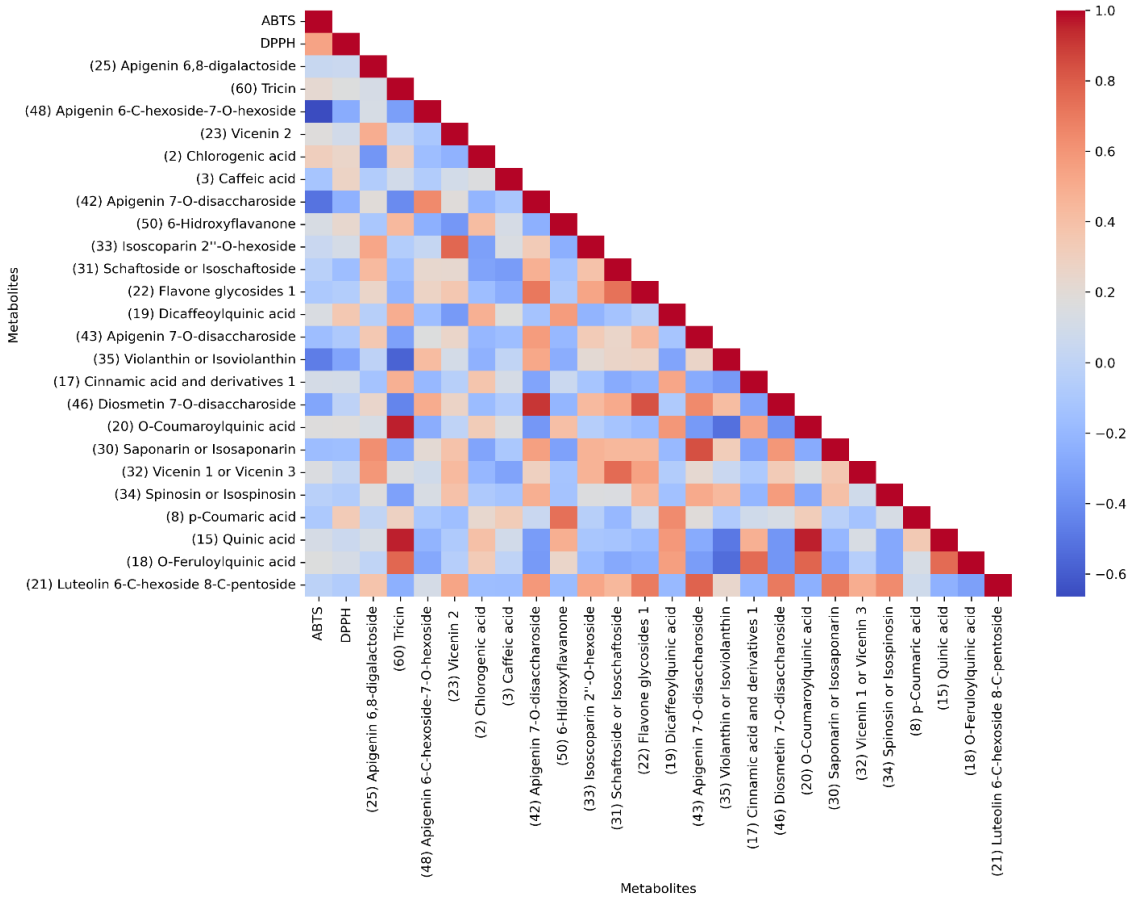



**Figure 3.11.** Heatmap representation of the Pearson's simple correlation coefficients for the top 24 statistically differential metabolites and antioxidant activities monocation of ABTS and DPPH of BLEs. The interpretation of the r values corresponds to very weak or no correlation (-0.65 to 0.00 or 0.00 to 0.25); weak correlation (0.25 to 0.50); moderate correlation (0.50 to 0.75) and strong or perfect correlation (0.75 to 1.00).

Figure 3.12 shows the relationship between anti-inflammatory activity values and the chemical composition of BLEs through simple Pearson correlation coefficients. We observe a positive statistical relationship between the anti-inflammatory activity variable and the metabolites, with a correlation coefficient higher than 0.50 for most of them. There is a significant increase in both variables in relation to activity, which is closely related to composition. From the correlation, metabolites positively correlated with activity stand out, including some flavonoids, particularly flavone glycosides.

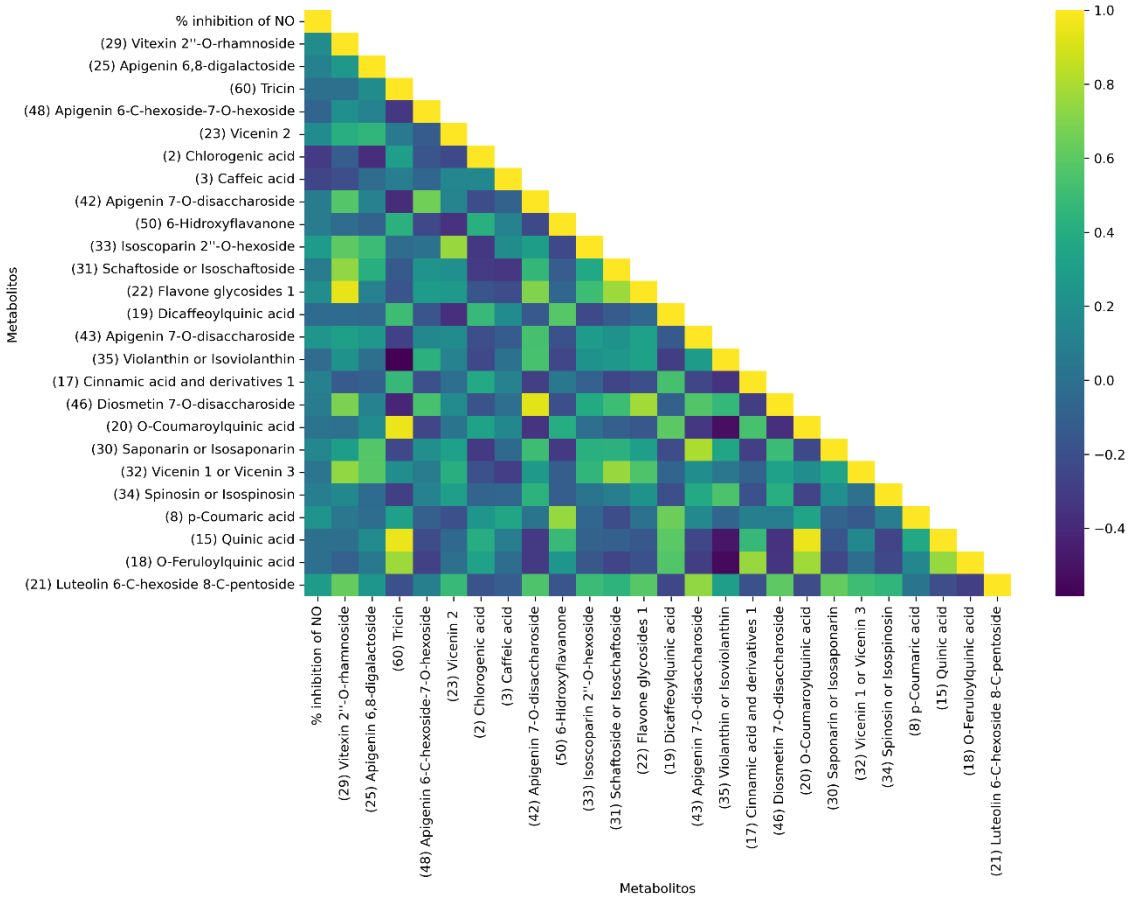



**Figure 3.12.** Heatmap representation of the Pearson's simple correlation coefficients for the top 24 statistically differential metabolites and the anti-inflammatory activity of BLEs. Interpretation of the r values corresponds to very weak or no correlation (-0.45 to 0.00 or 0.00 to 0.25); weak correlation (0.25 to 0.50); moderate correlation (0.50 to 0.75) and strong or perfect correlation (0.75 to 1.00).

To identify the differential metabolites associated with cytotoxic potential, a multivariate analysis was conducted to correlate the bioactivity data with the metabolic fingerprinting obtained from UHPLC-QTOF-MS and $^{1}$H-NMR (Figure 3.13A-B). Initially, an unsupervised principal component analysis (PCA) was employed to assess the quality and stability of the instrumental platform. Supporting Information Figure S3.6 illustrates the clustering of the QC samples, demonstrating the reproducibility of the analysis. For a detailed investigation of the correlation between bioactivity and metabolites, a supervised orthogonal partial squares discriminant analysis (OPLS-DA) analysis was applied, allowing discrimination of activity variability among samples. Figure 3.13A represent the

OPLS-DA plots for the UHPLC-QTOF-MS data in both negative and positive modes, as well as the $^{1}$H-NMR data. Notably, these plots highlight the discrimination between active and inactive sample groups within the specified activity range (>85% at 50 µg/mL with $IC_{50}$ <50 µg/mL). The established supervised models were validated through a permutation test, which assesses the quality of fit and predictive capability. In the case of cytotoxic activity against the colon cancer cell line (HCT-116), the $R^2X_{(cum)}$, $R^2Y_{(cum)}$, and $Q^2_{(cum)}$ values obtained from the OPLS-DA analysis were deemed acceptable, demonstrating excellent reproducibility and predictability on the analytical platforms used.

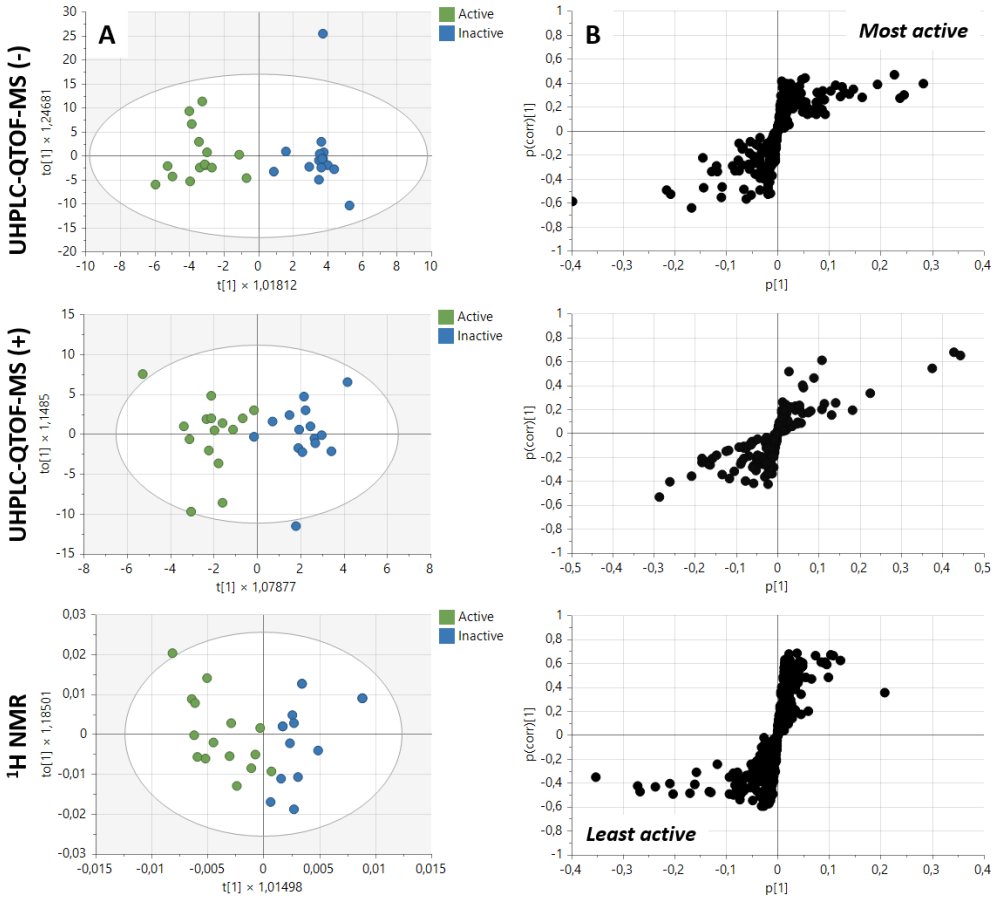



**Figure 3.13. (A)** OPLS-DA score plot demonstrating distinct separation between active (green) and inactive (blue) extracts against the colon cancer cell line (HCT-116). **(B)** S-loading plot depicting metabolites highly correlated with HCT-116 cytotoxicity. The prediction and quality values of the OPLS-DA model for each platform used were as follows: UHPLC-QTOF-MS (-) = $R^2X$(cum): 0.382; $R^2Y$(cum): 0.895; $Q^2$(cum): 0.226; UHPLC-QTOF-MS (+) = $R^2X$(cum): 0.216; $R^2Y$(cum): 0.795; $Q^2$(cum): 0.578, and $^{1}$H NMR = $R^2X$(cum): 0.815; $R^2Y$(cum): 0.680; $Q^2$(cum):

0.393. The corresponding loading plot displays metabolites on the right that contributed the most to activity and on the left the metabolites that contributed least to activity.

The variable importance in projection (VIP) plot was generated to calculate the influence intensity and interpretability of each metabolite's expression mode in distinguishing and classifying sample groups. In this case, this analysis facilitated the prediction of metabolites responsible for the activity, based on statistically significant changes between active and inactive sample groups. The s-plot is presented in Figure 3.13B, highlighting variables with a VIP score > 1.5, which serves as the prediction threshold. Additionally, we can observe regions where samples share a group of metabolites that contributed to cytotoxic activity to a lesser extent, and another region with metabolites contributing more significantly to cytotoxic activity. According to the above and from the OPLS-DA analysis, 27 differential metabolites were found between the active vs. inactive BLEs, as summarized in Table 3.5. These findings are linked to the MFs identified in the analysis conducted by MolNetEnhancer. Of the metabolites that correlated with the cytotoxic potential, it was found that flavone glycosides were the ones that statistically contributed to the bioactivity in the platforms used. In the case of UHPLC-QTOF-MS, it was evident that the noted flavonoids were those that correlated positively with cytotoxicity, while for $^{1}$H-NMR, the signals present in the aromatic and sugar regions ($\delta_H$ 6.50 – 8.50 ppm and $\delta_H$ 3.00 – 5.50 ppm, respectively in the identified buckets) showed a positive correlation. These results are consistent with those reported for a wide variety of flavonoid glycosides that exhibit cytotoxic activity against various cell lines, including MCF-7, HCT-116, HepG2, HeLa, among others.(SAK, 2014) We found that flavone glycosides particularly showed a positive relationship with increased cytotoxic activity, whereas caffeoylquinic acids did not.

**Table 3.4.** Significantly differential major metabolites correlating with cytotoxic activity determined by OPLS-DA model for UHPLC-QTOF-MS and $^{1}$H-NMR analysis. Direction of comparison: Active/Inactive. Statistical parameters: CV threshold < 20% for QC; FC threshold > 1 (increased

activity ↑) and FC threshold < 1 (decreased activity ↓); VIP threshold > 1 and *p*-value threshold < 0.05.

| Compound number | RT (min) | $\delta_H$ (ppm) | Multiplicity, *J* in Hz | Type of hydrogen | CV[a] for QC (%) | FC[b] | VIP[c] | *p*-value[d] |
|---|---|---|---|---|---|---|---|---|
| **2st** | 2.46 | 7.05<br>6.82 | d, *J* = 2.0 Hz<br>d, *J* = 7.6 Hz | Quinic acid derivatives aromatic, Ar-H | 7.25 | 0.35 ↓ | 1.86 | 3.67E-02 |
| **3st** | 2.74 | 7.10<br>6.75 | d, *J* = 2.0 Hz<br>d, *J* = 7.6 Hz | Phenolic acid aromatic, Ar-H | 1.97 | 0.52 ↓ | 1.67 | 3.67E-02 |
| **15** | 0.57 | 4.80 | s | Quinic acid derivatives α to oxygen, -CH-OH | 10.31 | 0.30 ↓ | 1.82 | 1.14E-02 |
| **16** | 1.20 | - | - | - | 3.60 | 0.44 ↓ | 1.82 | 2.09E-02 |
| **17** | 1.94 | - | - | - | 9.34 | 0.53 ↓ | 1.65 | 4.53E-02 |
| **18** | 1.98 | 5.05 | s | Quinic acid derivatives α to oxygen, -CH-OH | 17.46 | 0.35 ↓ | 1.60 | 1.61E-02 |
| **19** | 2.04 | 7.12<br>6.84 | d, *J* = 1.4 Hz<br>dd, *J* = 7.5, 2.0 Hz | Quinic acid derivatives aromatic, Ar-H | 3.40 | 0.35 ↓ | 2.00 | 4.53E-02 |
| **20** | 2.33 | 5.05 | s | Quinic acid derivatives α to oxygen, -CH-OH | 17.79 | 0.42 ↓ | 1.75 | 2.64E-02 |
| **21** | 2.36 | 7.47<br>6.92<br>6.60 | d, *J* = 2.0 Hz<br>d, *J* = 7.5 Hz<br>s | Luteolin derivatives aromatic Ar-H b-ring<br>Proton c-ring | 4.81 | 2.40 ↑ | 1.72 | 1.13E-02 |
| **22** | 2.51 | - | - | - | 1.26 | 4.98 ↑ | 1.73 | 1.28E-02 |
| **23** | 2.68 | 7.84<br>6.96<br>6.68 | m<br>m<br>s | Apigenin derivatives aromatic Ar-H b-ring<br>Proton c-ring | 4.50 | 2.44 ↑ | 1.41 | 1.45E-02 |

| | | | | | | | | |
|---|---|---|---|---|---|---|---|---|
| **25** | 2.71 | 7.83<br>6.95<br>6.68 | m<br>m<br>s | Apigenin derivatives aromatic Ar-H b-ring<br>Proton c-ring | 2.99 | 3.14 ↑ | 1.47 | 1.45E-02 |
| **29** | 2.87 | 7.83<br>6.95<br>6.68<br>6.28 | m<br>m<br>s<br>s | Apigenin derivatives aromatic Ar-H b-ring<br>Proton c-ring<br>Proton a-ring | 4.37 | 5.13 ↑ | 1.50 | 4.08E-02 |
| **30*** | 2.88 | 7.80<br>6.90<br>6.50 | m<br>m<br>s | Apigenin derivatives aromatic Ar-H b-ring<br>Proton c-ring | 6.32 | 3.38 ↑ | 1.79 | 1.61E-02 |
| **31*** | 2.91 | 7.83<br>6.95<br>6.68 | m<br>m<br>s | Apigenin derivatives aromatic Ar-H b-ring<br>Proton c-ring | 12.60 | 4.70 ↑ | 2.26 | 4.27E-03 |
| **32*** | 3.13 | - | - | - | 8.89 | 6.73 ↑ | 1.55 | 2.64E-02 |
| **33** | 3.16 | - | - | - | 13.65 | 3.52 ↑ | 1.41 | 6.18E-03 |
| **34*** | 3.18 | 7.87<br>6.98<br>6.75<br>6.65 | m<br>m<br>s<br>s | Apigenin derivatives aromatic Ar-H b-ring<br>Proton a-ring<br>Proton c-ring | 2.07 | 2.02 ↑ | 1.03 | 2.95E-02 |
| **8st** | 3.20 | 7.49<br>6.81<br>6.39 | m<br>m<br>d, *J* = 15.2 Hz | Phenolic acid aromatic, Ar-H<br>*trans* vinylic protons | 16.21 | 0.02 ↓ | 1.71 | 9.43E-03 |
| **35*** | 3.23 | 7.85<br>6.92<br>6.55 | m<br>m<br>s | Apigenin derivatives aromatic Ar-H b-ring<br>Proton c-ring | 8.99 | 1.72 ↑ | 1.25 | 1.13E-02 |
| **36** | 3.24 | 6.96<br>6.73<br>6.39 | m<br>d, *J* = 1.6 Hz<br>d, *J* = 1.6 Hz | Kaempferol derivatives aromatic Ar-H b-ring and a-ring | 13.97 | 2.61 ↑ | 1.34 | 2.48E-02 |

| | | | | | | | | | |
|---|---|---|---|---|---|---|---|---|---|
| **38** | 3.28 | - | - | - | 9.34 | 2.51 ↑ | 1.00 | 4.53E-02 |
| **42** | 3.54 | - | - | - | 10.33 | 2.14 ↑ | 1.34 | 1.86E-02 |
| **43** | 3.56 | - | - | - | 4.94 | 1.96 ↑ | 1.08 | 3.67E-02 |
| **46** | 3.61 | - | - | - | 6.39 | 1.36 ↑ | 1.68 | 8.64E-03 |
| **48** | 3.73 | 7.85<br>6.95<br>6.70<br>6.60 | m<br>m<br>s<br>s | Apigenin derivatives<br>aromatic Ar-H b-ring<br>Proton a-ring<br>Proton c-ring | 15.01 | 1.35 ↑ | 1.78 | 2.64E-02 |
| **50** | 4.57 | - | - | - | 1.07 | 0.28 ↓ | 1.78 | 2.09E-02 |

[a] CV: coefficient of variation in the metabolites in the QC samples; [b] FC: fold change in the comparison (average in active samples / inactive samples); [c] VIP: variable importance in projection; [d] *p*-value corresponding to the *p* values calculated by the Benjamini-Hochberg (<0.05); [st] The identification of compounds has been verified by using authentic standards; * Isomers. The assignments of the $^{1}$H-NMR signals were established by extracting signals with reference standards (STD) and based on literature reports.

The heatmap shows the abundance of the main statistically significant metabolites correlated with cytotoxic activity (Figure 3.14A). Hierarchical clustering analysis clearly reveals two clusters showing the differential chemical classes glycosidized flavonoids and caffeoylquinic acids (CQAs) derivatives with respect to activity groups. In terms of abundance, it is observed that the glycosidized flavonoids are present in the BLEs that presented a higher cytotoxic effect against the colon cancer cell line HCT-116, i.e., *G. incana* and *G angustifolia* species, respectively. Confirming these findings, we constructed a graph to search for patterns of metabolites correlated with cytotoxic activity (Figure 3.14B). It is observed that the group of glycosidized flavonoids presented positive

correlation coefficients, while the CQAs did not. Taken together, these data demonstrate that BLEs are a good source of new antioxidant and cytotoxic compounds. Although there are no studies on the effect of extracts of 8 *Guadua* species against HCT-116 colon cancer cell lines, the effect of extracts of bamboo shoots (*Dendrocalamus asper* and *Phyllostachys heterocycla* var. *pubescens*) against MCF-7 breast cancer cell lines has been reported, showing cytotoxic, antiproliferative, proapoptotic and proin-flammatory effects.(YANSEN et al., 2023)

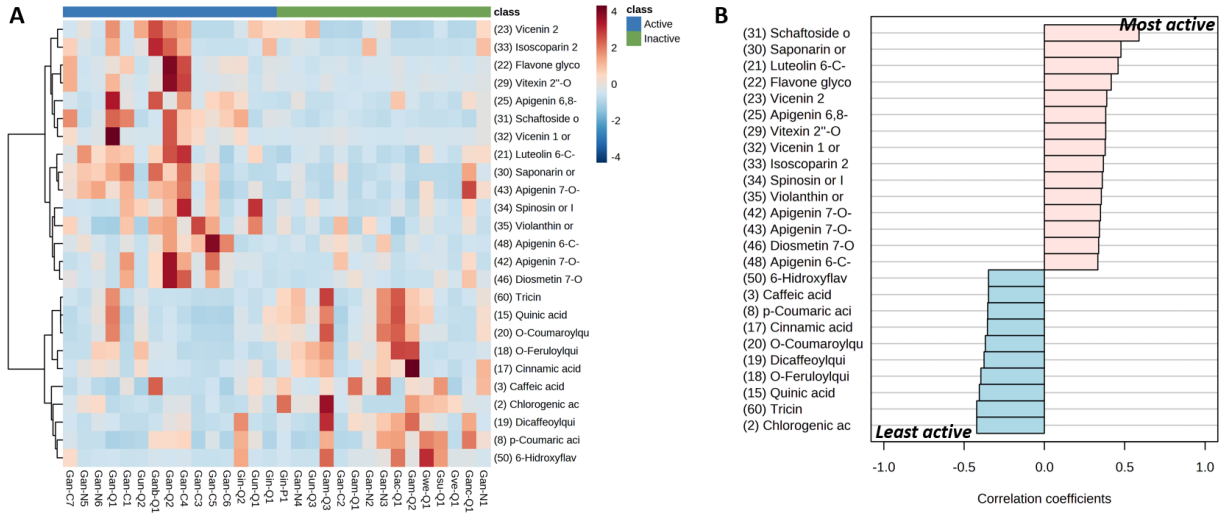



**Figure 3.14. A)** Hierarchical clustering analysis (HCA) with heatmap illustrating the difference in the compounds annotated abundance between active and inactive samples. The x-axis shows the clustering of all the samples and the y-axis shows the clustering of the 25 compounds significantly statistically. **B)** Pattern search for correlation analysis of metabolites correlated with cytotoxic activity. Compounds annotated significantly statistically by UHPLC-QTOF-MS from BLEs comparing Active/Inactive groups (p-value threshold < 0.05 and FC threshold > 2).

A recent study investigated the role of NO and inhibitors of apoptosis (IAPs) during the process of apoptosis induced by *Sasa quelpaertensis* Nakai leaf extracts (SQE) in p53 wild-type (WT) and p53 null HCT-116 colon carcinoma cells. SQE was shown to induce apoptosis independent of p53 status and was associated with modulation of endogenous NO in HCT-116 cells.(KIM, 2020) Particularly *S. argenteastriatus* E.G. Camus and *S. quelpaertensis* Nakai in another study performed on the changes in chemical composition based on seasonal and altitudinal variation showed a strong correlation with the increase

of phenolic compounds and flavonoids, being orientin, isoorientin, vitexin, homovitexin, and tricin the ones that notably exhibited a significant change increasing their antioxidant potential. In this context, and relating our findings, we could attribute this cytotoxic effect of BLEs to the high content of phenolic compounds present.(KO et al., 2018; NI et al., 2012) The major constituents were glycosylated flavones, showing a positive correlation with the cytotoxic potential. Thus, a straight-forward identification of potential biomarkers was achieved prior to any fractionation or isolation efforts. However, studies focused on the isolation of cytotoxic compounds are required to confirm our hypothesis.

### 3.2.10 Bioactivity score-based molecular networking

To complement the correlation analysis, the effectiveness of the molecular networking (MN) was evaluated together with the bioactivity variable of the extracts using the GNPS web platform. The MN containing the classification component of activity is represented in Figure 3.15. The constructed molecular networks show the two main molecular families (MFs) present in the BLEs. On one hand, the first molecular family (MF1) corresponds to flavonoid glycosides where three metabolites corresponding to luteolin 6-*C*-hexoside 8-*C*-pentoside (**21**, FC = 2.40; *p*-value = 1.13E-02), vitexin-2''-*O*-rhamnoside (**29**, FC = 5.13; *p*-value = 4.08E-02), and isoschaftoside (**31**, FC = 4.70; *p*-value = 4.27E-03) are represented correlating positively with cytotoxicity and the MF2 corresponds to CQAs including CGA (**2**, FC = 0.35; *p*-value = 3.67E-02), Feruloylquinic acid (**18**, FC = 0.35; *p*-value = 1.61E-02), and Dicaffeoylquinic acid (**19**, FC = 0.35; *p*-value = 4.53E-02), which in this case did not exhibit a correlation with cytotoxic activity against the colon cancer cell line HCT-116.

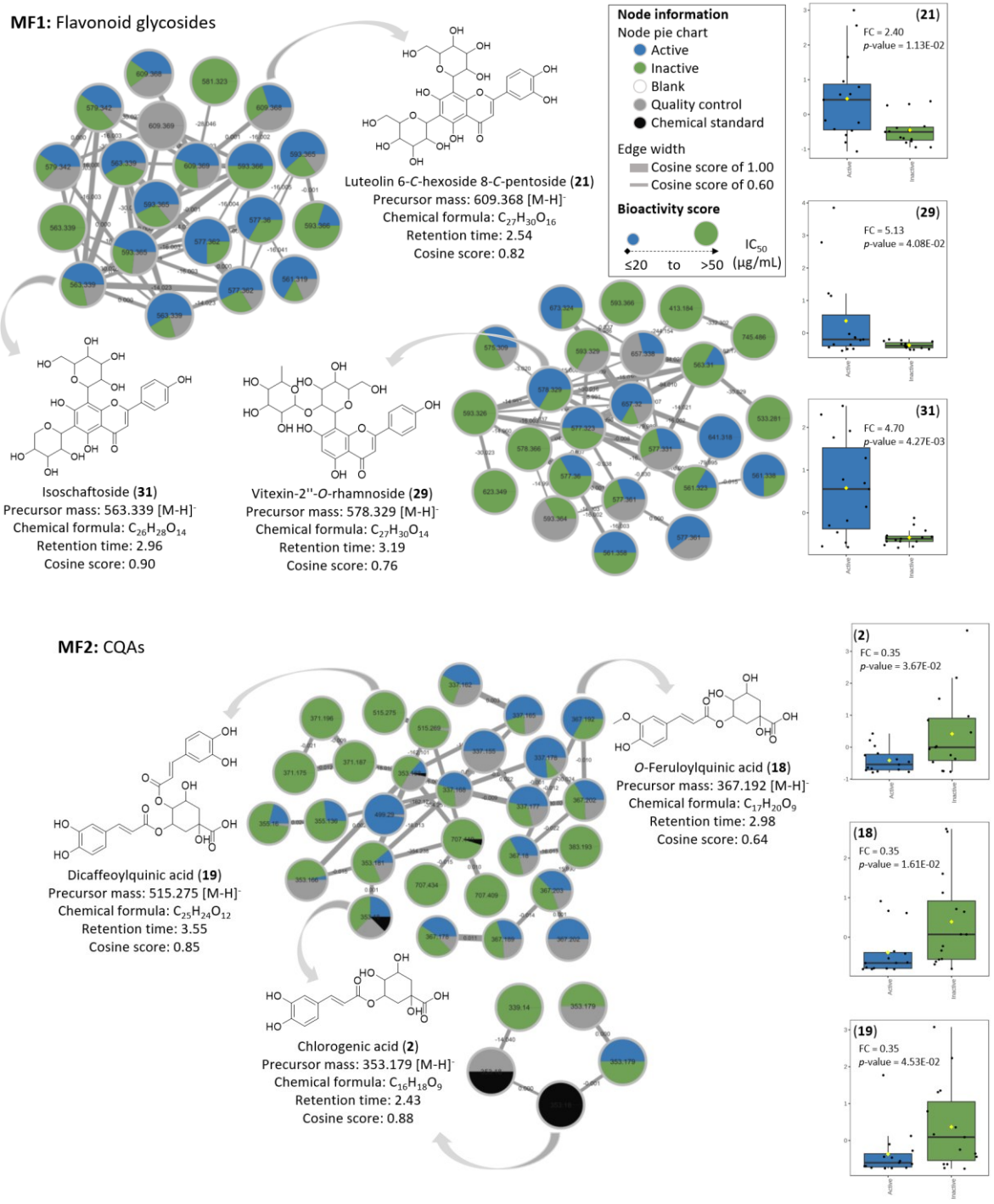



**Figure 3.15.** Bioactive molecular networking of the BLEs displays compounds that contribute most significantly to activity. Particularly, flavonoid glycosides are highlighted with a high bioactivity score, while CQAs present a low bioactivity score against the colon cancer cell line HCT-116. The nodes were colored based on the classification of active and inactive groups, considering the $IC_{50}$ value as a reference for the bioactivity score. Compounds **2**, **18**, **19**, **21**, **29**, and **31**, represented

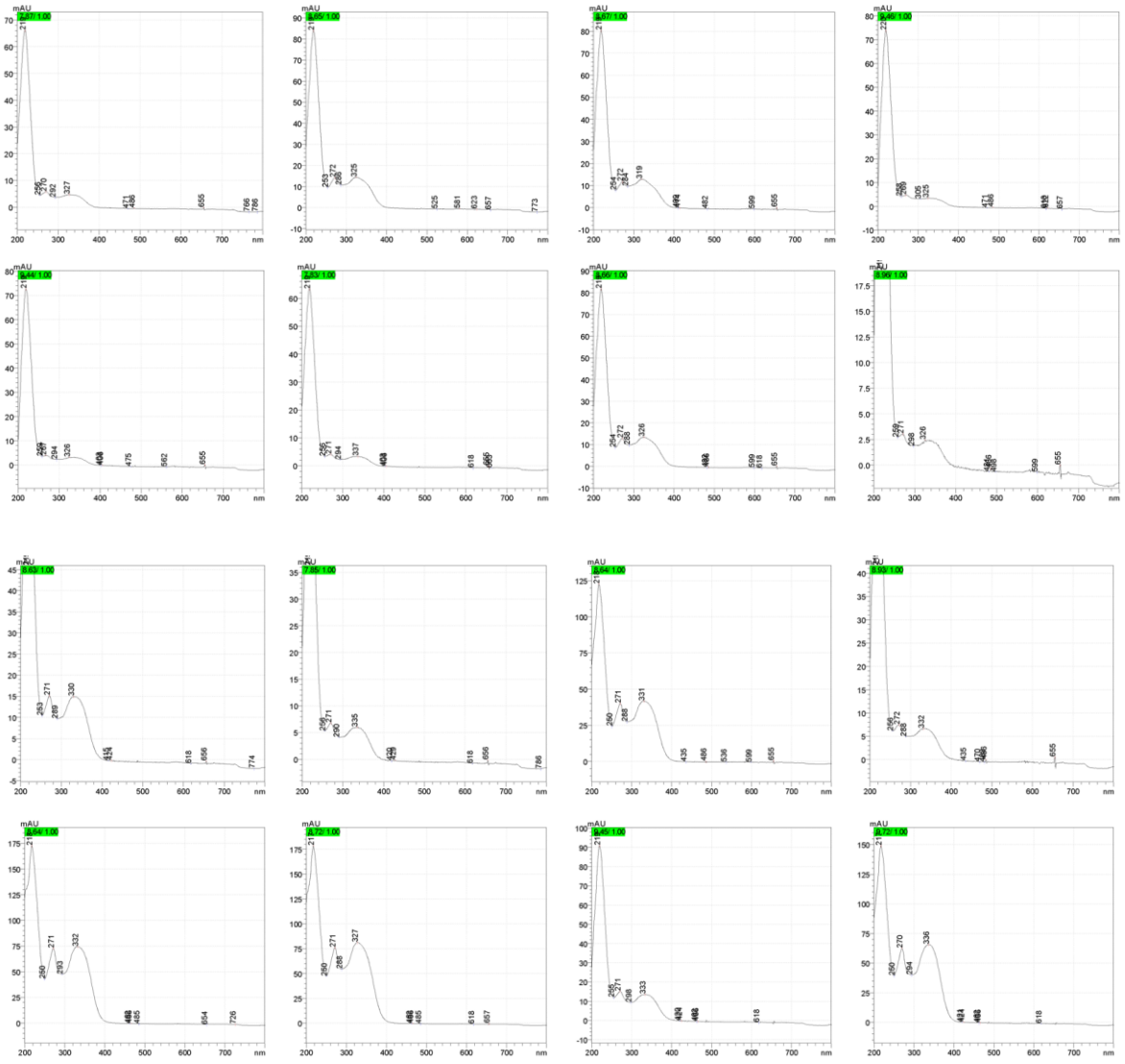
by the nodes, are the most representative according to the Pearson correlation coefficients determined by statistical analysis.

Molecular networking analysis has enabled the identification of bioactive molecules within BLEs, whose active constituents were previously unknown against colon cancer cells HCT-116. The present study demonstrated that the application of a metabolomics approach, based on correlation of chemical composition and biological activity, together with the construction of integrated molecular networks with bioactivity scores, can accelerate the search for bioactive molecules and rationalize the isolation procedure in bioassay-based phytoconstituent discovery. This innovative tool offers the possibility to narrow down the pool of candidate compounds for further isolation, thus minimizing the time required in this process. Further studies should be directed to isolate glycosylated flavones responsible for the cytotoxic activity of BLEs from the genus *Guadua*.

## 3.3 Conclusion

A metabolomic approach was successfully applied to investigate the identification of potential bioactive markers in BLEs. The fingerprinting conducted through HPTLC, HPLC-DAD, UHPLC-QTOF-MS, and NMR analyses, in combination with biochemometric analyses, facilitated the characterization and tentatively identification of 49 compounds in the extracts, with some of them being reported for the first time in some *Guadua* species, mainly flavonoids and phenolic acids derivatives. Most of the extracts exhibited significant antioxidant potential, and it was found that the extracts of *G. incana* and *G. angustifolia* showed the best cytotoxic effect, making them promising candidates for future investigation against the HCT-116 colon cancer cell lines. Correlation analysis highlighted those phenolic compounds contributed to the antioxidant potential, while glycosylated flavones showed a strong correlation with cytotoxic potential, making them candidates for further isolation. This study provides a new opportunity to explore novel biological properties from bamboo species extracts and emphasizes their significant medicinal potential.

## Supplementary information



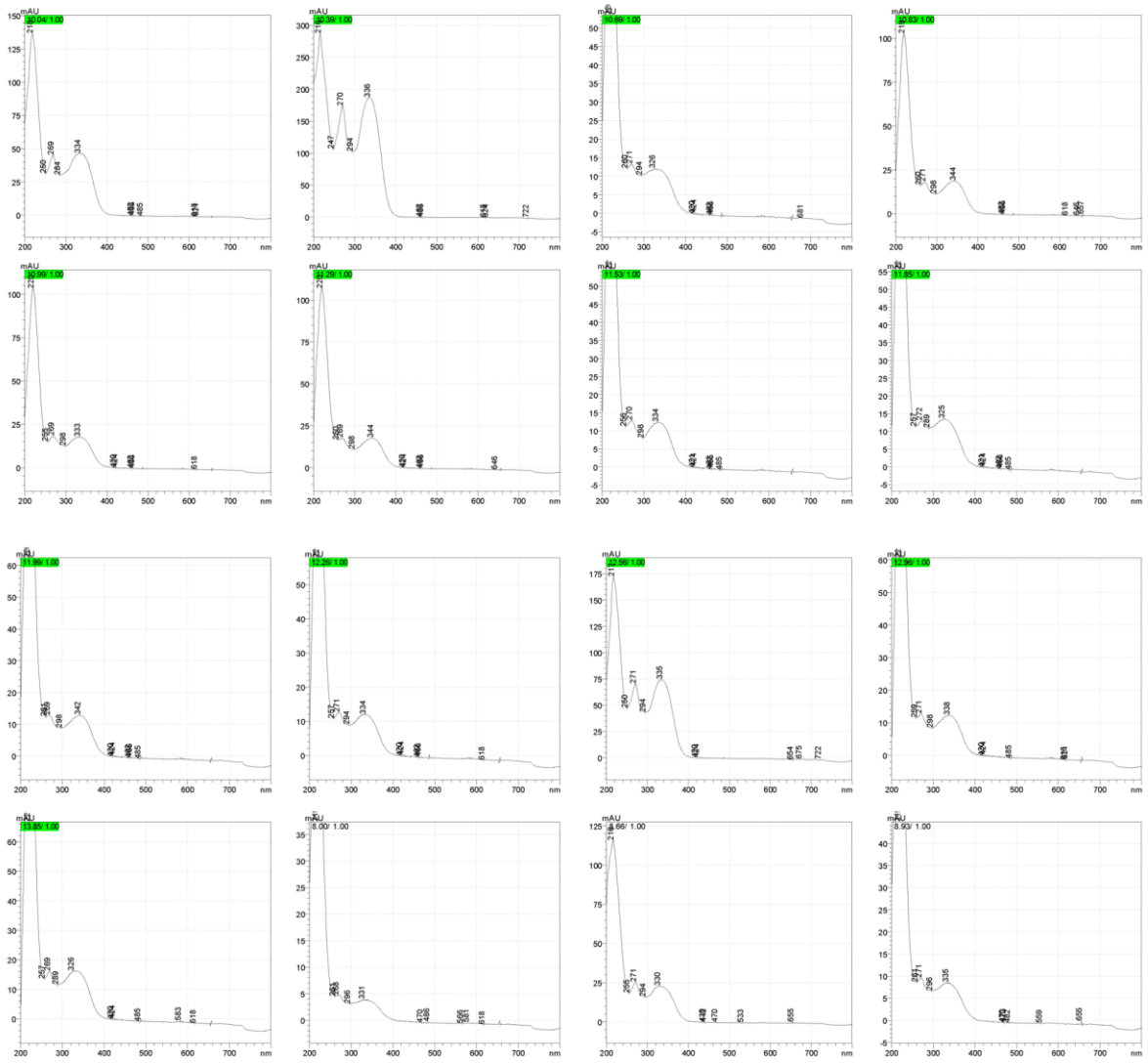


**Figure S3.1.** UV spectra of the major peaks found in the BLEs obtained by HPLC-DAD. The retention time of each peak and its corresponding spectrum are described in highlighted green ($t_R$/1.00).

**Table S3.1.** Phytochemicals tentatively identified in BLEs using UHPLC-QTOF-MS.

| Peak | $t_R$ (min) | UV $\lambda_{max}$ (nm) | Molecular formula | Adduct ion | Calculated mass (*m/z*) | Experimental mass (*m/z*) | Mass error (ppm) | Main fragment ions (MS/MS) | Identification confidence level | Tentative identification | Chemical class | Plant species | Reference or Database[a] |
|---|---|---|---|---|---|---|---|---|---|---|---|---|---|
| **15** | 0.57 | - | $C_7H_{12}O_6$ | $[M-H]^-$ | 191.0551 | 191.0543 | -4.2 | 175, 147, 129, 111 | 2 | Quinic acid | Organic acid | *G. aculeata*<br>*G. amplexifolia*<br>*G. angustifolia*<br>*G. angustifolia* biotype *San calixto*<br>*G. angustifolia* var. *bicolor*<br>*G. incana*<br>*G. superba*<br>*G. uncinata*<br>*G. venezuelae*<br>*G. weberbaueri* | (CAO et al., 2022; CHITIVA et al., 2023; JIANG et al., 2019) |
| **16** | 1.20 | Low intensity | $C_{16}H_{18}O_9$ | $[M-H]^-$ | 353.0878 | 353.0861 | -4.8 | 191, 179, 155, 135 | 3 | Not identified | Cinnamic acid and derivatives | *G. superba*<br>*G. weberbaueri* | |
| **17** | 1.94 | Low intensity | $C_{15}H_{16}O_{10}$ | $[M-H]^-$ | 355.0670 | 355.0669 | -0.3 | 209, 191, 163, 147, 129 | 3 | Not identified | Cinnamic acid and derivatives | *G. aculeata*<br>*G. amplexifolia*<br>*G. angustifolia*<br>*G. incana* | |
| **18** | 1.98 | Low intensity | $C_{17}H_{20}O_9$ | $[M-H]^-$ | 367.1034 | 367.1024 | -2.7 | 207, 193, 134 | 2 | *O*-Feruloylquinic acid | Cinnamic acid and derivatives | *G. angustifolia*<br>*G. superba*<br>*G. uncinata* | (HALDIPUR; SRIVIDYA, 2021; JIANG et al., 2019; VAN HOYWEGHEN; DEFORCE; HEYERICK, 2010; VAN HOYWEGHEN et al., 2012; WANG et al., 2020b) and GNPS |

| | | | | | | | | | | | | |
|---|---|---|---|---|---|---|---|---|---|---|---|---|
| **19** | 2.04 | 290[sh], 310 | $C_{25}H_{24}O_{12}$ | $[M-H]^-$ | 515.1195 | 515.1193 | -0.4 | 353, 191, 179, 137 | 2 | Dicaffeoylquinic acid | Cinnamic acid and derivatives | *G. aculeata*<br>*G. superba*<br>*G. venezuelae*<br>*G. weberbaueri* | (JIANG et al., 2019) and GNPS |
| **20** | 2.33 | Low intensity | $C_{16}H_{18}O_8$ | $[M-H]^-$ | 337.0928 | 337.0945 | 5.0 | 191, 173, 164, 119 | 2 | *O*-Coumaroylquinic acid | Cinnamic acid and derivatives | *G. aculeata*<br>*G. superba*<br>*G. venezuelae*<br>*G. weberbaueri* | (AKHTAR; PATOWARY, 2022; CHITIVA et al., 2023; GAGLIANO et al., 2022a; JIANG et al., 2019) and GNPS |
| **21** | 2.36 | 270, 327 | $C_{27}H_{30}O_{16}$ | $[M-H]^-$ | 609.1461 | 609.1466 | 0.8 | 547, 519, 489, 429, 399 | 3 | Luteolin 6-*C*-hexoside 8-*C*-pentoside | Flavone glycosides | *G. amplexifolia*<br>*G. angustifolia*<br>*G. angustifolia* biotype *San calixto*<br>*G. angustifolia* var. *bicolor*<br>*G. incana*<br>*G. uncinata* | |
| **2** | 2.46 | 292[sh], 326 | $C_{16}H_{18}O_9$ | $[M-H]^-$ | 353.0878 | 353.0864 | -4.0 | 191, 179, 135 | 1 | Chlorogenic acid[st] | Cinnamic acid and derivatives | *G. aculeata*<br>*G. superba*<br>*G. venezuelae*<br>*G. weberbaueri* | (HU; ZHANG; KITTS, 2000; MA et al., 2020a; NI et al., 2012; TANAKA et al., 2014) and GNPS |
| **22** | 2.51 | 274, 336 | $C_{21}H_{20}O_{10}$ | $[M-H]^-$ | 431.0983 | 431.0981 | -0.5 | 387, 341, 311, 179 | 3 | Not identified | Flavone glycosides | *G. aculeata*<br>*G. amplexifolia*<br>*G. angustifolia*<br>*G. angustifolia* biotype *San calixto*<br>*G. angustifolia* var. *bicolor*<br>*G. incana*<br>*G. superba*<br>*G. uncinata* | |

| | | | | | | | | | | | | |
|---|---|---|---|---|---|---|---|---|---|---|---|---|
| **23** | 2.68 | 272, 325 | $C_{27}H_{30}O_{15}$ | $[M-H]^-$ | 593.1511 | 593.1513 | 0.3 | 503, 473, 383, 353, 297 | 2 | Vicenin 2 | Flavone glycosides | *G. amplexifolia*<br>*G. angustifolia*<br>*G. angustifolia* biotype *San calixto*<br>*G. incana*<br>*G. superba*<br>*G. uncinata*<br>*G. venezuelae* | (CHITIVA et al., 2023; GAGLIANO et al., 2022b) and GNPS |
| **24** | 2.70 | 269, 325 | $C_{21}H_{20}O_{11}$ | $[M-H]^-$ | 447.0932 | 447.0931 | -0.2 | 327, 299, 285, 133, 109 | 3 | Not identified | Flavone glycosides | *G. amplexifolia*<br>*G. angustifolia*<br>*G. angustifolia* var. *bicolor*<br>*G. incana*<br>*G. uncinata* | |
| **25** | 2.71 | 268, 337 | $C_{27}H_{30}O_{15}$ | $[M-H]^-$ | 593.1511 | 593.1517 | 1.0 | 457, 383, 353, 297 | 2 | Apigenin 6,8-digalactoside | Flavone glycosides | *G. amplexifolia*<br>*G. angustifolia*<br>*G. angustifolia* biotype *San calixto*<br>*G. incana*<br>*G. superba*<br>*G. uncinata*<br>*G. venezuelae* | (GAGLIANO et al., 2022a) and GNPS |
| | | | | $[M+H]^+$ | 595.1668 | 595.1660 | -1.3 | 541, 481, 457, 379, 325, 295 | | | | | |
| **26** | 2.71 | 267, 326 | $C_{26}H_{28}O_{14}$ | $[M-H]^-$ | 563.1406 | 563.1411 | 0.9 | 473, 443, 383, 353, 325, 2.97 | 3 | Not identified | Flavone glycosides | *G. amplexifolia*<br>*G. angustifolia*<br>*G. angustifolia* var. *bicolor*<br>*G. incana*<br>*G. superba*<br>*G. uncinata*<br>*G. venezuelae*<br>*G. weberbaueri* | |

| | | | | | | | | | | | | |
|---|---|---|---|---|---|---|---|---|---|---|---|---|
| **3** | 2.74 | 311 | $C_9H_8O_4$ | $[M-H]^-$ | 179.0349 | 179.0352 | 1.7 | 135, 119 | 1 | Caffeic acid[st] | Cinnamic acid and derivatives | *G. aculeata*<br>*G. amplexifolia*<br>*G. angustifolia*<br>*G. angustifolia* biotype *San calixto*<br>*G. incana*<br>*G. superba*<br>*G. uncinata*<br>*G. venezuelae* | (HU; ZHANG; KITTS, 2000; NI et al., 2012, 2013) |
| **27** | 2.77 | 271, 333 | $C_{26}H_{28}O_{14}$ | $[M-H]^-$ | 563.1406 | 563.1410 | 0.7 | 445, 355, 325, 297 | 3 | Not identified | Flavone glycosides | *G. angustifolia*<br>*G. angustifolia* biotype *San calixto*<br>*G. angustifolia* var. *bicolor*<br>*G. incana*<br>*G. superba*<br>*G. uncinata* | |
| **28** | 2.80 | 269, 334 | $C_{26}H_{28}O_{14}$ | $[M-H]^-$ | 563.1416 | 563.1415 | -0.2 | 473, 443, 401, 383, 353, 311 | 3 | Not identified | Flavone glycosides | *G. aculeata*<br>*G. amplexifolia*<br>*G. angustifolia*<br>*G. angustifolia* biotype *San calixto*<br>*G. incana*<br>*G. superba*<br>*G. uncinata*<br>*G. venezuelae* | |
| **29** | 2.87 | 265, 341 | $C_{27}H_{30}O_{14}$ | $[M-H]^-$ | 577.1562 | 577.1565 | 0.5 | 413, 341, 293, 175 | 2 | Vitexin 2"-*O*-rhamnoside | Flavone glycosides | *G. angustifolia*<br>*G. angustifolia* biotype *San calixto*<br>*G. angustifolia* var. *bicolor*<br>*G. incana*<br>*G. superba*<br>*G. uncinata* | (CHITIVA et al., 2023) and GNPS |
| | | | | $[M+H]^+$ | 579.1719 | 579.171 | -1.6 | 433, 415, 367, 313, 283 | | | | | |

| | | | | | | | | | | | | |
|---|---|---|---|---|---|---|---|---|---|---|---|---|
| **30** | 2.88 | 269, 342 | $C_{27}H_{30}O_{15}$ | $[M-H]^-$ | 593.1511 | 593.1519 | 1.3 | 473, 431, 353, 311, 297, 282 | 2 | Saponarin or Isosaponarin | Flavone glycosides | *G. amplexifolia*<br>*G. angustifolia*<br>*G. angustifolia* var. *bicolor*<br>*G. incana*<br>*G. superba*<br>*G. uncinata*<br>*G. venezuelae*<br>*G. weberbaueri* | (CHITIVA et al., 2023; GAGLIANO et al., 2022a) and GNPS |
| **31** | 2.91 | 271, 335 | $C_{26}H_{28}O_{14}$ | $[M-H]^-$ | 563.1406 | 563.1401 | -0.9 | 473, 443, 383, 353, 325, 297 | 2 | Schaftoside or Isoschaftoside | Flavone glycosides | *G. amplexifolia*<br>*G. angustifolia*<br>*G. angustifolia* biotype *San calixto*<br>*G. angustifolia* var. *bicolor*<br>*G. incana*<br>*G. uncinata*<br>*G. venezuelae*<br>*G. weberbaueri* | (AKHTAR; PATOWARY, 2022; CHITIVA et al., 2023; GAGLIANO et al., 2022a; JIANG et al., 2019; WANG et al., 2020b, 2022b) and GNPS |
| | | | | $[M+H]^+$ | 565.1562 | 565.1563 | 0.2 | 547, 529, 499, 457, 427, 379 | | | | | |
| **32** | 3.13 | 273, 339 | $C_{26}H_{28}O_{14}$ | $[M+H]^+$ | 565.1562 | 565.1564 | 0.4 | 525, 481, 405, 337, 295 | 3 | Vicenin 1 or Vicenin 3 | Flavone glycosides | *G. amplexifolia*<br>*G. angustifolia*<br>*G. angustifolia* var. *bicolor*<br>*G. incana*<br>*G. superba*<br>*G. uncinata*<br>*G. venezuelae*<br>*G. weberbaueri* | |
| **33** | 3.16 | 270, 344 | $C_{28}H_{32}O_{16}$ | $[M-H]^-$ | 623.1617 | 623.1617 | 0.0 | 504, 443, 353, 323 | 3 | Isoscoparin 2''-*O*-hexoside | Flavone glycosides | *G. amplexifolia*<br>*G. angustifolia*<br>*G. angustifolia* biotype *San calixto*<br>*G. angustifolia* var. *bicolor*<br>*G. incana*<br>*G. uncinata* | |

| | | | | | | | | | | | | |
|---|---|---|---|---|---|---|---|---|---|---|---|---|
| **34** | 3.18 | 271, 342 | $C_{28}H_{32}O_{15}$ | $[M+H]^+$ | 609.1824 | 609.1824 | 0.0 | 430, 393, 327, 297, 267 | 3 | Spinosin or Isospinosin | Flavone glycosides | *G. amplexifolia*<br>*G. angustifolia*<br>*G. angustifolia* var. *bicolor*<br>*G. incana*<br>*G. superba*<br>*G. uncinata*<br>*G. venezuelae*<br>*G. weberbaueri* | |
| **8** | 3.20 | Low intensity | $C_9H_8O_3$ | $[M-H]^-$ | 163.0400 | 163.0400 | 0.0 | 119 | 1 | *p*-Coumaric acid[st] | Cinnamic acid and derivatives | *G. aculeata*<br>*G. amplexifolia*<br>*G. angustifolia*<br>*G. angustifolia* biotype *San calixto*<br>*G. incana*<br>*G. superba*<br>*G. uncinata*<br>*G. venezuelae* | (SILVA DE OLIVEIRA, 2019) and GNPS |
| **35** | 3.23 | 270, 341 | $C_{27}H_{30}O_{14}$ | $[M-H]^-$ | 577.1562 | 577.1569 | 1.2 | 533, 472, 413, 353, 293 | 2 | Violanthin or Isoviolanthin | Flavone glycosides | *G. amplexifolia*<br>*G. angustifolia*<br>*G. angustifolia* var. *bicolor*<br>*G. incana*<br>*G. superba*<br>*G. uncinata*<br>*G. venezuelae*<br>*G. weberbaueri* | (MORALES NOREÑA; SANCHEZ VALLEJO, 2008) |

| | | | | | | | | | | | | |
|---|---|---|---|---|---|---|---|---|---|---|---|---|
| **36** | 3.24 | 269, 332 | $C_{27}H_{30}O_{15}$ | $[M-H]^-$ | 593.1511 | 593.1512 | 0.2 | 285, 218, 151 | 2 | Kaempferol 7-*O*-neohesperidoside | Flavonol glycosides | *G. amplexifolia*<br>*G. angustifolia*<br>*G. angustifolia* biotype *San calixto*<br>*G. angustifolia* var. *bicolor*<br>*G. incana*<br>*G. uncinata* | (MORALES NOREÑA; SANCHEZ VALLEJO, 2008) and GNPS |
| **37** | 3.28 | 270, 325 | $C_{33}H_{40}O_{19}$ | $[M-H]^-$ | 739.2091 | 739.209 | -0.1 | 593, 431, 281 | 3 | Kaempferol 3-*O*-disaccharoside-7-*O*-pentoside | Flavonol glycosides | *G. amplexifolia*<br>*G. angustifolia*<br>*G. angustifolia* biotype *San calixto*<br>*G. angustifolia* var. *bicolor*<br>*G. incana*<br>*G. uncinata* | |
| **38** | 3.28 | 270, 326 | $C_{27}H_{30}O_{15}$ | $[M+H]^+$ | 595.1668 | 595.1667 | -0.2 | 449, 287 | 3 | Kaempferol 3-*O*-disaccharoside | Flavonol glycosides | *G. amplexifolia*<br>*G. angustifolia*<br>*G. angustifolia* biotype *San calixto*<br>*G. angustifolia* var. *bicolor*<br>*G. incana*<br>*G. uncinata* | |
| **39** | 3.35 | 272, 326 | $C_{21}H_{18}O_{13}$ | $[M-H]^-$ | 477.0674 | 477.0675 | 0.2 | 431, 301, 179 | 3 | Quercetin 3-*O*-hexoside | Flavonol glycosides | *G. amplexifolia*<br>*G. angustifolia*<br>*G. angustifolia* var. *bicolor*<br>*G. incana*<br>*G. superba*<br>*G. uncinata*<br>*G. venezuelae*<br>*G. weberbaueri* | |

| | | | | | | | | | | | | |
|---|---|---|---|---|---|---|---|---|---|---|---|---|
| **40** | 3.37 | 270, 325 | $C_{21}H_{20}O_{12}$ | $[M-H]^-$ | 463.0882 | 463.0880 | -0.4 | 372, 300, 271, 255, 243, 151 | 2 | Hyperoside | Flavonol glycosides | *G. aculeata*<br>*G. angustifolia*<br>*G. angustifolia* biotype *San calixto*<br>*G. angustifolia* var. *bicolor*<br>*G. incana*<br>*G. superba*<br>*G. uncinata*<br>*G. venezuelae* | (SILVA DE OLIVEIRA, 2019) |
| **41** | 3.41 | 271, 329 | $C_{28}H_{32}O_{17}$ | $[M-H]^-$ | 639.1566 | 639.1570 | 0.6 | 403, 328, 313, 285, 270, 242 | 3 | Isorhamnetin 3,4'-hexoside | Flavonol glycosides | *G. amplexifolia*<br>*G. angustifolia*<br>*G. angustifolia* var. *bicolor*<br>*G. incana*<br>*G. superba*<br>*G. uncinata*<br>*G. venezuelae*<br>*G. weberbaueri* | |
| **42** | 3.54 | 271, 344 | $C_{27}H_{30}O_{14}$ | $[M-H]^-$ | 577.1562 | 577.1561 | -0.2 | 269, 117 | 3 | Apigenin 7-*O*-disaccharoside | Flavone glycosides | *G. amplexifolia*<br>*G. angustifolia*<br>*G. angustifolia* biotype *San calixto*<br>*G. angustifolia* var. *bicolor*<br>*G. incana*<br>*G. uncinata*<br>*G. venezuelae* | |

| | | | | | | | | | | | |
|---|---|---|---|---|---|---|---|---|---|---|---|
| **43** | 3.56 | 269, 342 | $C_{27}H_{30}O_{14}$ | $[M+H]^+$ | 579.1719 | 579.1718 | -0.2 | 433, 363, 271, 153 | 3 | Apigenin 7-*O*-disaccharoside | Flavone glycosides | *G. amplexifolia*<br>*G. angustifolia*<br>*G. angustifolia* biotype *San calixto*<br>*G. angustifolia* var. *bicolor*<br>*G. incana*<br>*G. superba*<br>*G. uncinata*<br>*G. venezuelae*<br>*G. weberbaueri* |
| **44** | 3.58 | 268, 331 | $C_{22}H_{22}O_{11}$ | $[M-H]^-$ | 461.1089 | 461.1087 | -0.4 | 415, 341, 313, 298 | 3 | Not identified | Flavone glycosides | *G. amplexifolia*<br>*G. angustifolia*<br>*G. angustifolia* biotype *San calixto*<br>*G. angustifolia* var. *bicolor*<br>*G. incana*<br>*G. uncinata*<br>*G. venezuelae* |
| **45** | 3.59 | 270, 325 | $C_{28}H_{34}O_{15}$ | $[M-H]^-$ | 609.1824 | 609.1843 | 3.1 | 325, 301, 286, 151 | 3 | Hesperidin | Flavanone glycoside | *G. amplexifolia*<br>*G. angustifolia*<br>*G. angustifolia* biotype *San calixto*<br>*G. angustifolia* var. *bicolor*<br>*G. incana*<br>*G. uncinata* |

| | | | | | | | | | | | | |
|---|---|---|---|---|---|---|---|---|---|---|---|---|
| **46** | 3.61 | 271, 344 | $C_{28}H_{32}O_{15}$ | $[M+H]^+$ | 609.1826 | 609.1810 | -2.6 | 463, 301, 286, 258 | 3 | Diosmetin 7-*O*-disaccharoside | Flavone glycosides | *G. amplexifolia*<br>*G. angustifolia*<br>*G. angustifolia* biotype *San calixto*<br>*G. angustifolia* var. *bicolor*<br>*G. incana*<br>*G. superba*<br>*G. uncinata*<br>*G. venezuelae* | |
| **47** | 3.64 | 269, 326 | $C_{28}H_{32}O_{16}$ | $[M-H]^-$ | 623.1617 | 623.1620 | 0.5 | 329, 314, 299, 271, 243, 187 | 3 | Isorhamnetin 3-*O*-hexoside-6''-disaccharoside | Flavonol glycosides | *G. aculeata*<br>*G. angustifolia*<br>*G. angustifolia* biotype *San calixto*<br>*G. angustifolia* var. *bicolor*<br>*G. incana*<br>*G. superba*<br>*G. uncinata*<br>*G. venezuelae* | |
| **48** | 3.73 | 265, 341 | $C_{27}H_{30}O_{15}$ | $[M-H]^-$ | 593.1511 | 593.1512 | 0.2 | 473, 431, 353, 341, 311, 283 | 3 | Apigenin 6-*C*-hexoside-7-*O*-hexoside | Flavone glycosides | *G. amplexifolia*<br>*G. angustifolia*<br>*G. angustifolia* biotype *San calixto*<br>*G. angustifolia* var. *bicolor*<br>*G. incana*<br>*G. uncinata*<br>*G. venezuelae* | |
| | | | | $[M+H]^+$ | 595.1668 | 595.1667 | -0.2 | 415, 379, 337, 313, 283, 165 | | | | | |
| **49** | 4.47 | 264, 356 | $C_{15}H_{10}O_6$ | $[M-H]^-$ | 285.0404 | 285.0403 | -0.4 | 199, 169, 151, 133 | 2 | Luteolin | Flavone aglycones | *G. aculeata*<br>*G. incana*<br>*G. superba*<br>*G. uncinata*<br>*G. venezuelae*<br>*G. weberbaueri* | (CHENG et al., 2023; LI et al., 2021; MA et al., 2020a) |

| | | | | | | | | | | | | |
|---|---|---|---|---|---|---|---|---|---|---|---|---|
| **50** | 4.57 | 270, 319 | $C_{15}H_{12}O_3$ | $[M-H]^-$ | 239.0713 | 239.0699 | -5.9 | 211, 195, 179, 135 | 3 | 6-Hidroxyflavanone | Flavone aglycones | *G. amplexifolia*<br>*G. angustifolia*<br>*G. angustifolia* biotype *San calixto*<br>*G. angustifolia* var. *bicolor*<br>*G. incana* | |
| **51** | 4.88 | 264, 329 | $C_{23}H_{24}O_{12}$ | $[M-H]^-$ | 491.1195 | 491.1198 | 0.6 | 461, 328, 313, 285, 226 | 2 | Tricin 7-*O*-glucoside | Flavone glycosides | *G. aculeata*<br>*G. amplexifolia*<br>*G. angustifolia*<br>*G. angustifolia* var. *bicolor*<br>*G. incana*<br>*G. superba*<br>*G. uncinata*<br>*G. venezuelae* | (GAGLIANO et al., 2022a) |
| **52** | 4.92 | 264, 335 | $C_{27}H_{32}O_{14}$ | $[M-H]^-$ | 579.1719 | 579.1720 | 0.2 | 271, 177, 151, 119 | 3 | Naringenin-7-*O*-disaccharoside | Flavanone glycosides | *G. amplexifolia*<br>*G. angustifolia*<br>*G. angustifolia* biotype *San calixto*<br>*G. angustifolia* var. *bicolor*<br>*G. incana*<br>*G. uncinata* | |

| | | | | | | | | | | | | |
|---|---|---|---|---|---|---|---|---|---|---|---|---|
| **53** | 4.95 | 263, 334 | $C_{21}H_{22}O_{10}$ | $[M-H]^-$ | 433.1140 | 433.1145 | 1.2 | 271, 151, 119 | 3 | Naringenin-7-*O*-hexoside | Flavanone glycosides | *G. aculeata*<br>*G. amplexifolia*<br>*G. angustifolia*<br>*G. angustifolia* biotype *San calixto*<br>*G. angustifolia* var. *bicolor*<br>*G. incana*<br>*G. superba*<br>*G. uncinata*<br>*G. venezuelae*<br>*G. weberbaueri* | |
| **54** | 4.97 | 271, 358 | $C_{15}H_{10}O_5$ | $[M-H]^-$ | 269.0455 | 269.0460 | 1.9 | 227, 181, 151, 117 | 2 | Apigenin | Flavone aglycones | *G. incana*<br>*G. superba*<br>*G. uncinata*<br>*G. venezuelae*<br>*G. weberbaueri* | (LI et al., 2021) |
| **55** | 5.01 | 244, 315 | $C_{15}H_{10}O_6$ | $[M-H]^-$ | 285.0404 | 285.0405 | 0.4 | 211, 183, 149, 121 | 3 | 3,6,2',3'-Tetrahydroxyflavone | Flavone aglycones | *G. aculeata*<br>*G. amplexifolia*<br>*G. angustifolia*<br>*G. angustifolia* biotype *San calixto*<br>*G. angustifolia* var. *bicolor*<br>*G. incana*<br>*G. superba*<br>*G. uncinata*<br>*G. venezuelae*<br>*G. weberbaueri* | |

| | | | | | | | | | | | | |
|---|---|---|---|---|---|---|---|---|---|---|---|---|
| **56** | 5.03 | 245, 319 | $C_{15}H_{10}O_5$ | $[M-H]^-$ | 269.0455 | 269.0461 | 2.2 | 239, 211, 187, 143, 117 | 3 | 6,7,4'-Trihydroxyisoflavone | Flavone aglycones | *G. aculeata*<br>*G. amplexifolia*<br>*G. angustifolia*<br>*G. angustifolia* biotype *San calixto*<br>*G. angustifolia* var. *bicolor*<br>*G. incana*<br>*G. superba*<br>*G. uncinata*<br>*G. venezuelae*<br>*G. weberbaueri* | |
| **57** | 5.04 | 269, 354 | $C_{15}H_{10}O_6$ | $[M-H]^-$ | 285.0404 | 285.0420 | 5.6 | 255, 227, 187, 159, 143, 117 | 2 | Kaempferol | Flavonol aglycones | *G. aculeata*<br>*G. angustifolia* var. *bicolor*<br>*G. incana*<br>*G. superba*<br>*G. uncinata*<br>*G. venezuelae*<br>*G. weberbaueri* | (LI et al., 2021; MORALES NOREÑA; SANCHEZ VALLEJO, 2008) |
| **58** | 5.09 | 245, 319 | $C_{17}H_{14}O_7$ | $[M-H]^-$ | 329.0666 | 329.0671 | 1.5 | 271, 243, 227, 161, 133 | 3 | 4',5,7-Trihydroxy-3,6-dimethoxyflavone | Flavone aglycones | *G. aculeata*<br>*G. amplexifolia*<br>*G. angustifolia*<br>*G. angustifolia* biotype *San calixto*<br>*G. angustifolia* var. *bicolor*<br>*G. incana*<br>*G. superba*<br>*G. uncinata*<br>*G. venezuelae*<br>*G. weberbaueri* | |

| | | | | | | | | | | | | |
|---|---|---|---|---|---|---|---|---|---|---|---|---|
| **59** | 5.12 | 244, 325 | $C_{16}H_{12}O_6$ | $[M-H]^-$ | 299.0561 | 299.0561 | 0.0 | 256, 227, 212, 183, 151 | 3 | 3,5,7-Trihydroxy-4'-methoxyflavone | Flavone aglycones | *G. aculeata*<br>*G. amplexifolia*<br>*G. angustifolia*<br>*G. angustifolia* biotype *San calixto*<br>*G. angustifolia* var. *bicolor*<br>*G. incana*<br>*G. superba*<br>*G. uncinata*<br>*G. venezuelae*<br>*G. weberbaueri* | |
| **60** | 5.15 | 244, 354 | $C_{17}H_{14}O_7$ | $[M-H]^-$ | 329.0666 | 329.0669 | 0.9 | 229, 271, 227, 215, 161 | 2 | Tricin | Flavone aglycones | *G. incana*<br>*G. superba*<br>*G. uncinata*<br>*G. venezuelae*<br>*G. weberbaueri* | (LI et al., 2021) |
| | | | | $[M+H]^+$ | 331.0823 | 331.0820 | -0.9 | 313, 285, 270, 258, 203, 153 | | | | | |

[a] Database source: PubChem, METLIN, KEGG, GNPS; [st] The identification of compounds has been verified by using authentic standards; [sh] shoulder peak; *m/z* data were obtained by UHPLC-QTOF-MS based on time and peak areas. $\lambda_{max}$: UV maximum absorbance wavelength. The references described compounds found in the literature for leaves, culms, and shoots of several bamboos' plants; Phytochemicals were annotated with identification confidence levels as recommended by the Metabolomics Standards Initiative (MSI) according to: Level 0: *Unambiguous 3D Structure: isolated, pure compound, including full stereochemistry*; Level 1: *Confident 2D structure: uses reference standard match or full 2D structure elucidation;* Level 2: *Probable structure: matched to literature data or databases by diagnostic evidence*, Level 3: *Possible structure or class: most likely structure, isomers possible, substance class or substructure match*; Level 4: *Unknown feature of interest*.(BLAŽENOVIĆ et al., 2018).

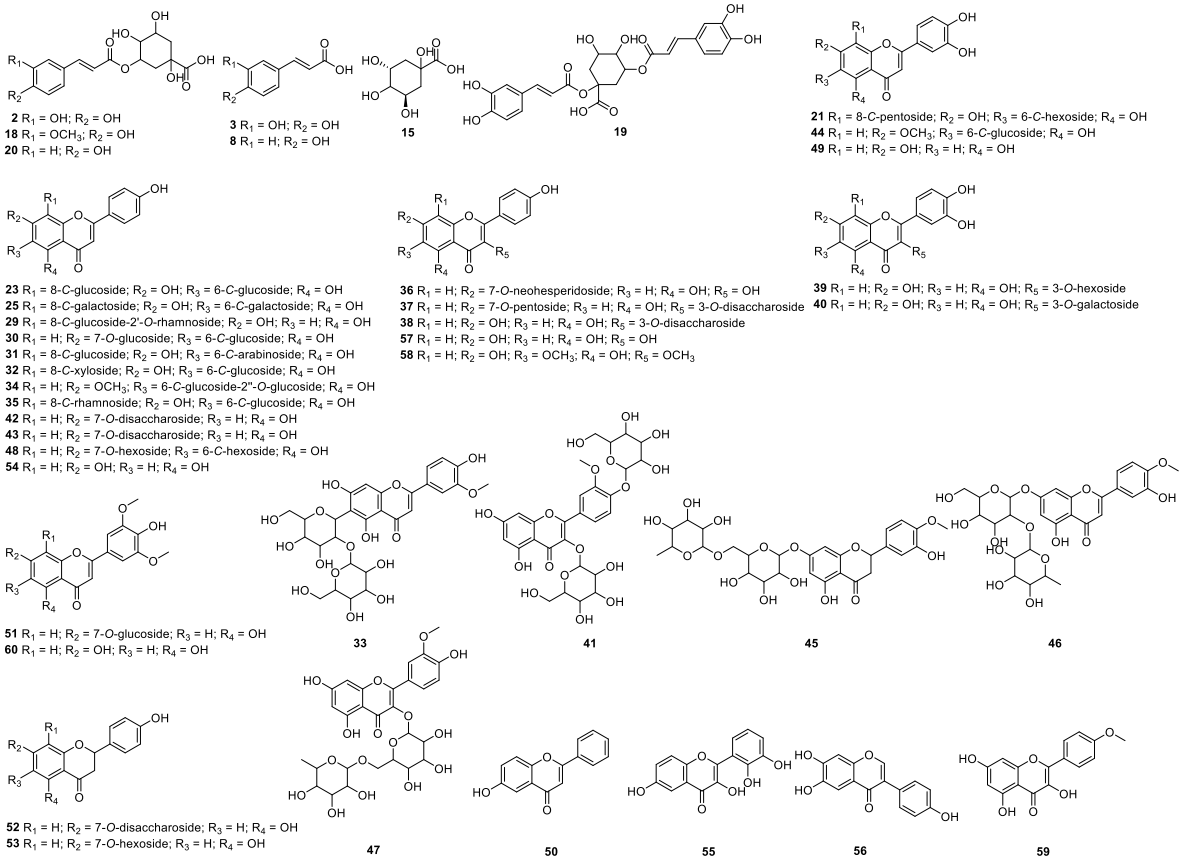
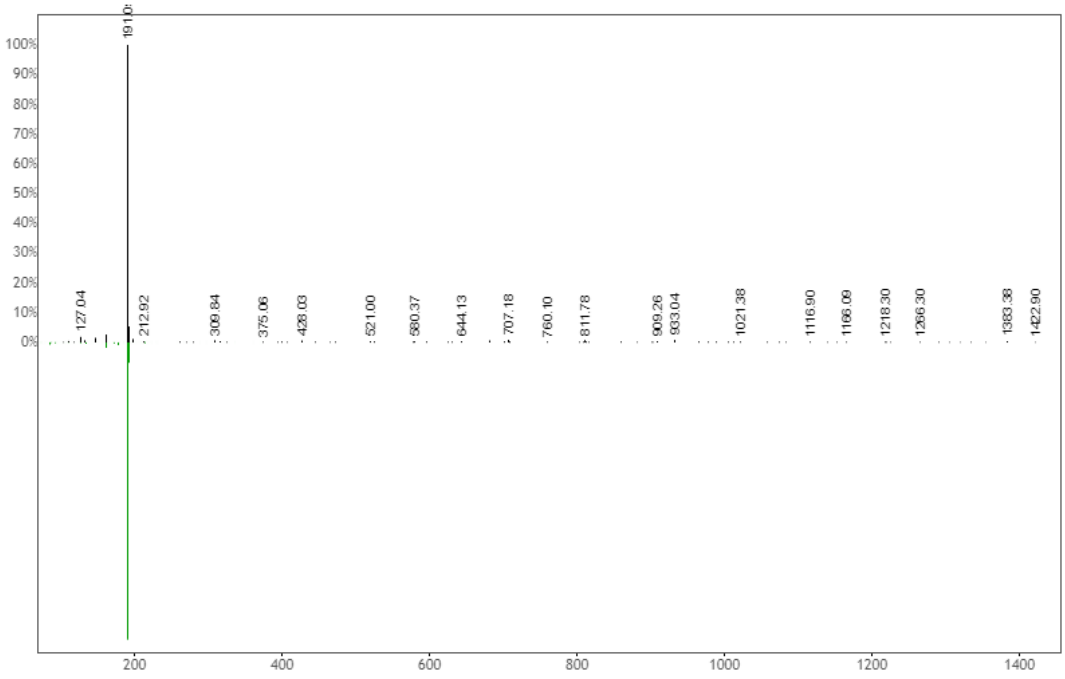
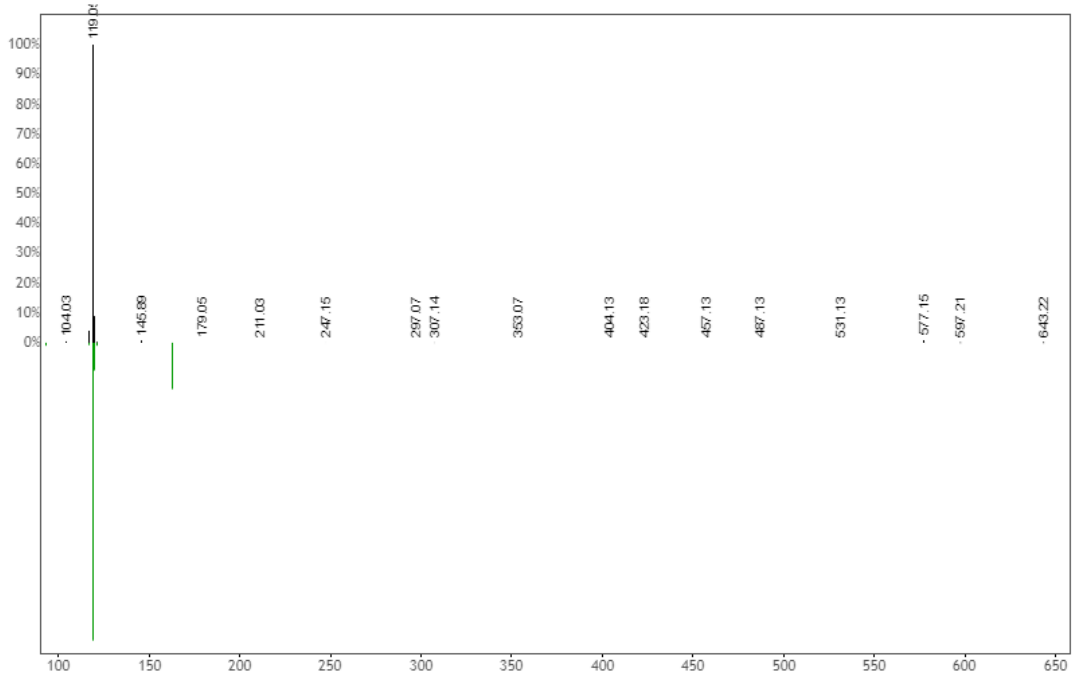



**Figure S3.2.** Chemical structures of the metabolites were found in BLEs.

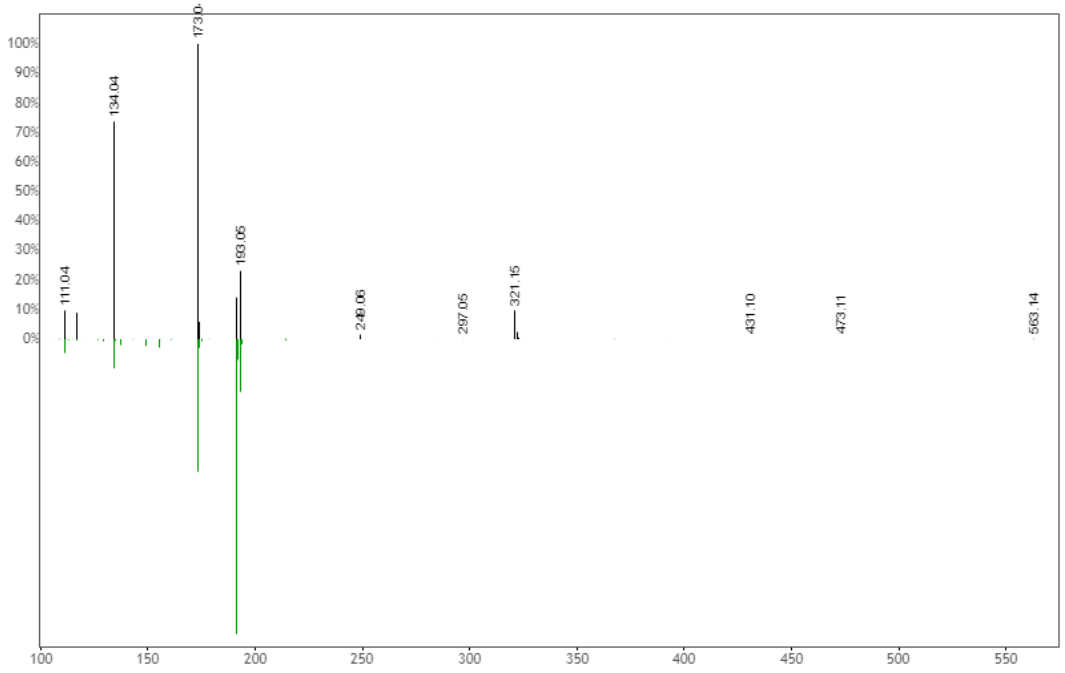
Compound **2**



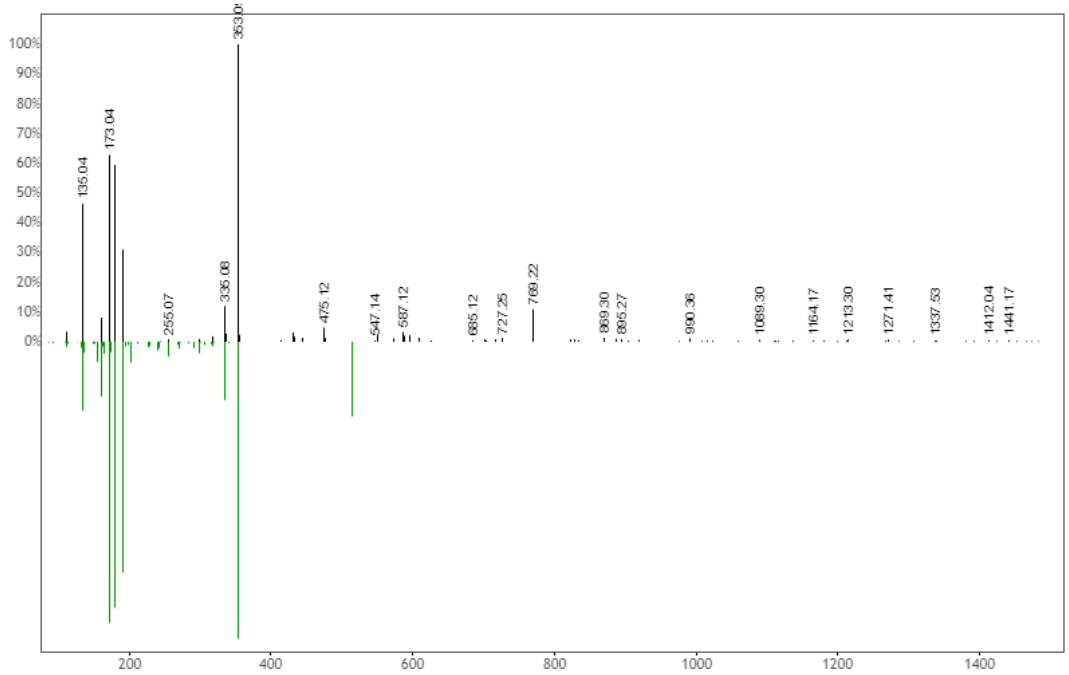

Compound **8**



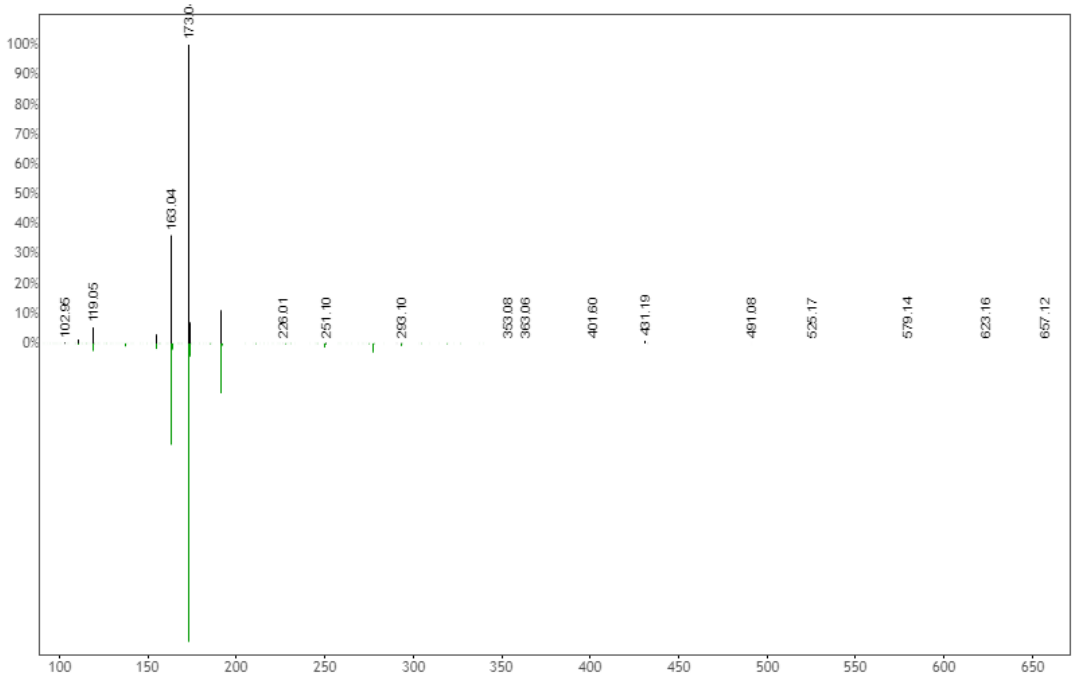
Compound **18**



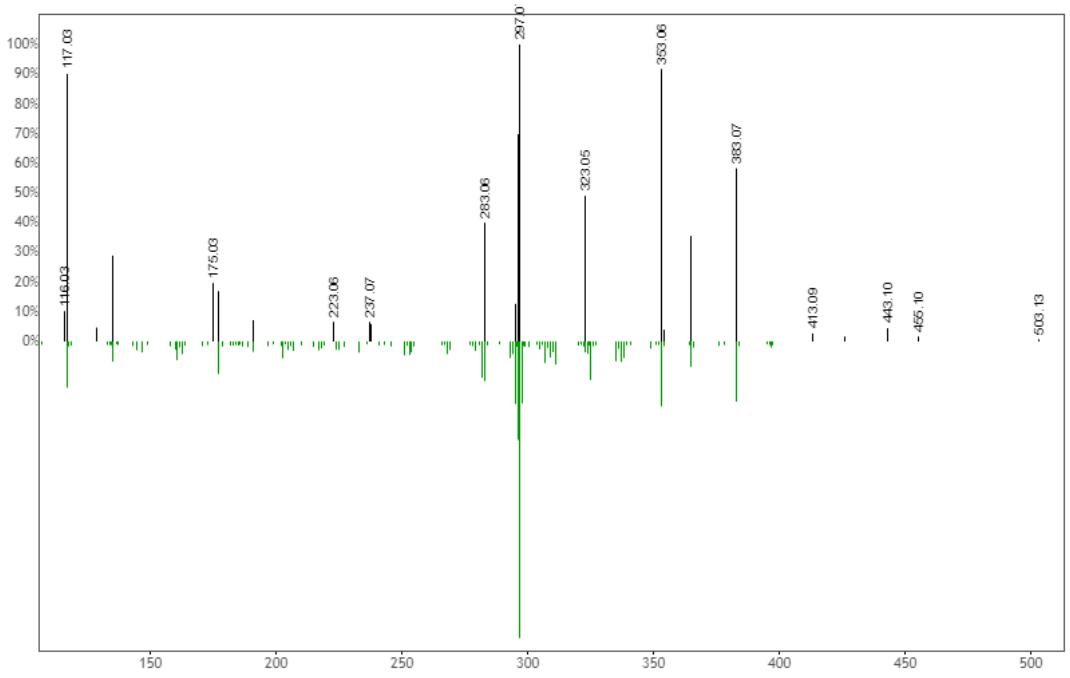

Compound **19**



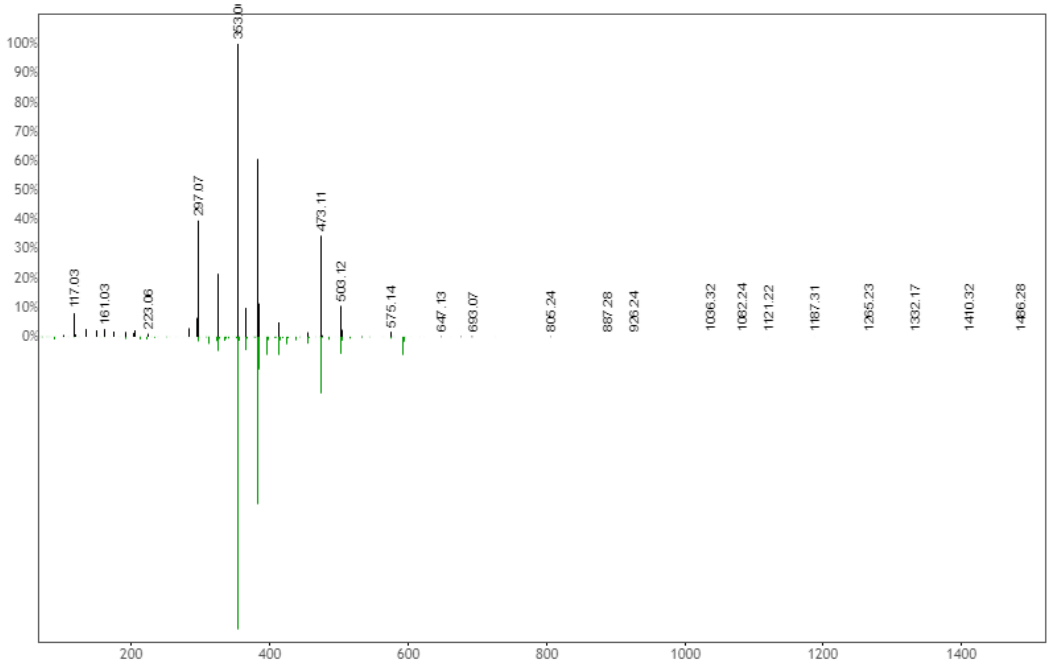
Compound **20**



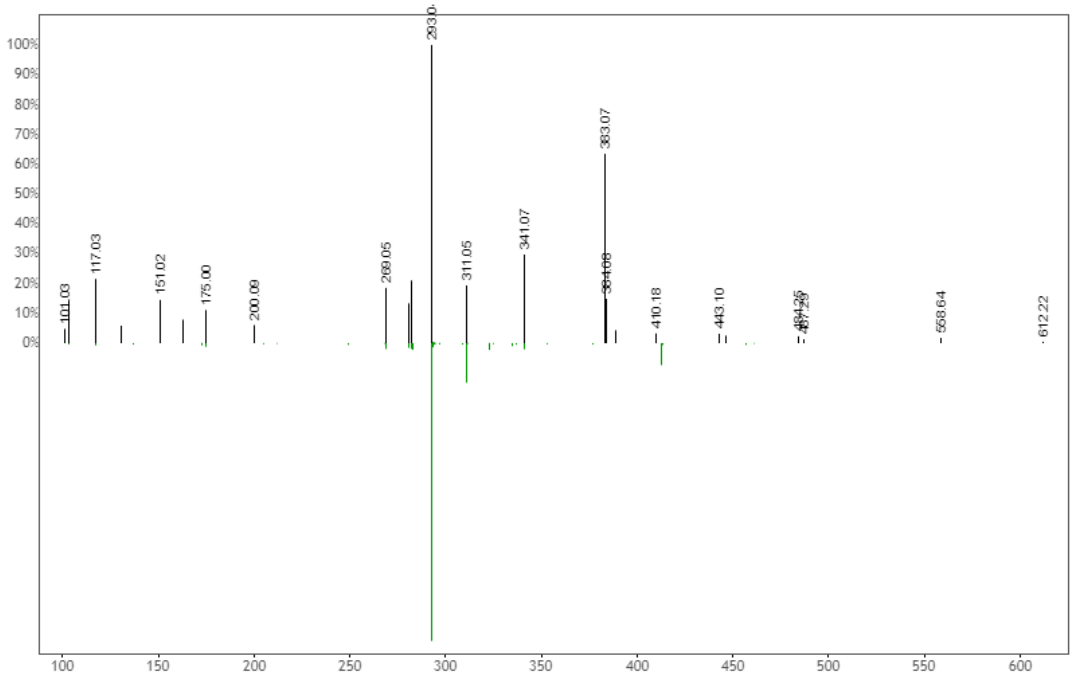

Compound **23**



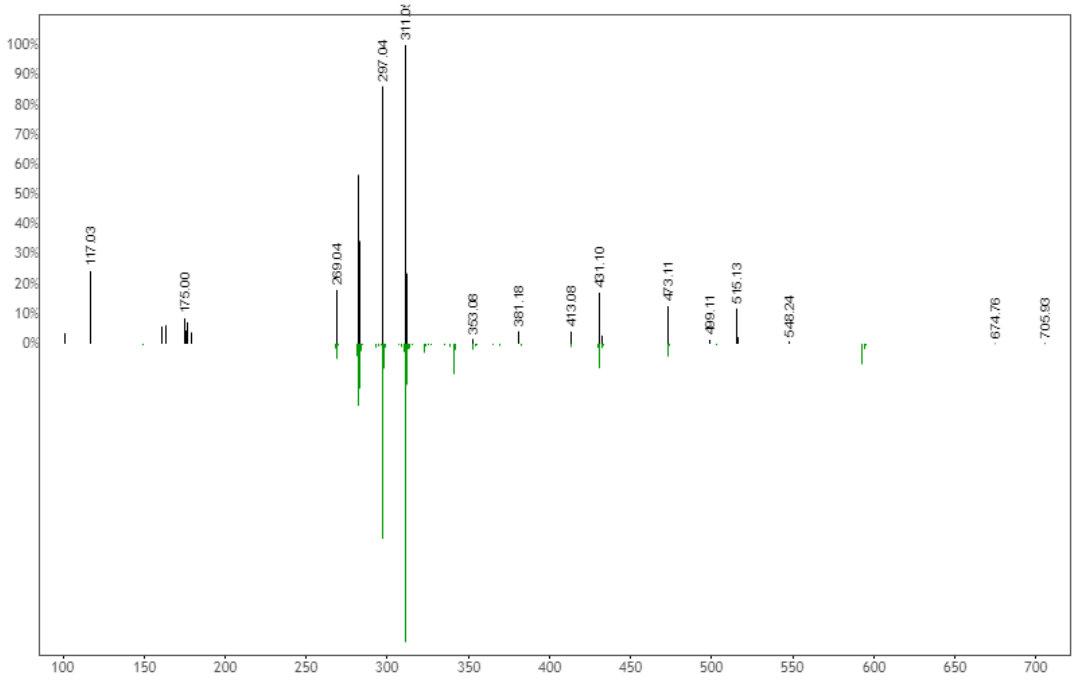
Compound **25**



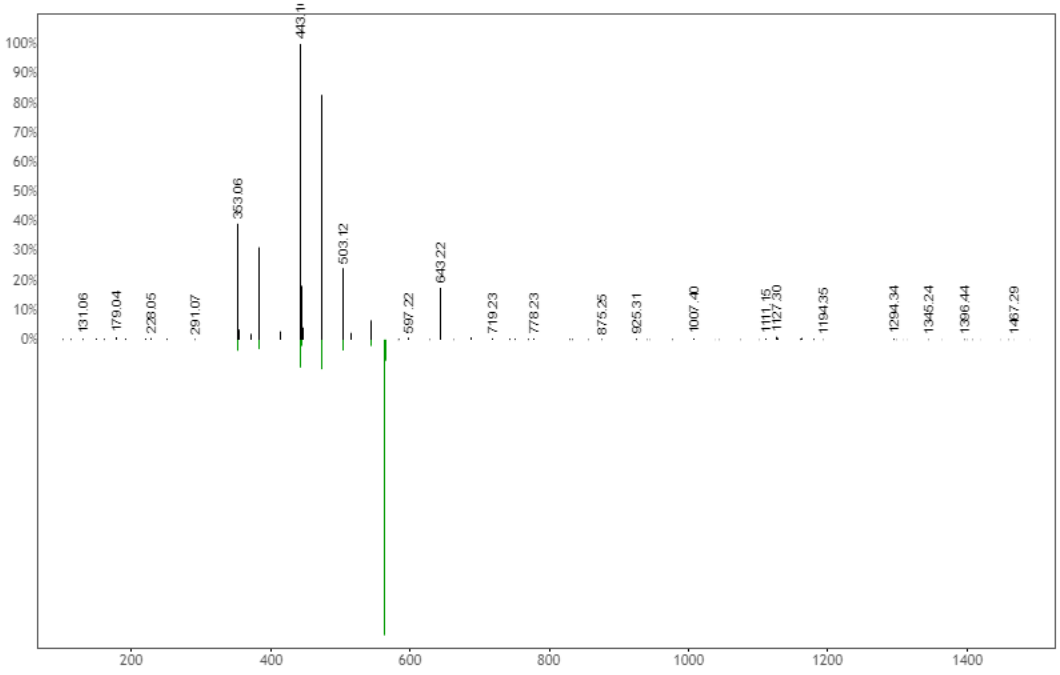

Compound **29**



Compound **30**




Compound **31**



Compound **36**

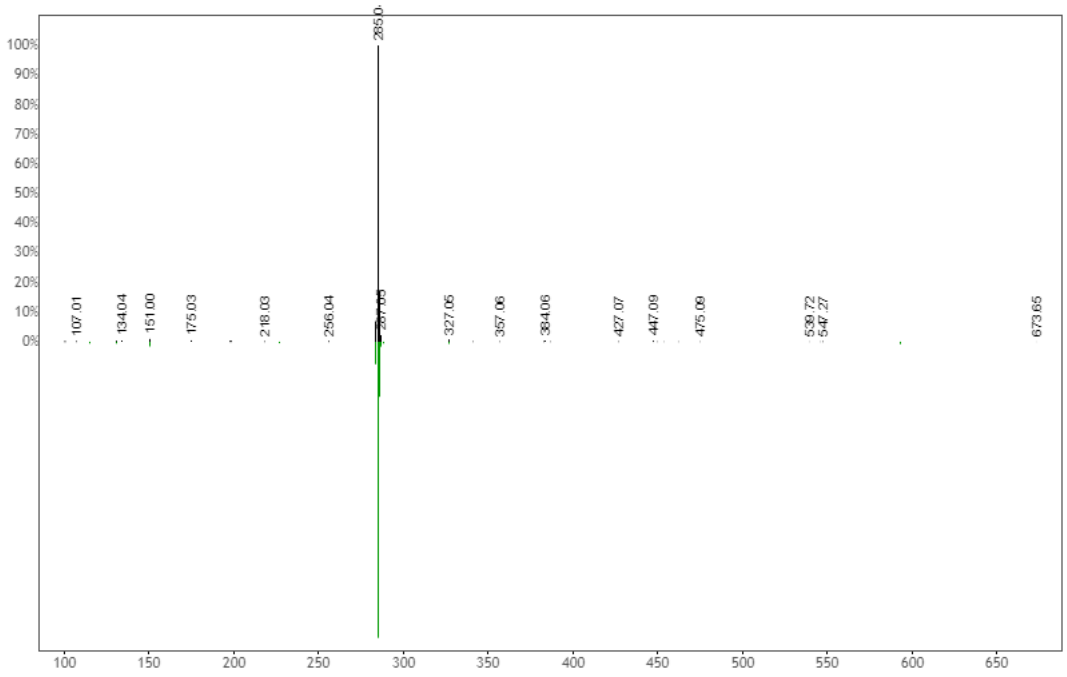



**Figure S3.3.** $MS^2$ spectrum match feature of GNPS showing the similarity of fragments patterns of the experimental and library data.

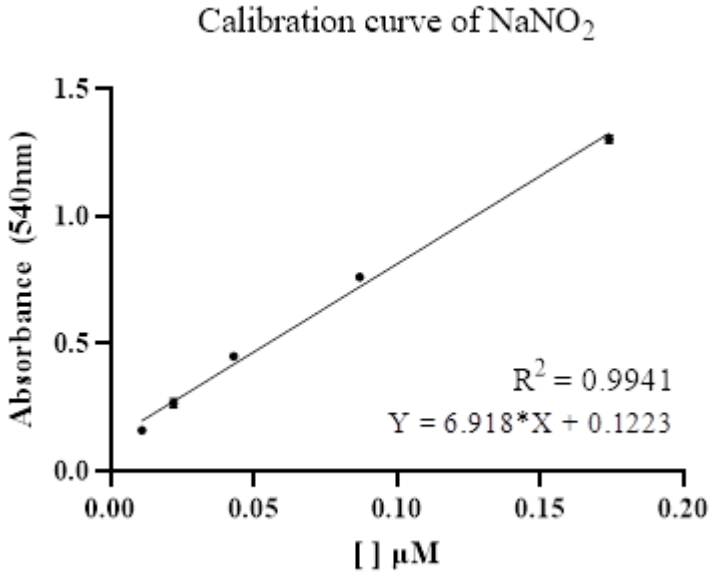



**Figure S3.4.** Calibration curve with sodium nitrite ($NaNO_2$) to represent the data in concentration of chemical $NO_2^-$ formed.

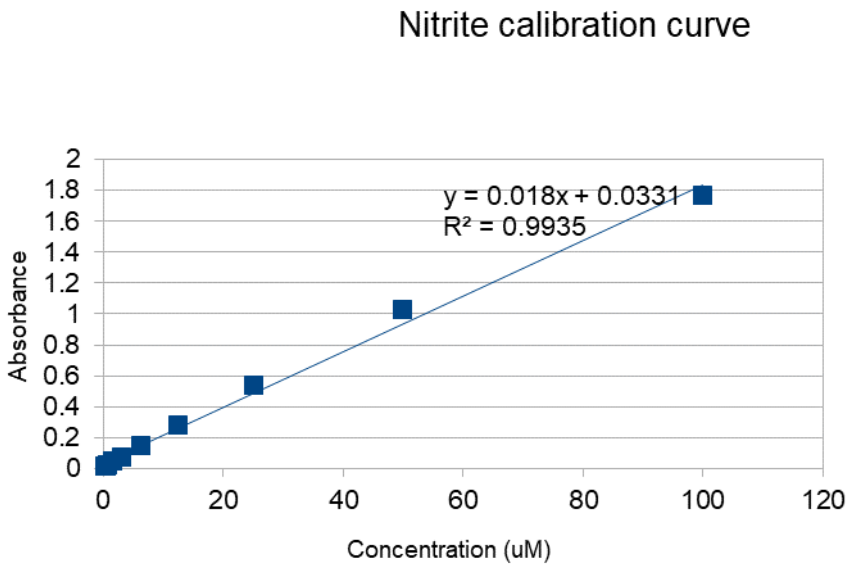



**Figure S3.5.** Calibration curve with sodium nitrite ($NaNO_2$) to represent the data in concentration of cellular $NO_2^-$ formed.

**Table S3.2.** Effect of L-NAME on NO inhibition in LPS-stimulated RAW 264.7 macrophage cells.

| Standard inhibitor | Concentrations tested (µg/mL) | | | | | |
|---|---|---|---|---|---|---|
| | **0.78125** | **1.5625** | **3.125** | **6.25** | **12.5** | **25** |
| L-NAME | 36.9% ± 0.28 | 41.7% ± 0.48 | 53.8 % ± 0.90 | 54.6% ± 4.40 | 74.5% ± 2.00 | 77.47 % ± 2.20 |

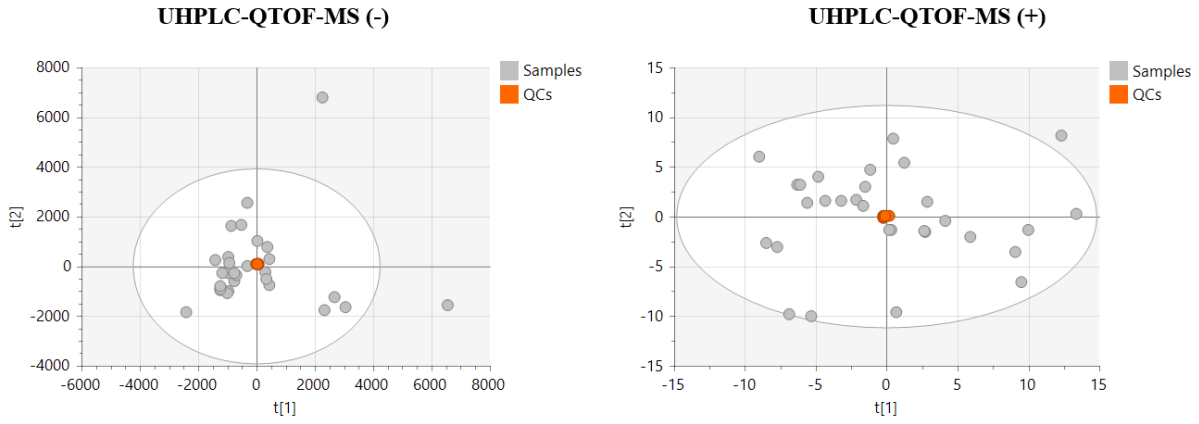



**Figure S3.6.** PCA score plot including Quality Controls (QCs) and all samples from UHPLC-QTOF-MS analysis in both negative and positive ion mode.

**Table S3.3.** List and information on the environmental variables of collection of the *Guadua* species used for the study.

| Species | Sample code | Location | Collection date | Latitude | Longitude | Altitude | AMAT (°C) | AMET (°C) | AMIT (°C) | MP (mm) | RH (%) |
|---|---|---|---|---|---|---|---|---|---|---|---|
| *G. aculeata* Rupr. ex E. Fourn. | *Gac-Q1* | Quindío | 12/2021 | 4.52086 | -75.80102 | 1256 | 28.0 | 24.0 | 21.0 | 200-300 | 82.0 |
| *G. amplexifolia* J.Presl | *Gam-Q1* | Quindío | 03/2021 | 4.52083 | -75.80108 | 1256 | 28.0 | 24.0 | 21.0 | 200-300 | 82.0 |
| | *Gam-Q2* | Quindío | 12/2021 | 4.52083 | -75.80108 | 1256 | 28.0 | 24.0 | 21.0 | 200-300 | 82.0 |
| | *Gam-Q3* | Quindío | 12/2021 | 4.52083 | -75.80108 | 1256 | 28.0 | 24.0 | 21.0 | 200-300 | 82.0 |
| *G. angustifolia* Kunth | *Gan-C1* | Cundinamarca | 09/2020 | 5.18127 | -74.19519 | 1343 | 31.5 | 25.5 | 23.5 | 100-200 | 82.5 |
| | *Gan-C2* | Cundinamarca | 09/2020 | 5.18127 | -74.19519 | 1343 | 31.5 | 25.5 | 23.5 | 100-200 | 82.5 |
| | *Gan-C3* | Cundinamarca | 09/2020 | 5.18127 | -74.19519 | 1343 | 31.5 | 25.5 | 23.5 | 100-200 | 82.5 |
| | *Gan-C4* | Cundinamarca | 10/2022 | 5.18127 | -74.19519 | 1343 | 31.5 | 25.5 | 23.5 | 100-200 | 82.5 |
| | *Gan-C5* | Cundinamarca | 09/2020 | 5.18127 | -74.19519 | 1343 | 31.5 | 25.5 | 23.5 | 100-200 | 82.5 |
| | *Gan-C6* | Cundinamarca | 09/2020 | 5.18127 | -74.19519 | 1343 | 31.5 | 25.5 | 23.5 | 100-200 | 82.5 |
| | *Gan-C7* | Cundinamarca | 10/2021 | 5.18127 | -74.19519 | 1343 | 31.5 | 25.5 | 23.5 | 100-200 | 82.5 |
| | *Gan-N1* | Nariño | 06/2021 | 1.37383 | -77.27988 | 1857 | 20.6 | 17.5 | 12.3 | 100-200 | 60.0 |
| | *Gan-N2* | Nariño | 12/2021 | 1.32755 | -77.48088 | 1720 | 21.8 | 16.8 | 13.6 | 100-200 | 65.0 |
| | *Gan-N3* | Nariño | 12/2021 | 1.32755 | -77.48088 | 1720 | 21.8 | 16.8 | 13.6 | 100-200 | 65.0 |
| | *Gan-N4* | Nariño | 01/2022 | 1.32755 | -77.48088 | 1720 | 21.8 | 16.8 | 13.6 | 100-200 | 65.0 |
| | *Gan-N5* | Nariño | 01/2022 | 1.54900 | -78.67738 | 21 | 28.0 | 26.0 | 24.0 | 200-300 | 85.0 |
| | *Gan-N6* | Nariño | 01/2022 | 1.54900 | -78.67738 | 21 | 28.0 | 26.0 | 24.0 | 200-300 | 85.0 |
| | *Gan-Q1* | Quindío | 12/2021 | 4.52053 | -75.79973 | 1256 | 28.0 | 24.0 | 21.0 | 200-300 | 82.0 |
| | *Gan-Q2* | Quindío | 04/2022 | 4.52053 | -75.79973 | 1256 | 28.0 | 24.0 | 21.0 | 200-300 | 82.0 |

| | | | | | | | | | | | |
|---|---|---|---|---|---|---|---|---|---|---|---|
| *G. angustifolia* Kunth biotype San Calixto | *Ganc-Q1* | Quindío | 04/2022 | 4.52063 | -75.80041 | 1256 | 29.0 | 23.0 | 18.0 | 200-300 | 80.0 |
| *G. angustifolia* var. *bicolor* Londoño | *Ganb-Q1* | Quindío | 04/2022 | 4.52018 | -75.80056 | 1256 | 29.0 | 23.0 | 18.0 | 200-300 | 80.0 |
| *G. incana* Londoño | *Gin-P1* | Putumayo | 12/2021 | 1.17730 | -76.66477 | 604 | 26.0 | 22.5 | 20.0 | 100-200 | 85.0 |
| | *Gin-Q1* | Quindío | 03/2021 | 4.52102 | -75.80013 | 1256 | 28.0 | 24.0 | 21.0 | 200-300 | 82.0 |
| | *Gin-Q2* | Quindío | 12/2021 | 4.52102 | -75.80013 | 1256 | 28.0 | 24.0 | 21.0 | 200-300 | 82.0 |
| *G. superba* Huber | *Gsu-Q1* | Quindío | 04/2022 | 4.52100 | -75.80036 | 1256 | 29.0 | 23.0 | 18.0 | 200-300 | 80.0 |
| *G. uncinata* Londoño & L.G.Clark | *Gun-Q1* | Quindío | 03/2021 | 4.51816 | -75.80033 | 1256 | 28.0 | 24.0 | 21.0 | 200-300 | 82.0 |
| | *Gun-Q2* | Quindío | 12/2021 | 4.51816 | -75.80033 | 1256 | 28.0 | 24.0 | 21.0 | 200-300 | 82.0 |
| | *Gun-Q3* | Quindío | 12/2021 | 4.51816 | -75.80033 | 1256 | 28.0 | 24.0 | 21.0 | 200-300 | 82.0 |
| *G. venezuelae* Munro | *Gve-Q1* | Quindío | 04/2022 | 4.52057 | -75.80005 | 1256 | 29.0 | 23.0 | 18.0 | 200-300 | 80.0 |
| *G. weberbaueri* Pilg. | *Gwe-Q1* | Quindío | 04/2022 | 4.52043 | -75.80057 | 1256 | 29.0 | 23.0 | 18.0 | 200-300 | 80.0 |

Annual Maximum Temperature (AMAT), Annual Mean Temperature (AMET), Annual Minimum Temperature (AMIT), Monthly Precipitation (MP), and Relative Humidity (RH).

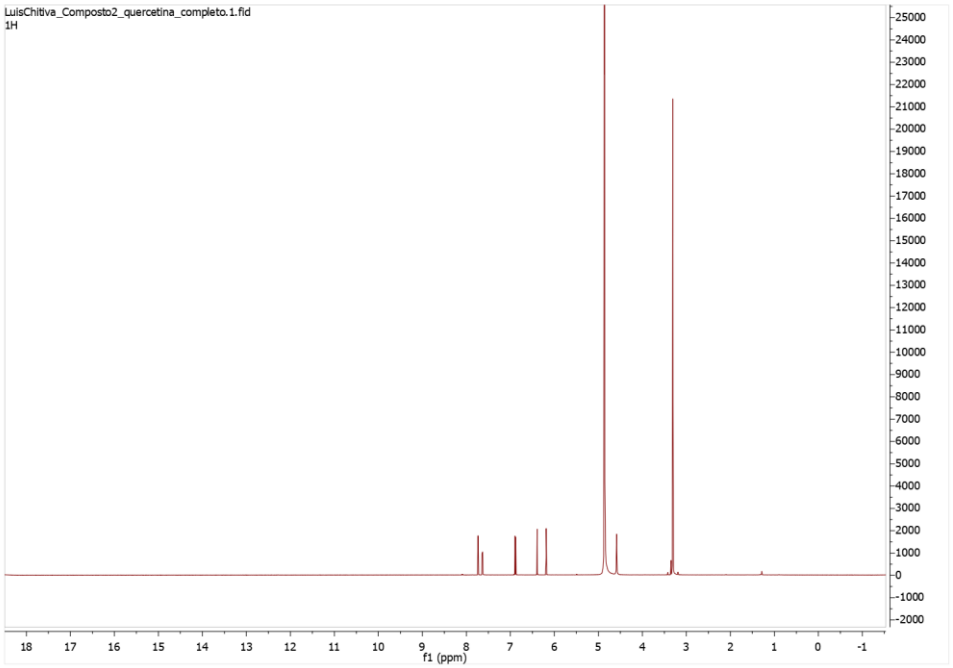
**Table S3.4.** Comparison of retention times of reference standards between HPLC-DAD and UHPLC-QTOF-MS analyses.

| No | Chemical standard | Chemical class | UV $\lambda_{max}$ (nm) | Molecular formula | $t_R$ (min) HPLC[a] | $t_R$ (min) UHPLC[b] | Exact mass | $[M-H]^-$ | $[M+H]^+$ |
|---|---|---|---|---|---|---|---|---|---|
| **1** | Gallic acid | Organic acid | 275 | $C_7H_6O_5$ | 4.36 | 1.09 | 170.0215 | 169.0132 | - |
| **2** | Chlorogenic acid (CGA) | Cinnamic acid and derivatives | 275sh, 325 | $C_{16}H_{18}O_9$ | 7.72 | 2.42 | 354.3095 | 353.0863 | - |
| **3** | Caffeic acid | Cinnamic acid and derivatives | 275 | $C_9H_8O_4$ | 9.08 | 2.55 | 180.0422 | 179.0344 | - |
| **4** | Isoorientin | Flavone glycosides | 274, 355 | $C_{21}H_{20}O_{11}$ | 9.39 | 2.96 | 448.3775 | 447.0954 | 449.1094 |
| **5** | Ampelopsin | Flavanonol aglycones | 300 | $C_{15}H_{12}O_8$ | 9.88 | 2.88 | 320.0532 | 319.0458 | - |
| **6** | Rutin | Flavonol glycosides | 274, 355 | $C_{27}H_{30}O_{16}$ | 10.42 | 3.20 | 610.1533 | 609.1531 | 611.1603 |
| **7** | Vitexin | Flavone glycosides | 273, 335 | $C_{21}H_{20}O_{10}$ | 10.56 | 3.26 | 432.1056 | 431.0923 | 433.1123 |
| **8** | *p*-Coumaric acid | Cinnamic acid and derivatives | 295sh, 310 | $C_9H_8O_3$ | 11.15 | 3.36 | 164.0473 | 163.0390 | - |
| **9** | Sinapinic acid | Cinnamic acid and derivatives | 325 | $C_{11}H_{12}O_5$ | 11.55 | 3.78 | 224.2101 | 223.0684 | - |
| **10** | Morin | Flavonol aglycones | 264, 354 | $C_{15}H_{10}O_7$ | 14.79 | 4.19 | 302.0426 | 301.0351 | 303.0512 |
| **11** | Coumarin | Coumarins | 275, 325 | $C_9H_6O_2$ | 15.19 | 4.35 | 146.1432 | - | 147.0377 |
| **12** | Quercetin | Flavonol aglycones | 275, 358 | $C_{15}H_{10}O_7$ | 15.86 | 4.49 | 302.0426 | 301.0344 | 303.0494 |
| **13** | Cinnamic acid | Cinnamic acid and derivatives | 275 | $C_9H_8O_2$ | 16.84 | 4.63 | 148.1597 | 147.0524 | - |
| **14** | Naringenin | Flavanone aglycones | 275, 325 | $C_{15}H_{12}O_5$ | 17.75 | 4.93 | 272.0684 | 271.0611 | 273.0764 |

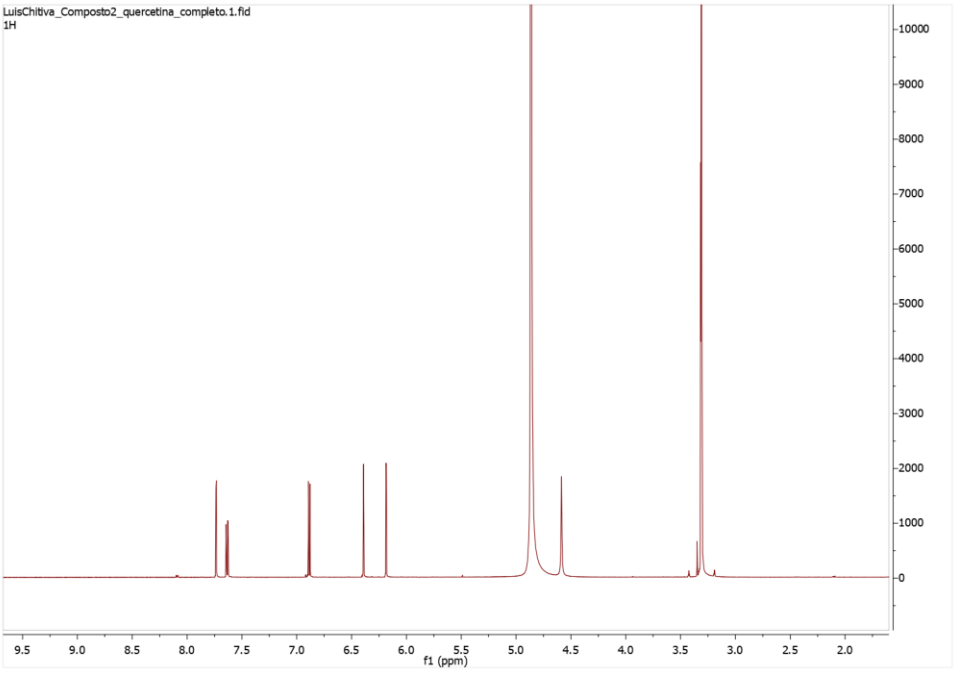
[a] Column: Luna C18 column (150 x 4.6 mm, 5 µm, 100 Å)

[b] Column: ACQUITY UPLC HSS T3 C18 column (2.1 × 100 mm, 1.8 µm)

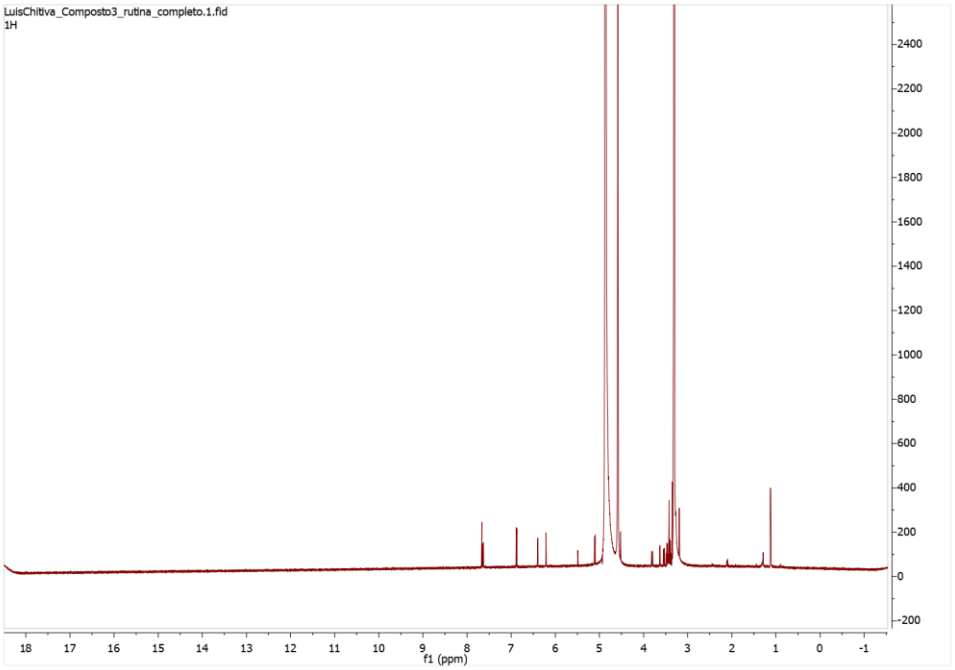
Quercetin (**STD 1**)




Quercetin (**STD 1**) expanded region



Rutin (STD 2)




Rutin (**STD 2**) expanded region

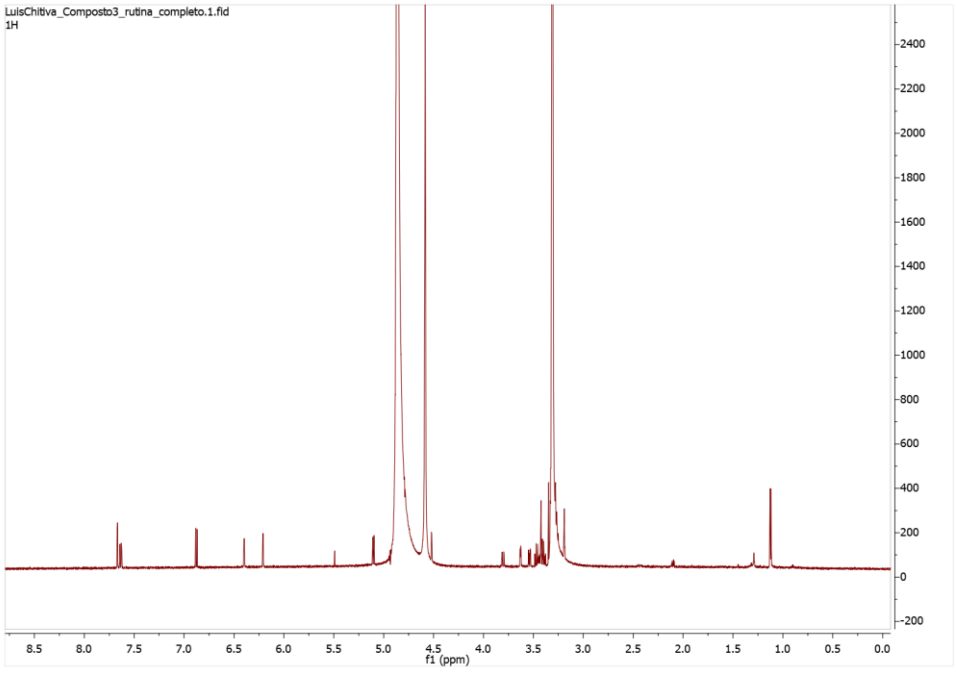



**Figure S3.7.** $^{1}$H-NMR spectra obtained for the reference standards (STD).

**Table S3.5.** Parameters used in the MZmine 2.53 software for processing the data obtained by UHPLC-QTOF-MS.

| MZmine version 2.53 software | |
|---|---|
| **Preprocessing step** | **Parameters** |
| ***Feature detection*** | *Mass Detection* |
| | MS level: 1 |
| | Set filters |
| | Retention time: 0.2 - 10 min |
| | Mass detector: Centroid |
| | Noise level: 1E3 |
| | MS level: 2 |
| | Set filters |
| | Retention time: 0.2 - 10 min |
| | Mass detector: Centroid |
| | Noise level: 1E2 |
| ***Chromatogram builder*** | *ADAP Chromatogram Builder* |
| | MS level: 1 |
| | Min group size in # of scans: 5 |
| | Group intensity threshold: 1E3 |
| | Min highest intensity: 3E3 |
| | *m/z* tolerance: 0 *m/z* or 20 ppm |
| ***Deconvolution*** | *Chromatogram deconvolution* |
| | Algorithm: Baseline cut-off |
| | Min peak height: 1E3 |
| | Peak duration range (min): 0 to 3 min |
| | Baseline level: 1E3 |
| | *m/z* range for MS2 scan pairing (Da): 0.01 |
| | RT range for MS2 scan pairing (min): 0.02 |
| ***Isotopes*** | *Isotopic peaks grouper* |
| | *m/z* tolerance: 0 *m/z* or 20 ppm |
| | Retention time tolerance: 0.02 min |
| | Max charge: 2 |
| | Representative isotope: Most intense |
| ***Alignment*** | *Join aligner* |
| | *m/z* tolerance: 0 *m/z* or 20 ppm |
| | Weight for *m/z*: 75 |
| | Retention time tolerance: 0.25 absolute (min) |
| | Weight for RT: 25 |
| ***Filtering*** | *Feature list rows filter* |
| | Minimum peaks in a row (X): 1 |
| | Minimum peaks in an isotope pattern (X): 1 |
| | *m/z* range: 75 to 2000 |
| | Reset peak number ID: True |
| | Keep only peaks with MS2 scan (GNPS): (X) |

| | |
|---|---|
| ***Gap Filling*** | *Peak finder* |
| | Intensity tolerance: 10% |
| | *m/z* tolerance: 0 *m/z* or 10 ppm |
| | RT tolerance: 0.05 min |
| ***Export*** | *Export to CSV file* |
| | (X) Export row |
| | (X) Export row *m/z* |
| | (X) Export row retention time |
| | (X) Peak area |
| ***Formula prediction*** | Charge: 2 |
| | Ionization type: M-H |
| | *m/z* tolerance: 0.01 *m/z* or 10 ppm |
| | Max best formulas per peak: 3 |
| | O 50 |
| | H 100 |
| | C 100 |

**Table S3.6.** Parameters used in the NMRProcFlow software for processing the data obtained by $^{1}$H NMR.

| **NMRProcFlow version 1.4.20 software** | |
|---|---|
| **Preprocessing step** | **Parameters** |
| ***PPM Calibration*** | *Range of the PPM reference:* |
| | Not applicable |
| | *PPM value of the center of resonance:* |
| | 0 |
| | *noisy PPM range:* |
| | 10.5 10.2 |
| ***Normalization*** | *Normalization Method:* |
| | Constant Sum Normalization |
| | *Reference PPM ranges:* |
| | Not applicable |
| ***Baseline correction*** | *Type of Correction:* |
| | Local Correction |
| | *noisy PPM range:* |
| | 10.5 10.2 |
| | *Restricted PPM range:* |
| | Not applicable |
| | *Level of Correction:* |
| | 1 |
| | *Order:* |
| | 1 |

| | |
|---|---|
| ***Alignment*** | *Align. Method:* |
| | Least Square |
| | *Relative max. shift:* |
| | 0.05 |
| | *Reference spectrum:* |
| | Auto reference |
| | *PPM Ranges to align:* |
| | Not applicable |
| ***PPM shift*** | *PPM shift value:* |
| | 0 |
| | *PPM Ranges to shift:* |
| | Not applicable |
| ***Zeroing*** | *PPM Ranges to clean:* |
| | 4.99 4.75 |
| ***Bucketing*** | |
| Bucketing Method | *Resolution Factor:* |
| *Intelligent Bucketing* | 0.5 |
| | *SNR threshold:* |
| | 3 |
| | *noisy PPM range:* |
| | 10.5 10.2 |
| | *PPM Ranges:* |
| | 10.0 0.0 |
| ***Data export*** | |
| Data matrix | *Export Format:* |
| | Comma Separator Value (CSV) |
| | *SNR threshold:* |
| | 3 |
| | *noisy PPM range:* |
| | 10.5 10.2 |
| | *Normalization Method:* |
| | Constant Sum Normalization |
| | *PPM range of the Reference:* |
| | Not applicable |
| ***Buckets table*** | *Export Format:* |
| | Comma Separator Value (CSV) |

# 4 CHAPTER 4. Uncovering metabolic alterations in HCT-116 colon cancer cells upon exposure to bamboo leaf extract obtained from *Guadua incana* Londoño

## Presentation

Considering the results of the previous chapters, which revealed that *Guadua* species have a high content of flavone glycosides in their chemical composition and that these compounds are responsible for their cytotoxic potential, Chapter 4 focused on applying a metabolomics analysis of the endometabolome and exometabolome of the HCT-116 cell line. The aim was to identify altered metabolic pathways after exposure to the active bamboo leaf extract obtained from *G. incana*, to understand possible mechanisms of action. The selection of the bamboo leaf extract was based on its cytotoxic potential and the richness of its chemical composition, particularly in flavonoid glycosides. The results in this chapter correspond to the manuscript:

*Molecules* 2024, *29(13), 2985*; DOI: 10.3390/molecules29132985

## 4.1 Materials and methods

### 4.1.1 Chemical and reagents

Methanol, Acetonitrile, and formic acid HPLC grade were acquired from Merck (Darmstadt, Germany). Ultra-pure water was used throughout and was produced by a Milli-Q Ultra-pure water system with a resistivity of 18.2 MΩ.cm at 25 °C (Millipore, Bedford, USA). For the NMR experiments, methanol-$d_4$ (>99.8 atom % D) and deuterium oxide (>99.8 atom % D) were purchased from Sigma-Aldrich USA (St. Louis, MO, USA). Dimethyl sulfoxide (DMSO) was purchased from Panreac AppliChem. RPMI-1640 medium, fetal bovine serum (FBS), and penicillin-streptomycin were obtained from Gibco BRL (Grand Island, NY, USA).

### 4.1.2 Plant material, extraction, and chemical characterization

Leaves of *Guadua incana* Londoño were collected in the bamboo collection of El Bambusal Farm, Quindío, Colombia (GPS 4°31'15'' N, 75°48'0'' W) and identified by Néstor García and Ximena Londoño at the Herbarium of the Pontificia Universidad Javeriana (HPUJ) and were deposited with voucher specimen number HPUJ-30723. The collection was performed under the permit of the Contract for Access to Genetic Resources and Derived Products (Contract No. 212/RGE 0287-6) granted by the Ministry of the Environment and Sustainable Development to the Pontificia Universidad Javeriana (PUJ) and the Colombia Científica/GAT Program. The plant material was dried in an oven with circulating air at 40 °C for 96 hours (about 4 days) for subsequent grinding. After grinding, extraction of the dried and ground plant material was carried out through percolation with ethanol (96% EtOH) at a ratio of 1:10 (*w/v*) at room temperature. The extraction process was conducted in 4 cycles of 24 hours each. The BLEGI obtained from the different cycles was combined and concentrated under reduced pressure at a temperature not exceeding 40 °C, using a rotary evaporator. The BLEGI extract was purified using a C18 cartridge to remove nonpolar interferences, such as lipids, fats, and other hydrophobic residues, aiming to obtain an extract enriched mainly in flavonoids and other compounds for subsequent biological assays and metabolomic analyses.

### 4.1.3 Chemical characterization of the BLEGI

#### 4.1.3.1 Chemical analysis through LC-MS

The samples were analyzed using a Waters ACQUITY UPLC high-resolution system in conjunction with a Waters Xevo G2-S QTOF mass spectrometer (Waters Corporation, Milford, MA, USA). A total of 2 µL of the sample was injected into a Waters ACQUITY UPLC HSS T3 C18 (2.1 x 100 mm, 1.8 µm) column (Waters Corporation, Wexford, Ireland) was used, maintaining the temperature at 30 °C. The separation was carried out using two mobile phases: eluent A (water with 0.1 % formic acid) and eluent B (acetonitrile with 0.1 % formic acid), at a flow rate of 0.5 mL/min. The elution gradient was programmed as follows: 10-100% B from 0 to 10 min, 100% B from 10 to 14 min, 100-5%

B from 14 to 15 min, and 5% B from 15 to 20 min. Mass spectrometry was performed on a Xevo G2-S QTOF instrument using electrospray ionization (ESI). Mass spectral data were acquired in negative ($ESI^-$) and positive ($ESI^+$) ionization modes, over a mass range of *m/z* 100-1500 Da using dependent data acquisition (DDA) mode at a scan rate set at 0.1 s, followed by MS/MS scanning of the most intense ions. For MS/MS fragmentation, a low collision energy ramp varying between 10 and 40 eV as well as a high collision energy ramp varying between 50 and 80 eV were applied to acquire the data in centroid format. The QTOF instrument operated at a frequency of 6.0 GHz and 76.0 µs, using high resolution calibrated with the reference mass correction for Leucine-enkephalin ($C_{28}H_{37}N_5O_7$) was used as a lock mass compound in positive ion mode ($[M+H]^+$ = 556.2771) and negative ion mode ($[M-H]^-$ = 554.2615), respectively. The spectrometer parameters were as follows: capillary voltage was set to 2.2 kV (ESI−) or 2.6 kV (ESI+), cone voltage was set to 40 V, source temperature was maintained at 120 °C, cone gas was set to 50 L/h, and desolvation gas was set to 800 L/h at 300 °C. Retention time data LC-MS analyzes of the chemical standards are detailed in Table S4.3.

#### 4.1.3.2 GNPS classical molecular MS/MS network analyses

The MS/MS data files in mzML format were submitted to the GNPS online platform (http://gnps.ucsd.edu). The molecular networking of BLEGI was obtained using parameters provided in the Table S4 and described by Aron et al., 2020 (ARON et al., 2020). The attribute table of the generated nodes was visualized in the Cytoscape version 3.7.2 software to analyze the molecular network.

### 4.1.4 Cell lines and culture conditions

The human colorectal cancer cell line HCT-116 was obtained from the American Type Culture Collection. Cells were routinely cultured in RPMI 1640 medium supplemented with 10% FBS and 1% penicillin-streptomycin. The cells were incubated at 37 °C in a humidified atmosphere with 5% $CO_2$. For all assays, HCT-116 cells were cultured and used at 80% confluency.

### 4.1.5 Cytotoxicity assay

Before the metabolomics experiment, an assessment of the cytotoxic potential of the BLE was conducted using the MTT assay. Briefly, HCT-116 cells were cultivated in 96-well plates at a density of 1 x $10^6$ cells per well in growth medium. Following a 24 h incubation period, the cells were rinsed with a PBS solution and treated with the extract at various concentrations (0.0032 to 50 µg/mL). Respective controls were included on each plate, comprising a blank (medium only), a solvent control (0.1% DMSO), and a positive control (doxorubicin). After a 72-h incubation, the cells underwent another PBS wash and were further maintained for an additional 3 hours in medium containing 0.5 mg/mL MTT. The resulting formazan was dissolved in 150 µL of DMSO, and absorbance was measured at 570 nm using reader Bio-Tek Synergy HTX multi-mode reader (BioTeck Instruments). Two independent experiments were performed in duplicates, and the $IC_{50}$ values and their 95% confidence interval were calculated by sigmoidal nonlinear regression using GraphPad Prism 8 software (San Diego, CA, USA).

### 4.1.6 Immunofluorescence Analysis

In the immunofluorescence assay, cells were cultured on coverslips in 35 mm Petri dishes at a concentration of 1 x $10^4$ cells/mL. After 24 hours, they were treated with a concentration of 1.23 µg/mL of BLEGI, and after the treatment time (72 hours), they were fixed in 3.7% formaldehyde for 20 minutes. Subsequently, they were washed with PBS, permeabilized with 0.5% Triton X-100 for 20 minutes and washed again. After permeabilization, the primary antibody (anti-a-tubulin, 1:50, Sigma-Aldrich, MO, USA) was added and left in contact with the cells overnight. Following the incubation period with the primary antibody, the cultures were washed with PBS, and the secondary antibody coupled to fluorescein (Alexa Fluor 488 Conjugate, 1:50, Cell Signaling Technology, MA, USA) was added and incubated for 2 hours. Subsequently, the nuclei were stained with DAPI (4′,6-diamidino-2-phenylindole) (1:100, Sigma-Aldrich, MO, USA). The slides were then mounted with Vecta-Shield anti-fading (Vector Laboratories, CA, USA). Images were acquired using a LionHeart FX fluorescence microscope (Biotek, VT, USA).

### 4.1.7 Nitric oxide (NO) inhibitory assay

In The evaluation of the NO scavenger was performed according to methodology adapted from Marcocci et al and Bates et al (MARCOCCI et al., 1994). The assay is based on the ability of sodium nitroprusside (NPS) molecules (commercial Neon code 02232; São Paulo, Brazil) to release NO spontaneously in PBS buffer when under the influence of light (BATES et al., 1995). NO, in turn, is transformed into nitrite ($NO_2^-$) when reacting with molecular oxygen in the medium and can therefore be quantified by adding Griess reagent (1% *w/v* sulfanilamide, 0.1% *w/v* of naphthyl ethylenediamine and 2.5% *v/v* of ortho-phosphoric acid) (Neon commercial code 02179, 01874 and 00232, respectively, São Paulo, Brazil) to form a pink chromophore with high absorption at 540 nm. To this end, NPS (1.25 mM) was prepared in phosphate buffer (0.1 M and pH 7.0) in the absence of light. In a 96-well plate, 50 µL of NPS and 50 µL of samples at different concentrations (25, 50, 100 and 200 µg/mL) were added and incubated for 40 minutes at room temperature with strong exposure to UV light. After incubation, 100 µL of Griess reagent was added and the reaction mixture was read at 540 nm. A calibration curve was also performed with sodium nitrite ($NaNO_2$) to represent the data in concentration of $NO_2^-$ formed (Figure S4.6).

### 4.1.8 Macrophages cell culture and viability

The murine macrophage cell line RAW 264.7 (ATCC TIB 71) was provided by the cell bank of Rio de Janeiro, Brazil. The cells were maintained in DMEM high glucose medium (Dulbecco's modified eagle medium) (Vitrocell code 02037, Campinas, Brazil) supplemented with 10% FBS (*v/v*) and incubated in an oven at 37 °C with atmosphere containing 5% $CO_2$ at different periods until reaching confluence of approximately 70 to 90%. Afterwards, the cells were removed with the aid of a cell scraper (RAW macrophages) and counted in a Neubauer chamber to obtain cell concentration values. After removing the medium and washing 3 times with PBS, the cells were detached with a cell scraper and counted in a Neubauer chamber. 100 µL of medium containing approximately $50 \times 10^4$ cells/mL was distributed in microplates (96 wells) incubated under

the same conditions as above. After 24 hours, the medium was removed, the wells were washed with PBS 3 times, and each well was treated with 3 concentrations of each sample (50 to 200 µg/mL) in triplicate. After incubation for 24 hours, cell viability was determined by the MTT test (Sigma-Aldrich, St. Louis, USA) (MOSMANN, 1983). The results were presented as mean ± standard deviation.

### 4.1.9 Inhibition of NO produced by macrophages

For NO assays, murine macrophage cultures RAW 264.7 (ATCC TIB-71) were used. Briefly, the cells were distributed in 96-well microplates at a concentration of 5 x $10^5$ viable cells/well/mL in complete DMEM medium and incubated for 2h (37 °C with 5% $CO_2$) for cell adhesion. After this period, the supernatant was discarded, and the cells were washed with sterile PBS. They were then stimulated with *Escherichia coli* Lipopolysaccharide (LPS) (SIGMA code L2630; St. Louis, MO, USA) at a concentration of 1 µg/mL, receiving, at the same time, different concentrations of samples (2 and 200 µg/mL) in supplemented DMEM, being the concentrations previously determined by the cytotoxicity assay. The plates were incubated overnight (37 °C with 5% $CO_2$). After this period, culture supernatants were collected for detection and quantification of NO using the Griess method (GREEN et al., 1982). Data were presented in $NO_2^-$ concentration (mM), using a standard curve for $NaNO_2$ (Figure S4.7). N(ω)-nitro-l-arginine methyl ester (L-NAME) was used as an inhibition control. Cytotoxicity evaluations were performed to determine the appropriate non-toxic concentrations of samples and after immunomodulatory assay through MTT method as described in item 4.3.5.

### 4.1.10 Statistical analysis

All results are represented as the mean ± standard deviation (SD) of triplicate data. Differences observed between the doses were achieved by one-way analysis of variance (ANOVA) followed by Tukey's pot hoc test and values of * $p$-value < 0.05 and ** $p$-value < 0.01 were considered significant. Statistical analyses were performed using GraphPad Prism 8 software (San Diego, CA, USA).

### 4.1.11 Untargeted metabolomic analysis

#### 4.1.11.1 Cell treatment

The cells were uniformly cultured in T75 cell culture flask under the same conditions. Ten replicates of both the BLE-treated group and the control group (untreated cells) were prepared for the metabolomic study. Additionally, a medium blank (process blank) without cells was placed on each plate. The minimum concentration of BLE that provides 50% survival of HCT-116 cells ($IC_{50}$) was determined to be 1.23 µg/mL. Therefore, this concentration was selected for treating the cells for metabolomic analysis. Cells were then seeded at a density of $3 \times 10^6$ cells/well in a 6-well cell culture plates using 5 ml of supplemented medium. Afterward, the plates were incubated for 24 hours to facilitate cell adhesion. Once the incubation was completed, fresh medium containing the selected concentration ($IC_{50}$ = 1.23 mg/mL) of the BLE for cell treatment was added. In all cases, the final concentration of DMSO in the medium did not exceed 0.01%. A control group of cells subjected to the same conditions was used. After a 72-hour incubation, the sampling process was carried out. Cell quenching was performed by placing the plates on an ice bucket, and 1 mL of methanol cooled to -80 °C was added to each well and left for a period of 10 minutes. Subsequently, the cells (endometabolome) were carefully scraped and placed in 2 mL Eppendorf tubes on dry ice for subsequent extraction. Later, the culture medium (exometabolome) was removed, and cells were washed with a pre-warmed PBS. In the case of the exometabolome, two aliquots of 500 µL each of the supernatants of the culture medium were centrifuged at 15.000 rpm for 10 minutes at 4 °C to eliminate suspended particles. Subsequently, the supernatant was lyophilized. All samples were stored at -80°C until metabolomic analysis. The workflow used in this study is summarized in Figure 4.1.

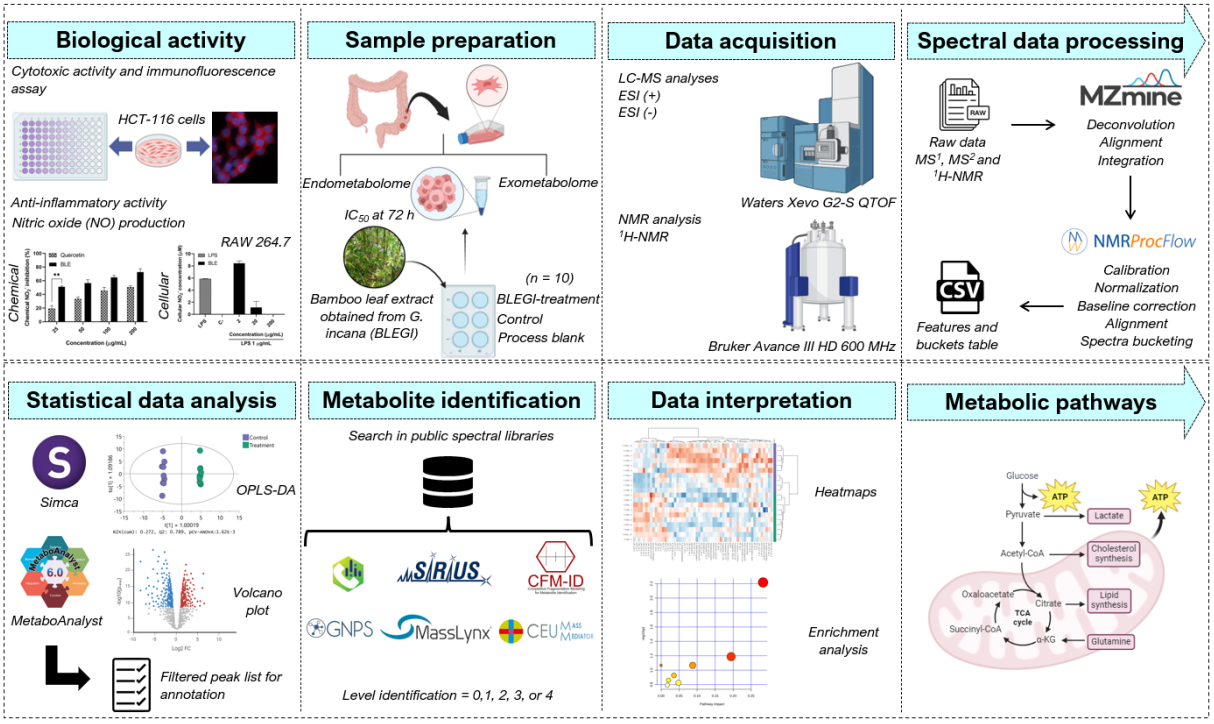



**Figure 4.1.** Schematic of the analytical workflow used in this cellular metabolomic study experiment.

### 4.1.11.2 Metabolite extraction

For the extraction of metabolites from the endometabolome, a cell lysis process was carried out using thermal shocks in liquid nitrogen and sonication of the samples for 5 minutes each procedure, respectively (This procedure was repeated three times). Subsequently, the samples were centrifuged at 15.000 rpm for 10 minutes at 4 °C. The resulting supernatants was divided into two aliquots of 500 µL and were lyophilized and stored at -80°C until metabolomic analysis.

### 4.1.11.3 Sample preparation for metabolomic analysis

For the analysis of endo- and exometabolome by LC-MS, the lyophilizate obtained above was resuspended in 500 µL of MeOH cooled to -20 °C, while for the analysis by $^{1}$H-NMR, the previously obtained lyophilizate was resuspended in 100 µL of methanol-*d4* ($CD_3OD$) and 100 µL of phosphate buffer ($KH_2PO_4$) in deuterium oxide ($D_2O$) (pH 6.0) from Sigma-Aldrich USA Isotope with 99.8% purity, solution was sonicated (frequency of

50 kHz/20 min) and centrifugated (10.000 rpm/5 min), and placed in a 3 mm NMR tubes for further 1D NMR analyses. Multiple QC samples were prepared by pooling and mixing identical volumes of each extract sample. This was done to verify system performance and ensure reproducibility in sample analysis. To evaluate instrument consistency, injections of the pooled QC samples were performed after every four sample injections.

#### 4.1.11.4 LC-MS metabolomic profiling analysis

LC-MS analysis of the endo- and exometabolome samples obtained from HCT-116 cells was performed under the same conditions described in Section 5.3.3.1.

#### 4.1.11.5 $^{1}$H-NMR fingerprinting analysis

$^{1}$H-NMR spectra were recorded at 25 °C on a Bruker Avance III HD 600 MHz spectrometer (Bruker, Karlsruhe, Germany) operating at a proton NMR frequency of 600.13 MHz. Each $^{1}$H NMR spectrum comprised 128 scans with the following parameters: 0.16 Hz/point, pulse width (PW) = 30 (11.3 μs), and relaxation delay (RD) = 1.5 s. Free induction decays (FIDs) underwent Fourier transformation with a line broadening (LB) of 0.3 Hz. Deuterated methanol was used as the internal lock. Chemical shifts were denoted in δ (ppm), and coupling constants were expressed in hertz.

#### 4.1.11.6 Data processing and statistical analysis

For the processing of the data obtained from LC-MS, the analysis was carried out using the software MZmine v2.53, to perform a deconvolution, alignment, and integration process. For the processing of the data obtained from $^{1}$H NMR, the analysis was carried out using the online software NMRProcFlow v1.4, in which a process of alignment and normalization of the data was performed. Additionally, the data were segmented and reduced using the clustering method with a window of 0.04 ppm. SIMCA 18.0 (Umetrics, Umea, Sweden) was used to perform multivariate analyses (MVA). MVA was used to build models such as PCA and OPLS-DA in relation to the VIP. The variables presenting statistical significance were determined by considering a *p*-value with FDR of less than

0.05, and a VIP greater than 1. This confirmation was based on the OPLS-DA models together with a significance assessment by means of CV-ANOVA with a value of less than 0.05. To establish *p*-valued characteristics, univariate analysis (UVA) was performed using MetaboAnalyst 6.0 server (LU; PANG; XIA, 2023; PANG et al., 2022).

#### 4.1.11.7 Metabolites identification

Differential annotation of metabolites was carried out considering mass accuracy with a maximum error of 10 ppm, as well as isotopic pattern distribution and adduct formation. For this purpose, several online public databases, such as METLIN (http://metlin.scripps.edu), KEGG (http://genome.jp/kegg), HMDB (https://hmdb.ca/), PubChem (https://pubchem.ncbi.nlm.nih.gov/), and ChEBI (https://www.ebi.ac.uk/chebi/), were used through the CEU mass mediation tool. Metabolite identification was based on the comparison between the obtained experimental MS/MS spectra and the predicted spectra present in the databases and other tools described in the literature.

#### 4.1.11.8 Mapping of altered metabolic pathways

The analysis of the metabolic pathways affected in the treated cells was conducted using the "Pathway Analysis" tool of the MetaboAnalyst 6.0 server (http://www.metaboanalyst.ca/). For this purpose, the altered compounds were annotated and compared with the *Homo sapiens* metabolome (KEGG) available on the same server.

## 4.2 Results and discussion

### 4.2.1 Chemical Characterization of Extract

The chemical characterization of BLEGI was carried out by LC-MS/MS in negative and positive ionization modes. The identified metabolites are shown in Table 4.1 along with their respective levels of identification accordance with Metabolomics Standards Initiative (MSI) (BLAŽENOVIĆ et al., 2018). From the BLEGI, a total of 46 compounds were recorded, distributed according to chemical classes, including flavonoids, and cinnamic acid derivatives, mainly. Additionally, a mapping of the chemical diversity of

BLEGI was carried out using the GNPS online platform, where compounds mainly related to flavonoids were found, including vicenin 2 (**6**), vitexin 2''-*O*-rhamnoside (**13**), saponarin or isosaponarin (**14**), schaftoside or isoschaftoside (**15**), kaempferol 7-*O*-neohesperidoside (**21**), and swertisin (**26**) related to the majority composition (Figure 4.2).

The molecular networking also highlights the presence of other molecular families, corresponding to fatty acids and derivatives for both ionization modes. Particularly in the negative ionization mode, molecular families such as flavonoids and cinnamic acid derivatives are the most abundant for BLEGI. Conversely, in the positive ionization mode, the molecular families of lipids and related molecules were found to a greater extent. The identification of the detected metabolites was based on the search for the main molecular ions (MS) and observed informative fragmentations (MS/MS), along with the use of standards when available, retention data, UV absorption, comparison with literature data, the GNPS web platform, and public databases. The MS/MS spectra for the related metabolites are represented in Figure S4.1.

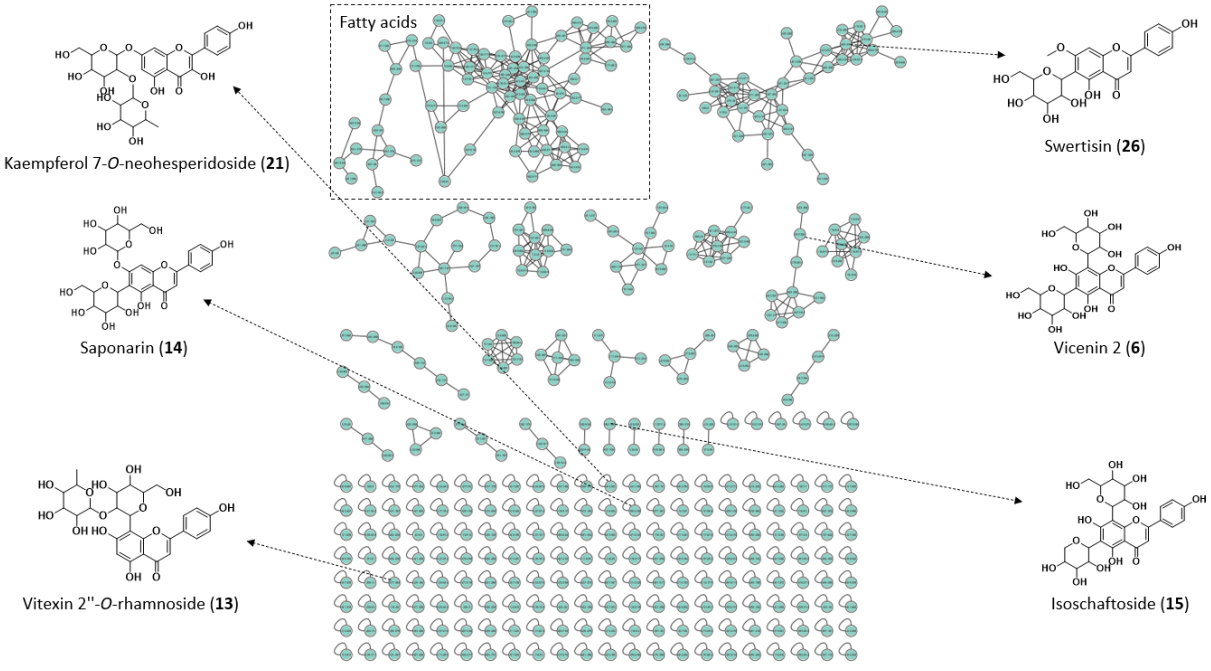



**Figure 4.2.** Molecular networking analysis of BLEGI highlighting flavonoids and other compounds, performed using the LC-MS/MS technique in negative mode.

From the UV spectra obtained, it was determined that most peaks corresponded to flavonoids, recognized by their characteristic bands and UV absorption maxima. Flavonoids exhibit two absorption maxima due to their two aromatic rings with conjugated double bonds, ring A and ring B. The first band (I) is associated with ring A, with UV absorption occurring between $\lambda_{max} \approx 300$ and 500 nm, while the second band (II) is associated with ring B, which absorbs between $\lambda_{max} \approx 240$ and 280 nm. Notably, we found that many of the flavonoids corresponded to glycosylated flavone scaffolds, in accordance with reports in the literature, highlighting a range of flavones with absorption between $\lambda_{max} \approx 275$ and 335 nm (GAGLIANO et al., 2022a).

**Table 4.1.** Metabolites tentatively identified in BLEGI using LC-MS/MS.

| No | $t_R$ (min) | UV $\lambda_{max}$ (nm) | Molecular formula | Adduct ion | Calculated mass (*m/z*) | Experimental mass (*m/z*) | Mass error (ppm) | Main fragment ions (MS/MS) | Identification confidence level | Metabolite | Reference or Database[a] |
|---|---|---|---|---|---|---|---|---|---|---|---|
| **1** | 0.57 | - | $C_7H_{12}O_6$ | $[M-H]^-$ | 191.0551 | 191.0543 | -4.2 | 175, 147, 129, 111 | 2 | Quinic acid | (CAO et al., 2022; CHITIVA et al., 2023; JIANG et al., 2019) |
| **2** | 1.94 | Low intensity | $C_{15}H_{16}O_{10}$ | $[M-H]^-$ | 355.0670 | 355.0669 | -0.3 | 209, 191, 163, 147, 129 | 4 | Not identified | |
| **3** | 2.33 | Low intensity | $C_{16}H_{18}O_8$ | $[M-H]^-$ | 337.0928 | 337.0945 | 5.0 | 191, 173, 164, 119 | 2 | *O*-Coumaroylquinic acid | (AKHTAR; PATOWARY, 2022; CHITIVA et al., 2023; GAGLIANO et al., 2022a; JIANG et al., 2019) and GNPS |
| **4** | 2.36 | 270, 327 | $C_{27}H_{30}O_{16}$ | $[M-H]^-$ | 609.1461 | 609.1466 | 0.8 | 547, 519, 489, 429, 399 | 3 | Luteolin 6-*C*-hexoside 8-*C*-pentoside | |
| **5** | 2.51 | 274, 336 | $C_{21}H_{20}O_{10}$ | $[M-H]^-$ | 431.0983 | 431.0981 | -0.5 | 387, 341, 311, 179 | 4 | Not identified | |
| **6** | 2.68 | 272, 325 | $C_{27}H_{30}O_{15}$ | $[M-H]^-$ | 593.1511 | 593.1513 | 0.3 | 503, 473, 383, 353, 297 | 2 | Vicenin 2 | (CHITIVA et al., 2023; GAGLIANO et al., 2022b) and GNPS |
| **7** | 2.70 | 269, 325 | $C_{21}H_{20}O_{11}$ | $[M-H]^-$ | 447.0932 | 447.0931 | -0.2 | 327, 299, 285, 133, 109 | 4 | Not identified | |
| **8** | 2.71 | 268, 337 | $C_{27}H_{30}O_{15}$ | $[M-H]^-$ | 593.1511 | 593.1517 | 1.0 | 457, 383, 353, 297 | 2 | Apigenin 6,8-digalactoside | (GAGLIANO et al., 2022a) and GNPS |
| | | | | $[M+H]^+$ | 595.1668 | 595.1660 | -1.3 | 541, 481, 457, 379, 325, 295 | | | |
| **9** | 2.71 | 267, 326 | $C_{26}H_{28}O_{14}$ | $[M-H]^-$ | 563.1406 | 563.1411 | 0.9 | 473, 443, 383, 353, 325, 2.97 | 4 | Not identified | |
| **10** | 2.74 | 311 | $C_9H_8O_4$ | $[M-H]^-$ | 179.0349 | 179.0352 | 1.7 | 135, 119 | 1 | Caffeic acid[st] | (HU; ZHANG; KITTS, 2000; NI et al., 2012, 2013) |
| **11** | 2.77 | 271, 333 | $C_{26}H_{28}O_{14}$ | $[M-H]^-$ | 563.1406 | 563.1410 | 0.7 | 445, 355, 325, 297 | 4 | Not identified | |
| **12** | 2.80 | 269, 334 | $C_{26}H_{28}O_{14}$ | $[M-H]^-$ | 563.1416 | 563.1415 | -0.2 | 473, 443, 401, 383, 353, 311 | 4 | Not identified | |
| **13** | 2.87 | 265, 341 | $C_{27}H_{30}O_{14}$ | $[M-H]^-$ | 577.1562 | 577.1565 | 0.5 | 413, 341, 293, 175 | 2 | Vitexin 2''-*O*-rhamnoside | (CHITIVA et al., 2023) and GNPS |
| | | | | $[M+H]^+$ | 579.1719 | 579.171 | -1.6 | 433, 415, 367, 313, 283 | | | |
| **14** | 2.88 | 269, 342 | $C_{27}H_{30}O_{15}$ | $[M-H]^-$ | 593.1511 | 593.1519 | 1.3 | 473, 431, 353, 311, 297, 282 | 2 | Saponarin or Isosaponarin | (CHITIVA et al., 2023; GAGLIANO et al., 2022a) and GNPS |

| | | | | | | | | | | | |
|---|---|---|---|---|---|---|---|---|---|---|---|
| **15** | 2.91 | 271, 335 | $C_{26}H_{28}O_{14}$ | $[M-H]^-$ | 563.1406 | 563.1401 | -0.9 | 473, 443, 383, 353, 325, 297 | 2 | Schaftoside or Isoschaftoside | (AKHTAR; PATOWARY, 2022; CHITIVA et al., 2023; GAGLIANO et al., 2022a; JIANG et al., 2019; WANG et al., 2020b, 2022b) and GNPS |
| | | | | $[M+H]^+$ | 565.1562 | 565.1563 | 0.2 | 547, 529, 499, 457, 427, 379 | | | |
| **16** | 3.13 | 273, 339 | $C_{26}H_{28}O_{14}$ | $[M+H]^+$ | 565.1562 | 565.1564 | 0.4 | 525, 481, 405, 337, 295 | 3 | Vicenin 1 or Vicenin 3 | |
| **17** | 3.16 | 270, 344 | $C_{28}H_{32}O_{16}$ | $[M-H]^-$ | 623.1617 | 623.1617 | 0.0 | 504, 443, 353, 323 | 3 | Isoscoparin 2''-*O*-hexoside | |
| **18** | 3.18 | 271, 342 | $C_{28}H_{32}O_{15}$ | $[M+H]^+$ | 609.1824 | 609.1824 | 0.0 | 430, 393, 327, 297, 267 | 3 | Spinosin or Isospinosin | |
| **19** | 3.20 | Low intensity | $C_9H_8O_3$ | $[M-H]^-$ | 163.0400 | 163.0400 | 0.0 | 119 | 1 | *p*-Coumaric acid[st] | (SILVA DE OLIVEIRA, 2019) and GNPS |
| **20** | 3.23 | 270, 341 | $C_{27}H_{30}O_{14}$ | $[M-H]^-$ | 577.1562 | 577.1569 | 1.2 | 533, 472, 413, 353, 293 | 2 | Violanthin or Isoviolanthin | (MORALES NOREÑA; SANCHEZ VALLEJO, 2008) |
| **21** | 3.24 | 269, 332 | $C_{27}H_{30}O_{15}$ | $[M-H]^-$ | 593.1511 | 593.1512 | 0.2 | 285, 218, 151 | 2 | Kaempferol 7-*O*-neohesperidoside | (MORALES NOREÑA; SANCHEZ VALLEJO, 2008) and GNPS |
| **22** | 3.28 | 270, 325 | $C_{33}H_{40}O_{19}$ | $[M-H]^-$ | 739.2091 | 739.209 | -0.1 | 593, 431, 281 | 3 | Kaempferol 3-*O*-disaccharoside-7-*O*-pentoside | |
| **23** | 3.28 | 270, 326 | $C_{27}H_{30}O_{15}$ | $[M+H]^+$ | 595.1668 | 595.1667 | -0.2 | 449, 287 | 3 | Kaempferol 3-*O*-disaccharoside | |
| **24** | 3.35 | 272, 326 | $C_{21}H_{18}O_{13}$ | $[M-H]^-$ | 477.0674 | 477.0675 | 0.2 | 431, 301, 179 | 3 | Quercetin 3-*O*-hexoside | |
| **25** | 3.37 | 270, 325 | $C_{21}H_{20}O_{12}$ | $[M-H]^-$ | 463.0882 | 463.0880 | -0.4 | 372, 300, 271, 255, 243, 151 | 2 | Hyperoside | (SILVA DE OLIVEIRA, 2019) |
| **26** | 3.38 | 271, 328 | $C_{22}H_{22}O_{10}$ | $[M-H]^-$ | 445.1140 | 445.1145 | 1.1 | 385, 325, 297, 282, 269 | 2 | Swertisin | (GAGLIANO et al., 2022a) |
| **27** | 3.41 | 271, 329 | $C_{28}H_{32}O_{17}$ | $[M-H]^-$ | 639.1566 | 639.1570 | 0.6 | 403, 328, 313, 285, 270, 242 | 3 | Isorhamnetin 3,4'-hexoside | |
| **28** | 3.54 | 271, 344 | $C_{27}H_{30}O_{14}$ | $[M-H]^-$ | 577.1562 | 577.1561 | -0.2 | 269, 117 | 3 | Apigenin 7-*O*-disaccharoside | |
| **29** | 3.56 | 269, 342 | $C_{27}H_{30}O_{14}$ | $[M+H]^+$ | 579.1719 | 579.1718 | -0.2 | 433, 363, 271, 153 | 3 | Apigenin 7-*O*-disaccharoside | |
| **30** | 3.58 | 268, 331 | $C_{22}H_{22}O_{11}$ | $[M-H]^-$ | 461.1089 | 461.1087 | -0.4 | 415, 341, 313, 298 | 4 | Not identified | |
| **31** | 3.59 | 270, 325 | $C_{28}H_{34}O_{15}$ | $[M-H]^-$ | 609.1824 | 609.1843 | 3.1 | 325, 301, 286, 151 | 3 | Hesperidin | |

| | | | | | | | | | | | |
|---|---|---|---|---|---|---|---|---|---|---|---|
| **32** | 3.61 | 271, 344 | $C_{28}H_{32}O_{15}$ | $[M+H]^+$ | 609.1826 | 609.1810 | -2.6 | 463, 301, 286, 258 | 3 | Diosmetin 7-*O*-disaccharoside | |
| **33** | 3.64 | 269, 326 | $C_{28}H_{32}O_{16}$ | $[M-H]^-$ | 623.1617 | 623.1620 | 0.5 | 329, 314, 299, 271, 243, 187 | 3 | Isorhamnetin 3-*O*-hexoside-6''-disaccharoside | |
| **34** | 3.73 | 265, 341 | $C_{27}H_{30}O_{15}$ | $[M-H]^-$ | 593.1511 | 593.1512 | 0.2 | 473, 431, 353, 341, 311, 283 | 3 | Apigenin 6-*C*-hexoside-7-*O*-hexoside | |
| | | | | $[M+H]^+$ | 595.1668 | 595.1667 | -0.2 | 415, 379, 337, 313, 283, 165 | | | |
| **35** | 4.47 | 264, 356 | $C_{15}H_{10}O_6$ | $[M-H]^-$ | 285.0404 | 285.0403 | -0.4 | 199, 169, 151, 133 | 2 | Luteolin | (CHENG et al., 2023; LI et al., 2021; MA et al., 2020a) |
| **36** | 4.57 | 270, 319 | $C_{15}H_{12}O_3$ | $[M-H]^-$ | 239.0713 | 239.0699 | -5.9 | 211, 195, 179, 135 | 3 | 6-Hidroxyflavanone | |
| **37** | 4.88 | 264, 329 | $C_{23}H_{24}O_{12}$ | $[M-H]^-$ | 491.1195 | 491.1198 | 0.6 | 461, 328, 313, 285, 226 | 2 | Tricin 7-*O*-glucoside | (GAGLIANO et al., 2022a) |
| **38** | 4.92 | 264, 335 | $C_{27}H_{32}O_{14}$ | $[M-H]^-$ | 579.1719 | 579.1720 | 0.2 | 271, 177, 151, 119 | 3 | Naringenin-7-*O*-disaccharoside | |
| **39** | 4.95 | 263, 334 | $C_{21}H_{22}O_{10}$ | $[M-H]^-$ | 433.1140 | 433.1145 | 1.2 | 271, 151, 119 | 3 | Naringenin-7-*O*-hexoside | |
| **40** | 4.97 | 271, 358 | $C_{15}H_{10}O_5$ | $[M-H]^-$ | 269.0455 | 269.0460 | 1.9 | 227, 181, 151, 117 | 2 | Apigenin | (LI et al., 2021) |
| **41** | 5.01 | 244, 315 | $C_{15}H_{10}O_6$ | $[M-H]^-$ | 285.0404 | 285.0405 | 0.4 | 211, 183, 149, 121 | 3 | 3,6,2',3'-Tetrahydroxyflavone | |
| **42** | 5.03 | 245, 319 | $C_{15}H_{10}O_5$ | $[M-H]^-$ | 269.0455 | 269.0461 | 2.2 | 239, 211, 187, 143, 117 | 3 | 6,7,4'-Trihydroxyisoflavone | |
| **43** | 5.04 | 269, 354 | $C_{15}H_{10}O_6$ | $[M-H]^-$ | 285.0404 | 285.0420 | 5.6 | 255, 227, 187, 159, 143, 117 | 2 | Kaempferol | (LI et al., 2021; MORALES NOREÑA; SANCHEZ VALLEJO, 2008) |
| **44** | 5.09 | 245, 319 | $C_{17}H_{14}O_7$ | $[M-H]^-$ | 329.0666 | 329.0671 | 1.5 | 271, 243, 227, 161, 133 | 3 | 4',5,7-Trihydroxy-3,6-dimethoxyflavone | |
| **45** | 5.12 | 244, 325 | $C_{16}H_{12}O_6$ | $[M-H]^-$ | 299.0561 | 299.0561 | 0.0 | 256, 227, 212, 183, 151 | 3 | 3,5,7-Trihydroxy-4'-methoxyflavone | |
| **46** | 5.15 | 244, 354 | $C_{17}H_{14}O_7$ | $[M-H]^-$ | 329.0666 | 329.0669 | 0.9 | 229, 271, 227, 215, 161 | 2 | Tricin | (LI et al., 2021) |
| | | | | $[M+H]^+$ | 331.0823 | 331.0820 | -0.9 | 313, 285, 270, 258, 203, 153 | | | |

[a] The references described compounds found in the literature for leaves, culms, and shoots of several bamboos' plants and database sources such as PubChem, METLIN, KEGG, GNPS; [st] The identification of metabolites has been verified by using authentic standards; *m/z* data were obtained by LC-MS based on time and peak areas. $\lambda_{max}$: UV maximum absorbance wavelength. Metabolites were annotated with identification confidence levels as recommended by the Metabolomics Standards Initiative (MSI) according to: Level 0: Unambiguous 3D Structure: isolated, pure compound, including full stereochemistry; Level 1: Confident 2D structure: uses reference standard match or full 2D structure elucidation; Level 2: Probable structure: matched to literature data or databases by diagnostic evidence, Level 3: Possible structure or class: most likely structure, isomers possible, substance class or substructure match; Level 4: Unknown feature of interest (BLAŽENOVIĆ et al., 2018).

### 4.2.2 Cell viability of HCT-116 cells

We evaluated the cytotoxic effect at two concentrations (5 and 50 µg/mL) to determine the percentage of cell viability against the HCT-116 colon cancer cell line. We found that at a concentration of 5 µg/mL it presented a cell viability percentage of 10%, while at 50 µg/mL it presented of 5% (Figure 4.3A). Considering these results, the $IC_{50}$ value was determined in a concentration range of 0.0032 to 50 µg/mL. BLEGI revealed significant cytotoxicity against the colon cell line with an $IC_{50}$ value of 1.23 µg/mL. Figure 4.3B shows the dose-response curve of cytotoxicity of HCT-116 cells after 72 hours of BLEGI treatment. Therefore, the $IC_{50}$ value was used for the treatment of cells in the metabolomics study.

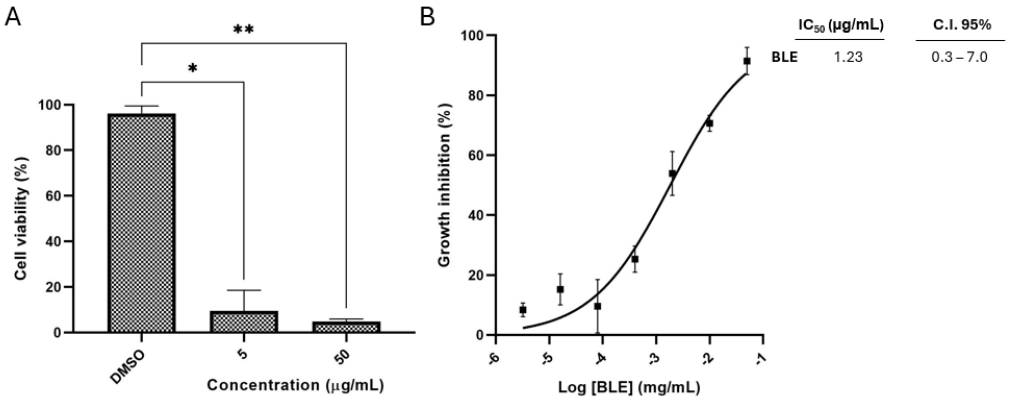



**Figure 4.3.** A) The cell viability after 72 h incubation at different concentrations. B) Dose-response curves of the cytotoxicity of HCT-116 cells after 72 h treatment with the BLEGI using concentrations of 0.0032 to 50 µg/mL. The data represent the mean of three independent biological replicates with at least technical duplicates ± SEM (standard error of the mean). All experiments employed 0.05% DMSO (vehicle) and doxorubicin (DOXO) ranging 0.00064 to 10 µM with $IC_{50}$ = 0.2 µM (C.I 95% 384 0.14 – 0.25) as negative and positive controls, respectively. One-way ANOVA analysis using Tukey's post hoc test was employed to indicate significance, denoted as follows: * $p < 0.05$ and ** $p < 0.01$ compared to DMSO.

### 4.2.3 Immunofluorescence assay

To determine whether BLEGI induced apoptosis in colon cancer cells, the a-tubulin antibody was evaluated, and cellular staining with DAPI was performed to examine cell morphology by immunofluorescence analysis. Treatment of HCT-116 cells with BLEGI significantly induced the formation of apoptotic bodies, and a tripolar mitosis process was

also observed, unlike the control used, DMSO. After 72 hours of treatment, the cytoskeleton of the cells (red) was observed with a-tubulin, while the cell nuclei (blue) and apoptotic bodies were observed with DAPI. By merging the images, the cellular processes involved are clearly observed (Figure 4.4). Doxorubicin was used as a positive control. These results imply that BLEGI can induce apoptosis of colon cancer cells.

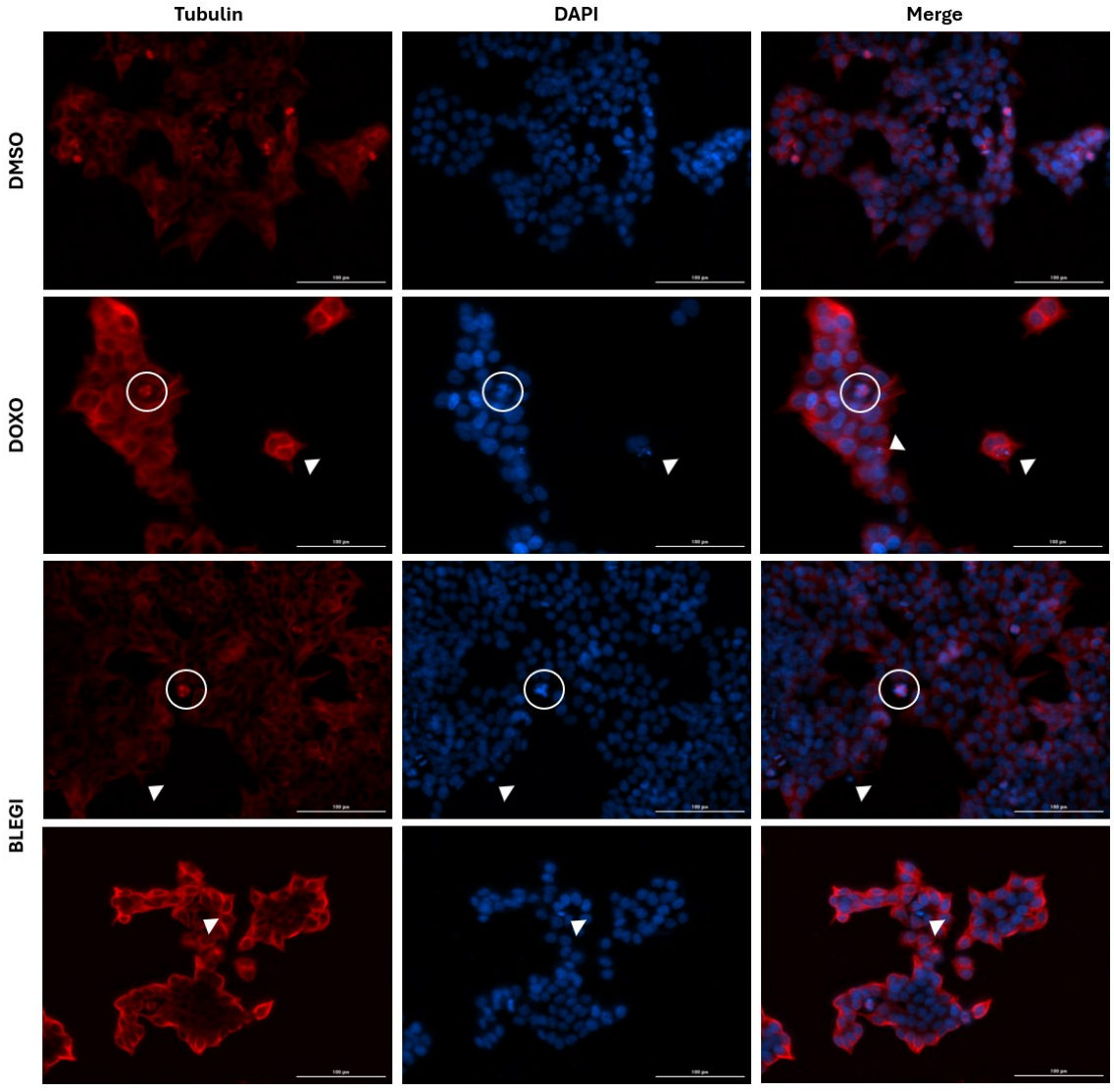



**Figure 4.4.** Immunofluorescence of a-tubulin and DAPI in HCT 116 cells after 72 h of incubation with DMSO 0.1%, DOXO 0.2 µM and BLEGI 1.23 µg/mL. Arrows indicate condensed chromatin (suggestive of apoptosis) and circles indicate tripolar mitosis.

### 4.2.4 Nitric Oxide (NO) Production Inhibition

To determine the percentage inhibition of NO by BLEGI, two methods were employed: first, the percentage inhibition of chemical NO was determined using the spectrophotometric method; second, the percentage inhibition of cellular NO was determined in macrophage cell lines treated with Lipopolysaccharide (LPS). Figure 4.5A shows the effect of BLEGI on the inhibition of NO. It is observed that at the four concentrations evaluated (25, 50, 100, and 200 µg/mL), it presented inhibition percentages greater than 50%, indicating a significant potential. Cell viability was first examined by 3-(4,5-dimethylthiazol-2-yl)-2,5-diphenyltetrazolium bromide (MTT) assay to exclude false positive results caused by possible cytotoxicity of BLEGI. The cytotoxicity of BLEGI was also evaluated in the macrophage cell line, where no cytotoxic effect was observed at the concentrations evaluated (50 to 200 µg/mL) since the $IC_{50}$ value of BLEGI was greater than 200 µg/mL in all concentrations analyzed. Figure 4.5B shows the effect of BLEGI on the production of NO in macrophage cells activated with LPS. It should be noted that, at the maximum concentration evaluated, it exhibits an inhibition percentage greater than 90%, indicating powerful inhibition of NO compared to the positive control. For the NO production assessed in macrophages inhibition tests, concentrations of 200 µg/mL, 20 µg/mL, and 2 µg/mL were used. Moreover, N(ω)-nitro-l-arginine methyl ester (L-NAME), an inhibitor of NO synthase, was used as a positive control (Figure 4.5C). Figure 4.5D displays the results of cellular NO levels in RAW 264.7 macrophage cells stimulated with LPS after BLEGI treatment. As a result, BLEGI showed significant inhibitory effects against NO production, with values of 8.44 ± 0.38 µM at a concentration of 2 µg/mL, comparable to the positive control.

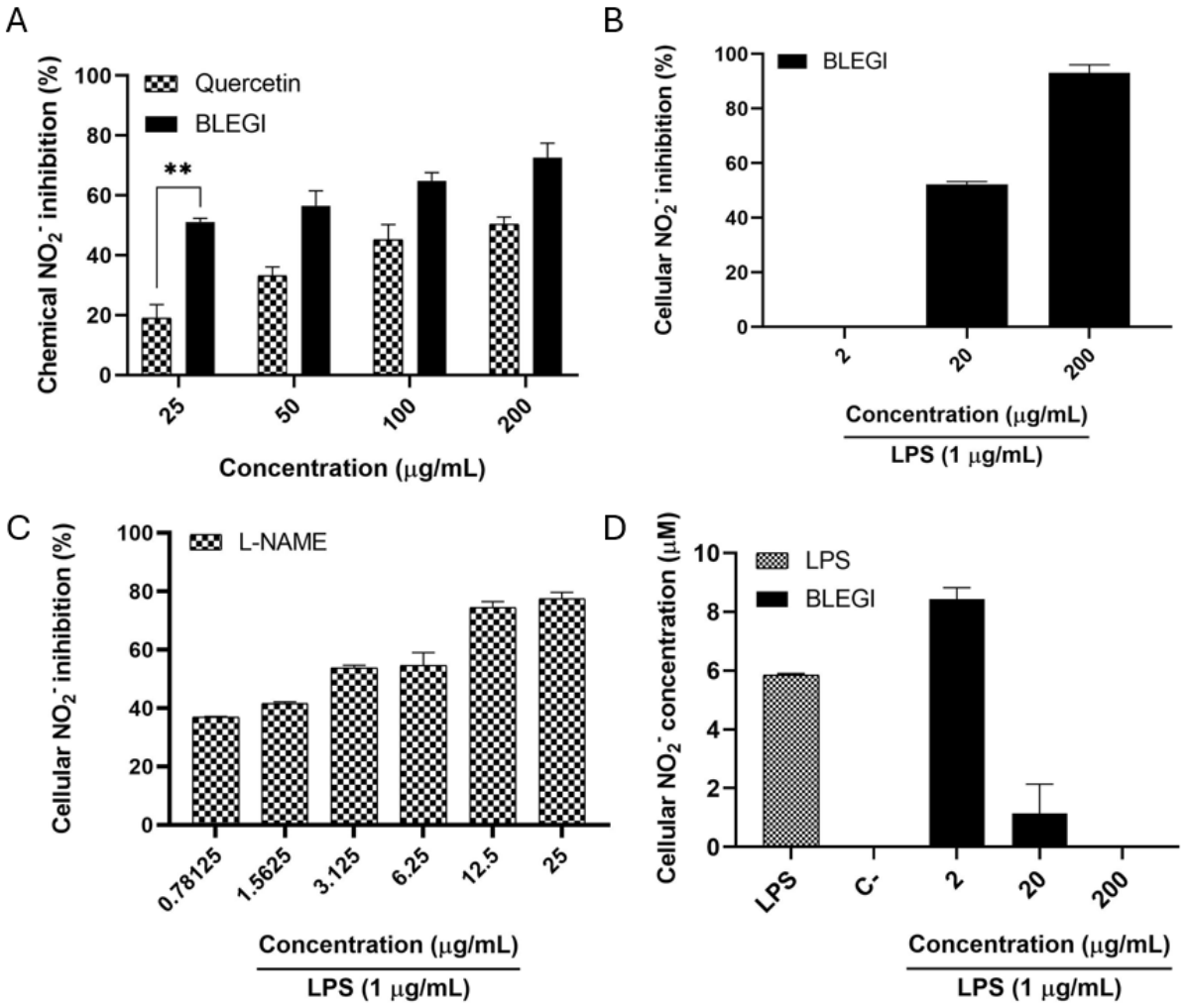



**Figure 4.5.** A) Determination of the percentage of chemical $NO_2^-$ after treatment with BLEGI, evaluated at four concentrations (25, 50, 100 and 200 µg/mL). B) Determination of the percentage of cellular $NO_2^-$ in the murine cell line RAW 264.7 after treatment with BLEGI, evaluated at three concentrations (2, 20 and 200 µg/mL). C) Level of cellular $NO_2^-$ in the murine cell line RAW 264.7 after treatment with L-NAME used as an inhibition control. D) Cellular $NO_2^-$ levels in the murine RAW 264.7 cell line stimulated with LPS after treatment with BLEGI, evaluated at three concentrations (2, 20 and 200 µg/mL).

### 4.2.5 Untargeted endo- and exometabolome analysis

To explore the metabolic profile of BLEGI-treated HCT-116 cells, we employed an untargeted metabolomics approach using LC-MS and $^1$H-NMR analyses. To elucidate the metabolic differences between BLEGI-treated and untreated cells, the endo- and exometabolome of the cells were profiled using the two analytical platforms. Multivariate

data analysis was conducted on the preprocessed data utilizing unsupervised principal component analysis (PCA) and supervised orthogonal partial least squares discriminant analysis (OPLS-DA) models. The quality and stability of the endo- and exometabolome profiling instrument were assessed by performing PCA of the quality control (QC) and samples. Figure S4.1 illustrates the groupings of the QC samples for each of the analytical platforms used, indicating the reliability and validity of the data, respectively. Furthermore, we observed notable separation trends between BLEGI-treated cells and untreated cells on the two platforms, indicating significant differences in the metabolites of HCT-116 cells after treatment. Additionally, all experimental clustering samples in the PCA score plots were within the 95% confidence interval.

Also, we built OPLS-DA models between the groups of BLEGI-treated cells and untreated cells, showing good quality parameters and complete separation of the groups for the endometabolome (Figure 4.6A) and exometabolome (Figure 4.6B), respectively. This allowed us to identify the significant variables contributing to the separation between the groups. Subsequently, to validate the analysis, we used the permutation test to assess the reliability of the OPLS-DA model by analyzing the values of $R^2$ and $Q^2$. Figure S4.2 shows the permutation test plots ($n$ = 200) of the OPLS-DA models for BLEGI-treated cells and untreated cells. For all OPLS-DA models, the values of $R^2$ and $Q^2$ demonstrated good robustness without overfitting, indicating that the OPLS-DA model can effectively distinguish each group of samples.

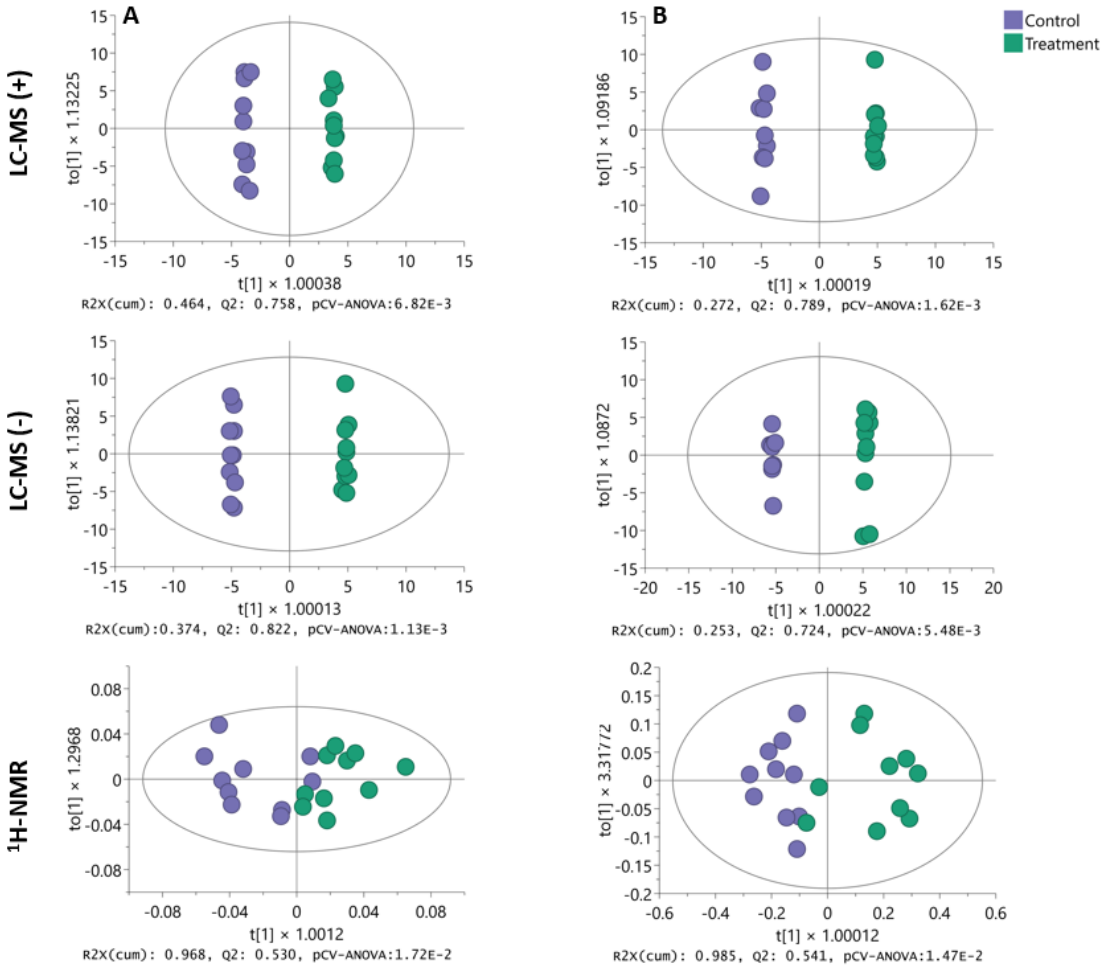



**Figure 4.6.** OPLS-DA score plots comparing the BLEGI-treated group (green) versus the control group (purple) for LC-MS and $^{1}$H-NMR data of the A) endometabolome and B) exometabolome of HCT-116 cells.

### 4.2.6 Analysis of altered metabolites in HCT-116 cells

A volcano plot was generated to identify the significantly differential metabolites in the endo- and exometabolome of HCT-116 cells. The differential metabolites were screened based on criteria such as variable of importance in the projection (VIP) >1, fold change (FC) > 1.2, or FC < 0.50, and false discovery rate (FDR) < 0.05 or *p*-value < 0.05 (Figure S4.4). This metabolites were identified according to the Metabolomics Standards Initiative (BLAŽENOVIĆ et al., 2018). A total of 57 altered metabolites were detected in the endometabolome of BLEGI-treated cells, with 14 up-regulated and 43 down-regulated.

Figure 4.7A shows the differential metabolites of the endometabolome corresponding to different classes including Glycerophospholipids (51%), carnitines (12%), peptides (9%), carboxylic acids and derivatives (7%), fatty acids (4%), glycerolipids (4%), sphingolipids (4%), organooxygen compounds (2%), nucleosides, nucleotides, and analogues (2%), pyrimidines and pyrimidine derivatives (2%), pyridines and derivatives (2%), steroids and steroid derivatives (2%), and sterol lipids (2%). A total of 42 altered metabolites were detected in the exometabolome of BLEGI-treated cells, with 27 up-regulated and 15 down-regulated. Figure 4.7B shows the differential metabolites identified in the exometabolome corresponding to different classes, including peptides (31%), fatty acids (21%), glycerophospholipids (12%), carboxylic acids and derivatives (7%), organooxygen compounds (5%), amino acid and derivatives (5%), sugar and derivatives (5%), carnitines (2%), nucleosides, nucleotides, and analogues (2%), pyrimidines and pyrimidine derivatives (2%), alcohols and polyols (2%), carbohydrates and carbohydrate conjugates (2%), and tryptamines (2%). The Table S4.1 and Table S4.2 show detailed information about the metabolites found. With the $^{1}$H-NMR analysis, it was possible to extract specific signals corresponding to derivatives of organic acids and fatty acids for the endo- and exometabolome, respectively. The signals for glutathione stand out with $\delta_H$ 2.91 (dd), 2.36 (m) and $\delta_H$ 4.46 (q), 3.86 (m), respectively, confirming the identification of this metabolite (Figure S4.5).

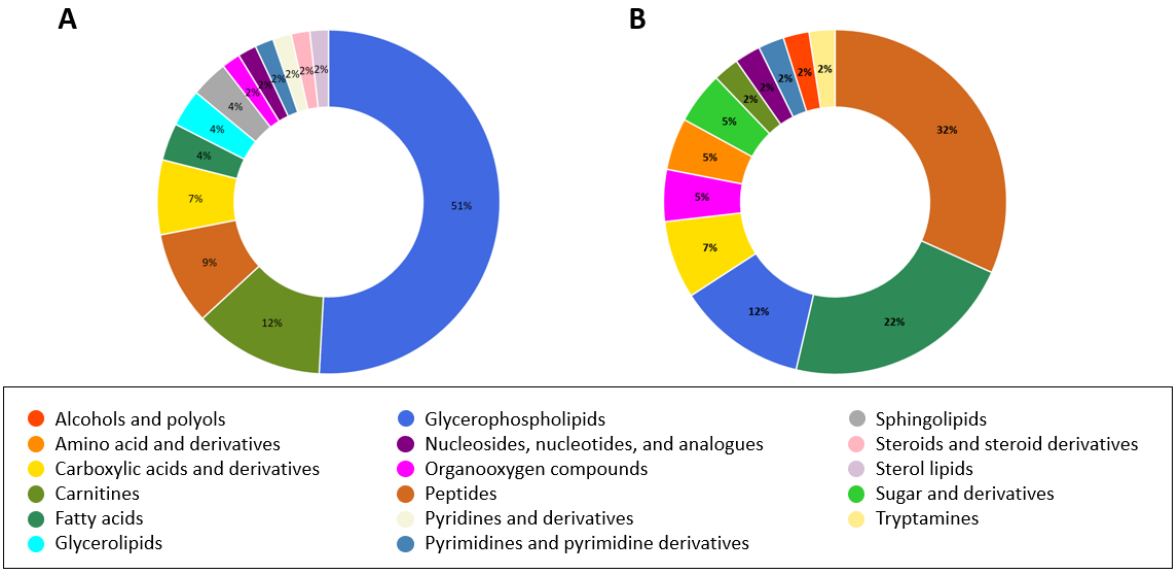



**Figure 4.7.** Altered A) endo- and B) exometabolome metabolites among BLEGI-treated versus untreated cells. Chemical classes are shown according to percentage and color.

The hierarchical clustering analysis and the heatmap based on the annotated metabolites comparing BLEGI-treated and untreated cells showed significant changes, generating a visualization of the distribution of the metabolites found. We highlight that the metabolites that presented a significant change with a FC greater than 1.2 in the group of BLEGI-treated cells were lysophosphatidylethanolamines (LPE) and phosphatidylserines (PS), while lysophosphatidylcholines (LPC), phosphatidylinositol (PI), and phosphatidylethanolamines (PE) presented a significant change with FC less than 0.5. It was determined that each group shares different patterns in terms of metabolic composition and levels of presence and abundance. A heatmap showing the top 40 metabolites altered in BLEGI-treated cells is presented in Figure 4.8A-B. Among the significantly decreased metabolites were fatty acyls, carboxylic acid and derivatives, PE, and PI, while the amino acid and derivatives.

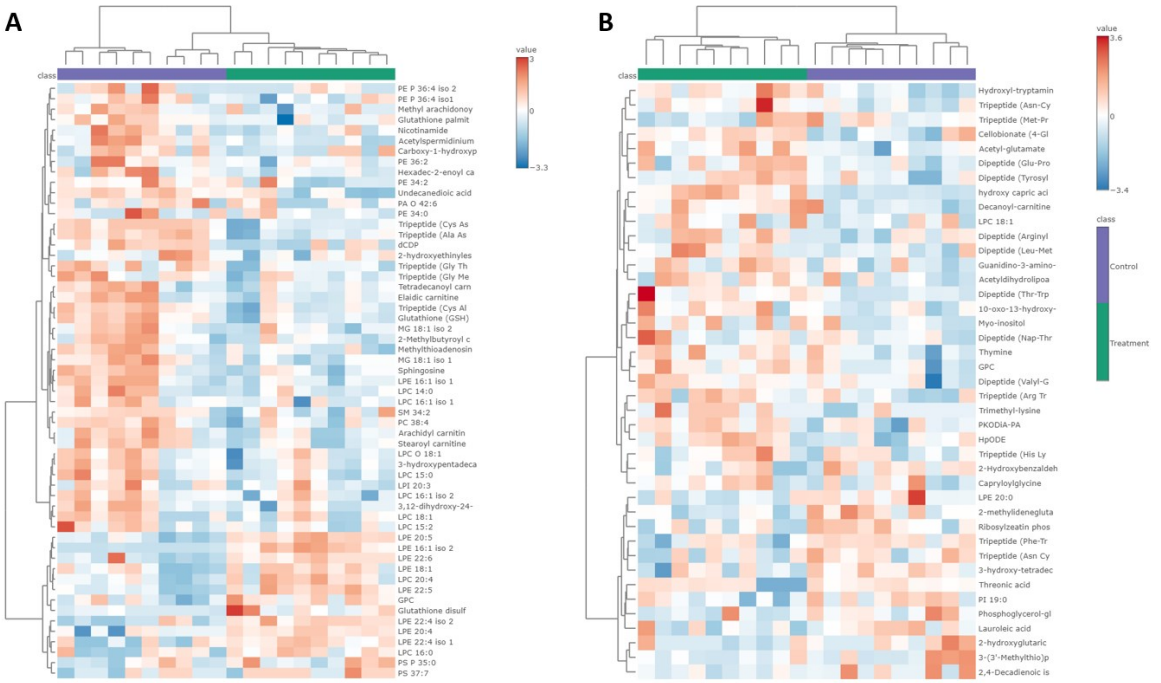



**Figure 4.8.** Hierarchical clustering with a heatmap illustrating the differences in the abundance of metabolites found in A) endometabolome and B) exometabolome between BLEGI-treated cells and untreated cells. The x-axis shows the clustering of all samples, and the y-axis shows the clustering of the metabolites found for the endo and exometabolome of HCT-116 cells.

Violin plots show the statistically significant and differential metabolites for BLEGI-treated and untreated cells. In Figure 4.9, we present the changes in the main metabolites that exhibited a significant change. We found that for the endometabolome, glutathione (GSH) (FC = 0.67; FDR-adjusted *p*-value = 2.87E-02), glutathione disulfide (GSSH) (FC = 1.32; *p*-value = 1.77E-02), and sphingosine (Sph) (FC = 0.77; *p*-value = 2.41E-02) exhibited significant changes. Our study also highlighted the importance of other metabolites with significant changes, which are described in Table S4.1 and Table S4.2.

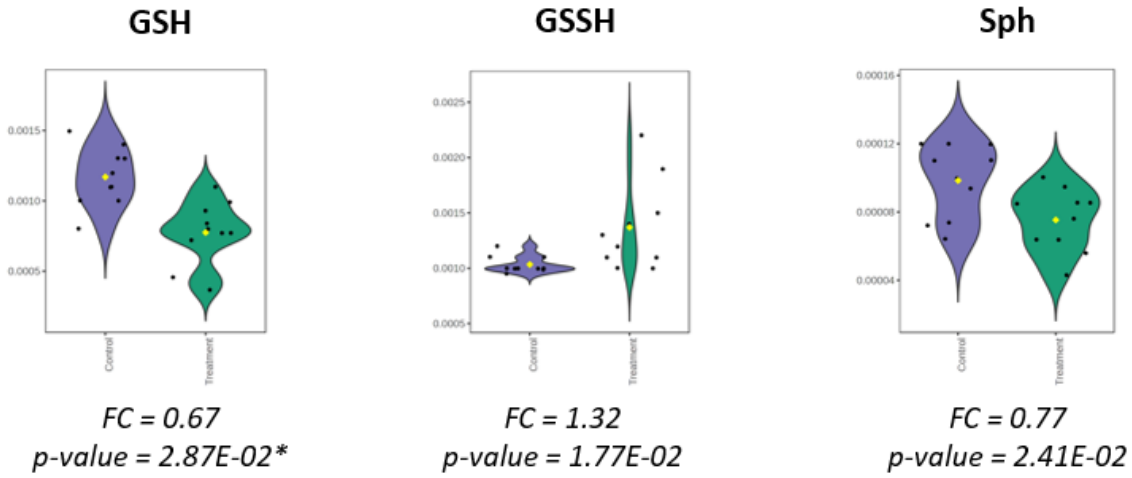



**Figure 4.9.** Violin plot for the altered metabolites corresponding to BLEGI-treated and untreated cells. Y-axes are represented as relative units. The date was normalized with respect to the total spectral area. Boxes range from the 5% and 95% percentiles are indicated as error bars; individual data points are in-dicated by circles. The medians are indicated by horizontal lines within each box.

### 4.2.7 Exploration of altered metabolic pathways in HCT-116 cells

Based on the observed variations of the metabolites found above, and to further elucidate the effect of BLEGI treatment on the metabolic processes of HCT-116 cells, it was necessary to explore the profoundly altered metabolic pathways. In this regard, the annotation of the differential pathways of the metabolites was performed using the KEGG database. Metaboanalyst was employed to identify the altered metabolic pathways and elucidate the metabolic differences between the BLEGI-treated and untreated cells. Different target metabolic pathways were found to be altered in HCT-116 cells. Through this analysis and as shown in Figure 4.10, possible pathways altered with BLEGI treatment included glutathione metabolism (*p*-value = 0.022, pi = 0.282), tricarboxylic acid cycle (*p*-value = 0.010, pi = 0.148), lipoic acid metabolism (*p*-value = 0.021, pi = 0.096), and pyrimidine metabolism (*p*-value = 0.039, pi = 0.053), among others. These metabolic pathways were found to be the most affected and the most influential in the enrichment analysis of HCT-116 cells after BLEGI exposure.

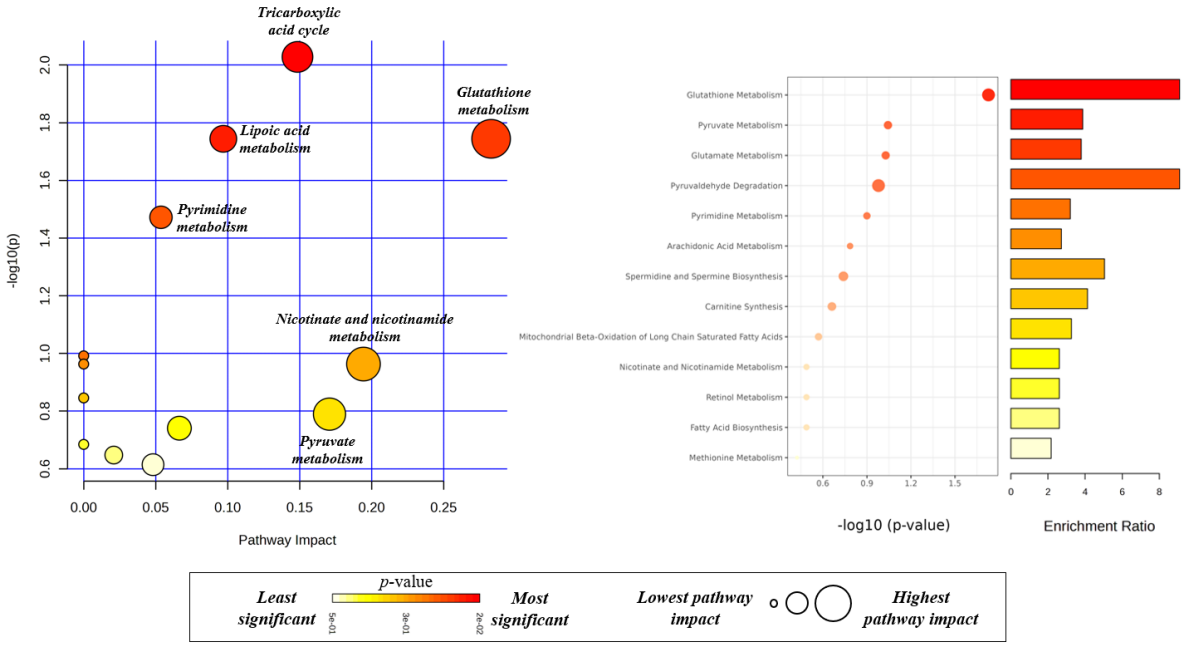



**Figure 4.10.** Metabolic pathway analysis based on the enrichment analysis procedure for metabolites found in the metabolome of HCT-116 cells after exposure to BLEGI. The most relevant biosynthesis pathways are represented according to *p*-value < 0.05 and pathway impact (pi) > 0. **1)** Glutathione metabolism (*p*-value = 0.022, pi = 0.282), **2)** Tricarboxylic acid cycle (*p*-value = 0.010, pi = 0.148), **3)** Lipoic acid metabolism (p-value = 0.021, pi = 0.096), **4**) and Pyrimidine metabolism (*p*-value = 0.039, pi = 0.053). Summary pathways biosynthesis identified in endo- and exometabolome generated with MetaboAnalyst 6.0 based on differential metabolites.

In the present study, the metabolome of HCT-116 cells was analyzed after the effect induced by BLEGI, using a metabolomic approach by LC-MS and $^{1}$H-NMR untargeted of the endometabolome and exometabolome. Initially, the cytotoxic effect of BLEGI on HCT-116 cells was determined considering an exposure time of 72 hours. The results showed a potent cytotoxic effect of BLEGI on HCT-116 cells with an $IC_{50}$ value of 1.23 µg/mL. These results were comparable to the ethanol extract obtained from the species *G. incana* in a previous study carried out on the same cells. In this regard, for the metabolomic analysis, the HCT-116 cells were treated with the $IC_{50}$ value obtained from the BLEGI.

Metabolomic analysis of the endo- and exometabolome of HCT-116 colon cancer cells demonstrated significant changes in several metabolites involved in various affected metabolic pathways. Among the main metabolic pathways affected, glutathione

metabolism, tricarboxylic acid cycle, lipoic acid metabolism, and pyrimidine metabolism stand out. When comparing the BLEGI-treated group with the untreated group, several metabolites associated with glutathione metabolism exhibited a notable impact value of 0.282. Metabolites produced in the context of glutathione metabolism comprised both reduced GSH and GSSG. The glutathione metabolism pathway plays a crucial role in intracellular antioxidant defense, redox regulation, and detoxification. This is achieved through the dynamic interaction of the GSH-GSSG redox pair together with various enzymes and glutathione-dependent transporter systems. GSH, which contains a crucial functional thiol group, functions as a key intercellular antioxidant by neutralizing free radicals and reactive oxygen compounds. It also acts by reducing oxidized or inactivated protein thiols to preserve their biological activities. Consequently, GSH is considered a vital indicator of oxidative stress (GAO et al., 2014; SHAO et al., 2016). As shown in Figure 4.11, GSH showed a decrease in BLEGI-treated cells compared to the untreated control, while GSSG showed an increase. These findings suggest that BLEGI influenced cellular redox status. Elevated GSSG levels provide valuable information supporting the induction of oxidative stress in BLEGI-treated cells. Furthermore, the marked reduction in glutathione levels implies a potentially diminished ability to maintain intercellular redox homeostasis. Studies have shown a close relationship between GSSG levels and loss of mitochondrial integrity and caspase activation (MUSAOGULLARI; MANDATO; CHAI, 2020). The adverse effects of BLEGI-induced oxidative stress could play a critical role in inhibiting cell proliferation, thus demonstrating its antitumor activity. Reactive oxygen species (ROS) are generated as byproducts of regular redox reactions that occur during cellular metabolism. However, when ROS levels exceed normal thresholds and are not efficiently removed, oxidative stress occurs, resulting in significant metabolic alterations and cellular damage. Elevated levels of ROS can interact with essential biomolecules such as lipids, nucleic acids, and proteins, disrupting their normal functions and contributing to chronic diseases, particularly colorectal cancer (DÜKEL; TAVSAN; KAYALI, 2021; SABHARWAL; SCHUMACKER, 2014). Under physiological conditions, there is a delicate balance between the antioxidant and pro-oxidant systems. Protective mechanisms include the glutathione system, where glutathione exists primarily in its

reduced form GSH within cells, with a smaller fraction in its oxidized state GSSG. This balance is maintained by the enzyme glutathione reductase (GR), which converts GSSG back to GSH, ensuring cellular redox homeostasis (BRZOZOWA-ZASADA et al., 2024; HEGEDŰS et al., 2018). Surprisingly, very low levels of GSH in cells treated with BLEGI compared to other studies demonstrate that high levels of GSH in tumor cells are associated with cancer progression and increased resistance to chemotherapeutic drugs. Several novel therapies targeting the GSH antioxidant system have recently been developed in different tumors as a means to increase response and decrease drug resistance (KENNEDY et al., 2020). The decrease in GSH in HCT-116 cells treated with BLEGI strongly supports the hypothesis of glutathione metabolism as a possible pathway responsible for the activity of the extract. This is consistent with what was observed in human liver HepG2 cells treated with a flavonoid derivative, where the low level of GSH in the treated cells indicated an increase in oxidative stress (GAO et al., 2014).

Nicotinamide (NAM) serves as a precursor to nicotinamide-adenine dinucleotide ($NAD^+$), which plays crucial roles in both redox and non-redox reactions regulating cellular energy metabolism. $NAD^+$ functions as a coenzyme in dehydrogenase reactions, facilitating the production of adenosine triphosphate (ATP). Elevated levels of $NAD^+$ (or a high $NAD^+$/NADH ratio) inhibit the generation of ROS and enhance mitochondrial function, thereby mitigating oxidative stress and promoting cell viability. Moreover, $NAD^+$ serves as a pivotal metabolite in cellular homeostasis, acting as an essential cofactor in oxidation-reduction (redox) reactions involved in various energy production pathways, including the Krebs cycle, fatty acid oxidation, glycolysis, and serine biosynthesis (CHEN et al., 2016; LI et al., 2022; NIKAS; PASCHOU; RYU, 2020). Similarly, elevated levels of $NAD^+$ are essential as they also participate in numerous non-redox molecular processes, including DNA repair, post-translational modifications, cell signaling, senescence, inflammatory responses, and apoptosis (YOON et al., 2023b; ZHANG et al., 2013b). Nicotinamide N-methyltransferase (NNMT) is an enzyme found in the cytoplasm that catalyzes the methylation of nicotinamide (NAM) and related compounds like pyridines. During this process, NNMT converts NAM into 1-methylnicotinamide (1-MNA). Subsequently, this

compound undergoes oxidation to produce N1-methyl-2-pyridone-5-carboxamide (2PY) and N1-methyl-4-pyridone-3-carboxamide (4PY) through the action of the AOX1 enzyme (RAMSDEN et al., 2017; WANG et al., 2022a).

In the context of HCT-116 tumor cell metabolism, this information could be relevant, since NNMT and its metabolic products could play a role in the regulation of certain metabolic aspects or specific pathways in these cells. NNMT and its metabolic products have been studied in the context of specific diseases and conditions, including some types of cancer, although the precise connection with the tumor-specific metabolism of HCT-116 may require further investigation. It has also been reported that NNMT participates in the regulation of autophagy to maintain the survival of cancer cells through the mTOR and AMPK pathways (CAMPAGNA et al., 2021; LU; LONG, 2018).

Dysregulated lipid metabolism is a significant metabolic alteration in cancer. Lipids encompass a complex group of biomolecules, including fatty acids, glycerides, non-glyceric lipids, and lipoproteins. Their diverse roles include serving as energy producers, signaling molecules, and source material for cell membrane biogenesis. Lipid metabolism generates various biological intermediates, many of which act as signaling molecules, regulating pathways controlling growth, proliferation, differentiation, apoptosis, motility, inflammation, survival, and cell membrane homeostasis (BROADFIELD et al., 2021; FU et al., 2021). A comprehensive understanding of how cancer cells reprogram lipid metabolism to support their malignant phenotype may unveil new therapeutic targets for cancer treatment. In our study, Sphingosine (Sph) levels decreased after BLEGI treatment, possibly due to cell membrane damage in HCT-116 cells. The cells then relied on sphingolipids to enhance membrane synthesis. Sph can undergo further phosphorylation, promoting cell proliferation and tumor survival. The results suggest that BLEGI may regulate apoptosis and the dysregulated metabolism of sphingolipids to exert its antitumor effect. Sphingolipids are essential molecules that comprise cell membranes and act as second messengers participating in numerous cellular functions, such as cell signaling, proliferation inhibition, cell cycle arrest, induction of apoptosis (programmed cell death), stress responses, necrosis, inflammation, senescence, and differentiation in

various types of cancer cells (CHOI; SONG, 2020; GOMEZ-LARRAURI et al., 2021; SANTOS; SCHULZE, 2012).

In this study, the results revealed an intracellular decrease in Sph, which could lead to the inhibition of cell growth and induction of apoptotic cell death in HCT-116 cells after BLEGI treatment. Sph has been implicated in various signaling pathways involved in the apoptotic process and acts as a second messenger in response to various cellular stress signals, such as DNA damage or cellular injury. Elevated levels of Sph promote cell cycle arrest and apoptosis, preventing uncontrolled cell growth (CUVILLIER, 2002). Therefore, these findings suggest that BLEGI-induced apoptosis of HCT-116 colon cancer cells could be due to the reduction of Sph levels in the endometabolome. Previous studies have suggested that sphingolipids, including Sph, play an important role in cancer development and progression. For example, Sph has been shown to play a specific role in ceramide-independent tumor cell death (ZHAO et al., 2023).

We present a comprehensive biochemical map illustrating the metabolites and metabolic pathways altered by BLEGI in HCT-116 colon cancer cells (Figure 4.11). Our findings reveal that BLEGI significantly impacts major metabolic pathways, including glutathione metabolism, the tricarboxylic acid cycle, lipoic acid metabolism, and pyrimidine metabolism. The endo- and exometabolomic profile of HCT-116 cells exhibits marked changes in metabolite concentrations following a 72-hour exposure to BLEGI. The integrated analysis allows us to suggest that BLEGI treatment may induce cell death by apoptosis. To confirm the findings regarding the induction of apoptosis in HCT-116 cells and its impact on the mechanism of action, we evaluated cell morphology and qualitative apoptosis induction using immunofluorescence assay. Through this analysis, we obtained qualitative information about cell structure and processes. In this assay, we used the antibody a-tubulin, which is one of the main cytosolic fibers constituting the cytoskeleton. Additionally, we used DAPI staining to visualize nuclear DNA in the cells and evaluate their macroscopic cell morphology. Notably, our immunofluorescence analysis revealed the presence of tripolar mitosis, a process of cell division driven by molecular mechanisms typical of mitosis. Additionally, we observed the formation of apoptotic bodies, which are

eventually phagocytosed, indicating an effect directly related to apoptotic cell death (XU; LAI; HUA, 2019) in HCT-116 cells after BLEGI treatment. These results highlight the promising therapeutic potential of BLEGI not only for colon cancer but also for other types of cancer. Considering that flavonoids, specifically flavone glycosides, are responsible for the cytotoxic effect on HCT-116 cells, in a previous study, a bioinformatic analysis and complete transcriptomic profile were performed with the aim of revealing regulatory pathways associated with cell apoptosis induced by quercetin in HCT-116 cells. It was determined that cell viability was markedly reduced with this flavonoid as a function of dose and time, respectively. Furthermore, it was confirmed that quercetin could inhibit proliferation and induce apoptosis. This could be associated with the transcriptome of HCT-116 cells, considering the differential expression of ncRNA and mRNA. Twelve deregulated ncRNAs and mRNAs were found related to two significantly enriched pathways, such as the PI3K-Akt and Ras signaling pathways, confirming that they may be related to the molecular mechanisms that quercetin exerts on CRC (ZHANG et al., 2019). These findings could help us elucidate the molecular mechanism role of BLEGI flavone glycosides and possible alterations in HCT-116 cells; however, further studies are required.

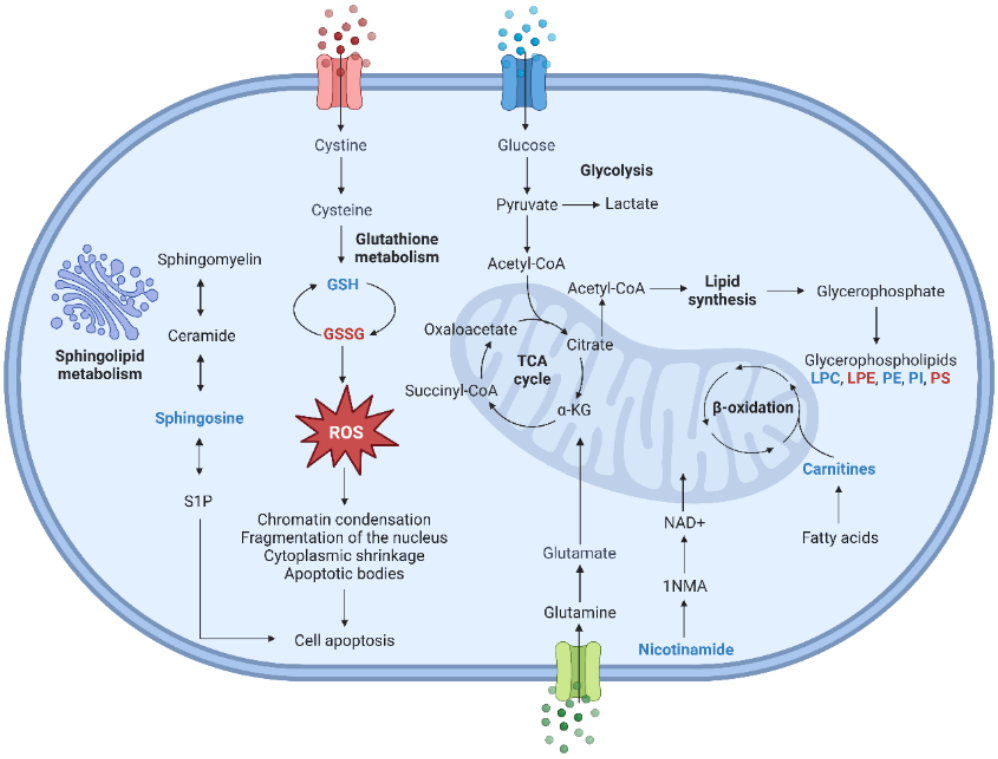



**Figure 4.11.** Schematic biochemical representation of the main altered metabolic pathways 72 hours after BLEGI treatment in HCT-116 cells. Red indicates potential up-regulated metabolites, while blue indicates potential down-regulated metabolites.

Furthermore, the anti-inflammatory activity of BLEGI was determined by calculating the percentage of inhibition of NO at the chemical level and at the cellular level in macrophage cells. Generally, BLEGI showed significant results for the inhibition of NO production, with an inhibition greater than 50%, which is considered an important result considering that NO is a factor involved in tumor progression. Considering the results of chemical NO and cellular NO, it is possible to infer that the samples can capture NO and inhibit iNOS (inducible nitric oxide synthase). The relationship of metabolomic analysis results with anti-inflammatory activity allows us to highlight a close relationship between inflammatory processes and tumor development. Thus, inflammation plays an important role in the development of different types of cancer. The enzyme iNOS is one of the three enzyme isoforms of nitric oxide synthase (NOS) being an enzyme expressed under inflammatory conditions that can produce high levels of NO, affecting the redox state of cells causing protein oxidation, lipid peroxidation and DNA damage. Thus, several iNOS

inhibitors have shown efficacy in reducing metastasis and inhibiting tumor cells (JIANG et al., 2018; KORDE CHOUDHARI et al., 2013; VANINI; KASHFI; NATH, 2015). Our hypothesis is since BLEGI may present a relevant anti-inflammatory capacity targeting iNOS and the regulation of oxidative stress, being a potential preventive agent against the growth of these tumor cells.

Based on the results of NO inhibitory activity of BLEGI, it has been reported that flavonoids normally have NO inhibitory activity (KIM et al., 1999). The chemical characterization of this extract allowed us to determine that phenolic compounds are the major compounds in the BLEGI. The presence of glycosylated flavonoids and phenolic acids and derivatives stands out mainly (CHITIVA et al., 2023). Consequently, and according to the reports described, it is established that flavonoids present anti-inflammatory and immunomodulatory properties in different tissues. Since NO produced by iNOS is one of the inflammatory mediators in cells, flavonoids can inhibit NO production, measured at the chemical and cellular level. NO production is a primary indicator of macrophage activation. NO is produced once the nuclear factor kappa B (NF-κB) complex has been activated by extracellular stimuli (JIANG et al., 2017). Therefore, BLEGI that suppresses NO production in macrophage cells can be expected to be a useful suppressor of inflammation (JIANG et al., 2017). Flavonoids can inhibit the synthesis and activities of different proinflammatory mediators (e.g. cytokines, chemokines, NO, eicosanoids etc.), and also have the ability to inhibit transcription factors such as nuclear factor kappa B (NF-κB) (ALVAREZ-SUAREZ et al., 2017; XU et al., 2002). Our study constitutes the first report on the anti-inflammatory properties of BLEGI. The results described in this study validate that the *G. incana* species is a remarkable source of bioactive compounds with important biological properties related to its anti-inflammatory and antioxidant capabilities.

Nevertheless, some limitations of our study should be noted. First, specific biological assays are needed to validate the mechanism of action in HCT-116 cells after BLEGI exposure. It is additionally recommended to continue performing tests specifically aimed at confirming the mechanism of cell death (e.g., assays focused on glutathione

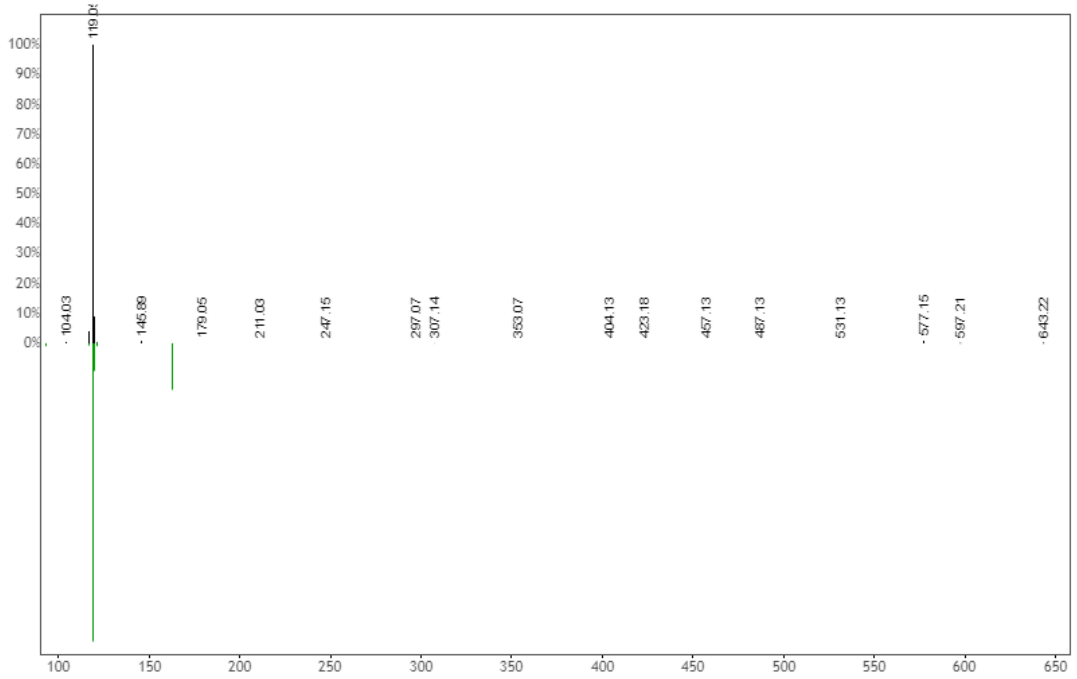
determination, quantitative apoptosis assay (Annexin V), glucose uptake, mitochondrial membrane potential, and evaluation of ROS levels). It is also worth noting that more research is needed to validate other potential therapeutic targets and fully understand the mechanism by which BLEGI exerts its effect. In summary, we identified multiple altered biological pathways after exposure to BLEGI, which shows us the possible altered metabolic pathways and provides insight into the possible mechanism of action in these tumor cells.

## 4.3 Conclusion

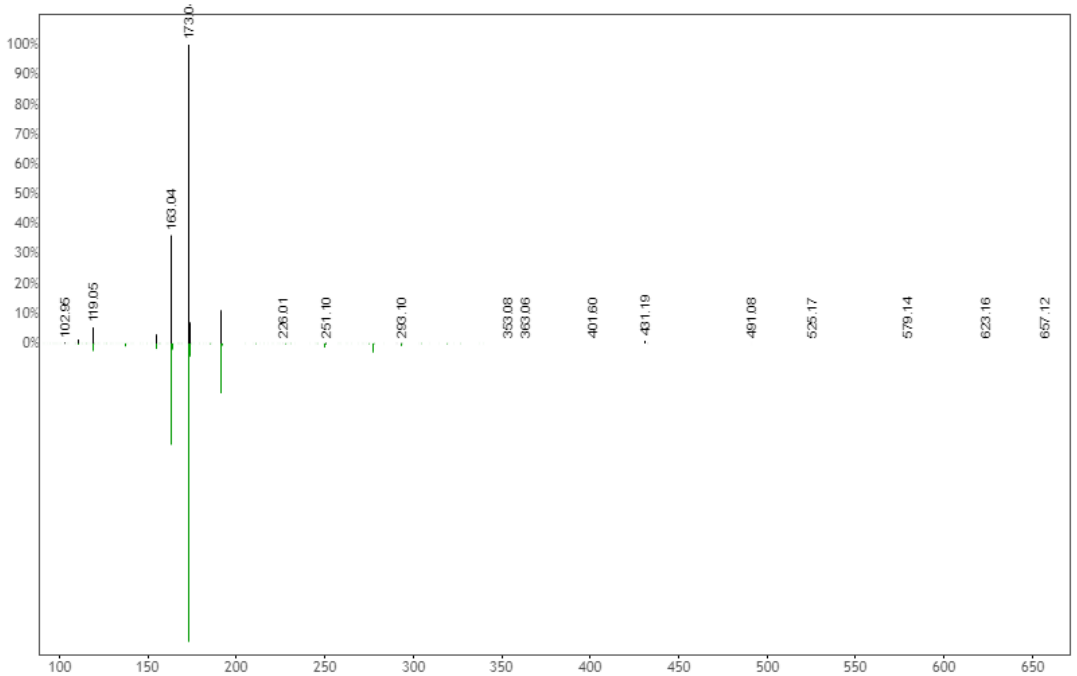
To the best of our knowledge, this is the first study to investigate possible alterations in metabolites associated with BLEGI-induced HCT-116 colon cancer cells. In this study, endo- and exometabolomic profiles were used to assess metabolite changes and identify altered metabolic pathways, proposing a possible mechanism of action. The tentatively identified metabolites suggest the possibility that the altered pathways are primarily associated with glutathione metabolism. Metabolomic analysis revealed that BLEGI may inhibit tumor progression, cause damage to tumor cells, and stimulate apoptosis. Furthermore, the identification of reduced levels of sphingosine and glutathione, along with increased levels of glutathione disulfide, potentially allows the activation of apoptosis signaling pathways, which may be one of the proposed mechanisms of action mediated by the induction of oxidative stress. However, more in-depth studies are needed to confirm these findings of altered metabolic pathways and the mechanisms of action through which the extract exerts its therapeutic effect. Moreover, the anti-inflammatory potential of BLEGI was demonstrated in the inhibition of nitric oxide in LPS-stimulated macrophage cells. Our results globally demonstrate the effect of BLEGI at the metabolic level in colon cancer lines, providing clues for the identification of new therapeutic targets in the treatment of this disease.

## Supplementary information

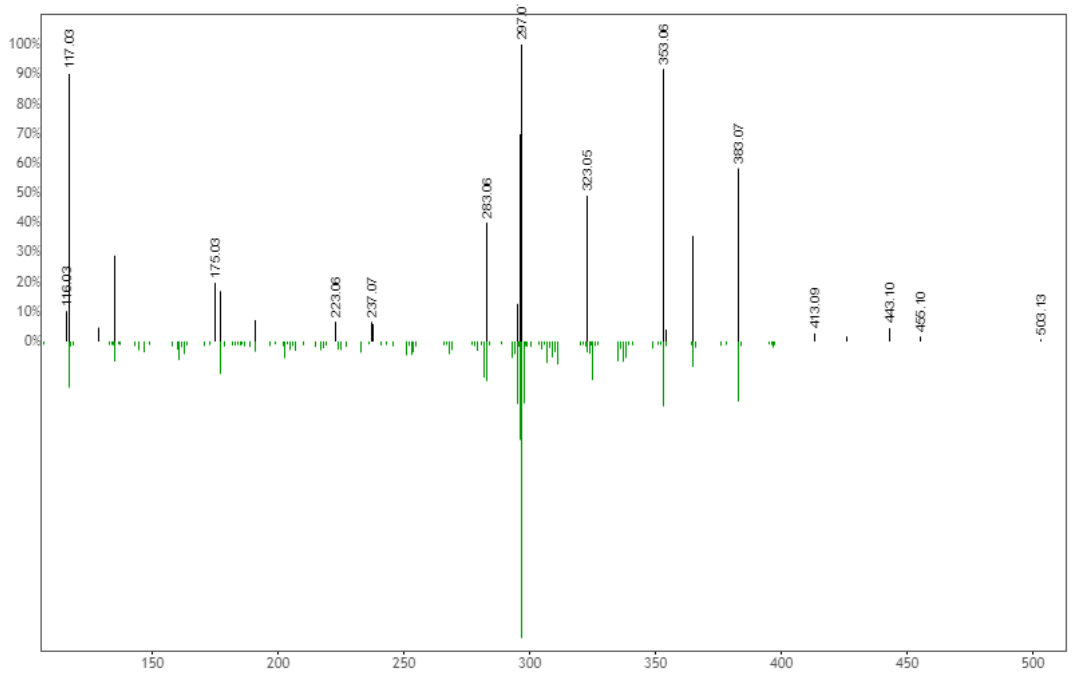
Compound 19



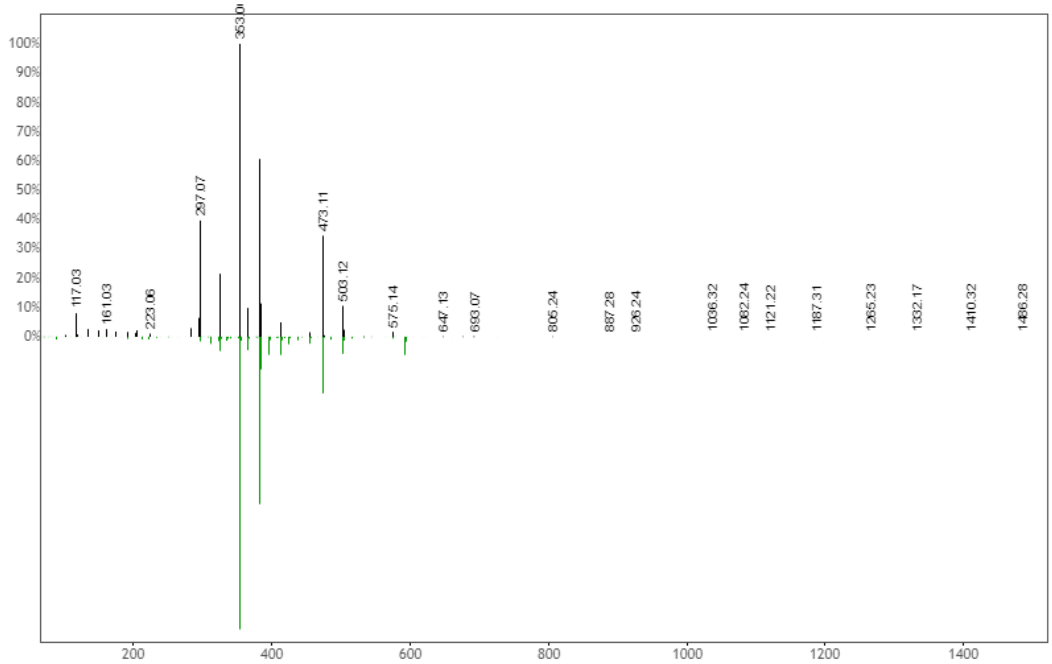

Compound 3



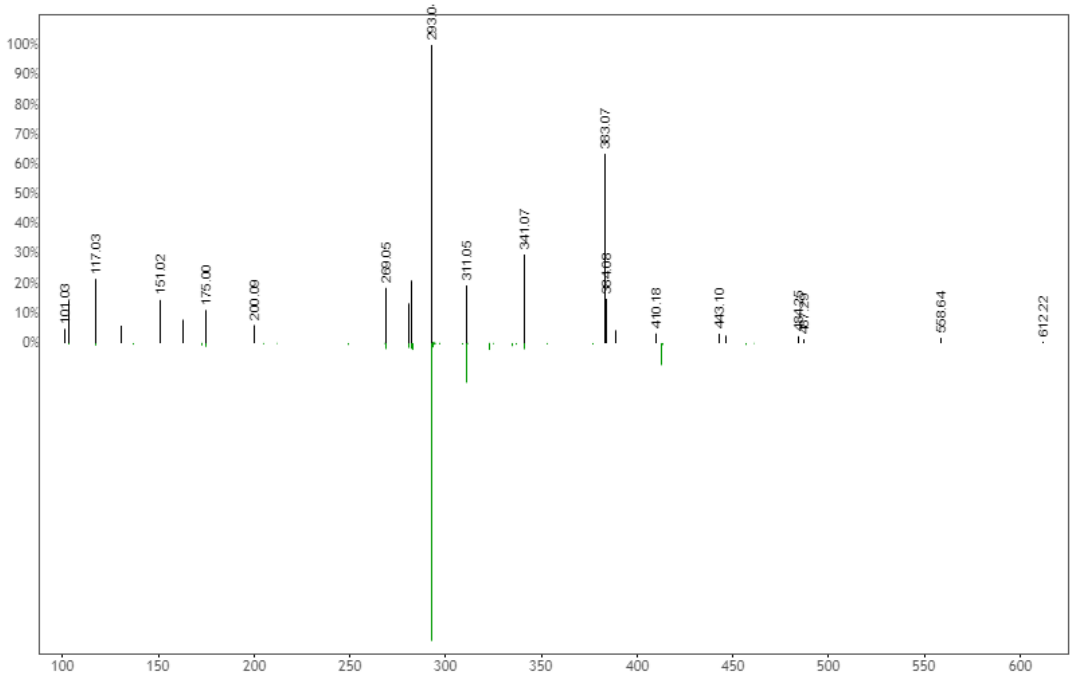
Compound 6



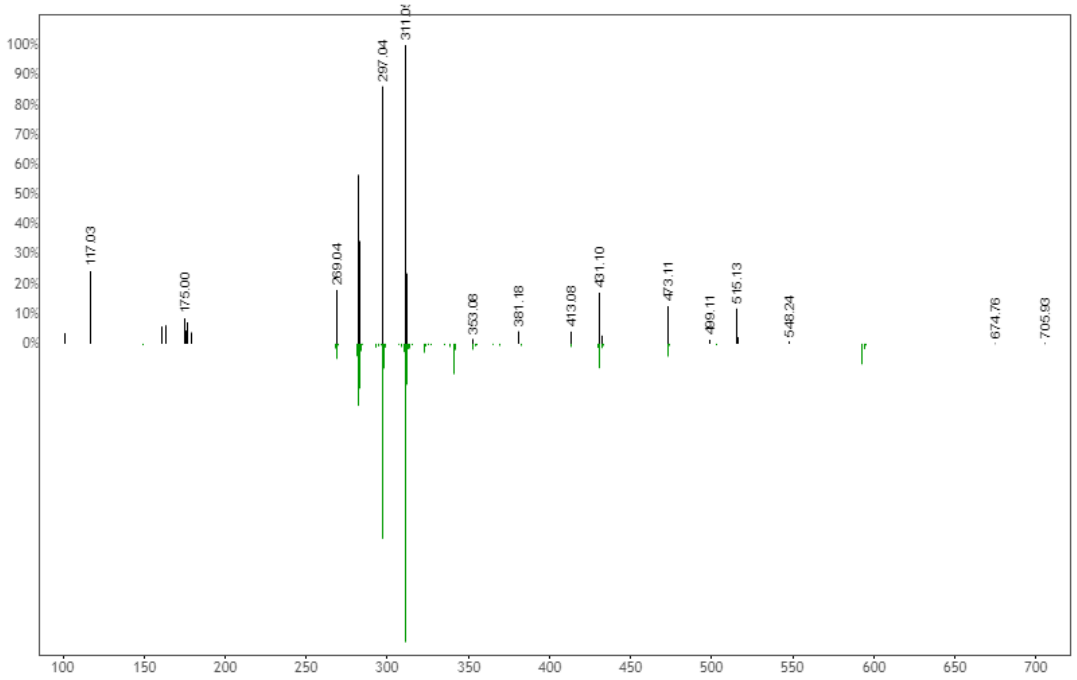

Compound 8



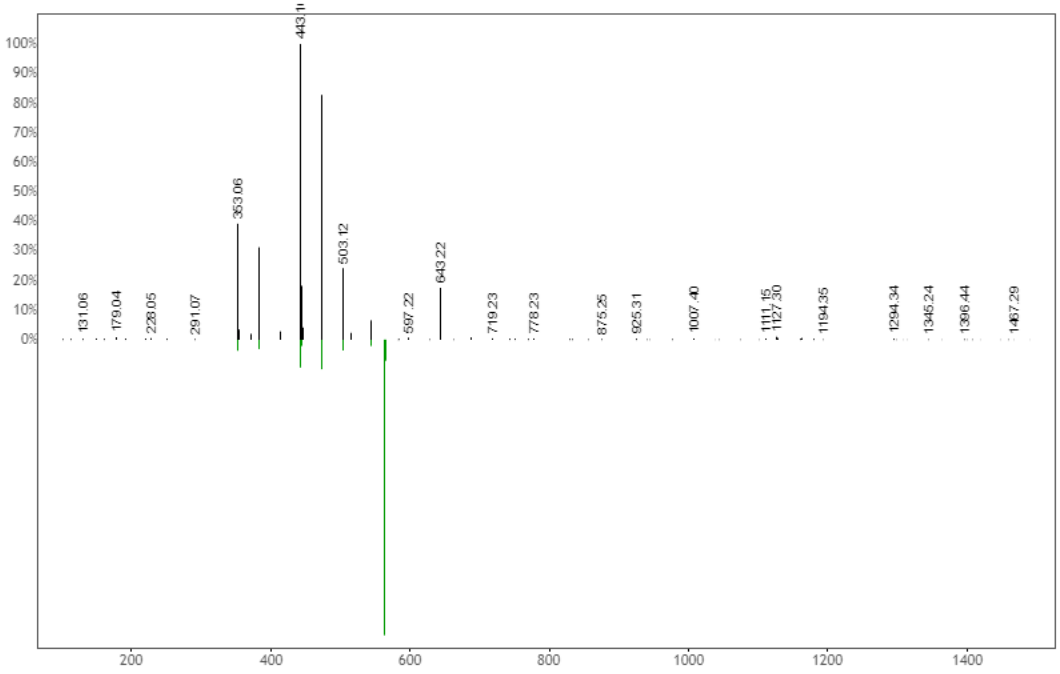
Compound 13



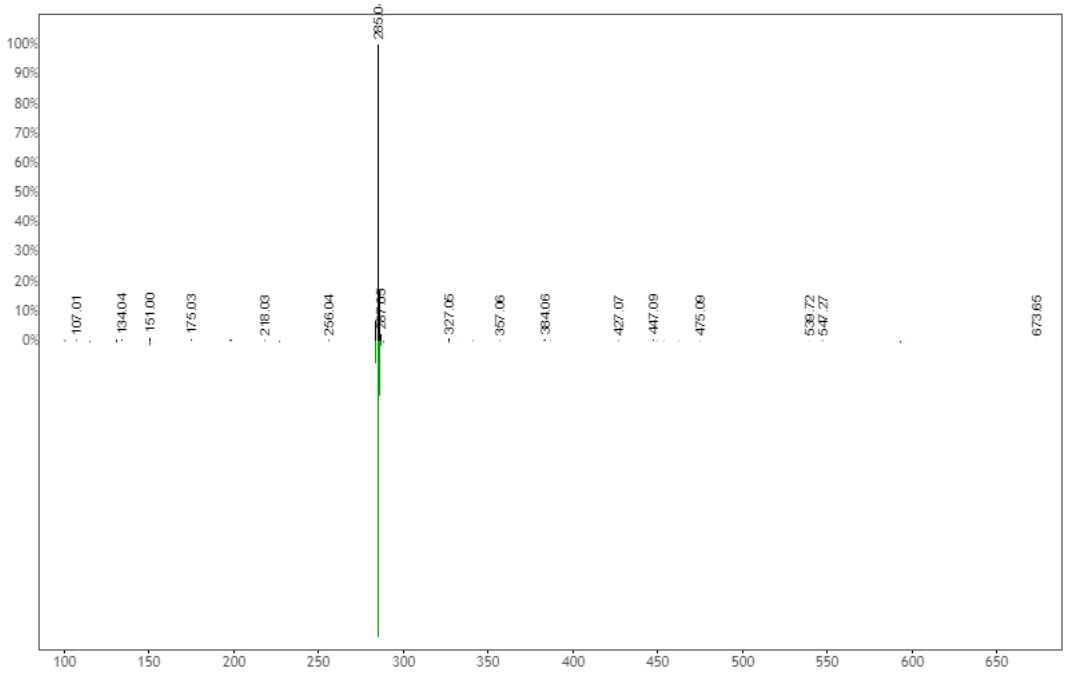

Compound 14



Compound 15




Compound 21



Compound 26

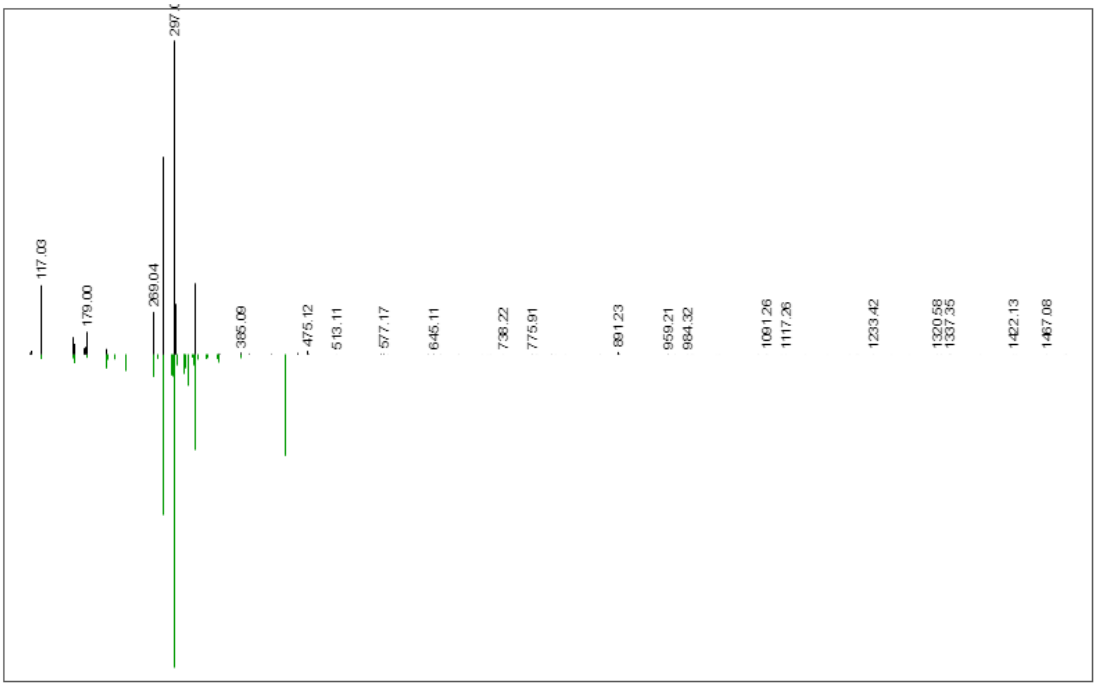



**Figure S4.1.** MS/MS spectrum match feature of GNPS showing the similarity of fragments patterns of the experimental and library data.

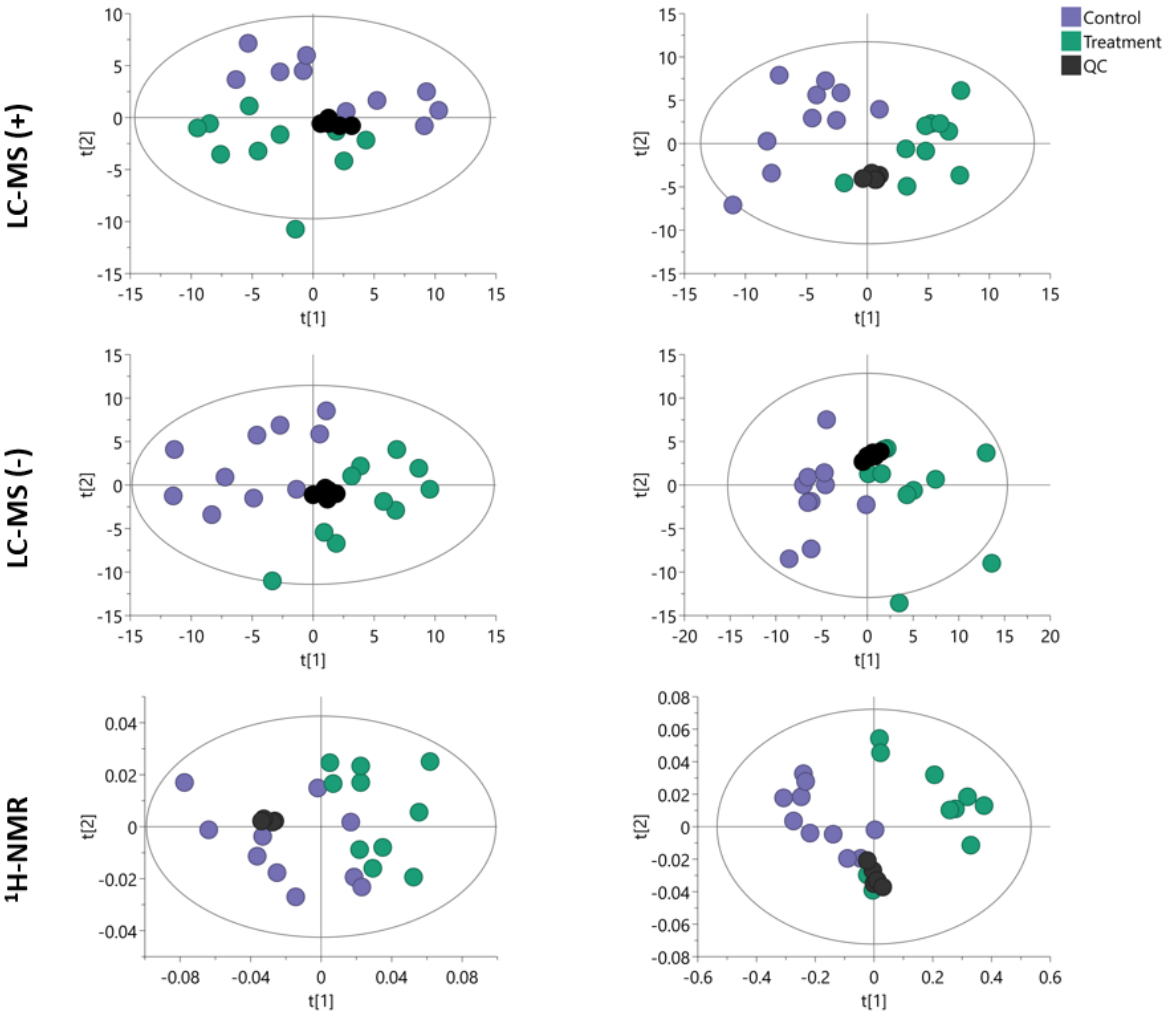



**Figure S4.2.** PCA score plot including quality controls (QCs) and all samples from LC-MS and $^{1}$H-NMR analysis.

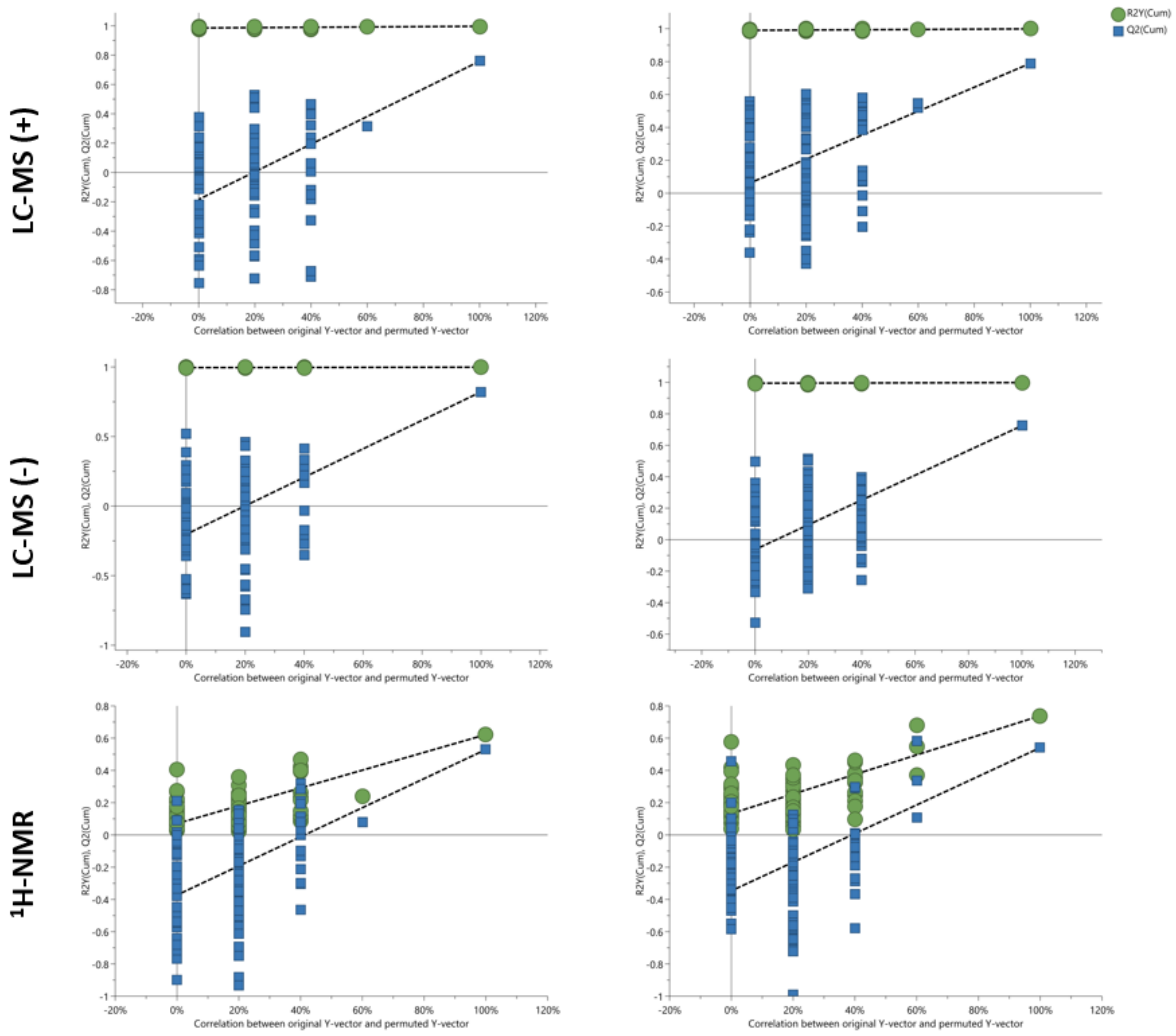



**Figure S4.3.** Cross-validation plots of the OPLS-DA models with 100 permutation tests. BLEGI-treated group ($n$ = 10) and untreated group ($n$ = 10).

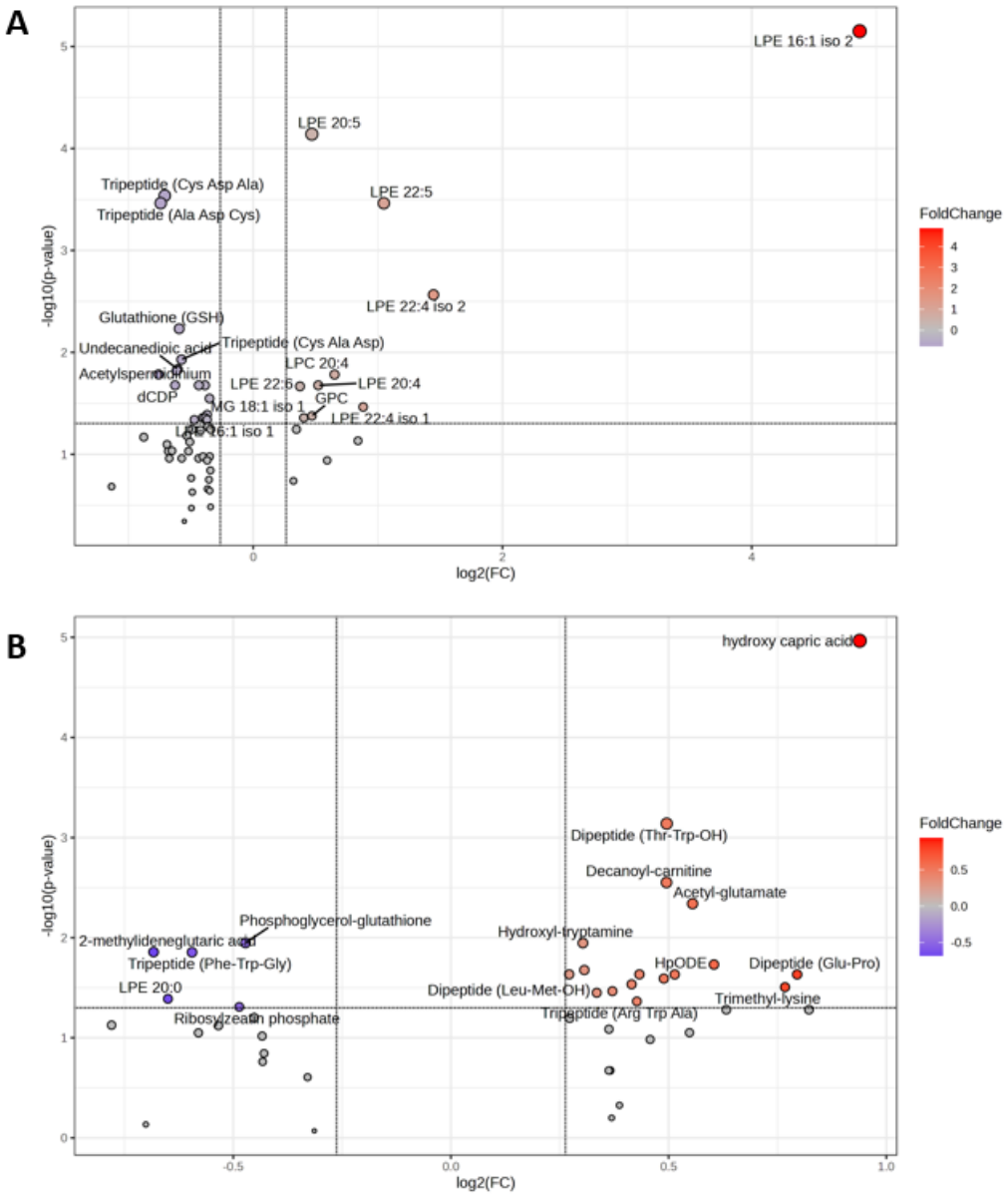



**Figure S4.4.** Volcano plot of metabolites from the A) endometabolome and B) exometabolome that met the *p*-value and fold change criteria, comparing the group of cells treated with BLEGI versus untreated cells.

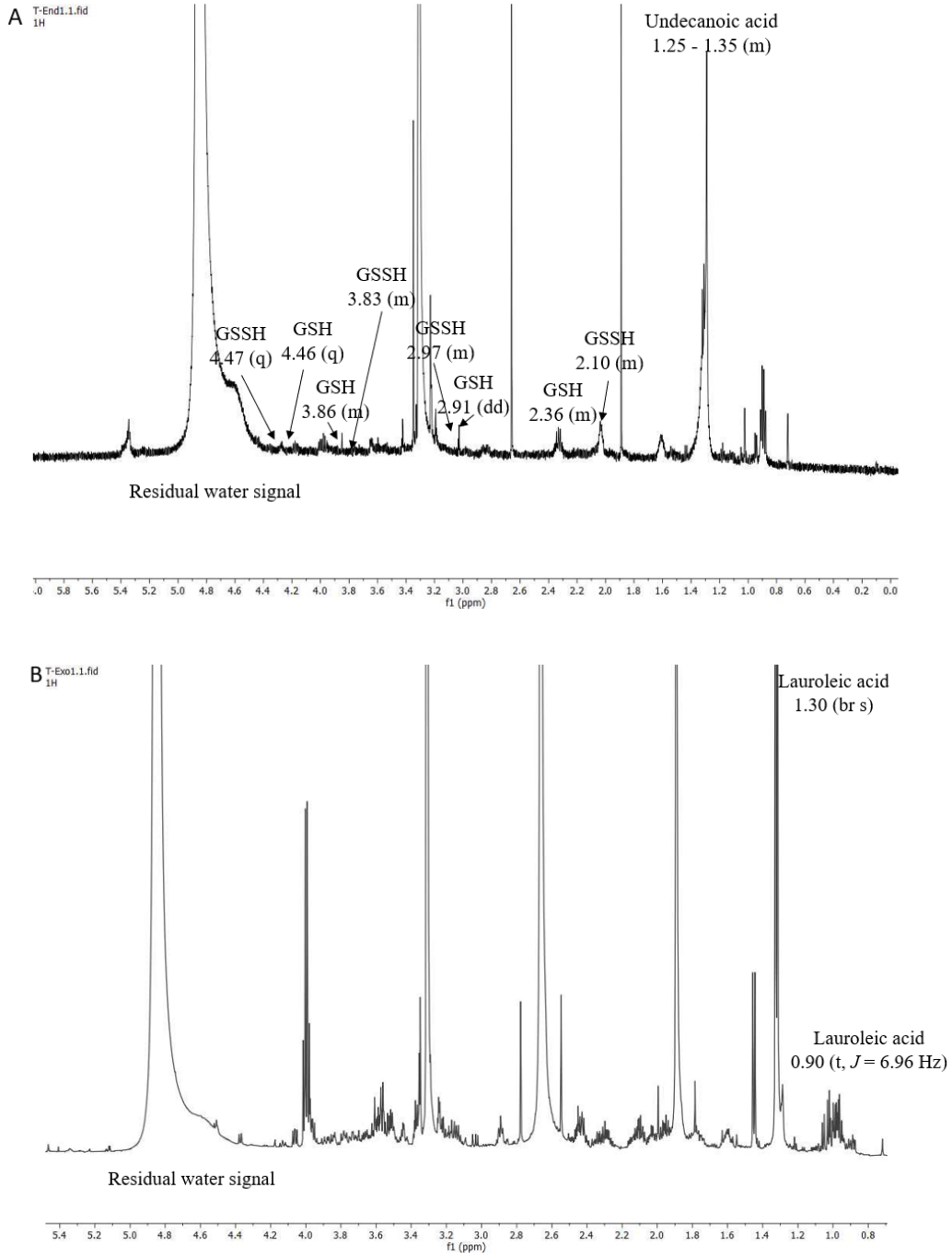



**Figure S4.5.** Representative $^{1}$H-NMR spectra of the A) endometabolome and B) exometabolome at 72 h of BLEGI-treated cells. The experimental data were compared with reports in the literature based on chemical shifts, multiplicities, and coupling constants for each metabolite, assigning the most representative signal for each molecule.

**Table S4.1.** List of all metabolites identified in the endometabolome of cancer cells HCT-116 treated with BLEGI.

| Compounds | Formula | Mass | RT (min) | Error (ppm) | Adduct | δ $^{1}$H (ppm) and Multiplicity, *J* in Hz | Assignments | [a]CV for QC (%) | Analytical platform | DET | [b]ID Level | [c]Fold Change | [d]*p* value* | [e]VIP |
|---|---|---|---|---|---|---|---|---|---|---|---|---|---|---|
| ***Organic acids and derivatives*** | | | | | | | | | | | | | | |
| Acetylspermidinium | $C_9H_{21}N_3O$ | 187.1685 | 1.10 | 1 | $[M+H]^+$ | - | - | 9.45 | LC-QTOF-MS | ESI + | 3 | 0.65 | 2.65E-03 | 1.64 |
| Glutathione (GSH) | $C_{10}H_{17}N_3O_6S$ | 307.0838 | 1.13 | 3 | $[M+H]^+$ | 2.91 (dd); 2.36 (m) 4.46 (q); 3.86 (m) | - | 9.65 | LC-QTOF-MS / NMR | ESI + / $^{1}$H | 2 | 0.67 | 2.87E-02* | 1.61 |
| Glutathione disulfide (GSSG) | $C_{20}H_{32}N_6O_{12}S_2$ | 612.1520 | 8.54 | 1 | $[M-H]^-$ | 2.10 (m); 2.97 (m) 4.47 (q); 3.83 (m) | - | 3.77 | LC-QTOF-MS / NMR | ESI - / $^{1}$H | 3 | 1.32 | 1.77E-02 | 1.24 |
| Glutathione palmitamide | $C_{26}H_{47}N_3O_7S$ | 545.3135 | 8.18 | 0 | $[M-H-H_2O]^-$ | - | - | 3.73 | LC-QTOF-MS | ESI - | 3 | 0.79 | 2.97E-02 | 1.05 |
| ***Carnitines*** | | | | | | | | | | | | | | |
| Hexadec-2-enoyl carnitine | $C_{23}H_{43}NO_4$ | 397.3192 | 8.86 | 1 | $[M+H]^+$ | - | - | 14.53 | LC-QTOF-MS | ESI + | 2 | 0.54 | 3.93E-02 | 1.26 |
| Elaidic carnitine | $C_{25}H_{47}NO_4$ | 425.3505 | 9.34 | 1 | $[M+H]^+$ | - | - | 10.13 | LC-QTOF-MS | ESI + | 2 | 0.76 | 1.84E-02 | 1.37 |
| Stearoyl carnitine | $C_{25}H_{49}NO_4$ | 427.3662 | 9.88 | 1 | $[M+H]^+$ | - | - | 9.62 | LC-QTOF-MS | ESI + | 2 | 0.77 | 5.04E-03 | 1.50 |
| Arachidyl carnitine | $C_{27}H_{53}NO_4$ | 455.3975 | 7.96 | 1 | $[M+H]^+$ | - | - | 10.37 | LC-QTOF-MS | ESI + | 2 | 0.74 | 5.61E-03 | 1.49 |
| Tetradecanoyl carnitine | $C_{21}H_{41}NO_4$ | 371.3036 | 3.3 | 1 | $[M+H]^+$ | - | - | 10.40 | LC-QTOF-MS | ESI + | 2 | 0.62 | - | 1.40 |
| 2-Methylbutyroylcarnitine | $C_{12}H_{23}NO_4$ | 245.1627 | 9.11 | 3 | $[M+H]^+$ | - | - | 7.23 | LC-QTOF-MS | ESI + | 2 | 0.62 | - | 1.36 |
| 3-hydroxypentadecanoyl carnitine | $C_{22}H_{43}NO_5$ | 401.3141 | 1.14 | 4 | $[M+Cl]^-$ | - | - | 4.18 | LC-QTOF-MS | ESI - | 2 | 0.71 | 2.06E-02 | 1.38 |
| ***Fatty acids*** | | | | | | | | | | | | | | |
| Methyl arachidonoyl amine | $C_{21}H_{35}NO$ | 317.2719 | 6.89 | 2 | $[M+H]^+$ | - | - | 10.92 | LC-QTOF-MS | ESI + | 3 | 0.76 | - | 1.10 |
| Undecanedioic acid | $C_{11}H_{20}O_4$ | 216.1362 | 5.77 | 8 | $[M-H]^-$ | 1.25 - 1.35 (m) | Aliphatic carbons | 10.21 | LC-QTOF-MS / NMR | ESI - / $^{1}$H | 3 | 0.66 | 2.32E-03 | 1.46 |
| ***Glycerophospholipids*** | | | | | | | | | | | | | | |
| LPC 14:0 | $C_{22}H_{46}NO_7P$ | 467.3012 | 7.67 | 1 | $[M+H]^+$ | - | - | 12.13 | LC-QTOF-MS | ESI + | 2 | 0.75 | - | 1.18 |
| LPC 15:0 | $C_{23}H_{48}NO_7P$ | 481.3168 | 9.37 | 2 | $[M-H-H_2O]^-$ | - | - | 5.73 | LC-QTOF-MS | ESI - | 2 | 0.78 | 1.43E-02 | 1.48 |
| LPC 15:2 | $C_{25}H_{52}NO_7P$ | 509.3481 | 9.99 | 3 | $[M-H]^-$ | - | - | 16.24 | LC-QTOF-MS | ESI - | 2 | 0.78 | - | 1.04 |

| | | | | | | | | | | | | | | |
|---|---|---|---|---|---|---|---|---|---|---|---|---|---|---|
| LPC 16:0 | $C_{24}H_{50}NO_7P$ | 495.3325 | 8.86 | 2 | $[M+Cl]^-$ | - | - | 5.57 | LC-QTOF-MS | ESI + | 2 | 1.80 | 4.39E-02 | 1.05 |
| LPC 16:1 iso 1 | $C_{24}H_{48}NO_7P$ | 493.3168 | 8.17 | 2 | $[M+HCOOH-H]^-$ | - | - | 4.66 | LC-QTOF-MS | ESI + | 2 | 0.73 | 3.16E-02 | 1.13 |
| LPC 16:1 iso 2 | $C_{24}H_{48}NO_7P$ | 493.3168 | 8.15 | 2 | $[M+HCOOH-H]^-$ | - | - | 4.03 | LC-QTOF-MS | ESI + | 2 | 0.71 | - | 1.24 |
| LPC 18:1 | $C_{26}H_{52}NO_7P$ | 521.3481 | 9.11 | 2 | $[M+HCOOH-H]^-$ | - | - | 4.01 | LC-QTOF-MS | ESI + | 2 | 0.79 | - | 1.06 |
| LPC 20:4 | $C_{28}H_{50}NO_7P$ | 543.3325 | 8.52 | 0 | $[M+H]^+$ | - | - | 10.76 | LC-QTOF-MS | ESI + | 2 | 1.58 | 3.50E-03 | 1.41 |
| LPC O-18:1 | $C_{26}H_{52}NO_7P$ | 521.3481 | 9.16 | 2 | $[M+HCOOH-H]^-$ | - | - | 3.97 | LC-QTOF-MS | ESI + | 3 | 0.78 | - | 1.23 |
| PC 38:4 | $C_{46}H_{84}NO_8P$ | 809.5935 | 9.69 | 2 | $[M+H]^+$ | - | - | 10.79 | LC-QTOF-MS | ESI + | 2 | 0.69 | - | 1.25 |
| GPC | $C_8H_{20}NO_6P$ | 257.1028 | 0.73 | 2 | $[M+H]^+$ | - | - | 13.86 | LC-QTOF-MS | ESI + | 3 | 1.38 | 1.57E-02 | 1.34 |
| LPE 16:1 iso 1 | $C_{21}H_{42}NO_7P$ | 451.2699 | 7.93 | 1 | $[M+H]^+$ | - | - | 9.36 | LC-QTOF-MS | ESI + | 3 | 0.78 | 2.09E-02 | 1.34 |
| LPE 16:1 iso 2 | $C_{21}H_{42}NO_7P$ | 451.2699 | 8.51 | 4 | $[M-H]^-$ | - | - | 12.49 | LC-QTOF-MS | ESI - | 2 | 52.50 | 2.31E-05* | 1.57 |
| LPE 18:1 | $C_{23}H_{46}NO_7P$ | 479.3012 | 8.46 | 5 | $[M+Na]^+$ | - | - | 9.40 | LC-QTOF-MS | ESI + | 3 | 1.28 | 2.74E-02 | 1.29 |
| LPE 20:4 | $C_{25}H_{44}NO_7P$ | 501.2855 | 8.41 | 2 | $[M-H]^-$ | - | - | 2.68 | LC-QTOF-MS | ESI - | 3 | 1.50 | 5.90E-03 | 1.30 |
| LPE 20:5 | $C_{25}H_{42}NO_7P$ | 499.2699 | 7.97 | 2 | $[M-H]^-$ / $[M+H]^+$ | - | - | 2.70 | LC-QTOF-MS | ESI - / ESI + | 2 | 1.38 | 2.36E-04* | 1.95 |
| LPE 22:4 | $C_{27}H_{48}NO_7P$ | 529.3168 | 9.17 | 5 | $[M-H]^-$ | - | - | 19.63 | LC-QTOF-MS | ESI - | 3 | 2.75 | 7.62E-03* | 1.69 |
| LPE 22:5 | $C_{27}H_{46}NO_7P$ | 527.3012 | 8.68 | 1 | $[M+H]^+$ | - | - | 11.35 | LC-QTOF-MS | ESI + | 2 | 2.08 | 3.78E-03* | 1.78 |
| LPE 22:6 | $C_{27}H_{44}NO_7P$ | 525.2855 | 8.43 | 1 | $[M-H]^-$ / $[M+H]^+$ | - | - | 2.41 | LC-QTOF-MS | ESI - / ESI + | 2 | 1.28 | 6.42E-03 | 1.42 |
| PE 34:0 | $C_{39}H_{76}NO_8P$ | 717.5309 | 9.62 | 2 | $[M+H]^+$ | - | - | 13.83 | LC-QTOF-MS | ESI + | 3 | 0.69 | - | 1.17 |
| PE 34:2 | $C_{39}H_{74}NO_8P$ | 715.5152 | 9.71 | 1 | $[M+H]^+$ | - | - | 18.47 | LC-QTOF-MS | ESI + | 3 | 0.64 | - | 1.28 |
| PE 36:2 | $C_{41}H_{78}NO_8P$ | 743.5465 | 9.54 | 1 | $[M-H]^-$ | - | - | 7.74 | LC-QTOF-MS | ESI - | 2 | 0.78 | - | 1.14 |
| PE P 36:4 iso 1 | $C_{41}H_{74}NO_7P$ | 723.5203 | 9.64 | 9 | $[M-H]^-$ | - | - | 15.46 | LC-QTOF-MS | ESI - | 3 | 0.70 | 4.64E-02 | 1.03 |
| PE P 36:4 iso 2 | $C_{41}H_{74}NO_7P$ | 723.5203 | 9.51 | 10 | $[M-H]^-$ | - | - | 8.21 | LC-QTOF-MS | ESI - | 3 | 0.45 | - | 1.00 |
| LPI 20:3 | $C_{29}H_{51}O_{12}P$ | 622.3118 | 9.08 | 2 | $[M-H]^-$ | - | - | 16.18 | LC-QTOF-MS | ESI - | 2 | 0.71 | - | 1.11 |
| PA O-42:6 | $C_{45}H_{79}O_7P$ | 762.5563 | 9.65 | 5 | $[M-H-H_2O]^-$ | - | - | 14.08 | LC-QTOF-MS | ESI - | 3 | 0.71 | - | 1.03 |
| PS 37:7 | $C_{43}H_{70}NO_{10}P$ | 791.4737 | 9.11 | 3 | $[M-H]^-$ | - | - | 5.52 | LC-QTOF-MS | ESI - | 3 | 1.55 | - | 1.05 |

| | | | | | | | | | | | | | | |
|---|---|---|---|---|---|---|---|---|---|---|---|---|---|---|
| PS P 35:0 | $C_{41}H_{80}NO_9P$ | 761.5571 | 9.64 | 0 | $[M-H-H_2O]^-$ | - | - | 15.86 | LC-QTOF-MS | ESI - | 3 | 1.26 | - | 1.02 |
| ***Glycerolipids*** | | | | | | | | | | | | | | |
| MG 18:1 iso 1 | $C_{21}H_{40}O_4$ | 356.2927 | 8.90 | 2 | $[M+H-H_2O]^+$ | - | - | 11.14 | LC-QTOF-MS | ESI + | 3 | 0.78 | 8.75E-03 | 1.49 |
| MG 18:1 iso 2 | $C_{21}H_{40}O_4$ | 356.2927 | 8.89 | 2 | $[M+H-H2O]^+$ | - | - | 13.46 | LC-QTOF-MS | ESI + | 3 | 0.66 | - | 1.10 |
| ***Sphingolipids*** | | | | | | | | | | | | | | |
| Sphingosine | $C_{18}H_{37}NO_2$ | 299.2824 | 2.74 | 2 | $[M+H]^+$ | - | - | 10.13 | LC-QTOF-MS | ESI + | 3 | 0.77 | 2.41E-02 | 1.38 |
| SM 34:2 | $C_{39}H_{77}N_2O_6P$ | 700.5519 | 0.82 | 1 | $[M+H]^+$ | - | - | 8.89 | LC-QTOF-MS | ESI + | 3 | 0.71 | - | 1.01 |
| ***Steroids and steroid derivatives*** | | | | | | | | | | | | | | |
| 2-hydroxyethinylestradiol | $C_{20}H_{24}O_3$ | 312.1725 | 9.40 | 6 | $[M-H]^-$ | - | - | 5.28 | LC-QTOF-MS | ESI - | 3 | 0.75 | - | 1.01 |
| ***Sterol Lipids*** | | | | | | | | | | | | | | |
| 3,12-dihydroxy-24-oxo-7-(sulfoxy)cholan-24-yl]-Glycine | $C_{26}H_{43}NO_9S$ | 545.2659 | 0.82 | 3 | $[M+Cl]^-$ | - | - | 4.17 | LC-QTOF-MS | ESI - | 3 | 0.70 | 2.80E-02 | 1.32 |
| ***Nucleosides, nucleotides, and analogues*** | | | | | | | | | | | | | | |
| Methylthioadenosine | $C_{11}H_{15}N_5O_3S$ | 297.0896 | 1.11 | 1 | $[M+H]^+$ | - | - | 9.68 | LC-QTOF-MS | ESI + | 3 | 0.78 | 2.53E-02 | 1.37 |
| ***Peptides*** | | | | | | | | | | | | | | |
| Tripeptide (Cys Ala Asp) | $C_{10}H_{17}N_3O_6S$ | 307.0838 | 1.12 | 2 | $[M+H]^+$ | - | - | 9.44 | LC-QTOF-MS | ESI + | 3 | 0.67 | 1.65E-03 | 1.49 |
| Tripeptide (Gly Met Cys) | $C_{10}H_{19}N_3O_4S_2$ | 309.0817 | 0.82 | 1 | $[M+H]^+$ | - | - | 11.29 | LC-QTOF-MS | ESI + | 3 | 0.69 | 4.22E-02 | 1.25 |
| Tripeptide (Gly Thr Asp) | $C_{10}H_{17}N_3O_7$ | 291.1067 | 1.11 | 5 | $[M-H-H_2O]^-$ | - | - | 15.41 | LC-QTOF-MS | ESI - | 3 | 0.59 | 3.17E-03 | 1.56 |
| Tripeptide (Ala Asp Cys) | $C_{10}H_{17}N_3O_6S$ | 307.0838 | 1.11 | 5 | $[M-H]^-$ | - | - | 5.68 | LC-QTOF-MS | ESI - | 3 | 0.60 | 1.17E-03* | 1.82 |
| Tripeptide (Cys Asp Ala) | $C_{10}H_{17}N_3O_6S$ | 307.0838 | 7.84 | 5 | $[M-H]^-$ | - | - | 5.41 | LC-QTOF-MS | ESI - | 3 | 0.61 | 9.46E-04* | 1.89 |
| ***Organooxygen compounds*** | | | | | | | | | | | | | | |
| dCDP | $C_9H_{15}N_3O_{10}P_2$ | 387.0233 | 9.62 | 0 | $[M-H]^-$ | - | - | 8.63 | LC-QTOF-MS | ESI - | 3 | 0.65 | 5.27E-03 | 1.38 |
| ***Pyrimidines and pyrimidine derivatives*** | | | | | | | | | | | | | | |
| Carboxy-hydroxypropyl thiamine diphosphate | $C_{16}H_{25}N_4O_{10}P_2S$ | 527.0767 | 9.4 | 8 | $[M+HCOOH-H]^-$ | - | - | 5.22 | LC-QTOF-MS | ESI - | 3 | 0.78 | - | 1.06 |
| ***Pyridines and derivatives*** | | | | | | | | | | | | | | |
| Nicotinamide | $C_6H_6N_2O$ | 122.0480 | 9.88 | 0 | $[M-H]^-$ | - | - | 17.17 | LC-QTOF-MS | ESI + | 2 | 0.63 | - | 1.06 |

RT: retention time; [a]CV, coefficient of variation in the metabolites in the QC samples; [b]Metabolites were annotated with identification confidence levels as recommended by the Metabolomics Standards Initiative (MSI) according to: Level 0: Unambiguous 3D Structure: isolated, pure compound, including full stereochemistry; Level 1: Confident 2D structure: uses reference standard match or full 2D structure elucidation; Level 2: Probable structure: matched to literature data or databases by diagnostic evidence, Level 3: Possible structure or class: most likely structure, isomers possible, substance class or substructure match; Level 4: Unknown feature of interest (BLAŽENOVIĆ et al., 2018); [c]Fold Change, change in the abundance of the specified comparison calculated as (BLEGI-treated cells/untreated cells); [d]p value* corresponding to the *p* values calculated by the Benjamini-Hochberg false discovery rate post hoc correction (FDR < 0.05); [e]VIP, variable importance in projection. [f]Overlapped. LC: liquid chromatography, QTOF-MS: quadrupole time-of-flight mass spectrometer, $^1$H NMR: proton nuclear magnetic resonance, br s: broad singlet, integrates for one proton.

**Table S4.2.** List of all metabolites identified in the exometabolome of cancer cells HCT-116 treated with BLEGI.

| Compounds | Formula | Mass | RT (min) | Error (ppm) | Adduct | δ $^1$H (ppm) and Multiplicity, *J* in Hz | Assignments | [a]CV for QC (%) | Analytical platform | DET | [b]ID Level | [c]Fold Change | [d]*p* value* | [e]VIP |
|---|---|---|---|---|---|---|---|---|---|---|---|---|---|---|
| ***Alcohols and polyols*** | | | | | | | | | | | | | | |
| Myo-inositol | $C_6H_{12}O_6$ | 180.0634 | 1.14 | 10 | $[M-H]^-$ | - | - | 10.59 | LC-QTOF-MS | ESI - | 3 | 1.21 | - | 1.29 |
| ***Amino acid and derivatives*** | | | | | | | | | | | | | | |
| Acetyl-glutamate | $C_7H_{11}NO_5$ | 189.0637 | 1.19 | 9 | $[M-H]^-$ | - | - | 7.00 | LC-QTOF-MS | ESI - | 2 | 1.50 | 6.52E-03 | 1.58 |
| Trimethyl -Lysine | $C_9H_{20}N_2O_2$ | 188.1525 | 3.86 | 9 | $[M+Na]^+$ | - | - | 12.08 | LC-QTOF-MS | ESI + | 3 | 1.78 | 2.58E-02 | - |
| ***Carboxylic acids and derivatives*** | | | | | | | | | | | | | | |
| 3-(3'-Methylthio)propylmalic acid | $C_8H_{14}O_5S$ | 222.0562 | 8.48 | 2 | $[M+H]^+$ | - | - | 8.61 | LC-QTOF-MS | ESI + | 3 | 0.62 | - | 1.14 |
| Phosphoglycerol-glutathione | $C_{13}H_{24}N_3O_{11}PS$ | 461.0869 | 1.16 | 3 | $[M-H]^-$ | - | - | 15.65 | LC-QTOF-MS | ESI - | 3 | 0.72 | - | 1.27 |
| Capryloyl glycine | $C_{10}H_{19}NO_3$ | 201.1365 | 5.06 | 9 | $[M+Na]^+$ | - | - | 12.37 | LC-QTOF-MS | ESI + | 3 | 1.29 | - | 1.29 |
| ***Carnitines*** | | | | | | | | | | | | | | |
| Decanoyl-carnitine | $C_{17}H_{33}NO_4$ | 315.2410 | 6.28 | 2 | $[M+H]^+$ | - | - | 12.59 | LC-QTOF-MS | ESI + | 2 | 1.41 | 3.06E-02 | 1.47 |
| ***Fatty acids*** | | | | | | | | | | | | | | |
| 2,4-Decadienoic isobutyl amide | $C_{14}H_{25}NO$ | 223.1936 | 9.67 | 8 | $[M+Na]^+$ | - | - | 15.04 | LC-QTOF-MS | ESI + | 2 | 0.74 | 3.03E-02 | - |
| 3-hydroxy-tetradecanedioic acid | $C_{14}H_{26}O_5$ | 274.1780 | 0.58 | 4 | $[M+K]^+$ | - | - | 9.35 | LC-QTOF-MS | ESI + | 3 | 0.72 | 3.38E-02* | - |
| 2-methylideneglutaric acid | $C_6H_8O_4$ | 144.0423 | 2.83 | 2 | $[M+H-H_2O]^+$ | - | - | 2.94 | LC-QTOF-MS | ESI + | 2 | 0.62 | 8.21E-03 | 1.50 |
| 2-hydroxyglutaric acid | $C_5H_8O_5$ | 148.0372 | 9.68 | 2 | $[M+H]^+$ | - | - | 19.93 | LC-QTOF-MS | ESI + | 3 | 0.57 | - | 1.20 |
| Acetyl dihydrolipoamide | $C_{10}H_{19}NO_2S_2$ | 249.0857 | 0.79 | 8 | $[M+HCOOH-H]^-$ | - | - | 11.85 | LC-QTOF-MS | ESI - | 3 | 1.29 | - | 1.15 |

| | | | | | | | | | | | | | | |
|---|---|---|---|---|---|---|---|---|---|---|---|---|---|---|
| Lauroleic acid | $C_{12}H_{22}O_2$ | 198.1620 | 6.84 | 9 | $[M+HCOOH-H]^-$ | 0.90 (t, *J* = 6.96 Hz)<br>1.30 (br s) | *t*-$CH_3$<br>$(CH_2)n$ | 13.08 | LC-QTOF-MS / NMR | ESI - / $^1H$ | 2 | 0.74 | - | 1.29 |
| 5-hydroxy capric acid | $C_{10}H_{20}O_3$ | 188.1412 | 6.63 | 8 | $[M-H]^-$ | - | - | 9.87 | LC-QTOF-MS | ESI - | 2 | 1.92 | 4.73E-04* | 2.30 |
| HpODE | $C_{18}H_{32}O_4$ | 312.2301 | 8.78 | 7 | $[M-H]^-$ | - | - | 18.70 | LC-QTOF-MS | ESI - | 3 | 1.43 | 2.17E-02 | - |
| 10-oxo-13-hydroxy-11-octadecenoic acid | $C_{18}H_{32}O_4$ | 312.2301 | 6.05 | 7 | $[M-H]^-$ | 0.89 (t, *J* = 6.95 Hz)<br>1.35 (br s) | *t*-$CH_3$<br>$(CH_2)n$ | 12.59 | LC-QTOF-MS / NMR | ESI - / $^1H$ | 3 | 1.78 | 2.68E-02 | 1.02 |
| ***Glycerophospholipids*** | | | | | | | | | | | | | | |
| GPC | $C_8H_{21}NO_6P$ | 258.1106 | 3.72 | 5 | $[M-H-H_2O]^-$ | - | - | 5.72 | LC-QTOF-MS | ESI + | 3 | 1.36 | 3.31E-02 | 1.30 |
| LPC 18:1 | $C_{26}H_{52}NO_7P$ | 521.3481 | 9.17 | 3 | $[M+Cl]^-$ | - | - | 11.91 | LC-QTOF-MS | ESI - | 2 | 1.29 | - | 1.16 |
| LPE 20:0 | $C_{25}H_{52}NO_7P$ | 509.3481 | 9.45 | 1 | $[M+H]^+$ | - | - | 10.89 | LC-QTOF-MS | ESI + | 3 | 0.64 | 3.03E-02 | 1.37 |
| PI 19:0 | $C_{28}H_{55}O_{12}P$ | 614.3431 | 7.29 | 8 | $[M+HCOOH-H]^-$ | - | - | 9.04 | LC-QTOF-MS | ESI - | 3 | 0.67 | 4.59E-02 | - |
| PKODiA-PA | $C_{27}H_{47}O_{11}P$ | 578.2856 | 4.37 | 4 | $[M+K]^+$ | - | - | 12.31 | LC-QTOF-MS | ESI + | 3 | 1.29 | 1.45E-02* | 1.15 |
| ***Organooxygen compounds*** | | | | | | | | | | | | | | |
| Guanidino-3-amino-1,3-dideoxy-scyllo-inositol | $C_7H_{16}N_4O_4$ | 220.1172 | 0.62 | 6 | $[M+H]^+$ | - | - | 19.42 | LC-QTOF-MS | ESI + | 3 | 1.52 | 1.76E-02 | 1.38 |
| 2-Hydroxybenzaldehyde | $C_7H_6O_2$ | 122.0368 | 9.37 | 2 | $[M+H-H_2O]^+$ | - | - | 19.66 | LC-QTOF-MS | ESI + | 3 | 0.67 | - | 1.16 |
| ***Peptides*** | | | | | | | | | | | | | | |
| Dipeptide 1 (Tyrosyl-Methionine) | $C_{14}H_{20}N_2O_4S$ | 312.1144 | 3.94 | 7 | $[M+Na]^+$ | - | - | 8.92 | LC-QTOF-MS | ESI + | 3 | 1.52 | 3.00E-02* | - |
| Dipeptide 2 (Leu-Met-OH) | $C_{16}H_{22}N_2O_6S$ | 370.1199 | 4.47 | 1 | $[M+H-H_2O]^+$ | - | - | 7.68 | LC-QTOF-MS | ESI + | 3 | 1.26 | 3.91E-02 | 1.29 |
| Dipeptide 3 (Valyl-Glutamate) | $C_{10}H_{17}N_2O_5$ | 245.1137 | 0.62 | 8 | $[M+H]^+$ | - | - | 9.31 | LC-QTOF-MS | ESI + | 3 | 1.26 | - | 1.24 |
| Dipeptide 4 (Arginyl-Serine) | $C_9H_{19}N_5O_4$ | 261.1437 | 0.81 | 8 | $[M+K]^+$ | - | - | 12.07 | LC-QTOF-MS | ESI + | 3 | 1.37 | - | 1.14 |
| Dipeptide 5 (Glu-Pro) | $C_{10}H_{16}N_2O_5$ | 244.1059 | 2.36 | 5 | $[M-H-H_2O]^-$ | - | - | 14.65 | LC-QTOF-MS | ESI - | 3 | 1.75 | 1.84E-02* | 1.74 |
| Dipeptide 6 (Thr-Trp-OH) | $C_{21}H_{21}N_3O_7$ | 427.1379 | 4.41 | 5 | $[M-H-H_2O]^-$ | - | - | 8.34 | LC-QTOF-MS | ESI - | 3 | 1.41 | 1.24E-02 | 1.73 |
| Dipeptide 7 (Nap-Thr-OH) | $C_{22}H_{20}N_2O_7$ | 424.1270 | 5.35 | 4 | $[M-H]^-$ | - | - | 14.98 | LC-QTOF-MS | ESI - | 3 | 1.29 | - | 1.04 |
| Tripeptide 1 (Asn Cys Cys) | $C_{10}H_{18}N_4O_5S_2$ | 338.0719 | 0.74 | 7 | $[M+Na]^+$ | - | - | 17.52 | LC-QTOF-MS | ESI + | 3 | 0.74 | - | 1.08 |
| Tripeptide 2 (Arg Trp Ala) | $C_{20}H_{29}N_7O_4$ | 431.2281 | 7.86 | 5 | $[M+H]^+$ | - | - | 3.86 | LC-QTOF-MS | ESI + | 3 | 1.34 | - | 1.20 |

| | | | | | | | | | | | | | | |
|---|---|---|---|---|---|---|---|---|---|---|---|---|---|---|
| Tripeptide 3 (His Lys Met) | $C_{17}H_{30}N_6O_4S$ | 414.2049 | 7.86 | 3 | $[M+Na]^+$ | - | - | 5.01 | LC-QTOF-MS | ESI + | 3 | 1.32 | - | 1.04 |
| Tripeptide 4 (Phe-Trp-Gly) | $C_{22}H_{24}N_4O_4$ | 408.1798 | 4.91 | 1 | $[M-H]^-$ | - | - | 12.42 | LC-QTOF-MS | ESI - | 3 | 0.64 | 1.52E-02 | 1.24 |
| Tripeptide 4 (Asn-Cys-Tyr) | $C_{16}H_{22}N_4O_6S$ | 398.1260 | 0.67 | 1 | $[M+HCOOH-H]^-$ | - | - | 12.06 | LC-QTOF-MS | ESI - | 3 | 1.55 | 4.70E-02* | 1.34 |
| Tripeptide 4 (Met-Pro-Pro) | $C_{15}H_{25}N_3O_4S$ | 343.1566 | 9.00 | 3 | $[M+HCOOH-H]^-$ | - | - | 7.07 | LC-QTOF-MS | ESI - | 3 | 0.80 | - | 1.03 |
| ***Nucleosides, nucleotides, and analogues*** | | | | | | | | | | | | | | |
| Ribosylzeatin phosphate | $C_{15}H_{22}N_5O_8P$ | 431.1206 | 4.54 | 1 | $[M+Na]^+$ | - | - | 13.69 | LC-QTOF-MS | ESI + | 3 | 0.71 | 9.49E-03* | 1.50 |
| ***Pyrimidines and pyrimidine derivatives*** | | | | | | | | | | | | | | |
| Thymine | $C_5H_6N_2O_2$ | 126.0429 | 1.51 | 2 | $[M+H]^+$ | - | - | 4.16 | LC-QTOF-MS | ESI + | 3 | 1.42 | 2.61E-02 | 1.41 |
| ***Sugar and derivatives*** | | | | | | | | | | | | | | |
| Cellobionate (4-Glucopyranosyl-gluconate) | $C_{12}H_{22}O_{12}$ | 358.1111 | 3.93 | 1 | $[M+Na]^+$ | - | - | 2.40 | LC-QTOF-MS | ESI + | 2 | 1.21 | 1.20E-02* | 1.53 |
| Threonic acid | $C_4H_8O_5$ | 136.0372 | 1.07 | 9 | $[M+H]^+$ | - | - | 1.74 | LC-QTOF-MS | ESI + | 3 | 0.75 | - | 1.30 |
| ***Tryptamines*** | | | | | | | | | | | | | | |
| Hydroxyl-tryptamine | $C_{10}H_{12}N_2O$ | 176.0950 | 2.83 | 3 | $[M+H-H_2O]^+$ | - | - | 5.65 | LC-QTOF-MS | ESI + | 3 | 1.23 | 1.58E-02 | 1.56 |

RT: retention time; [a]CV, coefficient of variation in the metabolites in the QC samples; [b]Metabolites were annotated with identification confidence levels as recommended by the Metabolomics Standards Initiative (MSI) according to: Level 0: Unambiguous 3D Structure: isolated, pure compound, including full stereochemistry; Level 1: Confident 2D structure: uses reference standard match or full 2D structure elucidation; Level 2: Probable structure: matched to literature data or databases by diagnostic evidence, Level 3: Possible structure or class: most likely structure, isomers possible, substance class or substructure match; Level 4: Unknown feature of interest (BLAŽENOVIĆ et al., 2018); [c]Fold Change, change in the abundance of the specified comparison calculated as (BLEGI-treated cells/untreated cells); [d]p value* corresponding to the *p* values calculated by the Benjamini-Hochberg false discovery rate post hoc correction (FDR < 0.05); [e]VIP, variable importance in projection; [f]Overlapped. LC: liquid chromatography, QTOF-MS: quadrupole time-of-flight mass spectrometer, $^1$H NMR: proton nuclear magnetic resonance, br s: broad singlet, integrates for one proton.

**Table S4.3.** Retention times of chemical standards in the LC-MS analyses.

| Chemical standard | Chemical class | UV $\lambda_{max}$ (nm) | Molecular formula | $t_R$ (min) LC-MS[a] | Exact mass | $[M-H]^-$ | $[M+H]^+$ |
|---|---|---|---|---|---|---|---|
| Gallic acid | Organic acid | 275 | $C_7H_6O_5$ | 1.09 | 170.0215 | 169.0132 | - |
| Chlorogenic acid | Cinnamic acid and derivatives | 275sh, 325 | $C_{16}H_{18}O_9$ | 2.42 | 354.3095 | 353.0863 | - |
| Caffeic acid | Cinnamic acid and derivatives | 275 | $C_9H_8O_4$ | 2.55 | 180.0422 | 179.0344 | - |
| Isoorientin | Flavone glycosides | 274, 355 | $C_{21}H_{20}O_{11}$ | 2.96 | 448.3775 | 447.0954 | 449.1094 |
| Ampelopsin | Flavanonol aglycones | 300 | $C_{15}H_{12}O_8$ | 2.88 | 320.0532 | 319.0458 | - |
| Rutin | Flavonol glycosides | 274, 355 | $C_{27}H_{30}O_{16}$ | 3.20 | 610.1533 | 609.1531 | 611.1603 |
| Vitexin | Flavone glycosides | 273, 335 | $C_{21}H_{20}O_{10}$ | 3.26 | 432.1056 | 431.0923 | 433.1123 |
| *p*-Coumaric acid | Cinnamic acid and derivatives | 295sh, 310 | $C_9H_8O_3$ | 3.36 | 164.0473 | 163.0390 | - |
| Sinapinic acid | Cinnamic acid and derivatives | 325 | $C_{11}H_{12}O_5$ | 3.78 | 224.2101 | 223.0684 | - |
| Morin | Flavonol aglycones | 264, 354 | $C_{15}H_{10}O_7$ | 4.19 | 302.0426 | 301.0351 | 303.0512 |
| Coumarin | Coumarins | 275, 325 | $C_9H_6O_2$ | 4.35 | 146.1432 | - | 147.0377 |
| Quercetin | Flavonol aglycones | 275, 358 | $C_{15}H_{10}O_7$ | 4.49 | 302.0426 | 301.0344 | 303.0494 |
| Cinnamic acid | Cinnamic acid and derivatives | 275 | $C_9H_8O_2$ | 4.63 | 148.1597 | 147.0524 | - |
| Naringenin | Flavanone aglycones | 275, 325 | $C_{15}H_{12}O_5$ | 4.93 | 272.0684 | 271.0611 | 273.0764 |

[a] Column: ACQUITY UPLC HSS T3 C18 column (2.1 × 100 mm, 1.8 µm)

**Table S4.4.** Parameters used in the GNPS Classical Molecular Networking.

| GNPS Classical Molecular Networking | |
|---|---|
| **Processing step** | **Parameters** |
| Basic options | Classical Molecular Networking<br>Precursor Ion Mass Tolerance: 0.02 Da<br>Fragment Ion Mass Tolerance: 0.02 Da |
| Advance Network Options | Min Pair Cos: 0.6<br>Network TopK: 10<br>Maximum Connected Component Size: 100<br>Minimun Matched Fragment Ions: 4<br>Minimum Cluster Size: 2<br>Maximum shift: 1999 Da<br>Run MSCluster: yes |
| Advance Library Search Options | Library Search Min Matched Peaks: 4<br>Search Analogs: Do Search<br>Score Threshold: 0.6<br>Maximum Analog Search Mass Difference: 100 Da |

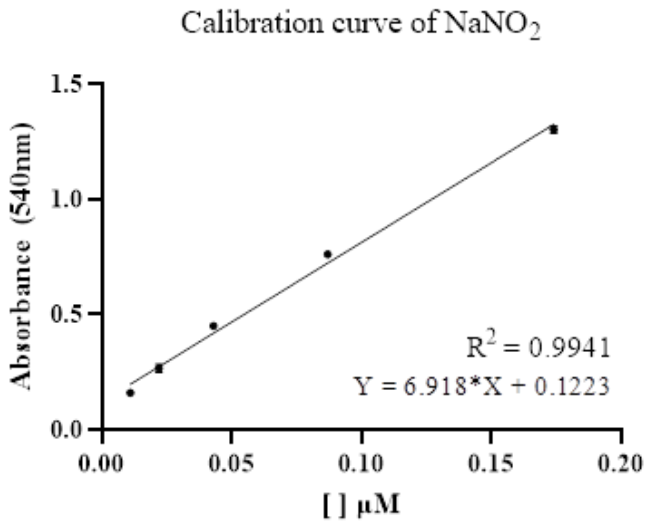



**Figure S4.6.** Calibration curve with sodium nitrite ($NaNO_2$) to represent the data in concentration of chemical $NO_2^-$ formed.

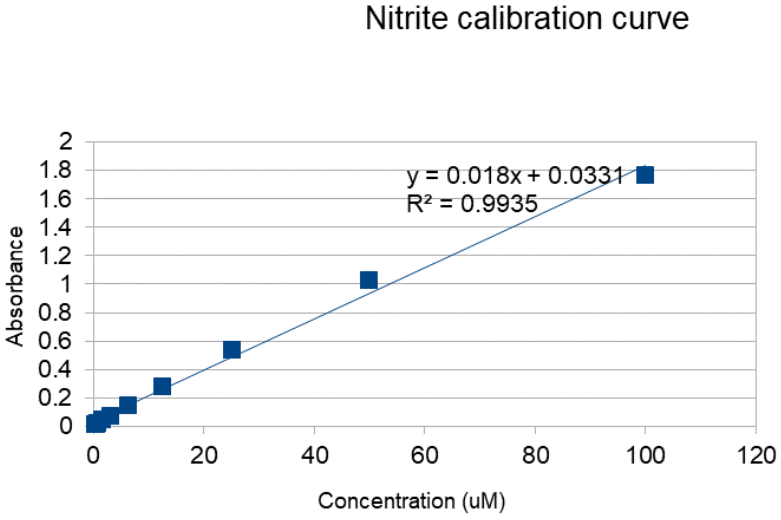



**Figure S4.7.** Calibration curve with sodium nitrite ($NaNO_2$) to represent the data in concentration of cellular $NO_2^-$ formed.

# 5 CHAPTER 5. Cytotoxic flavone glycosides from *Guadua incana* leaves

## Presentation

Once the results presented so far have been obtained, where it was found that flavone glycosides presented a positive correlation with the cytotoxic potential and in order to validate the results of the metabolic analysis and considering that the *G. incana* extract is the most promising in relation to cytotoxic activity, Chapter 5 presents the isolation of some of the main compounds present in the species *G. incana*, and verification of cytotoxic activity. For this purpose, a targeted isolation was carried out using centrifugal partition chromatography (CPC) and Sephadex LH-20, guided by the results of the metabolomic approach and bioactivity assays. As a result, the isolation of some flavones *C*-glycosides derived from the apigenin nucleous ws obtained, which presented good cytotoxic activity in HCT-116 cells.

## 5.1 Materials and methods

### 5.1.1 General experimental procedures

Thin-layer chromatography (TLC) was performed on Merck alumina silica gel 60 $F_{254}$ plates. Fractionation and purification were performed on a centrifugal partition chromatography CPC 250 / PLC 2250 equipment (Gilson, Plastic Valley, French). NMR measurements were conducted on a Bruker Avance III HD 600 MHz spectrometer (Bruker, Millerica, MA, USA). The 1D experiment were recorded at 600 MHz for $^{1}H$ using the solvent peaks as internal references. The spectra were recorded in Methanol-$d_4$ ($CD_3OD$). Chemical shifts (δ) are expressed in parts per million (ppm) and coupling constants (*J* values) are given in hertz (Hz). High-resolution mass spectrometry (HRMS) analysis was performed using Waters Xevo G2-XS QToF equipment. The ionization method operated with electrospray in negative mode (ESI-).

### 5.1.2 Plant material and extract preparation

Leaves of *Guadua incana* Londoño were collected in the bamboo collection of El Bambusal Farm, Quindío, Colombia (GPS 4°31'15'' N, 75°48'0'' W) and identified by Néstor García and Ximena Londoño at the Herbarium of the Pontificia Universidad Javeriana (HPUJ) and were deposited with voucher specimen number HPUJ-30723. The collection was performed under the permit of the Contract for Access to Genetic Resources and Derived Products (Contract No. 212/RGE 0287-6) granted by the Ministry of the Environment and Sustainable Development to the Pontificia Universidad Javeriana (PUJ) and the Colombia Científica-GAT Program. The plant material was dried in an oven with circulating air at 40 °C for 96 hours for subsequent grinding. After grinding, extraction of the dried and ground plant material was carried out through percolation with ethanol (96% EtOH) at a ratio of 1:10 (*w/v*) at room temperature. The extraction process was conducted in 4 cycles of 24 hours each. The bamboo leaf extract (BLE) obtained from the different cycles was combined and concentrated under reduced pressure at a temperature not exceeding 40 °C, using a rotary evaporator.

### 5.1.3 UHPLC-DAD-QTOF-MS analysis

For UHPLC-DAD-QTOF-MS analysis, the extract were dissolved in methanol at a concentration of 1 mg/mL. Samples were further diluted with methanol to obtain a final concentration of 500 ppm. Analyses were performed on an ACQUITY UPLC System (Waters, Milford, MA, USA) coupled with a Waters Xevo G2-XS QToF Mass Spectrometer. An ACQUITY UPLC HSS T3 C18 column (2.1 × 100 mm, 1.8 µm) from Waters (Waters Corporation, Wexford, Ireland) was used to carry on the chromatographic separation at 30 °C. The mobile phases consisted of eluent A (Water 0.1% formic acid) and eluent B (Acetonitrile 0.1% formic acid) with flow rate of 0.5 mL/min. The gradient was programmed as follows: 10-100% B from 0 to 10 min, 100% B from 10 to 14 min, 100-5% B from 14 to 15 min, 5% B from 15 to 20 min. Mass spectrometry was performed on a Xevo G2-XS QToF instrument using electrospray ionization (ESI). Data mass spectra were acquired in ionization negative (ESI−) and positive (ESI+) modes, in a mass range

of m/z 100–1500 Da in data dependent acquisition (DDA) mode at rate was set to 0.1 s scans, followed by an MS/MS scan of the most intense ions. For MS/MS fragmentation, a low collision energy ramp ranging from 10 to 40 eV and a high collision energy ramp ranging from 50 to 80 eV were applied to acquire the data in centroid format. The QTOF instrument was operated at a frequency of 6.0 GHz and 76.0 µs utilizing high resolution calibrated with the reference mass correction for Leucine-enkephalin ($C_{28}H_{37}N_5O_7$) was used as a lock mass compound in positive ion mode ($[M+H]^+$ = 556.2771) and negative ion mode ($[M-H]^-$ = 554.2615), respectively. The spectrometer parameters were as follows: capillary voltage was set to 2.2 kV (ESI−) or 2.6 kV (ESI+), cone voltage was set to 40 V, source temperature was maintained at 120 °C, cone gas was set to 50 L/h, and desolvation gas was set to 800 L/h at 300 °C.

### 5.1.4 $^1$H-NMR data acquisition

To the compound **1** and mixture **M1** were added 500 µL of methanol-$d_4$ ($CD_3OD$) and transferred to a 5 mm NMR tubes for further 1D NMR analyses. $^1$H NMR spectra were recorded at 25 °C on a Bruker Avance III HD 600 MHz spectrometer (Bruker, Karlsruhe, Germany) operating at a proton NMR frequency of 600.13 MHz. Each $^1$H-NMR spectrum consisted of 128 scans using the following parameters: 0.16 Hz/point, pulse width (PW) = 30 (11.3 µs), and relaxation delay (RD) = 1.5 s. Free induction decays (FIDs) were Fourier transformed with a line broadening (LB) = 0.3 Hz. Deuterated methanol was used as the internal lock. Chemical shifts were expressed in δ (ppm), and coupling constants were reported in hertz.

### 5.1.5 Extract fractionation and isolation of bioactive compounds

Crude ethanolic extract of *G. incana* (40 g) were dissolved with a hydromethanolic (HM) solution of methanol:water 7:3 (*v/v*) (500 mL) and liquid-liquid fractionated successively with *n*-hexane, ethyl acetate (EtOAc) and *n*-butanol (*n*-BuOH) (3 times x 500 mL for each one). Four fractions were obtained, after evaporation of solvents: *n*-hexane (8.6 g), EtOAc (4.8 g), *n*-BuOH (2.8 g) and residual HM (3.8 g).

The isolation was performed guided by previous correlation analysis and cytotoxic activity (CHITIVA et al., 2024). Initially, the solvent system for CPC was selected by dissolving a small amount of the *n*-BuOH fraction in test tubes containing variations of the EtOAc-*n*-BuOH-Water (EBuWat) system (Table S5.1) (COSTA et al., 2015; DAS NEVES COSTA; LEITÃO, 2010). Subsequently, the test tubes were shaken for 60 s and once rested and the sample was partitioned between phases, equal volumes of each phase was monitored by TLC. The selection of the solvent system was based on the visual distribution of the analyte between lower phase (LP) and the upper phase (UP) (Figure S5.1). The first separation was conducted in a gradient ascending mode, starting from the EBuWat 8:2:10 *v/v/v* system to EBuWat 2:8:10 *v/v/v*, gradually increasing, employing LP from EBuWat 8:2:10 system as the stationary phase, while the UP acted as the mobile phase. Column filling with stationary phase was performed at a rotation speed of 500 rpm and a flow rate of 25 mL/min. Mobile phase was pumped at 1800 rpm and 5 mL/min. After reaching hydrodynamics equilibrium, the retention of the stationary phase was calculated as 70%. Then, a sample of 500 mg from the extract, diluted in 5 mL of LP and 5 mL of UP, was injected into a 10 mL loop. This process was repeated several times injecting the same amount (500 mg x 5 times). From this process, a total of 65 fractions were obtained, which were combined into 5 fractions (F1 to F5) monitored by TLC analysis.

Then, fraction F5 (500 mg x 2 times) was fractionated in isocratic mode with EBuWat 2:8:10 *v/v/v* system, in ascending mode, with same conditions used previously. 53 fractions were obtained, which were combined by their TLC profile into 5 fractions (F5.1 to F5.5). Next, fraction F5.4 (750 mg) was purified on a Sephadex LH-20 column eluted with 100% MeOH, obtaining 41 fractions which were also monitored by TLC (Figure S5.2). From this analysis, fraction F5.4.4 (15.0 mg) was obtained with a mixture (**M1)** of compounds **4**, **6**, and **7**, and fraction F5.4.5 (8.5 mg) with the purified compound **1**. The fractionation and purification diagram are represented in Figure S5.3. The identification of compound **1** and compounds in **M1** was carried out using spectroscopic ($^1$H-NMR) and spectrometric (LC-MS/MS) techniques, complemented by comparison with the literature data.

### 5.1.6 Cell lines and maintance

The human colorectal carcinoma cell line HCT-116 was acquired from the American Type Culture Collection (ATCC, Rockville, MD, USA) and ground under standard cell culture conditions (37 °C, 95% with 5% $CO_2$ atmosphere) in RPMI-1640 medium supplemented with 10% fetal bovine serum (FBS), 2 g/L of $NaHCO_3$, and 1% antibiotics (penicillin and streptomycin). All assays were performed at least with duplicate two times.

### 5.1.7 Cytotoxic activity

Colorimetric 3-(4,5-dimethylthiazol-2-yl)-2,5-diphenyltetrazolium bromide (MTT) assay was used to evaluate metabolic activity. Almost $1x10^4$ cells per well were seeded in 96-well. 24 h after seeding, the cells were then treated with DMSO 0.05% (vehicle), doxorubicin 10 μM (control), and compound with a concentration of 0.0032 to 50 μg/mL (treatments) and incubated at standard cell culture conditions for 72 h again. Subsequently, MTT solution (150 μL, 10%) was added to each control and treated and incubated at again for three h. The medium was then poured out, and solubilization of the crystal formazan dye was done in 200 μL DMSO. The Bio-Tek Powerwave X microplate reader (BioTeck Instruments) was applied to read the absorbance at 570 nm.

### 5.1.8 Statistical analysis

Statistical analyses were performed using GraphPad Prism version 8 statistical software (GraphPad Software, San Diego, CA, USA) was used to analyze the data. All results were obtained from three independent experiments and expressed as mean ± SD ($n$ = 4).

## 5.2 Results and discussion

### 5.2.1 Chemical analysis of the crude extract and fractionation

From the chromatogram obtained by UHPLC-DAD analysis (Figure 5.1), some major peaks are observed with retention times (Rt) of 2.93 (**1**), 2.96 (**2**), 3.04 (**3**), 3.21 (**4**), 3.28 (**5**), 3.37 (**6**) and 3.95 (**7**) min. In the chromatogram obtained from the crude extract, it was acquired within a wavelength range of $\lambda \approx 200$ to 400 nm, where various major peaks are observed, corresponding to different compounds. From this chromatogram and the UV spectra obtained by the DAD detector, it was determined that these peaks correspond to flavonoids, considering the two maximum absorption bands reported in the literature, which are $\lambda_{max} \approx 275$ and 335 nm, respectively (Figure 5.1) (GAGLIANO et al., 2022a).

Flavonoids have two absorption maxima due to their two aromatic rings with conjugated double bonds, ring A and ring B. The first band (I) is associated with ring A, with UV absorption occurring between $\lambda \approx 300$ and 500 nm, while the second band (II) is associated with ring B, originating from cinnamic acid, which absorbs between $\lambda \approx 240$ and 280 nm (PINHEIRO; JUSTINO, 2012).

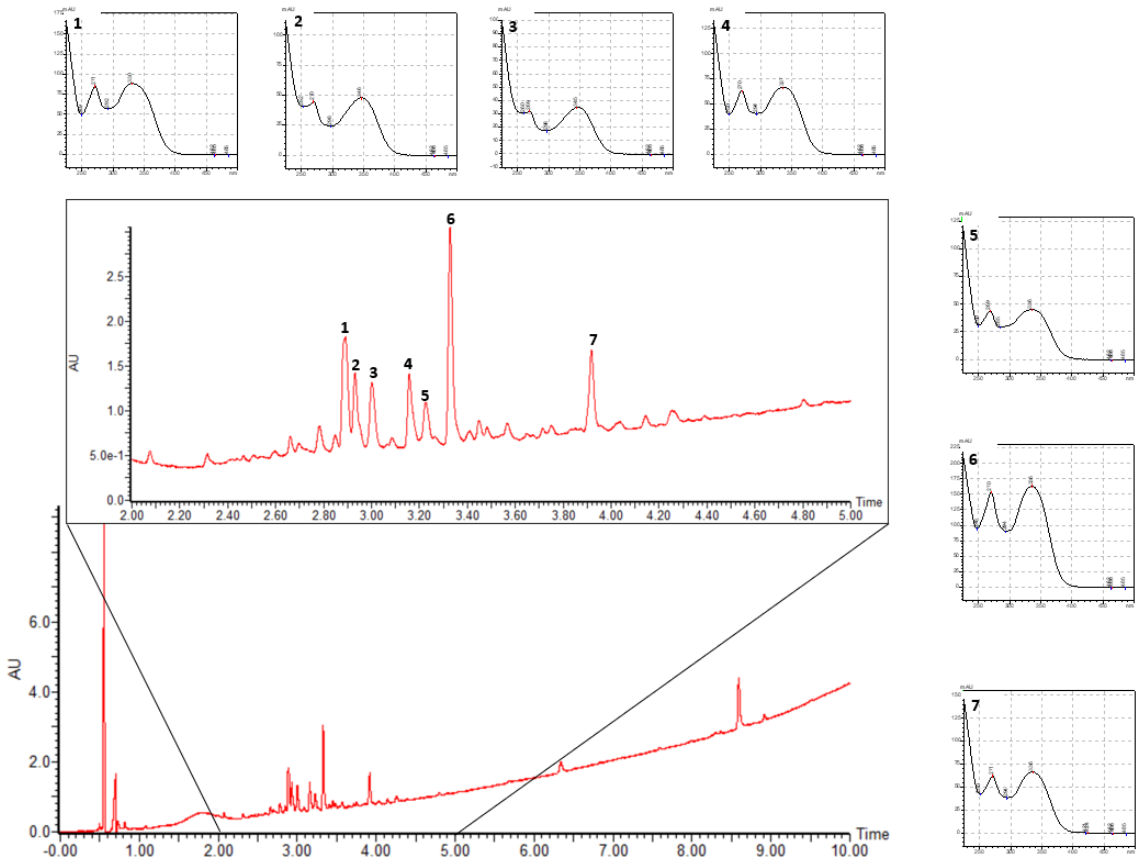



**Figure 5.1.** UHPLC-DAD chromatogram for the ethanolic extract of *G. incana* leaves obtained at a wavelength of 364 nm and ultraviolet absorption spectra for 7 major flavonoids present in extract. Expanded main area with retention time of 2.0 to 5.0 min.

On the other hand, the extract was analysed by UHPLC-QTOF-MS in negative and positive modes. As a result, chromatograms were obtained for the negative and positive mode (Figures 5.2A and 5.2B), showing the intensity of the peaks along with their respective *m/z* ratio values for each compound present in the extract.

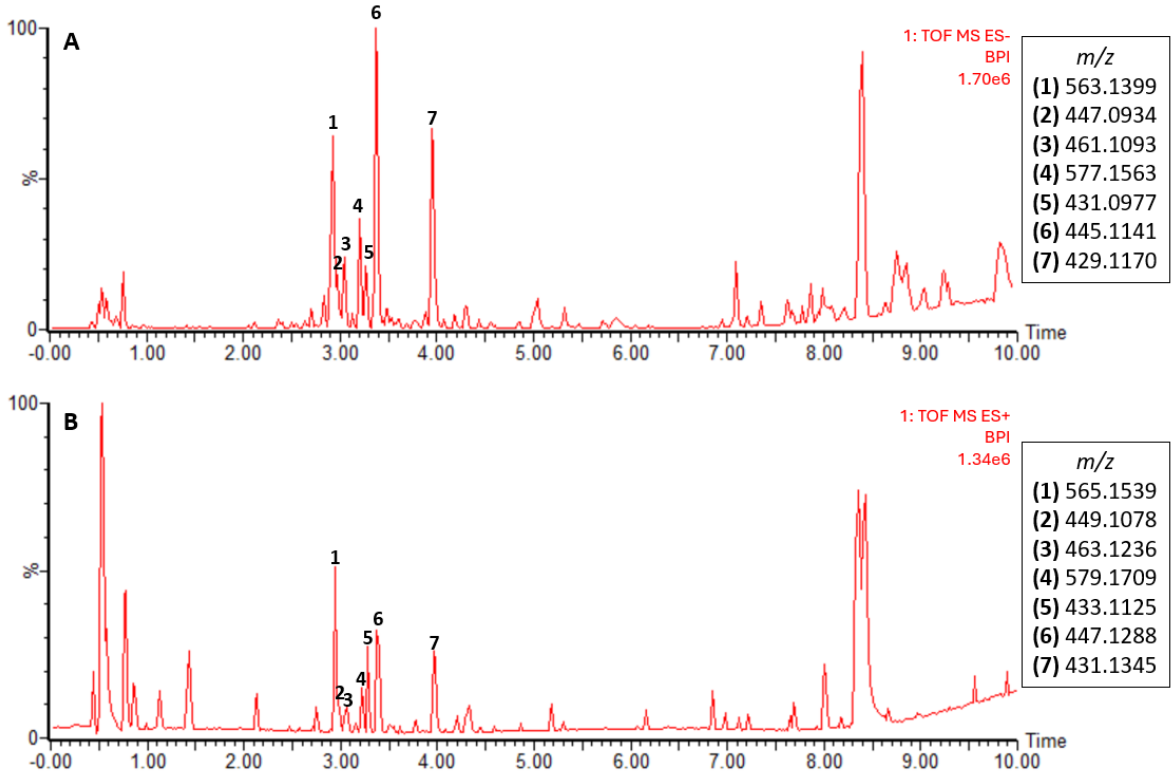



**Figure 5.2.** UHPLC-QTOF-MS base peak chromatogram (BPC) for the ethanolic extract of *G. incana* leaves obtained in A) negative and B) positive ionization modes.

As observed in the base peak chromatogram in negative mode in Figure 5.2A and positive mode Figure 5.2B, the *m/z* ratio values were found for majority of the peaks related to the UHPLC-DAD analysis. The related compounds are shown in Table 5.1.

**Table 5.1.** Compounds identified in the extract of *G. incana*.

| Compounds | Rt | $\lambda_{max}$ | $[M-H]^-$ | $[M+H]^+$ | Name | Ref. |
|---|---|---|---|---|---|---|
| **1** | 2.93 | 271, 330 | 563.1399 | 565.1539 | Isoschaftoside | (CHITIVA et al., 2023) |
| **2** | 2.96 | 270, 346 | 447.0934 | 449.1078 | - | - |
| **3** | 3.04 | 269, 345 | 461.1093 | 463.1236 | - | - |
| **4** | 3.21 | 270, 337 | 577.1563 | 579.1709 | Violanthin | (MORALES NOREÑA; SANCHEZ VALLEJO, 2008) |
| **5** | 3.28 | 269, 336 | 431.0977 | 433.1125 | - | - |
| **6** | 3.37 | 270, 336 | 445.1141 | 447.1288 | Swertisin | (GAGLIANO et al., 2022a) |
| **7** | 3.95 | 271, 336 | 429.1170 | 431.1345 | - | - |

Based on the results, a liquid-liquid partition was carried out using solvents of different polarities to obtain four fractions: *n*-hexane, EtOAc, *n*-BuOH, and residual HM, with yield percentages of 43%, 24%, 14%, and 19%, respectively. Subsequently, we evaluated the cytotoxic activity to select the most active fraction and proceed with the purification and isolation process of the bioactive compounds.

### 5.2.2 Cytotoxic activity of the fractions

The cytotoxic activity of the four fractions was evaluated at two concentrations, 5 and 50 µg/mL, against the HCT-116 colon cancer cell lines, determining the percentage of inhibition for each fraction. Figure 5.3 shows the percentage of inhibition of the fractions obtained, where it was found that the *n*-BuOH fraction presented the highest cytotoxic potential with 70.34% inhibition at the maximum concentration, while the hydromethanolic fraction presented 13.92% inhibition. The *n*-hexane fraction showed an inhibition of 16.55%, and the EtOAc fraction showed an inhibition of 45.17% at the maximum concentration evaluated. It should be noted that it was also found that the EtOAc fraction, at a concentration of 5 µg/mL, presented 31% inhibition, while the other fractions did not exceed 25%.

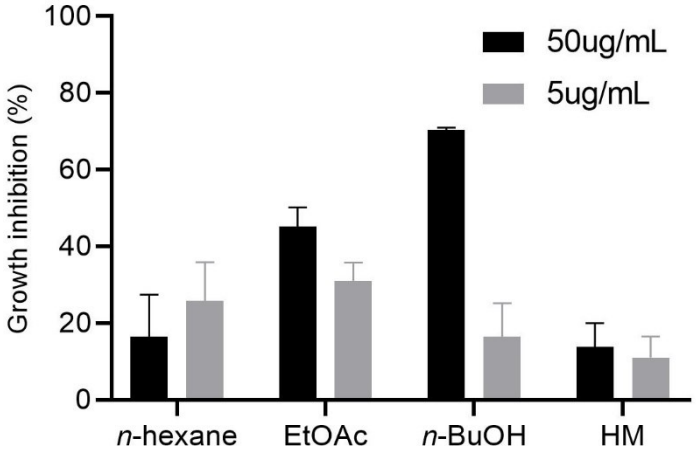



**Figure 5.3.** Percent growth inhibition of the four fractions obtained from the *G. incana* extract was evaluated at 50 and 5 µg/mL against HCT-116 using the MTT assay after 72 hours of exposure. The percentage of inhibition was calculated based on the growth of untreated cells. Data are presented as mean ± SEM (standard error of the mean) from three independent replicate

experiments. All experiments used 0.05% DMSO (vehicle) and doxorubicin (DOXO) as the negative and positive controls, respectively.

According to these results, the *n*-BuOH fraction was subjected to additional fractionation and purification to isolate some bioactive compounds. In a recent study on *Phyllostachys heterocycla* var. Pubescens, a bamboo considered a useful and commonly consumed food in the countries of Southeast Asia and East Asia, the cytotoxic effect was evaluated against the crude methanol extract and the fractions obtained from *n*-hexane, EtOAc, and *n*-BuOH, targeting five cell lines: HepG2, HeLa, A549, MCF-7, and THP-1. The *n*-BuOH fraction was reported to exhibit inhibition percentages greater than 60% against all cell lines at the maximum concentration of 100 µg/mL. Particularly, the *n*-BuOH fraction demonstrated the highest inhibition with 94.31% against the HeLa cell line (ABDELHAMEED et al., 2021), which is consistent with our study for the HCT-116 cell line. According to our findings and comparing the study carried out by Abdelhameed et al., 2021, the cytotoxic potential is related to the flavonoid content. These findings align with previous studies that employed correlation analysis through an untargeted metabolomic approach, reporting a positive correlation between flavone glycosides and cytotoxic potential (CHITIVA et al., 2024).

### 5.2.3 Isolation of flavonoids

The phytochemical study of *G. incana* leaves allowed the isolation of compound **1**, identified by spectroscopic and spectrometric methods, and by comparation with data described in the literature. Additionally, a mixture denominated **M1** (containing compounds **4**, **6**, and **7**) was obtained and analyzed by LC-MS/MS. The isolated and identified compounds correspond to four flavone glycosides, specifically isoschaftoside **1** and mixture **M1** of three flavone glycosides derived from apigenin, identified as violanthin **4**, swertisin **6**, and unidentified **7**. This is the first report of compounds **1**, **4** and **6**, in the leaves of *G. incana*. These compounds have been reported in other bamboo species, and these results are consistent with the chemotaxonomy of the genus. The presence of flavone glycosides is commonly reported in bamboo species (HASEGAWA et al., 2008; JIANG et al., 2019).

Compound **1** (8.5 mg) was obtained as yellow powder, which produced an orange, fluorescent band on TLC when sprayed with natural reagent (NP/PEG) at a wavelength of 365 nm, characteristic for visualizing flavonoids (WAGNER et al., 1996). The $^{1}$H-NMR analysis for compound **1** showed signals at $\delta_H$ 7.48 (d, *J* = 8.6 Hz, 2H) and 6.65 (d, *J* = 8.6 Hz, 2H), corresponding to two doublets (related protons), confirming the of a *para*-sustituted aromatic ring (ring B). Additionally, a single signal is shown at $\delta_H$ 6.71 (s, 1H), confirming the presence of an olefinic proton, and the absence of other singlets confirms a flavone with apigenin nucleous with substitutions at positions C6 and C8. Signals were also observed in the region $\delta_H$ 3.63 - 4.70, characteristic of the glycosides present in the apigenin scaffold, which by the number of signals indicate the presence of two sugar units. A characteristic signal was observed at $\delta_H$ 4.74 (d, *J* = 9.9 Hz, 1H), corresponding to the anomeric protons in the $\beta$ position of the respective glycosides (Figure S5.4). Comparison of the spectroscopic data obtained with those reported in the literature allowed the identification of compound **1** as isoschaftoside. Table S5.2 compares the chemical shifts obtained for compound **1** and those described for isoschaftoside according to Kun-Ping et al., 2020, taken for $^{1}$H-NMR (500 MHz in DMSO-*d*$_6$).

Additionally, an LC-MS/MS analysis was performed to complement the previous analysis and establish the structure. Its mass spectrum showed the precursor ion peak as the base peak at *m/z* = 563.1399 $[M-H]^-$ and *m/z* = 565.1539 $[M-H]^+$, consistent with the molecular formula $C_{26}H_{28}O_{14}$. The negative MS/MS spectrum of compound **1** (Figure 5.4) shows a precursor ion at *m/z* 563 $[M-H]^-$ and fragment ions at *m/z* 503 $[M-H-60]^-$ corresponding to the fragmentation of the sugar present in the C6 position, *m/z* 473 $[M-H-90]^-$, *m/z* 443 $[M-H-120]^-$ corresponding to the sugar fragmentations in the C8 position, *m/z* 413 $[M-H-150]^-$, *m/z* 383 $[M-H-180]^-$, *m/z* 353 $[M-H-210]^-$, *m/z* 325 $[M-H-238]^-$, *m/z* 297 $[M-H-266]^-$ and *m/z* 117 $[M-H-446]^-$ corresponding to characteristic retro-Diels-Alder (RDA) type fragmentation of the ring C for flavone. In general, RDA fragmentation involves the cleavage of two bonds in the C ring, forming negative ions that provide characteristic information. Particularly, these fragment ions contribute to the mass spectral fingerprint of

flavones in negative mode (KESKES et al., 2018; ŚLIWKA-KASZYŃSKA; ANUSIEWICZ; SKURSKI, 2022).

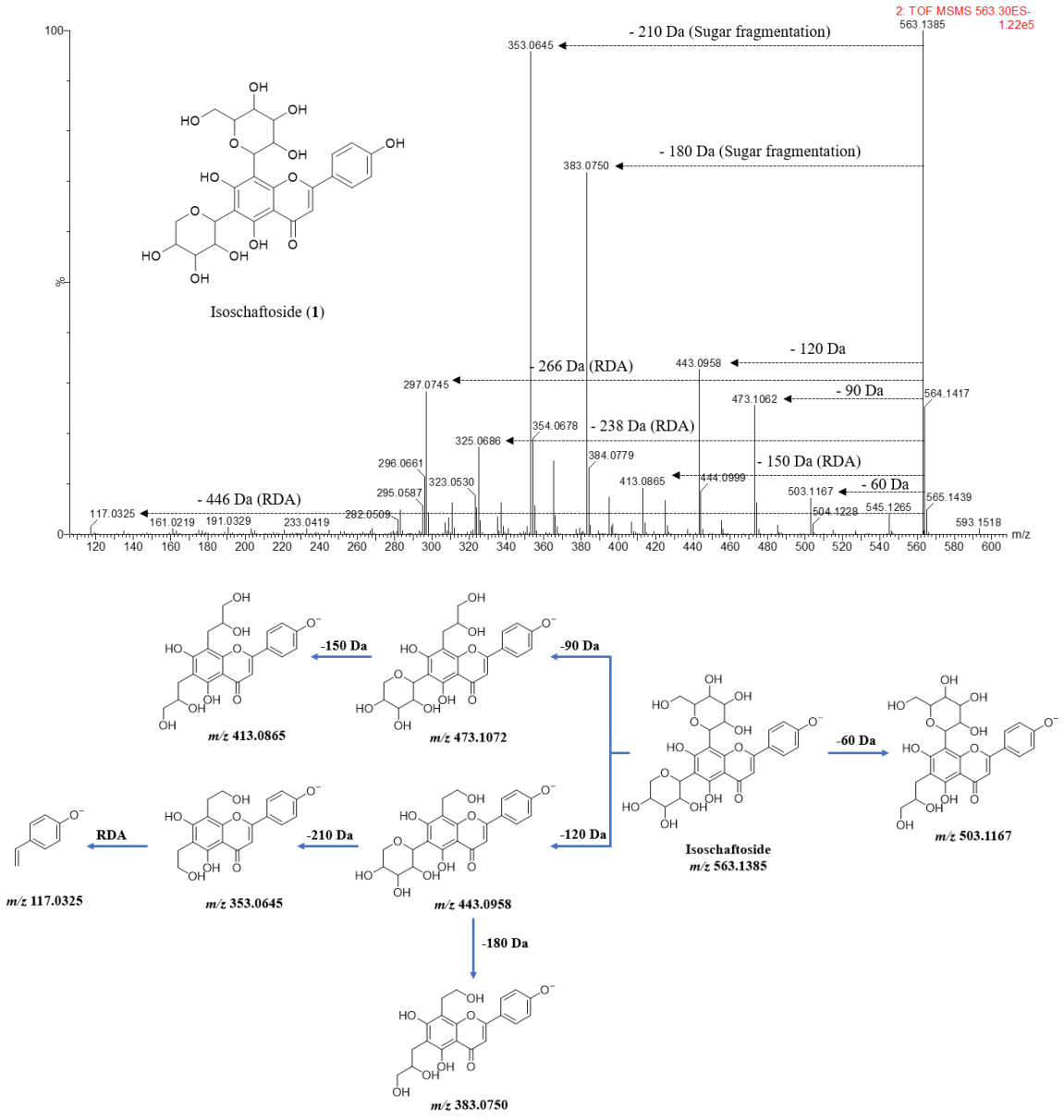



**Figure 5.4.** MS/MS spectra and proposed fragmentation pathway for isoschaftoside **1** isolated from *G. incana* leaves.

Mixture **M1** (15 mg) was obtained as yellow powder, which produced a yellow-orange, fluorescent bands in TLC when sprayed with natural reagent (NP/PEG) at a wavelength of 365 nm, characteristic for visualizing flavonoids (WAGNER et al., 1996).

$^{1}$H-NMR analysis for **M1** showed signals at $\delta_H$ 7.38 (d, *J* = 7.9 Hz, 6H) and 6.69 (d, *J* = 8.9 Hz, 6H), corresponding to two doublets (related protons), confirming the presence of protons aromatics on a flavone-like scaffold derived from apigenin with substitutions at positions C6 and C8. Furthermore, a signal is shown at $\delta_H$ 6.68 (s, 3H), confirming the presence of protons corresponding to the C ring of apigenin. Overlapping signals were also observed in the $\delta_H$ 3.60 - 4.75 region, characteristic of glycosides linked to the flavone (Figure S5.5). The DEPTQ analysis for **M1** showed signals at $\delta_C$ 60.0 to 80.0, corresponding to methine-type carbons (CH) present in sugars. In addition, signals are shown at $\delta_C$ 103.62, 104.55, 107.59, and 122.92 of the flavone's quaternary carbons (C) present in rings A and B. Likewise, signals are shown at $\delta_C$ 103.29 of the methine-type carbon (CH) present in the oxygen-containing $\gamma$-pyrone ring. Finally, signals are shown at $\delta_C$ 116.07 and 129.02, corresponding to methine-type carbons (CH) of the B ring of the flavone (Figure S5.6). Comparison of the spectroscopic data obtained with those reported in the literature allowed the identification of mixture **M1** as flavone glycosides derived from the apigenin scaffold (BLUNDER et al., 2017).

LC-MS/MS analysis allowed to be identified three compounds in the M1 mixture, being tentatively identified compound **4** as violanthin, compound **6** as swertisin, and compound **7** remains unidentified. (Figure S5.7 and S5.8). For compound **4**, the mass spectrum showed the pseudomolecular ion peak at *m/z* = 577.1563 $[M-H]^-$ and *m/z* = 579.1709 $[M-H]^+$, consistent with the molecular formula $C_{27}H_{30}O_{14}$. For compound **6**, the mass spectrum showed the peak of the pseudomolecular ion at *m/z* = 445.1141 $[M-H]^-$ and *m/z* = 447.1288 $[M-H]^+$, consistent with the molecular formula $C_{22}H_{22}O_{10}$. Compound **4**, identified as violanthin, has been reported for the species *G. angustifolia* (MORALES NOREÑA; SANCHEZ VALLEJO, 2008), while compound **6** identified as swertisin, has been reported for the bamboo *Parodiolyra micrantha* (Kunth) Davidse & Zuloaga with a relative percentage of 0.2% (GAGLIANO et al., 2022a).

### 5.2.4 Cytotoxic activity of the compounds

The cytotoxic activity against HCT-116 of compound **1** and mixture **M1** was evaluated using the MTT assay. First, the percentage of growth inhibition for compound **1** and mixture **M1** was determined at 5 and 50 µg/mL. It was found that both compound **1** and mixture **M1** exhibited inhibition percentages more significant than 90% at the maximum concentration evaluated, while only compound **1** showed 15% inhibition at the lowest concentration (Figure 5.5A). Finally, a concentration-response curve was determined to assess the potency of the cytotoxic effect of compound **1** (Figure 5.5B). Compound **1** presented an $IC_{50}$ value of 13.26 µM, which, compared to the positive control DOXO with an $IC_{50}$ value of 0.2 µM, demonstrated a significant cytotoxic effect. Furthermore, the high percentage of activity of **M1** indicates that flavone glycosides derived from apigenin have cytotoxic potential. However, further phytochemical studies of the *G. incana* species are necessary to identify other flavone glycosides with cytotoxic potential.

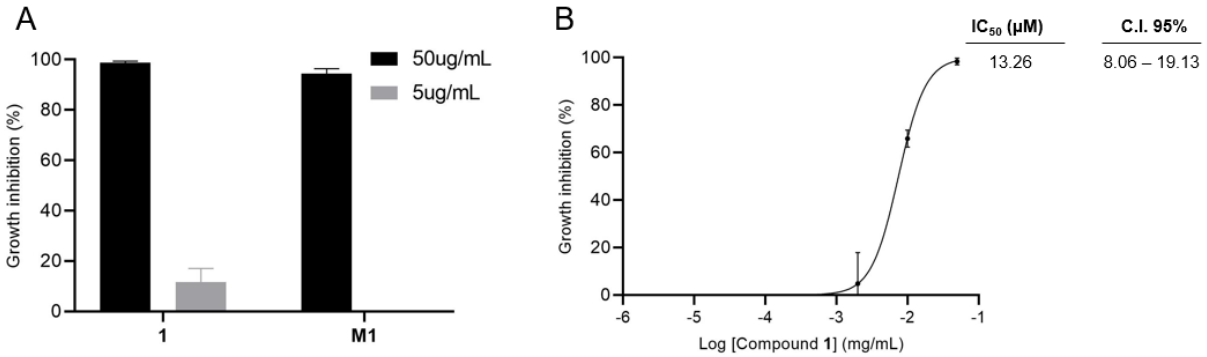



**Figure 5.5. A)** Cell viability after 72 hours of incubation at two concentrations: 5 and 50 µg/mL. B) Dose-response curve of the cytotoxicity in HCT-116 cells after 72 hours of treatment with isoschaftoside **1**, using concentrations from 0.0032 to 50 µg/mL. Data represent the mean of three independent biological replicates with at least two technical duplicates ± SEM (standard error of the mean). All experiments used 0.05% DMSO (vehicle) and doxorubicin (DOXO) in the range of 0.00064 to 10 µM, with $IC_{50}$ = 0.2 µM (95% CI 0.14–0.25) as negative and positive controls, respectively.

These results were consistent with previous reports of cytotoxic activity demonstrated in species of the *Guadua* genus. A recent study reported a positive correlation between flavonoid content and cytotoxic potential in the HCT-116 cell line. It was shown that

flavonoid glycosides, such as luteolin 6-*C*-hexoside 8-*C*-pentoside, isoschaftoside, and vitexin 2''-*O*-rhamnoside, presented a strong correlation with activity (CHITIVA et al., 2024). This results herein presented confirms that compound **1** is one of the compounds responsible for the cytotoxic activity of *G. incana*. Another previous study demonstrated that isoschaftoside had no significant impact on cell proliferation at a concentration below 500 µM after exposure on HepG2 cells, finding that isoschaftoside treatment did not significantly affect cells after 24 hours of exposure (SU et al., 2022). These data contrast with what was found in our study, where a 72-hour exposure of compound **1** showed cytotoxic potential. Furthermore, several reports focused on evaluating the biological potential of flavonoids, demonstrated potential cytotoxic activity against various tumor cell lines such as Caco-2, COL-2, HCT-115, HCT-116, and others (SAK, 2014).

## 5.3 Conclusion

This study represents the first report on isolating isoschaftoside from the leaves of *G. incana,* as well as the first study describing its activity against the colon cancer cell line HCT-116, with a potent $IC_{50}$ value that is comparable to the positive control (Doxorubicin). Our findings demonstrate the cytotoxic potential of flavone glycosides present in *G. incana* and provides information on previously unreported cytotoxic activity, aiding the search for new bioactive compounds.

## Supplementary information

**Table S5.1.** Phase system test of solvents used for separation by CPC.

| Solvent system | EBuWat | Separation time |
|---|---|---|
| I | 10:0:10 | > 60 s |
| II | 8:2:10 | 59 s |
| III | 6:4:10 | > 60 s |
| IV | 4:6:10 | > 60 s |
| V | 2:8:10 | 30 s |
| VI | 0:10:10 | 40 s |

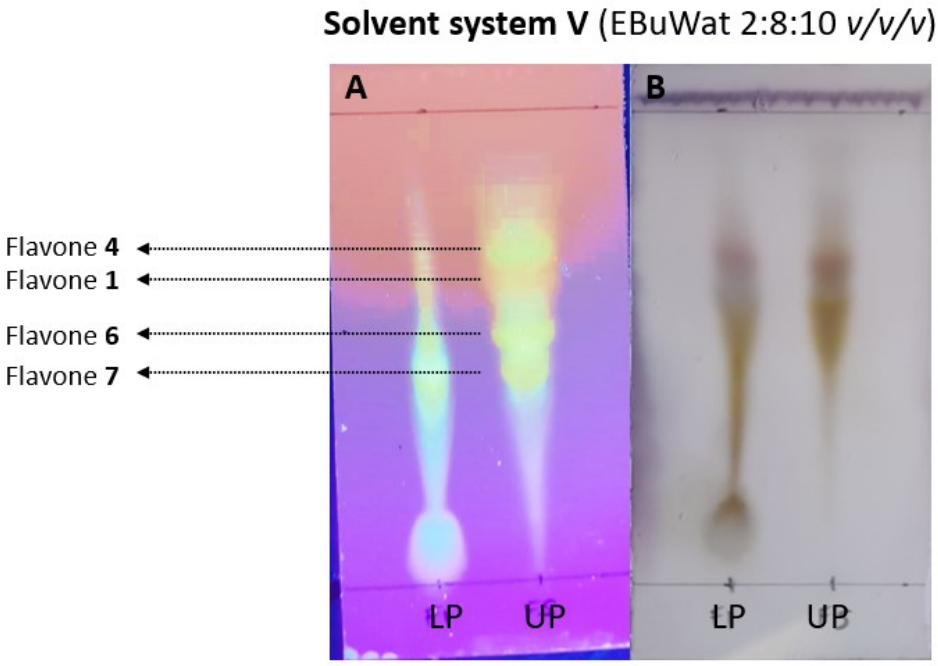



**Figure S5.1.** TLC chromatoplates eluted in specific solvent system for flavonoid glycosides (EtOAc:Formic acid:Acetic acid:$H_2O$ 100:11:11:27 *v/v/v/v*) for the lower phase (LP) and upper phase (UP) partition of the *G. incana* extract with the system (EBuWat 2:8:10 *v/v/v/v*) developed with A) Natural Product Reagent (NP/PEG UV-365 nm) and B) with *p*-anisaldehyde sulfuric acid and heated to 40 ºC.

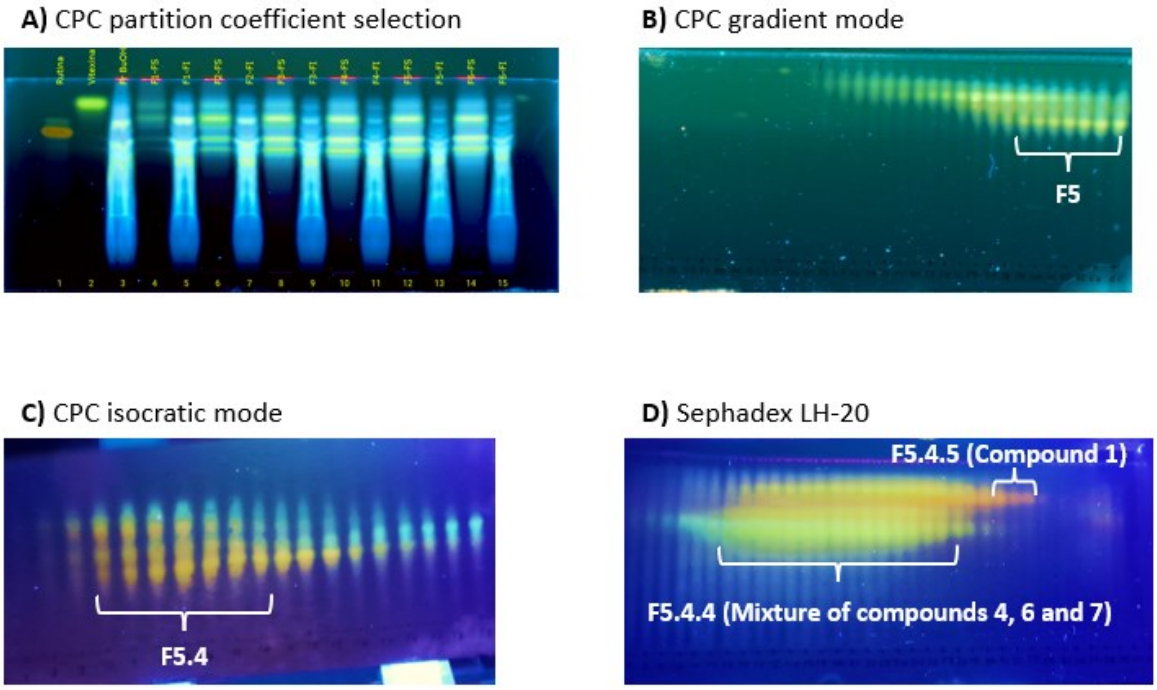



**Figure S5.2.** TLC chromatoplates eluted in specific solvent system for flavonoid glycosides (EtOAc:Formic acid:Acetic acid:$H_2O$ 100:11:11:27 *v/v/v/v*) for **A)** the selection of the gradient proportion, **B)** the fractions obtained from the first CPC separation (gradient mode), **C)** the fractions obtained from the second CPC separation (isocratic mode) and **D)** the fractions obtained from the Sephadex LH-20 column in the phytochemical analysis performed for the *G. incana* extract. All plates were developed with natural product reagent (NP/PEG UV-365 nm). The number of compound **1** and the mixture of compounds **M1** are related to the corresponding fractions in the flow chart used for the purification (Figure S5.3).

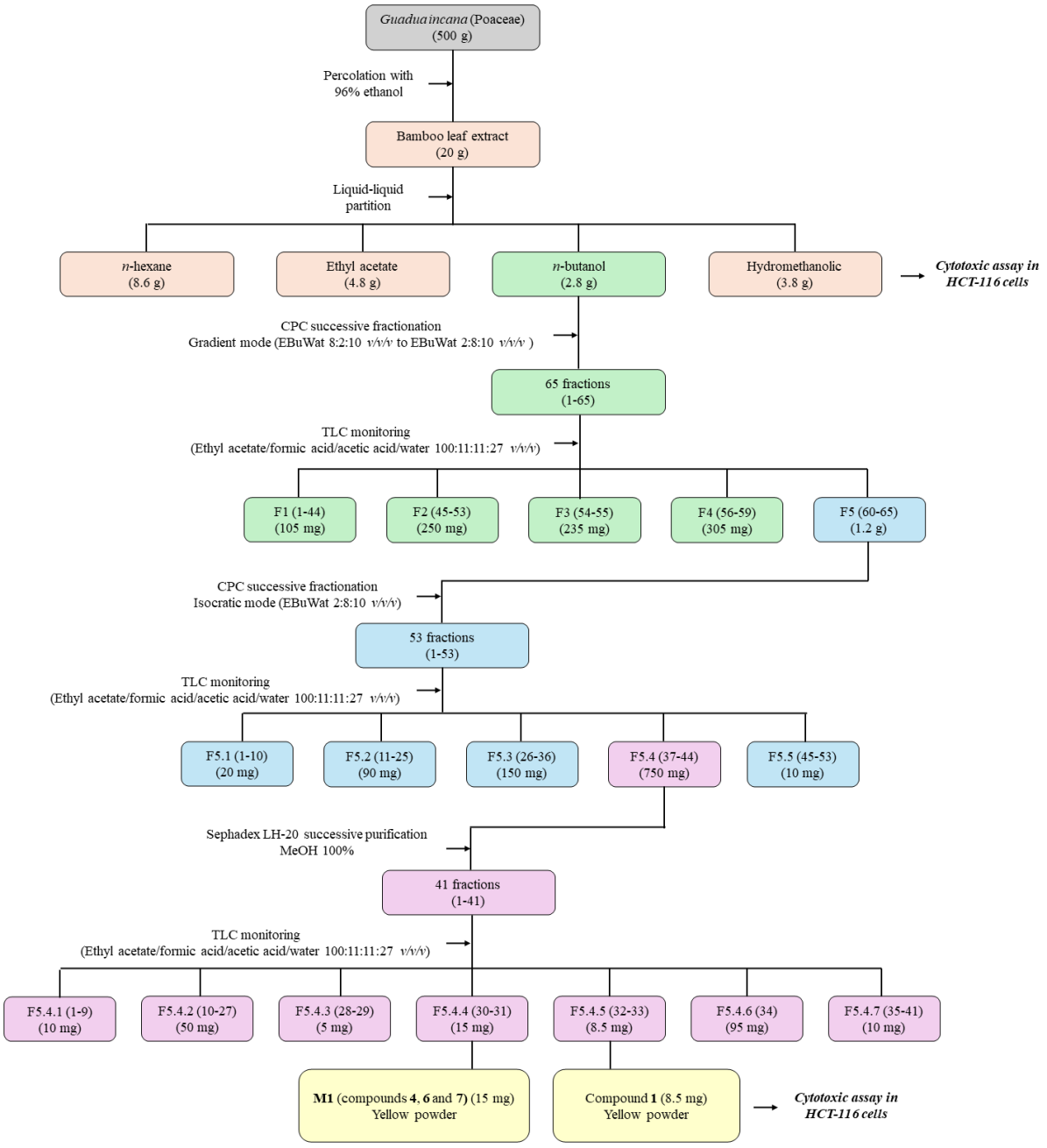



**Figure S5.3.** Diagram illustrating the extraction, fractionation, and purification by CPC and Sephadex LH-20 of the bamboo leaf extract obtained from *G. incana*.

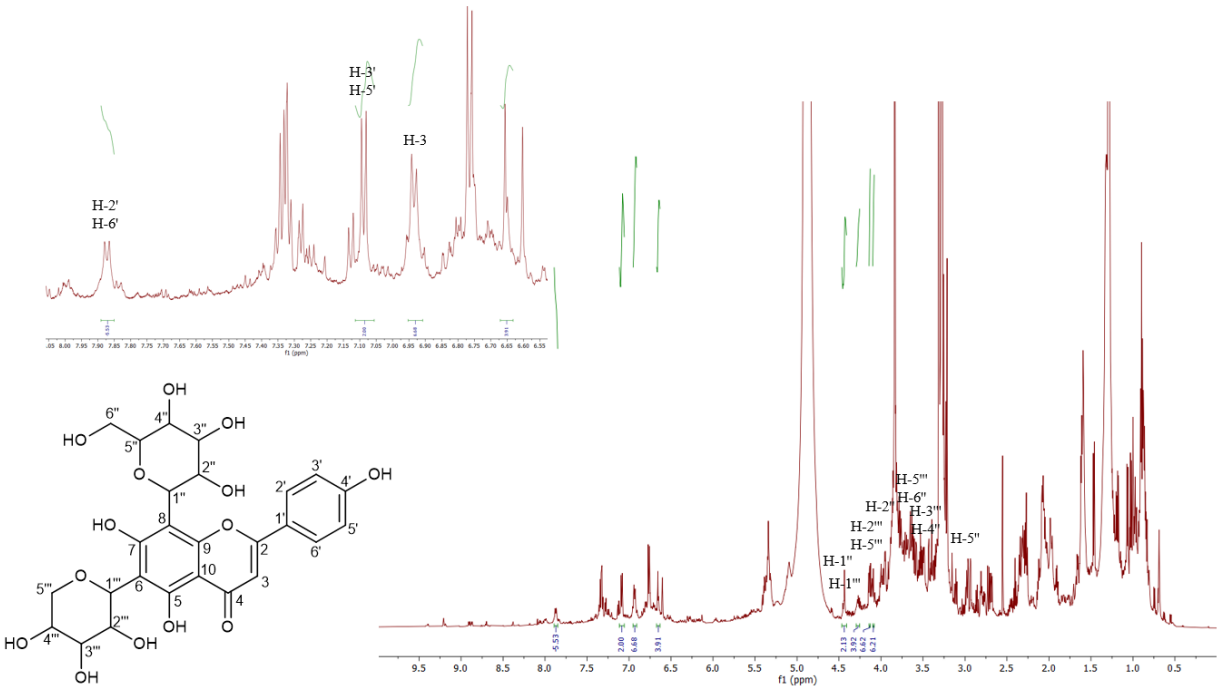
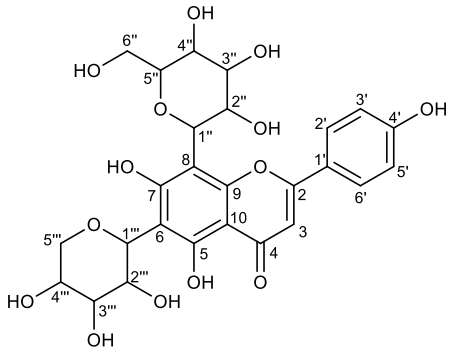



**Figure S5.4.** $^{1}$H-NMR spectrum of compound **1**.

**Table 5.2.** $^{1}$H-NMR data taken at 600 MHz for flavonoid **1** in Methanol-$d_4$ compared to the flavonoid isoschaftoside taken at 500 MHz in DMSO-$d_6$.

| Position | Compound 1[a] | Isoschaftoside[b] |
|---|---|---|
| | $\delta_H$ (ppm) | $\delta_H$ (ppm) |
| 2 | - | - |
| 3 | 6.71 (s) | 6.81 (s) |
| 4 | - | - |
| 5 | - | 13.67 (s, OH) |
| 6 | - | - |
| 7 | 7.37 (s, OH) | - |
| 8 | - | - |
| 9 | - | - |
| 10 | - | - |
| 1' | - | - |
| 2' | 7.48 (d, *J* = 8.6) | 8.03 (d, *J* = 8.8) |
| 3' | 6.65 (d, *J* = 8.8) | 6.90 (d, *J* = 8.8) |
| 4' | 7.37 (s, OH) | |
| 5' | 6.65 (d, *J* = 8.8) | 6.90 (d, *J* = 8.8) |
| 6' | 7.48 (d, *J* = 8.6) | 8.03 (d, *J* = 8.8) |
| 1'' | 4.70 (d, *J* = 9.6) | 4.70 (d, *J* = 9.6) |
| 2'' | 4.08 (m) | - |
| 3'' | 3.70 (m) | - |
| 4'' | 3.60 (m) | - |
| 5'' | 3.60 (m) | - |
| 6'' | 3.57 (m) | - |
| 1''' | 4.74 (d, *J* = 9.9) | 4.74 (d, *J* = 9.9) |
| 2''' | 4.08 (m) | - |
| 3''' | 3.70 (m) | - |
| 4''' | 3.70 (m) | - |
| 5''' | 3.63 (m) | - |




[a] Data obtained at 600 MHz for $^{1}$H-NMR in Methanol-$d_4$.
[b] Data obtained at 500 MHz for $^{1}$H-NMR in DMSO-$d_6$ (LI et al., 2020).

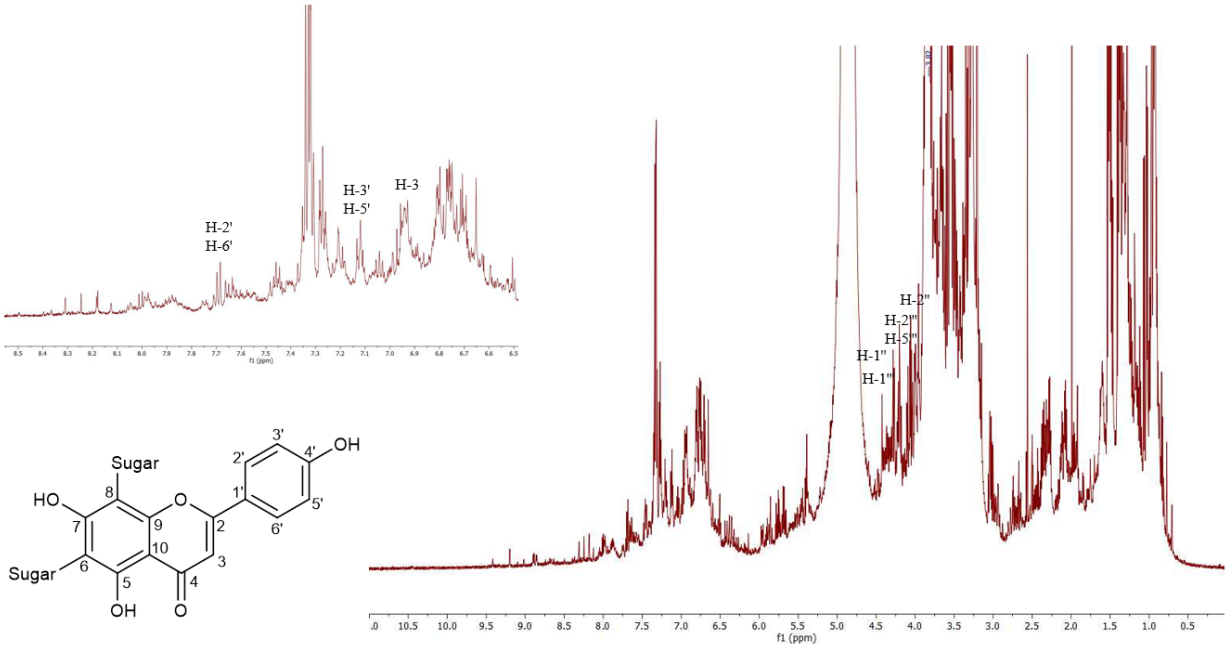



**Figure S5.5.** $^{1}$H-NMR spectrum of mixture **M1**.

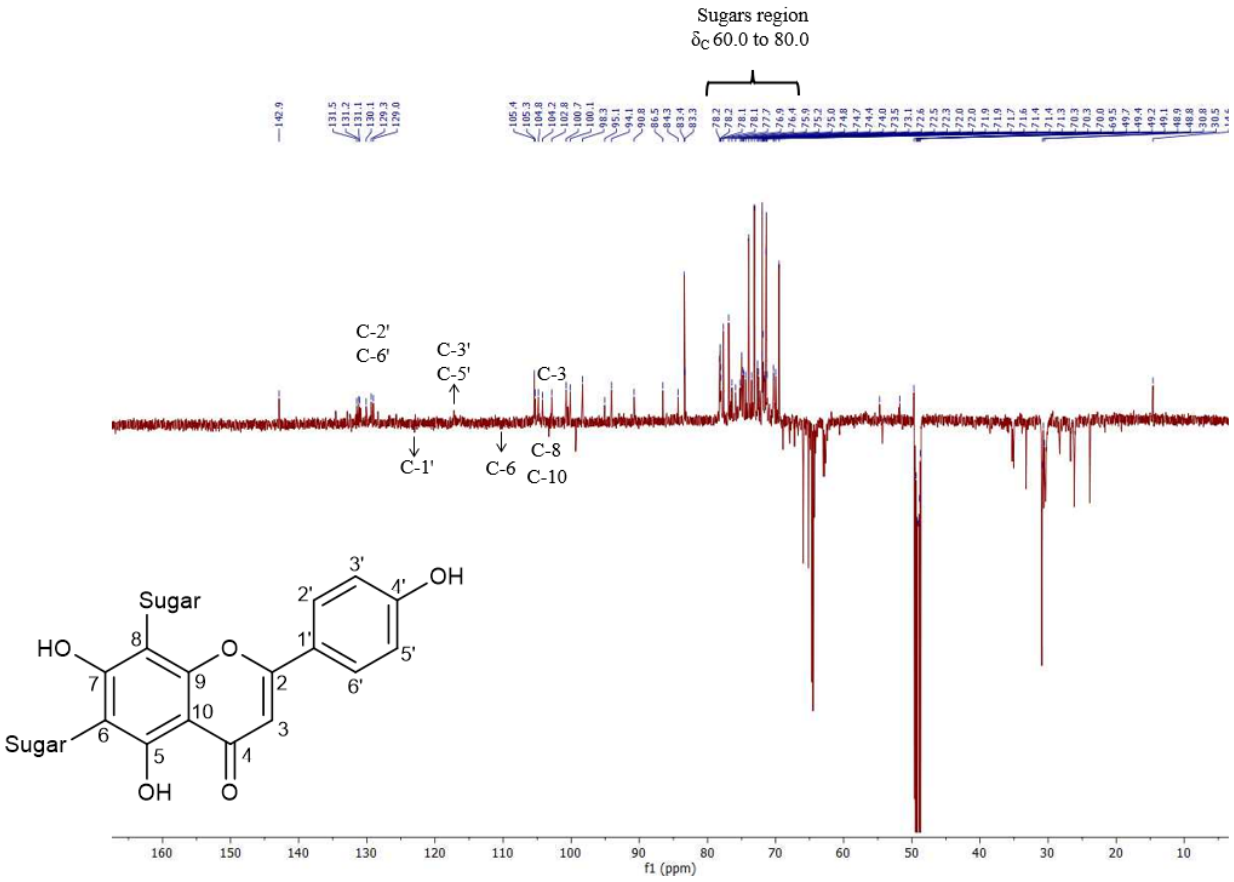



**Figure S5.6.** DEPTQ spectrum of mixture **M1**.

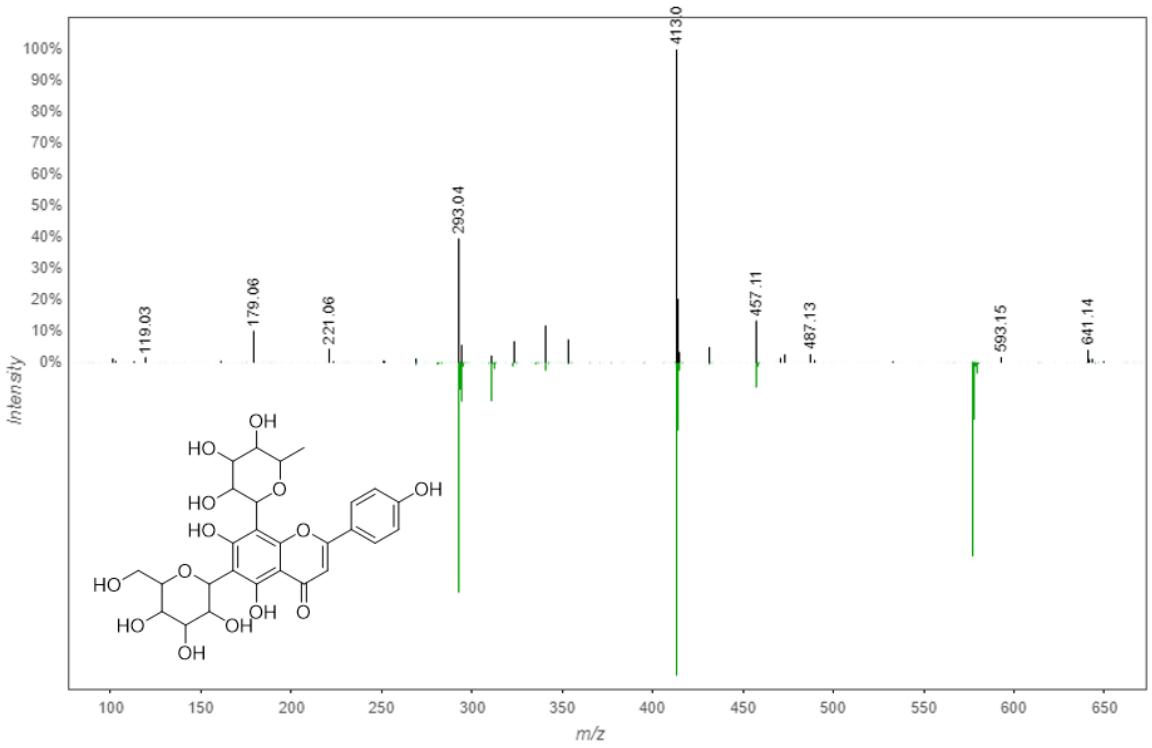



**Figure S5.7.** MS/MS spectra for violanthin **4** identified in *G. incana* leaves. MS/MS of the experimental compound **4** (black) and MS/MS of the compound obtained from the GNPS library (green).

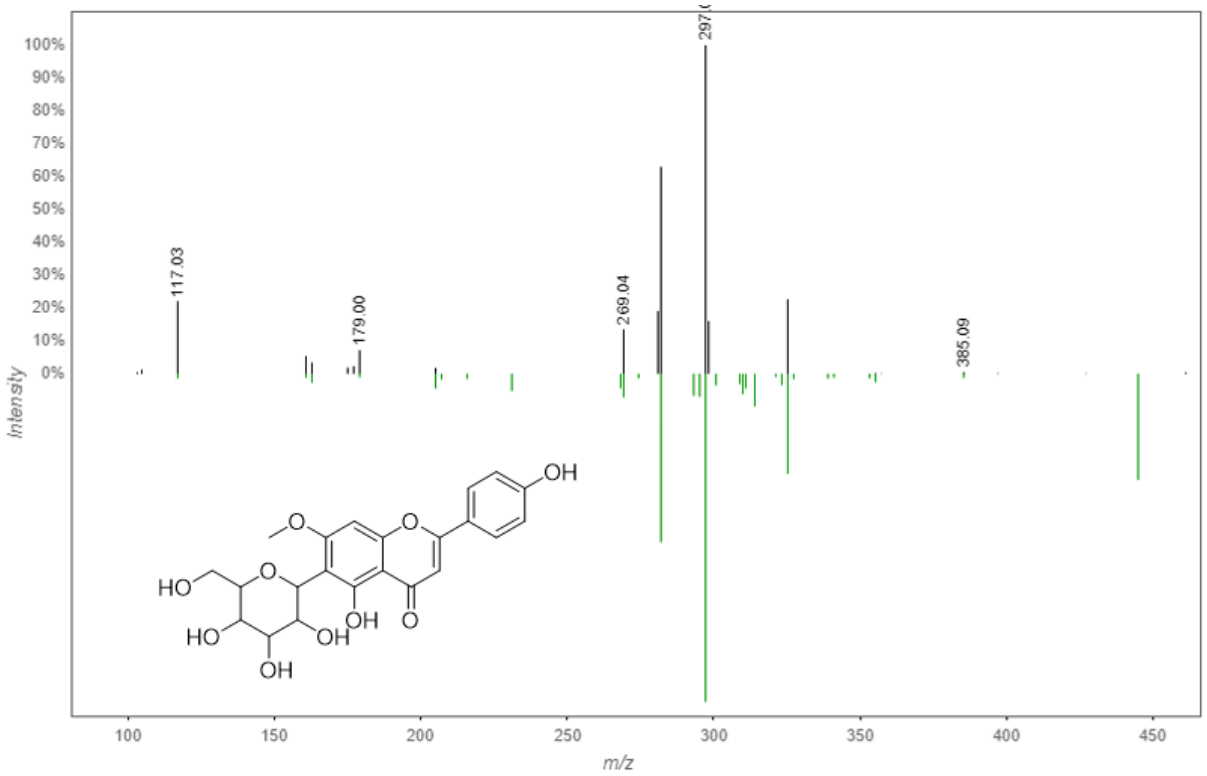



**Figure S5.8.** MS/MS spectra for swertisin **6** identified in *G. incana* leaves. MS/MS of the experimental compound **6** (black) and MS/MS of the compound obtained from the GNPS library (green).

## GENERAL DISCUSSION

The main bamboos studied in the world in terms of their chemical composition and biological activities are those of Asian origin. However, there is still limited information available in these aspects on bamboos occurring in South America (AKINLABI; ANANE-FENIN; AKWADA, 2017; EMAMVERDIAN et al., 2020; YU et al., 2015).

The results of **Chapter 2** showed that the main variation and difference observed in the chemical composition of the bamboo species was in the main groups of compounds found corresponding to flavonoids and cinnamic acid derivatives. Notably, flavonoids from *G. angustifolia* correlated positively with the high altitude group, while cinnamic acid derivatives from *G. angustifolia*, *G. incana*, *G. amplexifolia*, *B. vulgaris*. *G. angustifolia* var. *bicolor*, *G. angustifolia* biotype *San Calixto* and *P. aurea* with the low altitude group. Regarding the relationship between flavonoids and altitude, some studies indicate that plants grown at high altitudes tend to have higher levels of flavonoid content than plants grown at low altitudes (WANG et al., 2020a; ZHOU et al., 2021). Similarly, it has been reported that in the leaves of *Indocalamus latifolius* (Keng) McClure, the total content of flavonoids, phenols, triterpenoids, and eight compounds with biological potential (orientin, isoorientin, vitexin, isovitexin, *p*-coumaric acid, chlorogenic acid, caffeic acid, and ferulic acid) undergo significant changes with altitude. They observed a gradual decrease in these compounds below 700 m, followed by an increase at 1000 m. They showed that higher altitude led to the accumulation of secondary metabolites such as flavonoids. Among the eight characteristic compounds of bamboo, chlorogenic acid and orientin were found in the highest concentration for the leaves, being the most affected by altitude changes.

This effect occurs due to the increase of UV radiation, illumination time, and the delay of the plant's phenophase, together with the increase in elevation, being a protection system that plants use against adverse environmental conditions (NI et al., 2013).

Little is known to date, and studies on the variation of chemical composition in bamboo species need to be more comprehensive. Many studies have reported the influence of altitudinal variation on general flavonoid concentration in leaves. A recently

reported work on the influence of an altitudinal gradient on flavonoid variation in *Agriophyllum squarrosum* reported that flavonoids were enriched at higher altitudes. It was also shown that quercetin, tricin, and rutin contents were strongly positively correlated with environmental variables of latitude, longitude, and precipitation gradients (ZHOU et al., 2021). These compounds showed a preference for accumulation at higher elevation sites as opposed to lower elevation sites. These studies confirm our findings by providing valuable information about the variation in the chemical profile of bamboo when exposed to various abiotic factors such as altitude, temperature, light, soil, etc.

According to the results obtained, we hypothesize that the accumulation of flavonoids at high altitudes is due to the adaptability of bamboo species to environmental conditions. These species are considered as giant grasses and biosynthesize, mostly flavonoid-type phenolic compounds used as a defence. They are also considered potential antioxidants (FALCONE FERREYRA; RIUS; CASATI, 2012; PANCHE; DIWAN; CHANDRA, 2016; WANG; LI; BI, 2018). It is essential to highlight that, considering the results of this study, the pathway that has been altered possibly corresponds mainly to the phenylpropanoid biosynthesis pathway, which directly involves flavonoid biosynthesis. The phenylpropanoid biosynthesis pathway is the starting point for producing many essential compounds, such as flavonoids, coumarins, lignans, and hydroxycinnamic acid conjugates (FRASER; CHAPPLE, 2011).

Flavonoid production occurs mainly through a diverse biosynthetic pathway involving the shikimate and polyketide pathways (Liu et al., 2021; Mouradov & Spangenberg, 2014). Incidentally, there are analysis models to determine the possible altered pathways, such as the *Arabidopsis thaliana* (thale cress) (KEGG) model, which has helped to elucidate details in the phenylpropanoid pathway (FALCONE FERREYRA; RIUS; CASATI, 2012; SAITO et al., 2013). We found it interesting that when mapping the phenylpropanoid biosynthetic pathway, quinic acid (QA) presented a significant change (FC: 5.05, VIP: 1.42, and *p*-value with FDR: 3.14E-03) and is a metabolite related to the caffeoylquinic acids (CQAs) biosynthesis pathway, essential precursors in flavonoid biosynthesis. CQAs are specialized bioactive metabolites derived from the phenylpropanoid biosynthesis pathway. Consequently, this compound is a critical

intermediate in the biosynthesis of many flavonoids through cinnamic acid, a necessary precursor (ALCÁZAR MAGAÑA et al., 2021; LIU et al., 2021).

Furthermore, the study revealed an interesting chemical diversity in these species. In this respect, a large part of the global chemical composition of these species was visualized with the mapping of the chemical space (including information about known reference spectra). However, the GNPS platform presented a low annotation rate, generating many no-matches. Additionally, and to complement the study of changes in chemical composition under the influence of altitude, the specific cluster for flavonoids was analyzed with the molecular network, comparing low and high altitudes. The study showed that the flavonoids annotated as vitexin 2"-*O*-rhamnoside, vicenin-2, and saponarin at high altitudes showed a positive tendency to increase. This is mainly because these compounds protect against UV rays in this type of giant grass (YESHI et al., 2022). Consequently, a close relationship was evidenced between the concentration of phenolic compounds (flavonoids and cinnamic acid derivatives) in bamboo species. Visual inspection of the metabolites found related in a heatmap reveals a clear difference between the content of flavonoids and cinnamic acid derivatives among the groups compared under the effect of the altitudinal gradient, which could be considered marker compounds for chemical classification. A significant difference was observed among the metabolites exposed to the variable altitude, indicating that environmental factors previously influenced plants' genetic and chemical diversity (PACHECO-HERNÁNDEZ et al., 2021).

Comparing the metabolome between species, it was observed that*G. angustifolia* has an abundant flavonoid *C*-glucosides profile. These metabolites had already been reported for other bamboo species corresponding to *P. nigra* var. *henonis* (IBRAHIM et al., 2021; ZHANG et al., 2008) *P. pubescens* Mazel ex J.Houz. (TANAKA et al., 2014) and *B. vulgaris* Schrad. (AKHTAR; PATOWARY, 2022). Other species such as *G. aculeata*, *G. angustifolia* biotype *San Calixto*, *G. incana*, *G. uncinata*, and *G. venezuelae* shared some flavonoids in their chemical composition. Considering the limited information in the literature and the results obtained from the metabolomic analysis, this study opened a

new opportunity to explore the metabolome of these species, specifically those belonging to the genus *Guadua* found in the Latin American continent.

**Chapter 3** presents the results obtained from a correlation study employing metabolomic approaches for identifying potential bioactive markers, correlating chemical composition and biological activity. The studies reported to date provide a basis for comparing and confirming our chemical composition and biological activity findings. Previously, some flavonoid compounds were identified in polar extracts of *G. angustifolia* leaves, including quercetin, kaempferol, violanthin, and kaempferol-7-*O*-neohesperidoside (MORALES NOREÑA; SANCHEZ VALLEJO, 2008). Additional studies explored vinegar obtained from *G. angustifolia*, emphasizing its antioxidant and antimicrobial activity against *Pseudomonas aeruginosa* and *Staphylococcus aureus*, attributed to the high content of phenolic compounds (MEJÍA GALLÓN et al., 2011; MEJÍA GALLÓN; CADAVID TORRES; GALLARDO CABRERA, 2011)). Another study focused on the essential oil from *G. angustifolia* and *G. chacoensis*. The researchers analyzed the chemical composition and assessed antimicrobial activity against *Aspergillus brasiliensis*, *Candida albicans*, *Escherichia coli*, *P. aeruginosa,* and *S. aureus*. Most of the essential oil composition in both essential oils primarily consisted of terpenes and related compounds. For the essential oil of *G. angustifolia*, the major compounds were hexahydrofarnesyl acetone (23.1%) and (Z)-phytol (21.3%), while for *G. chacoensis*, the main compounds included (E)-β-ionone (8.8%), hexadecanoic acid (6.8%), hexadecenoic acid (6.5%), (Z)-phytol (5.3%), and (E)-α-ionone (5.0%). Some of these essential oils exhibited significant activity, with a MIC < 100 µg/mL, suggesting their potential as candidates for developing new antimicrobial agents (MORENO et al., 2018). Other studies involving *G. angustifolia* var. *bicolor* evaluated leaf and culm extracts' antioxidant and anti-tyrosinase potential. The *n*-butanol fraction exhibited the highest antioxidative activity, while the dichloromethane fraction showed tyrosinase inhibition, with inhibition percentages of 86.39% and 40.66%, respectively. Finally, the metabolites responsible for the evaluated activities were tentatively identified as *p*-coumaric acid, catechin, epicatechin, quercetagetin 7-*O*-glucoside, and genistein (CAETANO CORRÊA; HRIHOROWITSCH MORENO, 2020; CORRÊA; MORENO, 2022). Per the above, several

compounds identified in this thesis through chemical profiling had already been reported in BLEs, demonstrating antioxidant (MOSQUERA et al., 2016), antimicrobial (MORENO et al., 2018), and anti-tyrosinase (CAETANO CORRÊA; HRIHOROWITSCH MORENO, 2020; CORRÊA; MORENO, 2022) activities.

The results obtained in chapter 3 were consistent with what was discussed in the previous chapter. These compounds, widely distributed as secondary metabolites in most plants, are important due to their ability to act as antioxidants. Many phenolic compounds have been reported to possess potent antioxidant activity, which may impact anticancer, antibacterial, antiviral, or anti-inflammatory properties to varying degrees (ABOU BAKER, 2022; KUMAR; PANDEY, 2013; PANCHE; DIWAN; CHANDRA, 2016).

The findings of this work demonstrate that BLEs have antioxidant potential, which aligns with data collected for certain species of bamboo leaves, such as *G. angustifolia* (VALENCIA et al., 2011). In their study, different extraction methods were employed with solvents of varying polarity, including ethyl acetate, diethyl ether, and 50% ethanol, using three separate extraction techniques: reflux, Soxhlet, and ultrasound. Additionally, they evaluated the antioxidant capacity using the DPPH methodology in their extracts at a concentration of 50 mg/mL. It was highlighted that the medium and high polarity extracts, corresponding to ethyl acetate and 50% ethanol, presented the highest antioxidant activity. This observation could indicate the presence of polyphenolic compounds, such as flavonoids, to which antioxidant activity has been attributed and that have been found in bamboo leaves, specifically *Phyllostachys nigra* var. *henonis* (KIM et al., 2014; MA et al., 2020a). It is important to highlight that our study used a concentration of 1 mg/mL to evaluate antioxidant activity through the ABTS and DPPH assays. Therefore, compared with the previous study, our results for antioxidant activity indicate that most of the BLEs presented a substantial antioxidant potential, with values greater than 100 and 30 µmol TE/g of extract for ABTS and DPPH, respectively. Another study assessed the antioxidant potential of bamboo vinegar obtained through the pyrolysis process of *G. angustifolia*. Both methods determined the antioxidant activity in the vinegar. In this study, the concentration of syringol was quantified in the different formulations obtained from the vinegar, revealing that this compound, along with others such as guaiacol, exhibited

antioxidant capacity (ARBOLEDA ECHAVARRÍA; JARAMILLO YEPES; PALACIO TORRES, 2012).

Considering that only previous reports have been found for some species of the genus *Guadua*, and to strengthen our discussion, a search was carried out at the Bambusoideae subfamily level for related studies to compare our results of chemical composition and biological activity. In this sense, it was found that the dried leaves of *Sasa veitchii* bamboo, a species traditionally used in Asian folk medicine, reveal its use as a source of antioxidant food supplements in Japan. As well, the Chinese Food Additives Standardization Committee approved an extract of *Phyllostachys nigra* var. *henonis* known as an antioxidant of bamboo leaves (AOB) as a novel kind of natural antioxidant due to its potent antioxidant capacity attributed to phenolic compounds (VAN HOYWEGHEN et al., 2010; VAN HOYWEGHEN; DEFORCE; HEYERICK, 2010). Products derived from bamboo extracts, coupled with the increased production of reactive oxygen species (ROS), are believed to play a significant role in preventing disease development and reducing the impact of oxidative stress when disease occurs (CHOI et al., 2018; YU et al., 2019).

Additionally, we evaluated the anti-inflammatory potential of BLEs by measuring the percentage of NO inhibition both chemically and in RAW 264.7 macrophage cell lines. Overall, BLEs demonstrated significant inhibition of NO production, exceeding 50%, which is noteworthy considering NO's involvement in tumor progression. Analysis of chemical and cellular NO levels suggests that BLEs may effectively capture NO and inhibit iNOS (inducible nitric oxide synthase). Previous findings suggest flavonoids, typically found in BLEs, exhibit NO inhibitory activity (KIM et al., 1999). As evidenced by prior research, flavonoids influence the inflammatory process and possess anti-inflammatory and immunomodulatory properties both *in vitro* and *in vivo*. Given that NO production is a key indicator of macrophage activation, the ability of flavonoids to inhibit NO production at both chemical and cellular levels underscores their potential as anti-inflammatory agents (JIANG et al., 2017). Flavonoids also demonstrate the ability to inhibit various proinflammatory mediators and transcription factors, further supporting their anti-inflammatory effects (ALVAREZ-SUAREZ et al., 2017; XU et al., 2002). This study

represents the first documentation of BLEs' anti-inflammatory properties, confirming *Guadua* species as a significant source of bioactive compounds with notable anti-inflammatory and antioxidant capacities.

We highlight that according to our results, to date, the BLEs included in this research do not present any report of cytotoxic activity; this being the first report. Despite the absence of reports on cytotoxicity in these bamboos, it is striking that, in general, other bamboo species such as *Phyllostachys heterocycla* and *Dendrocalamus asper* have shown anticancer effects against various cell lines, including HepG2, MCF-7, HeLa, A549, and THP-1, which are directly associated with the high content of polyphenols (CHENG et al., 2023; GAGLIANO et al., 2022b). For example, in a previous study, the polar fraction of *Phyllostachys heterocycla* var. *pubescens* (Pradelle) Ohwi was shown to exhibit selectivity by inhibiting the epidermal growth factor receptor (EGFR) in HepG2 cells. In this study, the isolation of 7-hydroxy-5-methoxy-methylcinnamate showed $IC_{50}$ values of 7.43 and 10.65 μM against HepG2 and MCF-7 cell lines, respectively. Moreover, it induced apoptotic cell death in HepG2 cells, with a total apoptotic rate of 58.6% compared to 4.71% in the control, achieved by arresting cell cycle progression in the G1 phase (ABDELHAMEED et al., 2021). Previous studies in other bamboo species have reported cytotoxic activity, e.g., in the crude methanol extract obtained from the skin of the shoots of the bamboo *Phyllostachys heterocycla*. The crude extract was evaluated against five cell lines-four of them tumorigenic (HepG2, HeLa, A549, and MCF-7) and one non-tumorigenic cell line. The results showed that the crude extract presented a moderate cytotoxic effect against HepG2 and MCF-7, with $IC_{50}$ values of 48.4 and 38.9 μg/mL, respectively, while against HeLa, it showed a weak effect with an $IC_{50}$ value of 50 μg/mL (ABDELHAMEED et al., 2022). In a more recent study on *P. heterocycla* var. *pubescens*, the cytotoxic effect was evaluated against the crude methanol extract and the fractions obtained from *n*-hexane, ethyl acetate, and *n*-butanol, targeting five cell lines: HepG2, HeLa, A549, MCF-7, and THP-1. It was reported that the *n*-butanol fraction exhibited inhibition percentages exceeding 60% against all cell lines at the maximum 100 μg/mL concentration. Notably, the *n*-butanol fraction demonstrated the highest inhibition at 94.31% against the HeLa cell line (ABDELHAMEED et al., 2021).

In the broader context of our research on the chemical and biological properties of *Guadua* species, our study significantly expands the existing knowledge base, particularly concerning cytotoxic activity. Although previous reports have been scarce, our results of the activity of BLEs against HCT-116 cells represent a novel contribution to understanding these bamboos' anticancer potential and confirming that these extracts may be promising candidates for bioactive compounds, specifically as anticancer agents. Our interest in HCT-116 cells and the need for further research on the antioxidant and cytotoxic potential of *Guadua* species led us to establish a correlation between the chemical composition and the antioxidant and cytotoxic activities of BLEs to identify bioactive compounds responsible for these effects. This holistic approach improves our understanding of BLEs and lays the foundation for developing new therapeutic agents with potential applications in cancer research and treatment.

Based on this context and considering that it is the first approach in bamboo, it is highlighted that the compounds corresponding to flavonoids and derivatives of phenolic acids correlated positively with the antioxidant potential previously highlighted in the studies described. Particularly, in a study conducted by Ni et al., 2012 on the species *Sasa argenteastriatus*, it was found that they correlated the chemical composition with antioxidant activity, determining that the content of total flavonoids (TF) and total phenols (TP) obtained from the leaves of this ornamental bamboo exhibited a high correlation with antioxidant activity. Additionally, eight characteristic compounds of this bamboo were identified, including orientin, isoorientin, vitexin, homovitexin, *p*-coumaric acid, chlorogenic acid, caffeic acid, and ferulic acid. In general, it is highlighted that seasonal variation and the content of TF and TP influence the DPPH radical scavenging capacity. The correlation coefficient between TF, TP, and DPPH radical scavenging is TF > TP, indicating that TF in bamboo leaves plays a primary role in the DPPH radical scavenging capacity. The correlation coefficient between TF, TP, and antioxidant capacity obtained by the FRAP assay is TP > TF (NI et al., 2012).

According to the above, our correlation results of the chemical composition and antioxidant activity align with this previous study. Although the total flavonoid and total phenolic content were not determined, it was established that about 50% of the chemical

composition of the BLEs corresponds to flavonoids and derivatives of phenolic acids. On the other hand, compounds reported in this work, such as vicenin-2, chlorogenic acid, caffeic acid, schaftoside or isoschaftoside, saponarin or isosaponarin, etc., presented a higher correlation coefficient (> 0.5), demonstrating powerful antioxidant activity, in agreement with the findings reported and compared by Ni et al., 2012. Similarly, a recent study by Ko et al., 2018 on the effect of seasonal variations on phenolic compounds and the antioxidant and anti-inflammatory activity of *S. quelpaertensis* Nakai through a correlation study demonstrated that phenolic compounds (*p*-coumaric acid, tricine, TP, and TF content) in ethanol extracts of leaves (ESL) showed an excellent correlation with antioxidant activities, indicating that ESL contained the highest levels of antioxidant and anti-inflammatory substances (KO et al., 2018). However, in our study, the flavone tricine showed correlation coefficients < 0.5, indicating a negative correlation with antioxidant activity, unlike the findings reported by Ko et al., 2018. The above allows us to determine that the effect is possibly attributed to the synergistic effect (CRESPO et al., 2019; ZHANG et al., 2022) of the compounds present in the BLEs or other specific phenolic compounds, such as *p*-coumaric acid and Luteolin 6-*C*-hexoside 8-*C*-pentoside, presenting a coefficient of correlation > 0.7, indicating a potent antioxidant effect for both methods.

On the other hand, flavonoid glycosides presented a positive correlation with cytotoxic activity. These results are consistent with those reported where some flavones, including apigenin, baicalein, chrysin, luteolin, nobiletin, tangeretin, and wogonin, have shown cytotoxic potential against various colon cancer cell lines, such as Caco-2, COL-2, COLO201, COLO205, COLO320, HCT-115, HCT-116, HT-29, etc., with $IC_{50}$ values < 100 µM (SAK, 2014). We found that glycosated flavones particularly showed a positive relationship with increased cytotoxic activity, whereas caffeoylquinic acids did not. Although there are no studies on the effect of BLEs against HCT-116 colon cancer cell lines, the effect of extracts of bamboo shoots (*Dendrocalamus asper*, *Phyllostachys heterocycla* var. *Pubescens* and *S. quelpaertensis*) against MCF-7 breast cancer cells and HCT-116 colon cancer cells lines has been reported, showing cytotoxic, antiproliferative, proapoptotic and proinflammatory effects (KIM, 2020; YANSEN et al., 2023). A recent study investigated the role of $NO^{\bullet}$ and inhibitors of apoptosis (IAPs) during

the process of apoptosis induced by *S. quelpaertensis* leaf extracts (SQE) in p53 wild-type (WT) and p53 null HCT-116 colon carcinoma cells. SQE induce apoptosis independent of p53 status and was associated with the modulation of endogenous $NO^{\bullet}$ in HCT-116 cells (KIM, 2020).

Sak, 2014 reported that flavonoids, such as quercetin and baicalein, are recognized as beneficial agents for preventing and treating colon cancer. However, in contrast to their glycosides, rutin and baicalin, respectively, they did not exhibit growth-inhibitory effects on colon cancer cells. This observation highlights the substantial impact of the sugar fraction on the bioactivity of flavonoids (SAK, 2014). Interestingly, our correlation study contradicts this finding, especially concerning glycosylated flavones identified as vicenin-1 or vicenin-3 (FC = 6.73; *p*-value = 2.64E-02), vitexin 2''-*O*-rhamnoside (FC = 5.13; *p*-value = 4.08E-02), , isoschaftoside (FC = 4.70; *p*-value = 4.27E-03), and saponarin or isosaponarin (FC = 3.38; *p*-value = 1.61E-02), which demonstrated significant changes and are associated with cytotoxic potential in the most active BLEs. Other recent study, by Vukovic et al., 2018, evaluated the cytotoxicity of eleven flavonoids isolated from propolis against colon cancer cell lines (HCT-116) and breast cancer cells (MDA-MB-231). Six flavonoids induced cytotoxic effects in both cell lines. Luteolin exhibited cytotoxicity, especially in HCT-116 cells, with an $IC_{50}$ value after 72 h of exposure of 66.86 µM. Myricetin demonstrated cytotoxicity with an $IC_{50}$ value of 114.75 µM, inducing apoptosis in MDA-MB-231 cells (VUKOVIC et al., 2018). The preceding data, related to the correlation study and bioactivity of glycosylated flavones against the colon cancer cell line HCT-116, align consistently with our results. Thus, a straightforward identification of potential biomarkers was achieved before any fractionation or isolation efforts.

Molecular networking analysis identified bioactive molecules within BLEs, whose active constituents were previously unknown against colon cancer cells HCT-116. The study emphasized that compounds luteolin 6-*C*-hexoside 8-*C*-pentoside, vitexin 2”-*O*-rhamnoside, and isoschaftoside exhibited a better positive correlation, affirming the earlier observations. The present study demonstrated that the application of a metabolomics approach, based on the correlation of chemical composition and biological activity,

together with the construction of integrated molecular networks with bioactivity scores, can accelerate the search for bioactive molecules and rationalize the isolation procedure in bioassay-based phytoconstituent discovery (TAHIR et al., 2019). This innovative tool allows narrowing down the pool of candidate compounds for further isolation, thus minimizing the time required in this process.

Considering that the bamboo leaf extract obtained from *G. incana* (BLEGI) showed potent cytotoxic activity, in **Chapter 4**, HCT-116 colon cancer cells were treated with the BLEGI to evaluate the metabolic alterations of the endometabolome and exometabolome of the cells. We highlight that cancer results from accumulated molecular changes, such as the activation of oncogenes, inhibition of tumor suppressor genes, and epigenetic alterations, leading to deregulated intracellular signaling pathways (NIKAS; PASCHOU; RYU, 2020). Cancer cells adapt their metabolism to favor survival, growth, and metastasis, involving altered nutrient uptake, intracellular metabolism, gene expression, and interactions with the tumor microenvironment (DI GREGORIO et al., 2022; GYAMFI; KIM; CHOI, 2022).

Metabolomic analysis of HCT-116 colon cancer cells revealed significant alterations in key metabolites within various metabolic pathways. Notably affected pathways include glutathione metabolism, the tricarboxylic acid cycle, lipoic acid metabolism, and pyrimidine metabolism. Comparison between the BLEGI-treated and untreated groups highlighted a significant impact on metabolites associated with glutathione metabolism, notably reduced GSH and GSSG. Glutathione metabolism plays a crucial role in antioxidant defense, redox regulation, and detoxification through the interplay of the GSH-GSSG redox pair and related enzymes and transporter systems. GSH, with its essential thiol group, functions as a critical intracellular antioxidant, counteracting free radicals and preserving protein activity by reducing oxidized thiols, making it a key indicator of oxidative stress (GAO et al., 2014; SHAO et al., 2016).

These findings suggest that BLEGI affects cellular redox status, as evidenced by elevated GSSG levels, indicating the induction of oxidative stress in treated cells. The significant reduction in glutathione levels implies a potential disruption of intercellular redox balance, which may lead to compromised mitochondrial integrity and caspase

activation-known to inhibit cell proliferation and exhibit antitumor effects (MUSAOGULLARI; MANDATO; CHAI, 2020). Excessive generation of reactive oxygen species (ROS) during cellular metabolism can lead to oxidative stress, causing metabolic disturbances and cellular damage, particularly in colorectal cancer (DÜKEL; TAVSAN; KAYALI, 2021; SABHARWAL; SCHUMACKER, 2014). Under normal conditions, a delicate balance between antioxidant and pro-oxidant systems, such as the glutathione system, maintains cellular redox homeostasis, with glutathione primarily in its reduced form (GSH), regulated by glutathione reductase (GR) (BRZOZOWA-ZASADA et al., 2024; HEGEDŰS et al., 2018). Compared to previous studies, low levels of GSH observed in BLEGI-treated cells suggest a potential link between high GSH levels in tumor cells, cancer progression, and resistance to chemotherapy (KENNEDY et al., 2020). Targeting the GSH antioxidant system has emerged as a novel therapeutic approach in various cancers to enhance treatment response and reduce drug resistance. The reduction in GSH levels in BLEGI-treated HCT-116 cells strongly supports the hypothesis of glutathione metabolism as a potential pathway underlying the extract's activity. This finding is consistent with observations in HepG2 liver cells treated with a flavonoid derivative, where decreased GSH levels indicated heightened oxidative stress (GAO et al., 2014).

Another altered metabolite observed in our results corresponds to Nicotinamide (NAM), which serves as a precursor to nicotinamide-adenine dinucleotide (NAD+), crucial for cellular energy metabolism and participating in redox and non-redox reactions. Elevated $NAD^+$ levels or a high $NAD^+$/NADH ratio inhibit the generation of ROS, enhancing mitochondrial function and cell viability by mitigating oxidative stress (CHEN et al., 2016; LI et al., 2022; NIKAS; PASCHOU; RYU, 2020). Additionally, $NAD^+$ is vital for cellular homeostasis, acting as a coenzyme in various energy production pathways and participating in non-redox processes such as DNA repair, post-translational modifications, and cell signaling (YOON et al., 2023b; ZHANG et al., 2013b). Nicotinamide N-methyltransferase (NNMT) catalyzes the methylation of NAM, producing 1-methyl nicotinamide (1-MNA), which further oxidizes to N1-methyl-2-pyridone-5-carboxamide

(2PY) and N1-methyl-4-pyridone-3-carboxamide (4PY) through AOX1 enzyme action (RAMSDEN et al., 2017; WANG et al., 2022a).

Dysregulated lipid metabolism is a significant feature of cancer, involving a complex array of biomolecules such as fatty acids, glycerides, and lipoproteins. These lipids play diverse roles in energy production, signaling, and cell membrane formation, influencing pathways governing growth, proliferation, and survival (BROADFIELD et al., 2021; FU et al., 2021). Understanding how cancer cells reprogram lipid metabolism could reveal new therapeutic avenues. In our study, BLE treatment reduced Sphingosine (Sph) levels, possibly due to cell membrane damage in HCT-116 cells. Sphingolipids, including Sph, play crucial roles in cell signaling, proliferation, and apoptosis regulation (CHOI; SONG, 2020; GOMEZ-LARRAURI et al., 2021; SANTOS; SCHULZE, 2012), suggesting BLEGI may influence these processes to exert its antitumor effects.

The results suggest that BLEGI may regulate apoptosis and the dysregulated metabolism of sphingolipids to exert its antitumor effect. This finding was verified by an immunofluorescence assay performed on HCT-116 lines, in which the formation of apoptotic bodies related to the effect exerted by BLEGI was determined. This indicates that the cells are in fact undergoing cell death by apoptosis, but despite this result, it is necessary to confirm this mechanism of action with other specific assays.

Connecting anti-inflammatory activity with metabolomic analysis of HCT-116 colon cancer cells reveals a significant link between chronic inflammation and tumor development. Inflammation is pivotal in various cancer types of pathogenesis, with iNOS, an enzymatic isoform of nitric oxide synthase (NOS), playing a key role. iNOS, expressed in inflammatory conditions, produces high levels of NO, impacting cell redox balance and inducing damage to proteins, lipids, and DNA. iNOS inhibitors have shown promise in reducing metastasis and inhibiting cancer cells (JIANG et al., 2018; KORDE CHOUDHARI et al., 2013; VANINI; KASHFI; NATH, 2015). We hypothesize that BLE's anti-inflammatory properties, targeting iNOS and oxidative stress, could potentially prevent colon cancer growth. Our research demonstrates that BLEGI profoundly affects key metabolic pathways, including glutathione metabolism, the tricarboxylic acid cycle, lipoic acid metabolism, and pyrimidine metabolism. After a 72-hour exposure to BLEGI, significant

alterations in metabolite concentrations were observed in both the endo- and exometabolomic profiles of HCT-116 cells. These results suggest that BLEGI treatment may trigger apoptotic cell death, although additional studies are needed to confirm this hypothesis. Overall, these findings underscore the potential therapeutic efficacy of BLEGI not only for colon cancer but maybe for dfferent types of cancer cells.

Lastly, to confirm the findings of the correlation study and the cytotoxic potential of BLEGI, **Chapter 5** presents the phytochemical study guided by the metabolomic approach of the most active species *G. incana*, to isolate some compounds with cytotoxic potential against HCT-116 cells. Therefore, this chapter of the Thesis presents the first phytochemical report for the plant species *G. incana*. The isolated metabolites are described for the first time for the species, and this work is the first isolation reported for the species. Of note is isoschaftoside, a flavone di-*C*-glycoside with a history of reports in literature closely related to the flavones reported in other bamboo species (ANDRESSA ALMEIDA FARIAS et al., 2024).

Several studies have determined that flavonoid *C*-glycosides are the main flavonoids reported in the bamboos of the genus *Guadua* (ÁLVAREZ et al., 2015; LOZANO-PUENTES et al., 2023). It is important to highlight that from the chemotaxonomic point of view, these bamboos are characterized by the presence of flavone *C*-glycosides together with their respective aglycones apigenin and luteolin (YE et al., 2022; YUAN et al., 2021). Furthermore, the presence of flavone *C*-glycosides has been observed in other genera of the family Poaceae (Bambusoideae): *Phyllostachys*, *Sasa*, *Fargesia*, *Bambusa* and *Dendrocalamus* (GAGLIANO et al., 2022b).

Particularly, flavonoids in plants are biosynthesized by the mixed path from the hydroxyl cinnamic acid (Ring B) and the malonyl residue (Ring A) through a sequence of reactions with a $C_6$-$C_3$-$C_6$ skeleton, including flavones, flavonols, flavanones, isoflavones, etc. Most flavonoids in plants present various substituents, such as hydroxylation, methylation, acylation, and glycosylation in the form of *O*-glycosides or *C*-glycosides (XIE et al., 2022). Flavonoids *O*-glycosides are the most reported, while *C*-glycosides are much more restricted in plants. However, they have been shown to have antidiabetic, anti-inflammatory, anti-Alzheimer, antioxidant, antiviral, cytotoxic, and anxiolytic effects

(CHUA; ABDULLAH; AWANG, 2020; PANCHE; DIWAN; CHANDRA, 2016). Interestingly, it has been found that flavones *C*-glycosides in plants help to absorb the UV rays to which they are exposed for protection. The biosynthetic pathway of flavonoid *C*-glycosides compared to flavonoid *O*-glycosides is still unclear. According to the above and considering the high growth of these bamboos, the high chemical composition related to flavonoids could be related to these effects, using these metabolites for their defense against UV rays. This finding was confirmed with the study of chemical composition variation under the influence of an altitudinal gradient reported for *Guadua* species in the first chapter. Finally, the potent cytotoxic effect presented by isoschaftoside is highlighted, which supports the results obtained in the correlation study described in chapter 3. Previously it was reported that the evaluation of this compound against HepG2 cells showed that isoschaftoside did not have a significant impact on cell proliferation at a concentration lower than 500 µM (SU et al., 2022), however in this study its cytotoxic potential is highlighted.

In summary, our research contributes to the chemical composition of species belonging to the *Guadua* genus and explores their biological potential related to antioxidant, anti-inflammatory, and cytotoxic activity, revealing potential applications in various fields. An importante highlight is given to the species *G. incana* and its flavonoid composition, where the data could lead to discover the main compound responsible for its cytotoxicity. Our results shed light on the importance of bamboo in the medicinal field, offering new perspectives for its use in Colombia.

## CONCLUSIONS

The present study contributes to research on the chemical composition and biological properties of bamboos of the genus *Guadua* present in Colombia through a metabolomic analysis of the chemical composition under the influence of an altitudinal gradient; the evaluation of antioxidant, anti-inflammatory and cytotoxic activities and their correlation with the chemical composition; the evaluation of metabolic alterations in HCT-116 cells after exposure to the *G. incana* extract; and the isolation and characterization of some bioactive compounds present in *G. incana* leaves. The results obtained in this research allow us to conclude:

- The untargeted metabolomics approach and molecular networking analysis revealed that at high altitudes, flavonoid profiles increased, while at low altitudes, the content of cinnamic acid derivatives increased. This research on bamboo metabolomics enhances our understanding of its chemical composition and metabolic conservation, and identifies patterns related to environmental and cultivation factors. These findings have practical implications for the cultivation and utilization of bamboos in different altitudinal regions.

- The comparative analysis of bamboo species by molecular networks on the GNPS platform showed great chemical diversity among species, including flavonoid glycosides, cinnamic acid derivatives, lignans, alkaloids, carbohydrates, and fatty acids. The species corresponding to *G. angustifolia* showed greater distinction in their chemical composition concerning the other bamboos influenced by the presence of isoschaftoside, isovitexin, isorhamnetin 7-rhamnoside, and rhoifolin.

- The study of antioxidant activity with ABTS and DPPH showed that the *G. angustifolia*, *G. amplexifolia*, *G. incana*, and *G. uncinata* species exhibit promising activity where their antioxidant effect is related to the high content of phenolic compounds.

- The ethanolic extracts of *G. amplexifolia*, *G. angustifolia*, *G. angustifolia* var. *bicolor*, *G. incana*, and *G. uncinata* showed anti-inflammatory activity, where *G. incana* was the most promising species, demonstrating potential for the inhibition of the chemical production of NO with percentages greater than 70%, while for inhibition of the cellular production of NO presented percentages greater than 90% in LPS-stimulated macrophages.

- The study of cytotoxic activity showed that the species *G. amplexifolia*, *G. angustifolia*, *G. angustifolia* var. *bicolor*, *G. incana*, and *G. uncinata* exhibit promising activity, where *G. incana* was the most promising species on the HCT-116 cell line.

- The correlation study between the chemical composition and the antioxidant, anti-inflammatory, and cytotoxic activity of *Guadua* species demonstrated that the high phenolic composition related to flavonoid compounds and cinnamic acid derivatives strongly correlated with antioxidant and anti-inflammatory activities. At the same time, the flavone glycosides correlated with cytotoxic activity.

- The metabolomic analysis of the endo- and exometabolome of HCT-116 cells after treatment with *G. incana* extract revealed different altered metabolites related to glutathione metabolism, tricarboxylic acid cycle metabolism and lipoic acid metabolism. Furthermore, it was determined that the mechanism of action by which the extract exerts its effect on cells is possibly mediated by oxidative stress-induced cell apoptosis.

- The phytochemical study developed on the leaves of *G. incana* guided by the metabolomic approach allowed the isolation of a flavone glucoside named isoschaftoside **1** and a mixture of three flavones derived from the apigenin scaffold identified as violanthin **4**, swertisin **6**, and unidentified **7**. Compound **1** presented

a powerful cytotoxic effect and has been reported for other species related to the Bambusoideae subfamily, while this is the first report for *G. incana*.

## PERSPECTIVES

It is necessary to validate with specific assays the mechanism of action by which the bamboo leaf extract obtained from *G. incana* exerts the effect on HCT-116 cells.

It is necessary to standardize the extract of *G. incana* related to its physical properties and chemical composition to propose a coadjuvant phytomedicine for cancer treatment in the future.

It is necessary to continue phytochemical research on species of the genus *Guadua* to isolate and identify more bioactive constituents, which would give more robustness to the chemical composition that is so unknown in these bamboos.

It is necessary to continue with the bioactivity screening in different models to explore other biological properties that these bamboo species could present.

It is necessary to strengthen metabolomic studies related to the variation of chemical composition considering other environmental variables to which these bamboos are exposed.

Further anti-inflammatory activity assays are recommended to explore other mechanisms related to cancer pathology.

It is recommended that a metabolomic study with the compound isoschaftoside on HCT-116 cells be performed to understand the metabolic alterations and propose possible molecular mechanisms.

## REFERENCES


ABDELHAMEED, R. F. A. et al. Cytotoxic, apoptosis-inducing activities, and molecular docking of a new sterol from bamboo shoot skin Phyllostachys heterocycla var. Pubescens. **Molecules**, v. 25, n. 23, p. 5650, 2020.

ABDELHAMEED, R. F. A. et al. Chemical constituent profiling of *Phyllostachys heterocycla* var. *Pubescens* with selective cytotoxic polar fraction through EGFR inhibition in HepG2 cells. **Molecules**, v. 26, n. 4, p. 940, 2021.

ABDELHAMEED, R. F. A. et al. Chemical profiling, cytotoxic activities through apoptosis induction in MCF-7 cells and molecular docking of *Phyllostachys heterocycla* bark nonpolar extract. **Journal of Biomolecular Structure and Dynamics**, v. 40, n. 20, p. 9636–9647, 2022.

ABOU BAKER, D. H. An ethnopharmacological review on the therapeutical properties of flavonoids and their mechanisms of actions: A comprehensive review based on up to date knowledge. **Toxicology Reports**, v. 9, p. 445–469, 1 jan. 2022.

ACOSTA-LEAL, D. et al. **La guadua (*Guadua angustifolia*) Kunth: El oro verde por descubrir**. Bogotá: Corporación Universitaria Minuto de Dios, 2021.

ACS. American Cancer Society Cancer Statistics 2021 Report. **Journal of nuclear medicine : official publication, Society of Nuclear Medicine**, v. 62, n. 3, 2022.

AKHTAR, J.; PATOWARY, L. *Bambusa vulgaris*: A comprehensive review of its traditional uses, phytochemicals and pharmacological activities. **Sciences of Phytochemistry**, v. 1, n. 2, p. 11–21, 2022.

AKINLABI, E. T.; ANANE-FENIN, K.; AKWADA, D. R. Applications of Bamboo. In: **Bamboo: the multipurpose plant**. [s.l.] Springer International Publishing, 2017. p. 179–219.

ALCÁZAR MAGAÑA, A. et al. Caffeoylquinic acids: chemistry, biosynthesis, occurrence,

analytical challenges, and bioactivity. **The Plant journal**, v. 107, n. 5, p. 1399, 1 set. 2021.

ALVAREZ-SUAREZ, J. M. et al. Anti-inflammatory effect of Capuli cherry against LPS-induced cytotoxic damage in RAW 264.7 macrophages. **Food and Chemical Toxicology**, v. 102, p. 46–52, 2017.

ÁLVAREZ, E. S. D. et al. Estudios para el aprovechamiento potencial de hojas de *Guadua angustifolia* Kunth (Poaceae), para el sector cosmético. **Revista Cubana de Farmacia**, v. 49, n. 3, p. 535–542, 2015.

AMERICAN CANCER SOCIETY. American Cancer Society: Cancer Facts and Figures 2021. **Atlanta, Ga: American Cancer Society**, 2021.

ANDRESSA ALMEIDA FARIAS, C. et al. Phenolic diversity and antioxidant potential of different varieties of bamboo leaves using LC-ESI-QTOF-MS/MS and LC-ESI-QqQ-MS/MS. **Food Research International**, v. 179, 1 mar. 2024.

ARBOLEDA ECHAVARRÍA, C.; JARAMILLO YEPES, F.; PALACIO TORRES, H. Determinación del potencial antioxidante en extractos de vinagre *Guadua angustifolia* Kunth para aplicaciones alimenticias. **Revista cubana de plantas medicinales**, v. 17, n. 4, p. 330–342, 2012.

ARON, A. T. et al. Reproducible molecular networking of untargeted mass spectrometry data using GNPS. **Nature Protocols**, v. 15, n. 6, p. 1954–1991, 2020.

BAHARUM, Z. et al. In vitro antioxidant and antiproliferative activities of methanolic plant part extracts of *Theobroma cacao*. **Molecules**, v. 19, n. 11, p. 18317–18331, 10 nov. 2014.

BATES, T. E. et al. Immunocytochemical evidence for a mitochondrially located nitric oxide synthase in brain and liver. **Biochemical and Biophysical Research Communications**, v. 213, n. 3, p. 896–900, 1995.

BELAY, A.; GHOLAP, A. V. Characterization and determination of chlorogenic acids (

CGA ) in coffee beans by UV-Vis spectroscopy. **African Journal of Pure and Applied Chemistry**, v. 3, n. 11, p. 234–240, 2009.

BENIWAL, S. S. et al. Current Status and Emerging Trends in Colorectal Cancer Screening and Diagnostics. **Biosensors**, v. 13, n. 10, p. 926, 2023.

BHATT, K. et al. Comprehensive Insight into Colorectal Cancer Metabolites and Lipids for Human Serum: A Proof-of-Concept Study. **International Journal of Molecular Sciences**, v. 24, n. 11, p. 9614, 2023.

BINGOL, K. Recent advances in targeted and untargeted metabolomics by NMR and MS/NMR methods. **High-throughput**, v. 7, n. 2, p. 9, 2018.

BLACKADAR, C. B. Historical review of the causes of cancer. **World Journal of Clinical Oncology**, v. 7, n. 1, 2016.

BLAŽENOVIĆ, I. et al. **Software tools and approaches for compound identification of LC-MS/MS data in metabolomics**. **Metabolites**, 2018.

BLUNDER, M. et al. Efficient identification of flavones, flavanones and their glycosides in routine analysis via off-line combination of sensitive NMR and HPLC experiments. **Food Chemistry**, v. 218, p. 600–609, 2017.

BONAM, S. R. et al. What has come out from phytomedicines and herbal edibles for the treatment of cancer? **ChemMedChem**, v. 13, n. 18, p. 1854–1872, 2018.

BREDENOORD, J. Bamboo as a Sustainable Building Material for Innovative, Low-Cost Housing Construction. **Sustainability (Switzerland)**, v. 16, n. 6, 2024.

BROADFIELD, L. A. et al. Lipid metabolism in cancer: New perspectives and emerging mechanisms. **Developmental Cell**, v. 56, n. 10, p. 1363–1393, 2021.

BRZOZOWA-ZASADA, M. et al. Glutathione Reductase Expression and Its Prognostic Significance in Colon Cancer. **International Journal of Molecular Sciences**, v. 25, n. 2,

p. 1097, 1 jan. 2024.

CAETANO CORRÊA, J. K.; HRIHOROWITSCH MORENO, P. R. **Isolamento e identificação de compostos com atividade antioxidante e anti-tirosinase em extratos de *Guadua angustifolia* var. *bicolor* Londoño**. 29º SIICUSP. **Anais**...2020.

CAMPAGNA, R. et al. Beyond nicotinamide metabolism: Potential role of nicotinamide n-methyltransferase as a biomarker in skin cancers. **Cancers**, v. 13, n. 19, p. 4943, 2021.

CAO, X. et al. High-Yield Recovery of Antioxidant Compounds from *Bambusa chungii* Culms Using Pressurized Hot Water Extraction. **Antioxidants**, v. 11, n. 11, 1 nov. 2022.

CASTRO, C. B. et al. Metabolomics-Based Discovery of Biomarkers with Cytotoxic Potential in Extracts of Myracrodruon urundeuva. **Journal of the Brazilian Chemical Society**, v. 31, n. 4, p. 775–787, 2020.

CÉSPEDES PRIETO, N. E. et al. Análisis del desarrollo innovador para el aprovechamiento de la *Guadua angustifolia* Kunth) en la sustitución de cultivos ilícitos. **Ciencia en Desarrollo**, v. 11, n. 2, p. 97–109, 2020.

CHEN, C. et al. Nicotinamide n-methyltransferase: A potential biomarker for worse prognosis in gastric carcinoma. **American Journal of Cancer Research**, v. 6, n. 3, p. 649–663, 2016.

CHENG, Y. et al. Bamboo leaf: A review of traditional medicinal property, phytochemistry, pharmacology, and purification technology. **Journal of Ethnopharmacology**, v. 306, p. 116166, 2023.

CHITIVA, L. C. et al. Untargeted metabolomics approach and molecular networking analysis reveal changes in chemical composition under the influence of altitudinal variation in bamboo species. **Frontiers in Molecular Biosciences**, v. 10, p. 1192088, 2023.

CHITIVA, L. C. et al. Metabolomic Profiling of *Guadua* Species and its Correlation with

Antioxidant and Cytotoxic Activities. **ACS Omega**, 2024.

CHOI, M. H. et al. Antioxidative and anti-melanogenic activities of bamboo stems (*Phyllostachys nigra* variety *henosis*) via PKA/CREB-mediated MITF downregulation in B16F10 melanoma cells. **International Journal of Molecular Sciences**, v. 19, n. 2, p. 409, 2018.

CHOI, M. K.; SONG, I. S. **Recent advances in the formulation of sphingolipid anticancer therapeutics**. **Journal of Pharmaceutical Investigation**, 2020.

CHUA, L. S.; ABDULLAH, F. I.; AWANG, M. A. Potential of natural bioactive C-glycosyl flavones for antidiabetic properties. In: **Studies in Natural Products Chemistry**. [s.l: s.n.]. v. 64p. 241–261.

COOPER, G. M.; HAUSMAN, R. E. **The Cell: A Molecular Approach 2nd Edition**. [s.l: s.n.].

CORNEJO-BÁEZ, A. A. et al. Chemometrics: a complementary tool to guide the isolation of pharmacologically active natural products. **Drug discovery today**, v. 25, n. 1, p. 27–37, 2019.

CORRÊA, J. K. C.; MORENO, P. R. H. **Atividade antioxidante e anti-tirosinase nas folhas de *Guadua angustifolia* var. *bicolor* Londoño (Bambusoideae:Poaceae)**. 10º Workshop do Mestrado Profissional – Universidade de São Paulo, Instituto de Química. **Anais**...2022.

COSTA, G. M. et al. Isolation of C-glycosylflavonoids with α-glucosidase inhibitory activity from *Passiflora bogotensis* Benth by gradient high-speed counter-current chromatography. **Journal of Chromatography B: Analytical Technologies in the Biomedical and Life Sciences**, v. 990, p. 104–110, 2015.

CRAGG, G. M.; PEZZUTO, J. M. Natural products as a vital source for the discovery of cancer chemotherapeutic and chemopreventive agents. **Med. Princ. Pract.**, v. 25, n. 25,

p. 41–59, 2016.

CRESPO, Y. A. et al. Evaluation of the synergistic effects of antioxidant activity on mixtures of the essential oil from *Apium graveolens* L., *Thymus vulgaris* L. and *Coriandrum sativum* L. using simplex-lattice design. **Heliyon**, v. 5, n. 6, 1 jun. 2019.

CUELLAR BAHAMON, A. Estudio prospectivo de la cadena productiva de la guadua en el sur del departamento del Huila, Colombia. **Revista de Investigación Agraria y Ambiental**, v. 7, n. 2, 2016.

CUVILLIER, O. Sphingosine in apoptosis signaling. **Biochimica et Biophysica Acta**, v. 1585, p. 153–162, 2002.

CVETKOVIĆ, M. et al. Integration of dry-column flash chromatography with NMR and FTIR metabolomics to reveal cytotoxic metabolites from *Amphoricarpos autariatus*. **Talanta**, v. 206, p. 120248, 2020.

DA SILVA, R. R. et al. Propagating annotations of molecular networks using in silico fragmentation. **PLoS Computational Biology**, v. 14, n. 4, p. e1006089, 2018.

DAHABIYEH, L. A. et al. Mass spectrometry-based metabolomics approach and in vitro assays revealed promising role of 2,3-dihydroquinazolin-4(1H)-one derivatives against colorectal cancer cell lines. **European Journal of Pharmaceutical Sciences**, v. 182, 1 mar. 2023.

DAS NEVES COSTA, F.; LEITÃO, G. G. Strategies of solvent system selection for the isolation of flavonoids by countercurrent chromatography. **Journal of Separation Science**, v. 33, n. 3, p. 336–347, fev. 2010.

DEBORDE, C. et al. Plant metabolism as studied by NMR spectroscopy. **Progress in Nuclear Magnetic Resonance Spectroscopy**, v. 102, p. 61–97, 2017.

DEMAIN, A.; VAISHNAV, P. Natural products for cancer chemotherapy. **Microbial Biotechnology**, v. 4, n. 6, p. 687–699, 2011.

DEMARQUE, D. P. et al. Mass spectrometry-based metabolomics approach in the isolation of bioactive natural products. **Scientific Reports**, v. 10, n. 1, p. 1051, 2020.

DEMARQUE, D. P.; ESPINDOLA, L. S. Challenges, Advances and Opportunities in Exploring Natural Products to Control Arboviral Disease Vectors. **Frontiers in Chemistry**, v. 9, p. 979, 15 nov. 2021.

DI GREGORIO, J. et al. Mitochondrial and metabolic alterations in cancer cells. **European Journal of Cell Biology**, v. 101, n. 3, p. 151225, 2022.

DIAS, D. A.; URBAN, S.; ROESSNER, U. A historical overview of natural products in drug discovery. **Metabolites**, v. 2, n. 2, p. 303–336, 2012.

DJOUMBOU FEUNANG, Y. et al. ClassyFire: automated chemical classification with a comprehensive, computable taxonomy. **Journal of Cheminformatics**, v. 8, n. 1, p. 1–20, 2016.

DOS REIS LUZ, L. et al. Metabolomic profile of *Schinopsis brasiliensis* via UPLC-QTOF-MS for identification of biomarkers and evaluation of its cytotoxic potential. **Journal of Chromatography B: Analytical Technologies in the Biomedical and Life Sciences**, v. 1099, n. April, p. 97–109, 2018.

DÜKEL, M.; TAVSAN, Z.; KAYALI, H. A. Flavonoids regulate cell death-related cellular signaling via ROS in human colon cancer cells. **Process Biochemistry**, v. 101, p. 11–25, 2021.

EMAMVERDIAN, A. et al. Application of Bamboo Plants in Nine Aspects. **The Scientific World Journal**, v. 2020, p. 1–9, 2020.

ERNST, M. et al. MolNetEnhancer: Enhanced Molecular Networks by Integrating Metabolome Mining and Annotation Tools. **Metabolites**, v. 9, n. 7, 1 jul. 2019.

ESPINOSA PÉREZ, D. C. **La cadena de la guadua en Colombia**. [s.l: s.n.].

FALCONE FERREYRA, M. L.; RIUS, S. P.; CASATI, P. Flavonoids: Biosynthesis, biological functions, and biotechnological applications. **Frontiers in Plant Science**, v. 3, n. SEP, p. 222, 28 set. 2012.

FRASER, C. M.; CHAPPLE, C. **The Phenylpropanoid Pathway in *Arabidopsis***. [s.l.] American Society of Plant Biologists, 2011. v. 9

FU, Y. et al. Lipid metabolism in cancer progression and therapeutic strategies. **MedComm**, v. 2, n. 1, p. 27–59, 2021.

GAGLIANO, J. et al. Are Brazilian bamboo species helpful for cognition and memory? **Phytomedicine Plus**, v. 2, n. 1, p. 100183, 2022a.

GAGLIANO, J. et al. What is known about the medicinal potential of bamboo? **Advances in Traditional Medicine**, v. 22, n. 3, p. 467–495, 1 set. 2022b.

GAGLIANO, J.; GROMBONE-GUARATINI, M. T.; FURLAN, C. M. Antioxidant potential and HPLC-DAD profile of phenolic compounds from leaves and culms of *Merostachys pluriflora*. **South African Journal of Botany**, v. 115, p. 24–30, 2018.

GANESAN, R.; PRABHAKARAN, V. S.; VALSALA GOPALAKRISHNAN, A. Metabolomic Signatures in Doxorubicin-Induced Metabolites Characterization, Metabolic Inhibition, and Signaling Pathway Mechanisms in Colon Cancer HCT116 Cells. **Metabolites**, v. 12, n. 11, 1 nov. 2022.

GAO, D. et al. Metabonomic study on the antitumor effect of flavonoid derivative 3d in HepG2 cells and its action mechanism. **Talanta**, v. 118, p. 382–388, 2014.

GAO, D. et al. Metabolomics study on the antitumor effect of marine natural compound flexibilide in HCT-116 colon cancer cell line. **Journal of Chromatography B-Analytical Technologies in the Biomedical and Life Sciences**, v. 1014, p. 17–23, 2016.

GLOBOCAN. **Global Cancer Observatory. International Agency for Research on Cancer 2023**.

GOMEZ-LARRAURI, A. et al. **Ceramide metabolism enzymes—therapeutic targets against cancer**. **Medicina (Lithuania)**, 2021.

GOMEZ, J. P. et al. Chemical characterization and antiradical properties of pyroligneous acid from a preserved Bamboo, *Guadua angustifolia* Kunth. **Brazilian Archives of Biology and Technology**, v. 64, p. 1–13, 2021.

GORROCHATEGUI, E. et al. Data analysis strategies for targeted and untargeted LC-MS metabolomic studies: Overview and workflow. **TrAC Trends in Analytical Chemistry**, v. 82, p. 425–442, 2016.

GOVINDAN, B. et al. Secondary metabolites from the unique bamboo, Melocanna baccifera. **Natural Product Research**, v. 33, n. 1, p. 122–125, 2019.

GREEN, L. C. et al. Analysis of nitrate, nitrite, and [15N]nitrate in biological fluids. **Analytical Biochemistry**, v. 126, n. 1, p. 131–138, 1982.

GROMBONE-GUARATINI, M. T. et al. Antioxidant and Photoprotective Properties of Neotropical Bamboo Species. In: **Plant Antioxidants and Health**. [s.l: s.n.]. p. 1–35.

GYAMFI, J.; KIM, J.; CHOI, J. Cancer as a Metabolic Disorder. **International Journal of Molecular Sciences**, v. 23, n. 3, p. 1155, 2022.

HALDIPUR, A. C.; SRIVIDYA, N. A comparative evaluation of in vitro antihyperglycemic potential of Bamboo seed rice (*Bambusa arundinacea*) and Garudan samba (*Oryza sativa*): An integrated metabolomics, enzymatic and molecular docking approach. **Journal of Cereal Science**, v. 99, p. 103200, maio 2021.

HANAHAN, D. **Hallmarks of Cancer: New Dimensions**. **Cancer Discovery**, 2022.

HANAHAN, D.; WEINBERG, R. Hallmarks of Cancer: The Next Generation. **Cell**, v. 144, n. 5, p. 646–674, 2011.

HASEGAWA, T. et al. Antioxidant C-glycosyl flavones from the leaves of Sasa kurilensis

var. gigantea. **Phytochemistry**, v. 69, n. 6, p. 1419–1424, 2008.

HEGEDŰS, C. et al. Redox control of cancer cell destruction. **Redox Biology**, v. 16, 2018.

HOLSER, R. A. Principal Component Analysis of Phenolic Acid Spectra. **ISRN Spectroscopy**, v. 2012, p. 1–5, 2012.

HOSSAIN, M. S. et al. Colorectal Cancer: A Review of Carcinogenesis, Global Epidemiology, Current Challenges, Risk Factors, Preventive and Treatment Strategies. **Cancers**, v. 14, n. 7, p. 1732, 2022.

HU, C.; ZHANG, Y.; KITTS, D. D. Evaluation of antioxidant and prooxidant activities of bamboo *Phyllostachys nigra* var. *Henonis* leaf extract in vitro. **Journal of Agricultural and Food Chemistry**, v. 48, n. 8, p. 3170–3176, 2000.

HUBERT, J.; NUZILLARD, J.-M.; RENAULT, J.-H. Dereplication strategies in natural product research: How many tools and methodologies behind the same concept? **Phytochemistry Reviews**, v. 16, n. 1, p. 55–95, 2017.

IBRAHIM, A. et al. Biological Activities of Different Species of the Genus *Phyllostachys*. **Records of Pharmaceutical and Biomedical Sciences**, v. 5, n. 1, p. 64–73, 2021.

JIANG, L. et al. Extraction and characterization of phenolic compounds from bamboo shoot shell under optimized ultrasonic-assisted conditions: A potential source of nutraceutical compounds. **Food and Bioprocess Technology**, v. 12, p. 1741–1755, 2019.

JIANG, W. J. et al. Stereospecific inhibition of nitric oxide production in macrophage cells by flavanonols: Synthesis and the structure-activity relationship. Part 2. **Bioorganic and Medicinal Chemistry**, v. 25, n. 16, p. 4277–4284, 2017.

JIANG, Y. X. et al. Total Flavonoids from Radix Glycyrrhiza Exert Anti-Inflammatory and Antitumorigenic Effects by Inactivating iNOS Signaling Pathways. **Evidence-based Complementary and Alternative Medicine**, v. 2018, p. 6714282, 2018.

KAESER, M. D.; PEBERNARD, S.; IGGO, R. D. Regulation of p53 Stability and Function in HCT116 Colon Cancer Cells. **Journal of Biological Chemistry**, v. 279, n. 9, p. 7598–7605, 27 fev. 2004.

KATIYAR, C. et al. Drug discovery from plant sources: An integrated approach. **Ayu**, v. 33, n. 1, p. 10–19, 2012.

KENNEDY, L. et al. Role of glutathione in cancer: From mechanisms to therapies. **Biomolecules**, v. 10, n. 10, p. 1–27, 2020.

KESKES, H. et al. LC–MS–MS and GC–MS analyses of biologically active extracts of Tunisian Fenugreek (*Trigonella foenum-graecum* L.) Seeds. **Journal of Food Measurement and Characterization**, v. 12, n. 1, p. 209–220, 1 mar. 2018.

KIM, C. Y. et al. Rapid Identification of Radical Scavenging Phenolic Compounds from Black Bamboo Leaves using High-Performance Liquid Chromatography Coupled to an Online ABTS+-Based Assay. **Journal of the Korean Society for Applied Biological Chemistry**, v. 52, n. 6, p. 613–619, 2009.

KIM, H. K. et al. Effects of naturally occurring flavonoids on nitric oxide production in the macrophage cell line RAW 264.7 and their structure-activity relationships. **Biochemical Pharmacology**, v. 58, n. 5, p. 759–765, 1999.

KIM, J. S. et al. Evaluation of antioxidant and anticancer activity of steam extract from the bamboo species. **Journal of the Korean Wood Science and Technology**, v. 42, n. 5, p. 543–554, 2014.

KIM, M. Y. Sasa quelpaertensis Nakai extract induces p53-independent apoptosis via the elevation of nitric oxide production in human HCT116 colon cancer cells. **Oncology Letters**, v. 19, n. 4, p. 3027–3034, 2020.

KO, H. C. et al. Seasonal variations in the phenolic compounds and antioxidant activity of *Sasa quelpaertensis*. **Industrial Crops and Products**, v. 122, p. 506–512, 15 out. 2018.

KOPARDE, A. A.; DOIJAD, R. C.; MAGDUM, C. S. Natural products in drug discovery. In: **Pharmacognosy-medicinal plants**. [s.l.] IntechOpen, 2019.

KORDE CHOUDHARI, S. et al. Nitric oxide and cancer: A review. **World Journal of Surgical Oncology**, v. 11, p. 118, 2013.

KUMAR, R. et al. Metabolomics for Plant Improvement: Status and Prospects. **Frontiers in Plant Science**, v. 8, p. 1302, 2017.

KUMAR, S.; PANDEY, A. K. Chemistry and biological activities of flavonoids: An overview. **The Scientific World Journal**, v. 2013, 2013.

KUMBHARE, V. HPLC estimation of phenolic acids in leaves of some central indian bamboo species. **Journal of Bamboo and Rattan**, v. 8, n. 1–2, p. 23–29, 2009.

LI, K. P. et al. Variations of flavone glycosides profile underscore the necessity of quality control of prepared Microctis folium slices. **Evidence-based Complementary and Alternative Medicine**, v. 2020, p. 8887489, 2020.

LI, X. et al. Simultaneous determination of flavonoids from bamboo leaf extracts using liquid chromatography-tandem mass spectrometry. **Revista Brasileira de Farmacognosia**, v. 31, p. 347–352, 2021.

LI, X. Y. et al. Nicotinamide N-Methyltransferase: A Promising Biomarker and Target for Human Cancer Therapy. **Frontiers in Oncology**, v. 12, p. 894744, 2022.

LIU, W. et al. The Flavonoid Biosynthesis Network in Plants. **International Journal of Molecular Sciences**, v. 22, n. 23, 1 dez. 2021.

LONDOÑO, X. El bambú en Colombia. **Biotecnología Vegetal**, v. 11, n. 3, p. 143–154, 4 jul. 2011.

LONDOÑO, X. Hidden treasures in the Amazon region of Colombia, Ecuador and Peru: Diversity and uses (Poaceae: Bambusoideae). **Proceedings of 12th World Bamboo**

**Congress 12 th World Bamboo Congress Taiwan**, p. 1–38, 2024.

LONDOÑO, X.; RUIZ-SANCHEZ, E. A new species of *Guadua* (Poaceae: Bambusoideae: Bambuseae: Guaduinae) from the Colombian Amazon. **Phytotaxa**, v. 638, n. 3, p. 227–236, 5 mar. 2024.

LOZANO-PUENTES, S. H. et al. *Guadua angustifolia* Kunth leaves as a source for bioactive phenolic compounds: Optimization of ultrasound-assisted extraction using response surface methodology and antioxidant activities. **SSRN Heliyon**, p. 1–14, 2023.

LU, X. M.; LONG, H. Nicotinamide N-methyltransferase as a potential marker for cancer. **Neoplasma**, v. 65, n. 5, p. 656–663, 2018.

LU, Y.; PANG, Z.; XIA, J. Comprehensive investigation of pathway enrichment methods for functional interpretation of LC-MS global metabolomics data. **Briefings in Bioinformatics**, v. 24, n. 1, p. 1–15, 2023.

LUAN, H. et al. statTarget: A streamlined tool for signal drift correction and interpretations of quantitative mass spectrometry-based omics data. **Analytica Chimica Acta**, v. 1036, p. 66–72, 2018.

LUO, G. Y. et al. Antioxidant compounds from ethanol extracts of bamboo (Neosinocalamus affinis) leaves. **Journal of Asian Natural Products Research**, v. 17, n. 3, p. 248–255, 2015.

MA, J. et al. Interactions of Flavonoids with Biomacromolecules. **Current Organic Chemistry**, v. 15, n. 15, p. 2627–2640, 2011.

MA, N. et al. Antioxidant and compositional HPLC analysis of three common bamboo leaves. **Molecules**, v. 25, n. 2, p. 409, 2020a.

MA, Y. et al. Phenolics and antioxidant activity of bamboo leaves soup as affected by in vitro digestion. **Food and Chemical Toxicology**, v. 135, p. 110941, 1 jan. 2020b.

MADJI HOUNOUM, B. et al. Liquid chromatography-high-resolution mass spectrometry-based cell metabolomics: Experimental design, recommendations, and applications. **TrAC - Trends in Analytical Chemistry**, v. 75, p. 118–128, 1 jan. 2016.

MARCOCCI, L. et al. The nitric oxide-scavenging properties of Ginkgo biloba extract EGb 761. **Biochemical and Biophysical Research Communications**, v. 201, n. 2, p. 748–755, 1994.

MARKLEY, J. L. et al. The future of NMR-based metabolomics. **Current Opinion in Biotechnology**, v. 43, p. 34–40, 2017.

MCGURK, S. The Molecular Biology of Cancer: A Bridge from Bench to Bedside – Second edition The Molecular Biology of Cancer: A Bridge from Bench to Bedside – Second edition. **Nursing Standard**, v. 28, n. 1, 2013.

MEJÍA GALLÓN, A. et al. Identificación de compuestos volátiles del vinagre de *Guadua angustifolia* Kuth. **Revista Cubana de Plantas Medicinales**, v. 2, n. 16, p. 190–201, 2011.

MEJÍA GALLÓN, A.; CADAVID TORRES, E.; GALLARDO CABRERA, C. Actividad antiséptica de vinagre de *Guadua angustifolia* Kunth. **Revista cubana de plantas medicinales**, v. 16, n. 3, p. 244–252, 2011.

MOHIMANI, H. et al. Dereplication of peptidic natural products through database search of mass spectra. **Nature Chemical Biology**, v. 13, n. 1, p. 30–37, 2017.

MORALES NOREÑA, N.; SANCHEZ VALLEJO, L. **Contribución al estudio fitoquímico de las hojas de *Guadua angustifolia* Kunth**. [s.l.] Universidad del Quindío, 2008.

MORENO, P. R. H. et al. **PP11. Chemical composition and antimicrobial properties of the essential oils of two *Guadua* Kunth species (Poaceae-Bambusoideae)**. Chemistry and Technology. **Anais**...2018.

MOSMANN, T. Rapid colorimetric assay for cellular growth and survival: Application to

proliferation and cytotoxicity assays. **Journal of Immunological Methods**, v. 65, n. 1–2, p. 55–63, 1983.

MOSQUERA MARTÍNEZ, O. M. et al. Caracterización fitoquímica de los extractos de acetona y contenido de lignina en culmos de *Guadua angustifolia*. **Recursos Naturales y Ambiente**, v. 65, n. 65, p. 10–15, 2012.

MOSQUERA, O. M. et al. Caracterización fitoquímica, determinación del contenido de lignina y la actividad antioxidante de los culmos de *Guadua angustifolia* Kunth. **Revista Facultad de Ciencias Básicas**, v. 11, n. 2, p. 124–135, 2016.

MOURADOV, A.; SPANGENBERG, G. Flavonoids: a metabolic network mediating plants adaptation to their real estate. **Frontiers in Plant Science**, v. 5, n. November, p. 1–16, 10 nov. 2014.

MUSAOGULLARI, A.; MANDATO, A.; CHAI, Y. C. Role of Glutathione Depletion and Reactive Oxygen Species Generation on Caspase-3 Activation: A Study With the Kinase Inhibitor Staurosporine. **Frontiers in Physiology**, v. 11, p. 998, 2020.

MUSHTAQ, S. et al. Natural products as reservoirs of novel therapeutic agents. **EXCLI journal**, v. 17, p. 420–451, 2018.

NEWMAN, D. J.; CRAGG, G. M. Natural products as sources of new drugs over the nearly four decades from 01/1981 to 09/2019. **J. Nat. Prod.**, v. 83, n. 3, p. 770–803, 2020.

NI, Q. et al. Seasonal variations of the antioxidant composition in ground bamboo *Sasa argenteastriatus* leaves. **International Journal of Molecular Sciences**, v. 13, n. 2, p. 2249–2262, 20 fev. 2012.

NI, Q. et al. Altitudinal variation of antioxidant components and capability in *Indocalamus latifolius* (Keng) McClure leaf. **Journal of Nutritional Science and Vitaminology**, v. 59, n. 4, p. 336–342, 2013.

NIKAS, I. P.; PASCHOU, S. A.; RYU, H. S. The role of nicotinamide in cancer

chemoprevention and therapy. **Biomolecules**, v. 10, n. 3, p. 477, 2020.

NORDIN, M. L. et al. In vitro investigation of cytotoxic and antioxidative activities of *Ardisia crispa* against breast cancer cell lines, MCF-7 and MDA-MB-231. **BMC Complementary and Alternative Medicine**, v. 18, n. 1, p. 1–10, 12 mar. 2018.

OWOLABI, M. S.; LAJIDE, L.; MOSES OWOLABI, C. S. Preliminary phytochemical screening and antimicrobial activity of crude extracts of Bambusa vulgaris Schrad. Ex J.C. Wendl. (Poaceae) from southwestern Nigeria. **American Journal of Essential Oils and Natural Products**, v. 3, n. 1, p. 42–45, 2015.

OZAROWSKI, M. et al. Comparison of bioactive compounds content in leaf extracts of *Passiflora incarnata*, *P. caerulea* and *P. alata* and in vitro cytotoxic potential on leukemia cell lines. **Revista Brasileira de Farmacognosia**, v. 28, n. 2, p. 179–191, 2018.

PACHECO-HERNÁNDEZ, Y. et al. Influence of environmental factors on the genetic and chemical diversity of *Brickellia veronicifolia* populations growing in fragmented shrublands from Mexico. **Plants**, v. 10, n. 2, p. 1–21, 8 fev. 2021.

PANCHE, A. N.; DIWAN, A. D.; CHANDRA, S. R. Flavonoids: An overview. **Journal of Nutritional Science**, v. 5, p. 1–15, 8 jan. 2016.

PANDA, A.; PARIDA, A. K.; RANGANI, J. Advancement of Metabolomics Techniques and Their Applications in Plant Science: Current Scenario and Future Prospective. In: **Plant Metabolites and Regulation Under Environmental Stress**. [s.l.] Elsevier, 2018. p. 1–36.

PANG, Z. et al. Using MetaboAnalyst 5.0 for LC–HRMS spectra processing, multi-omics integration and covariate adjustment of global metabolomics data. **Nature Protocols**, v. 17, n. 8, p. 1735–1761, 17 jun. 2022.

PARK, H. S. et al. Antioxidant flavone glycosides from the leaves of Sasa borealis. **Archives of Pharmacal Research**, v. 30, n. 2, p. 161–166, 2007.

PINHEIRO, P.; JUSTINO, G. Structural Analysis of Flavonoids and Related Compounds - A Review of Spectroscopic Applications. In: **Phytochemicals - A Global Perspective of Their Role in Nutrition and Health**. [s.l: s.n.].

PLATZER, M. et al. Radical Scavenging Mechanisms of Phenolic Compounds: A Quantitative Structure-Property Relationship (QSPR) Study. **Frontiers in Nutrition**, v. 9, 4 abr. 2022.

PRIYA, S.; SATHEESHKUMAR, P. Natural products from plants: Recent developments in phytochemicals, phytopharmaceuticals, and plant-based neutraceuticals as anticancer agents. **Functional and Preservative Properties of Phytochemicals**, p. 145–163, 2020.

RAJPUT, A. et al. Characterization of HCT116 Human Colon Cancer Cells in an Orthotopic Model. **Journal of Surgical Research**, v. 147, n. 2, p. 276–281, 15 jun. 2008.

RAMSDEN, D. B. et al. Nicotinamide N-methyltransferase in health and cancer. **International Journal of Tryptophan Research**, v. 10, p. 1–19, 2017.

RE, R. et al. Antioxidant activity applying an improved ABTS radical cation decolorization assay. **Free Radical Biology and Medicine**, v. 26, n. 9–10, 1999.

RINSCHEN, M. M. et al. Identification of bioactive metabolites using activity metabolomics. **Nature Reviews Molecular Cell Biology**, v. 20, n. 6, p. 353–367, 2019.

RUIZ-SANCHEZ, E. et al. **Diversity, distribution, and classification of neotropical woody bamboos (Poaceae: Bambusoideae) in the 21st/s century**. **Botanical Sciences**, 2021.

SABHARWAL, S. S.; SCHUMACKER, P. T. Mitochondrial ROS in cancer: Initiators, amplifiers or an Achilles' heel? **Nature Reviews Cancer**, v. 14, n. 11, p. 709–721, 2014.

SAEED, N.; KHAN, M. R.; SHABBIR, M. Antioxidant activity, total phenolic and total flavonoid contents of whole plant extracts *Torilis leptophylla* L. **BMC Complementary and**

**Alternative Medicine**, v. 12, 16 nov. 2012.

SAITO, K. et al. The flavonoid biosynthetic pathway in Arabidopsis: Structural and genetic diversity. **Plant Physiology and Biochemistry**, v. 72, p. 21–34, 1 nov. 2013.

SAK, K. Cytotoxicity of dietary flavonoids on different human cancer types. **Pharmacognosy Reviews**, v. 8, n. 16, p. 122–146, 2014.

SANTOS, C. R.; SCHULZE, A. Lipid metabolism in cancer. **FEBS Journal**, v. 279, n. 15, p. 2610–2623, ago. 2012.

SCHYMANSKI, E. L. et al. **Identifying small molecules via high resolution mass spectrometry: Communicating confidence**. **Environmental Science and Technology**, 18 fev. 2014.

SHAO, S. et al. Characterization and Identification of the Major Flavonoids in Phyllostachys edulis Leaf Extract by UPLC-QTOF-MS/MS. **Acta Chromatographica**, v. 32, n. 4, p. 228–237, 1 dez. 2020.

SHAO, X. et al. Application of metabolomics to investigate the antitumor mechanism of flavopiridol in MCF-7 breast cancer cells. **Journal of Chromatography B: Analytical Technologies in the Biomedical and Life Sciences**, v. 1025, p. 40–47, 1 jul. 2016.

SHARIFI-RAD, J. et al. Natural Coumarins: Exploring the Pharmacological Complexity and Underlying Molecular Mechanisms. **Oxidative Medicine and Cellular Longevity**, v. 2021, p. 6492346, 2021.

SILVA, C. F. M. et al. Challenges with chromone as a privileged scaffold in drug discovery. **Expert Opinion on Drug Discovery**, v. 13, n. 9, p. 795–798, 2018.

SILVA DE OLIVEIRA, D. C. **Composição química e atividades biológicas de extratos de *Guadua angustifolia* Kunth**. [s.l.] Universidade de São Paulo, 2019.

ŚLIWKA-KASZYŃSKA, M.; ANUSIEWICZ, I.; SKURSKI, P. The Mechanism of a Retro-

Diels–Alder Fragmentation of Luteolin: Theoretical Studies Supported by Electrospray Ionization Tandem Mass Spectrometry Results. **Molecules**, v. 27, n. 3, p. 1032, 2022.

SU, Y. et al. Isoschaftoside Reverses Nonalcoholic Fatty Liver Disease via Activating Autophagy In Vivo and In Vitro. **Evidence-based Complementary and Alternative Medicine**, v. 2022, 2022.

SUGA, A. et al. Two lignan dimers from bamboo stems (*Phyllostachys edulis*). **Phytochemistry**, v. 64, n. 5, p. 991–996, 2003.

SULTANA, N.; LEE, N. H. New phenylpropanoids from Sasa quelpaertensis Nakai with tyrosinase inhibition activities. **Bulletin of the Korean Chemical Society**, v. 30, n. 8, p. 1729–1732, 2009.

SULTANA, N.; LEE, N. H. A new alkene glycoside from the leaves of *Sasa quelpaertensis* Nakai. **Bulletin of the Korean Chemical Society**, v. 31, n. 4, p. 1088–1090, 2010.

SUN, J. et al. Simultaneous HPTLC analysis of flavonoids in the leaves of three different species of bamboo. **Journal of Planar Chromatography - Modern TLC**, v. 23, n. 1, p. 40–45, 2010.

SUNG, H. et al. Global Cancer Statistics 2020: GLOBOCAN Estimates of Incidence and Mortality Worldwide for 36 Cancers in 185 Countries. **CA: A Cancer Journal for Clinicians**, v. 71, n. 3, 2021.

TAHIR, A. T. et al. Metabolomic approaches in plant research. In: **Essentials of Bioinformatics, Volume III: In Silico Life Sciences: Agriculture**. [s.l: s.n.]. p. 109–140.

TANAKA, A. et al. Biological Activities and Phytochemical Profiles of Extracts from Different Parts of Bamboo (*Phyllostachys pubescens*). **Molecules**, v. 19, n. 6, p. 8238–8260, 2014.

TAWFIKE, A. F.; VIEGELMANN, C.; EDRADA-EBEL, R. Metabolomics and dereplication strategies in natural products. In: **Metabolomics Tools for Natural Product Discovery**.

[s.l.] Springer, 2013. p. 227–244.

THEODORIDIS, G. A. et al. Liquid chromatographic methods combined with mass spectrometry in metabolomics. In: **Proteomic and Metabolomic Approaches to Biomarker Discovery**. [s.l.] Elsevier, 2020. p. 149–169.

TROALEN, L. G. et al. Historical textile dyeing with *Genista tinctoria* L.: A comprehensive study by UPLC-MS/MS analysis. **Analytical Methods**, v. 6, n. 22, p. 8915–8923, 21 nov. 2014.

TUNDIS, R. et al. Anti-Inflammatory and Antioxidant Effects of Leaves and Sheath from Bamboo (*Phyllostacys edulis* J. Houz). **Antioxidants**, v. 12, n. 6, p. 1239, 8 jun. 2023.

VALENCIA, M. et al. Extracción de fracciones con actividad antioxidante en hojas de *Guadua angustifolia* Kunth. **Revista Cubana de Plantas Medicinales**, v. 16, n. 4, p. 364–373, 2011.

VAN HOYWEGHEN, L. et al. Antioxidant flavone glycosides from the leaves of *Fargesia robusta*. **Journal of Natural Products**, v. 73, n. 9, p. 1573–1577, 2010.

VAN HOYWEGHEN, L. et al. In vitro inhibition of the transcription factor NF-κB and cyclooxygenase by Bamboo extracts. **Phytotherapy Research**, v. 28, n. 2, p. 224–230, 2014.

VAN HOYWEGHEN, L.; DEFORCE, D.; HEYERICK, A. **Antioxidant Capacity and Secondary Metabolites of 12 Bamboo Species**. I International Symposium on Genetic Resources of Bamboos and Palms and III International Symposium on Ornamental Palms 1003. **Anais**...2010.

VAN HOYWEGHEN, L. VAN et al. Phenolic compounds and anti-oxidant capacity of twelve morphologically heterogeneous bamboo species. **Phytochemical Analysis**, v. 23, n. 5, p. 433–443, 2012.

VANINI, F.; KASHFI, K.; NATH, N. The dual role of iNOS in cancer. **Redox Biology**, v. 6,

2015.

VERPOORTE, R.; CHOI, Y. H.; KIM, H. K. Metabolomics: what's new? **Flavour and Fragrance Journal**, v. 25, n. 3, p. 128–131, 2010.

VINAIXA, M. et al. Mass spectral databases for LC/MS- and GC/MS-based metabolomics: State of the field and future prospects. **Trac-Trends in Analytical Chemistry**, v. 78, p. 23–35, 2016.

VORONTSOVA, M. S. et al. **World Checklist of Bamboos and Rattans**. Beijing: [s.n.].

VUKOVIC, N. L. et al. Cytotoxic, proapoptotic and antioxidative potential of flavonoids isolated from propolis against colon (HCT-116) and breast (MDA-MB-231) cancer cell lines. **Food Research International**, v. 106, p. 71–80, 1 abr. 2018.

WAGNER, H. et al. **Plant drug analysis: A Thin Layer Chromatography Atlas**. 1. ed. Munchen, Germany: Springer Science & Business Media, 1996.

WANG, J. et al. Rapid Screening for Flavone *C*-Glycosides in the Leaves of Different Species of Bamboo and Simultaneous Quantitation of Four Marker Compounds by HPLC-UV/DAD. **International Journal of Analytical Chemistry**, v. 2012, p. 1–8, 2012a.

WANG, J. et al. TLC screening for antioxidant activity of extracts from fifteen bamboo species and identification of antioxidant flavone glycosides from leaves of bambusa. textilis mcclure. **Molecules**, v. 17, n. 10, p. 12297–12311, 2012b.

WANG, L. et al. A protocol to compare methods for untargeted metabolomics. In: **Metabolic Signaling**. [s.l.] Springer, 2019. p. 1–15.

WANG, L. et al. Dietary flavonoids and the altitudinal preference of wild giant pandas in Foping National Nature Reserve, China. **Global Ecology and Conservation**, v. 22, p. e00981, 2020a.

WANG, M. et al. **Sharing and community curation of mass spectrometry data with**

**Global Natural Products Social Molecular Networking**. **Nature Biotechnology**Nature Publishing Group, , 9 ago. 2016. Disponível em: <https://www.nature.com/articles/nbt.3597>. Acesso em: 2 dez. 2022

WANG, S. et al. Simultaneous determination of 12 coumarins in bamboo leaves by HPLC. **Journal of AOAC International**, v. 96, n. 5, p. 942–946, 2013.

WANG, T. YANG; LI, Q.; BI, K. SHUN. Bioactive flavonoids in medicinal plants: Structure, activity and biological fate. **Asian Journal of Pharmaceutical Sciences**, v. 13, n. 1, p. 12–23, 2018.

WANG, W. et al. Complex roles of nicotinamide N-methyltransferase in cancer progression. **Cell Death and Disease**, v. 13, n. 3, p. 267, 2022a.

WANG, Y. et al. A systematic review on the composition, storage, processing of bamboo shoots: Focusing the nutritional and functional benefits. **Journal of Functional Foods**, v. 71, p. 104015, 2020b.

WANG, Y. et al. Efficient purification of flavonoids from bamboo shoot residues of *Phyllostachys edulis* by macroporous resin and their hypoglycemic activity. **Food Chemistry: X**, v. 16, p. 100505, 2022b.

WRÓBLEWSKA, K. B. et al. Medicinal properties of bamboos. In: PERVEEN, S. (Ed.). **Pharmacognosy-medicinal plants**. Saudi Arabia: IntechOpen, 2018. p. 1–18.

WRÓBLEWSKA, K. B. et al. In vitro antioxidant and photoprotective activity of five native Brazilian bamboo species. **Industrial Crops and Products**, v. 130, p. 208–215, 1 abr. 2019.

XI, Y.; XU, P. Global colorectal cancer burden in 2020 and projections to 2040. **Translational Oncology**, v. 14, n. 10, 2021.

XIA, X. et al. Anti-Colon Cancer Activity of Dietary Phytochemical Soyasaponin I and the Induction of Metabolic Shifts in HCT116. **Molecules**, v. 27, n. 14, 1 jul. 2022.

XIE, L. et al. Comparison of Flavonoid O-Glycoside, C-Glycoside and Their Aglycones on Antioxidant Capacity and Metabolism during In Vitro Digestion and In Vivo. **Foods**, v. 11, n. 6, 2022.

XU, W. et al. The role of nitric oxide in cancer. **Cell Research**, v. 12, n. 5–6, p. 311–320, 2002.

XU, X.; LAI, Y.; HUA, Z. C. Apoptosis and apoptotic body: Disease message and therapeutic target potentials. **Bioscience Reports**, v. 39, n. 1, 2019.

YANG, J. H. et al. Potent Anti-Inflammatory and Antiadipogenic Properties of Bamboo (Sasa coreana Nakai) Leaves Extract and Its Major Constituent Flavonoids. **Journal of Agricultural and Food Chemistry**, v. 65, n. 31, p. 6665–6673, 2017.

YANSEN, I. A. et al. Potential of Bamboo Shoots against Breast Cancer: A Review. **Malaysian Journal of Medicine and Health Sciences**, v. 19, n. SUPP3, p. 144–148, 2023.

YE, S. et al. Isolation, Characterization of Bamboo Leaf Flavonoids by Size Exclusion Chromatography and Their Antioxidant Properties. **Chemistry and Biodiversity**, v. 19, n. 9, p. e202200506, 1 set. 2022.

YESHI, K. et al. **Plant Secondary Metabolites Produced in Response to Abiotic Stresses Has Potential Application in Pharmaceutical Product Development**. **Molecules**Multidisciplinary Digital Publishing Institute (MDPI), , 2022.

YI, L. et al. Chemometric methods in data processing of mass spectrometry-based metabolomics: A review. **Analytica Chimica Acta**, v. 914, p. 17–34, 2016.

YOON, D. et al. Metabolomics reveals that *Curcuma longa* and demethoxycurcumin inhibit HCT116 human colon cancer cell growth. **Applied Biological Chemistry**, v. 66, n. 1, 1 dez. 2023a.

YOON, H. et al. Nicotinamide enhances osteoblast differentiation through activation of the

mitochondrial antioxidant defense system. **Experimental and Molecular Medicine**, v. 55, n. 7, 2023b.

YU, Y. et al. Fabrication, material properties, and application of bamboo scrimber. **Wood Science and Technology**, v. 49, n. 1, p. 83–98, 1 jan. 2015.

YU, Y. et al. Bamboo Leaf Flavonoids Extracts Alleviate Oxidative Stress in HepG2 Cells via Naturally Modulating Reactive Oxygen Species Production and Nrf2-Mediated Antioxidant Defense Responses. **Journal of Food Science**, v. 84, n. 6, p. 1609–1620, 1 jun. 2019.

YUAN, T. et al. Characterization and identification of flavonoids from Bambusa chungii leaves extract by UPLC-ESI-Q-TOF-MS/MS. **Acta Chromatographica**, v. 33, n. 3, p. 281–294, 2021.

YULIANA, N. D. et al. Metabolomics for bioactivity assessment of natural products. **Phytotherapy Research**, v. 25, n. 2, p. 157–169, 2011.

ZEB, A. Concept, mechanism, and applications of phenolic antioxidants in foods. **Journal of Food Biochemistry**, v. 44, n. 9, 1 set. 2020.

ZHANG, A. et al. Cell metabolomics. **OMICS A Journal of Integrative Biology**, v. 17, n. 10, p. 495–501, 1 out. 2013a.

ZHANG, J. G. et al. Nicotinamide prohibits proliferation and enhances chemosensitivity of pancreatic cancer cells through deregulating SIRT1 and Ras/Akt pathways. **Pancreatology**, v. 13, n. 2, p. 140–146, 2013b.

ZHANG, L. et al. Study on Synergistic Antioxidant Effect of Typical Functional Components of Hydroethanolic Leaf Extract from *Ginkgo Biloba* In Vitro. **Molecules**, v. 27, n. 2, 1 jan. 2022.

ZHANG, Y. et al. Isolation and purification of four flavone *C*-glycosides from antioxidant of bamboo leaves by macroporous resin column chromatography and preparative high-

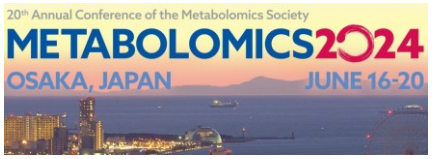
performance liquid chromatography. **Food Chemistry**, v. 107, n. 3, p. 1326–1336, 2008.

ZHANG, Z. et al. Integrated Whole Transcriptome Profiling and Bioinformatics Analysis for Revealing Regulatory Pathways Associated With Quercetin-Induced Apoptosis in HCT-116 Cells. **Frontiers in Pharmacology**, v. 10, p. 446985, 2019.

ZHAO, J. et al. Promoting liver cancer cell apoptosis effect of Tribulus terrestris L. via reducing sphingosine level was confirmed by network pharmacology with metabolomics. **Heliyon**, v. 9, n. 6, p. e17612, 1 jun. 2023.

ZHOU, S. et al. Variations in Flavonoid Metabolites Along Altitudinal Gradient in a Desert Medicinal Plant *Agriophyllum squarrosum*. **Frontiers in Plant Science**, v. 12, p. 683265, 30 jun. 2021.

## PARTICIPATION IN SCIENTIFIC EVENTS AND AWARDS




**20th Annual Conference of the Metabolomics Society – Metabolomics 2024**, Osaka – Japan, June 16-20, 2024. Metabolomic analysis of chemical composition and exploration of biological potential in bamboo of the genus *Guadua*. Luis Carlos Chitiva, Paula Rezende Teixeira, Hair Santiago Lozano-Puentes, Jessica Rodrigues Pereira de Oliveira Borlot, Rodrigo de Almeida Romagna, Rodrigo Rezende Kitagawa, Lucía Ana Díaz-Ariza, Ximena Londoño, Leticia Costa-Lotufo, Juliet Angélica Prieto, Geison Modesti Costa, **Ian Castro-Gamboa**. *Oral presentation – Co-author.*




**1st Latin American Metabolic Profiling Society Podium,** Bogotá – Colombia, November 24, 2023. Metabolomics-Based Correlation Analysis of Chemical Profiles and Cytotoxic Activity in Bamboo Leaf Extracts (BLEs) of the Genus *Guadua* Kunth. **Luis Carlos Chitiva**, Paula Rezende Teixeira, Tiago F. Leao, Ximena Londoño, Leticia Lotufo, Juliet Angélica Prieto, Geison Modesti Costa, Ian Castro-Gamboa. *Oral presentation – Author.*




**9th Brazilian Conference on Natural Products / XXXV RESEM**, Salvador – Bahía, Brazil, October 24-27, 2023. Metabolomics Approach Applied to the Analysis of the Chemical Composition of Bamboos Belonging to the Genus *Guadua* and its Correlation with Cytotoxic Activity. **Luis Carlos Chitiva**, Paula Rezende Teixeira, Tiago F. Leao, Ximena Londoño, Leticia Lotufo, Juliet Angélica

Prieto, Ian Castro-Gamboa, Geison Modesti Costa. *Oral presentation – Author.*




**IV Lamps Meeting Latin American Metabolic Profiling Society (LAMPS)**, Cartagena, Colombia, November 2-4, 2022. Untargeted phyto-metabolomics using LC-MS-QTOF reveals the influence of altitudinal variation in chemical composition of bamboo species. **Luis Carlos Chitiva**, Santiago Lozada, Tiago Leao, Mónica Cala, Juliet Angélica Prieto, Ian Castro-Gamboa, Geison Modesti Costa. *Poster presentation – Author.*




**IV Lamps Meeting Latin American Metabolic Profiling Society (LAMPS)**, Cartagena, Colombia, November 2-4, 2022. Metabolic profiling of ethanolic extracts from Colombian species of *Guadua* (Poaceae). **Luis Carlos Chitiva**, Ximena Londoño, Joao Bronzel, Juliana Rodrigues, Ian Castro-Gamboa, Geison Modesti Costa. *Poster presentation – Author.*




**7 SIBGUADUA Simposio Internacional del Bambú y la Guadua**, Lima, Perú, September 15-17, 2022. Análisis del perfil químico de *Guadua* spp. encontrada en guaduales colombianos. Luis Carlos Chitiva, Hair Santiago Lozano, Ximena Londoño, Juliet A. Prieto Rodríguez, Lucía Ana Díaz, **Geison Modesti Costa**. *Presentación oral – Co-author.*




**I Congreso Internacional Programa GAT**, Bogotá, Colombia, November 30, and December 1, 2021. Perfil metabólico preliminar de extractos vegetales con posible potencial citotóxico. **Luis Carlos Chitiva**, Laura Rojas, Susana Fiorentino, Juliet Angélica Prieto, Geison Modesti Costa. *Oral presentation – Author.*




**8th Brazilian Conference on Natural Products**, Goiás, Brasil, November 9-12, 2021. Cytotoxic activity and preliminary metabolic profile of Colombian plant extracts. **Luis Carlos Chitiva**, Laura Rojas, Susana Fiorentino, Juliet Angélica Prieto, Geison Modesti Costa. *Poster presentation – Author.*




**XVI Congreso La Investigación en la Pontificia Universidad Javeriana**, Bogotá, Colombia, September 15-16, 2021. Perfilamiento químico de plantas colombianas con posible potencial citotóxico. **Luis Carlos Chitiva**, Laura Rojas, Susana Fiorentino, Geison Modesti Costa. *Oral presentation – Author.*

## TRAINING COURSES

- Curso Metabolómica por espectrometría de masas: Fundamentos, diseño experimental y herramientas de procesamiento de datos (22 al 25 de marzo de 2022). Universidad de los Andes – MetCore – Educación Continuada.

- Curso Resonancia Magnética Nuclear de Productos Naturales y Metabolómica (28 de marzo al 08 de abril de 2022). Universidad Autónoma del Estado de Morelos y Universidad de Costa Rica.

- Seminario Taller RMN y Metabolómica (26 al 27 de mayo de 2022). Universidad Nacional de Colombia.

- Curso Mass spectrometry as an important tool in multiomics analysis llevado a cabo durante los días 20 de julio al 01 de agosto de 2023 en el Instituto de Química de la Universidad Estadual Paulista “Júlio de Mesquita Filho” en la ciudad de Araraquara – São Paulo / Brasil.

- Curso First school of integrated metabolomics llevado a cabo durante los días 11 al 15 de septiembre de 2023 en el Instituto de Química de la Universidad Estadual Paulista “Júlio de Mesquita Filho” en la ciudad de Araraquara – São Paulo / Brasil.

**FINANCED PROJECTS**

- Proyecto Vicerrectoría de Investigación presentado en la convocatoria interna Apoyo a proyectos de tesis doctorales “Evaluación de las alteraciones metabólicas en células de cáncer de colon HCT-116 inducidas por un extracto de bambú” (Propuesta ID 20834).

- Proyecto MINCIENCIAS-FAPESP convenio Colombia-Brasil “Estudio de la diversidad química de Passifloras en Colombia y Brasil: aproximación metabolómica y potencial biológico de subproductos agroindustriales”. (En ejecución)

- Proyecto Banco de la República “Aporte a la estandarización de un extracto citotóxico de hojas foliares de *Guadua incana* Londoño” (En evaluación).

**AWARDS**

- Beca de doctorado 2ª Convocatoria Ecosistema Científico - Colombia Científica 792-2017, Programa “Generación de alternativas terapéuticas en cáncer a partir

de plantas a través de procesos de investigación y desarrollo traslacional, articulados en sistemas de valor sostenibles ambiental y económicamente" (Contrato no. FP44842-221-2018). De agosto 2020 – noviembre 2023.

## PUBLICATIONS AND OTHER CONTRIBUTIONS

### Article 1

frontiers | Frontiers in Molecular Biosciences

TYPE Original Research
PUBLISHED 24 May 2023
DOI 10.3389/fmolb.2023.1192088

Check for updates

OPEN ACCESS

EDITED BY
Guillermo Moyna,
Universidad de la República, Uruguay

REVIEWED BY
Andrés Perez Parada,
Universidad de la República, Uruguay
Ying Liu,
Canadian Food Inspection Agency (CFIA), Canada
Wilton Ricardo Sala-Carvalho,
University of São Paulo, Brazil

*CORRESPONDENCE
Ian Castro-Gamboa,
ian.castro@unesp.br
Geison M. Costa,
modesticosta.g@javeriana.edu.co

†These authors have contributed equally to this work and share first authorship

RECEIVED 22 March 2023
ACCEPTED 10 May 2023
PUBLISHED 24 May 2023

CITATION
Chitiva LC, Lozano-Puentes HS, Londoño X, Leão TF, Cala MP, Ruiz-Sanchez E, Díaz-Ariza LA, Prieto-Rodríguez JA, Castro-Gamboa I and Costa GM (2023), Untargeted metabolomics approach and molecular networking analysis reveal changes in chemical composition under the influence of altitudinal variation in bamboo species.
*Front. Mol. Biosci.* 10:1192088.
doi: 10.3389/fmolb.2023.1192088

COPYRIGHT
© 2023 Chitiva, Lozano-Puentes, Londoño, Leão, Cala, Ruiz-Sanchez, Díaz-Ariza, Prieto-Rodríguez, Castro-Gamboa and Costa. This is an open-access article distributed under the terms of the Creative Commons Attribution License (CC BY). The use, distribution or reproduction in other forums is permitted, provided the original author(s) and the copyright owner(s) are credited and that the original publication in this journal is cited, in accordance with accepted academic practice. No use, distribution or reproduction is permitted which does not comply with these terms.

# Untargeted metabolomics approach and molecular networking analysis reveal changes in chemical composition under the influence of altitudinal variation in bamboo species

Luis Carlos Chitiva[1,2†], Hair Santiago Lozano-Puentes[1,3†], Ximena Londoño[4], Tiago F. Leão[2], Mónica P. Cala[5], Eduardo Ruiz-Sanchez[6], Lucía Ana Díaz-Ariza[3], Juliet A. Prieto-Rodríguez[1], Ian Castro-Gamboa[2*] and Geison M. Costa[1*]

[1]Department of Chemistry, Faculty of Sciences, Pontificia Universidad Javeriana, Bogotá, Colombia, [2]Institute of Chemistry, São Paulo State University (UNESP), Araraquara, Brazil, [3]Department of Biology, Faculty of Sciences, Pontificia Universidad Javeriana, Bogotá, Colombia, [4]Faculty of Agricultural Sciences, Universidad Nacional de Colombia, Palmira, Colombia, [5]Metabolomics Core Facility-MetCore, Universidad de los Andes, Bogotá, Colombia, [6]Department of Botany and Zoology, Universidad de Guadalajara, Jalisco, México

Bamboo species have traditionally been used as building material and potential source of bioactive substances, as they produce a wide variety of phenolic compounds, including flavonoids and cinnamic acid derivatives that are considered biologically active. However, the effects of growth conditions such as location, altitude, climate, and soil on the metabolome of these species still need to be fully understood. This study aimed to evaluate variations in chemical composition induced by altitudinal gradient (0–3000 m) by utilizing an untargeted metabolomics approach and mapping chemical space using molecular networking analysis. We analyzed 111 samples from 12 bamboo species collected from different altitudinal ranges using liquid chromatography coupled with quadrupole time-of-flight mass spectrometry (LC-QTOF-MS). We used multivariate and univariate statistical analyses to identify the metabolites that showed significant differences in the altitude environments. Additionally, we used the Global Natural Products Social Molecular Networking (GNPS) web platform to perform chemical mapping by comparing the metabolome among the studied species and the reference spectra from its database. The results showed 89 differential metabolites between the altitudinal ranges investigated, wherein high altitude environments significantly increased the profile of flavonoids. While, low altitude environments significantly boosted the profile of cinnamic acid derivatives, particularly caffeoylquinic acids (CQAs). MolNetEnhancer networks confirmed the same differential molecular families already found, revealing metabolic diversity. Overall, this study provides the first report of variations induced by altitude in the chemical profile of bamboo species. The findings may possess fascinating active biological properties, thus offering an alternative use for bamboo.

**Article 2**

*molecules*

MDPI

*Article*

# Uncovering Metabolic Alterations in HCT-116 Colon Cancer Cells upon Exposure to Bamboo Leaf Extract Obtained from *Guadua incana* Londoño

**Luis Carlos Chitiva [1,2], Mary Andrea Santamaría-Torres [3], Paula Rezende-Teixeira [4], Jessica Rodrigues Pereira de Oliveira Borlot [5], Rodrigo de Almeida Romagna [5], Ximena Londoño [6], Rodrigo Rezende Kitagawa [5], Leticia V. Costa-Lotufo [4], Juliet A. Prieto-Rodríguez [1], Ian Castro-Gamboa [2,*] and Geison Modesti Costa [1,*]**

[1] Grupo de Investigación Fitoquímica Universidad Javeriana (GIFUJ), Department of Chemistry, Faculty of Sciences, Pontificia Universidad Javeriana, Bogotá 110231, Colombia; chitival@javeriana.edu.co (L.C.C.); juliet.prieto@javeriana.edu.co (J.A.P.-R.)
[2] Núcleo de Bioensaios, Biossíntese e Ecofisiologia de Produtos Naturais (NuBBE), Institute of Chemistry, São Paulo State University (UNESP), Araraquara 14800-900, Brazil
[3] Universidad de los Andes, Bogotá 111711, Colombia; m.santamariatorres@uniandes.edu.co
[4] Laboratório de Farmacologia de Produtos Naturais Marinhos, Institute of Biomedical Sciences, University of São Paulo, São Paulo 05508-000, Brazil; paularez@usp.br (P.R.-T.); costalotufo@usp.br (L.V.C.-L.)
[5] Laboratório de Triagem Biológica de Produtos Naturais, Department of Pharmaceutical Sciences, Federal University of Espírito Santo (UFES), Vitoria 29047-105, Brazil; jessicacarpo@hotmail.com (J.R.P.d.O.B.); rodrigoromagna@gmail.com (R.d.A.R.); rodrigo.kitagawa@ufes.br (R.R.K.)
[6] Faculty of Agricultural Sciences, Universidad Nacional de Colombia, Palmira 763533, Colombia; ximelondo@gmail.com
* Correspondence: ian.castro@unesp.br (I.C.-G.); modesticosta.g@javeriana.edu.co (G.M.C.)

check for updates

**Citation:** Chitiva, L.C.; Santamaría-Torres, M.A.; Rezende-Teixeira, P.; Borlot, J.R.P.d.O.; Romagna, R.d.A.; Londoño, X.; Kitagawa, R.R.; Costa-Lotufo, L.V.; Prieto-Rodríguez, J.A.; Castro-Gamboa, I.; et al. Uncovering Metabolic Alterations in HCT-116 Colon Cancer Cells upon Exposure to Bamboo Leaf Extract Obtained from *Guadua incana* Londoño. *Molecules* **2024**, *29*, 2985. https://doi.org/10.3390/molecules29132985

Academic Editor: José Rubén Tormo

Received: 7 May 2024
Revised: 5 June 2024
Accepted: 10 June 2024
Published: 23 June 2024

**Copyright:** © 2024 by the authors. Licensee MDPI, Basel, Switzerland. This article is an open access article distributed under the terms and conditions of the Creative Commons Attribution (CC BY) license (https://creativecommons.org/licenses/by/4.0/).

**Abstract:** Metabolic alterations are increasingly recognized as important aspects of colorectal cancer (CRC), offering potential avenues for identifying therapeutic targets. Previous studies have demonstrated the cytotoxic potential of bamboo leaf extract obtained from *Guadua incana* (BLEGI) against HCT-116 colon cancer cells. However, the altered metabolic pathways in these tumor cells remain unknown. Therefore, this study aimed to employ an untargeted metabolomic approach to reveal the metabolic alterations of the endometabolome and exometabolome of HCT-116 cells upon exposure to BLEGI treatment. First, a chemical characterization of the BLEGI was conducted through liquid chromatography coupled with mass spectrometry (LC-MS). Next, we assessed cell viability via MTT and morphological analysis using an immunofluorescence assay against colon cancer cells, and anti-inflammatory activity using an LPS-stimulated macrophage model. Subsequently, we employed LC-MS and proton nuclear magnetic resonance ($^1$H-NMR) to investigate intra- and extracellular changes. Chemical characterization primarily revealed the presence of compounds with a flavone glycoside scaffold. Immunofluorescence analysis showed condensed chromatin and subsequent formation of apoptotic bodies, suggesting cell death by apoptosis. The results of the metabolomic analysis showed 98 differential metabolites, involved in glutathione, tricarboxylic acid cycle, and lipoic acid metabolism, among others. Additionally, BLEGI demonstrated significant nitric oxide (NO) inhibitory capacity in macrophage cells. This study enhances our understanding of BLEGI's possible mechanism of action and provides fresh insights into therapeutic targets for treating this disease.

**Keywords:** bamboo leaf extract; *Guadua incana*; cytotoxic activity; HCT-116 cells; endometabolome; exometabolome; anti-inflammatory activity; metabolomics

## 1. Introduction

Cancer is a multiphase process caused by the accumulation of molecular alterations, including the activation of oncogenes, inhibition of tumor suppressor genes, and changes

**Article 3**

Journal of *Fungi*

MDPI

*Article*

# Evaluation of Anti-*Candida* Potential of *Piper nigrum* Extract in Inhibiting Growth, Yeast-Hyphal Transition, Virulent Enzymes, and Biofilm Formation

**Claudia Patrícia Bravo-Chaucanés [1], Yerly Vargas-Casanova [1], Luis Carlos Chitiva-Chitiva [2], Andrés Ceballos-Garzon [1,3], Geison Modesti-Costa [2] and Claudia Marcela Parra-Giraldo [1,*]**

[1] Unidad de Proteómica y Micosis Humanas, Grupo de Enfermedades Infecciosas, Departamento de Microbiología, Facultad de Ciencias, Pontificia Universidad Javeriana, Bogotá 110231, DC, Colombia; claub06@gmail.com (C.P.B.-C.); y.vargasc@javeriana.edu.co (Y.V.-C.); andress1224@hotmail.com (A.C.-G.)
[2] Grupo de Investigación Fitoquímica Universidad Javeriana (GIFUJ), Departamento de Química, Facultad de Ciencias, Pontificia Universidad Javeriana, Bogotá 110231, DC, Colombia; chitival@javeriana.edu.co (L.C.C.-C.); modesticosta.g@javeriana.edu.co (G.M.-C.)
[3] UMR 0454 MEDIS, INRAE, Université Clermont Auvergne, 63000 Clermont-Ferrand, France
* Correspondence: claudia.parra@javeriana.edu.co

**Abstract:** Due to the increased incidence of fungal infections and the emergence of antifungal resistance mainly by *Candida* species, the need for safe and effective novel therapies is imperative. Consequently, plants and herbs are a powerful source to combat infections. Here, we evaluated the anti-*Candida* potential of an ethanolic extract from *Piper nigrum*. The phytochemical analysis of *P. nigrum* revealed bioactive compounds such as alkaloids, terpenoids, and tannis. Our results showed that *P. nigrum* extract suppressed the virulence factors of *C. albicans* strains, including hyphae formation in both liquid and solid media, reduced secretion of phospholipases/proteinases, and affected biofilm formation. Furthermore, the *P. nigrum* extract showed no hemolytic effect in vitro and exhibited reduced cytotoxicity on Vero cells and *G. mellonella* larvae at concentrations that inhibited hyphae and biofilm in *C. albicans*. Moreover, the extract demonstrated antifungal activity against *C. auris* strains. In conclusion, the *P. nigrum* extract affected the growth and morphogenesis of *Candida* (even in resistant strains), demonstrating that this plant has an anti-candida activity and represents a promising resource for discovering novel antifungal compounds.

**Keywords:** *Piper nigrum*; *Candida albicans*; *C. auris*; morphogenesis; antibiofilm; enzyme activity; toxicity

check for updates

**Citation:** Bravo-Chaucanés, C.P.; Vargas-Casanova, Y.; Chitiva-Chitiva, L.C.; Ceballos-Garzon, A.; Modesti-Costa, G.; Parra-Giraldo, C.M. Evaluation of Anti-*Candida* Potential of *Piper nigrum* Extract in Inhibiting Growth, Yeast-Hyphal Transition, Virulent Enzymes, and Biofilm Formation. *J. Fungi* **2022**, *8*, 784. https://doi.org/10.3390/jof8080784

Academic Editors: Hyang Burm Lee, Kerstin Voigt and André Luiz Cabral Monteiro de Azevedo Santiago

Received: 22 June 2022
Accepted: 22 July 2022
Published: 27 July 2022

**Publisher's Note:** MDPI stays neutral with regard to jurisdictional claims in published maps and institutional affiliations.

**Copyright:** © 2022 by the authors. Licensee MDPI, Basel, Switzerland. This article is an open access article distributed under the terms and conditions of the Creative Commons Attribution (CC BY) license (https://creativecommons.org/licenses/by/4.0/).

## 1. Introduction

*Candida* species represent the most common cause of invasive fungal infections (IFIs), particularly in immunocompromised patients [1], *Candida albicans* being the most frequently isolated of them. This fungus, which co-exists as a commensal organism of the skin, the vaginal and oral cavities, and gastrointestinal microbiota, usually causes no harm in healthy individuals, as its growth is restrained by the immune barriers and other residents of the microbiota [2,3]. However, it will likely change when tissue homeostasis is disrupted [4], causing superficial but more severe, life-threatening systemic infections [5]. The associated mortality is about 50% [6,7]. In general, the poor prognosis is partly attributable to the limited antifungal armamentarium, i.e., azoles, polyenes, and echinocandins, that exhibit disadvantages such as side effects, toxicity, and complex drug interactions, and the ongoing problem of antifungal resistance [8–10]. Due to these limitations, current research has focused on developing alternative therapies for treating *Candida* infections [7,11,12].

The pathogenicity of *Candida* spp. derives from multiple factors, including its high ability to adapt to stressful conditions [13,14]. Moreover, virulence attributes such as the

**Article 4**

Univ. Sci. 28(2): 217–229, 2023
doi: 10.11144/Javeriana.SC282.besv
ORIGINAL ARTICLE

# Black-eyed Susan vine (*Thunbergia alata*): chemical and antifungal potential evaluation of an invasive plant species in Colombia

**Miguel Ángel Vanegas Romero[1], Luis Carlos Chitiva[1], Claudia Patrícia Bravo-Chaucanés[2], Andrea Ximena Hernández[1], Claudia Marcela Parra-Giraldo[2], Geison Modesti Costa*[1]**

**Edited by**
Angela Johana Espejo Mojica
editorus@javeriana.edu.co

**1**. Pontificia Universidad Javeriana, Faculty of Science, Department of Chemistry, Grupo de Investigación Fitoquímica Universidad Javeriana (GIFUJ), Carrera 7 # 43-82, Bogotá D.C., Colombia, 110231.

**2**. Pontificia Universidad Javeriana, Faculty of Science, Department of Microbiology, Unidad de Proteómica y Micosis Humanas, Grupo de Enfermedades Infecciosas, Carrera 7 # 43-82, Bogotá D.C., Colombia, 110231.

*modesticosta.g@javeriana.edu.co

**Received:** 28-11-2022
**Accepted:** 11-05-2023
**Published online:** 03-07-2023

**Citation:** Vanegas-Romero MA, Chitiva-Chitiva LC, Bravo-Chaucanés CP, Hernández AX, Parra-Giraldo CM, Costa GM. Black-eyed Susan vine (Thunbergia alata): chemical and antifungal potential evaluation of an invasive plant species in Colombia, *Universitas Scientiarum*, 28(2): 217–227, 2023.
doi: 10.11144/Javeriana.SC282.besv

**Funding:** n.a.

**Electronic supplementary material:** n.a.

## Abstract

*Thunbergia alata* (Black-eyed Susan) is a plant species from East Africa and grows in tropical regions worldwide, including Colombia, being considered an invasive species in some countries. Even though it is used by local communities to treat several illnesses, including malaria, there are few biological and chemical studies on *T. alata*. Therefore, this study aimed to explore the chemical composition and *in vitro* antimycotic (against *Candida* strains) activity of *T. alata* crude ethanolic stem and leaf extracts. This was achieved via phytochemical analyses and chromatographic profiling (HPTLC, UPLC-DAD, and LC-MS). A two-fold serial microdilution method was used to determine the minimum inhibitory concentration (MIC) against selected Candida strains. Results showed the presence of saponins, terpenes, and flavonoids in the *T. alata* crude ethanolic stem and leaf extracts, although rutin and chlorogenic acid were the main components of stem and leaf extracts, respectively. Concerning biological assays, *T. alata* leaf extracts demonstrated moderate antimycotic activity, with MIC values between 5.00 mg $mL^{-1}$ and 1.25 mg $mL^{-1}$ against *C. albicans* and *C. auris* strains. The results indicate that *T. alata* extracts, including some of their major identified compounds, possess promising antifungal properties against two significant microorganisms.

**Keywords:** Antifungal activity; *Candida albicans*; *Candida auris*; HPTLC, LC-MS, *Thunbergia alata*, UPLC.

## 1. Introduction

Human societies have used plants for the treatment of many diseases. According to the World Health Organization (WHO), over 80 % of the world's population depends on traditional medicine or herbs for their primary healthcare needs [1]. To date, searching for natural products obtained from plants is one of the strategies used for developing new drug leads due to the unmatched chemical diversity within the plant kingdom [1, 2, 3]. Plant extracts boast a broad array of secondary metabolites, such as flavonoids, tannins, alkaloids, and terpenoids, which are anti-infective agents and generate fewer side effects than those of synthetic antimicrobial drugs [1, 4, 5, 6].

*Universitas Scientiarum*, Journal of the Faculty of Sciences, Pontificia Universidad Javeriana, is licensed under the Creative Commons Attribution 4.0 International Public License

**Article 5**

Cancer Immunology, Immunotherapy (2023) 72:3279–3292
https://doi.org/10.1007/s00262-023-03487-3

RESEARCH

# *Piper nigrum* extract suppresses tumor growth and enhances the antitumor immune response in murine models of breast cancer and melanoma

Paola Lasso[1] · Laura Rojas[1] · Cindy Arévalo[1] · Claudia Urueña[1] · Natalia Murillo[1] · Paula Nossa[1] · Tito Sandoval[1] · Luis Carlos Chitiva[2] · Alfonso Barreto[1] · Geison M. Costa[2] · Susana Fiorentino[1]

Received: 28 November 2022 / Accepted: 26 June 2023 / Published online: 18 July 2023
© The Author(s) 2023

**Abstract**

Although the antitumor effect of *P. nigrum* has been widely studied, research related to its possible immunomodulatory effects is relatively scarce. Here, the antitumor and immunomodulatory activity of an ethanolic extract of *P. nigrum* were evaluated in the murine models of 4T1 breast cancer and B16-F10 melanoma. In vitro evaluations showed that the *P. nigrum* extract has cytotoxic activity, induces apoptotic cell death, and has a pro-oxidant effect in both cell lines, but it regulates glucose uptake differently in both lines, decreasing it in 4T1 but not in B16-F10. *P. nigrum* extract significantly reduced tumor size in both models and decreased the occurrence of macrometastases in 4T1 model. Evaluation of immune subpopulations by flow cytometry revealed that the *P. nigrum* extract significantly increases the frequency of dendritic cells and activated $CD8^+$ T cells and decreases the frequency of myeloid-derived suppressor like cells and Tregs in the tumor microenvironment of both models but with different dynamics. Our findings strongly suggest that the *P. nigrum* extract exerts immunomodulatory functions, slightly related to the modulation of cellular energy metabolism, which could ultimately contribute to the promising antitumor effect of *P. nigrum*.

**Keywords** Breast cancer · Melanoma · *Piper nigrum* · Immunomodulation · Antitumor · Plant extracts

## Introduction

*Piper* species, widely distributed in tropical and subtropical regions of the world, are used in the Ayurvedic system of medicine in India as well as in folk medicine in Latin America and the West Indies. Some species, like *P. aduncum* and *P. hispidum* are used for stomach pain and insect repellants. *P. amalago* distributed from Mexico to Brazil is used to relieve chest pain and as an anti-inflammatory agent [1, 2]. The roots and fruits of *P. chaba* and *P. futokadsura* are useful in asthma, bronchitis, fever, and hemorrhoidal conditions [3].

✉ Susana Fiorentino
susana.fiorentino@javeriana.edu.co

[1] Grupo de Inmunobiología y Biología Celular, Pontificia Universidad Javeriana, Carrera 7a. No. 43-82, Ed. 50, Lab. 101, Bogotá C.P. 110211, Colombia

[2] Grupo de Investigación en Fitoquímica, Pontificia Universidad Javeriana, Bogotá, Colombia

*P. nigrum* is widely used in folk medicine and has been used for diarrhea, indigestion, and respiratory system problems [4]. Surprisingly, *P. nigrum* has also shown significant in vitro and in vivo anticancer activity in many cancer models, including breast, prostate, colon, rectal, lung, melanoma, ovarian, and cervical cancers, among others [5]. The major compounds found in *P. nigrum* extract are alkaloids, including piperine, chavicine, piperidine, pellitorine, and piperedine, while flavones, flavanones, terpenes, steroids, lignans, neolignans, and alkamides are other main compounds [6, 7]. Interest in piperines and their biological activity is not recent, these compounds have been characterized for their anti-inflammatory, immunomodulatory, and anticancer effects [5].

The ethanolic extract as well as the one obtained by supercritical fluids extraction, rich in piperines, present interesting cytostatic activity by inducing arrest in the G1 or G2/M phases of the cell cycle, respectively, in addition to differential cytotoxicity depending on the cell line, apparently due to a p53-dependent effect. Interestingly, the complete extract is more cytotoxic than the two main

**Article 6**

molecules

MDPI

*Article*

# Dendritogenic Potential of the Ethanol Extract from *Lippia alba* Leaves in Rat Cortical Neurons

**María Marcela Velásquez [1,*], María Claudia Lattig [2], Luis Carlos Chitiva [3], Geison M. Costa [3], Jhon Jairo Sutachan [4] and Sonia Luz Albarracin [4,*]**

[1] Instituto de Genética Humana, Facultad de Medicina, Pontifica Universidad Javeriana, Bogotá 110911, Colombia
[2] Facultad de Ciencias, Universidad de los Andes, Bogotá 110911, Colombia
[3] Departamento de Química, Pontificia Universidad Javeriana, Bogotá 110911, Colombia
[4] Departamento de Nutrición y Bioquímica, Pontificia Universidad Javeriana, Bogotá 110911, Colombia
* Correspondence: mariamvelasquez@javeriana.edu.co (M.M.V.); albarra@javeriana.edu.co (S.L.A.)

**Abstract:** A reduced dendritic complexity, especially in regions such as the hippocampus and the prefrontal cortex, has been linked to the pathophysiology of some neuropsychiatric disorders, in which synaptic plasticity and functions such as emotional and cognitive processing are compromised. For this reason, the identification of new therapeutic strategies would be enriched by the search for metabolites that promote structural plasticity. The present study evaluated the dendritogenic potential of the ethanol extract of *Lippia alba*, an aromatic plant rich in flavonoids and terpenes, which has been widely used in traditional medicine for its presumed analgesic, anxiolytic, and antidepressant potential. An in vitro model of rat cortical neurons was used to determine the kinetics of the plant's effect at different time intervals. Changes in morphological parameters of the neurons were determined, as well as the dendritic complexity, by Sholl analysis. The extract promotes the outgrowth of dendritic branching in a rapid and sustained fashion, without being cytotoxic to the cells. We found that this effect could be mediated by the phosphatidylinositol 3-kinase pathway, which is involved in mechanisms of neuronal plasticity, differentiation, and survival. The evidence presented in this study provides a basis for further research that, through in vivo models, can delve into the plant's therapeutic potential.

**Keywords:** structural plasticity; dendritic complexity; neurotrophins; PI3Ks; MAPKs; flavonoids; terpenes; *Lippia alba*; neuropsychiatric disorders

check for updates

**Citation:** Velásquez, M.M.; Lattig, M.C.; Chitiva, L.C.; Costa, G.M.; Sutachan, J.J.; Albarracin, S.L. Dendritogenic Potential of the Ethanol Extract from *Lippia alba* Leaves in Rat Cortical Neurons. *Molecules* **2023**, *28*, 6666. https://doi.org/10.3390/molecules28186666

Academic Editor: Ladislav Kokoska

Received: 13 July 2023
Revised: 29 August 2023
Accepted: 30 August 2023
Published: 16 September 2023

**Copyright:** © 2023 by the authors. Licensee MDPI, Basel, Switzerland. This article is an open access article distributed under the terms and conditions of the Creative Commons Attribution (CC BY) license (https://creativecommons.org/licenses/by/4.0/).

## 1. Introduction

Dendritic arborization is a relevant morphological factor that influences the identity and number of presynaptic stimuli that neurons can integrate, thus affecting their overall functionality [1]. Changes in dendritic complexity are decisive for neuronal plasticity dynamics in the central nervous system [2,3]. Accordingly, it has been suggested that irregularities in the formation of spines and dendritic branches, which are the basis of the postsynaptic excitatory machinery, are related to the pathophysiology of multiple neuropsychiatric disorders [4,5]. Specifically, morphological abnormalities of the dendritic tree have been identified in conditions such as autism spectrum disorder, Alzheimer's disease, schizophrenia, Down syndrome, fragile X syndrome, and Rett syndrome [6,7]. Likewise, considering that dendritic complexity is susceptible to responding to intrinsic and extrinsic factors, such as trauma or stress, it has been related to cognitive and mood disorders, including anxiety and major depression [8,9]. In this regard, chronic stress has been reported to induce neuro-histological changes, especially in regions such as the hippocampus and prefrontal cortex, significantly reducing dendritic arborization and, thus, affecting the glutamatergic neurotransmission system [8,10].

**Article 7**

ACS OMEGA

Open Access

This article is licensed under CC-BY-NC-ND 4.0

http://pubs.acs.org/journal/acsodf

Article

# Changes in Phenolic Profile and Total Phenol and Total Flavonoid Contents of *Guadua angustifolia* Kunth Plants under Organic and Conventional Fertilization

*Published as part of the ACS Omega virtual special issue "Phytochemistry".*

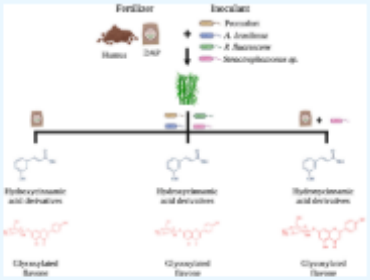
David A. Villamarin-Raad,[#] Hair S. Lozano-Puentes,[#] Luis Carlos Chitiva, Geison M. Costa, Sergio A. Díaz-Gallo, and Lucía A. Díaz-Ariza[*]

Cite This: *ACS Omega* 2023, 8, 41223−41231

Read Online

ACCESS | Metrics & More | Article Recommendations | Supporting Information

**ABSTRACT:** Agronomic management of a crop, including the application of fertilizers and biological inoculants, affects the phenol and flavonoid contents of plants producing these metabolites. *Guadua angustifolia* Kunth, a woody bamboo widely distributed in the Americas, produces several biologically active phenolic compounds. The aim of this study was to evaluate the effect of chemical and organic fertilizers together with the application of biological inoculants on the composition of phenolic compounds in *G. angustifolia* plants at the nursery stage. In 8-month-old plants, differences were observed in plant biomass (20.27 ± 7.68 g) and in the content of total phenols and flavonoids (21.89 ± 9.64 mg gallic acid equivalents/plant and 2.13 ± 0.98 mg quercetin equivalents/plant, respectively) when using the chemical fertilizer diammonium phosphate (DAP). No significant differences were found owing to the effect of the inoculants, although the plants with the application of *Stenotrophomonas* sp. on plants fertilized with DAP presented higher values of the metabolites (24.12 ± 6.72 mg gallic acid equivalents/plant and 2.39 ± 0.77 mg quercetin equivalents/plant). The chromatographic profile of phenolic metabolites is dominated by one glycosylated flavonoid, the concentration of which was favored by the application of the inoculants *Azospirillum brasilense*, *Pseudomonas fluorescens*, and *Stenotrophomonas* sp. In the case study, the combined use of DAP and bacterial inoculants is recommended for the production of *G. angustifolia* plant material with a high content of promising biologically active flavonoids or phenolics.



## 1. INTRODUCTION

*Guadua angustifolia* is a bamboo species with high economic value for Colombia.[1] The culm has been the main organ of interest for this plant because it can be used for the manufacture of structures, handicrafts, flooring, and woodwork.[2] Likewise, it has been found that byproducts of the culm production process, such as chips and leaves, are used for pulp and biochar production.[3,4] Additionally, its chemical composition and biological activity, associated with secondary metabolites present in the culms and leaves of this plant, have been studied;[5,6] furthermore, phenolic compounds such as caffeoylquinic acid and caffeic acid 3-glucoside and flavonoids such as quercetin 3,7-dirhamnoside, kaempferol-3-O-rutinoside, violanthin, vitexin 6″-(3-hydroxy-3-methylglutarate), and kaempferol 7-sophoroside have been reported in these leaves,[7] showing the potential of this plant as a source of secondary metabolites of interest in different industries.

In addition, the use of agronomic management that improves the content of phenolic compounds is a strategy for crop production with greater phytochemical value.[8,9] For this purpose, the use of different fertilizers has been evaluated, such as organic fertilizers[10] and conventional fertilizers,[11,12] which have been effective in increasing the content of phenols and flavonoids in different plant species.[13−15] In addition, inoculants can encourage the formation of phenolic compounds, which are naturally occurring poisons that help protect plants from harmful organisms.[16] Bacteria, such as *Azotobacter* sp., *Azospirillum* sp., *Bacillus* sp., and *Pseudomonas* sp., also increase the content of phenolic compounds. These organisms can act in conjunction with fertilizers to promote higher phenolic and flavonoid contents, as well as higher biomass.[14,17−19]

Received: June 26, 2023
Revised: October 4, 2023
Accepted: October 9, 2023
Published: October 25, 2023



ACS Publications

© 2023 The Authors. Published by American Chemical Society



https://doi.org/10.1021/acsomega.3c04579
ACS Omega 2023, 8, 41223−41231

**Article 8**

biomolecules

MDPI

*Article*

# Exploring the Potential Mechanism of Action of Piperine against *Candida albicans* and Targeting Its Virulence Factors

**Claudia Patricia Bravo-Chaucanés [1], Luis Carlos Chitiva [2], Yerly Vargas-Casanova [1], Valentina Diaz-Santoyo [1], Andrea Ximena Hernández [2], Geison M. Costa [2] and Claudia Marcela Parra-Giraldo [1,3,*]**

[1] Unidad de Proteómica y Micosis Humanas, Grupo de Enfermedades Infecciosas, Departamento de Microbiología, Facultad de Ciencias, Pontificia Universidad Javeriana, Bogotá 110231, DC, Colombia; claub06@gmail.com (C.P.B.-C.); y.vargasc@javeriana.edu.co (Y.V.-C.); valentina_diaz@javeriana.edu.co (V.D.-S.)

[2] Grupo de Investigación Fitoquímica Universidad Javeriana (GIFUJ), Departamento de Química, Facultad de Ciencias, Pontificia Universidad Javeriana, Bogotá 110231, DC, Colombia; chitival@javeriana.edu.co (L.C.C.); hernandez_a@javeriana.edu.co (A.X.H.); modesticosta.g@javeriana.edu.co (G.M.C.)

[3] Departamento de Microbiología y Parasitología, Facultad de Farmacia, Universidad Complutense de Madrid, 28040 Madrid, Spain

* Correspondence: claudpar@ucm.es or claudia.parra@javeriana.edu.co

**Abstract:** Plant-derived compounds have proven to be a source of inspiration for new drugs. In this study, piperine isolated from the fruits of *Piper nigrum* showed anti-*Candida* activity. Furthermore, the mechanisms of action of piperine and its impact on virulence factors in *Candida albicans*, which have not been comprehensively understood, were also assessed. Initially, piperine suppressed the hyphal transition in both liquid and solid media, hindered biofilm formation, and resulted in observable cell distortions in scanning electron microscope (SEM) samples, for both fluconazole-sensitive and fluconazole-resistant *C. albicans* strains. Additionally, the morphogenetic switches triggered by piperine were found to rely on the activity of mutant *C. albicans* strains. Secondly, piperine treatment increased cell membrane permeability and disrupted mitochondrial membrane potential, as evidenced by propidium iodine and Rhodamine 123 staining, respectively. Moreover, it induced the accumulation of intracellular reactive oxygen species in *C. albicans*. Synergy was obtained between the piperine and the fluconazole against the fluconazole-sensitive strain. Interestingly, there were no hemolytic effects of piperine, and it resulted in reduced cytotoxicity on fibroblast cells at low concentrations. The results suggest that piperine could have a dual mode of action inhibiting virulence factors and modulating cellular processes, leading to cell death in *C. albicans*.

**Keywords:** antifungal activity; *Candida albicans*; mechanism of action; piperine; virulence factors

check for updates

**Citation:** Bravo-Chaucanés, C.P.; Chitiva, L.C.; Vargas-Casanova, Y.; Diaz-Santoyo, V.; Hernández, A.X.; Costa, G.M.; Parra-Giraldo, C.M. Exploring the Potential Mechanism of Action of Piperine against *Candida albicans* and Targeting Its Virulence Factors. *Biomolecules* **2023**, *13*, 1729. https://doi.org/10.3390/biom13121729

Academic Editors: Nurhayat Tabanca and Jen-Tsung Chen

Received: 8 September 2023
Revised: 1 November 2023
Accepted: 9 November 2023
Published: 30 November 2023

**Copyright:** © 2023 by the authors. Licensee MDPI, Basel, Switzerland. This article is an open access article distributed under the terms and conditions of the Creative Commons Attribution (CC BY) license (https://creativecommons.org/licenses/by/4.0/).

## 1. Introduction

*Candida* is a yeast that naturally exists in the human microbiota as a commensal organism [1]. However, under certain favorable conditions or predisposing circumstances, it can transform an opportunistic pathogen, giving rise to various types of infections, which can span from superficial to systemic and can manifest in various parts of the body. Notably, candidiasis can lead to substantial morbidity and mortality, particularly among individuals with compromised immune systems [2,3]. Currently, there are some broad-spectrum antifungal drugs accessible for treating infections caused by *Candida*. Nonetheless, the emergence of adverse side effects and the growing problem of antifungal resistance have raised concerns regarding the efficacy of existing antifungal treatments. Consequently, a pressing demand exists for novel and enhanced antifungal agents to effectively tackle these issues [4].

An innovative approach in the search for *Candida* inhibitors is to target the virulence factors of the pathogen. This strategy aims to disable *Candida's* ability to infect without

## Undergraduate thesis supervision

Pontificia Universidad JAVERIANA Bogotá | Facultad de Ciencias Carrera de Biología

**A QUIEN CORRESPONDA**

Respetados señores reciban un cordial saludo.

Me permito informar que **Luis Carlos Chitiva Chitiva,** Estudiante de Doctorado de Ciencias Biológicas de la Facultad de Ciencias de la Pontificia Universidad Javeriana, participó como **Director** del siguiente trabajo de grado. Este fue sustentado y aprobado satisfactoriamente en junio de 2022, por el estudiante de la carrera de Biología **Miguel Quintero Correa.**

Título Trabajo de Grado: "Aporte quimiotaxonómico para tres especies vegetales del género Piper (Piperaceae) mediante el uso de técnicas HPTLC y CPC."

La presente comunicación se expide a los veintitrés (23) días del mes de agosto del año dos mil veintidós (2022).

Atentamente,

**JORGE JÁCOME, PhD**
Director
Carrera de Biología

Carrera 7ª 43-82, Piso 5. Edificio Carlos Ortiz, S.I. (52) Oficina 508 – Bogotá, D.C., Colombia
Teléfono: 57 (1) 3208320 ext. 4054